Determination of Hydro-Mechanical Characteristics of Biodegradable Waste- Laboratory and Landfill Site

Kiran Nousheen Arif

UNIVERSITE DE GRENOBLE

THESE

préparée au

Laboratoire d'étude des Transferts en Hydrologie et Environnement (LTHE)

dans le cadre de
L'Ecole Doctorale Terre, Univers, Environnement

pour obtenir le grade de

DOCTEUR DE L'UNIVERSITE DE GRENOBLE

Spécialité : Sciences de la Terre, de l'Univers et de l'Environnement
(Earth, Universe and Environmental Sciences)

présentée par

Kiran NOUSHEEN ARIF

intitulée

Determination of Hydro-Mechanical Characteristics of Biodegradable Waste- Laboratory and Landfill Site

Soutenue le 20 Avril 2010 devant la commission d'examen

Mounir BOUASSIDA	Rapporteur	Professeur, ENI Tunis
Guy MATEJKA	Rapporteur	Professeur, ENSI Limoges
Jean-Pierre GOURC	Directeur de thèse	Professeur, LTHE
Philippe DELMAS	Examinateur	Professeur, CNAM Paris
Franck OLIVIER	Examinateur	Ingénieur, ECOGEOS

ACKNOWLEDGEMENTS

One year of Masters leading to more than three and a half years of doctoral work have finally culminated into the point where I can express my gratitude to those who made it possible for me to get through what I set out for. Needless to say how tiring this phase becomes especially towards its end, of essence is the fact that it ended well, giving way to, hopefully, a promising life and new chapters of life.

Those having gone through the tedious doctoral work know how important a role one's supervisor plays. Say it my luck or whatever anyone wishes to name it, I had Mr. Jean-Pierre GOURC as my supervisor. The man, being a giant in the field, taught me a lot. He helped me wade through the difficult times, at times pushing and at times encouraging. I am profoundly obliged to him for all the support he lent me.

I am highly thankful to the jury members specially the referees, Mr. Mounir BOUASSIDA and Mr. Guy MATEJKA, for their detailed and sincere remarks that they managed to send back while the time was of essence. The valuable comments from the examiners, Mr. Philippe DELMAS and Mr. Franck OLIVIER, were of great help enabling me to further improve my report. I stand indebted to them, particularly to Mr. OLIVIER, my erstwhile senior colleague at the laboratory, with whose gracious support I could incorporate the new version of ISPM model into my thesis report, an important contribution to the scientific community of my domain.

Guillaume STOLTZ, a senior colleague and a friend, illuminated me with technical and pedagogical reasoning in long and tireless discussions. Had it not been for his well-disposed nature, my efforts would have increased manifold in order to comprehensively grasp the subject. I am deeply grateful to him.

As my work encompassed experimental work all along, I needed the help of technical staff on regular basis. For facilitating my work, Mr. Henri MORA was always there. Without him, it would have been extremely difficult to successfully complete a hectic schedule of experiments. I appreciate him for everything he did for me.

It is difficult to name everyone who eased my way to this point, however, this note of gratitude would be incomplete if I don't mention my friends at my workplace: Lucile TARTARD, Elisabeth CANET, Matthias STAUB, and Anne-Juile TINET, to name a few. Indeed the off and on badinage is indispensable to lighten up the otherwise usually dry and sombre research environment. Their moral support and our confabs left unforgettable memories in my mind. I wish them all the success in their endeavours.

Hailing from a distant place, far from the family of origin and culture, a logical outcome is nostalgia which is itself quite difficult to bear if one falls a victim to it. Owing to a very supportive and active Pakistani students community, I didn't have to face anything of that sort. Be it a local festivity or our traditional events, we were always together. I wish them all the best of luck. Their combined efforts to put forward the true image of Pakistan, as progressive, tolerant, and moderate country are highly appreciative.

I take this opportunity to thank the Higher Education Commission of Pakistan with whose funding I have been able to come abroad and complete my studies. It has been a worthwhile experience and I am sure that with the broadened vision and developed competencies, I'll be able to serve my country in a better manner.

Last but not the least, I'd like to express my gratitude to my family: my husband for his non-judgmental and tolerant attitude, and my kids, Khuzemah and Rawahah, whose lovable and innocent faces, gestures and talk brushed off all the cumulated fatigue of the usually tiring day.

DEDICATION

To my mother

Due to whom I am where I am today

TABLE OF CONTENTS

CHAPTER III

I- INTRODUCTION

As long as there is the need for disposal of household waste there will be the need to understand the phenomena taking place at the other end i.e. a landfill or incinerators. The understanding of landfill technology is of great importance because of its ever changing state, whether physical, chemical or hydrological. Despite the increasing rates of recycling and reuse, population and economic growth will still render landfill as necessary component of solid waste management. Landfills can either be technically engineered structure or an open dump as the case may be in less developed countries, but the burial of domestic waste has been practiced since ages and remains one of the most common processes of disposal. In the context of our proposed research topic there is a need to elaborate various aspects concerning municipal solid waste, its typical composition, characteristics and behaviour concerning its disposal at landfill sites.

I-1 TYPES OF SOLID WASTES

According to the regulatory legislation, solid waste is classified according to their origin and their toxicity. The type of storage structure depends on the nature and characteristics of waste. The current regulations distinguish three broad classes of waste:

1) Hazardous Waste: According to European Directive No. 2002-540 of April 18, 2002 on classification of wastes, is the type of waste which displays one or more of the following properties: Explosive, oxidizing, easily flammable, flammable, irritant, harmful, carcinogenic, corrosive, infectious, mutagenic, toxic for reproduction substances and chemical compounds which on contact with water, air or an acid, emit toxic gas or highly toxic substances and chemical compounds which, after disposal, may yield by any means another substance, e.g. the leachate which might possess any eco-toxic characteristics listed above.
The directive of January 19, 2006 amending the directive of September 9, 1997 concerns storage of household or similar waste without distinguishing household waste and assimilated waste, and only defines non-hazardous waste.

2) Non-hazardous waste: is defined in the directive of January 19, 2006 amending the directive of September 9, 1997 as any waste not defined as hazardous by No. 2002-540 of 18 April 2002. The non-hazardous waste is divided into two categories according to predictable behaviour under storage conditions and alternative disposal:

- **Category D:** Waste whose behaviour within the storage evolves and leads to the production of leachate and biogas. This category includes household garbage, bulky items of domestic origin with fermentable components as green waste. This type of waste is not considered ultimate refuse because their pollution intensity can further be reduced.
- **Category E:** waste whose behaviour in storage is indolent and the degradation capacity is low. This category presents a moderate pollutant nature and includes waste plastics and scrap metals, glass, ash and slag.

3) Inert waste: is defined by European Directive 1999/31/EC of April 26, 1999, as undergoing "no change physical, chemical or biological" in time. Inert waste does not decompose, burn and have no physical or chemical reaction. It is not biodegradable and do not deteriorate. Furthermore materials with which come into contact with them are not likely to cause environmental pollution or harm to the human health. The total leachate production, content of waste pollutant and the eco-toxicity of the leachate should be negligible and, especially, should not affect the quality of surface water and / or groundwater. This class mainly incorporates mineral waste or similar to natural unpolluted substrate.

The French law on waste disposal and recovery materials July 13, 1992 prohibits the storage of raw waste that can not be considered as ultimate waste or stabilized. This prohibition is effective in France since 1 July 2002. A waste is considered as the ultimate refuse whether treated or not if it is not likely to be treated in technical and economic conditions of the moment. Considering the present economic state, the waste is considered as stable when its liquid permeability and leaching fraction has been reduced.

I-1.1 Municipal Solid Waste

Municipal Solid Waste (MSW) is the type of the waste which includes primarily household waste with sometimes the addition of ordinary commercial waste containing either solids or semi solids. According to IFEN (2006) each year 31 million tons of domestic waste is generated in France with a generation rate of 457 kg/capita/year. In Figure I-1 the generation trends for member countries of the economic cooperation organisation are presented including the expected generation rate for the year 2020, where as Table I-1 details the MSW waste composition according to the income level.

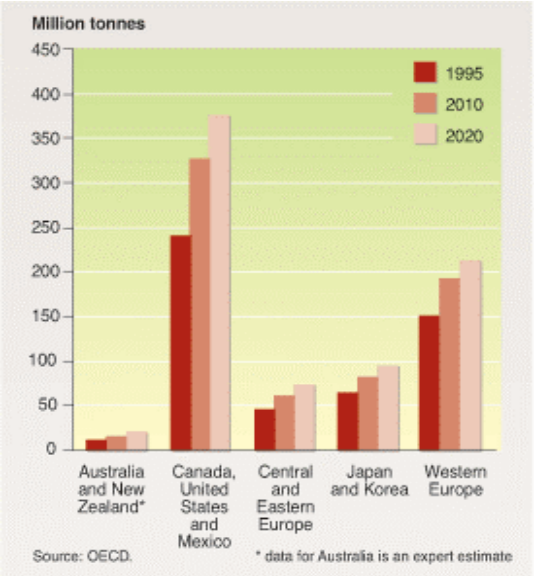

Figure I-1 : Municipal solid waste generation trends around the world (OECD, 2004).

Table I-1: MSW composition for different income levels (Tchobanoglous et al., 2003)

Waste Component (% $_{MH}$)	Countries Income		
	High	Medium	Low
Organic			
Food Waste	6-30	20-65	40-85
Paper/Cardboard	20-45	8-30	1-10
Plastics	2-8	2-6	1-5
Textile	2-6	2-10	1-5
Rubber & leather	0-2	1-4	1-5
Wood & yard waste	10-20	1-10	1-5
Misc organic waste	< 1	< 1	< 1
Inorganic			
Glass	4-12	1-10	1-10
Tin cans	2-8	1-5	1-5
Aluminium	0-1	1-5	1-3
Other metals	1-4	1-5	1-5
Dirt, ash etc.	0-10	1-30	1-40

I-1.2 Multi-Criterion Municipal Solid Waste Composition

If the solid waste is considered as a material demonstrating the properties of a geological material, it is certainly important to explain its environmental impacts in reference to its disposal as it concerns the geotechnical experts as well as the field operators.

Household waste is a mixture of particles each of which is differently classified from organic to granular and inert to putrescibles. Because of the heterogeneous nature of the waste mass there is always uncertainty for the parameters determined for the whole mass as it comprises many elements each unique in its nature. But together the technical experts, engineers and researchers work in collaboration to unite these all aspects in a manner to formulize in general the whole mass. The aim of the study always is to estimate the waste mechanical characteristics in correlation with the composition of waste which is modified because of change in the bio-chemical properties resulting in change of the mechanical properties. Depending upon the composition of the specific waste material the mechanical characteristics may differ from those of typical soils and may require special geotechnical consideration. Relating the changes in its chemical and biological form to the mechanical properties can be done through some laws of mechanics which has not yet been well established. There are models proposed by researchers which take into account these various aspects of biological, chemical and mechanical properties but their authenticity is still to be acknowledged.

Numerous approaches to characterize the waste components exist, which mainly depend upon the type of study under discussion. In terms of biochemical classification of the waste it is subdivided into two classes, namely organic and inorganic components as shown in Table I-1. Furthermore these components can be sub- classified as Aran (2001) proposed the classification of organic waste on the function of their degradation activity, with the following subdivision:

Readily Degradable waste: This class includes the kitchen and garden waste (fruits, vegetables, animal waste) etc.
Normally degradable waste: In this class sludge and fatty waste is considered
Slow degradable waste: Paper, cardboard and wood is included in this class.

In Figure I-2 the waste composition for the developed countries is presented in comparison with the composition of major cities in the less developed countries of Asia.

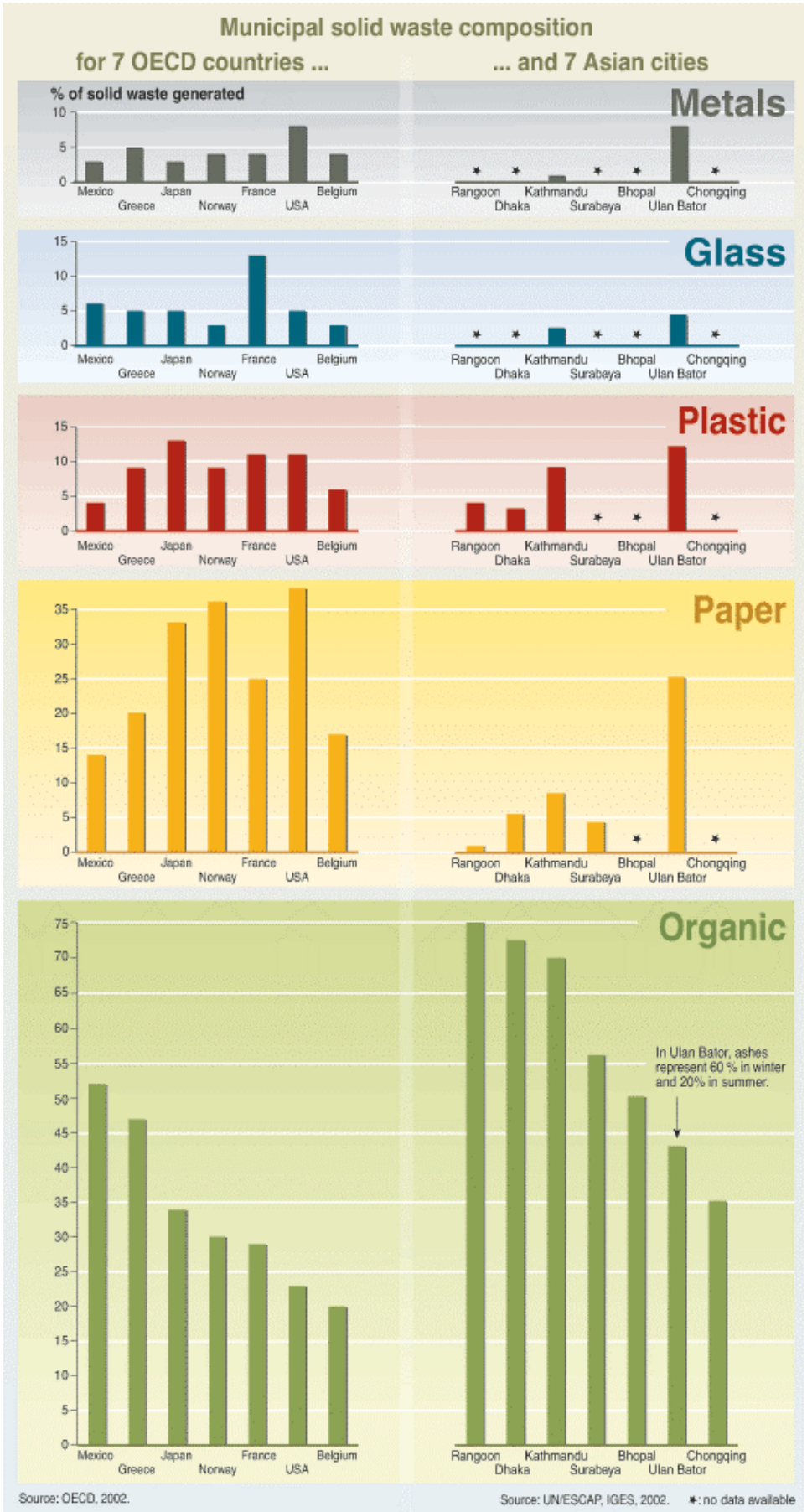

Figure I-2 : Comparison of waste composition (UNESCAP, 2002).

Different types of particles are present in a solid waste mass, classified (Landva & Clark, 1990, Kölsch, 1995) according to their geo-mechanical properties. Grisolia et al. (1995) proposed their classification as under:

Class A: Inert stable materials (rigid) are regrouped in this class whose composition do not vary over the course of time and have high resistance to deformation. These materials are considered to have mechanical behaviour similar to soils. This category includes different soil materials as well as aggregates and debris, glass, ceramics, metal, plastics and wood.

Class B: Highly deformable materials include those materials which tend to go under instantaneous compression under the application of load and some of them continue to deform over the period of time under the applied load but on the contrary their degradation is a very slow process. Within this class the waste materials are further subdivided into

- crushable/breakable
- compressible/bendable/deformable

The overall influence of these materials on the waste body is generally dependent upon their size, pre-treatment (shredding) and the load applied.

Class C: Biodegradable, which change in volume or change from solid to liquid or gas phase on decomposition. This class of waste materials comprises mainly of kitchen and garden waste. Their decomposition highly affects the material structure of the landfill over the long run as their degradation reduces the total volume of solids, increasing the over all density and generates by products such as leachate and biogas. This classification for various regions of the world is presented in Figure I-3.

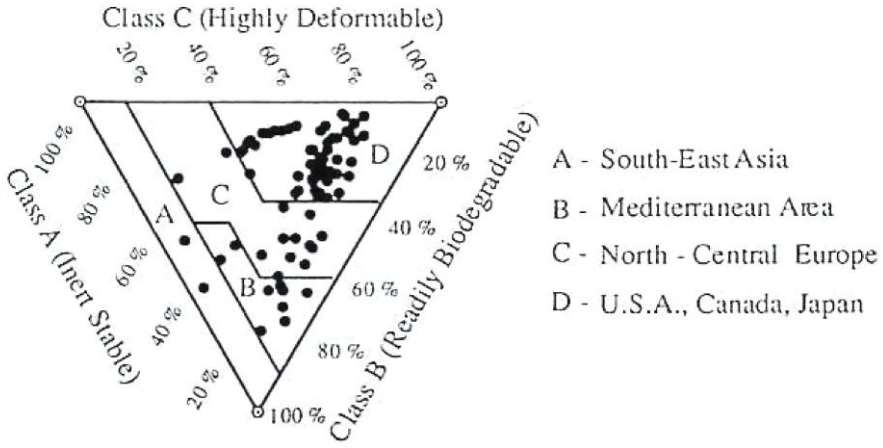

Figure I-3 : Ternary diagram of waste classification as presented by Grisolia et al. (1995).

Some classification systems e.g. as proposed by Langer (2005) separate different components as follows:

- Material groups (papers, plastics, metals)
- Mechanical properties of material groups (shear, tensile and compressive strength)

With further subdivision according to

- shape
- Reinforcing components
- Compressible components (high & low)
- Incompressible components
- Size of the components
- Degradation potential within the material groups

I-1.3 Four Stage Bacterial Decomposition of MSW

Bacteria decompose landfill waste in four phases and the composition of the gas produced changes with each of the four phases of decomposition. Landfills often accept waste over a long period of time, so the waste in a landfill may be undergoing several stages of decomposition at once. This means that older waste in one section of the landfill might be in a different phase of decomposition than more recently buried waste in another section (Figure I-4, I-5).

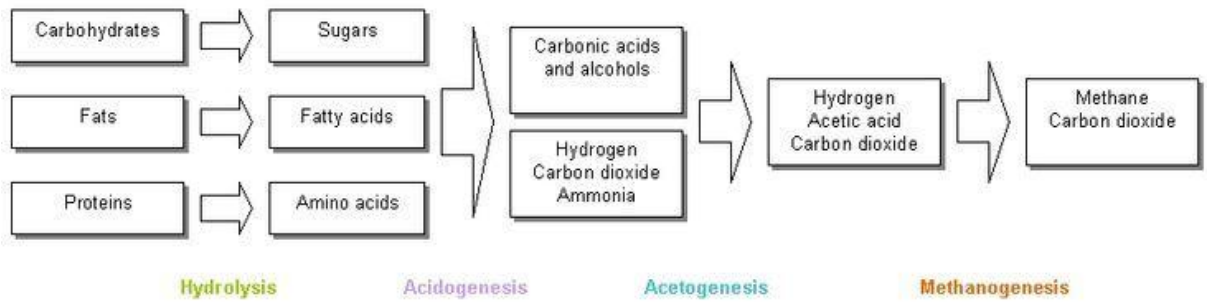

Figure I-4 : Chemical processes occurring during the four stages of decomposition (Marshal, 2007).

Stage I: During the first phase of decomposition, aerobic bacteria consume oxygen while breaking down the long molecular chains of complex carbohydrates, proteins, and lipids that comprise organic waste. The primary by-product of the process is carbon dioxide. Nitrogen content is high at the beginning of this phase, but declines as the landfill moves through the four stages. Stage I continues until available oxygen is depleted. Decomposition during the stage I can last for days or months, depending on how much oxygen is present when the waste is disposed of in the landfill. Oxygen levels vary according to factors such as how loose or compressed the waste was when it was buried.

Stage II: Stage II decomposition starts after the oxygen in the landfill has been used up. Using an anaerobic process, bacteria convert compounds created by aerobic bacteria into acetic, lactic, and formic acids and alcohols such as methanol and ethanol. As the acids mix with the moisture present in the land-fill, they cause certain nutrients to dissolve, like nitrogen and phosphorus. The gaseous by-products of these processes are carbon dioxide and hydrogen.

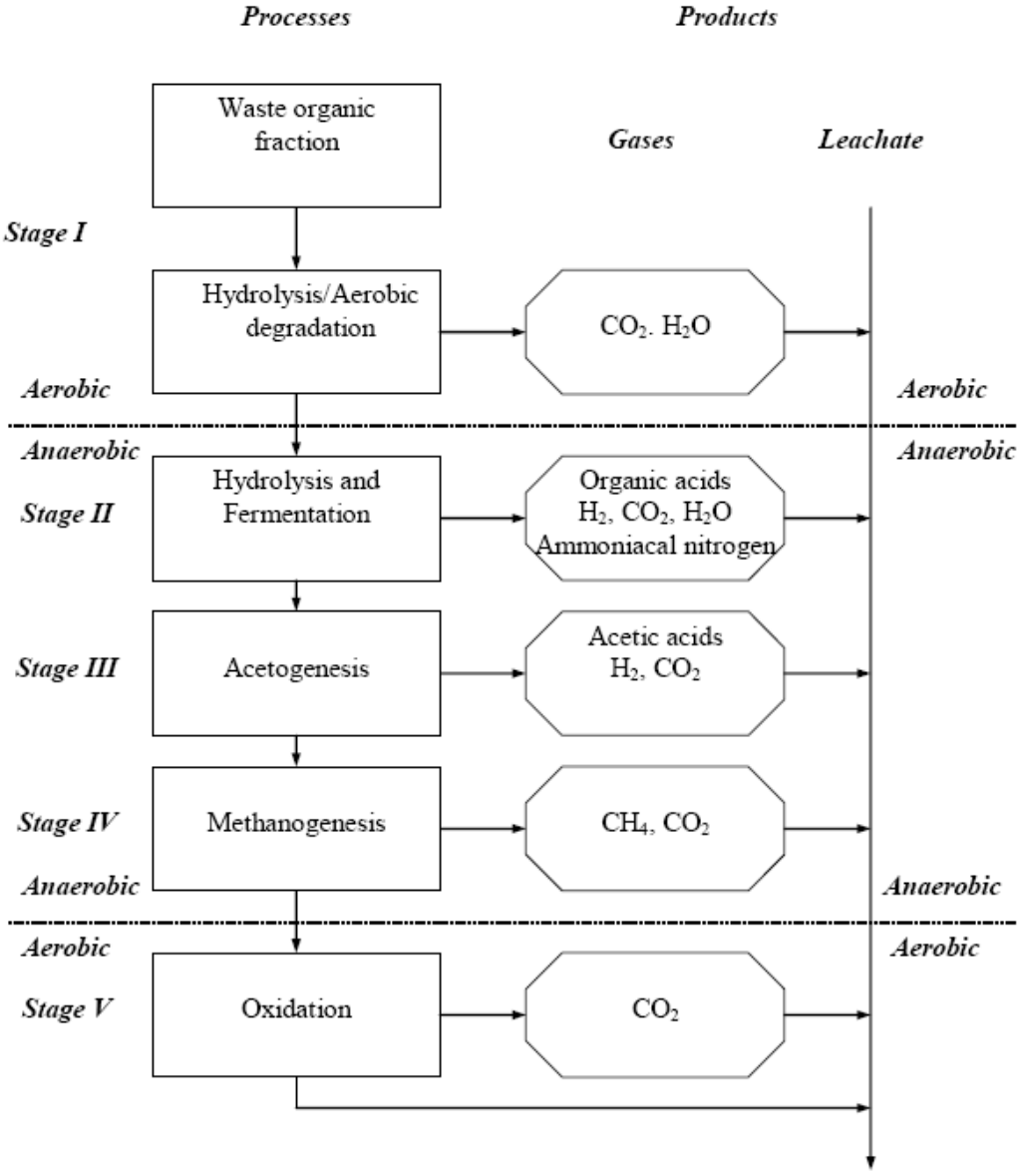

Figure I-5 : The degradation process of the organic matter (William 2005).

Stage III: Stage III decomposition starts when certain kinds of anaerobic bacteria consume the organic acids produced in stage II and form acetate, an organic acid. This process causes the landfill to become a more neutral environment in which methane producing bacteria begin to establish themselves. Methane and acid producing bacteria have a symbiotic, or mutually beneficial, relationship. Acid-producing bacteria create compounds for the methanogenic bacteria to consume.

Methanogenic bacteria consume the carbon dioxide and acetate, too much of which would be toxic to the acid producing bacteria.

Stage IV: Stage IV decomposition begins when both the composition and production rates of landfill gas remain relatively constant. Gas is produced at a stable rate in stage IV, typically for about 20 years; however, gas will continue to be emitted for 50 or more years after the waste is placed in the landfill. Gas production might last longer, for example, if greater amounts of organics are present in the waste, such as at a landfill receiving higher than average amounts of domestic animal waste.

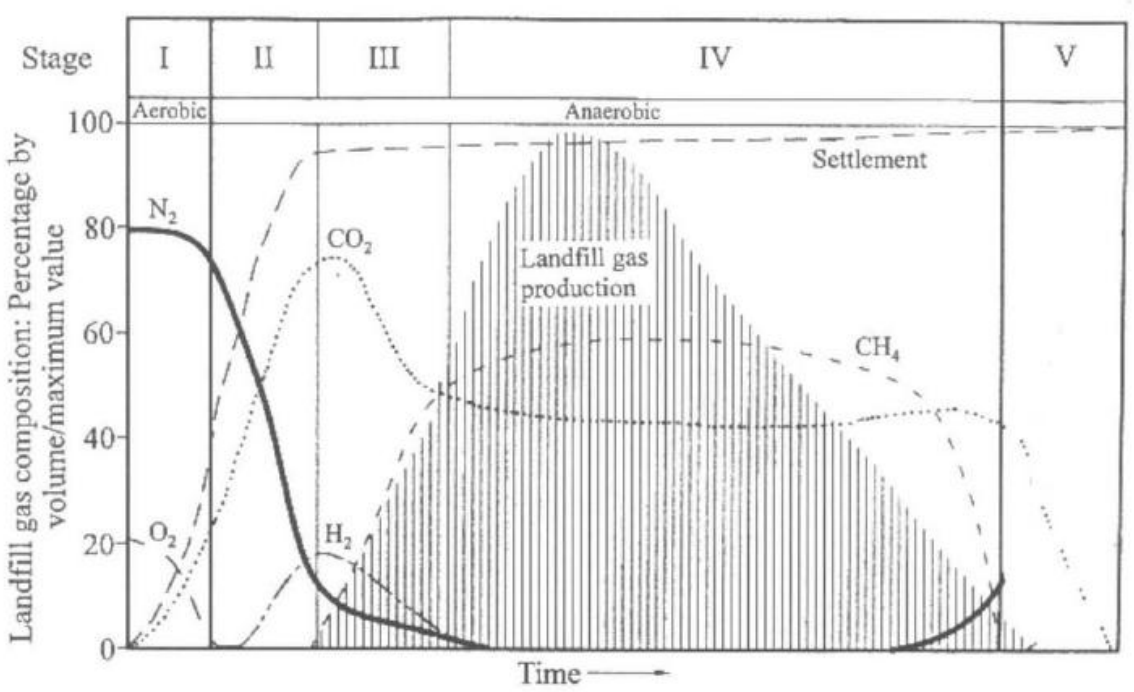

*Time scale variable for different stages of biodegradation.

Figure I-6 : Gas production trends for all four phases of decomposition (William, 1998).

Landfill gas typically has methane concentrations around 50%. Advanced waste treatment technologies can produce biogas with 55-75%CH_4 (Figure I-6). Landfill gas production results from chemical reactions and microbes acting upon the waste as the putrescibles begin to break down in landfill. Due to the constant production of landfill gas, pressure increases within the landfill provoke its release into the atmosphere. Such emissions lead to important environmental, security and hygiene problems in the landfill. Landfill gas production must be managed to control the discharge of potentially dangerous gases into the atmosphere. Venting and/or gas collection systems must be installed to control and monitor the gas production in the landfill. All new landfills must be assessed for the viability of energy recovery from the gas production.

Initially these gases were vented and burned to avoid nuisance to the surrounding atmosphere but then more economical and productive solution in the form of energy production gave rise to installation of

piping system within the waste body to collect and use biogas for energy generation. And now there are a number of landfill sites capable of managing its energy requirement from the generation of biogas.

I-1.4 Effects of Degradation on Biochemical Properties of MSW

Though not well defined and understood, the bio-chemical aspects of a solid waste are very important to understand its behaviour in a landfill. These bio-chemical properties are interconnected with the mechanical and hydrological properties in such a way that ignoring them for the sake of future predictions alone lead to misinterpretation of the situation. To see the nature of these impacts some observations need to be carried out at site and determination of certain parameters needs to be done in the laboratory to homogenise these parameters for their scope of work. Most important factors with respect to biological and chemical reactions are the temperature and moisture content. Rates of biodegradation and chemical reaction depend on factors such as waste composition, moisture content, leachate mobility and temperature. When the solid wastes are placed in the landfills the following biological, chemical and physical events occur simultaneously:

- Biological decay of organic materials (aerobic/anaerobic) with evolution of gases and leachate (chemical oxidation of waste materials)
- Leaching of organic and inorganic materials by water and movement of leachate through the fill
- Movement of dissolved materials by concentration gradient and osmosis, Movement of liquids caused by differential heads
- Escape of gases
- Differential settlements caused by consolidation of materials into voids

I-1.4.1 Composition

For the evaluation of landfill management, information regarding the composition of solid waste is very important. Considering only the bio-chemical properties of the domestic waste and the reactions taking place inside the waste body, the state of decomposition can be defined. Biochemical parameters such as biochemical oxygen demand (BOD), chemical oxygen demand (COD), total oxygen demand (TOD), total organic carbon (TOC) and volatile organic compounds (VOC) are analysed to determine the decomposition phase. Another theoretical method is to use organic carbon content (OCC) of waste components (IPCC, 2006). However these experiments do not reflect the biodegradability in the anaerobic conditions. In contrast to these experiments the biochemical methane potential (BMP) test is

an experiment that examines the gas production and the waste degradation under the optimal anaerobic condition.

I-1.4.2 Temperature & pH

Temperature plays an important role in degradation of a waste body. The rate of methane generation can be increased, up to 100 times, when the temperature raises from 20 to 40 ºC (Christensen et al, 1989). Moreover, in a deep landfill with a moderate water flux, landfill temperature of 30 to 45 ºC can be expected for temperate climates. The heat is a result of aerobic decomposition process that can result in a temperature rise within the landfill environment.

The optimum pH range for microbial activity is generally between 6 and 8. pH values available for the aerobic degradation of solid waste are near neutral values. Nakasaki et al. (1993) determined an optimum pH range of 7–8 while testing the pH dependency of active microorganisms in the composting process. Cossu et al. (2003), in the column study, determined the pH 6 for anaerobic landfill leachate, while it was almost 7.5 for an aerobic landfill reactor. The pH of the waste body and leachate significantly influences the chemical and biological processes. An acidic pH increases the solubility of many constituents, decreases adsorption, and increase the ion exchange between the leachate and organic matter. During the initial stages of anaerobic decomposition, organic acids are formed and result in an acidic pH. Furthermore the pH should rise as the acids are converted to methane.

The optimum pH range for anaerobic reaction is 6.7 to 7.5. Within the optimum pH range, methanogens grow at high rate leading to maximum methane production. The rate of methane production is seriously limited when the pH level is lower than 6 or higher than 8 (Barlaz et al, 1987) which affects the activity of the sulphate reducing bacteria as well. The presence of industrial wastes, alkalinity and groundwater infiltration may affect the pH level in a landfill.

I-1.4.3 Leachate

Leachate may be defined as a liquid that has percolated through solid waste and has extracted dissolved or/and suspended materials from it. In most of the landfills leachate is composed of decomposition related produced liquid and liquid entered from external source (rainfall, groundwater). According to Kjeldsen et al. (2002) a landfill that receives a mixture of municipal, commercial, and mixed industrial waste, but excludes significant amounts of concentrated specific chemical waste, landfill leachate may be characterized as a water-based solution of four groups of contaminants ; dissolved organic matter (alcohols, acids, aldehydes, short chain sugars etc.), inorganic macro

components (common cations and anions including sulphate, chloride, Iron, aluminium, zinc and ammonium), heavy metals (Pb, Ni, Cu, Hg), and organic compounds such as halogenated organics, (PCBs, dioxins, etc.) and the organic compounds of sulphate. The physical appearance of leachate when it emerges from a typical landfill site is a strong-odour brown or black cloudy liquid. The smell is acidic and offensive and may be very pervasive because of hydrogen, nitrogen and sulphur rich organic species.

Only a decade ago effluent from the landfill was considered useless, nuisance and problematic in proper landfill operations but as soon as its importance in relation to biodegradation and further stabilisation of landfill was explored, its utilisation has become state of the art technique in any landfill operation management. Moreover with the development of the bioreactors leachate recirculation and constituent or concentration modification has yet opened new doors to landfill management strategies. None the less profound study of leachate is a tool to understand hydrological parameters of the waste body, where its piping system serves both the purposes of circulation/re-injection and settlement measurements.

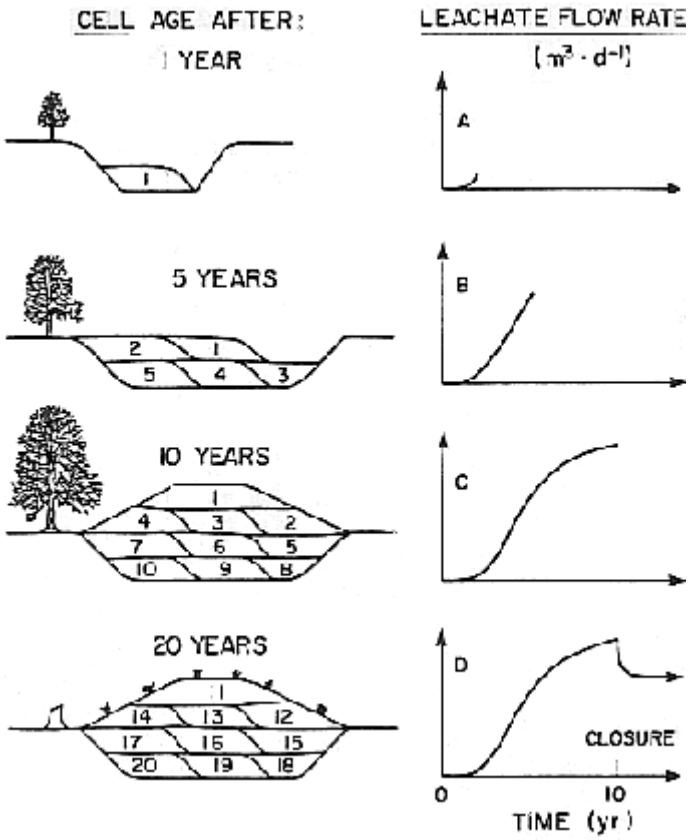

Figure I-7 : Leachate flow rate for different waste component categories (A, B, C and D) as a function of time (Farquhar, 1989).

In Figure I-7 leachate flow rate is shown as a function of landfill progression as suggested by Farquhar (1989). The component compositions are presented as ranges of percent wet weight of refuse. Category A consists of readily biodegradable food and garden wastes which produce high concentrations of organic matter (as BOD or TOC) and total nitrogen (TN) in the leachate. Category B is also organic but contains fewer biodegradables than A. It includes primarily paper with much smaller amounts of wood and rubber. Because of reduced biodegradability, these components yield organics to the leachate at concentrations much lower than for Category A but for much longer times measured in years. Category C includes metallic wastes composed mainly of iron, aluminium, and zinc. In time, these and other metals appear in the leachate and do so for many years because of slow rates of release. Category D includes non-metallic inorganic components such as glass, soil, and salts.

I-1.4.4 Biogas

Another yet important biological/chemical parameter is the production of biogas during the decomposition. Biogas generally refers to a gas produced by the anaerobic digestion or fermentation of organic matter present in a municipal solid waste, biodegradable waste or any other biodegradable feedstock, under anaerobic conditions. Biogas is comprised primarily of methane and carbon dioxide. Landfill gas is produced from organic waste dumped in landfill. The principal gaseous products resulting from the bacterial decomposition of the waste are methane, nitrogen, carbon dioxide, hydrogen and hydrogen sulphide. Around 100-200 m^3 (with theoretical values going up to 400 m^3) biogas is produced per ton of MSW in the methanogenic phase. In Table I-2 typical composition of the biogas components as found in the conventional landfills is presented.

Table I-2: Typical composition of gases in landfills (Tchobanoglous et al., 1995).

Component	Percent by volume
Methane	45-60
Carbon dioxide	40-60
Nitrogen	2-5
Oxygen	0.1-1
Ammonia	0.1-1
Carbon mono-oxide	0-0.2
Non methane organic compounds	0.01-0.6
Hydrogen	0-0.2
Sulphides	0-1

I-2 LANDFILLS

According to legislative regulations in France regarding landfilling several classes of landfills are defined in terms of waste stored:

- Class I: for special industrial waste or hazardous. For non-biodegradable waste
- Class II: for non-hazardous household waste and treated industrial waste.
- Class III: for inert waste.

The present study concerns the municipal solid waste of class II.

Landfills or Sanitary landfills are disposal sites for non-hazardous solid wastes spread in layers, compacted to the smallest practical volume, and covered by material applied at the end of each operating day (Figure I-8). Whereas secure chemical landfills are disposal sites for hazardous waste, selected and designed to minimize the chance of release of hazardous substances into the environment.

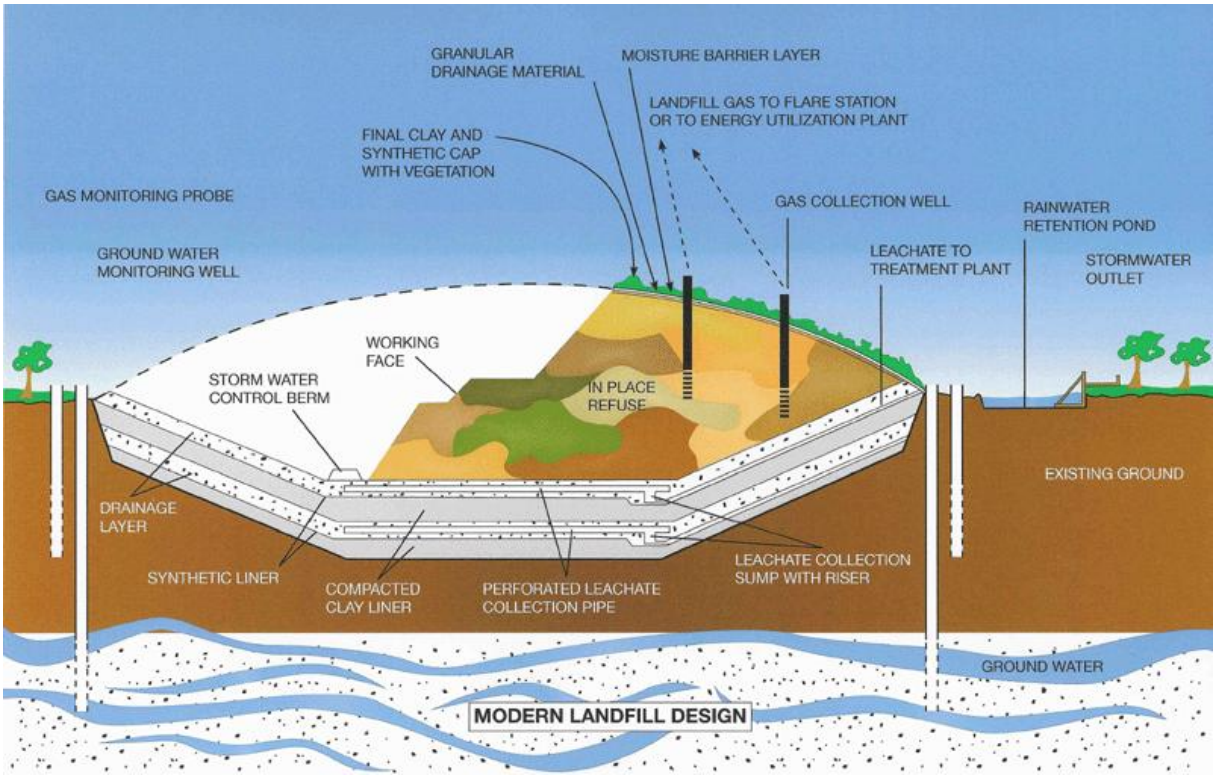

Figure I-8 : Landfill components (RUNCO, 2007).

It can be noted in Figure I-9 that even at the present time landfilling is one of the dominant methods of waste disposal in comparison to the incineration.

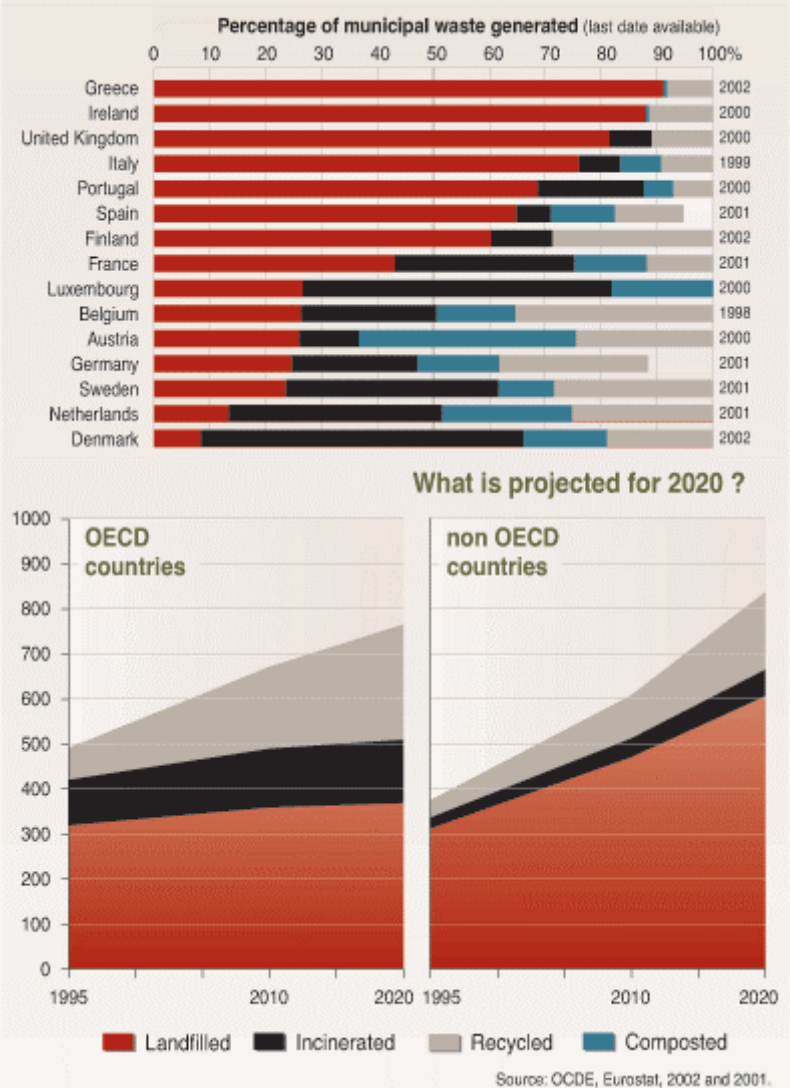

Figure I-9 : General trends of waste management in European countries and comparison of waste management techniques implemented in OECD member countries with those followed in non OECD countries. (OECD, 2002).

I-2.1 Landfill Construction and Operation

Landfills are properly designed and constructed structures according to the regional or national directives. Primarily the construction of any landfill is studied as a viable solution in accordance with specific requirements; such as location, capacity and stability. The cost and nuisances are also of great importance regarding the landfill construction. Landfill management strategy defines certain waste laying practices followed at landfills, for different cell heights, daily covers and the lining systems to integrate into the system in a manner to; use as small area as possible, exploit it to its maximum capacity and reduce as much adverse affects to the surrounding environment as possible.

The construction and the sequence of operation in a sanitary landfill are mainly based on the topography of the land. They also depend on the source of the covering material and the depth of the water table. There are two different ways to construct a sanitary landfill: the trench method and the area method (Jaramillo J., 1993).

The trench or ditch method: is used in flat regions and consists of periodically digging trenches two or three meters depth with an excavator or tracked dozers. It should be noted that there have been trenches dug up to seven meters depth. The soil taken out is stockpiled for later use as covering material for a subsequent trench. Wastes are placed in the trench, and then they are spread, compacted and covered with soil. Ditch excavation requires favourable conditions regarding water table depth and adequate soil. Lands with a high water table or very close to the surface are not suitable because groundwater would be contaminated. Rocky soil is not adequate since excavation is very difficult.

The area method: In flat areas where pits or trenches cannot be dug, refuse can be deposited directly on top of the original soil, elevating the level a few meters. Cover soil should be brought in or extracted from the surface layer. In both cases, the first cells are constructed with a smooth gradient to prevent slides and create stability as the landfill rises. (Figure I-10)

Figure I-10 : Construction of landfill cell according to area method (French landfill site).

This method can be used for filling natural depressions or abandoned quarries a few meters depth. The cover material is dug from the slopes or from a nearby place to avoid increased transportation costs. The unloading operation and construction of the cells should be done from the bottom up. The cells of the landfill are supported on the natural gradient of the land, the incoming refuse is spread and compacted at the base of the slope and covered daily with a layer of 0.10 m to 0.20 m of soil. The operation continues along the terrain maintaining a smooth gradient of about 30 degrees on the slope and 1 to 2 degrees on the surface.

I-2.1.1 Waste Compaction and Pre-Consolidation

At a given time only some portion of the landfill is used for construction of the waste layers, this is termed as waste cell. The waste is placed on the daily basis in layers, each compacted to a certain degree and covered with soil which is termed as a daily cover. This process is repeated till a predefined height is reached, namely, the cell height. At the end of the cell construction it is covered with a lining system comprising of geosynthetic membranes, clays and pipes for gas recovery and leachate recirculation. The compaction effort is applied keeping in mind the objective of bringing the loose waste layers in dense form so that

- Landfill capacity is increased
- Later settlements are reduced
- Shear resistance is increased
- Internal combustion possibility is reduced
- Hydraulic conductivity is reduced

The act of compacting waste in place should be viewed as a construction effort. The goal of this effort is to construct the highest-density cell volume in the safest possible manner. For most landfills, a small fleet of vehicles is required to manage the working face and ensure that compaction is performed properly. Tractor-type vehicles are useful for spreading waste in thin layers over the working face and for providing a secondary compaction prior to direct compaction. Track loaders are occasionally used on area fills to load and deposit earth materials such as gravel or daily cover soil. Wheel loaders, though not used for waste handling, are useful of cleanup tasks and for keeping the working face tidy. These materials are usually loaded onto articulated trucks for hauling to the working face or wherever the material is needed. Wheel tractor scrapers are best at performing cover operations, pushing soil cover deposited at the toe of the working face up and over the exposed waste at the end of the working day (Figure I-11). All this work is performed so that the waste compactors can effectively and efficiently perform their task.

Waste compactors both spread and compact deposited waste. They operate at relatively high operating speeds and torques. The minimum preferred operating weight for landfill compactors is over 45,000 lbs. Several factors besides equipment weight affect the results of compaction. First, waste should be spread out in thin layers by the tracked dozers prior to direct compaction by the waste compactors. These equipments shred of the waste components, triturate and restructure them resulting in the voids reduction of the layer.

A certain minimum number of passes with the compactor is required to achieve maximum density. This number is usually 3 - 4 passes, with a full pass being defined as rolling over and backing down from the working face. After 4 - 5 passes, no more significant densification can usually be obtained, and further compactor operations are not economical (Figure I-12). The final result depends on the type of the equipment and the number of passes applied to the layer thickness of the waste layer but as well the moisture content of the waste.

Figure I-11 : Spreading and compaction vehicle (Sheep foot roller).

As a matter of fact the compaction effort has many empirical rules such as mixing of big and small elements, mixing dry waste with the humid and the rough and hard elements with the soft and slack. Application of any/all of these combinations of waste compaction depends on the opinion of the landfill operator. The effectiveness of the compaction is generally evaluated from the density of the compacted layers; however it remains relative as a function of the landfill specificity (waste composition, layer thickness). Figure I-12 describes the interrelation of number of passes and the layer thickness with the density achieved. However it should be kept in mind that compaction effort is difficult to quantify as a part of the compaction effort goes wasted as there is some reversible deformation of the waste layer due to the elastic components such as; plastics and paper. Nevertheless the importance of compaction is twofold as it increases the landfill capacity as well as reduces the post construction settlement of the waste mass.

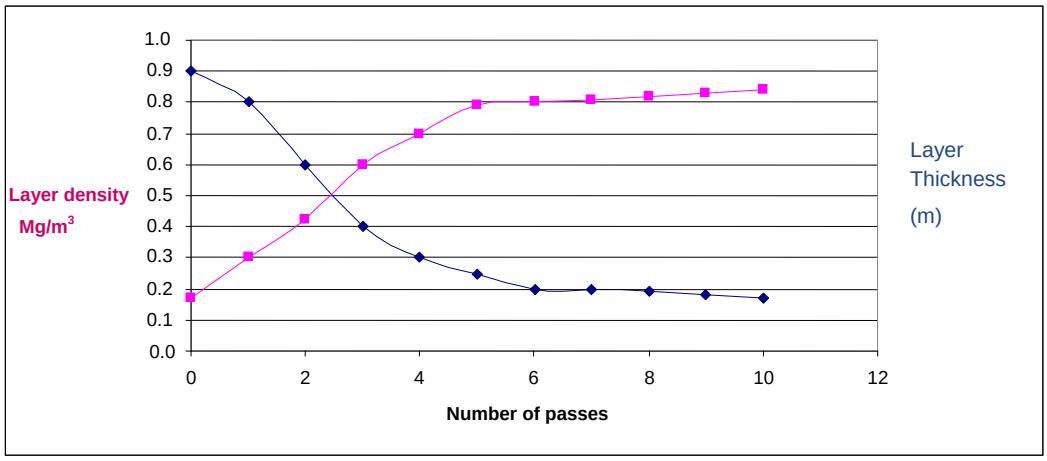

Figure I-12 : Effect of number of passes and the layer thickness over the layer density (Oweis et al., 1990).

In the waste cell construction, each layer initially compacted undergoes further compression due to overload of layer placed and compacted on top. It is observed that waste layers without compaction reach a maximum density of 0.9 Mg/m^3 at the end of operation whereas the maximum density of compacted layers may reach around 1.3 Mg/m^3 (Figure I-13).

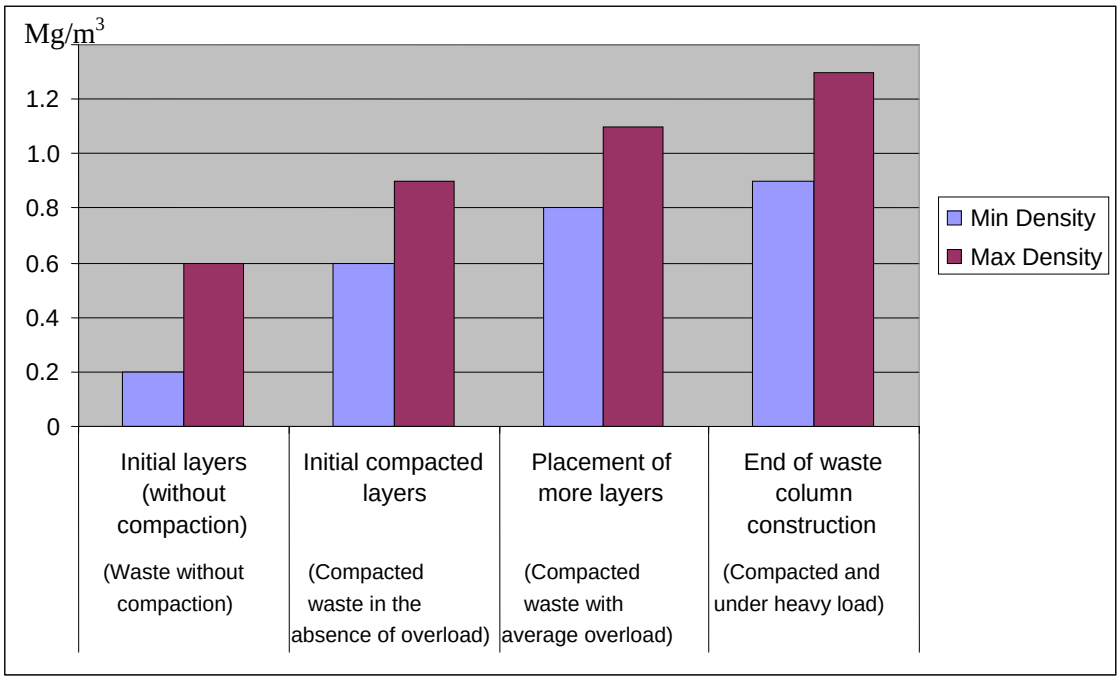

Figure I-13 : Comparison of improved waste density as a function of compaction effort and surcharge due to layers on top.

I-2.1.2 Bottom Lining System

The general structure of landfill consists of a lateral and basal lining system, a drainage system for leachate and gas (and a leachate re-circulation system in some cases), a top cover and the waste body. As the waste body is the largest structural element of a landfill, changes to its biological, physical and mechanical properties have important impact on the remaining elements. The fact that the waste is a "live" element subjected to constant load and that it is not fully stabilised after years, emphasises the need for knowing and controlling its behaviour.

The regulations for the confinement of the waste in France has the main objective to control any transfers between the waste and the environment (atmosphere, soil, water), including inputs and outputs of water from the site and ensure effective drainage of leachate to avoid percolation in the soil. The barriers differ depending on the class and the nature of waste. For example, in the case of hazardous waste, there should be practically zero percolation while in the case of degradable waste, a minimum percolation should be ensured to allow degradation of waste. The durability of the confinement system must be ensured for decades, depending on the evolution of waste. The directive of September 9, 1997 as amended specifies the components of lining facilities for storage of non-hazardous waste (Class II). Figure I-14 shows a scheme of the structural elements of a landfill lining system with terms employed in the Landfill Directive and Guidance defined by Environment Agency (2002).

Regarding the bottom and slope lining systems of landfills, two security levels are established:
Active barrier: it ensures the hydraulic autonomy of the waste body for drainage and leachate collection, and avoids the stress of passive barrier. It consists of a complex combination of geosynthetic (geomembrane, geotextile) and natural materials (drainage layer, soil).
Passive barrier: it must ensure long-term prevention of soil, surface and groundwater from the pollution of waste and leachate. At the bottom of waste body, this lining may comprise of the natural or artificial geological material; reconstituted and / or treated.
For non-hazardous waste: one meter of clay layer with a permeability less than 10^{-9} m / s overlying five meters of silt layer with a permeability less than 10^{-6} m / s.
For hazardous waste: five meters of clay layer with a permeability less than 10^{-9} m / s (Figure I-14).

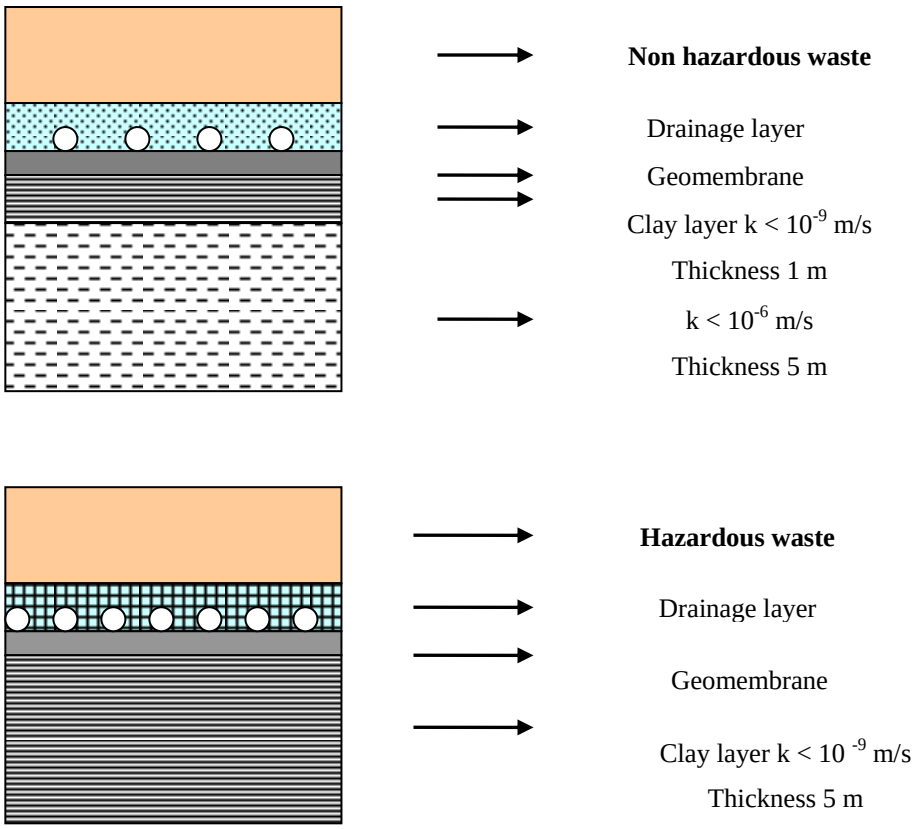

Figure I-14 : French environment legislation authority recommendation for landfill bottom liner system as a function of type of waste.

A key product that can replace partially the clay layer is the geosynthetic bentonite (GSB) respecting a minimum thickness of the overall active barrier of 0.5 m (Regulatory Authority, France). The GSB is composed of a layer of bentonite between two geotextiles and has a thickness of about one centimetre. To compare different configurations of passive barriers, it is possible to define the mass flow (mass emitted per unit time) for each configuration. Another method is to determine the balance equation that describes mass transfer of particles dissolved in water and calculate their effect on groundwater resources.

It is important to note that these two levels of security are complementary. The security barrier allows the active collection, including for treatment, of pollutants liquid flow at least during the period when flows are highest i.e. when the leachate is highly pollutant. However, consider the case where the active barrier would not work during long term, drainage layers can clog over time. Geomembranes are aging and may have breaks of various kinds. The passive barrier is sought in this case, at least in the long term, but at a time when the leachate will be less noxious (most of the pollution load has been treated). To verify the hydraulic performance of the bottom and side linings of the landfill, the technical guidance of November 1997 of the Ministry of Planning and Environment relating to landfills and related wastes recommends at least one point of permeability measurement per hectare,

however, due to heterogeneity it is necessary to intelligently place the permeability probes. On the same location measurement must be performed every meter from 0 to 5 m.

I-2.1.3 Cover System (Cap Liner)

Once the operation is completed at the landfill, the cover layer is installed at the top of the waste body. Primarily the landfill cap cover barrier enables (ADEME BRGM, 2001):

- Waste containment
- Regulation of inflow of water
- Limiting the gas escape into atmosphere
- Enhance the mechanical stability of the landfill
- Integrate the landfill as a landscape environment

The constraints taken into account to define the characteristics of cover system to fill these functions are numerous:

- The nature of waste (biodegradation potential, compressibility, characteristic pollutant, radioactive)
  The geometry of the cover layer (slope, thickness)
- The configuration of the site (pit, embankment)
- The availability of the material
- The conditions of the site development and the future of the site
- Climatic conditions (precipitation, evapotranspiration, erosion, frost, drought)

The analysis of features and required performances of a final cover led to advocate five layers; each of which ensures at least one function: (from top to bottom)

- Surface layer: allows site integration with its natural environment, reduces the effects of fluctuating temperatures and humidity and protects the cover system from erosion.
- Protection layer: protects the layer of low permeability against the intrusion of animals or plants and climate cycles (freeze-thaw, wetting-drought)
- Drainage layer: collects rainwater which is not evacuated by surface runoff, reduces the hydraulic gradient on the low permeability layer, increases the stability of the cover system by reducing the pore pressure
- Low permeability layer: prevents or limits the water infiltration into the waste body and prevents the rise in gas content
- Support layer immediately on top of the waste: ensures a consistent level base, stable for the cover system.

Different types of cover systems

Two main concepts of cover liners are recommended depending on the nature of degradable or non-degradable waste underneath.

Non-biodegradable waste: The regulations require, as part of the implementation of a landfill for non-degradable waste (inert waste or Class E) to implement an impervious cover liner. Any transport phenomenon between the waste and the outside environment is minimized.

In practice, a waterproof cover type is composed of a geomembrane or equivalent (with a permeability less than or equal to 10^{-11} m / s, or thickness > 1.5 mm), on top a clay layer of thickness greater than or equal to one meter and permeability less than or equal to 10^{-9} m / s. This layer acts on an interface layer with the layer of waste. Often a geotextile is used as a protection layer to avoid any puncture or possible penetration in the geomembrane. Rainwater seeped into the cover system is drained by a drainage layer of permeability greater than or equal to 10^{-4} m / s placed over the impervious barrier cover (Figure I-15).

Degradable waste: La degradable or treated waste (category D) requires a minimum moisture content and only the controlled infiltration is allowed. Two types of cover system can be implemented for this type of waste (Figure I-15):

Cover layer (semi-impervious): It is composed of altered natural materials and compacted soil of at least one meter and a maximum permeability of 10^{-6} m / s. A drainage layer allows higher limit infiltration water. Another lower layer can drain the biogas. The drainage layers are generally composed of granular material or geo-composite drainage. Impervious cover itself, similar to the one presented in the case of non-degradable waste, plus a piping system for the recirculation of fluids to promote biological activity and thus the degradation of waste.

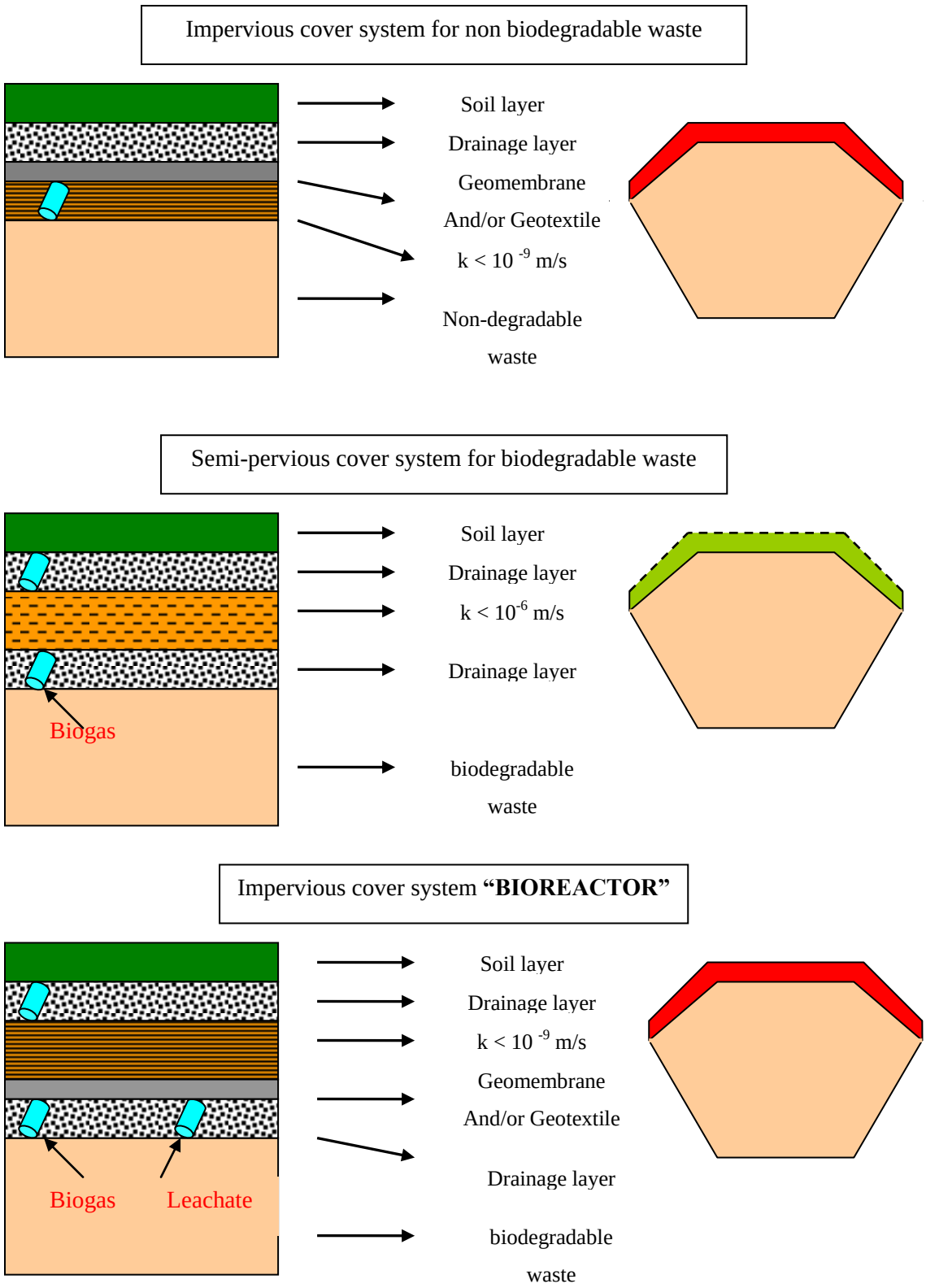

Figure I-15 : Types of cover lining systems in reference with the waste landfilled.

I-2.2 Post-Construction Behaviour

Completed sanitary landfills generally require maintenance because of uneven settlement or stability concerns. Maintenance consists primarily regarding the surface; to maintain good drainage and filling in small depressions to prevent water ponding and subsequent groundwater pollution. Completed landfills have been used for recreational purposes such as parks, play grounds or golf courses, parking and storage areas, botanical gardens are other final uses. Because of the differential settlement and gas escape from landfill, construction of buildings on landfills should be avoided. Data of physical composition is important for the equipment operation and facilities at landfills as well as for assessing the feasibility of resources and energy recovery. In all cases, when operation is completed, it is being monitored for:

- The ground water quality
- Leachate analysis
- Biogas analysis
- Mechanical instability, subsidence, cracking, erosion and settlement

Large scale instrumentation can be implemented to monitor the behaviour of the cover system over the course of time, including the monitoring of subsidence, temperature, and pore pressure. These post operation controls change with time depending on the age of storage and the frequency and network of measurements tend to decrease with age because the waste becomes less and less pollutant reducing the risk of pollution of the surroundings.

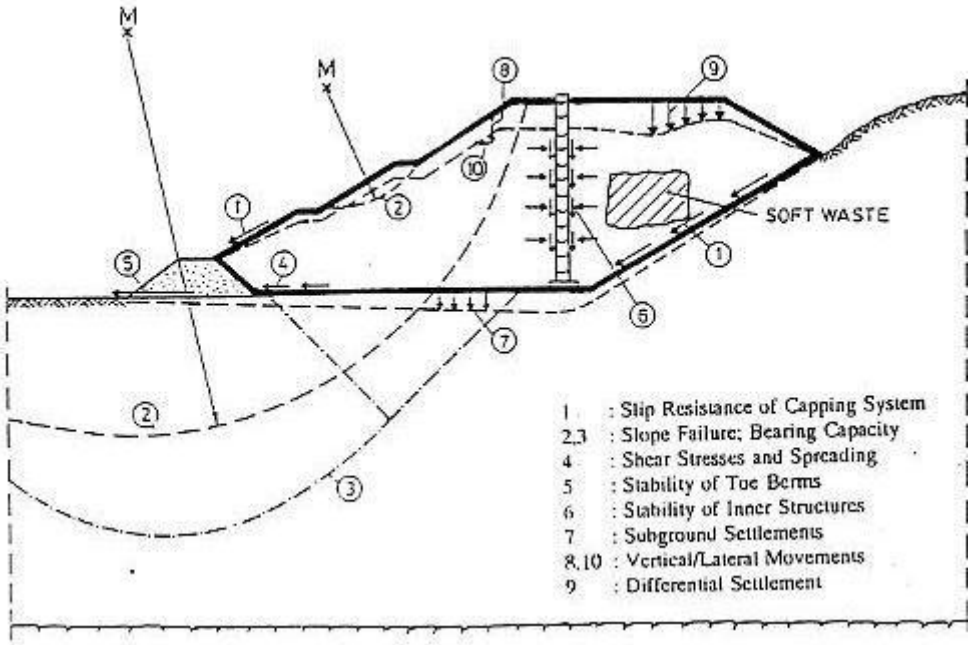

Figure I-16 : Cross-sections of possible stability and deformation concerns in a landfill (Jessberger, 1993).

Jessberger (1993) outlined briefly how to assess the amount of deformation in a landfill and whether unacceptable cracking will develop as a result. Design of landfill involves consideration of numerous stability concerns as delineated in Figure I-16, such as slope failure due to inadequate bearing capacity (#2 and #3 in Figure I-16) vertical and/or lateral movements (#8 and #10 in Figure I-16) and differential settlement (#9 in Figure I-16). Differential settlement can cause surface maintenance problems and damage the integrity of the landfill cover, allowing excessive infiltration of surface water, accelerated local settlement, increased leachate generation and high concentrations of landfill gas to escape causing odour nuisance or breach of consent conditions.

The knowledge generated by a better assessment of waste settlement over time should allow a better estimate of stresses and deformation induced in the barrier system, drainage is a basis for the design of modern landfill facilities for its dual function; sealing (which prevents the dispersion of leachate) and drainage (which allows the sewage effluent liquids and gases produced by decomposition. Waste compresses due to increase in effective stress (primary settlement) and due to mass loss from biodegradation (secondary settlement). Estimation of settlement is important mainly for the purposes of calculating internal settlement of buried pipelines (leachate and gas collection and liquid distribution pipes), as well as to calculate landfill capacity and post-closure settlement estimations. Secondary settlement of MSW is important from the viewpoint of cover stability and end-use of the landfill site. The stability of landfilled waste is related to the shear strength of the material and for both the static and dynamic slope stability evaluation shear strength of MSW is required.

I-3 WASTE TREATMENT MODES RELATED TO LANDFILLING

Ever since the need for larger landfill sites drew attention of the engineers, maximum material recovery gained importance in the solid waste management and now together with recycling it is one of the most important steps in the solid waste management strategy. It is pertinent from the term of pre-treatment that there is change in the physical and/or chemical properties of the solid waste due to application of various processes. Pre-treatment of the waste is either carried out at source which is termed as sorting, or it is done once the waste has reached the landfill site where it is mechanically biologically treated to reduce the load of waste. Numerous options are available for mechanical and biological treatment ranging from switching their arrangement to skipping one type of pre-treatment altogether.

I-3.1 Mechanical Biological Pre-treatment (MBP)

Mechanical biological pre-treatment is defined as the processing or conversion of waste from human settlements with biologically degradable components by the use of the combination of mechanical and other physical processes (for example, cutting or crushing, sorting) with biological processes (aerobic "rotting", anaerobic fermentation). MBP is a term referring to a number of processes that further treat residual waste before disposal (Figure I-17).

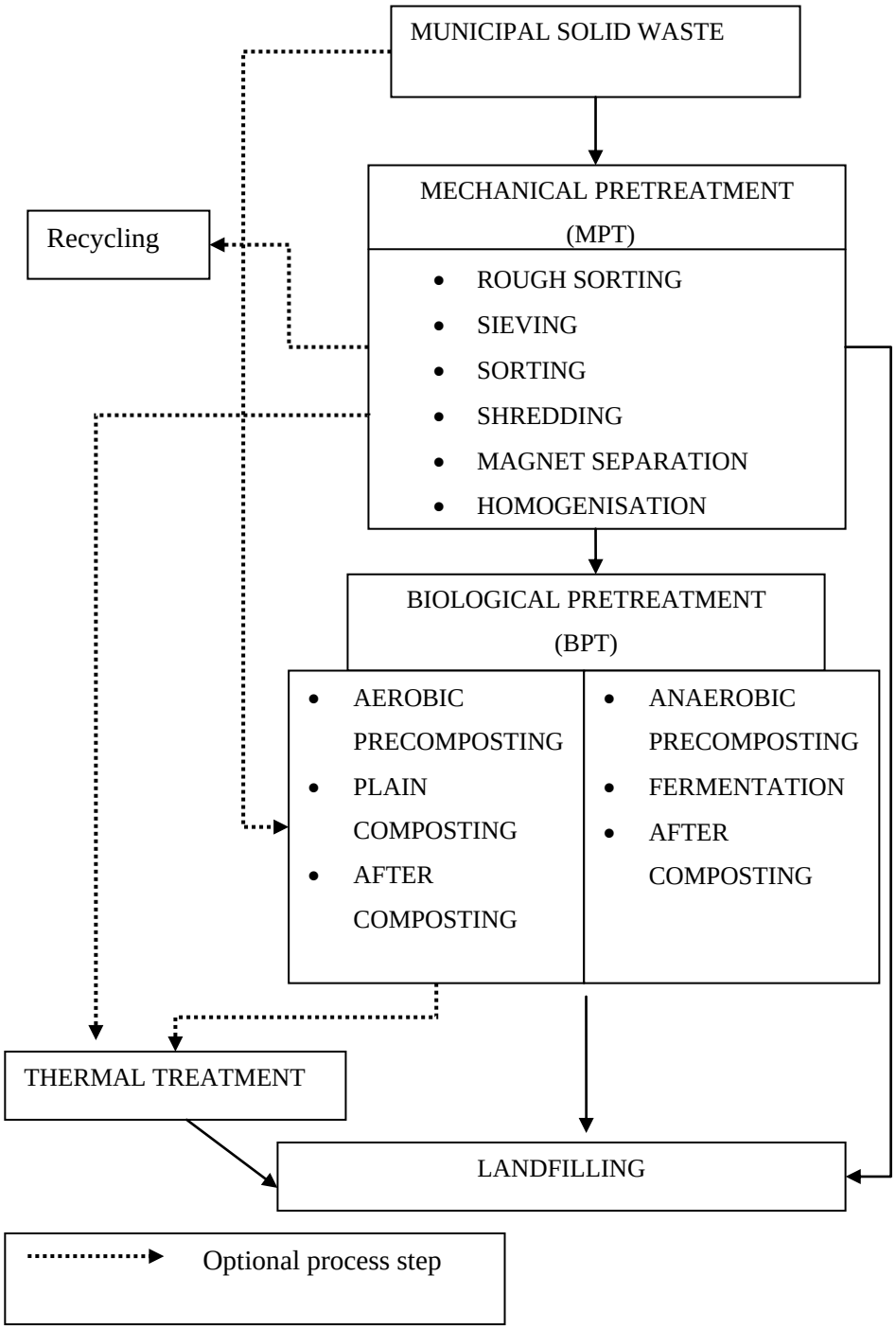

Figure I-17 : Mechanical Biological Pretreatment plan.

The aim of MBP is to minimise the environmental impacts of ultimate disposal and to improve some gain value from the waste through the recovery of metals etc.and, in some cases, energy. It aims to reduce the mass and the volume of the waste and a lower environmental impact of the waste after its deposition, i.e. low emissions of landfill gas, small amounts of leachate, and a reduced settlement of the landfill body. Furthermore, MBP includes the separation of useful waste components for industrial reuse, such as metals and plastics as well as refuse derived fuel (RDF).

I-3.1.1 Control of Waste Input and Pre-treatment before Disposal

The first step in the waste control strategy is to minimize the amount of waste to be landfilled; this can be achieved by waste avoidance, separate collection activities and recycling, incineration and mechanical biological pre-treatment of residual municipal solid waste (Figure I-18).

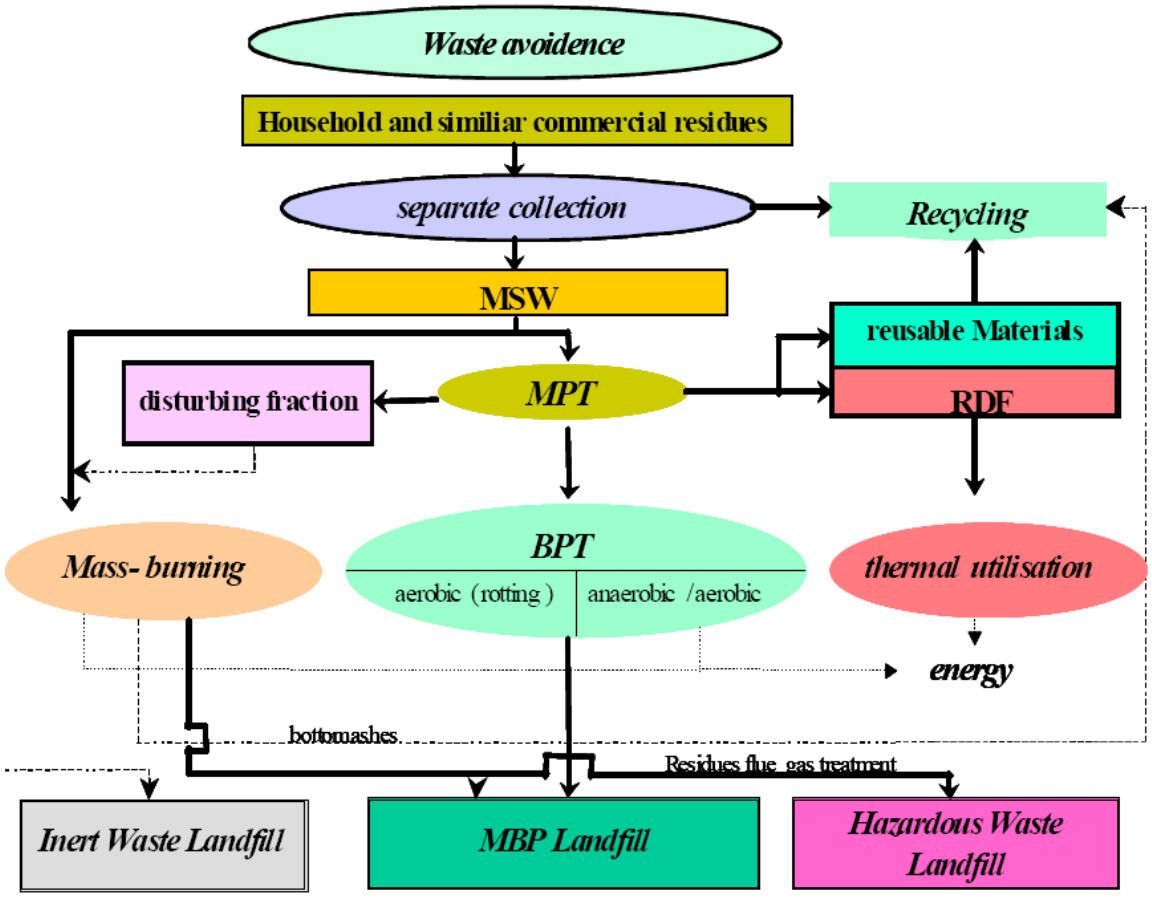

Figure I-18 : General concept of municipal solid waste management (Stegmann R., 2005).

Regarding its properties, waste can be divided into different fractions, fractions of high calorific value, mineral fraction or a fraction rich in organic matter. Some of these fractions have reutilization potential. MBP can be used within a waste management concept as a single process or in combination with thermal pre-treatment. Significant reductions in the remaining emissions in terms of loads and concentrations are achievable after the MBP.

The *mechanical pre-treatment* (MPT) step includes the removal of contaminants and components, which impede the technological process. Reusable material is separated. The whole waste is fractionated into two or more fractions defined by material qualities, which are then handled specifically. The whole waste is fractionated into two or more fractions defined by material qualities. Mechanical treatment consists mainly of screening and shredding devices. Specialities of residual waste are partly considered, but there is a good potential for further improvements. Most plants aim to separate the components with high calorific value, as plastics, paper, timber, and composites, for energy recovery.

The *biological pre-treatment* (BPT) step relies on aerobic rotting, anaerobic fermentation or combined processes. At present all the existing landfills are anaerobic landfills, and research suggests that aerobic practices should be introduced to accelerate the decomposition processes within the landfill to attain early stabilization. The biological pre-treatments which mainly involves the aerobic pre-treatments include; composting or aerobisation. Aerobic systems in widespread use comprise of windrows with or without aeration, containers or boxes, drums, or tunnels. Anaerobic pre-treatment includes anaerobic digestion for biogas production for energy recovery and reduction in odour.

I-3.1.2 Potential Advantages of MBP

Mechanical Pre-treatment (MPT): Even with a successful sorting at resource scheme in place there are some recyclable materials in the residual waste, which could be captured at the mechanical treatment stage. MBP reduces the volume of residual waste and therefore the landfill space, thus reducing the cost to the local authority of disposal. Moreover potential hazardous waste contaminants of the waste stream, such as batteries, solvents, paints, fluorescent light bulbs etc, will not reach municipal landfill sites due to the sorting.

Biological Pre-treatment (BPT): It reduces the biodegradability of the waste, thus reducing the methane and leachate production once the residue is landfilled. Stabilisation of the waste reduces side-effects at the landfill such as odour, dust and windblown paper and plastics. The plants tend to be modular. They are made up of small units which can be added to or taken away as waste streams or volumes change. These plants can be built on a small scale, which would not drag waste in from a large surrounding area.

Table I-3: Comparison of different pre-treatment option focusing on the related advantages and disadvantages.

Scenario	Description	Advantages	Disadvantages
1	BPT of raw waste (no MPT)	- Organic matter (OM) stabilisation - Simple processes	- No resource recovery
2	BPT (without MPT) + Thermal pre-treatment (TPT) before landfilling	- Thermal Stabilisation	- Incinerator required
3	MBP with sorting of recyclables	- OM stabilisation - Material recovery	- No heat energy recovery
4	MBP with high calorific value sorting and TPT resulting in rich OM with low calorific value for landfilling	- OM stabilisation - Heat energy recovery	- Incinerator required - No material recovery
5	MBP with TPT, sorting high calorific value fraction and recyclables resulting in low calorific value fraction rich in OM for landfilling	- OM stabilisation - Heat energy recovery - Material recovery	- Incinerator required
6	MBP with sorting of recyclables and OM. BPT of OM with TPT before incineration reducing moisture content and homogenising the material plus reduction of waste quantity for incineration	- Material recovery - Heat energy recovery - Only residue from incinerator to be landfilled	- Incinerator required

Lorber et al. (2001) compared the biochemical properties of untreated waste to those of treated waste (Table I-4) and to the treated waste of age 2 years. It can be noted that these biochemical properties improve considerably for the treated waste and the biochemical methane potential of the treated waste reduced to 17.6 %, the BMP of the treated waste after 2 years was not available.

Table I-4: Comparison of biochemical characteristics of untreated and treated waste (Lorber et al., 2001), with biochemical terms defined in § I-1.4.1.

Analysis	Units	Un-treated waste	Treated waste	Treated waste (2 yr)
Oxygen consumption	mg O_2/g MS	55.8	6.6	1.9
TOC	$\%_{MS}$	31.2	18.9	11.7
VOC	$\%_{MS}$	52.1	33.0	22.0
BMP	Nl/kg MS	200	35.2	-

Stegmann (2005) studied the parameters of chemical oxygen demand, total nitrogen and biogas generation for the treated and untreated waste and showed that 90% reduction was possible if the pre-treatment was adopted (Table I-5).

Table I-5: Comparison of biochemical parameters as measured by Stegmann, 2005 (with biochemical terms defined in § I-1.4.1).

Analysis	Units	Un-treated waste	Treated waste	%Reduction
COD	mg O_2/kg MS	25,000-40,000	1000-3000	90%
TN	mg / kg MS	1500-3000	150-300	90%
Biogas generation	Nl / kg MS	150-200	0-20	90%

Laboratory studies carried out by Cossu et al. (2003) in 1 m waste columns of 18 cm diameter suggested similar results as presented in table I-6.

Table I-6: Comparison of biochemical parameters (Cossu et al., 2003), with biochemical terms defined in § I-1.4.1.

Analysis	Units	Un-treated waste		Treated waste	
		Start	End	Start	End
BOD	mg / l	50,000	20,000	30,000	1300
COD	mg / l	20,000	10,000	3000	300
NH_4+	mg / l	900	400	2000	50

I-3.2 In Situ Aerobic Treatment

The aerobisation can stop the emissions from landfills and waste storage areas and eliminate potential pollution by biodegradable compounds. It is mainly applied to sites contaminated by landfills. The realization of an in situ aeration measure, especially on existing landfills without base liner, aims at the stabilization of biodegradable organics through degradation and degradation of nitrogen compounds within the landfill body. For this purpose, air is injected into the landfill body via aeration wells. Depending on the aeration rate and its duration a gradual aerobisation of the landfill body can be realized (Ritzkowski et al. 2005).

I-3.2.1 Fundamentals and Objectives of Aerobic Stabilisation

The aerobisation is the process of active introduction of air inside a landfill in a manner to target the processing of biogenic organic matter with the oxygen present in air. The air is introduced into the waste mass by suction from wells specially installed at the base of the landfill. The further distribution within the landfill body is realized by means of convection and diffusion processes. There is a uniform suction throughout the whole deposit and the organic matter is gradually degraded, starting from the outside to inside of the waste mass. By applying a combined aeration – extraction operation the air supply and distribution effect can even be increased. The extracted off-gas is collected by means of a gas collection system and discharged into the atmosphere after a final treatment (Figure I-19).

Recent scientific investigations have shown that aerobic in situ stabilisation measures can help achieve sustained improvement of the emission and settlement behaviour of landfills when the process technology is adapted to the conditions of the landfill body and operated in a qualified manner (Ritzkowski et al. (2005), Heyer et al. (2005)). This objective can be achieved through the low pressure aeration which has been applied for several years now on landfills and old deposits. This process is applied in large landfills which have a significant deposition thickness and are equipped with a bottom sealing. Over-suction methods for aeration may also be used, provided that the landfill body meets certain boundary conditions (e.g. less tickness of landfill body). The aerobisation helps obtain the following effects:

- accelerating the degradation of pollutants and elimination of methane emissions;
- shortening the period of monitoring of abandoned landfills and storage areas;
- reduced pollution potential and water pollution from leaching within the discharges;

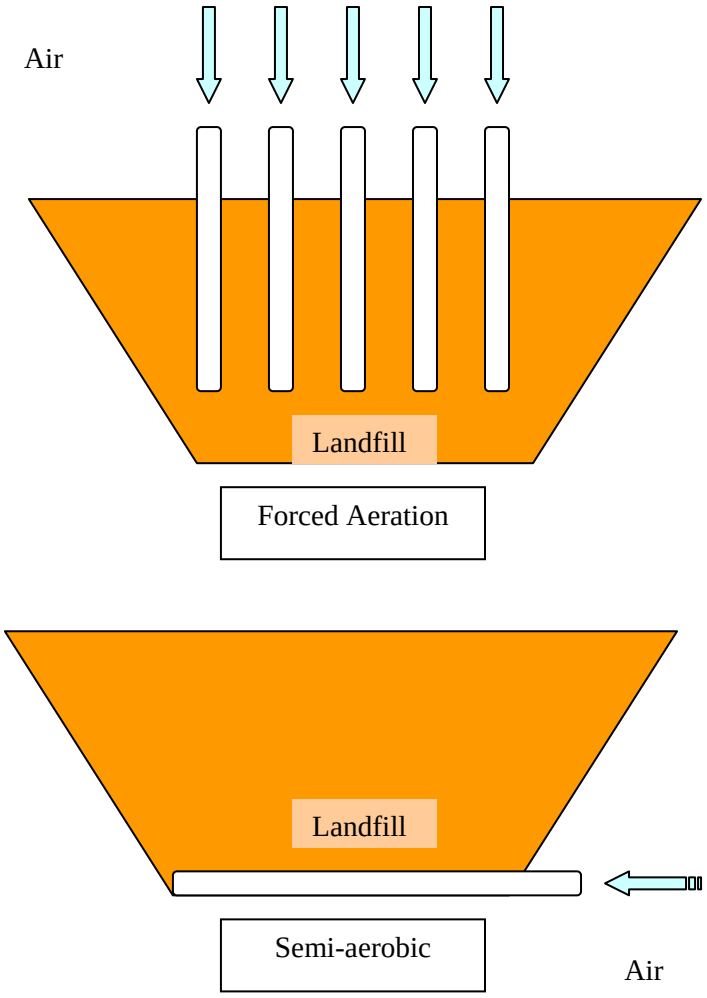

Figure I-19 : Comparison of two in-situ aeration processes.

I-3 .2.1.1 Low Pressure Aeration

The basic technical concept comprises a system of gas wells, through which atmospheric oxygen is introduced into the landfill body to accelerate the aerobic stabilisation of the deposited waste. The contaminated air coming out from the waste body is collected simultaneously and treated in a controlled manner in corresponding gas wells. Aeration is implemented using low pressures and is continuously adjusted to the oxygen demand, so that the stabilisation operation is constantly optimised (Heyer et al., 2005).

I-3 .2.1.2 Over Suction Method

As far as the over-suction methods are concerned, the effect of aerobisation is achieved through the suction operation including drawing-in of the atmospheric oxygen over the surface of the landfill and/or through passive aeration wells. In general, this is implementable only at sites with emission relevant deposition thicknesses of < 10 m because otherwise the oxygen supply and thus aerobisation may not be guaranteed (Heyer et al., 2001).

I-3.2.2 Processes and Effects of Aerobic Stabilisation

Under average landfill conditions, in situ aeration operation is intended for a period of 3 to 6 years. Basically, aeration includes the following processes:

- A changeover for the waste medium from anaerobic to aerobic conditions takes place, which results in an accelerated degradation of the biologically active waste components.
- At the end of stabilisation, organic compounds consist of only persistent or non-degradable organic compounds with a very low gas formation potential.

As a result of the accelerated biodegradation processes, the change in settlement course is also anticipated.

I-3 .2.2.1 Effects on the Water Path

Aerobic degradation of organic compounds releases the gas (carbon dioxide) and there is an accelerated decrease of the COD parameters and nitrogen (TKN or NH_4-N) can be observed in the leachate path as a result of aeration. In comparison with the strictly anaerobic conditions, the aftercare periods for the leachate emission path are reduced by at least several decades when applying in situ aeration.

I-3 .2.2.2 Effects on the Gas Path

The accelerated carbon degradation and discharge leads to an increased carbon dioxide formation rate. Prevention or reduction of the methane content in waste air through reduced gas production at old landfills at the end of the stable methane phase results in a lower explosion risk and fewer costs with regard to long-term waste air treatment. The carbon conversion and discharge may serve as the measure of intensity and of the acceleration of the biodegradation processes and can be determined through the mass balance in connection with the waste air consistency.

I-3.2.3 Future Applications of Aerobisation

I-3 .2.3.1 Processes

In situ aeration changes the principle processes inside the landfill body which are fundamentally different from those occurring in the conventional anaerobic landfills. The oxygen level and the temperature dynamic are the main parameters controlling these processes. The questions are; how and to what extent these parameters influence biodegradation processes and how they might be controlled in order to optimise the aeration process.

I-3 .2.3.2 Stabilisation Criteria

To define the stabilisation criteria the endpoint of in situ landfill aeration is crucial, respecting the planning and calculation of these measures. Again parameters to be applied and what values to be reached (either on a case to case decision or for landfill aeration in general) is questionable. Certain stabilisation criteria might be defined for aeration to contribute towards the landfill sustainability as landfill aeration is one of the existing tools for the accelerated and controlled reduction of the remaining emission potential of landfills.

I-3 .2.3.3 GHG Emissions and CO_2 Emission Trading

This aspect covers two main parts, firstly the question of relevance (How much green house gasses GHG are actually emitted from old landfills and what is the proportion related to the global GHG production?) and then the question of a possible re-financing in future for the in situ aeration projects through the emission trading market. The answer to the first question is pertinent as the landfills contribute significantly towards the GHG-gases emissions while the second one mainly depends on legal and statistical requirements. For instance in situ aeration projects are not included in the CO_2 emission trading but their insertion and a reliable method for the calculation of the emission savings should be developed and implemented.

I-3.3 Bioreactor Landfills

In contrast to the traditional landfill approach, the bioreactor landfill operates to rapidly transform and degrade the organic components of the waste mass. This goal is accomplished through the liquid and gas injection into the system (Figure I-20).

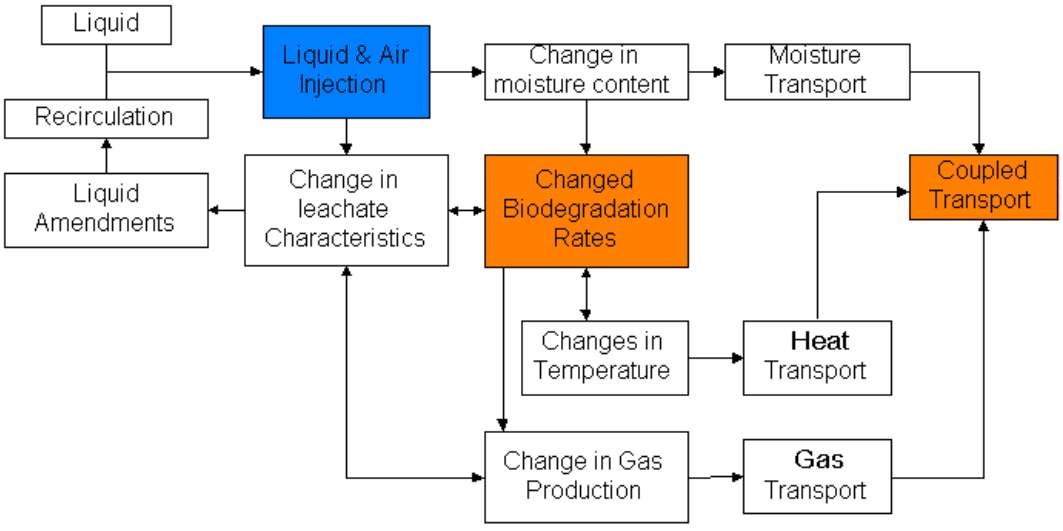

Figure I-20 : Interdependent biochemical and physical processes in a bioreactor landfill (Gawande, 2008).

I-3.3.1 Anaerobic Bioreactor Landfill

Anaerobic conditions develop naturally in nearly all landfills without any intervention. The waste mass in typical MSW landfills contains between 10 and 25 percent water. To optimize anaerobic degradation, moisture conditions at or near field capacity, or about 85 to 185 percent moisture are required and thus increased through injection. In an anaerobic bioreactor landfill leachate is re-circulated, however the biodegradation occurs in the absence of oxygen (Figure I-21).

The amount of leachate produced at many sites is insufficient to achieve optimal moisture conditions in the waste, therefore, additional sources of moisture such as sewage sludge, storm water, and other non-hazardous liquid wastes are used. Without air, methanogenic bacteria are promoted to accelerate waste degradation. As moisture content of the waste approaches optimal levels, the rate of waste degradation increases, this in turn leads to an increase in the amount of landfill gas produced. An increase in the density of the waste is also observed during the process. The rate of gas production in an anaerobic bioreactor can be twice as high as a normal landfill, but the duration of gas production is significantly shorter. The by-products of anaerobic degradation are methane (CH_4) that can be used as an alternative energy source and CO_2.

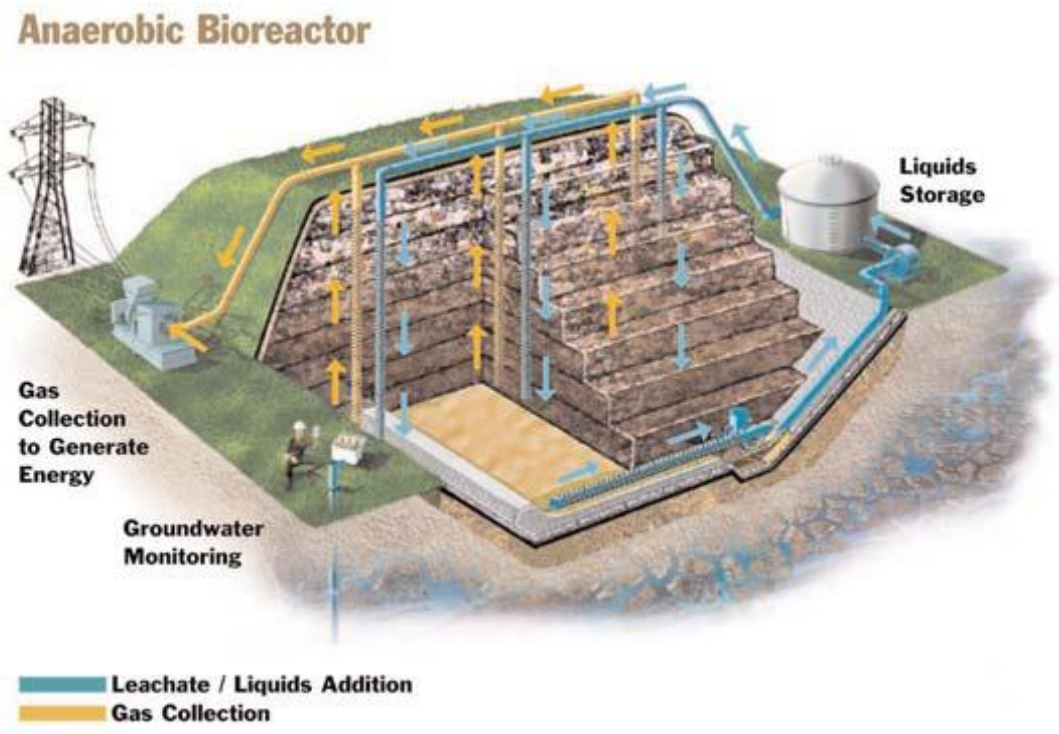

Figure I-21 : Anaerobic Bioreactor (Waste Management, 2000).

I-3.3.2 Hybrid (Aerobic-Anaerobic) Bioreactor Landfill

The hybrid bioreactor landfill accelerates the process of biodegradation by employing a sequential aerobic-anaerobic treatment to rapidly stabilize the waste mass through attainment of degradation in the upper layers and collect gas from the lower layers of the waste mass. The waste is first degraded under aerobic conditions followed by anaerobic conditions. Aerobic conditions usually occur in the newly placed waste in the upper sections of the landfill, while anaerobic conditions occur in the lower sections (Figure I-22) resulting in methane production.

The principle advantage of the hybrid approach is that it combines the operational simplicity of the anaerobic process with the treatment efficiency of the aerobic process, with the added benefits of an expanded potential for destruction of volatile organic compounds (VOCs), hazardous air pollutants (HAPs) and non-methane organic compounds (NMOCs) in the waste mass.

Figure I-22 : Hybrid bioreactor landfill (Waste Management, 2000).

Aerobic bioreactor landfills: Another option for the aerobic bioreactor landfill works on the principle of leachate removal from the bottom layer, piped to liquid storage tanks and re-circulated into the landfill in controlled manner with simultaneous air injection into the waste mass using vertical or horizontal wells to promote aerobic activity and accelerate biological stabilization (Figure I-23). A vacuum can also be applied to the waste mass to pull air in through a permeable cap. The degradation

of waste occurs under conditions similar to compost operations thus no methane is generated in this type of landfill.

The byproducts of aerobic degradation are carbon dioxide (CO_2) and water (H_2O). One drawback of the aerobic bioreactors is the increased potential for landfill fires. To avoid such hazards monitoring and controlling the temperature, moisture content and oxygen level within the landfill must be done constantly. Due to the higher level of operations management and higher moisture requirement aerobic reactors are more expensive to implement.

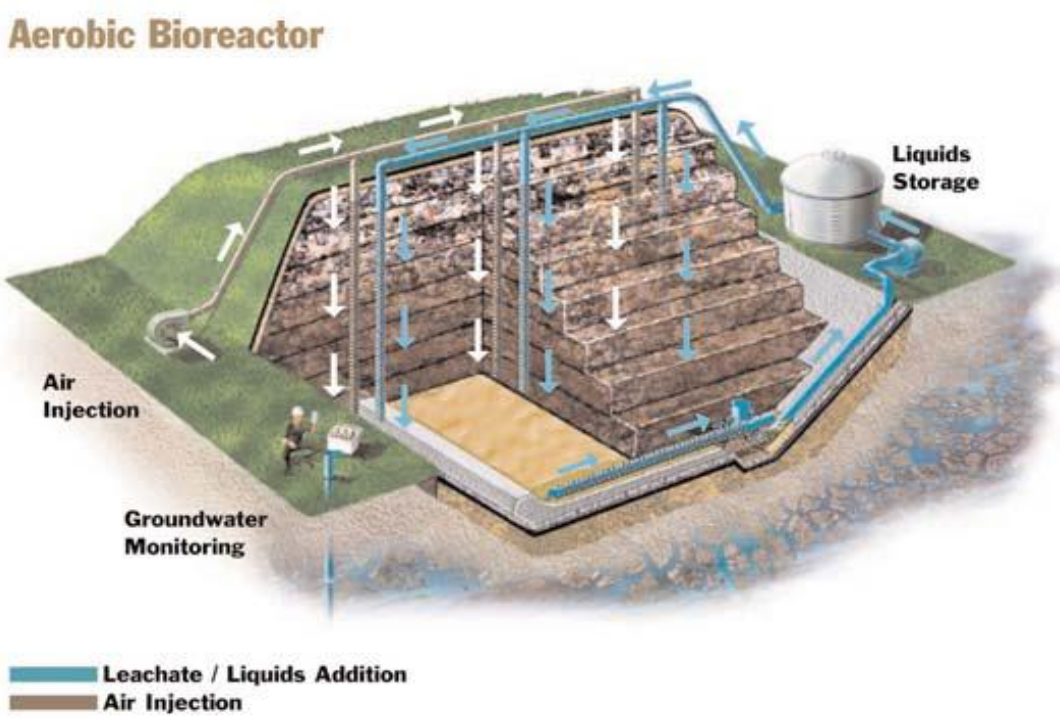

Figure I-23 : Aerobic Bioreactor (Waste Management, 2000).

I-3.3.3 Potential Advantages of the Bioreactor Landfill

- Accelerated decomposition and biological stabilization.
- Lower waste toxicity and mobility due to both aerobic and anaerobic conditions.
- Reduced leachate treatment and disposal cost.
- 15-30% increase in landfill space due to increased density of the waste mass.
- Increased landfill gas generation, which can be used for energy generation.
- Reduced post closure management.

I-4 STATUS OF MSW MANAGEMENT IN PAKISTAN

The discussion relating to the municipal solid waste of Pakistan is produced here with the objective to relate the present research study with the possible future field application in Pakistan. According to the NCS (Pakistan) the waste generation rate Pakistan in 1992 was 47,290 tons per day with a growth rate of 2.61% per annum. Presently it is estimated that 77,021 tons per day waste is generated in Pakistan with no separation of hospital, hazardous and industrial waste before disposal. A few exceptions for hospital incinerators in working condition though exist, but open burning and open disposal are much in practice.

Figure I-24 : Waste collection and disposal in Karachi (Pakistan) (IGES, 2005).

I-4.1 Disposal Trend in Pakistan

Keeping in view that only 50-69% of the waste generated is collected, there is a huge potential in recycling and involvement of the private sector which, unfortunately, is being overlooked for the moment. The separation practices are well established and a quantity of certain wastes such as; bottles, papers, glass and metal is considerably reduced in the waste stream. PEPA (Pakistan Environmental Protection Agency) and provincial EPA's work for the implementation of Pakistan Environmental Protection Act 1997, whereas the Town Municipal Authorities are responsible for waste collection, transportation and disposal. Unfortunately none of the cities in Pakistan has a proper solid waste management system starting from collection of waste to the disposal point. Even in the big cities, where this system exists, due to lack of collection and transport facilities and huge population density it still is impossible to cater for all the waste generated.

I-4.2 MSW Composition in Pakistan

In general the composition of MSW in Pakistan comprises of more than 50% of organic waste and due to local level recycling activities lesser percentage of paper, glass and metal is present in the waste. Per capita generation rate varies from 0.29 kg/day to 0.62 kg/day depending on the type of municipal area, while in France an average per capita generation rate 1 kg/day. In Table I-7 typical composition of MSW of Pakistan is presented in comparison with the waste composition of France.

Table I-7: MSW composition for France and Pakistan.

Waste Component	France (ADEME, 2002)	Pakistan (EPMC, 1996)
Organic	29	59
Paper/cardboard	25	5
Plastics	11	5
Textiles/Sanitary textiles	6	5
Glass	13	1
Metals	4	0
Miscellaneous	12	25

It should be noted here that this difference of composition especially due to high percent of organic components may need the characterisation of MSW of Pakistan separately. On the other hand the lower percentage of recyclable may have significant effects on the mechanical behaviour of MSW in landfills which will need their analyses through modification in the already defined parameters of determination and protocols as detailed in the present study.

I-4.3 Context and Objectives of the Present Study

According to a World Bank report, Pakistan has responded to its environmental problems by developing laws, establishing Government agencies and accepting technical assistance from donors, including the World Bank. Despite this, the response remains fragmented and environmental institutions, laws, and other initiatives do not solve the whole problem. Environmental legislation is still not well developed in Pakistan, especially in comparison to the developed world. For example, there are no national quality standards for MSW.

Keeping in mind the present state of the municipal solid waste management in Pakistan, the study presented here has been formulated in such a way that once this report is finalised it could be used as a reference to start different research projects in Pakistan. At the present time it is aimed to accumulate the possible experimental and analytical expertises in the field of MSW management which would in

turn serve as a baseline for the improvement in state of affairs of MSW characterisation back in Pakistan.

This brief introduction of the status of MSW management in Pakistan has been provided here with the objective to prepare a line of action for the future endeavours for the betterment of the living standard of the common people in Pakistan. Right now it is envisaged that this study will help develop a data base for the characterisation of the MSW as well as the techniques of landfilling at site starting from the barrier systems to the overall environmental safety concerning the settlement and stability issues.

II- PHYSICAL MECHANICAL AND HYDROLOGICAL PROPERTIES OF MUNICIPAL SOLID WASTE

Municipal Solid Waste (MSW) is a porous medium, consisting of all three phases; solids, liquids and gases, with heterogeneous properties. It seemed very important to define the concerned physical/mechanical properties of the medium before discussing in detail the research work carried out by other authors available in the literature and analysing in detail the experimental data of the present study. In the present chapter a review of the physical, mechanical and hydrological properties is presented including some biochemical notation which are related to the biodegradation of the MSW without discussing in detail the later as some of these phenomena are important in relation with the mechanical properties of compression and settlement of the medium as well as the fluid flow in the medium.

II-1 PRESENTATION OF THE MUNICIPAL SOLID WASTE MEDIUM

Municipal solid waste is any non-hazardous, solid waste from a combination of domestic, commercial and industrial sources. This can include food and garden waste, rubble and timber. Industrial waste is specific to industry or industrial processes. The municipal solid waste medium is a unique porous medium which comprises of a number of constituents, each one different in its physical, chemical and mechanical properties. This complexity is even more prominent with respect to its mechanical characteristics due to the presence of organic constituents which undergo the biodegradation over a period of time changing the structure of the medium and its mechanical/ hydrological behaviour.

The composition of the municipal solid waste placed in a landfill is difficult to define and depends on a variety of factors such as:

- Origin of the waste (domestic, industrial, hazardous etc.)
- Regulations of the landfilling agency
- Period of the year
- Any municipality or national environmental agency laws
- Landfilling techniques/management (including any prior pre-treatments)

In general the composition of waste is characterised on the basis of its grain size distribution and the percentage of all the constituents. These constituents for the percent calculation of the composition of municipal solid waste vary depending on the concerned regulatory authority. Most frequently characterised constituents include organic, inert, glass, metal, paper, plastic and metal but there can also be wood/garden trimming, cardboard, construction material, textile and rubber.

In Table II-1 the waste analysis protocol as defined by USEPA and other developed countries is detailed. In France the determination of the composition is carried out by MODECOM according to the French environmental agency ADEME legislation. It has thirteen primary categories and the composition can be defined up to thirty three categories including the sub classes of the composition.

Table II- 1: Waste analysis protocol (USEPA, 2008)

Waste Analysis Protocol primary category	Solid Waste Analysis Protocol primary category	Description
Paper	Paper	Recyclable paper, as newspaper and cardboard, non-recyclable paper, as milk containers and waxed paper
	Diapers and sanitary	Disposable nappies, feminine hygiene products and paper towels
Plastics	Plastic	Both recyclable and non-recyclable plastics
Organic	Putrescibles	Kitchen/food waste, green waste, other organic waste such as food processing waste
Metal	Ferrous metal	Metal products predominately made from steel
	Non ferrous metal	Other metal, such as aluminium, copper, lead
Glass	Glass	Recyclable glass, such as bottles and jars, and other products including glass, televisions and computer monitors
Construction and demolition	Rubble	Concrete, rocks, plasterboard and ceramics
	Timber	Timber lengths, furniture, sawdust
Other	Textile	Clothing, carpet
	Rubber	Tyres, foam mattresses
Potentially hazardous	Potentially hazardous	Material with potentially toxic or eco-toxic properties or properties requiring special disposal techniques (includes sewage sludge, paint, medical waste, solvents, asbestos and oil)

For the purpose of the multidimensional study of the hydro-mechanical behaviour of the waste, the composition of the waste can help understand numerous aspects of the medium such as:

- Organic constituent proportion is important in the study of the mechanical behaviour of the waste with respect to the settlement phenomenon.
- Deformable materials like paper, cardboard and textile which undergo the mechanical compaction and plastics influence the stability and strength parameters of the waste as well as the permeability parameters of the medium.

The information on waste composition can help develop waste minimisation policies, target waste minimisation programmes and improve recycling schemes. As an example, local authorities can use waste composition information to target reuse or recycling schemes for materials that make up a large part of the waste stream in their area. Within the unit volume of the waste material, the medium can be divided into four categories: gas, liquid and solids further subdividing the solids into organic and inert material.

II-2 PHYSICAL PARAMETERS

Household waste is a particulate material, heterogeneous in composition and thus in properties but its mechanical behaviour is always attempted to be quantified on the basis of soil mechanics. Compression, consolidation, shear strength and hydraulic conductivity are studied making use of laws applicable to soils with little or no modification. Following properties are discussed in a broader spectrum of geotechnical characteristics of a MSW:

- Unit weight
- Moisture content
- Permeability
- Settlement behaviour
- Shear strength

Due to large range of data, inconsistency in components is sometimes seen, thus it is most important to note the boundary conditions with each parameter presented.

II - 2.1 Leachate

II- 2.1.1 Liquid Density

The density intervenes in calculations of fluid flows as in the determination of liquid volume present in the sample (mass flow, measured by weighing, or volume). In the present study the liquid density is denoted as ρ_L. The liquid phase is mainly consists of water but contains other dissolved compounds as well. There are very few data in the literature concerning measurement of the leachate density. Vigneron (2005) measured the leachate density ranging between 1.013 and 1.016 Mg/m^3. In the absence of precise measurements, the density ρ_L = 1 Mg/m^3 identical to that of pure water is (exact value with 4°C) retained. That produces an error of about 1% compared to the measurements carried out by Vigneron (2005).

II- 2.1.2 Dynamic Viscosity

The dynamic viscosity of the liquid phase, denoted as η_L in the present study, is used in the flow rates calculations. The dissolved organic mass contained in the leachate can modify the value of dynamic viscosity. In the absence of any data relating to the leachate viscosity in the literature, this viscosity is considered equal to that of water.

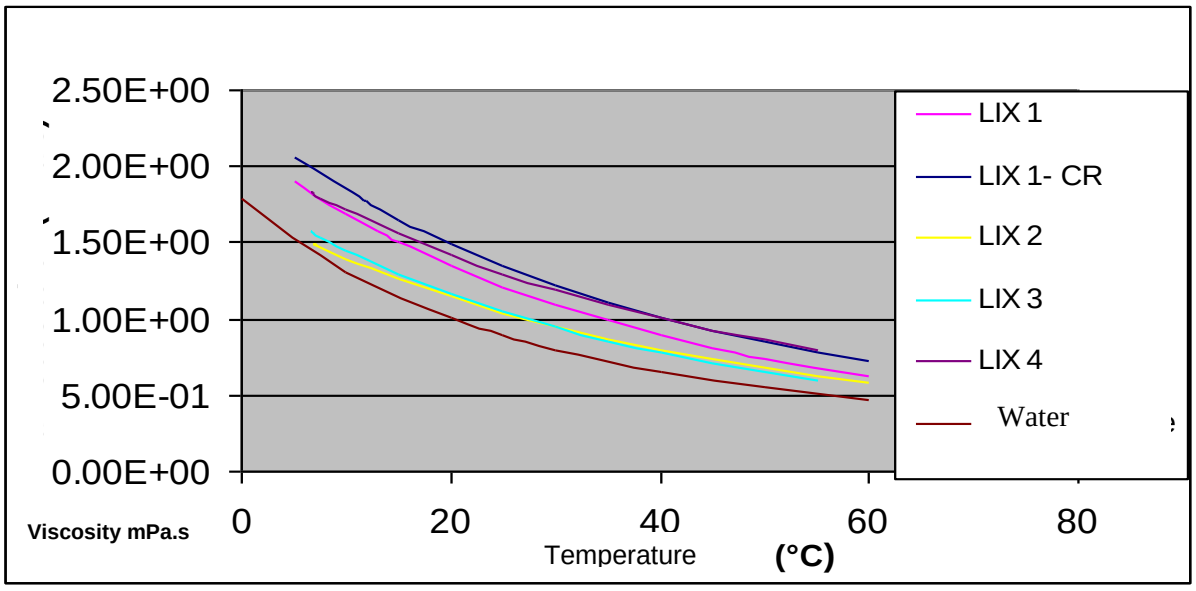

Figure II- 1: Dynamic viscosity of leachate as a function of temperature.

The effect of temperature on the viscosity of the liquids requires corrections to be applied for the temperature change in laboratory measurements. In a recent study in the laboratory (LTHE) a number

of leachate samples of different composition and ages were analysed for the dynamic viscosity of the liquid medium of the waste as a function of temperature which confirms this relationship. The results suggested higher values of dynamic viscosity in comparison with the dynamic viscosity of water as shown in Figure II-1.

II - 2.2 Biogas

The parameters of the gas phase are complex to define and even more to determine experimentally, this is the probable reason that very few parameters of gas phase are cited in the literature. The gas phase of the municipal solid waste mainly consists of methane (CH_4) and carbon dioxide (CO_2), termed as biogas, with varying percentage over the course of time depending on the phase of biodegradation.

There are many other molecules present in the gas phase with the character more or less like the pollutant, like H_2S (hydrogen sulphide) NH_3 (ammonia), the N_2O (nitrogen peroxide), *VOC* (Volatile Organic compound). Lornage (2006) studied the presence of *VOC* in biogas, their origin and their toxicity. Biogas also contains toxic compounds type *BTEX* (benzene, Toluene, Methylbenzene, Xylene). Manoukian (2008) studied the quantification of these *BTEX* in biogas and in particular showed that the stage of methanogenesis is preceded by a key emission of *BTEX*. The concerned parameters of gas phase such as gas density ρ_G and dynamic viscosity η_G of the gas are the parameters which evolve with the course of time.

II- 2.2.1 Gas Density

In site temperature and pressure range is small enough to apply the law of perfect gases for the determination of the density of the biogas. The law of perfect gases applied to the mixture of chemical components makes it possible to obtain the density of biogas according to the temperature, the pressure and the molar fractions. Either for a mixture of x_i^{molar} or $x_i^{molar} = \frac{n_i}{n_G}$ of CO_2 and at a temperature *T*, the average density is given by:

$$\rho_G = \frac{P_G M_G^{molar}}{RT}$$

P_G is generally taken at the atmospheric pressure, determined with the molar fractions;
M_G^{molar} is the molar mass of the gas
R is the constant of perfect gases.

II- 2.2.2 Dynamic Viscosity

The viscosity of biogas, noted η_G, can be calculated from the viscosities of pure gases comprising the mixture, their mass fraction and the temperature. For a mixture with 40°C of 50% carbon dioxide and 50% methane (in molar fraction), average dynamic viscosity η_G is approximately 14.10^{-6} Pa.s (Townsend et al, 2005).

II - 2.3 Solids Density

Since the municipal solid waste is composed of various solid constituents where each constituent has its own dry density, the dry density of the whole medium is not equivalent to the dry density of all the solids. The density of the solid constituents is thus defined as the sum of the dry density of all the constituents $\overline{\rho}_S = \dfrac{1}{\sum_i \dfrac{\mu_i}{\rho_{Si}}}$ where $\mu_i = \dfrac{m_{Si}}{M_S}$

μ_i is the percent mass of the constituent '*i*'
m_{si} is the dry weight of the constituent '*i*'
M_s is the dry weight of the solid mass

$\rho_{Si} = \dfrac{m_{Si}}{V_{Si}}$ corresponds to the dry density of the constituent '*i*'

Very few data regarding the solids density (ρ_s) is available in the literature e.g. Zornberg et al. (1999) give a values of 2.3 Mg/m^3 for the solids density of the waste sample without mentioning the method of determination of the parameter. They only state that the solids density is measured from the composition of the waste sample however it is worth mentioning that for each constituent even if the moisture content is known for that constituent determination of the solid density is an approximation as the saturation of that constituent is unknown.

II-3 STATE PARAMETERS

After defining the medium of municipal solid waste as a whole on the basis of three phases, solid, liquid and gas, now the solid phase of the municipal solid waste is classified on the basis of the types of elements present therein. This classification (Figure II-2) is presented in reference with the fluid flow through the medium and is different from the previous classification.

- Elements of the organic matter with the voids filled with water in micro pores. These elements are deformable under mechanical compression and are evolutionary in time due to

degradation. This category included waste of kitchen, green waste, papers and paperboards and textiles. These elements are compared with a matrix of fine elements is. A suggestion regarding the size of the elements constituting this matrix was made following the experimental measurements carried out in cell of laboratory by Stoltz (2009).

- Plastic elements (plastic fibres) are represented in the form of sheets. These elements are regarded as inert in time but deformable under mechanical compression.
- Contrary to the plastics, the textiles do not behave like impervious barriers (although they interact as reinforcement fibres).
- Inert elements (inorganic/non degradable), considered as non deformable with compression. This category includes wood, glass, metal.

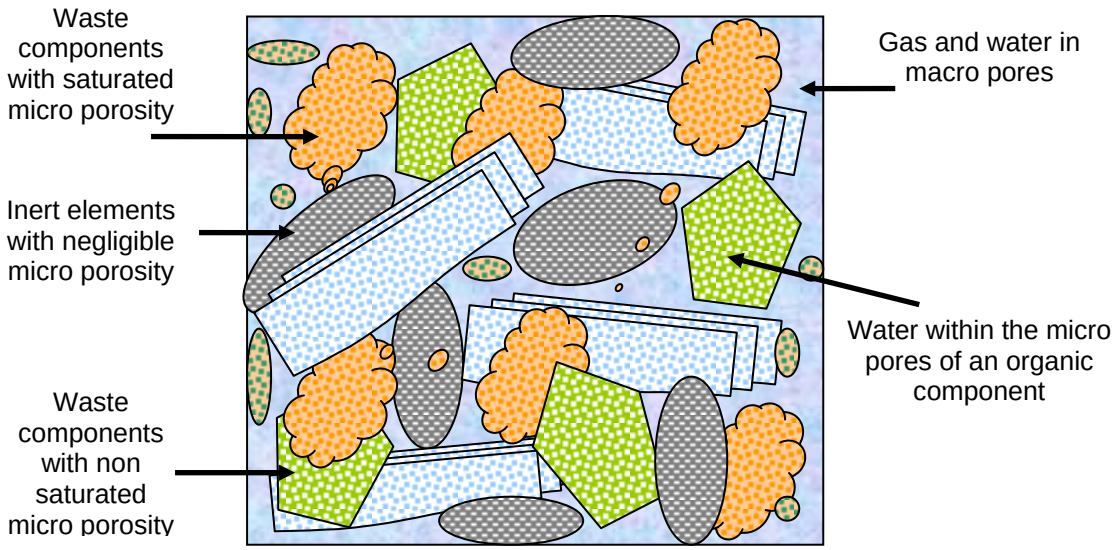

Figure II- 2: Waste medium distinguishing the liquid and gas phase within the solid phase.

II - 3.1 Definitions of various Densities associated with MSW

For the physical properties of the municipal solid waste two parameters are of basic importance and need to be defined prior to any further discussion. They are namely the solid content and the moisture content of the medium. In Figure II-3 the unit volume of the waste material is detailed with the mathematical notations which will further be used frequently in the present study.

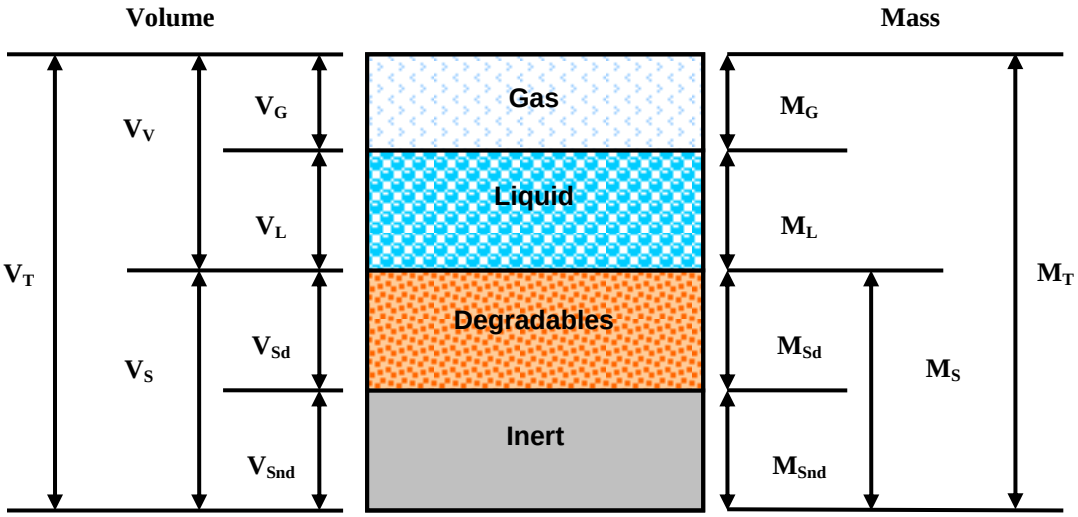

Figure II- 3: Description of different phases for the unit volume of MSW.

Unit weight of municipal solid waste is influenced by waste composition, cover between different layers and compaction effort. Composition specially the organic content plays an important role in defining the unit weight since decomposition governing the gas and leachate production affects the unit weight. Because the densities of solid waste vary markedly with geographic locations, season of the year and length of time in storage so the selection of the typical values with most appropriate assumptions for its component percent should be done carefully.

The overall density of the waste can be estimated by summation of all the densities of its components. Mass of the solid waste can be calculated separately for each component and accumulation of all densities is a better estimation of the density of the waste as a whole.

$$\rho_d = \frac{M_S}{V_T} \text{ or } \rho_d = \frac{M_S}{V_S + eV_S}$$

ρ_d = dry density

Ms = mass of solids

Vs = volume of the waste solids and

e = void ratio

$$M_S = \rho_S . V_S = \sum \rho_{Si} . V_{Si}$$

where

ρ_{si} = density of single component

V_{si} = volume of respective component

Waste particles undergo significant changes in density as the overburden stress is increased this is in contrast to some conventional theories of soil mechanics, in which soil particles are assumed to be

incompressible. Normally the values of 0.8 to 1.0 Mg/m^3 are used for unit weight of MSW however it may be an under estimation of relatively dry landfills as well as for degraded waste it might be greater than 1.5 Mg/m^3 or sometimes exceeds 2.0 Mg/m^3.

This dry density is defined with respect to the dry state; it thus depends on the measurement of the moisture content $w = \frac{V_L \cdot \rho_L}{V_S \cdot \rho_S} = \frac{M_L}{M_S}$.

ρ_d is calculated by the equation: $\rho_d = \frac{\rho}{1 + w_{MS}}$

where w_{MS} is the gravimetric moisture content . In addition to these densities the density of leachate and the gas density as defined in previous section are used. The leachate density ρ_L is defined by the equation $\rho_L = \frac{M_L}{V_L}$ while the gas density can be calculated making use of the formula $\rho_G = \frac{M_G}{V_G}$.

Finally the saturated density (ρ_{sat}) of the medium is defined by the following equation:

$$\rho_{sat} = \frac{M_S + V_V \times \rho_L}{V_T}$$

II - 3.2 Definitions of Moisture Content in reference with the Waste Mass

Moisture content of the municipal solid waste depends upon the initial waste composition, environmental conditions, biological decomposition rates as well as operating procedure and leachate collection system capacity performance. Moisture content is observed to increase with increase in organic component. It is one of the most important parameters of the solid waste since it directly affects a waste's mechanical, chemical and hydrological properties. Because of its influence on all aspects its relative determination for one factor alone can be confusing. If it is considered in context with the shear strength of a waste body it is not possible to neglect its affect on the slope stability, likewise its affect on biodegradation is inter-related with settlement or the affect of change in hydraulic conductivity on leachate circulation and gas extraction.

The moisture content of the medium is defined either on the basis of total wet mass of the medium where it is denoted as $\%_{MH}$, or it is calculated on the basis of the total solid mass of the medium where it is denoted as $\%_{MS}$. In literature both terms are used frequently however within the scope of the present study the moisture content is defined on the dry mass basis. The moisture content of solid waste is usually expressed as the mass of the liquid per unit mass of the wet or dry material. In both cases it is expressed as a percentage of weight.

w_{MS} (%) = M_L/M_S

Where; M_L = mass of the liquid in the sample

M_S = dry mass of sample

Moisture content present in the waste an be divided into two type;

- Free moisture (within the voids)
- Constitutive moisture content (which makes a part of the solid matrix) in the micro porosity

For the determination of moisture content of the waste drying in the oven can eliminate the free water but drying the constitutive moisture is not a function of heating in the oven rather it depends on the degradation, compression and other interrelated phenomena. The gravimetric moisture content (w_0) is the ratio of mass of water to the mass of solids $w_0 = \frac{M_L}{M_S}$, where M_L is the mass of water and M_S is the dry mass of the material likewise the initial moisture content can be determined through $\left(w_0 = \frac{M_{T0} - M_S}{M_S} \times 100 \right)$ where M_{TO} is the initial total mass of the material.

- Gravimetric moisture content as a ratio of mass of water to the dry solid mass w_{MS} expressed in percent mass $\%_{MS}$

$$w_{MS} = \frac{M_L}{M_S}$$

- Gravimetric moisture content as a ratio of mass of water to the total solid mass w_{MH} expressed in percent mass $\%_{MH}$

$$w_{MH} = \frac{M_L}{M_T}$$

These two ratios are interrelated through the following equation

$$w_{MS} = \frac{w_{MH}}{1 - w_{MH}}$$

In the present study, it is the gravimetric moisture content w_{MS} which will be used for all analyses however to avoid huge notations it will be denoted as 'w' hereafter.

Moisture Content at Field Capacity

The concept of moisture content at "field capacity" is usually employed in the field of waste; it represents the quantity of maximum water that waste can retain. This concept seems easy to conceive and well defined but the misconception lies with its representativeness keeping in view that its measurement is far from being simple. In reality, the field capacity of a waste column is not

characterized by a single value but by a profile which depends on the moisture retention properties of each layer (increasingly compressed towards the bottom of the column) and especially on the variation of the capillary pressure on the overall length of the column.

II - 3.3 Definition of Porosity and Corresponding Volumetric Content Parameters

In literature, the measurement of the porosity of solid waste sample is employed without defining the term "porosity". Different types of porosities are mentioned from drainage porosity to effective porosity and field capacity without giving reference to the total porosity which results in a percent error of 1% for drainage porosity to an error of 50% when it is the effective (open) porosity which is measured, hence no comparison of measured values is possible. Here these parameters are defined so as to develop their comprehension in reference with the present study (Figure II-4).

II- 3.3.1 Total Porosity

Total porosity of the medium is defined as the volume of voids (V_V) in the total volume (V_T) of the medium (expressed as a percent).

$$n = \frac{V_V}{V_T}$$

Another volumetric parameter is the void ratio (e) which is the ratio of volume of voids (V_V) to the volume of solids (V_S) and it is expressed as a decimal.

$$e = \frac{V_V}{V_S}$$

Both of these parameters are interrelated as expressed below:

$$e = \frac{n}{1 - n}$$

The parameter of void ratio is used in the analyses in the soil mechanics where the solids volume is constant. This is not the case when the municipal solid waste is concerned as the biodegradation affects the volume of solids which changes in time (reduction in V_S), therefore, the parameter of void ratio is not considered plausible for the present study.

On the other hand porosity is dependent upon the grain size distribution of the material as well as their arrangement in the given volume so that the material with the spread around the average will decrease the porosity and a skewed average will result in increased porosity. Similarly the shredding of municipal solid waste changes the porosity of the material to a lower value or the compaction results

in the decreased porosity. Likewise the volumetric solid content (θ_S) can also be used for the purpose of hydro-mechanical analysis of the medium as defined by the equation $\theta_S = \frac{V_S}{V_T}$. This parameter is of interest since the compaction of the solid mass does not necessarily result in decrease in porosity as the loss of mass due to biodegradation at the same time results in the increase in porosity. It is relative to porosity through $n + \theta_S = 1$.

The quantity of degradable solid (θ_{Sd}), differs from that non degradable (θ_{Snd}). These two parameters can be evaluated if the biochemical methane potential (BMP) of the sample is known. In Figure II-4 these parameters are detailed with reference to the volume of the waste medium.

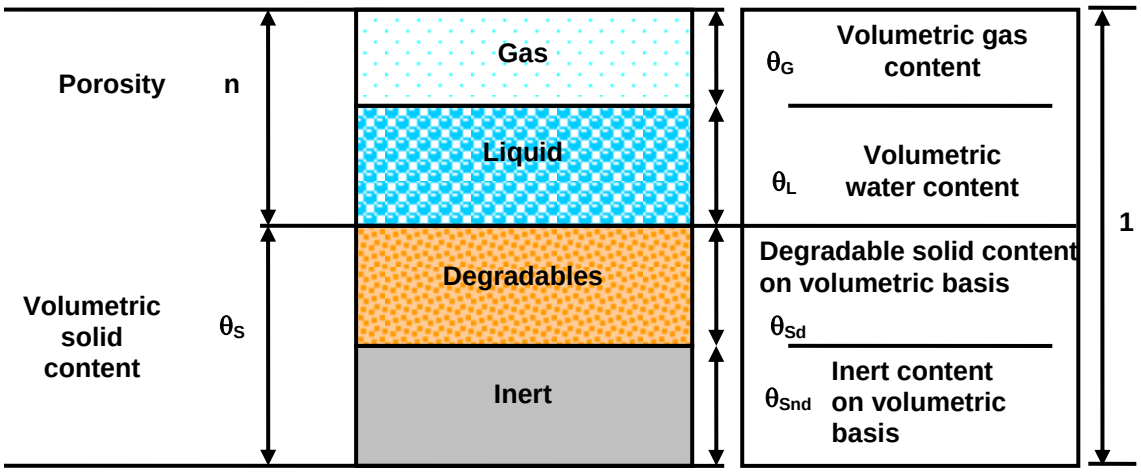

Figure II- 4: Phase definition on volumetric bases V_T of the waste.

II- 3.3.2 Volumetric Liquid Content

Volumetric water content (θ_L) is defined as the ratio of the volume of liquid (V_L) present in the pores to the total volume of the medium.

$$\theta_L = \frac{V_L}{V_T}$$

This parameter can indirectly be calculated from the gravimetric moisture content using the following equation:

$\theta_L = w \times \frac{\rho_d}{\rho_L}$ or $\theta_{L0} = w_0 \frac{\rho_{d0}}{\rho_L}$ for initial volumetric water content or $\frac{M_L \cdot \rho_d}{M_S \cdot \rho_L} = \frac{V_L}{V_T} = \theta_L$

II- 3.3.3 Volumetric Gas Content

Volumetric gas content is the ratio of the voids filled with gas (V_G) to the total volume of the medium $\theta_G = \frac{V_G}{V_T}$

Hereafter this parameter will be termed as the gas porosity. Together these two volumetric contents result in the total porosity of the medium $\theta_L + \theta_G = \frac{V_L + V_G}{V_T} = \frac{V_V}{V_T} = n$.

II- 3.3.4 Degree of Saturation

The two mathematical terms used frequently in the models of non saturated permeability are the degree of liquid and gas saturation. The degree of liquid saturation (S_L) is the ratio of pores filled with liquids (V_L) to the total volume of the voids (V_V)

$$S_L = \frac{V_L}{V_V} = \frac{\theta_L}{n}$$

Likewise the degree of gas saturation (S_G) is defined as the ratio of pores filled with gas (V_G) to the total volume of voids (V_V)

$$S_G = \frac{V_G}{V_V} = \frac{\theta_G}{n}$$

The sum of these two saturation degrees is expressed as $S_L + S_G = \frac{\theta_L + \theta_G}{n} = 1$.

II- 3.3.5 Interrelation of the State Parameters

The state parameters, as interrelated to each other, allow the calculation of all the parameters from a few measurements. Direct measurement of all of these parameters is not necessary to obtain their values. In general following three parameters are sufficient to determine all the others:

- Dry density (ρ_d) of the sample or the humid density, ρ_d
- Moisture content (w) of the sample
- Total porosity (n) of the sample

II-4 MECHANICAL PARAMETERS

II - 4.1 Settlement

With respect to time the settlement may be broadly divided into 3 phases; instantaneous, primary and secondary settlement. While instantaneous and primary settlements are not a function of time and secondary settlement is dependent upon time. Prediction of long term settlement behaviour is important for a successful future development of the site. Prediction of settlement rate is more important than the total settlement. With a total settlement range of 25% to 50% of the initial waste height, more than half is attributed to secondary settlement.

Primary Settlement: It is load induced instantaneous consolidation in landfill compared to the consolidation settlement of fine grained soils. Many researchers have investigated its characteristics Jessberger et al. (1993), Beaven et al. (1995). In general it is dependent upon composition, age and the compaction effort applied to the waste. The compressibility of the waste is characterised by the coefficient of primary compression C^*_R which is derived from the one dimensional consolidation theory of the pre-consolidated soil. The equation of C^*_R is $\frac{\Delta H}{H_0} = C^*_R \log \frac{\sigma'}{\sigma'_C}$ where H_0 is the height of the sample for the pre-consolidation pressure, ΔH is the primary settlement for the unidirectional compression stress σ' (Figure II-5) assuming that there are no lateral strains and σ'_c = Pre-consolidation stress.

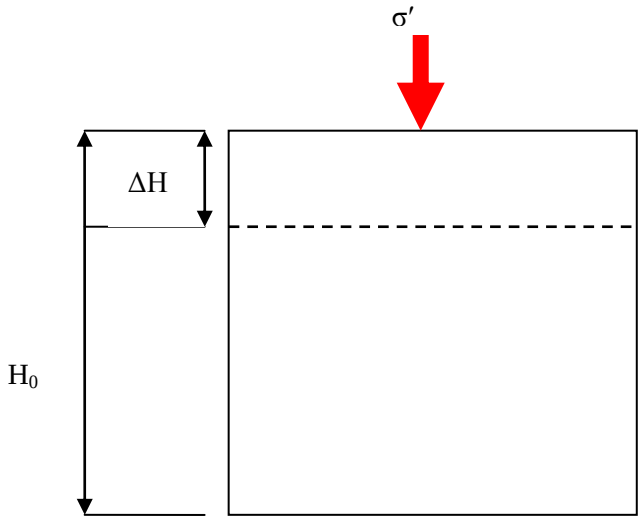

Figure II- 5: Primary settlement with the application of a unidirectional vertical load.

The parameter of settlement utilised for the calculation of other hydro-mechanical parameters are;

- Dry density $\rho_d = \dfrac{\rho_{d0}}{1 - \dfrac{\Delta H}{H_0}}$
- Porosity $n = n_0 - \Delta n$ with $\dfrac{\Delta H}{H_0} = \dfrac{\Delta n}{1 - \Delta n - n_0}$
- Volumetric moisture content $\theta_L = \left(w_0 - \dfrac{M_{LC}}{M_S} \right) \dfrac{\rho_{d0}}{\rho_L} \left(\dfrac{1}{1 - \dfrac{\Delta H}{H_0}} \right)$
- where moisture content $w = w_0 - \dfrac{M_{LC}}{M_S}$ (M_{LC} being the leachate drained out during the test)

Secondary Settlement: Long term settlement of a landfill is referred to as the secondary settlement which is assumed to be independent of the load but is dependent upon time and biodegradation effects. For the post operation settlement it is not the primary settlement which is important since it is almost completely incorporated before landfill closure, but is the component of secondary settlement which play an important role throughout the life time of a waste body.

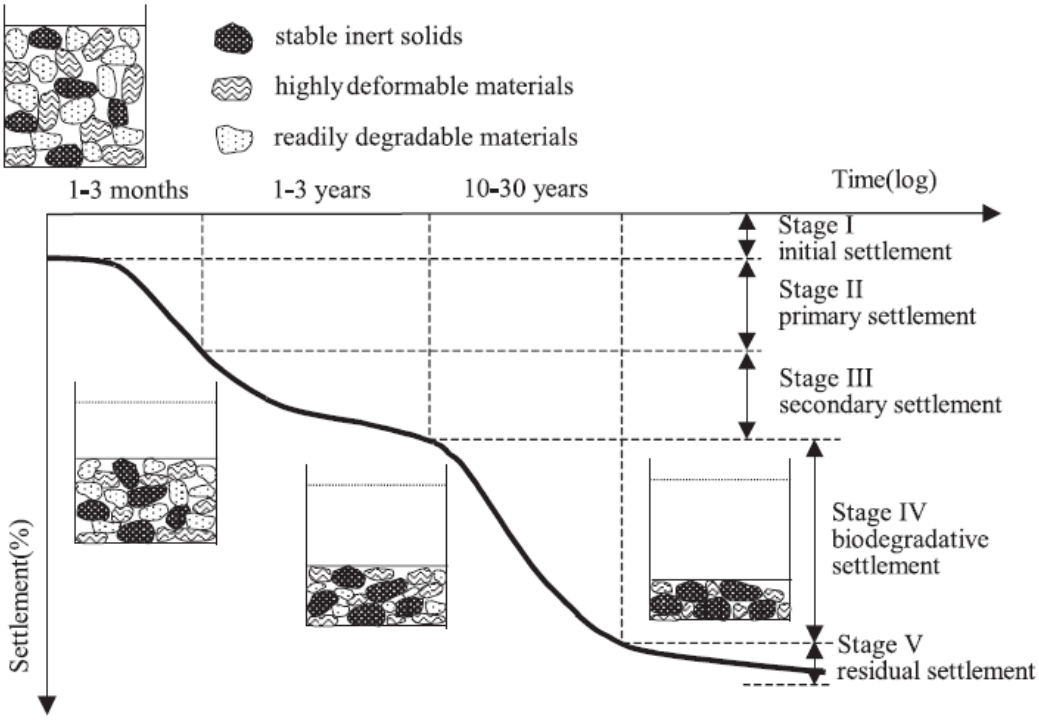

Figure II- 6: The typical time–settlement data for a landfill under vertical stress (Grisolia et al., 1995).

The long term settlement prediction is carried out using one dimensional consolidation theory of soils, with the coefficient of secondary compression $C_{\alpha\varepsilon}$ which in turn depends on other parameters namely time of construction of the waste body, initial degree of compression, recirculation of leachate and other bio-chemical factors yet to be correlated with the phenomenon of time dependent settlement. According to the Buisman (1936) the secondary settlement can be calculated as $\frac{\Delta H^{S}}{H_0} = C^{*}_{\alpha\varepsilon} \log \frac{t}{t_p}$ where ΔH_S is the secondary settlement and t_p is the time at the end of primary settlement (Figure II-6).

II - 4.2 Shear Strength Parameters

Shear strength is one of the two important mechanical parameters of the waste, other being the compression, studied for last two decades. The laws of soil mechanics are applied to the waste with a little or no modification. In case of shear behaviour the same approach of soil shear strength is followed. The difference between the two is that for the soils it is only non-linear but for the waste it is time dependent as well. However the Coulomb's theory and that of Mohr's are most commonly used. For a unit area with normal effective stress σ', shear strength is expressed in terms of friction angle and cohesion as;

$\tau = c + \sigma' \tan \varphi$

where cohesion "c" is the binding force between the fine particles of soils and "φ" the friction angle is the friction between the particles.

Cohesion is considered to be stress-independent while the friction is stress-dependent. However for the waste the term of apparent cohesion is applied which is related to the capillary forces. A critical combination of normal and shear stresses results in failure of a plane and failure planes joined together through a curve define a Coulomb failure envelope. A straight line along the curve for approximation known as Mohr-Coulomb rupture line is also used. The effective stresses concept proposed by Terzaghi is often used concerning the fracture and deformation behaviour of soils as;

$\tau'_{max} = c' + \sigma' \tan \varphi'$

where $\sigma' = \sigma - u$, u is the pore water pressure

However for the waste (with larger particle size and heterogeneous nature), Kölsh (1995) explained the shear behaviour of the waste with the concept of tensile resistance that is caused by the fibrous particles interlocking various materials when shear stresses are mobilised. This tensile strength adds up to the Coulomb's equation as a percentage of both the angle of tensile strength and fibre cohesion. These physico-mechanical parameters are discussed in detail in Chapter VI.

II-5 FLUID TRANSPORT PARAMETERS

Previously the physical properties and the state parameters of the MSW are defined and discussed; now the fluid flow within this porous medium is discussed. To the present date the fluid flow in the MSW has not been studied in detail and less is known about the water and gas permeability of the municipal solid waste especially in unsaturated state. As there exist different phases in a waste medium i.e. solid, liquid and gas, with fluid phase consisting of liquid and gas both, there is a dire need to analyze this dual phase of the porous medium. Any fluid transport taking place in the medium is affected by these two phases which in turn is influenced by the presence of moisture content and the deformation of the waste column layers due to compression.

Moreover in a landfill, the biogas generated due to the degradation of the organic matter is collected at the top of the waste cell but the leachate produced during the process as well as any rain water percolated in the mass is collected at the bottom of the waste body under the effect of gravity. In bioreactor landfills the leachate is re-circulated generating a fluid flow through the medium and the flow rate of biogas and leachate are affected by the intrinsic permeability of the medium and the degree of saturation of both phases.

II - 5.1 Definition of Fluid Transport Parameters

II- 5.1.1 Darcy's Law for Saturated and Unsaturated Conditions

Darcy's law describes the fluids flow in a porous medium. Darcy's law is a simple proportional relationship between the instantaneous discharge rate through a porous medium, the viscosity of the fluid and the pressure drop over a given distance for a given cross-sectional area. It is expressed as follows;

$V = q/A$ OR $V = -K\left(\frac{dH}{dL}\right)$

Where dH/dL is the hydraulic gradient;

K is the hydraulic conductivity

V is the filtration rate (m/s)

A is the filtration area (m^2)

H is the hydraulic head $H_{fluid} = \frac{u}{\gamma_w} - z + \frac{v^2}{2g}$

And two different hydraulic and pneumatic heads exist as $h_L = \frac{P_L}{\rho_L g}$ and $h_G = \frac{P_G}{\rho_G g}$

ρ_{fluid} is the unit weight of fluid

Darcy's law is applicable to a Reynolds number up to 10 with the following assumptions;

- This law is applicable for flows caused only by the frictional forces between the fluids and the particles surface considering the inertial forces to be negligible.
- The fluids are considered to be inert with respect to the porous medium through which they percolate thus there is no chemical or physical change involved during the flow.
- For small filtrations, $V^2/2g$ is considered negligible for liquids, thus the following relationship remains $H_L = \frac{P_L}{\rho_L g} - z$

And for the gases because of their small densities, the effect of gravity and corresponding pneumatic head $Z = 0$, the equation reduces to; $H_G = \frac{p_G}{\rho_G g}$

$$RN = \frac{v\bar{d}_p \rho}{\eta}$$

$\bar{d}_p$ is the average pore diameter and η is the dynamic viscosity of the fluid.

The coefficient of permeability primarily depends on the size of pores which in turn is dependent on the distribution of particle sizes, shape and soil structure. Permeability is a function of void ratio and determination of coefficient of permeability is carried out in laboratory through 'constant head' permeability test for coarse grained soils and 'falling head' permeability test for the fine grained soils. The same is applicable for the solid waste with no major modification.

II- 5.1.2 Intrinsic Permeability (at Saturation)

In saturated state the coefficient of intrinsic permeability denoted as k_i is defined by

$$k_i = \frac{\eta_{fluid}}{\rho_{fluid}\, g} K_{fluid} \quad (S_{fluid} = 1).$$

k_{fluid} depends upon the dynamic viscosity and the unit weight of the fluid. The parameter k_i is a hydrodynamic characteristic of the porous medium and is independent of the nature of the fluid flowing through it. Thus for saturated state the Darcy's law becomes;

For liquids $v = -k_i \frac{\rho_L g}{\eta_L} \times \frac{dH_L}{dL}$

For gases $v = -k_i \frac{\rho_G g}{\eta_G} \times \frac{dH_G}{dL}$

Both the dynamic viscosity η_{fluid} and the density ρ_{fluid} depend on the temperature which needs to be measured to calculate these parameters. Generally in geotechnical engineering, only the coefficient termed as hydraulic conductivity is determined, denoted as K_w, because the fluid considered is always water. K_w is used for a standard temperature of 20°C and expressed in m/s. The correlation between K_w and k_i is described as $K_W = k_i \frac{\rho_w(20\,°C) \times g}{\eta_w(20\,°C)} = 10^7 k_i$.

II- 5.1.3 Fluid Permeability (Unsaturated State)

For unsaturated state of the porous medium, there exist two permeabilities, one for the liquids with a coefficient of permeability for liquids and the other for the gases with a permeability coefficient for gas with relationships defined as under;

For liquids $v_L = -k_L(S_L) \times \frac{\rho_L g}{\eta_L} \times \frac{dH_L}{dL}$

For gases $v_G = -k_G(S_G) \times \frac{\rho_G g}{\eta_G} \times \frac{dH_G}{dL}$

In applications, relative permeability is often represented as a function of water saturation, however due to capillary hysteresis one often resorts to one function or curve measured under drainage and one measured under imbibitions. As the flow of each phase is inhibited by the presence of the other phases, the sum of relative permeabilities over all phases is always less than 1. The following expressions define the relative permeabilities of liquids and gases respectively with respect to the intrinsic permeability;

$k_{rL}(S_L) = \frac{1}{k_i} k_L(S_L)$ so the Darcy's law becomes $v = -k_i k_{rL}(S_L) \times \frac{\rho_L g}{\eta_L} \times \frac{dH_L}{dL}$,

$k_{rG}(S_G) = \frac{k_G(S_G)}{k_i}$ so the Darcy's law is defined as $v = -k_i k_{rG}(S_G) \times \frac{\rho_G g}{\eta_G} \times \frac{dH_G}{dL}$.

k_{rL} and k_{rG} are non-dimensional parameters. For saturated conditions, $S_L = 1$ or $S_G = 1$ so the relative coefficients of permeability k_{rL} or k_{rG} are equal to one as well, thus intrinsic permeability k_i can be determined with $k_G(1) = k_L(1) = k_i$.

For a compressible medium, with porosity 'n', Figure II-7 describes the diminishing porosity with the modification of its relative permeability curve for example in the case of municipal solid waste. However as indicated earlier, the sum of liquid and gas permeability in unsaturated condition does not result in intrinsic permeability ($k_{rL} + k_{rG} < 1$) as the flow in a unsaturated state of any porous medium has two flow phases i.e. for liquids and for gases which occurs in different flow paths. This is why the relative permeability curve for liquid and gas is not symmetrical and it can be noticed in the Figure II-

7 that relative permeability of the gas is more important than that of the liquid. Furthermore the existing residual liquid and gas saturations (S_{rL} and S_{rG}) will be discussed in detail in chapter IV within the scope of double porosity.

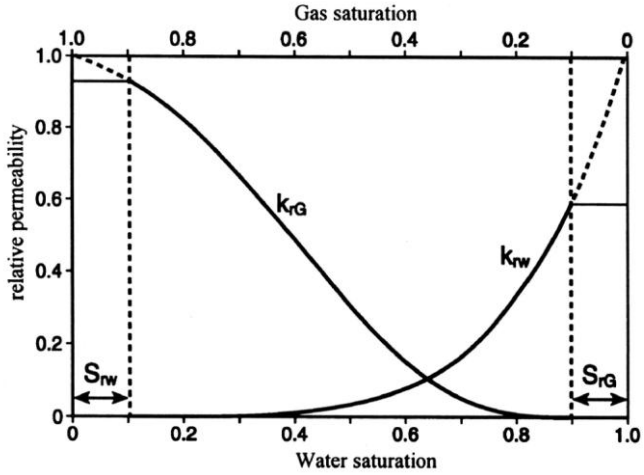

Figure II- 7: Relative permeability trends for soil as discussed by Warrick (2001).

The determination of k_i which is an intrinsic parameter of the porous structure of the medium, which implies that the same value must be found whether by a permeability test performed with water (saturating the medium) or a permeability test through gas (saturating the medium) due to the presence of these residual saturations becomes complicated because the certainty of the saturated condition is not always obvious.

II - 5.2 Previous Research on Fluid Transport Parameters

In this section traditional unsaturated flow laws in porous medium are reviewed and discussed according to their application in conventional landfills. Any relation between the settlement and liquid and gas flow in the bioreactor landfill needs to be explored. The present section deals with the study of the flows of liquids and gas in the porous media of solid waste. In the literature the study of fluid flows in waste material is fewer in number and lacks information (in particular the measurements of permeability of water and gas in unsaturated conditions, there is almost no data available in the literature).

Waste is a poly-phase porous medium containing two fluid phases: a liquid and a gas phase. The transfers of fluids are thus of diphase nature. These transports are influenced by the moisture of the medium but also by the deformation of the various compressed layers (settlement). The origin of the flows in waste can be described briefly as: biogas which is a product of the biological breakdown and which is collected by difference in pressure at the top of the waste column, and the leachate resulting from precipitation and the product of waste degradation, which percolates towards the bottom of the

waste column under the effect of gravity. The management of a landfill site as a bioreactor leads to the recirculation of the leachate within the solid mass of waste and there is a di-phase flow in the reverse direction (upwards). The porous space in which the fluids run are significantly tiny voids and the rates of flow of biogas and the leachate, thus are entirely conditioned by the intrinsic permeability of the medium and the degree of saturation of each one of these phases. The description of this settlement - flow of liquid - flow of gas interaction is essential in the case of a management as a bioreactor mode.

II- 5.2.1 Permeability/Hydraulic Conductivity Measurements

Hydraulic conductivity of saturated soils is measured through 'rigid-wall or flexible-wall' permeameters in the laboratory. For the wastes in general the same Darcy's law is applicable without any modification. According to Beaven et al. (1995) flow through saturated domestic waste is reasonably characterized by Darcy's Law. But the hydraulic conductivity of domestic waste depends upon density which in turn depends upon the vertical stress to which it is subjected. And again degradation of waste reduces particle size increasing its density affecting the hydraulic conductivity. Moreover there is a difference of vertical and horizontal conductivity because of the layered structure of the domestic waste in landfills. Liquid flow in unsaturated waste needs further research as well as the double porosity flow models.

Powrie et al. (2000) performed experiments for the quantification of relationship between;

- Drainable porosity and vertical stress
- Hydraulic conductivity and vertical stress

and concluded;

- Wastes approach saturation even if they are free to drain under gravity.
- Hydraulic conductivity of different waste types (processed, unprocessed and household) have insignificant differences in comparisons with order of magnitude change in hydraulic conductivity that results from waste compression.
- Hydraulic conductivity of the waste is governed by maximum equivalent vertical stress to which waste has been subjected (unloading doesn't have any influence), however, stress history/density of waste must be considered while assessing hydrological and geological properties (Figure II-8).
- Layered structure of waste has anisotropy of hydraulic conductivity, where degree of anisotropy increases with increasing stress.

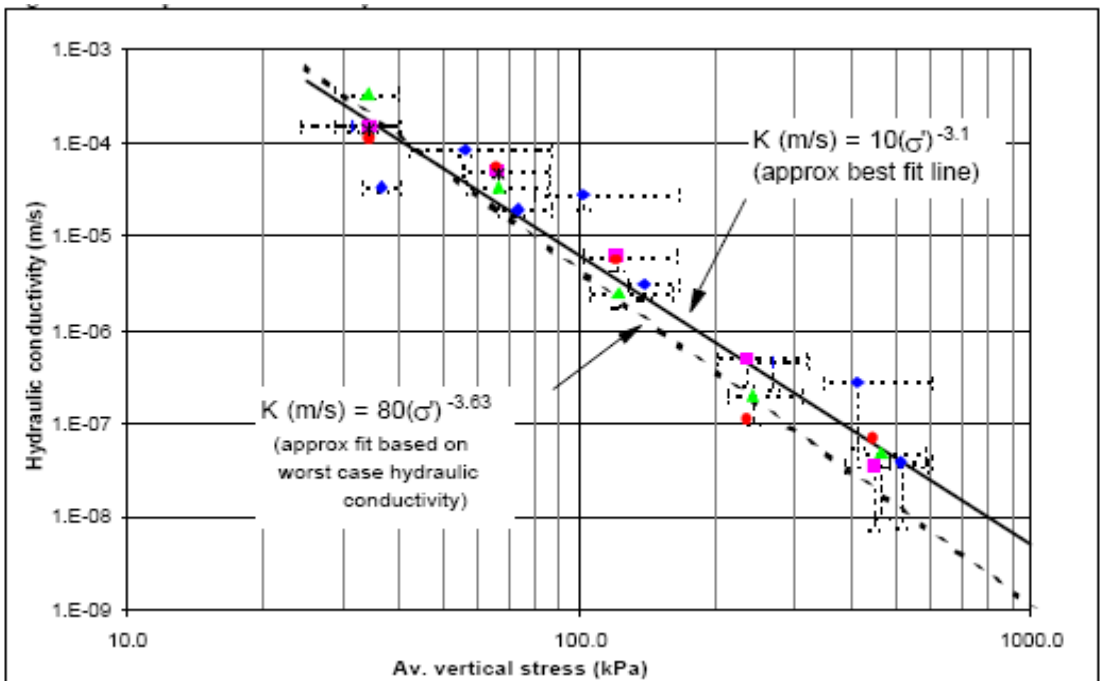

Figure II- 8: Reduction in hydraulic conductivity with increasing effective stress (Powrie et al., 2000).

Durmusoglu et al. (2005) studied the permeability of typical solid waste sample in two different scale devices (small & large). They used conventional consolidometers of ASTM D2435 specification for smaller scale study with a water tight body and base for submerging the waste sample. While for the larger samples they made use of a consolidometer with an internal diameter of 71.12 cm with a height of 55.88 cm. The results are in conformity with the other ongoing and already done research (Table II-2), however, they had a large scale of variation and they did not offer any conclusion.

Table II- 2: Published permeability values for MSW samples (Durmusoglu et al., 2005)

Source	K (m/s)
Fungaroli and Steiner (1979)	1.0×10^{-5} - 2.0×10^{-4}
Oweis and Khera (1986)	1.0×10^{-5} - 1.0×10^{-4}
Ettala (1987)	5.9×10^{-5} - 2.5×10^{-3}
Landva and Clark (1990)	1.0×10^{-5} - 4.0×10^{-4}
Oweis et al. (1990)	1.0×10^{-6} - 1.0×10^{-5}
Edgers et al. (1992)	1.0×10^{-5} - 2.0×10^{-4}
Gabr and Valero (1995)	1.0×10^{-7} - 1.0×10^{-5}
Present Study (Durmusoglu et al. 2005)	4.7×10^{-6} - 1.24×10^{-4}

Permeability decreases with increase in hydraulic gradient, but larger values were measured in small scale device which may be due to sensitivity to boundary or generation of paths within the specimen (Figure II-9). The authors suggested that there might be no linear relationship between permeability

and moisture content conditions and the only conclusion is that higher the waste density, lower will be the permeability.

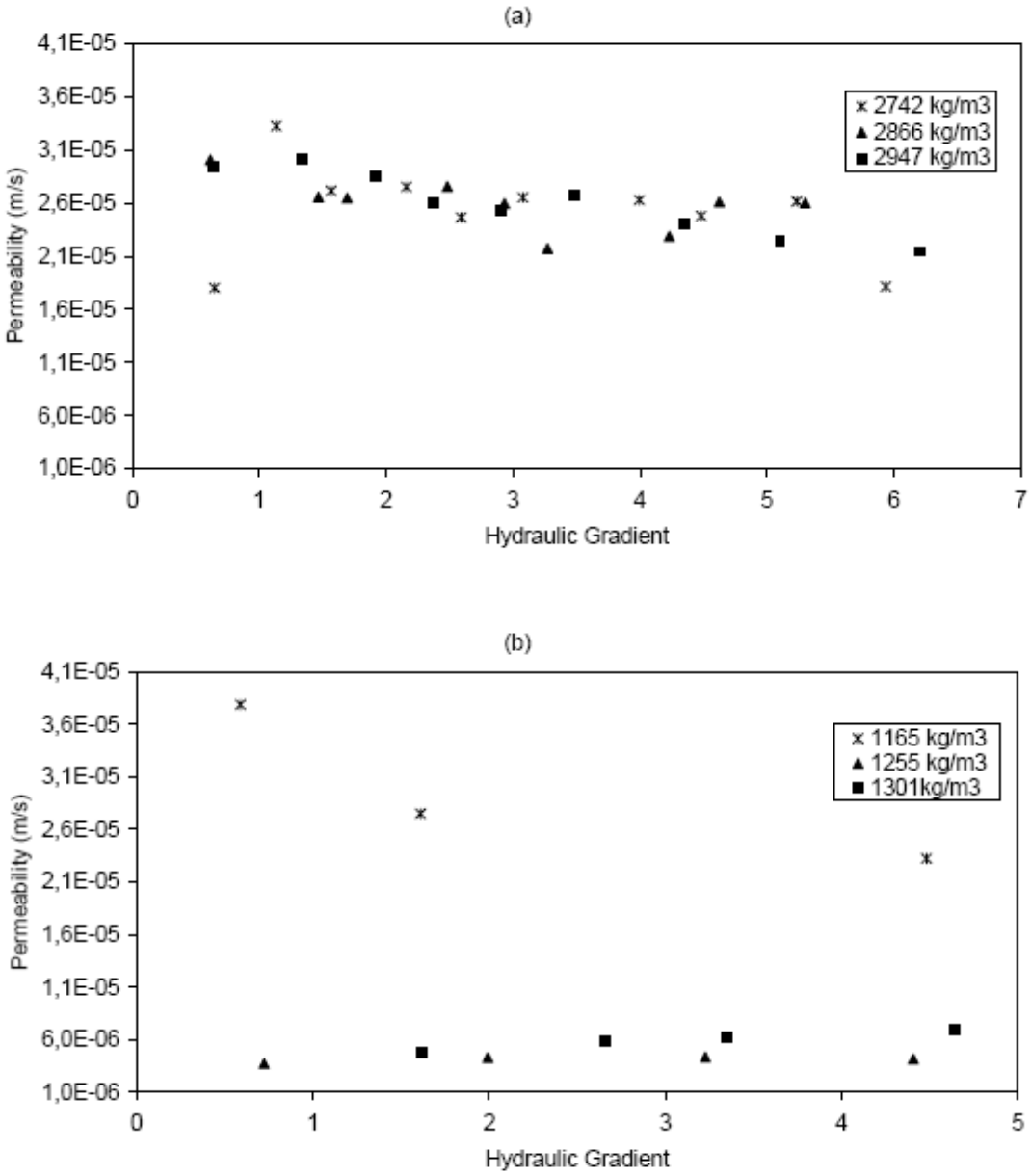

Figure II- 9: The values of permeability for MSW samples at field capacity (saturated and drained under the effect of gravity) tested under different densities and hydraulic gradients in (a) small-scale device; (b) large-scale device (Durmusoglu et al., 2005).

II- 5.2.2 Effects of Degradation on Physical Parameters of MSW

For a realistic comparison, the geotechnical properties are studied for both conditions of the waste (fresh and degraded) and the parameters are modified likewise. For a fresh waste density is less than that for a degraded waste as the mass decomposition results in reduction in volume and emission of gases gives rise to formation of voids leading to compressibility of the waste as a whole, making it

denser. Watson et al. (2007) investigated the change in structure of biodegradable waste. The main purpose of the study was to develop the techniques for non-invasive investigation of the anaerobic degradation of MSW. As all the "undisturbed" samplings involve disturbance thus new techniques have been explored and tested to propose future modification in the field testing options. To better understand the structure of the waste and distribution of liquid, gas and solid phase within the medium, X-ray computed tomography (CT scanning) could be an attractive non-invasive method of structure visualisation. The authors have performed test on a degrading waste with installation of the CT scanners within the reactors, they suggest that it may be a promising technique for future to study the structural change in the MSW.

Figure II-10 shows voids present after degradation in one of the reactors; some of the void areas are quite large (up to about 5cm^3). Some of the larger voids match areas visible in the pre-degradation scans (samples were dry for the initial scan, high proportion of gas-filled void than seen in the saturated waste shown in figure) but whether these voids were never filled with water or if gas produced by the degrading waste has become trapped, displacing water during the course of the experiment is unclear. Similar features are seen in the scans of reactors 1 and 3 but the void volumes are significantly smaller in reactor 3, as would be expected with the much smaller particle size.

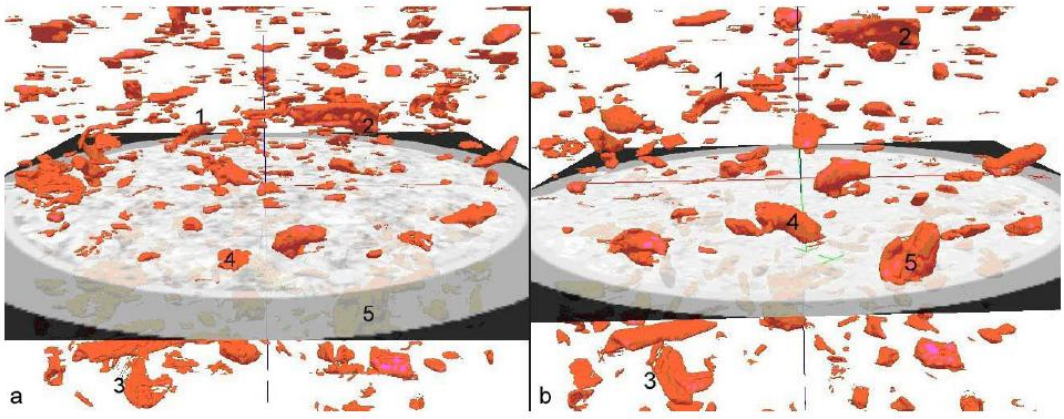

Figure II- 10: 3D image of reactor 2 showing only objects with CT number between 200 and 900, corresponding to bone and other dense materials. The uniform grey area represents the plane at the centre of the midpoint piezometer port to provide absolute location (Watson, et al., 2007) Figure 'a' is related to the scan prior to degradation while 'b' shows the scan after 2 months of degradation.

Figure II-11 shows that gas is present mainly in discrete major pockets which are reasonably evenly distributed through the sample (the sample has a more or less uniform void ratio and density even though it is a heterogeneous material). This scan image might suggest that relatively large gas pockets may play a major role in gas transport. The CT scanning data shows presence of dry voids, probably

created by gas production of the waste during degradation; it is visible that relatively large gas pockets play a role in gas transport, although further investigations are needed to identify the mechanism (Figure II-11).

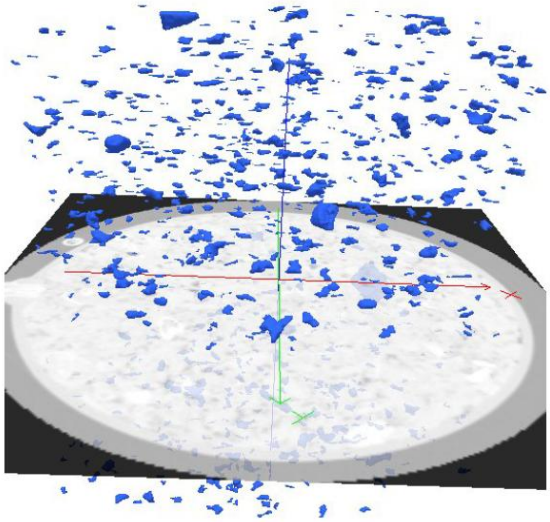

Figure II- 11: 3D image of reactor 2 after degradation showing only objects with CT number less than -500, corresponding to gas-filled voids. The uniform grey area represents the plane of the centre of the midpoint piezometer port to provide absolute location (Watson et al., 2007).

II- 5.2.3 Anisotropy of Permeability in Relation with MSW

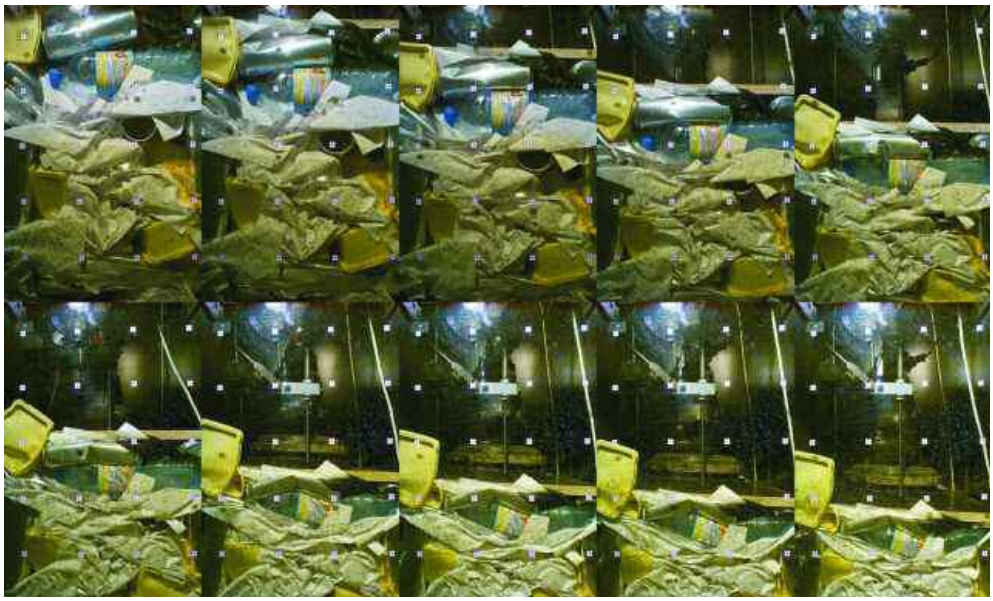

Figure II- 12: Compression of plastic components in the horizontal direction during the compaction of synthetic waste (Langer, 2005).

In practice, the municipal solid waste is placed in layers at site with plastic components being placed at horizontal orientation. This results in an isotropy of permeability in horizontal and vertical direction with vertical permeability having much smaller values due to the fact that the fluid needs to move laterally before going down vertically every time it encounters an impermeable plastic component. This provision is observed in the photos (Figure II-12) as observed during the compression behaviour studied for the synthetic waste comprising mainly of plastics, textiles and papers (Langer, 2005).

II - 5.3 Flow Models for Saturated and Unsaturated Porous Media

As the settlement is a characteristic to observe the evolution of physical as well as bio-mechanical parameters of the waste, laws governing the flow of liquids or gases are studied to characterize the permeability with respect to settlement to better understand the evolution of MSW. Certain authors like Powrie et al. (2000) proposed a law of reduction in the saturated hydraulic permeability as a function of the applied pressure but this is an empirical law because it makes no use of the structural parameters of the waste.

II- 5.3.1 Laws of Intrinsic Permeability

II - 5.3.1.1 Carman-Kozeny Model

Poiseuille's equation for laminar flow was further developed by Carman-Kozeny as capillary tube model to predict the flow rates through porous passages, filters etc. In this model the porous medium is represented as a bunch of cylindrical capillaries of different radii. The capillaries may be tortuous but their radii remain invariable along their extent. This excludes hysteresis related to different locations of the menisci in the same capillary. It is expressed as follows:

$$v_P = \frac{d_p^2}{32\eta}\frac{\Delta H}{L_e}$$

Here v_P is the rate of flow in interstitial spaces, ΔH is the difference of pressure at the entrance and the exit points of the tube, η is the viscosity, d_p is the hydraulic diameter of the tube and L_e is the tube length which could be different from the thickness of the medium and caters for the medium tortuousity. The hydraulic diameter can further be expressed as a function of capillary tube as;

d_p = 4x (volume of voids/ internal surface) = $4\frac{1}{S_S}\frac{n}{1-n}$ with S_s being the specific surface of the material defined with respect to the volume of solids i.e. $S_S = \frac{Surface of grains}{V_S}$

From this relationship Darcy's law of filtration becomes $v = \frac{k_{KC}}{\eta}\frac{\Delta H}{L}$

k_{kc} is the Carman-Kozeny's intrinsic permeability
L is the thickness of the porous medium, η is the viscosity.

The interstitial speed of fluid 'v_P' and the filtration rate 'v' are inter-related through $v_P \frac{L_e}{L} = \frac{v}{n}$.

This relationship is based on the Dupuit-Forchheimer hypothesis, according to which the interstitial flow speed is correlated to filtration rate through porosity. However the ratio L_e/L is introduced by Carman and is commonly known as tortuosity (τ) with a value close to 5 for soils. Finally the coefficient of intrinsic permeability proposed by Carman-Kozeny is expressed as $k_{KC} = \frac{1}{\tau}\frac{1}{S_s^2}\frac{n^3}{(1-n)^2}$. However τ and S_s can not be measured directly.

II - 5.3.1.2 Application of Carman-Kozeny's Model to the Gas Permeability

For a gas flow in an unsaturated medium, the gas uses the pores available for gas movement. The medium can be defined to have two parts: one made up of the solid and the liquid, and the other corresponding to the gas flow. The formula of Carman- Kozeny can be used by replacing porosity 'n' by porosity with the gas θ_G $k_G = \frac{1}{\tau}\frac{1}{S_s^2}\frac{\theta_G^3}{(1-\theta_G)^2}$. The assumption of immobile water like the solid depends on several factors like the absolute pressure of gas, the capillary pressure etc. Nevertheless this assumption is considered within the framework of this study.

II- 5.3.2 Relative Permeability Models

For the models of relative permeability, the structure of the porous medium is defined with a given porosity and a given intrinsic permeability k_i. The gas and water permeability is determined according to the degree of saturation of liquid (with $S_L + S_G = 1$). In addition to that it is the coefficient of relative permeability k_r for the liquid or gas is calculated as needed on the case to case basis making use of relationship

for liquids $k_{rL}(S_L) = \frac{k_L(S_L)}{k_i}$

for the gases $k_{rG}(1-S_L) = \frac{k_G(1-S_L)}{k_i}$

Models of relative permeability with reference to pore size and saturation degree are discussed in detail in the thesis report of Stoltz (2009).

II- 5.3.3 Application of Permeability Models to MSW Landfills

Within the scope of permeability measurement, information available in the literature seems insufficient and incomplete with reference to the MSW. Moreover data on saturated hydraulic conductivity are only available with measurement performed with the help of piezometer in unsaturated conditions considering the capillary action. The liquid and gas flow are then characterized with the help of two coefficients of permeability one for each phase within unsaturated conditions, neglecting on one hand the effect of intrinsic permeability coefficient of the medium and the degree of saturation of both phases on the other.

Furthermore the research with the objective of modelling the permeability within the domain of municipal solid waste is rare. Arigala et al. (1995) proposed a model for saturated state with only two permeability aspects in consideration, horizontal and vertical permeability without any focus on unsaturated conditions. Durmusoglu et al. (2005) proposed a settlement model with fluids circulation taking into account the intrinsic permeability at unsaturated state. They have made use of Carman-Kozeny's model for intrinsic permeability and the model of Brooks et al. (1964) governing the laws of unsaturated permeability as follows:

$$S_e = \frac{w - S_{rL}}{S_{sL} - S_{rL}} = \left(\frac{h_d}{h}\right)^{\alpha} \text{ for } h \geq h_d$$

And $S_e = 1$ for $h \leq h_d$

S_e is the effective degree of saturation

w is the sample moisture content

S_{rL} is the degree of relative liquid saturation

S_{sL} is the saturated degree of liquid saturation

And h_d is the air entry suction for the samples and h is the pressure head. However they noted that their study was not calibrated for waste materials.

McDougall et al. (2007) proposed a bio-hydro-mechanical model for prediction of settlements making use of Richards's formula for unsaturated transport phenomenon and used the Van Genuchten (1980) equation for retention curves, but they have not considered the gas flow in their model. This is why to address this incomplete information and to propose a newer technique; an apparatus named "oedopermeameter" was conceived and designed at LTHE laboratory, in order to measure the gas permeability in unsaturated conditions.

The description of the complex permeability according to the depth is illustrated in Figure II-13. To characterize the capacity fluids transport in a waste column, it is necessary to define a law giving the

evolution of the intrinsic permeability according to the depth (Stoltz, 2009). Keeping in mind that the deeper a sample is in the waste column, the more it will undergo the settlement because of constraint imposed by the overlying column of waste. Porosity decreases thus according to the depth. The evolution of the intrinsic permeability with porosity must thus be characterized. Then for a given level (and thus for a given porosity), one needs the laws of relative permeability kr_L (S_L) and kr_G (S_G). To discuss the permeability of a waste column, profiles of the permeability will be considered for the whole length of the waste column. The decrease in intrinsic permeability as a function of depth of the waste column is illustrated in Figure II-13 where it is defined for a saturated state waste sample. It is worth noticing that the flow paths are influenced by the voids thus porosity, hence it is the function of permeability with respect to porosity which will further be discussed in detail.

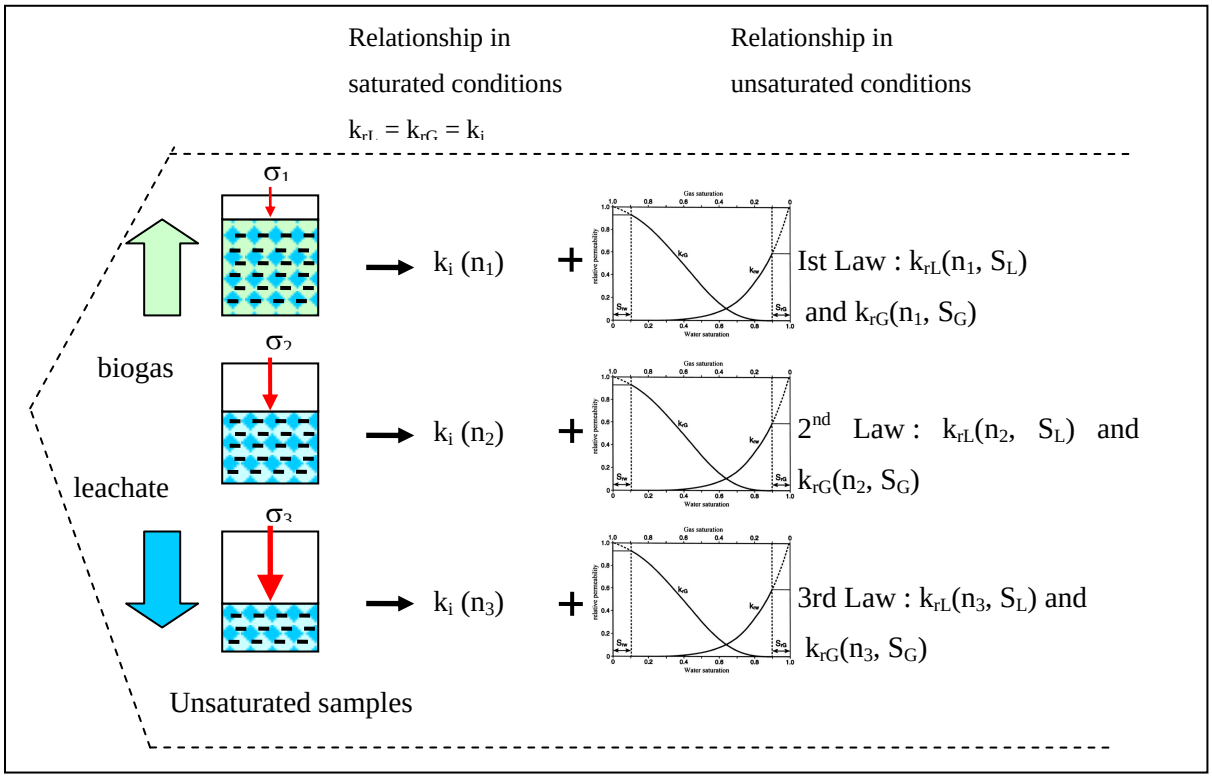

Figure II- 13: Evolution of intrinsic permeability as a function of waste column depth (Stoltz, 2009).

II-6 OEDOPERMEAMETER, HYDRO-MECHANICAL PARAMETERS' MEASUREMENT AND THE PRINCIPLE APPLIED

Liner systems, daily covers as wall as gas and leachate collection systems are installed in the landfill facilities which necessitate the assessment of hydraulic characteristics. Weight density and moisture content relationship affects the hydraulic conductivity from case to case basis. Compacted fine grained soils are widely used in the liners and covers for the waste containment structures, their primary purpose is to minimize flow, hence low hydraulic conductivity is most concerned. Hydraulic conductivity is the coefficient of proportionality in the Darcy's law. Civil engineers traditionally call '*K*' the coefficient of permeability while soil scientists refer to it as the hydraulic conductivity. Hydraulic conductivity is one of the hydraulic properties of the soils. More specifically, the hydraulic conductivity determines the ability of the soil fluid to flow through the soil matrix system under a specified hydraulic gradient.

The present section discusses in detail the traditional laws of flow in porous media, saturated and unsaturated, and their applications to the domestic landfill sites are presented. In the present study hydro-mechanical parameters of settlement and liquid flow are analyzed simultaneously keeping in view the following objectives:

- Verification of the hydro-mechanical model initially proposed and presented by Stoltz (2009).
- To propose various directions for future analyses mainly focusing on the bioreactor landfills' optimization.

The hydro-mechanical analyses in the present study were performed in the laboratory LTHE in a device named 'oedopermeameter" specially designed and conceived for these analyses. The principle of oedopermeameter consists of compacting a waste sample at various compression loads with permeability measurements done at each compression load.

II - 6.1 Apparatus Description

The oedopermeameter cell consists of a stainless steel cylinder with two porous plates, one at each end of the cylinder. The cell has a diameter of 27 cm and an effective height of 29 cm (which is the initial height of the sample) with total height of more than 32 cm. The porous plates have pores of 5 mm diameter at a spacing of 1 cm centre to centre. In order to minimize any solids transport along with the leachate, a geo-synthetic membrane having square openings of 1 mm width is placed between the

porous plates and the waste sample. Two opening in the outer cover of the cylinder at both ends facilitate the placement of pressure sensors as well as the gas entrance and the leachate collection (Figure II-14). The top cover plate is equipped with the piston which connects the pneumatic loading system with the support structure. This support structure is capable of supporting a force up to 12kN equivalent to a compression stress of 300 kPa.

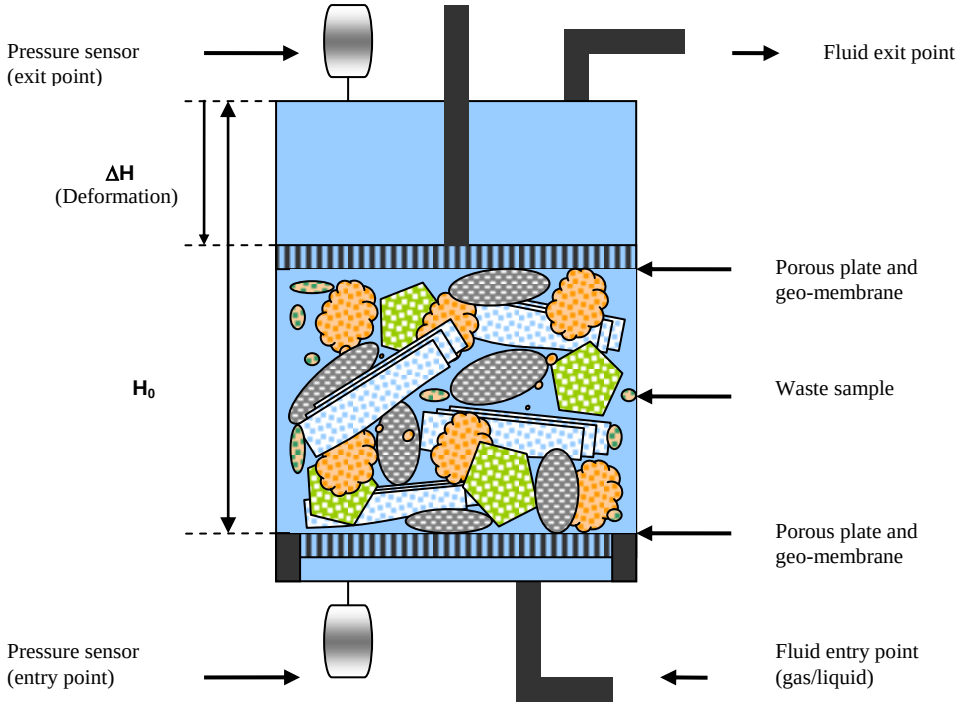

Figure II- 14: Schematic diagram of the Oedopermeameter.

II- 6.1.1 Complimentary Equipment

These materials consist of a number of sensors attached to the oedopermeameter (Figure II-15)

- A force sensor (25 kN capacity)
- A displacement sensor (15 mm course)
- A flow meter for nitrogen with a minimum limit of 5 l / min. This flow meter is converted from massflow into volumetric flow at standard temperature (273 K) and pressure (101.32 kPa).
- Two pressure sensors, one at each end of the cell with a range between -6.6 to +6.6 kPa.
- An atmospheric pressure sensor
- A mercury thermometer (0-35°C) for ambient temperature measurement applied for dynamic viscosity correction
- An oven (727 liters) is available for the moisture content determination of the samples at the end of each test series in order to interpret the porosity of the sample.

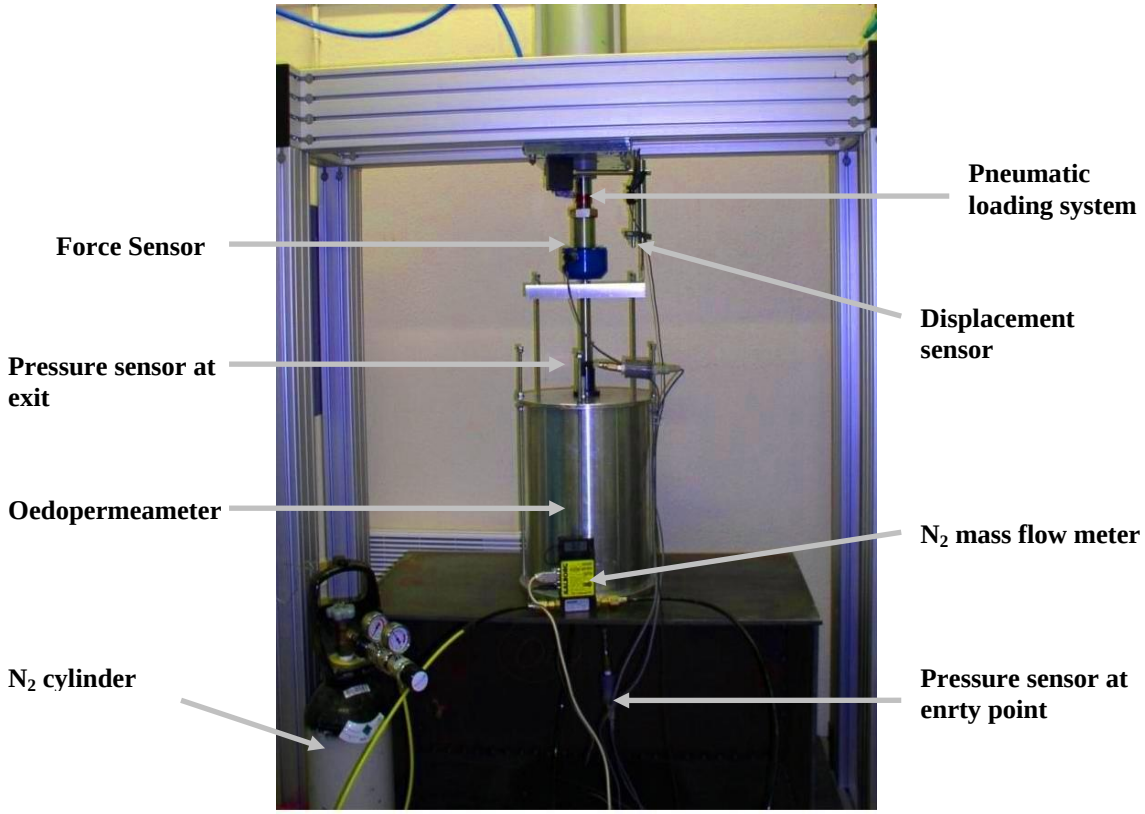

Figure II- 15: Oedopermeameter connected with complimentary equipment.

II- 6.1.2 Sample Preparation

In the waste sample, there are number of components which are different in size shape and nature. To have a representative sample it is important that each component is present in the same proportion as at site. However due to size limitation of the laboratory equipment those waste samples are used which either are initially shredded when placed in landfill or are shredded or sieved (6 cm) in the laboratory prior to testing. In this manner a ratio of 6 between the largest sample component and the diameter of the cell is obtained. The waste already shredded at site made it possible to use a major portion of the waste as retrieved from site with the exception of some plastic or metal parts which were cut smaller.

II - 6.2 Physical and State Parameters

II- 6.2.1 Volumetric Moisture Content

A waste sample with known initial mass M_T is placed in the oedopermeameter. The known volume of the sample V_T allows the calculation of the initial unit weight of the sample ($\rho = M_T/V_T$). At the end of the test the whole sample is put into the oven and dried at 80°C until the stabilization of the weight of

the sample is attained, this permits the determination of total dry mass as well as the moisture content of the sample. The volumetric moisture content of the sample is determined through $\theta_L = \frac{\rho_d}{\rho_L} w$.

II- 6.2.2 Gas Porosity Measurement through Pycnometer (gas saturation)

This procedure consists of connecting a known volume under pressure (V_r) with the volume of the gas voids to be determined. Once the equilibrium is attained, law of perfect gases is applied to determine the volume of gas voids. In Figure II-16, V_r is the volume of the reservoir and V_G is the volume of gas voids in the waste sample in oedopermeameter which is to be determined. Within the oedopermeameter, the total voids volume is not only that in the waste sample but also the volume corresponding to the pores volume in the porous plates and of that volume which is present at the top and bottom of the porous plates, referred to as the volume of chambers (V_c). Figure II-16 demonstrates different stages of the measurement as follows:

Initial State: the two volumes V_r and V_G are connected to achieve a thermal equilibrium while maintaining the atmospheric pressure for the two volumes.

1st Stage: with the valve connecting the volume V_r and V_G at closed position, the reservoir volume V_r is put under a known pressure as $p_1 = P_1 - P_{atm}$ where p_1 is the relative pressure and P_1 is the absolute pressure.

2nd Stage: with the connecting valve between the two volumes at open position and all the exit points closed, the relative pressure at equilibrium is measured as $p_2 = P_2 - P_{atm}$.

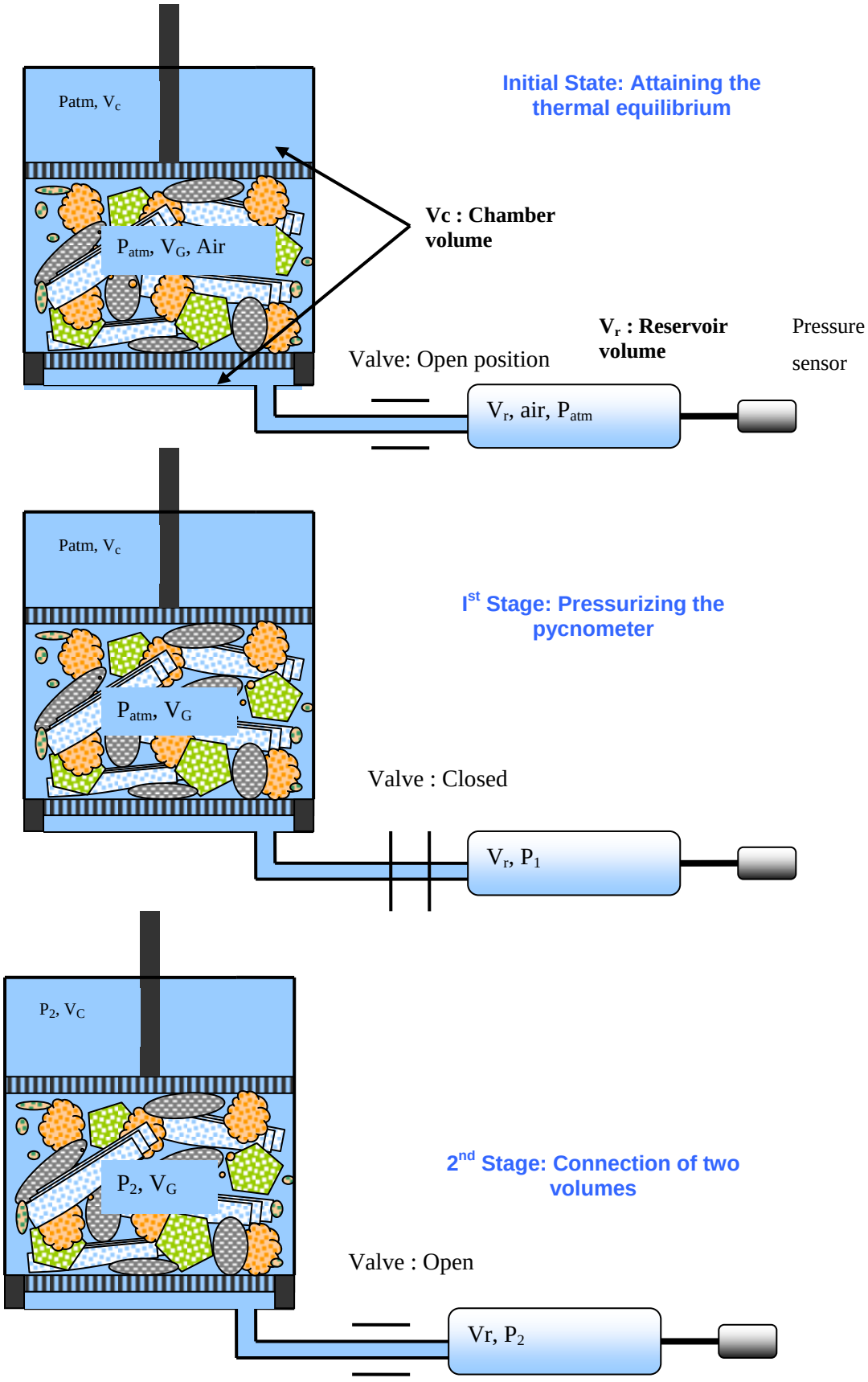

Figure II- 16: Steps for gas porosity measurement.

It is notable that the equilibrium pressure p_2 is not attained simultaneously but it is rather a stabilization process of pressure between the two volumes. When the valve is turned to open position, there is a decrease in pressure of the reservoir p_1 probably due to dynamic effects and then the pressure gradually increases until a stabilized value is achieved over a period of 30 seconds giving the desired equilibrium pressure p_2. The data acquisition is set at an interval of 1 second so as to have a number of values to determine an average for the equilibrium pressure.

From the Boyle-Mariotte equation $(P_{atm} + p_1) \times V_r = (P_{atm} + p_2) \times (V_r + V_G + V_c)$ which is written as $p_1 \times V_r = p_2 \times (V_r + V_G + V_c)$ with respect to relative pressures.

The volume of gas voids is determined as $V_G = \frac{p_1 V_r}{p_2} - (V_r + V_c)$. The gas used for the determination of porosity is Nitrogen N_2. The reservoir volume V_r is influenced by p_1 and V_G. With a high ratio of $\frac{V_r}{V_G + V_c}$ a small pressure variation is observed but in the inverse case of small ratio of $\frac{V_r}{V_G + V_c}$ the equilibrium is attained at a pressure close to the atmospheric pressure. As the pressure sensor has a limit of 6 kPa, the volume of the reservoir is selected close to 5600 cm^3 which gives a value around 0.6 for $\frac{V_r}{V_G + V_c}$ ratio.

Through the pycnometer method, the porosity of the gas $\theta_G = \frac{V_G}{V_T}$ is measured and knowing the volumetric moisture content θ_L, the total porosity $n = \theta_L + \theta_G$ can be calculated. The precision of the gas porosity measurement was verified through the measurement of settlement of the sample at various compression loadings. With only the known initial volume of voids further change in volume due to settlement and resulting change in total porosity corresponding to that compression loading was determined and compared against the measured porosity values. This comparison is discussed in section III-7.

II- 6.2.3 Total Porosity Measurement

Total porosity is the total voids present in the waste sample as well as the voids present within the elements on a microscopic scale. This measurement is performed through the saturation of the sample with known initial moisture content. However due to the presence/formation of bubbles it may lead to an underestimation of the total porosity which may not be negligible. Contrary to this traditional method of total porosity measurement, a new protocol of porosity measurement through pycnometer with gas saturation as defined by Stoltz (2009) was applied. The method of measurement of total porosity through pycnometer can be performed with gas or water and the results are comparable for

these two methods but they give higher values of porosity when compared with the values obtained through traditional measurement method. These procedures of measurement are still not cited in literature.

Importance of porosity measurement in hydro-bio-mechanical analyses of MSW: The measurement of the total porosity makes part of the overall determination of the solids density. It makes possible the determination of many other physical parameters as well as helping in providing a base for the application of laws of fluids flow.

II- 6.2.4 Conclusions on Total Porosity Measurement

Measurement of the total porosity is of interest because;

- This parameter is indispensible for the determination of constitutive solids density ρ_S as well as other parameters of the state.

$$\rho_S = \left(\frac{\rho_d}{1 - n} \right)$$

- If the model of double porosity is considered applicable for the domestic waste (fine matrices for micro porosity and preferential paths/macro pores), then the total porosity is the sum of these two porosities and determination of one of them along with the total porosity would lead to the determination of the other.

It is mentioned in the thesis report of Stoltz (2009) that the determination of total porosity through water saturation is better than the method of total porosity determination through gas. However there is only a difference of 1% between the values determined through these two methods with those determined through gas on the inferior side. Moreover it is worth mentioning that if the measurement of porosity is carried out in a waste column which is 'saturated' with leachate, then the presence of gas bubbles within the waste column would render the liquid porosity values to be smaller than it actually is.

II - 6.3 Gas Permeability Measurement

There are two possible methods of measurement of gas permeability in the oedopermeameter cell. One of the methods is the 'Permanent flow method' and the other is 'transitory flow method' or method of differential pressure (Figure II-17). The gas used for the measurement is Nitrogen N_2. Though the experiments performed can be termed as short term experiments without the phenomenon of biodegradation but air was not used as fluid due to following reasons; Presence of the humidity within the compressed air can modify the value of dynamic viscosity. Nitrogen is used as a fluid when it comes to the experimentation of waste materials on long term basis, therefore, the experiments of

short term duration performed with Nitrogen make it possible to compare these both types of experiments. The density of Nitrogen N_2 is ρ_{N2} = 1.25 kg/m^3 and the dynamic viscosity of N_2 is η = 16x 10^{-6} Pa.S (Weast, 1981) at normal temperature (273 K) and pressure (101.32 kPa).

II- 6.3.1 Permanent Flow Method

Darcy's law which is generally applied for liquids is modified to be used for the measurement of permeability with gas. Due to the change in density of the gas with the change in pressure, the law of conservation of mass can not be applied but as the mass flow rate (q_m) remains constant the relationship is modified to obtain the following equation;

$$\frac{q_v}{A} = -\frac{k_G}{\eta_{N2}} \frac{1}{2L} \frac{P_s^2 - P_e^2}{P_e}$$

q_V is volumetric flow rate

A is sample cross-section

L is the length of the sample

P_e is pressure at entrance

P_S is pressure at exit

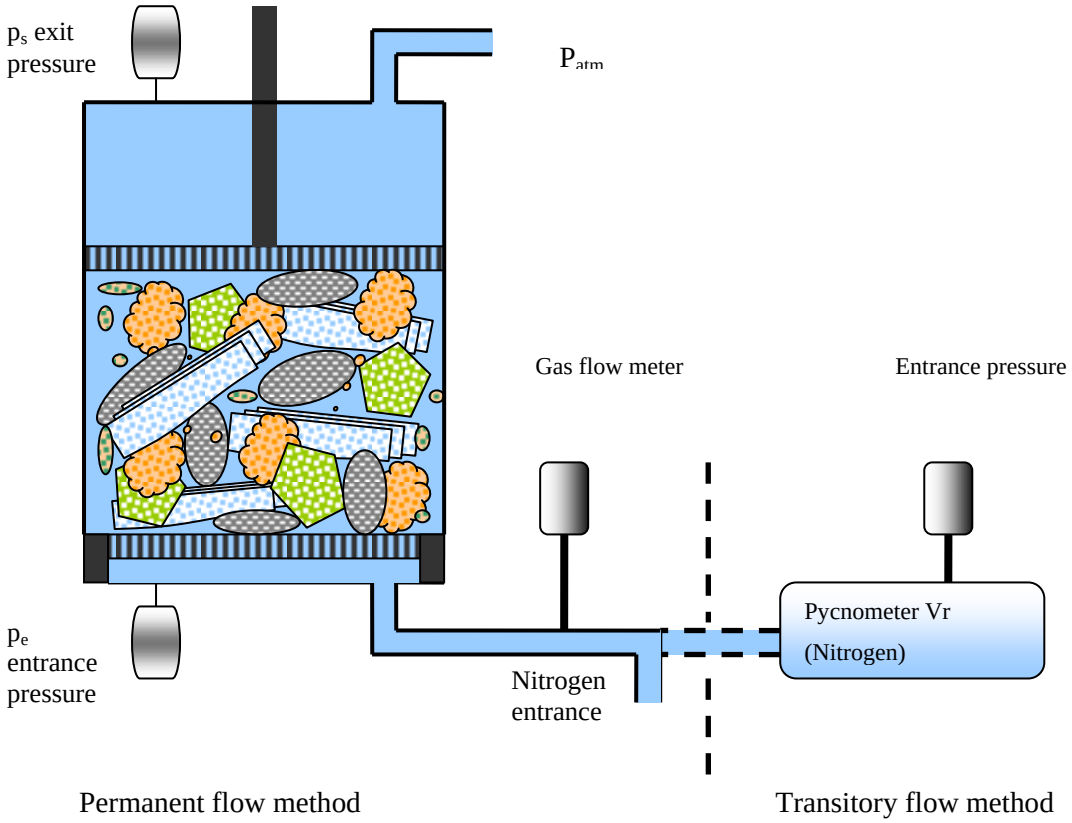

Figure II- 17: Apparatus arrangement for gas permeability measurement for permanent and transitory flow methods.

The pressures used in the equation are absolute pressures with the flow direction taken from entrance to exit. Considering the difference of pressure at entrance and exit as very small (inferior to 1 kPa) and the variation in densities at both ends to be negligible, the above equation reduces to

$$\frac{q_v}{A} = -\frac{k_G}{\eta_{N2}} \frac{p_s - p_e}{L}.$$

The pressures p_s and p_e are the relative pressures with reference to the atmospheric pressure. Stabilization of pressure is attained before the measurement of these pressures at entrance and exit and a series of measurement is carried out for different flow rates and differential pressures keeping in view the limit of pressure sensor to be 5 l/min. Moreover an entrance pressure higher than 4 kPa may cause the expulsion of leachate from the sample, thus it is maintained around 2 kPa for all the measurements.

II- 6.3.2 Transitory Flow Method

The limitation of entrance pressure of 2 kPa makes it impossible to measure the permeability of any sample which is highly compressed and has high moisture content with the help of constant flow regime. Therefore these measurements are performed with another technique of variable flow regime termed as 'transitory flow method'. It applies the same principle and system of measurement as that of total porosity with the reservoir. In this method nitrogen is left to flow and fill the reservoir and the sample in a manner that the pressure in reservoir is within the range of 2 kPa. The nitrogen feed is then cut (t = 0) and the decrease in pressure is measured as a function of time [p_1 (t)]. Assuming that the density of nitrogen to be independent of the pressure, the Darcy's law is applied taking into account the time and pressure relation as follows;

$$\ln\left(\frac{P_1(t) - P_s}{P_1(t_0) - P_s}\right) = -\frac{k_G}{\eta_{N2}} \frac{A}{V_r L} p_{atm} (t - t_0)$$

V_r is volume of the reservoir

L is the length of the waste sample

A is cross-section of the sample

P_S is the absolute pressure at exit (equals the partial pressure of N_2 in air ~ 80 kPa)

and P_1 (t) is the absolute pressure of N_2 in the reservoir.

During the measurement of gas permeability through constant flow regime, pressures are measured at the entrance and exit points of the cell and any pressure drop due to porous plates is considered to be negligible. Likewise for variable pressure method, any pressure losses between the reservoir and the sample due to connecting tubes are not considered due to the fact that the flow rates during these measurements are very small.

II - 6.4 Permeability Measurement with Water at Saturated Condition

In literature the method applied most frequently for the permeability measurement is through water at saturated condition. But this method of measurement is complicated as the complete saturation of the sample is necessary, but any such protocol is not cited in the literature. Stoltz (2009) used the following protocol as standard for the measurement of permeability with water at saturated condition;

- Initially the sample is washed with CO_2 with a volume which is six to seven times the volume of the sample to remove any gases and air bubbles.
- Then the sample is saturated with water having an upstream pressure head (< 1 cm above the upstream surface of the sample).
- A series of compression stresses is applied with measurements of water permeability carried out at each stage of compression stress.

Since the measurements were completed within 12 hrs, the biodegradation effects were neglected. The temperature of water was measured at the upstream and downstream points of the sample to apply any corrections for the dynamic viscosity if needed.

II- 6.4.1 At Constant Head

For this method of measurement two water tanks at constant height are added to the conventional apparatus of the oedopermeameter (Figure II-18). The flow rate is measured with the help of a weighing balance connected with the digital acquisition. The difference of water level ΔH_L corresponds to the difference in pressure head which is measured through the piezometer at the upstream and downstream level. In the above arrangement ΔH_L was equal to 80 cm. The hydraulic permeability is measured through Darcy's law

$$\frac{q}{A} = k_L \frac{\rho_L . g}{\eta_L} \frac{\Delta H_L}{L}$$

k_L is the liquid permeability, A is the cross-section of the sample and L is the sample length

The temperature of water at the upstream and downstream is noted for any leachate viscosity corrections. Even though leachate and water have definitely different chemical characteristics and the probably do not have the same viscosity. But due to unavailability of leachate viscosity values in literature, the viscosity of the leachate was taken equal to that of water.

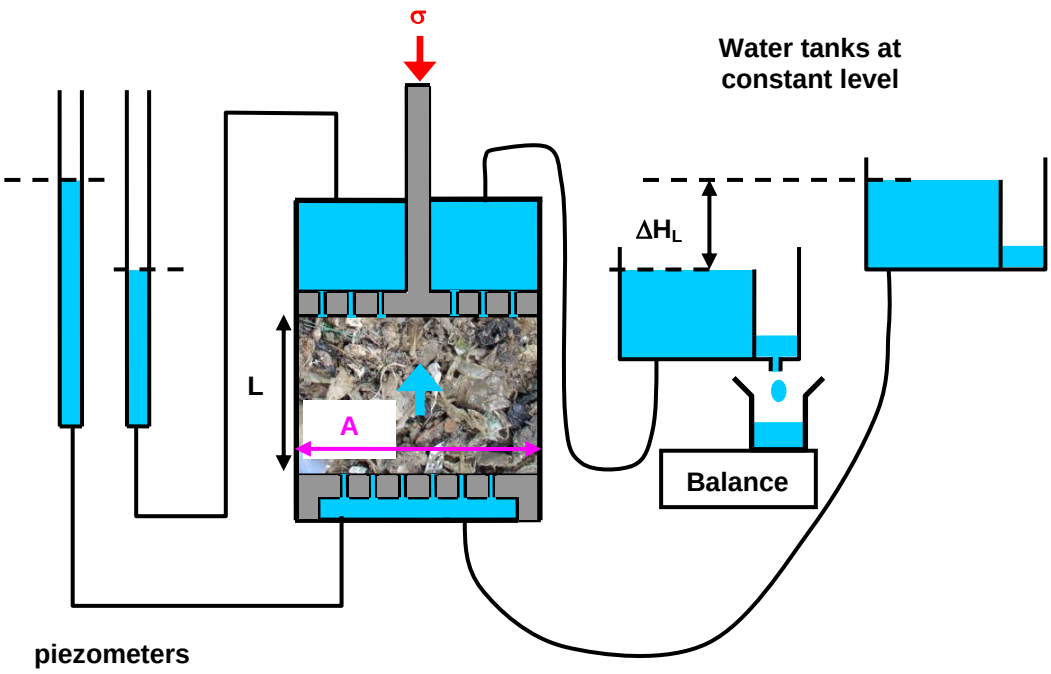

Figure II- 18: Measurement of permeability with water at constant pressure (Stoltz, 2009).

II- 6.4.2 At Variable Head with Back Pressure

For a sample initially saturated with water, hydraulic permeability at variable head with backpressure was measured according to the protocol shown in Figure II-19. The hydraulic permeability is determined through Darcy's law at variable head as follows

$$\ln\left[\frac{\Delta H_L(t)}{\Delta H_L(t_0)}\right] = -k_L \frac{\rho_L g}{\eta_L}\frac{A}{a.L}(t - t_0)$$

A is the sample cross-section

a is the cross section of the tube

L is the length of the sample

For apparatus arrangement for this case $\Delta H_L(t = 0)$ is equal to 50 cm. A back pressure of 50 kPa was decided to be sufficient for the dissolution of air bubbles, after a number of back pressures were tried. This minimum back pressure was fixed because of the certainty of maintaining saturated state of the sample.

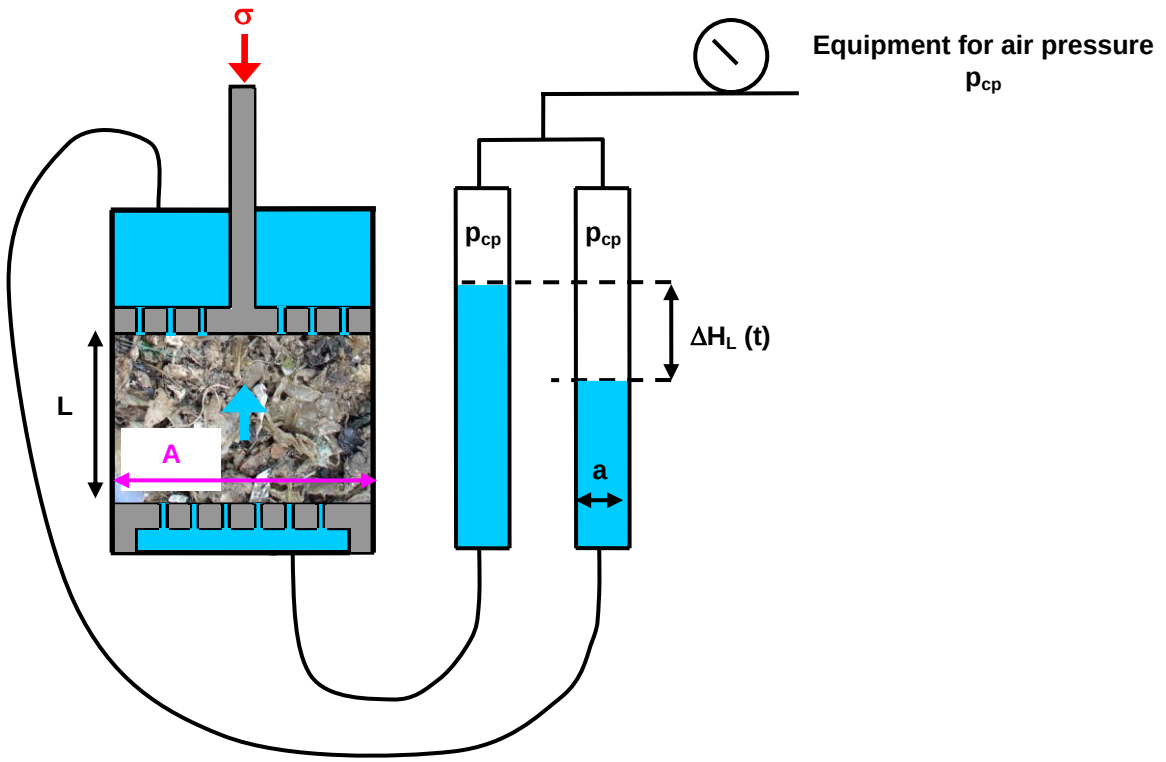

Figure II- 19: Permeability measurement with water at back pressure (Stoltz, 2009).

II- 6.4.3 Head Losses within the Apparatus

For the hydraulic permeability measurement at constant head, the piezometer measurements are taken at the upstream and downstream level of the sample so any corrections for head losses are considered as negligible. However for the measurements performed for variable head method, the calculation for head losses is complicated. The head losses within the tubular system at voids was determined and it was noted that if the intrinsic permeability of the waste sample is greater than $2x10^{-11}$ m^2. Then for a given fluid circulation speed the head losses due to tubular system is higher than that produced by the waste sample. Thus for any waste sample with an intrinsic permeability smaller than $2x10^{-12}$ m^2, the measurements of hydraulic permeability with back pressure can be carried out with the head losses deducted from the total values.

III- GAS - PERMEABILITY TESTS IN OEDOPERMEAMETER

III-1 LABORATORY SCALE PERMEABILITY ANALYSES

All the tests discussed in this Chapter are short-term tests i.e. the experiments of compression-permeability were never prolonged over more than one week. The phenomenon of biological degradation of waste was not considered for the measurement analyses. Regarding the tests, several wastes were tested. First waste (Waste 'B') was used within the framework of verification of the model of double porosity proposed by Stoltz (2009). Within this waste type, called B, some samples belonging to CICLADE (test bioreactor cells at LTHE) were also analysed for the effects of re-circulation of leachate on hydrological parameters. These tests made it possible to validate the double porosity model, the results corresponding to the waste 'B', are discussed in Chapter IV. Another campaign, followed these preliminary tests, on the waste of tests cells (waste 'C') built under the supervision of Véolia Environment, to analyse various landfilling techniques; such as Bioreactor or MBP waste cells.

Figure III- 1: Apparatus arrangement for gas permeability measurement.

III - 1.1 Tests Program for a Fresh Waste

The tests of total porosity and permeability were carried out on the waste samples extracted from a French landfill site operated by Véolia Environment. This waste was initially shredded at site before its placement in the waste cells to a size of 40 mm. The composition according to MODECOM criterion of waste characterization is shown in Figure III-2. For the purpose of experimentation the waste was divided into following categories;

- Waste samples retrieved from the big waste containers brought to the laboratory from the landfill one and a half year ago. These containers are closed cover bins with two small holes at their side for the ease of biogas escape from the bin.
- Waste samples taken out from the lab scale 'Bioreactor Cells CICLADE' where they were put during Sept 2007 for the purpose of the study of settlement behaviour with leachate recirculation with a recirculation rate of 17 lit/day for a period of 500 days.

The comparison of BMP values of both these types of samples suggest that the samples which belong to the bioreactor cell CICLADE are the waste samples in the phase IV of biodegradation and are highly methanogenised samples.

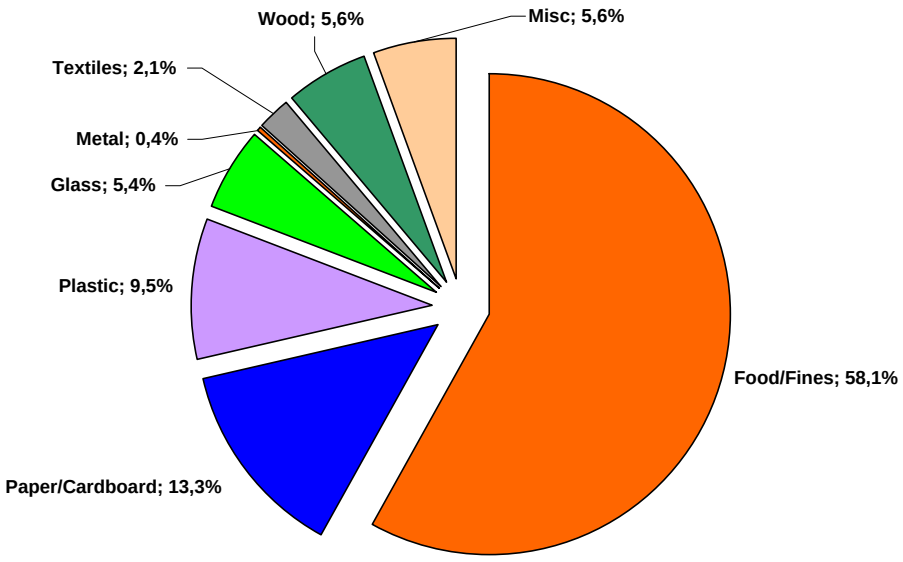

Figure III- 2: Composition of waste samples used for compression-permeability tests (waste 'B').

The series of experiments carried out on these waste samples can be classified as under:

- Series of compression-gas permeability tests at various initial moisture content
- Series of tests for compression-total porosity analysis

Table III- 1: Composition of Waste Samples (B1-B9).

Waste constituent	% wet mass	% dry mass
Paper/cardboard	13.3	17.0
Plastics	9.5	13.2
Metal	0.4	0.7
Glass	5.4	9.8
Textiles	2.1	2.7
Wood	5.6	8.2
Food/Fines	58.1	39.0
Miscellaneous	5.6	9.4

III - 1.2 Sample Preparation

To achieve the objective of different initial moisture content for every series of compression-permeability test, the samples were prepared according to the following procedure

- To obtain low initial moisture content, samples (B6, B7) were dried at 35°C during 7 days in the oven.
- To obtain medium moisture content range, samples (B4, B5) were air dried for 7 days in rectangular containers with large surface areas.
- To obtain moisture content higher than the natural moisture content of the samples at storage, water was added with the help of sprinkler while overturning the samples with hands a number of times and left for imbibitions for 48 hours. The samples were then taken out from the container pressing with hands to remove any access water before filling the oedopermeameter cell.

The waste ‘B’ being the shredded waste, simplified the process of sample preparation regarding the separation of bigger particles however some plastic or metallic components were removed now and then. The samples were placed in the oedopermeameter with hands in layers of 2 to 2.5 kg with compaction effort applied to each layer (4 to 6 layers) with the help of compaction rod of mass 8 kg and a free fall of 70 cm which produces a compaction effort of 5.5 kN. 30 blows were applied over all the cross-section of the sample as an average compaction effort for each layer. All the tests were carried out as series of one experiment with the same sequence of compression loading for all the series of compression-permeability tests which is as follows; 20 kPa, 40 kPa, 80 kPa, 140 kPa and 200 kPa. All of these compression loads were maintained during a period of time ranging from 24 hours to 96 hours.

Table III- 2: Waste samples of compression-permeability tests.

Test No	Notation	Initial Gravimetric Moisture Content 'w' ($\%_{MS}$)	Observations
1	B1	80	Natural moisture content, air dried during 7 days
2	B2	94	Natural moisture content, air dried during 7 days
3	B3	116	Natural moisture content (Field capacity)
4	B4	55	B3 oven dried at 35°C during 7 days
5	B5	6	B4, oven dried at 35°C during 7 days
6	B6	50	Initially at natural moisture content, oven dried at 35°C during 7 days
7	B7	275 to144	Water injection for 48 hrs, excess water drained before compression
8	B8	66	Waste sample retrieved from bioreactor cell at natural moisture content
9	B9	24	Oven dried at 45°C during 7 days

For each compression loading following measurements were obtained:

- Settlement measurement from the vertical displacement sensor
- Gas permeability measurement
- Leachate collection and determination of its mass

Other measurements performed during various stages of the test are as follows;

- Initial mass (M_{T0}) and initial volume (V_{T0}) to obtain initial bulk density of the samples.
- Dry mass (M_S) obtained at the end of each series through drying the whole sample in the oven at 80°C until the stabilization of the mass to calculate the initial dry density of the sample and the initial gravimetric moisture content.
- Before starting the compression loading sequence one measurement of the gas porosity (θ_G) is carried out through pycnometer in order to calculate the total porosity of the sample.
- For next compression loads during the experiment, the rest of the parameters are calculated making use of the settlement measurement (ΔH) and any leachate collected (M_{LC}).

Remark: Initial bulk density is not fixed to any desired value but the oedopermeameter cell was filled in a manner to achieve the maximum height of the cell i.e. ~29 cm.

1st Stage: V_r put under pressure p_1 with connecting valve at closed position

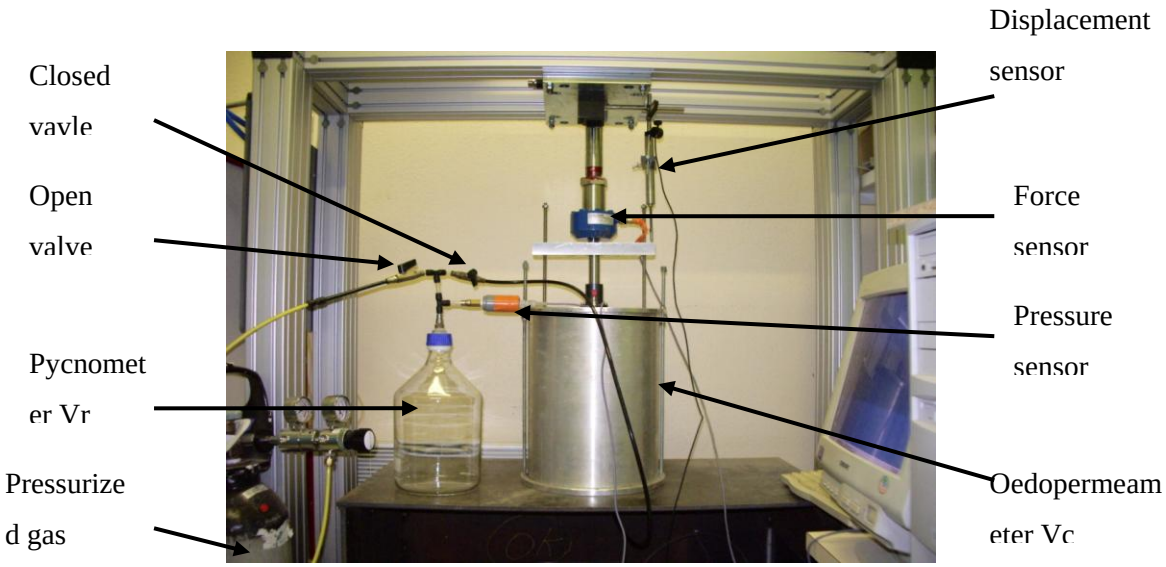

2nd Stage: Measurement of relative equilibrium pressure p_2 with connecting valve at open position

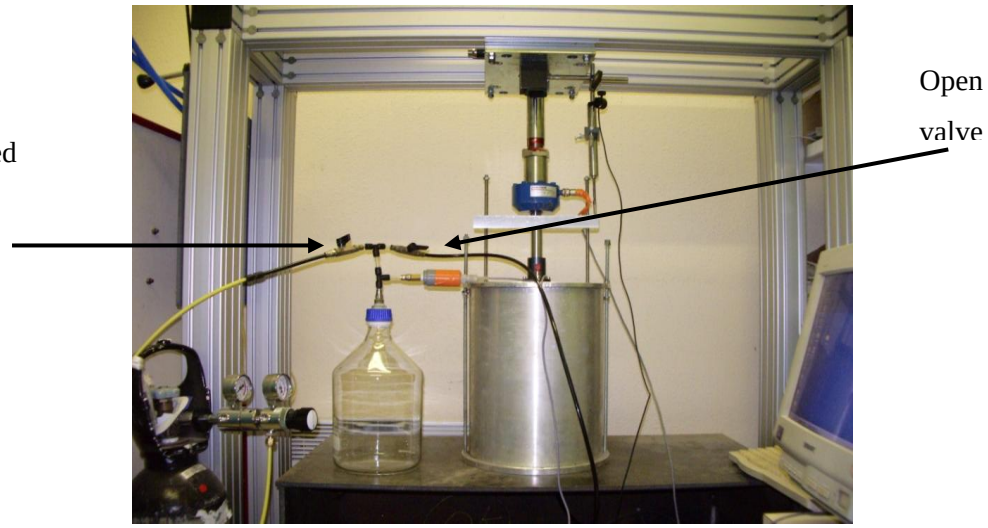

Figure III- 3: Two stages for the determination of gas porosity (θ_G) with the help of oedopermeameter and pycnometer.

III - 1.3 Analysis of Compressibility

All the waste samples are supposed to be collected from different locations and due to heterogeneous nature of municipal solid waste; they are all different in density. In Graph III-1 the dry density of all

the samples of waste B at 20 kPa compression stress are plotted against their initial moisture content and it can be observed that for the moisture content increasing up to 66% there is a direct effect on the dry density of the sample however, after that limit any further increase in moisture content does not increase the dry density of the sample.

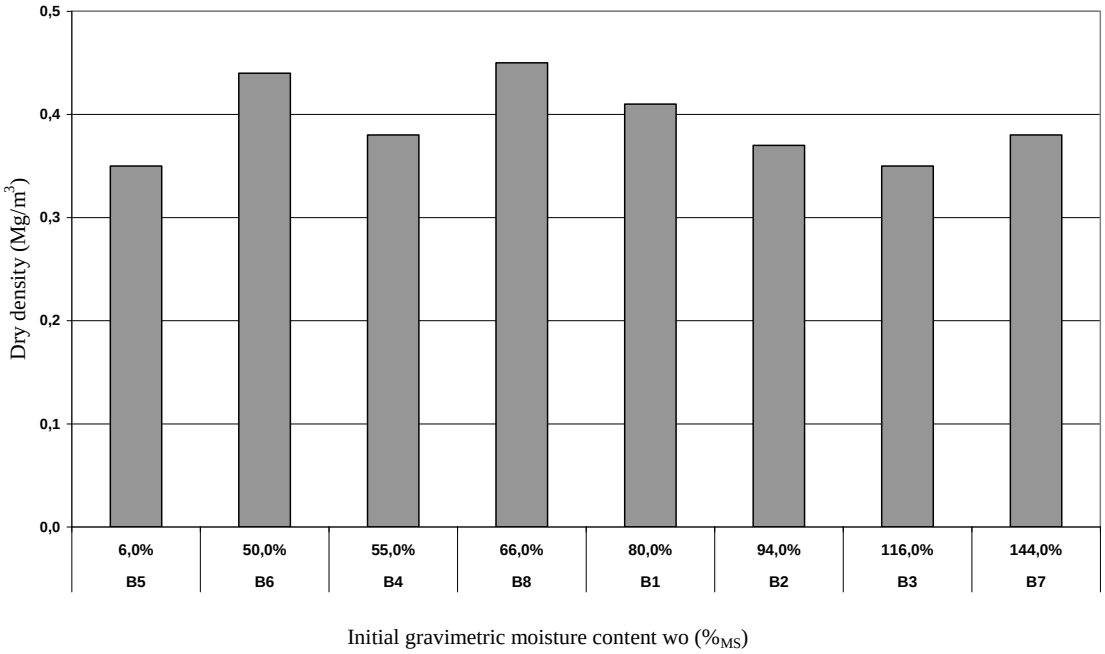

Graph III- 1: Dry density of various samples at 20 kPa compression stress as a function of respective initial gravimetric moisture content for the waste 'B'.

The same relation is studied in Graph III-2, but this time the dry density is plotted against the compression stress of 20 kPa with its increase due to the compression stages for the compression stress of 200 kPa in order to observe any contrary observations as made in Graph III-1. The compression stress of 200 kPa is the maximum compression limit maintained during all the compression-permeability tests carried out and it is worth noting that the same trend exists for the compression stress of 200 kPa.

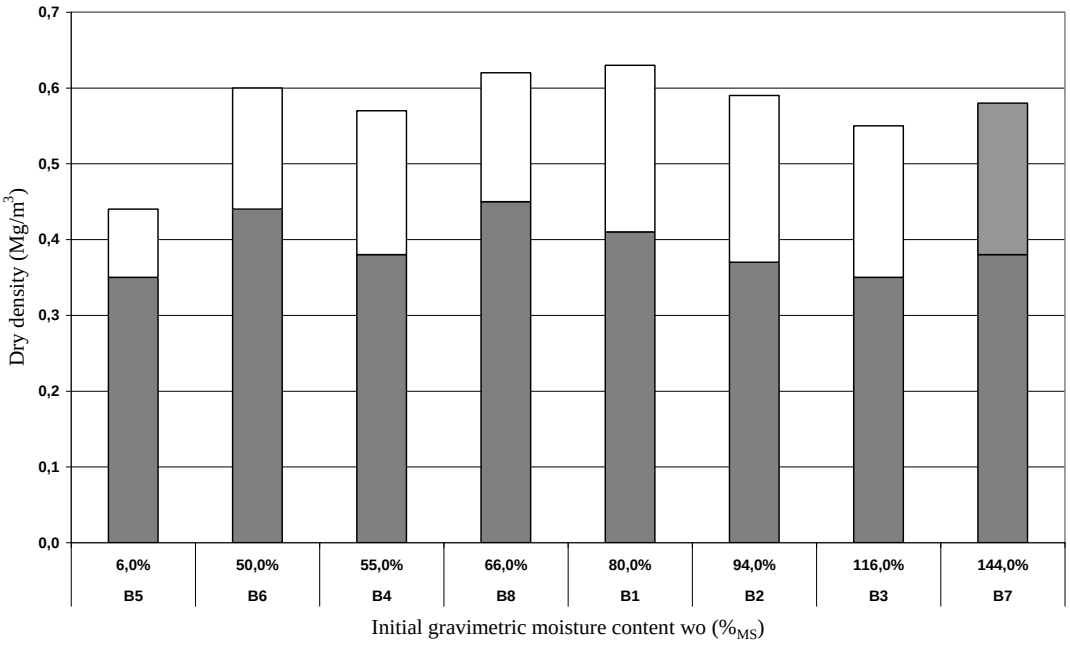

Graph III- 2: Dry density at 20 kPa and 200 kPa as a function of initial moisture content for the compression-gas permeability experiments carried out for the Waste 'B'.

There is some similarity with the proctor tests that: if the proctor test is carried out for the MSW samples as it is done for the soils, it may be interesting to develop any correlation. But in that case the same sample is compacted at various moisture contents whereas in the present study each sample was different and thus can only compared on the basis of its initial moisture content and respective dry density at the same compaction effort.

In Graph III-2 the effect of initial moisture content on the dry density of the sample is similar to that in Graph III-1 and it can be noticed that up to the range of 66% and 80% of the initial moisture content the sample becomes more and more dense after which there is no direct effect on the dry density of the sample for example for the sample with moisture content 116% the dry density is smaller than the sample with the moisture content of 144%. From this analysis it can be suggested that the optimum moisture content for MSW as in the case of soils helps attain better compaction of the sample.

Moreover it can be noticed that the dry density of the sample with least moisture content is smaller than other samples with higher moisture content which is in accordance with the proposition of presence of optimum moisture content-dry density relation but to define any moisture content to be the optimum moisture content is still not possible with these experiments and a detailed study of any such relation might be interesting with a goal to propose such a relation if exists.

Determination of Coefficient of Primary Compression: A pre-consolidation stress is needed to analyze the sample compressibility with reference to the primary compression coefficient C^*_R. This pre-consolidation stress corresponds to the compaction effort applied during the placement of the waste at site. As for the soils it is well known that the soils initially consolidated do not go under further consolidation until the compression stress greater than initial consolidation stress is applied, the same law is assumed to stand true for the case of MSW. To determine this consolidation stress for this study, all the pre-consolidation stresses were calculated for each compression-gas permeability test from the graphs plotted for settlement ($\Delta H/H$) as a function of log (σ). On the graph the slope of the line gives the value of C^*_R. The line extended back to x coordinate at 'x=0' gives the value of σ'_c (Figure III-4). From this graph horizontal bisector tangents is taken as the pre-consolidation pressure (σ'_C). The equation used for the calculation of C^*_R is $\frac{\Delta H^P}{H_0} = C^*_R \log \frac{\sigma}{\sigma'_C}$ where H_0 is the height of the sample for the pre-consolidation pressure.

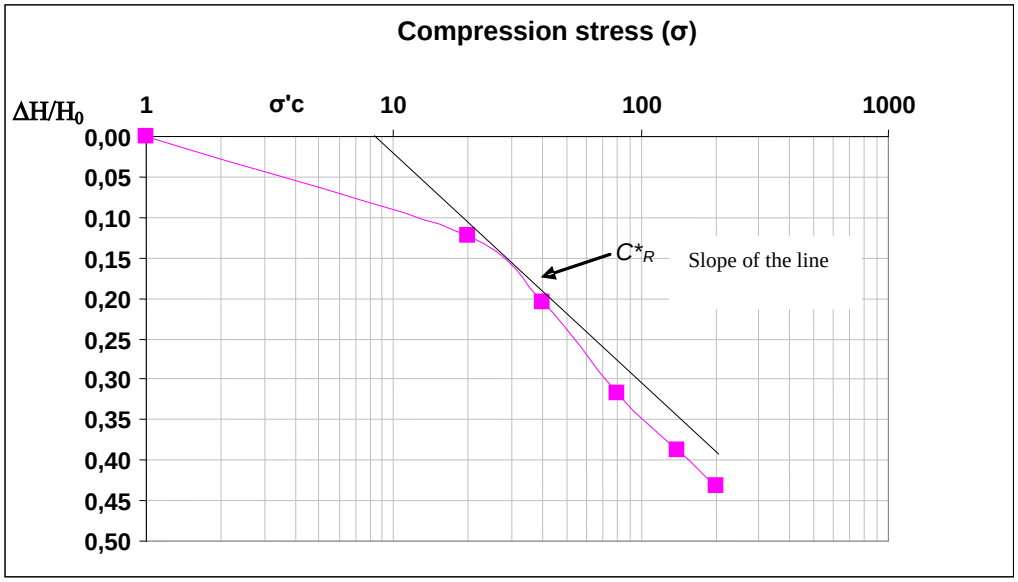

Figure III- 4: Determination of pre-consolidation stress.

ΔH^P is the primary settlement for each compression loading σ' and measured at the end of each loading stage ranging from 24 hrs to 72 hrs. Graph III-3 represents the calculation of the pre-consolidation compression stress for all the samples while in Graph III-4 the calculated C^*_R for all the samples of MSW 'B' is presented. The intersection of the line on the x-axis (x_0) is used to calculate the corresponding pre-consolidation stress for the respective experiment. An average value of C^*_R = 0.31 is calculated from the given data. The pre-consolidation (σ'_c) stress is further used to plot the graph for the analysis of effect of initial moisture content on the pre-consolidation stress (Graph III-7).

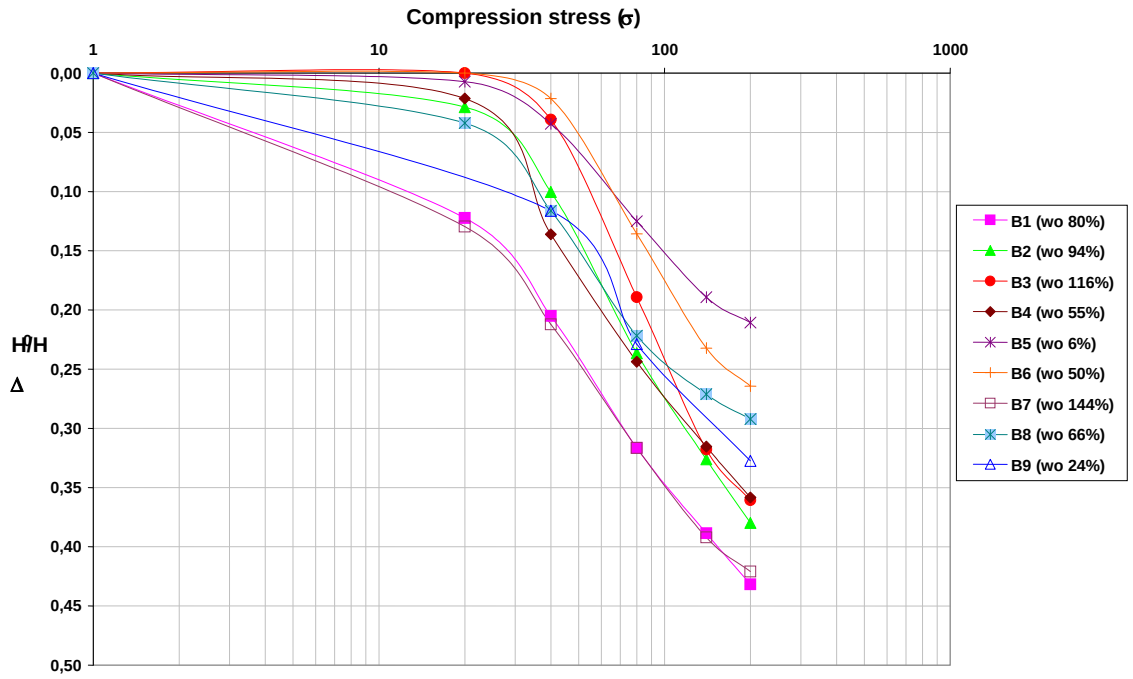

Graph III- 3: Determination of pre-consolidation compression stress for all the samples of waste 'B'.

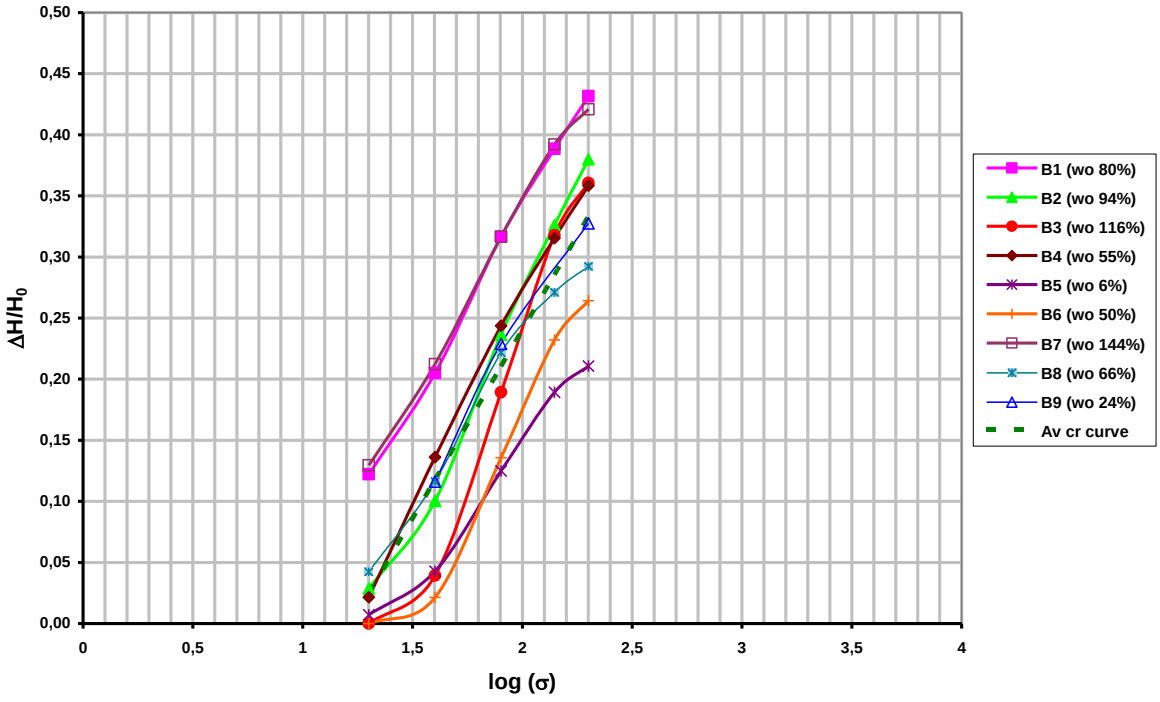

Graph III- 4: Determination of coefficient of primary compression.

With an objective of defining a relation between various physical parameters of the state of MSW and C^*_R, different relationships are studied in each of the graphs below;

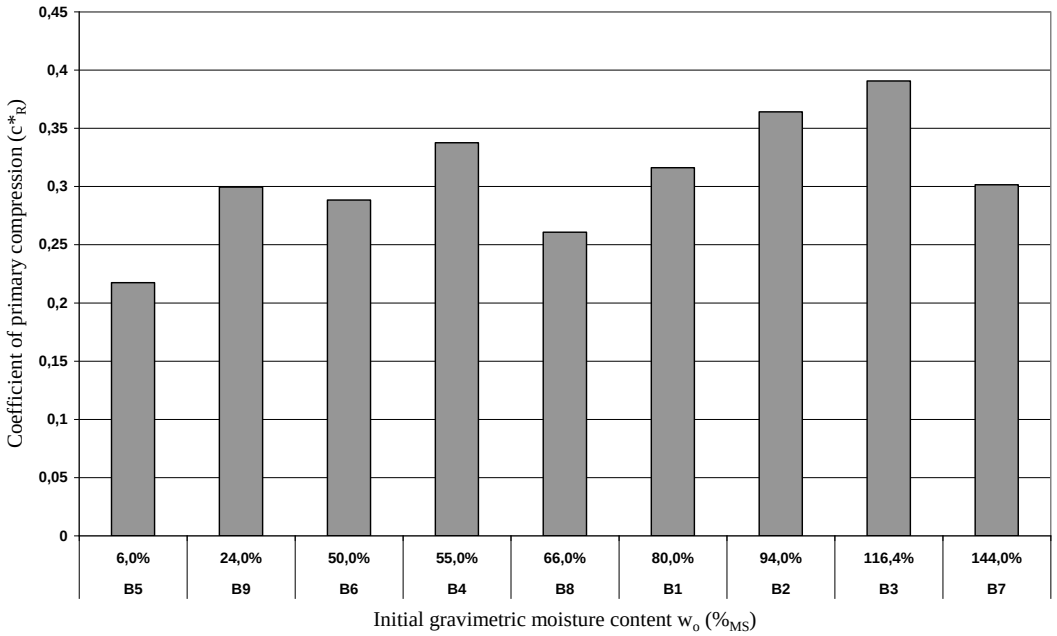

Graph III- 5: Coefficient of primary compression C^*_R as a function of initial gravimetric moisture content for the compression-gas permeability experiments carried out in the oedopermeameter (waste 'B').

In Graph III-5 the calculated value of C^*_R for each sample is plotted against the initial moisture content of the sample, however any direct relation between the two parameters is not quite visible.

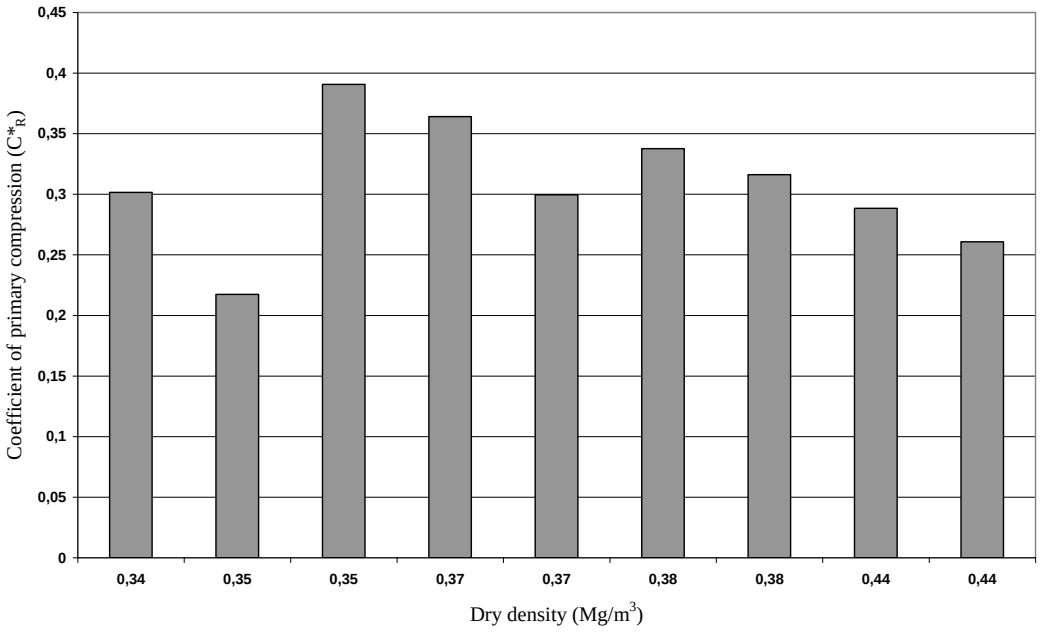

Graph III- 6: Coefficient of primary compression C^*_R as a function of initial dry density at the pre-consolidation compression stress of respective waste sample for the compression-gas permeability tests carried out in oedopermeameter cell (Waste 'B').

The correlation of coefficient of primary compression and initial moisture content is affected also by the initial dry density, therefore, in Graph III-6 C^*_R is plotted against ρ_d at the pre-consolidation stress (σ_c) in order to define any distinguishable relation. It may be said that for a range of initial moisture content between 6% and 66% higher compaction of the sample is achieved and that a sample which is most dense at pre-consolidation stress is the sample which is least compressible. However due to the limited number of experiments and complex nature of municipal solid waste, it is quite difficult to reach any conclusion regarding the definition of a correlation between coefficient of primary compression C^*_R and the initial dry density ρ_d. As a matter of fact ρ_d not only depends on the porosity but also on the value of solids density ρ_S which could be different for all the samples.

Finally in order to analyze the correlation of density under the calculated pre-consolidation stress (σ'_c) and the initial moisture content Graph III-7 is presented. It is interesting to note here that the effect of initial moisture content on the dry density at pre-consolidation stress is more prominent than the relation already observed in Graph III-1 where a correlation between the initial moisture content and the initial dry density at 20 kPa compression stress was analyzed. It can be noted that there is a direct effect of the initial moisture content on the dry density of the sample for a given pre-consolidation pressure and that this initial moisture content is probably the equilibrium moisture content of the waste sample.

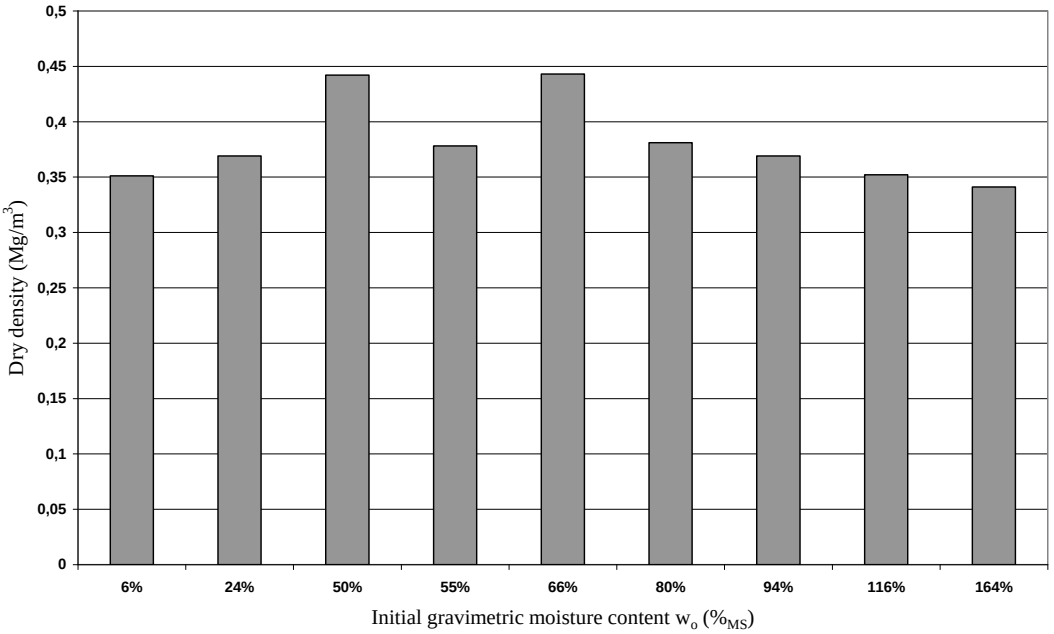

Graph III- 7: Dry density of all the samples (B1-B9) of the Waste 'B' at calculated pre-consolidation stress (σ'_c) as a function of their initial moisture content.

From the Graph III-7 it can be deduced that up to the range of 66% of the initial moisture content the dry density increases with the increase in the moisture content (with the exception of sample B4) after

which the presence of additional water has an inverse effect on the compression of the sample. This relation may also stand true for the model of double porosity with a distinct effect of two porosities (micro and macro porosity of the sample) and will be discussed later in chapter IV in detail.

III - 1.4 Determination of Constitutive Solid Density

III- 1.4.1 Average Solid Density

Different methods of calculation of constitutive density have been discussed in detail in chapter II. Within the framework of this study the solid density of a given sample of municipal solid waste with the known dry density was determined through the measurement of total porosity with pycnometer;

$$\rho_S = \left(\frac{\rho_d}{1 - n} \right)$$

Measurements of solid density were carried out for two samples of waste 'B'. One of the measurements was carried out for the waste sample retrieved from the waste container while the other was carried out for the waste sample taken from the bioreactor cell 'CICLADE'. It enabled the comparison of three different values of the same type of municipal solid waste with the third value of solid density being the one quoted by Stoltz (2009). The average value for the solid density for the waste sample of the bioreactor cell 'CICLADE' was measured to be 1.95 Mg/m^3 and the average value for the waste retrieved from the container was determined to be 1.81 Mg/m^3. Finally the value of solid density for the same waste tested one and a half year ago was quoted as 1.62 Mg/m^3.

The increase in the solid density over one and a half year is quite evident as the waste stored in the waste container has undergone degradation with the organic mass reducing into biogas and leachate; resulting in the disappearance of the organic components lighter than the mineral ones. The degradation leaves behind the materials which are less degradable like paper cardboard and inert like glass and metal. All these materials have higher constituent density as compared to the constitutive density of the waste thus increasing the amount of the latter. The same reason is applicable for the waste retrieved from the bioreactor, with the possible justification of more completed biodegradation related to the recirculation of the leachate for still higher solid density.

III- 1.4.2 Determination of Solid Density from the Waste Composition

For the calculation of solid density from the composition of the MSW, dry density of all constituent is summed to obtain the average solid density of the sample;

$\mu_i = \frac{m_{si}}{M_s}$ for each constituent and the average solid density is calculated using the following equation

$$\overline{\rho_s} = \frac{1}{\sum_i \frac{\mu_i}{\rho_{si}}}$$

Where m_{si} is the dry weight of the constituent 'i', M_s is the dry weight of the whole sample and $\rho_{si} = \frac{m_{si}}{V_{si}}$ corresponds to the dry density of the constituent 'i'.

Table III-3 gives details of the calculation of solid density for the waste 'B'. The parameters of ρ_{dSi} and ρ_{satSi} are taken from the Beaven and Powrie (1995) and Landva and Clark (1990). These values are not all calculated but estimated as well. In addition to that these values are calculated taking account of the open porosity 'n_{Si}' with a dry density 'ρ_{dSi}' however metal, plastics or glass are considered to have no open porosity. For the calculation of average density from the composition of the waste following hypotheses are made; Categories of combustibles, putrescibles and fines were considered to have the same values of densities by the authors and for the category of miscellaneous or inert materials, they used the dry density of 2.6 Mg/m^3. ρ_{Si} is calculated taking into account the following equation: $\rho_{Si} = \frac{\rho_{dSi}}{1 - n_{Si}}$ whereas n_{Si} is calculated from the equation $n_i = \frac{\rho_{satSi} - \rho_{dSi}}{\rho_L}$.

Table III- 3: Various constituents' parameters for the determination of ρ_{Si} (waste 'B').

Waste constituent	μ_{Si} (%$_{MS}$)	ρ_{dSi} (Mg/m^3)	ρ_{satSi} (Mg/m^3)	n_{Si} (%)	ρ_{Si} (Mg/m^3)
Paper/cardboard	17.0	0.4	1.2	80	2.0
Plastics	13.2	1.0	1.0	0	1.0
Metal	0.7	6.0	6.0	0	6.0
Glass	9.8	2.9	2.9	0	2.9
Textiles	2.7	0.3	0.6	30	0.43
Wood	8.2	1.0	1.2	20	1.25
Food/Fines	39.0	1.0	1.2	20	1.25
Miscellaneous	9.4	2.6	2.6	0	2.6

The value of average solid density calculated from the waste composition results in 1.372 Mg/m^3. The value obtained from the pycnometer was 1.81 Mg/m^3. The following observations are made:

- The values given by Beaven et al. (1995) and Landva et al. (1990) are in reference with the 30% of textile porosity and 20% wood and putrescibles, only if a higher porosity value was

considered for these components it would have resulted in higher value of constitutive solid density.

- Kazimoglu et al. (2005) have determined a value of solid density ρ_S = 1.33 Mg/m^3 while making use of the data provided by Landva et al. (1990). This method is only appreciable if the precise composition of the waste sample is known.

At this time of research some detailed analysis of solid density is needed for better understanding of the subject.

III - 1.5 Analysis of Equilibrium Moisture Content

Leachate Drainage under Compression

Since the waste 'B' used for the compression-gas permeability experiments had high initial moisture content so whenever at a compression stage some leachate was drained, it was collected and weighed. This reduction in moisture content when plotted as a function of dry density is expressed as moisture content of equilibrium. The drainage results in the decrease in moisture content as a function of compression stress and increase in the dry density of the sample (Graph III-8).

The samples which were less humid, did not drain any leachate, even for the higher stages of compression stress, whereas, the samples with less initial moisture content (lower than the equilibrium moisture content) drained the leachate for the stages of compression approaching the limits i.e. 140 kPa or 200 kPa. In Graph III-8 only sample B7 with an initial moisture content of 166% drained leachate right from the beginning of the sample compaction during its placement in the oedopermeameter. This leachate content was deduced from the calculated initial gravimetric moisture content (144%). It is worth mentioning that this is the same sample which was initially sprinkled with water to attain high initial moisture content. As marked on Graph III-8 this sample was left to drain for 48 hrs before the start of compression-gas permeability test which brought down the moisture content to 144%. Sample B3 drained leachate for the compression stress stages of 140 kPa and 200 kPa which has initial moisture content of 116%. Other samples, though, having initial moisture content approximately 94% and 80% did not drain any leachate at any stage of compression which emphasizes that the equilibrium moisture content of the waste 'B' might be higher than the normal expected range, around 100% of the dry mass (*Ms*).

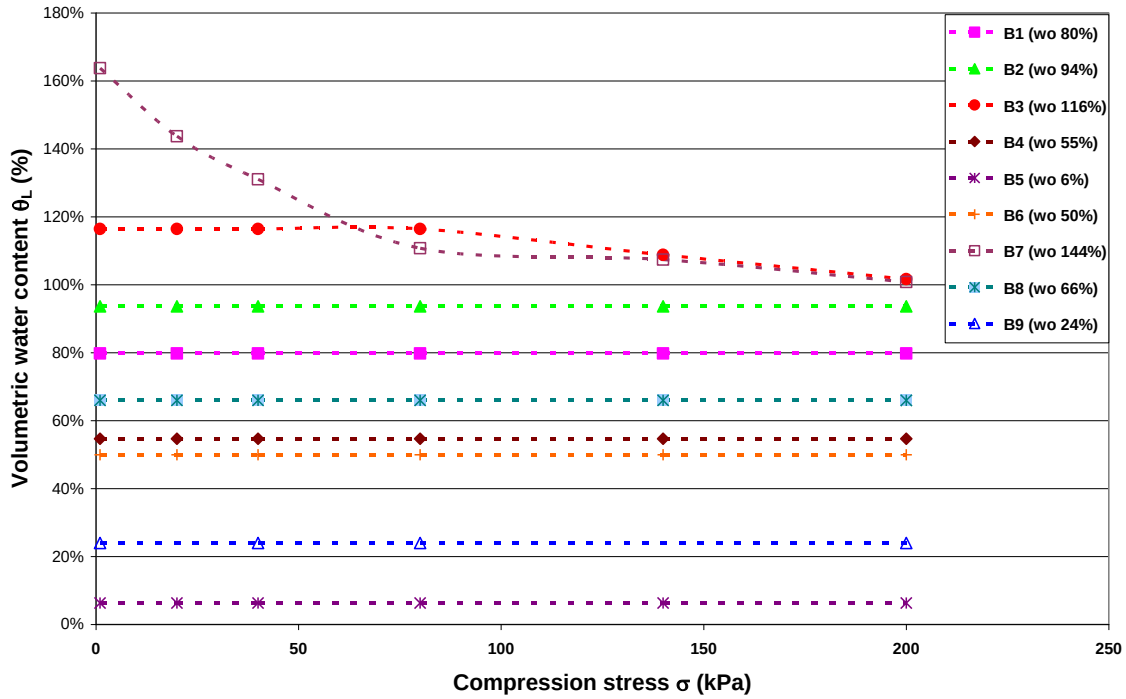

Graph III- 8: Change in the gravimetric moisture content of the waste samples as a function of applied compression stresses (Waste 'B').

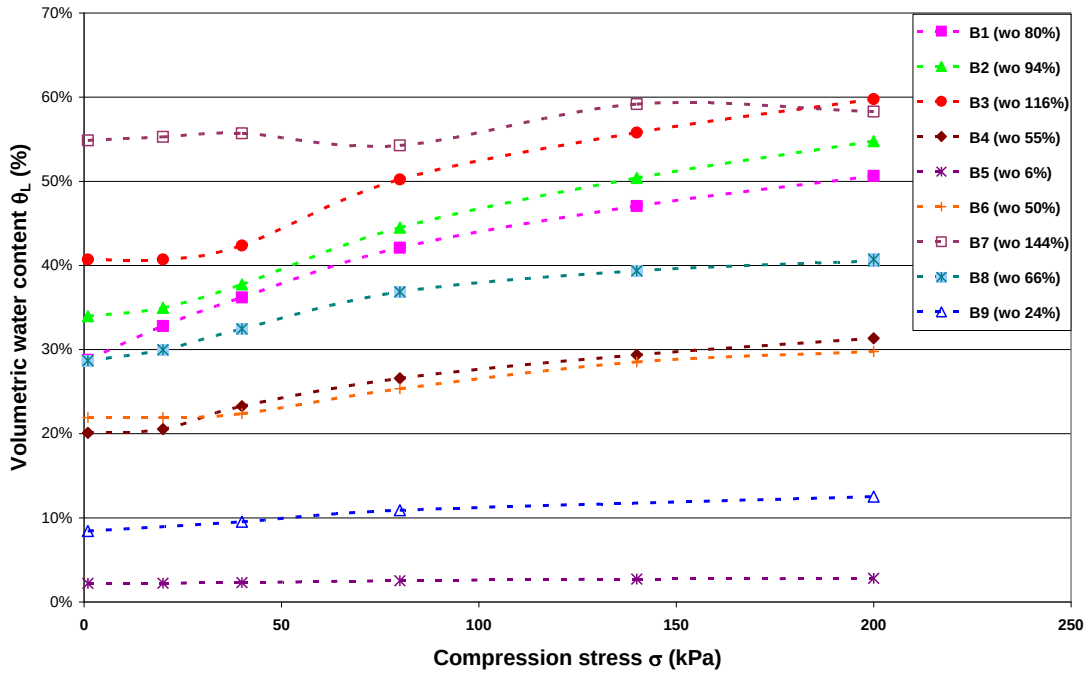

Graph III- 9: Volumetric water content of the waste samples as a function of applied compression stress (Waste 'B').

The evolution of moisture content of the sample throughout the experiment can be studied as a function of volumetric moisture content $\theta_L = w \frac{\rho_d}{\rho_S}$ and the decrease in the moisture content of the sample does not actually result in the decrease in the volumetric moisture content of the sample along the compression process as it can be seen in Graph III-9. In fact for the samples which do not loose water during the compression stages, the volumetric moisture content increases with the increase in settlement since the total volume of the sample is decreasing; however no linear relation is observed between the two as noted in Graph III-9 for sample B3 and B7.

Nevertheless the volumetric moisture content when plotted as a function of dry density gives the precise point of the start of leachate drainage from the sample as shown in Graph III-10. This phenomenon is more complex than any simple or direct relation between the dry density and the volumetric moisture content of the sample. The curve of sample B7 emphasizes on the presence of hysteresis for equilibrium moisture content. There may be the reason of different pore occupation of water for the same dry density of different samples which plays an important role in defining the equilibrium moisture content. Or may be the initial moisture content of the sample has an effect on equilibrium volumetric moisture content of the sample which needs to be analyzed in detail.

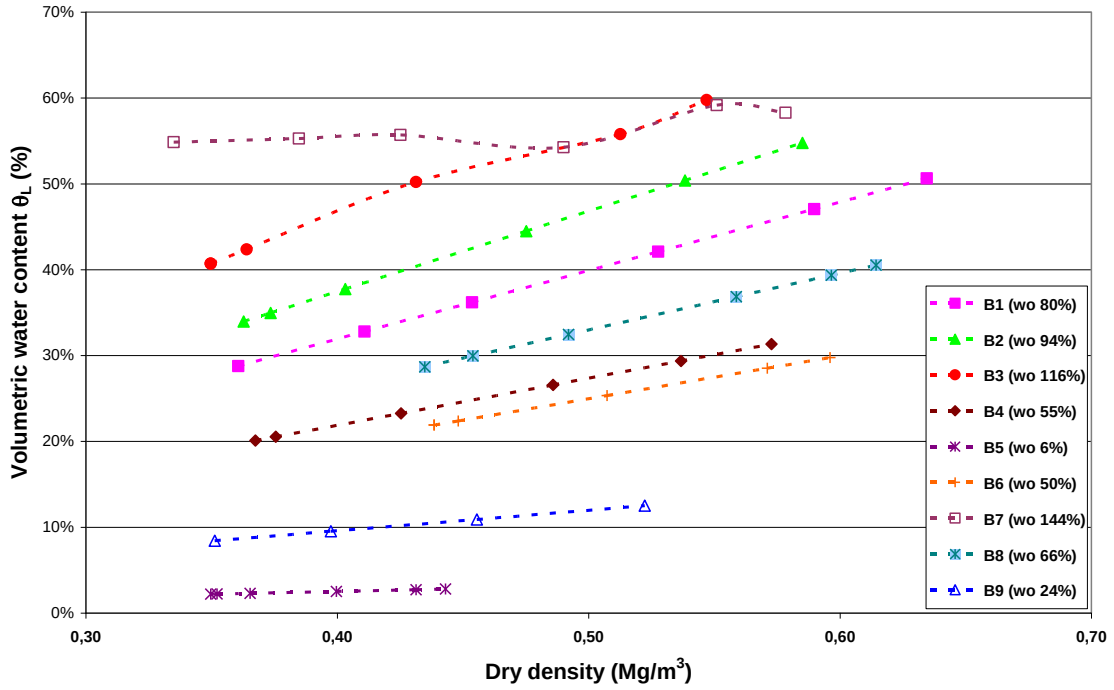

Graph III- 10: Evolution of volumetric moisture content as a function of dry density.

III - 1.6 Analysis of Gas Permeability Tests

During the compression-gas permeability tests, measurement of gas permeability was carried out at each compression stage and the change in gas permeability is analyzed as a function of gas porosity. For a given porosity there is a decrease in gas permeability for increasing gravimetric moisture content to the increase in the volumetric moisture content at the same time. Various parameters of the state can be used to analyze the gas permeability values such as dry density, porosity or the degree of saturation.

- Dry density (ρ_d) the porosity (n) and the gravimetric moisture content are the parameters which take into account any change in the gas permeability but on the other hand they not explicitly represent the change in volumetric moisture content which takes place in all unsaturated samples.
- The degree of gas saturation $S_G = \frac{V_G}{V_V} = \frac{\theta_G}{n}$ represents the pores available for the gas within the void volume. For a sample with S_G =1 (a dry sample) for a given sample porosity n, application of compression load decreases its total porosity n and thus its gas permeability while the degree of gas saturation is constant at 1.
- Volumetric gas content $\theta_G = \frac{V_G}{V_T}$ represents the pores available for gas within the total volume of the sample. According to Darcy's Law $\frac{q}{S} = K\frac{\Delta H}{L}$ the permeability is directly proportional to the sample length and inversely proportional to the surface area of the sample. This ratio takes account of the total volume of the sample therefore the volumetric moisture content θ_G is a characteristic state parameter of the gas permeability.

Graph III-11 presents all the gas permeability values measured for the waste 'B'. In a general overview it can be noticed that all the graph lines are clustered together except for the sample B5 and B9 which are the dry samples with moisture content of 6% and 24% respectively. For these samples initial drying was carried out in order to decrease their natural moisture content before the placement in the oedopermeameter.

This cluster of lines highlights the fact that whichever the method of reduction of porosity either through increase in moisture content or by the decrease in total porosity through compression, the values of gas permeability obtained are in the same scale of variation depending mainly on the gas porosity θ_G. In Figure II-7 typical curves of relative permeability as a function of degree of saturation (S_L and S_G with $S_L + S_G = 1$) are shown for a sample with a given porosity. In Graph III-11 the gas permeability values are presented as a function of volumetric gas content, however due to the fact that

for one sample the decrease in permeability is a function of decrease in the total porosity during compression, for all the samples, this graph can not be directly compared with the Figure II-7 where the relative permeability trends for soils are plotted as a function gas and liquid saturation.

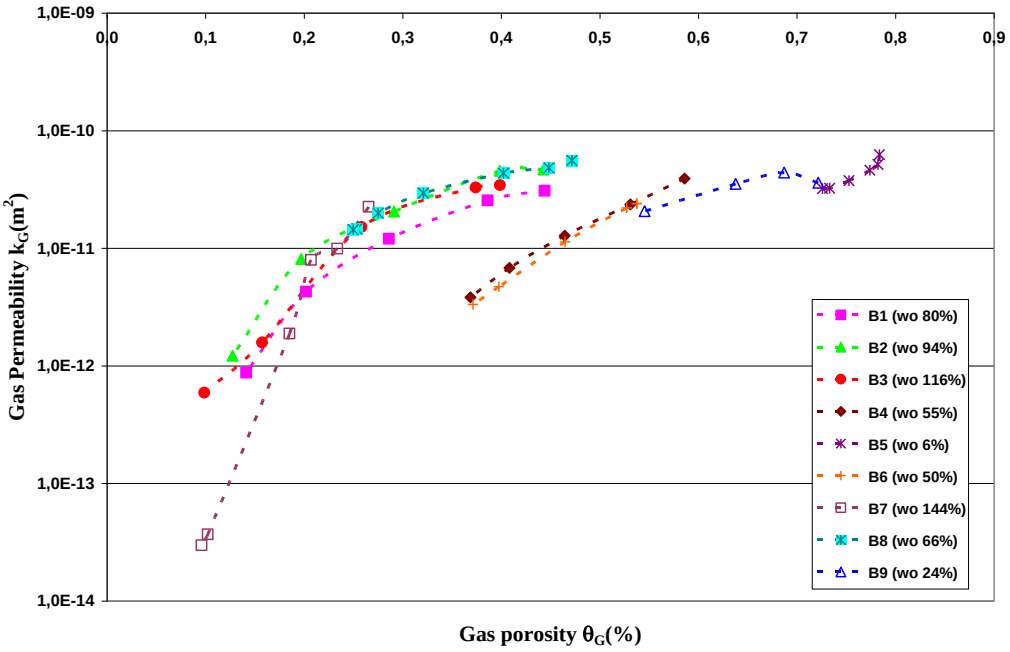

Graph III- 11: Evolution of gas permeability as a function of gas porosity for compression-gas permeability tests of waste 'B'.

For a given total porosity '*n*' for the compressed samples the decrease in degree of gas saturation S_G through the increase in initial moisture content 'w_0' produces a decrease in the gas permeability over a larger scale. For less compressed samples, the decrease in the degree of gas saturation (from 80% to 35%) has a lesser effect over the decrease in the gas permeability (from $4x10^{-10}$ m^2 to $5x10^{-11}$ m^2). For given initial moisture content the effect of compression is twofold

- Decrease in the total porosity
- Increase in the volumetric moisture content

These two effects result in the decrease in gas permeability. The more the volumetric moisture content present in a given sample, more it will occupy the free macro pores thus reducing the passage of gas through the medium. In Graph III-12 it can be observed that the volumetric moisture content of sample 'B7' remained constant, however, it was still in such a high range that its effect on gas permeability is noticeable.

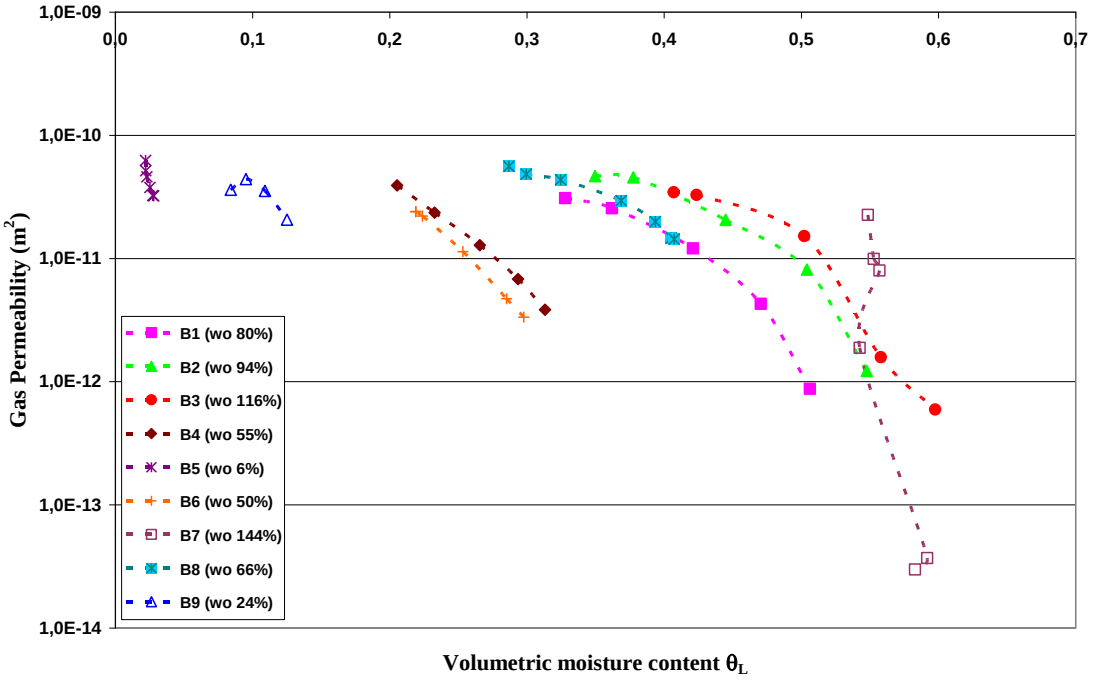

Graph III- 12: Evolution of gas permeability as a function of volumetric moisture content for compression-gas permeability tests of waste 'B'.

III - 1.7 Analysis of Different Hydrological Parameters

The evolution of the total porosity, the volumetric moisture content and the volumetric gas content under a compression stress is a key issue for leachate and biogas flows. In an attempt to interrelate these parameters, the evolution of the gravimetric moisture content *w*, total porosity *n*, the volumetric moisture content θ_L and the volumetric gas content θ_G as a function of compression stress for the samples 'B6' and 'B7' is presented on Graph III-13 (the total porosity is the sum of the volumetric moisture content and the volumetric gas content). It should be kept in mind that the gravimetric moisture content for sample 'B7' is almost three times higher than the moisture content of sample 'B6'.

The total porosity, for both the samples in the same range, decreases similarly with increasing stress which confirms that these samples have a very similar structure. For σ' between 0 and 200 kPa, approximately 15 % of the total porosity is lost. This variation should generate a drastic change in the hydraulic properties of the waste material. No liquid is drained out of the sample 'B6' thus, its volumetric moisture content increases during the test. On the other hand, sample B7 loses the leachate during compression and the gravimetric moisture content is observed to be decreasing. it can be observed that the volumetric moisture content of sample 'B7' remains almost constant after the compression stage of 100 kPa upto 200 kPa. This sample appears to be close to its maximum water

storage capacity. Furthermore it can be noted that at higher compression stages, the volumetric moisture content and the volumetric gas content of sample 'B6' are almost equal. On the other hand, for the same compression stages, the volumetric gas content of sample 'B7' is significantly lower because of its very high volumetric moisture content.

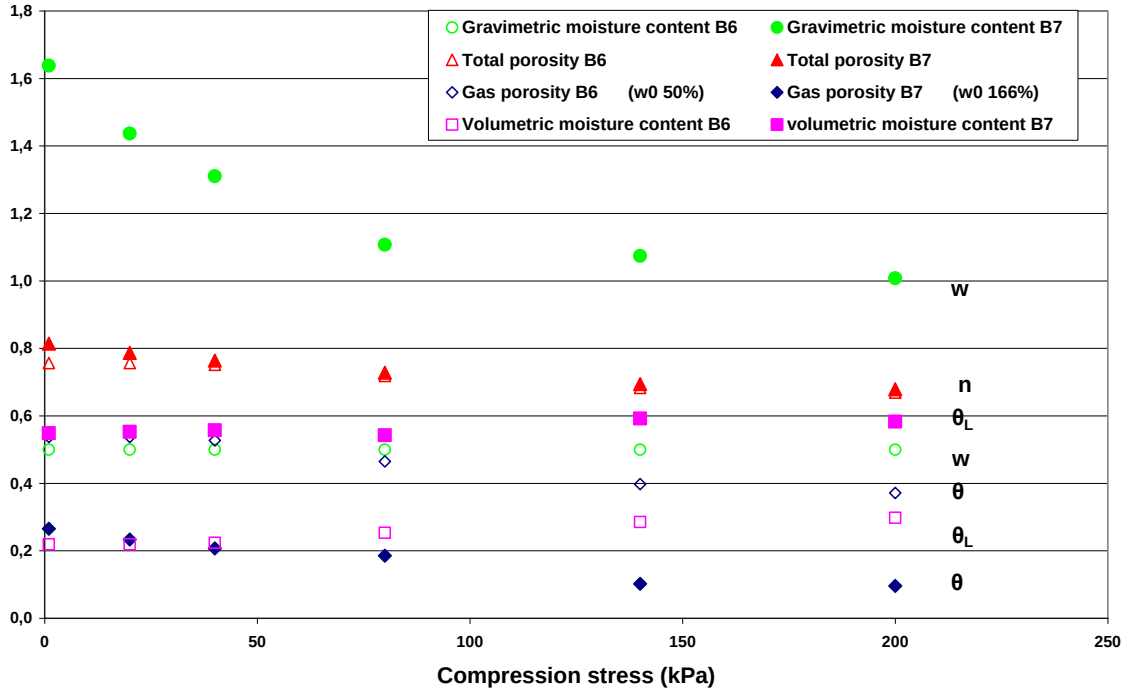

Graph III- 13: Comparison of evolution of various parameters of sample B6 and B7 as a function of compression stress.

III-2 TEST PROGRAM FOR AN OLD WASTE

III - 2.1 Presentation of the Cells

The part of the study is based primarily on the analysis of hydrological characteristics of 4 test cells constructed under the project ELIA (Lornage, 2006). The conventional storage/landfill methodology of Municipal Solid Waste (MSW) has been compared to two "new" processes of storage: Bioreactor Landfill and Mechanical and Biological Pre-treatment (MBP) before landfilling. The imperative to compare the behaviour of waste under the three different processes required the use of a waste product from the same deposit at the beginning of the study, the duration of the test was almost 5 years..

Four test cells were constructed namely C1, C2, C3 and C4 with the same volume (Figure III-5). The height of the cells is 4 m with a cross-section of 2.5 m x 2.5 m. The placement of waste was carried out with leachate drainage layers at the bottom of the cell. Settlement probes were installed in the waste as well as the gas collection pipes (Figure III-6) for the determination of amount and characteristics of the biogas collected throughout the period of the study. One of the four cells was dedicated to the conventional MSW “C2” another cell “C1”was reserved for study of the MSW as a bioreactor test cell and the remaining two cells “C3” and “C4” received MSW after the mechanical and biological pre-treatment.

Figure III- 5: Study Cells of ELIA before and after the placement of cover compost.

Active processes within the waste are relatively complex and multi-phase, it is important to monitor as many parameters in the liquid phase (leachate) as in the gas phase (biogas) and where possible directly in the solid matrix. Information collected through the monitoring of gas emissions and liquid drainage is essential for understanding the bio-physical and chemical processes taking place in waste. For the

present study, mechanical preparation of the waste (coarse grinding) was done before storage. Then recirculation of leachate was carried out, more or less intensively as a function of production rate of leachate.

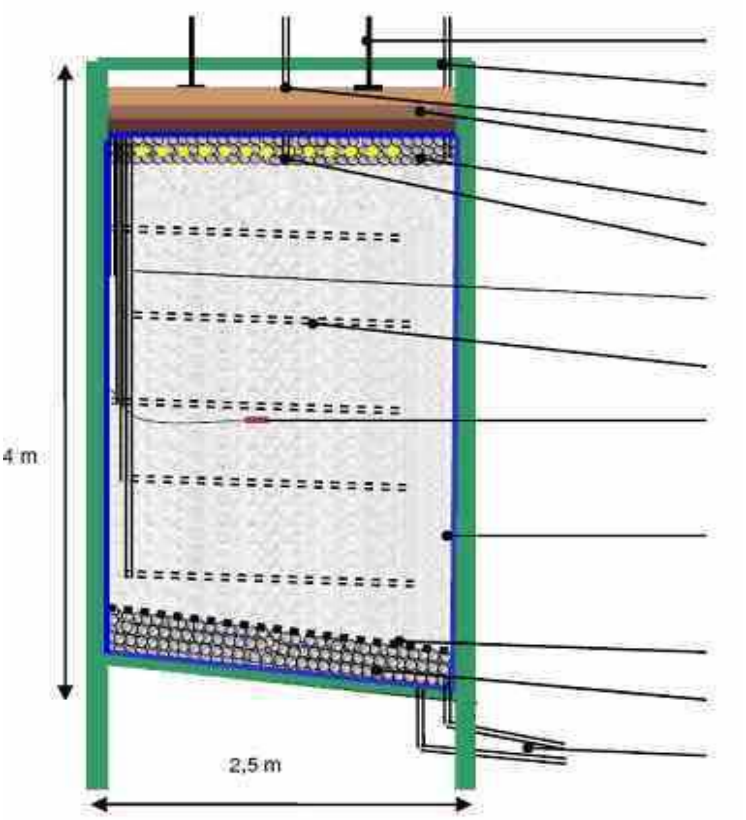

Figure III- 6: Schematic diagram of the test cell with different systems of devices in place (Lornage, 2006).

III- 2.1.1 Experimental Variations

To achieve the objective of experimental study in the best possible way, it was necessary to choose the parameters and characteristics for each of the three types of test cells, in a manner so as to ensure the best match with actual site conditions, taking into account the specificities and constraints related to pilots cells and to conduct experiments.

III- 2.1.1.1 Conventional Waste Cell “C2”

In the conventional cell, the waste was buried "as received". Once the desired height of the waste column was achieved, the waste was covered with a final cover made of low permeable clay.

III - 2.1.1.2 Bioreactor Waste Cell “C1”

The methodology of the bioreactor landfill is based on the principle of providing the micro-organisms responsible (in particular by leachate recirculation) for the degradation of the waste an environmental condition which is optimal for their development.

The preparation (mechanical, biological) of waste before landfilling is possible, like wise it is possible to change the moisture content of solid waste by adding water or recirculation of leachate and playing on the content of different inhibiting nutrients or compound elements or treating leachate prior to reinjection. The degree of sophistication in processing, which defines the composition and stability of final waste to be buried, is directly related to the regulatory force and the fixed cost of processing generated. The main objective of shredding is to increase the storage capacity of landfills. The size reduction due to the coarse grinding of the waste allow better contact between microorganisms, nutrients and organic matter as well as the increase of specific surface area of waste (Barlaz et al., 1990). As part of the mechanical treatment its particularity is to treat all the mass without separation of waste before landfilling, while the aerobic modality was chosen for the biological treatment.

III - 2.1.1.3 Pre-treated Waste Cells “C3 & C4”

The Mechanical and Biological Pre-treatment (MBP) of the waste before burial can be of many forms depending on the objectives of stabilization, opportunities for recyclable materials and of course on the type of waste. The mechanical preparation of the waste is almost always a combination crushing / screening which materializes at least two size fractions (sometimes 3 or 4). The fine fraction destined to be stabilized may undergo either an aerobic biological treatment, or anaerobic, moreover the combination of both is also possible. To test two scenarios, corresponding to two degrees of stability of waste in landfill, biological treatment was performed for 12 weeks before the burial of half of the treated waste (Test cell C3). For the second part of the waste the biological treatment continued for another 13 weeks (total 25 weeks of pre-treatment) prior to its placement in the pilot cell (Test cell 4). Figure III-7 shows the chronology of various important phases of placement of waste in all four test cells.

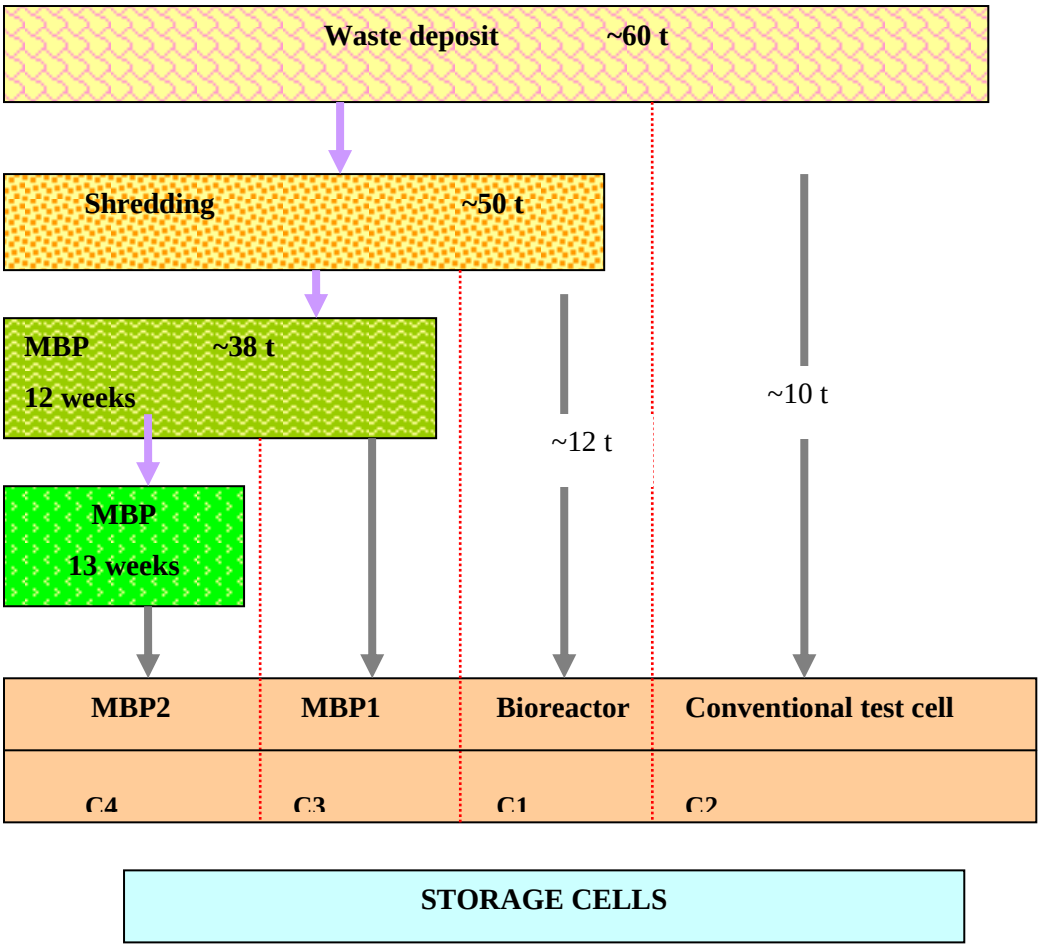

Figure III- 7: Waste preparation procedure for all four experimental cells ELIA.

III- 2.1.2 Municipal Solid Waste under Study

The MSW used for the study came from a compost sorting plant located at Auquemesnil near Dieppe (Seine Maritime). Approximately 60 tons of waste from the collection of communities across the region was collected on August 27, 2003. After homogenization, 500 kg of waste was collected for characterization of type MODECOM. At the same time, 10 tons were levied for the filling of test cell representing the conventional household waste (C2), the rest of the lot had to undergo mechanical processing. There it was divided into two parts, first part filling the bioreactor test cell (C1) and second part for the biological pre-treatment through aeration in windrows. After 12 weeks of treatment, half of the waste in windrow was used to fill the cell (C3) while the other half was used to rebuild a windrow of smaller size for further pre-treatment. The final waste, aged 25 weeks, was used to fill the (C4) cell (Table III-4).

Table III- 4: Preparation of the waste placed in the four test cells of ELIA.

Waste Cell	Raw Waste	Mechanical pre-treatment	Leachate recycling	Biological pre-treatment	Extended biological pre-treatment
C1		X	X		
C2	X				
C3		X		X	
C4		X		X	X

III - 2.1.2.1 Un-treated Waste

The composition of the waste and its size distribution (in $\%_{MH}$) calculated from 500 kg of waste sample is given in Figure III-8 (Table III-5). The initial gravimetric moisture content (w_0) of the waste was 39 $\%_{MS}$. The gravimetric moisture content is the ratio of mass of water to the mass of solids $w_0 = \frac{M_L}{M_S}$, where M_L is the mass of water in the sample and M_S is the dry mass of the sample.

The fraction (54.7%) of organic waste studied was composed of 54% kitchen and garden waste while 46% accounted for papers / cardboards.

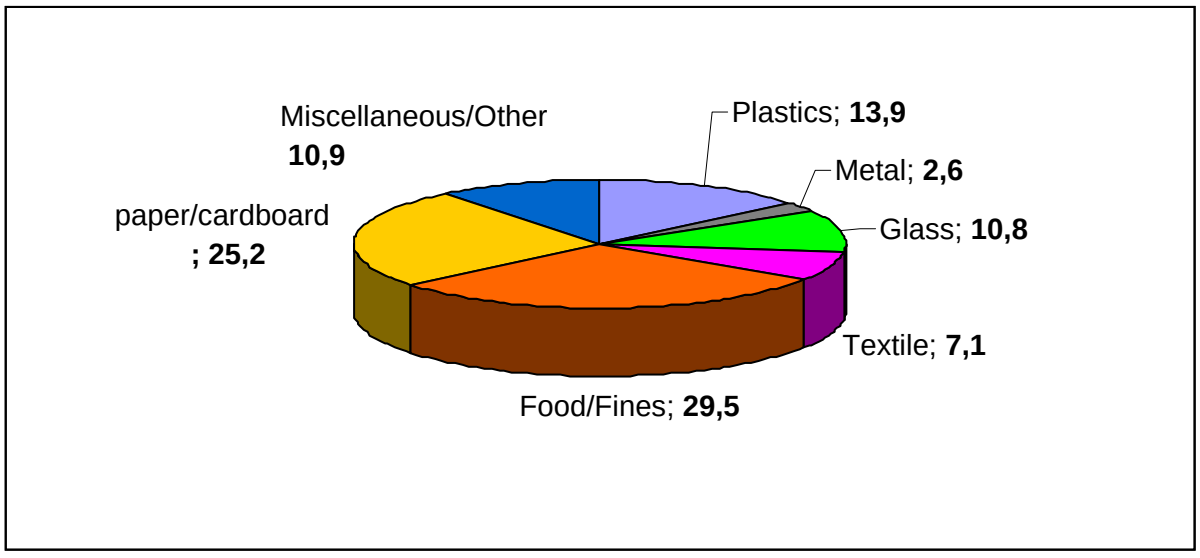

Figure III- 8: Composition of raw waste material prior to placement in the test cells.

Table III- 5: Composition of Waste Samples (C1-C4).

Waste constituent	$\%_{MH}$
Plastics	13.9
Metal	2.6
Glass	10.8
Textiles	7.1
Food/Fines	29.5
Paper & Cardboard	25.2
Miscellaneous	10.9

III - 2.1.2.2 Mechanical Treatment

The mass composition of the waste after mechanical treatment remains the same (the moisture loss by evaporation during grinding is negligible) and only its size distribution changes. Initially the waste fraction above 100 mm was 54% by wet mass of waste while the fraction 20-100 mm was 27%. After the shredding the fraction > 100 mm reduced to 27% whereas the fraction 20-100 mm increased to 40%, therefore, the waste fraction < 20 mm accounted for 33% after the shredding. The actual initial dry and wet densities were respectively equal to 0.34 and 0.47 t/m^3.

III - 2.1.2.3 Biological Treatment (C3 & C4)

A total of 37.46 tons of waste charges (± 20 kg), having undergone mechanical pre-treatment, was arranged in windrows 21 m long, 6 m wide and 2 m high. The initial moisture content($\%_{MT}$), too low to ensure optimal conditions for development of biological activity, was increased from 39% to 93% by the addition of 385 $L.t^{-1}$. The initial wet density in the windrows was estimated to be 0.2 t/m^3. The windrow was turned and moistened once in the 10^{th} week of treatment with 120 L/t^1 added. At the 12^{th} week of treatment, 11.30 tons (± 10 kg) were placed in the cell "C3". On this occasion, the remaining waste was reconstituted in another windrow with the length of about 7 m, 6 m wide and 3.5 m height. The biological treatment was then continued for 13 weeks with controlled ventilation significantly reduced in order to simulate a period of maturation. After 25 weeks of biological treatment, 10.66 tons (± 10 kg) of waste were buried in the cell "C4". In total water was added two times (at the start and at week 10) with the total addition of 505 L/t^1. The wet and dry densities were initially 0.43 and 0.59 t/m^3 respectively.

III-2.1.2.4 Sample Retrieval at the end of Test Period

For the purpose of hydrological analysis of the waste buried in the test cells for the last 6 years, a total of 300 kg of waste was brought to the LTHE laboratory in July 2009 for the permeability tests. From

each cell three samples were excavated from three different depths. In addition to that one sample comprising of all three depths termed as 'mixed' was also collected. The details of all the samples are given in Table III-6. The moisture content for each sample depth prior to compression-gas permeability test determined by ECOGEOS is noted as the in situ moisture content 'w_0^{is}' while the initial moisture content (deduced at the end of the compression-gas permeability tests in LTHE, Laboratory) is termed as 'w_0'. Furthermore the average dry density, assessed for the global cell, is used as the in-situ value $\overline{\rho_d^{is}}$ for the comparison with the densities achieved in the oedopermeameter.

Table III- 6: Details of samples collected from "ELIA" test cells.

Waste Cell	Sample Depth	Av. Dry Density ($\overline{\rho_d^{is}}$)	Gravimetric Moisture Content (w_0^{is}) %	Initial Gravimetric Moisture Content (w_0) %: reception LTHE ('natural moisture content)
C1	70 cm below the soil cover	0.711	72.4	77.0
	Middle of the cell height		94.3	
	50 cm above the drainage layer		96.8	
C2	70 cm below the soil cover	0.713	86.2	92.5
	Middle of the cell height		102.0	
	50 cm above the drainage layer		140.0	
C3	70 cm below the soil cover	0.738	79.4	75.2
	Middle of the cell height		90.3	
	50 cm above the drainage layer		90.4	
C4	70 cm below the soil cover	0.689	59.5	67.1
	Middle of the cell height		62.6	
	50 cm above the drainage layer		75.7	

III - 2.2 Sample Preparation

For each series of compression-gas permeability test, the samples were prepared according to the following procedure (Figure III-9):

- First test was performed for the samples with the initial moisture content as received from site, close to w_0^{is}.
- For the second series of test measurement, sample removed from the first test was dried at 35°C in the oven and/or in air over a period of 2 or 3 days to reduce its moisture content.

- Third test was performed in the same manner as the second test with a further drying of the same sample in the oven at 35°C for another 2 to 3 days. (Table III-7)
- For each type of sample (C1 to C4), the initial wet mass of the waste is the same for three series of compression-gas permeability tests (before alteration of the gravimetric moisture contents).

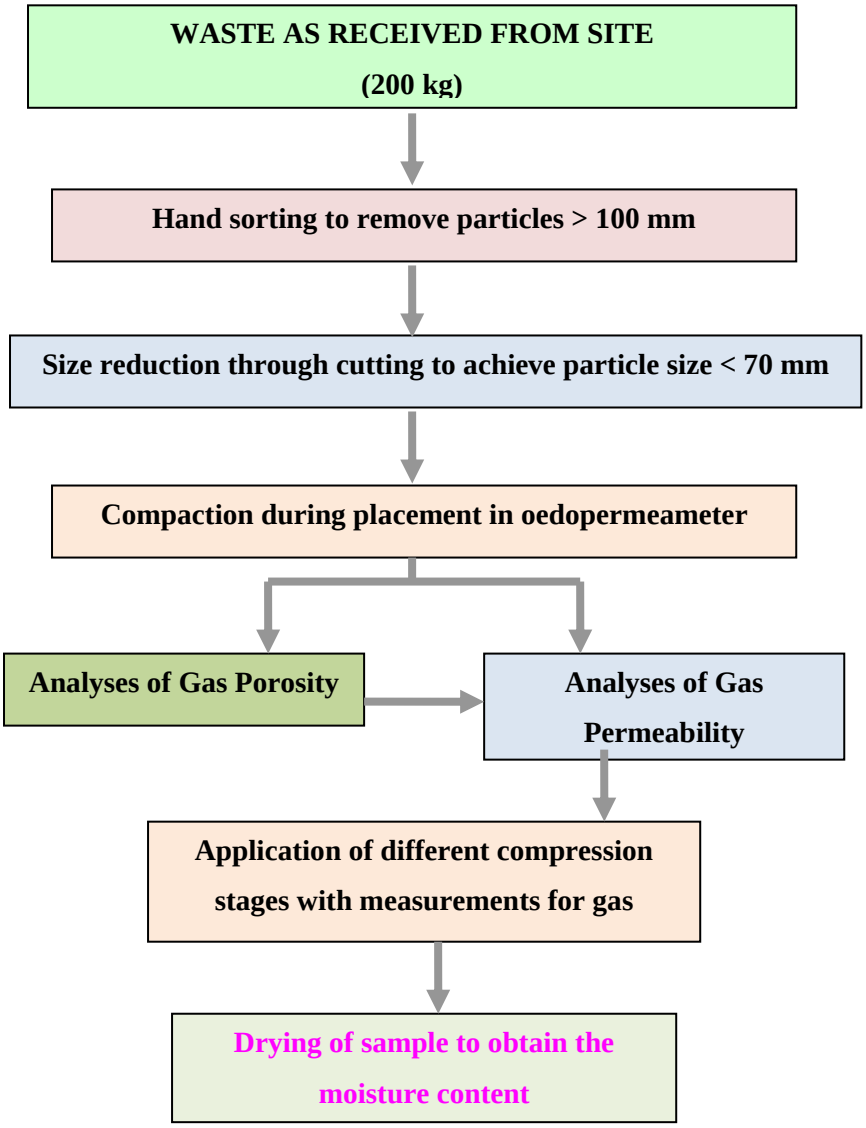

Figure III- 9: Schematic diagram for the oedopermeameter tests.

Table III- 7: Various observations regarding sample preparation.

Test No	Notation	Initial moisture content w_0 (%)	Observations
1	C1- 1	77.0	Sample at natural moisture content
2	C1- 2	30.1	Sample C1- 1, oven dried at 35°C during 3 days
3	C1- 3	15.6	Sample C1- 2, oven dried at 35°C during 3 additional days
4	C2- 1	92.5	Sample at natural moisture content
5	C2- 2	48.0	Sample C2- 1, oven dried at 35 °C during 2 days
6	C2- 3	26.1	Sample C2- 2, oven dried at 35 °C during 2 additional days
7	C3- 1	75.2	Sample at natural moisture content
8	C3- 2	26.6	Sample C3- 1, oven dried at 35°C during 3 days
9	C3- 3	13.7	Sample C3- 2, oven dried at 35 °C during 2 additional days and further air dried during 3 days
10	C4- 1	67.1	Sample at natural moisture content
11	C4- 2	45.4	Sample C4- 1, air dried at 25°C during 5 days
12	C4- 3	24.2	Sample C4- 2, oven dried at 35°C during 2 additional days

The compaction protocol follows the same procedure as used earlier for the fresh waste (§ III-1.2). Since the waste samples were not received shredded, bigger particles needed to be removed however some plastic or textile components were cut with the help of scissors to maintain the proportion of all the components. All the measurements were carried out in the series of one experiment with the same sequence of compression stresses (σ) for compression-permeability tests which is as follows: 0 kPa, 40 kPa, 80 kPa, 140 kPa and 200 kPa. All of these compression stresses were maintained during a period of time ranging from 4 hours to 72 hours.

For each compression stress, following measurements were obtained (Figure III-9):

- Settlement measurement from the vertical displacement sensor (ΔH)
- Gas permeability measurement
- Leachate loss and corresponding mass

III - 2.3 Analysis of Compressibility

All the samples were put under same sequence of compression stress with a varying time for each stage (ranging from 4 to 72 hrs). Initial dry density of the samples achieved was different for some

samples due to difference in initial moisture content. These values are detailed in Table III-8. Below in Graph III-14 to Graph III-17 the relative settlement over the whole period of compression is plotted as a function of time to observe the correlation of initial moisture content and the relative settlement achieved.

Table III- 8: Measured values of initial moisture content, initial wet and dry density, pre-consolidation stresses, and coefficient of primary compression for samples ELIA.

Sample	ρ_0 (g/cm^3)	w_0 (%)	ρ_{d0} (g/cm^3)	$\sigma'c$ (kPa)	C^*_R
C1-1	0.96	77.0	0.542	11.1	0.20
C1-2	0.70	30.1	0.540	22.9	0.36
C1-3	0.63	15.6	0.542	06.5	0.17
C2-1	0.72	92.5	0.375	11.4	0.31
C2-2	0.56	48.0	0.379	10.1	0.33
C2-3	0.48	26.1	0.383	03.3	0.22
C3-1	0.89	75.2	0.510	10.1	0.24
C3-2	0.66	26.6	0.520	07.1	0.15
C3-3	0.59	13.7	0.520	10.0	0.20
C4-1	0.83	67.1	0.496	05.3	0.22
C4-2	0.72	45.4	0.496	09.3	0.24
C4-3	0.62	24.2	0.496	12.8	0.26

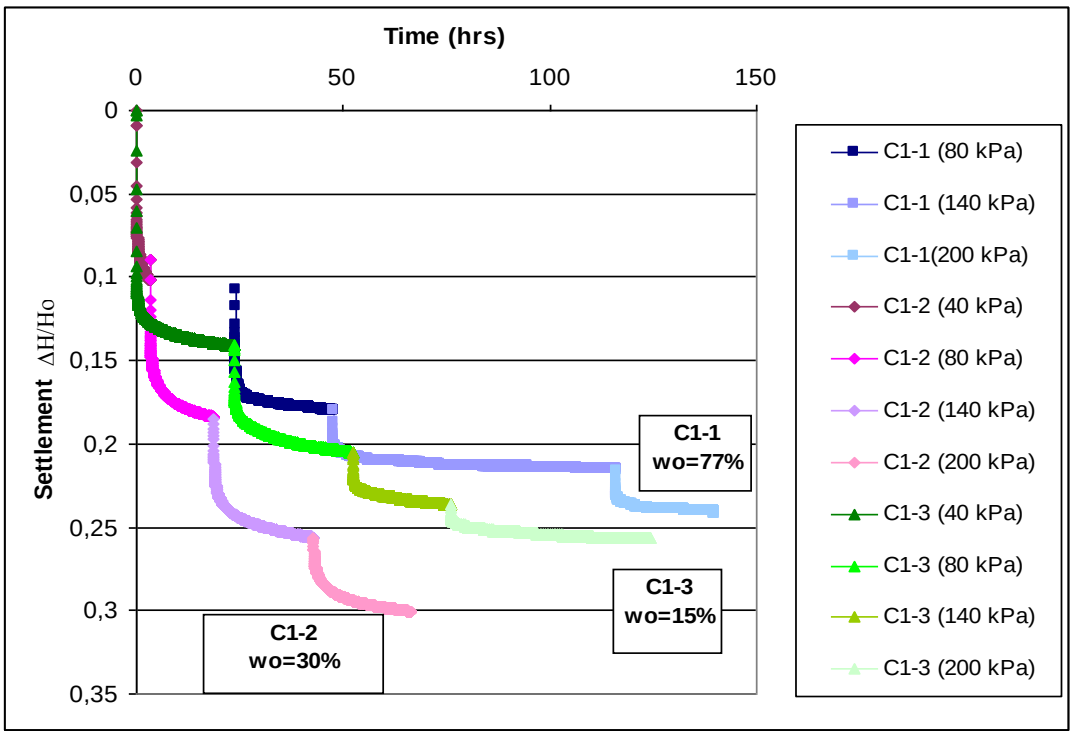

Graph III- 14: Settlement graph of sample 'C1' for three different initial moisture contents for compression-gas permeability test.

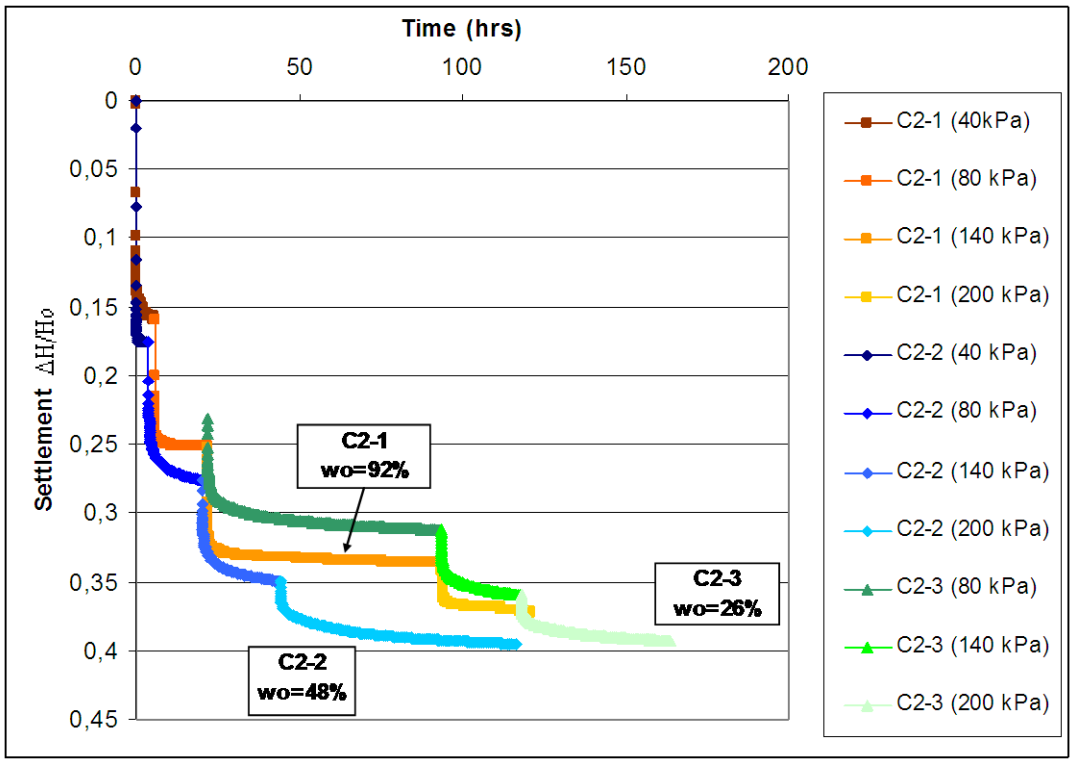

Graph III- 15: Settlement graph of sample 'C2' for three different initial moisture contents for compression-gas permeability test.

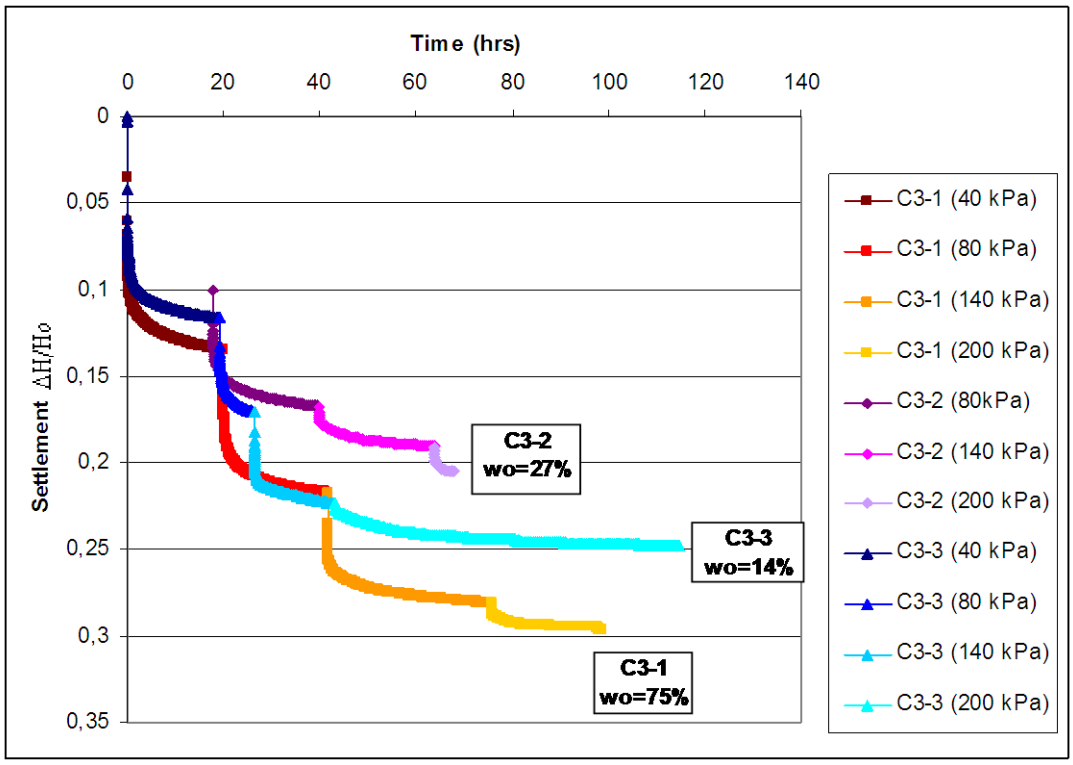

Graph III- 16: Settlement graph of sample 'C3' for three different initial moisture contents for compression-gas permeability test.

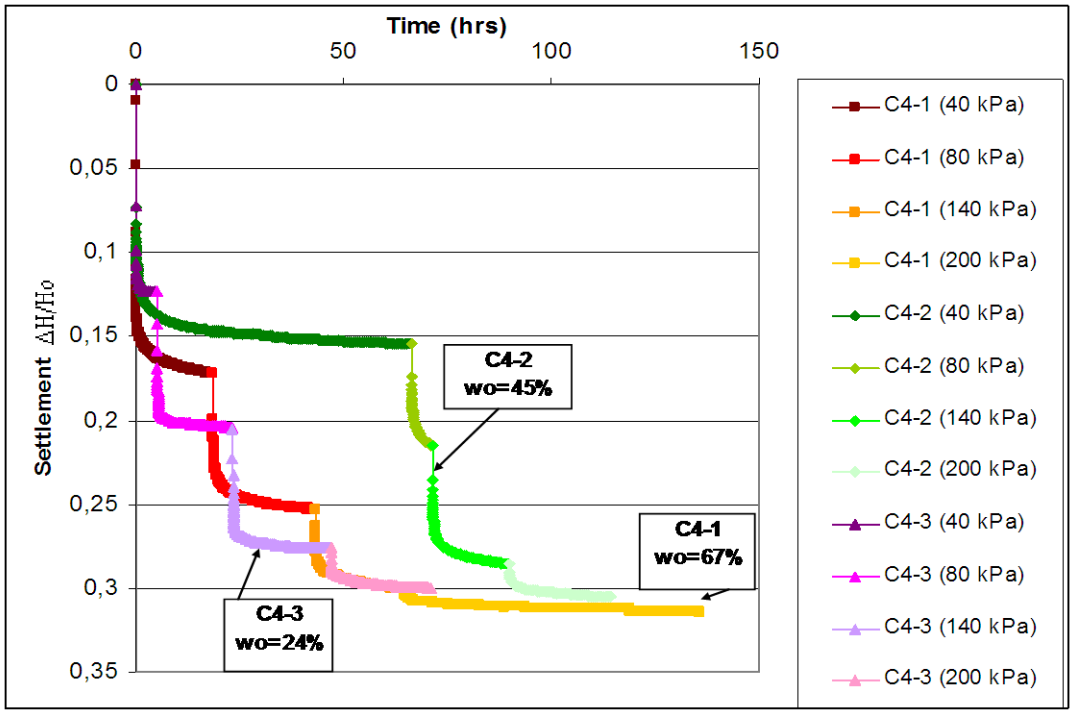

Graph III- 17: Settlement graph of sample 'C4' for three different initial moisture contents for compression-gas permeability test.

Determination of Coefficient of Primary Compression

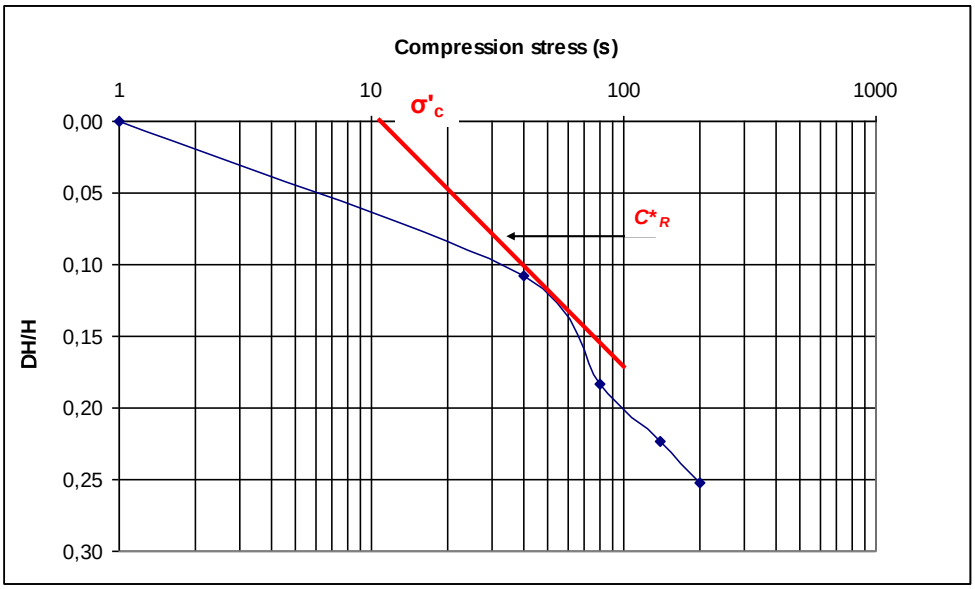

Figure III- 10: Determination of pre-consolidation stress (σ'_c) and the coefficient of primary compression (C^*_R).

To determine the coefficient of primary compression for the present study, all the pre-consolidation stresses were calculated for each compression-gas permeability test from the graphs plotted for settlement ($\Delta H/H_0$) and log (σ). On the same graph the slope of the line gives the value of C^*_R. The line extended back to x coordinate at 'x=0' gives the value of $\sigma'c$ (Figure III-10).

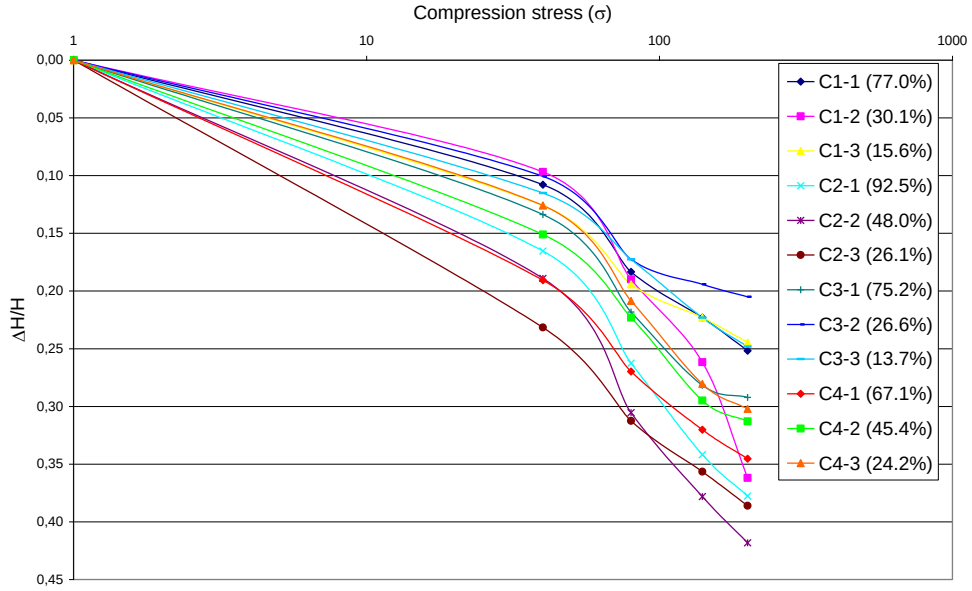

Graph III- 18: Compression of the samples as a function of various compression stages during the compression-gas permeability tests.

It can be noted in Table III-8 that the pre-consolidation stress (σ'_c) is generally less than 12 kPa, which in comparison with the samples of the fresh waste tested for waste 'B' is in the lower limit. The average value for pre-consolidation calculated for the latter was 16.6 kPa whereas the average σ'_c for test cells ELIA is 9.9 kPa. The initial dry density for different samples is around 0.5 t/m^3 except for the sample C2 corresponding to the raw waste which is more difficult to compact due to coarse elements. The values of the coefficient of primary compression (C^*_R) are in the range of values determined by Olivier (2003) however the raw waste sample appears to be more compressible.

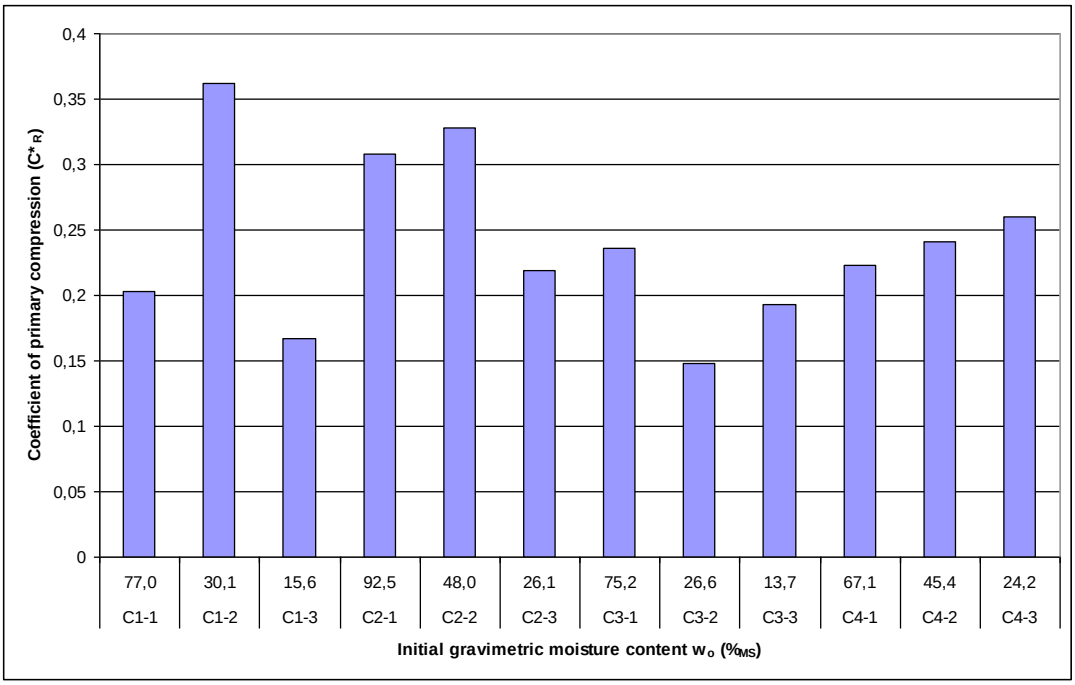

Graph III- 19: Comparison of coefficient of primary compression (C^*_R) of different samples as a function of initial gravimetric moisture content (w_0) and treatment (C1 to C4).

III-2.4 Comparison of the In-situ Density with the Density attained in Oedopermeameter

All the waste samples tested were the mixture of samples coming from different depth and due to heterogeneous nature of MSW, they are all different in density. In Graph III-20 the evolution of dry density (ρ_{is}) during the compression-permeability of all four samples is plotted against the in-situ density of the waste. The in-situ density (ρ_{is}) is plotted on the same graph corresponding to the mean compression stress in the test cell [at mid depth of the cell z = 2 m, $\sigma' = \rho.z = (1+w_0).\rho^{is}_d.z$].

It can be noted in Graph III-20 that the compaction effort applied while the placement of sample in oedopermeameter does not suffice to reproduce the same field density. In the case of sample C2 it is

not attained even at 200 kPa compression stress, however for the sample C4 it is achieved at 80 kPa. It seems clearly easier to compact the pre-treated waste (C4) than the raw waste (C2). The values of permeability for this material correspond to the high limit of permeability monitoring of the oedopermeameter device.

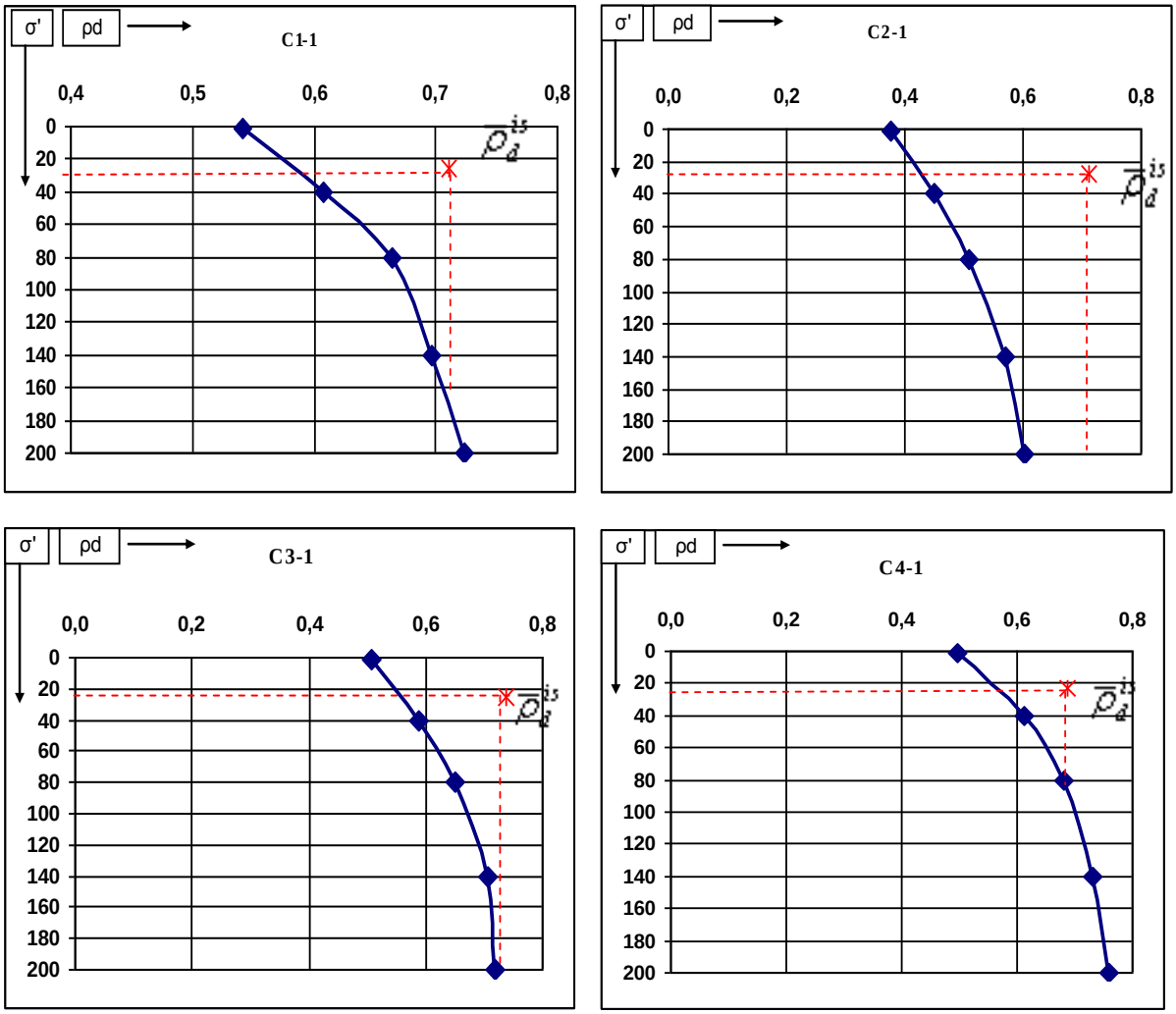

Graph III- 20: Evolution in dry density (ρ_d) of samples (C1-C4) at natural moisture content (w_0) as a function of compression stress (σ) during the compression-permeability test in comparison with the in-situ density ($\overline{\rho}_d^{is}$).

Influence of the Initial Moisture Content and Waste Treatment on the Dry Density

The relation between the initial moisture content (w_0) and the change in the dry density with increasing compression stress is studied in Graph III-21, the dry density (ρ_d) is plotted against the compression

stress (σ') of 40 kPa and 200 kPa in order to observe any possible direct influence. The compression stress of 200 kPa is the maximum compression limit maintained during all the compression-Permeability tests carried out.

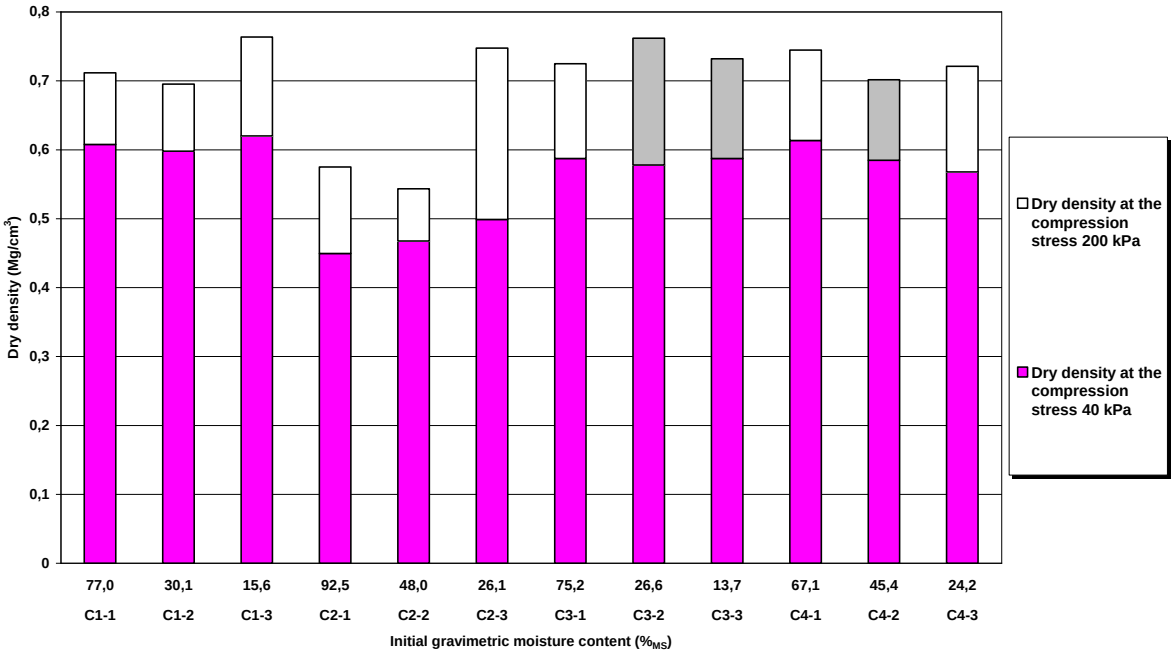

Graph III- 21: Change in dry density (ρ_d) between the compression stress of 40 kPa and 200 kPa as a function of initial moisture content (w_0) and waste treatment (C1 to C4).

In Graph III-21 no direct relation is observed, which is plausible keeping in view that all four samples belong to different test cells and more importantly all these samples, before their placement in the test cells, have undergone different treatment processes affecting their bio-hydro-mechanical properties.

III-2.5 Analysis of Equilibrium Moisture Content

Leachate Drainage under Compression

When the waste samples used for the compression-gas permeability experiments had high initial moisture content so whenever at a compression stage some leachate was squeezed out, it was collected and weighed. This reduction in moisture content when presented as a function of compression is noted with a moisture content at that stage termed here as the moisture content of equilibrium. This drainage as a function of compression stress results in the decrease in the gravimetric moisture content and increase in the dry density of the sample (Graph III-22).

The samples which were less humid, did not drain any leachate, even for the higher stages of compression stress, whereas, the samples with higher initial moisture content (however lower than the equilibrium moisture content i.e. field capacity) drained the leachate for higher stages of compression stress i.e. 140 kPa or 200 kPa: C1, C2 and C3 were subjected to the drainage of leachate under high compression stress when they were at their natural gravimetric moisture content unlike C4 which exhibited a lower natural moisture content. In Graph III-22 sample C1-1 and sample C2-1 with an initial moisture content of 77.0% and 92.5% respectively drained leachate starting from the compression stage of 40 kPa during the test. Sample C3-1 drained leachate for the compression stages of 140 kPa and 200 kPa which had initial moisture content of 75.2%. Other sample, though, having initial moisture content around 67.0% did not drain any leachate at any stage of compression which emphasizes that the equilibrium moisture content of the waste might be higher than the normal expected range, around 90% of the dry mass (*Ms*).

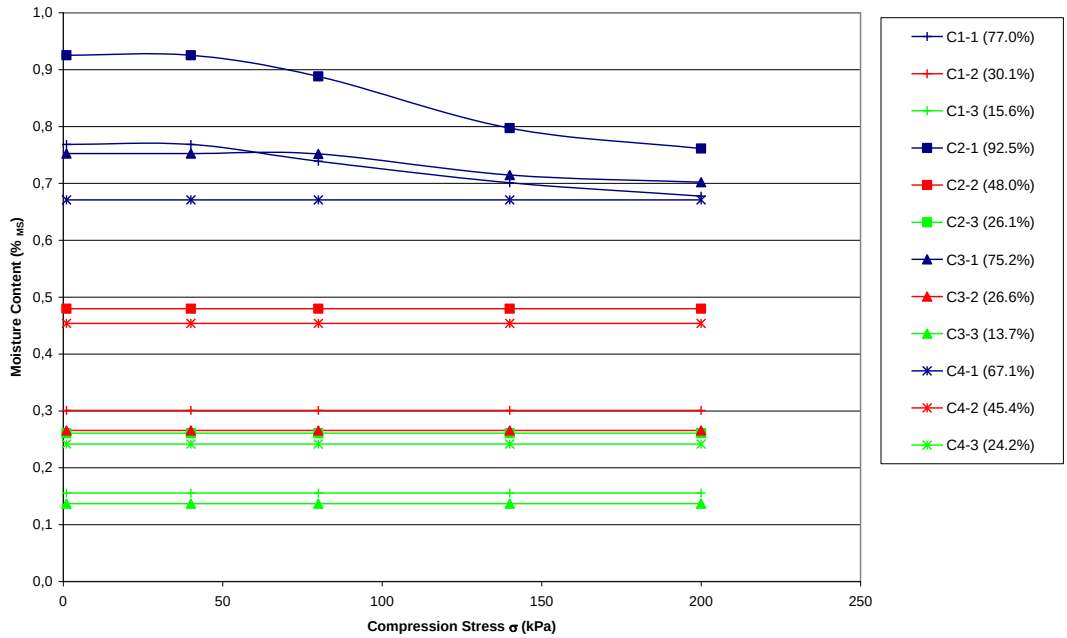

Graph III- 22: Change in gravimetric moisture content during the compression-gas permeability tests.

The evolution of water content of the sample throughout the experiment can be studied as a function of volumetric moisture content $\theta_L = w \frac{\rho_d}{\rho_s}$ and the decrease in the gravimetric moisture content of the sample does not actually result in the decrease in the volumetric moisture content of the sample along the compression process as it can be seen in Graph III-23. As a matter of fact the volumetric moisture content increases with the increase in settlement however no linear relation is observed between the two as observed in Graph III-23 for sample C1-1, C2-1 and C3-1. There is a maximum value of

volumetric liquid content θ_L which is around 0.5 for all the sample types, C1 to C4. A limit on θ_L seems more relevant than the limit on gravimetric moisture content *w* considered in Graph III-22.

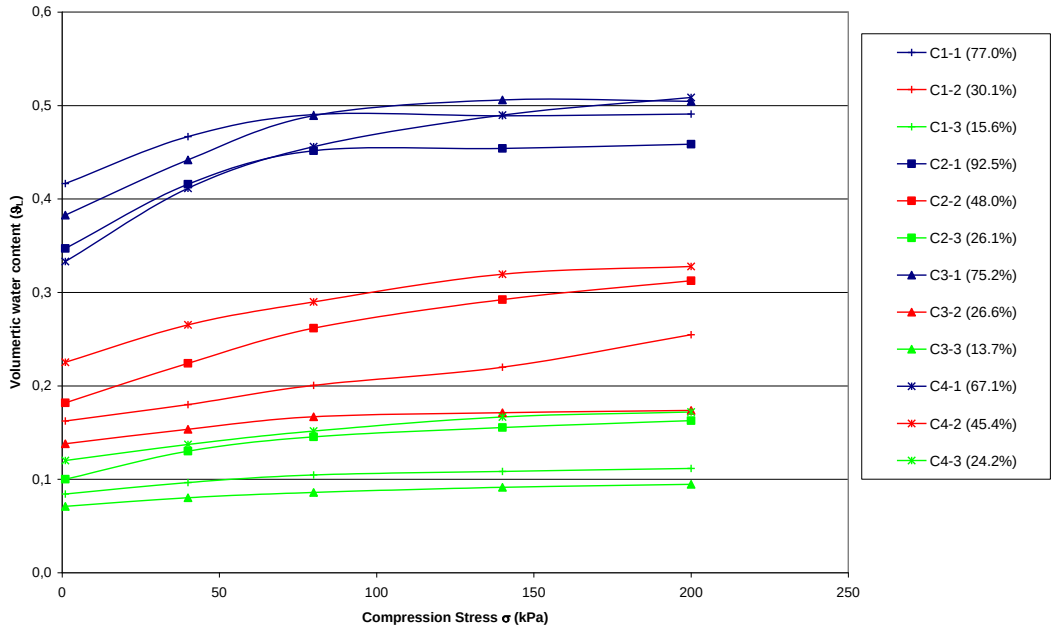

Graph III- 23: Volumetric moisture content as a function of dry density for the compression-gas permeability tests.

Table III- 9: Details of different parameters measured and calculated during the compression-gas permeability tests.

Sample	Moisture content ($\%_{MS}$)	Solid density (ρ_s)	Compression stress					
			40 kPa			200 kPa		
			n (%)	θ_G (%)	k_G (m^2)	n (%)	θ_G (%)	k_G (m^2)
C1	76.8	2.14	0.70	0.24	$8.6E^{-10}$	0.65	0.16	$4.8E^{-11}$
	30.0		0.74	0.56	$5.6E^{-10}$	0.63	0.38	$4.2E^{-10}$
	15.5		0.70	0.61	$4.3E^{-10}$	0.66	0.55	$3.5E^{-10}$
C2	92.5	2.02	0.76	0.34	$4.6E^{-10}$	0.67	0.21	$3.3E^{-11}$
	47.9		0.79	0.57	$3.9E^{-10}$	0.71	0.39	$2.4E^{-10}$
	26.1		0.75	0.62	$4.9E^{-10}$	0.69	0.52	$2.5E^{-10}$
C3	75.2	2.12	0.73	0.29	$2.7E^{-11}$	0.67	0.16	$1.2E^{-11}$
	26.6		0.72	0.57	$4.1E^{-11}$	0.68	0.51	$2.5E^{-11}$
	13.7		0.73	0.64	$6.1E^{-11}$	0.68	0.58	$1.9E^{-10}$
C4	67.1	2.14	0.71	0.43	$2.9E^{-11}$	0.64	0.13	$1.4E^{-11}$
	45.4		0.73	0.46	$3.9E^{-10}$	0.67	0.34	$1.3E^{-10}$
	24.2		0.73	0.59	$9.5E^{-10}$	0.66	0.49	$2.2E^{-10}$

III-2.6 Analysis of Gas Permeability Tests

The measurement of gas permeability was carried out at each compression stage of the compression-gas permeability tests, and the change in gas permeability is analyzed as a function of gas porosity. Various parameters of the state can be used to analyze the gas permeability values starting from dry density, porosity to the degree of saturation parameter.

Graph III-24 presents all the gas permeability values measured for the waste samples (C1-C4) separately, with the measured values detailed in Table III-9, while in Graph III-25 all these samples are put together in one graph to observe the presence of any possible correlation between these different samples. These samples can be compared to the Graph III-11 obtained for the fresh waste.

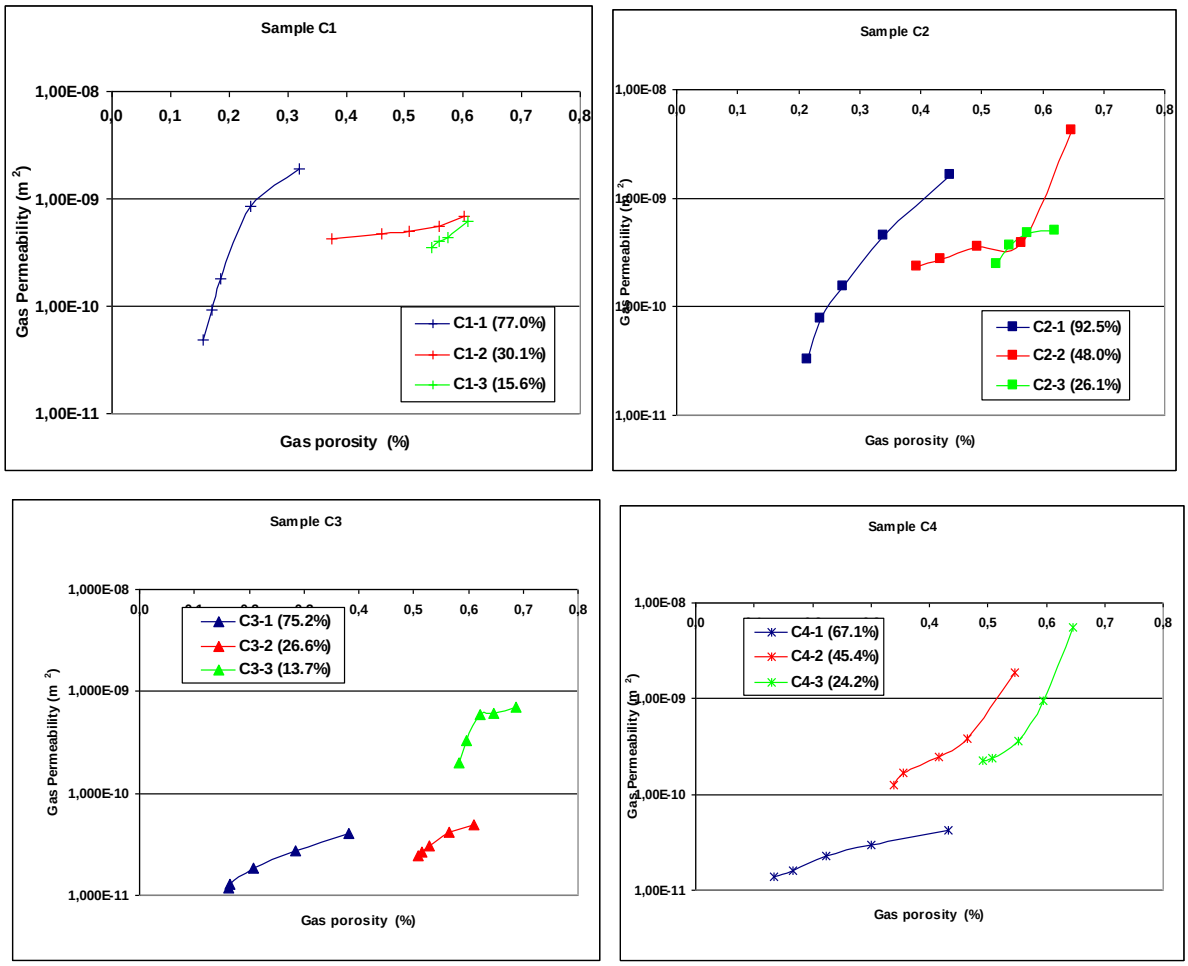

Graph III- 24: Effect of gas porosity over the change in the range of gas permeability for all samples (C1-C4) with different initial moisture content.

In a general overview of Graph III-25 it can be noticed that all the curves are clustered together except for the sample C3-1, C3-2, C4-1 which have the initial moisture content of 75.2% and 26.6% and

67.1% respectively. These samples were retrieved from the test cells with mechanically biologically pre-treated waste. That is to say that the samples have not only high percentage of smaller components but they are more stabilized samples than the other two mixed samples (C1 and C2).

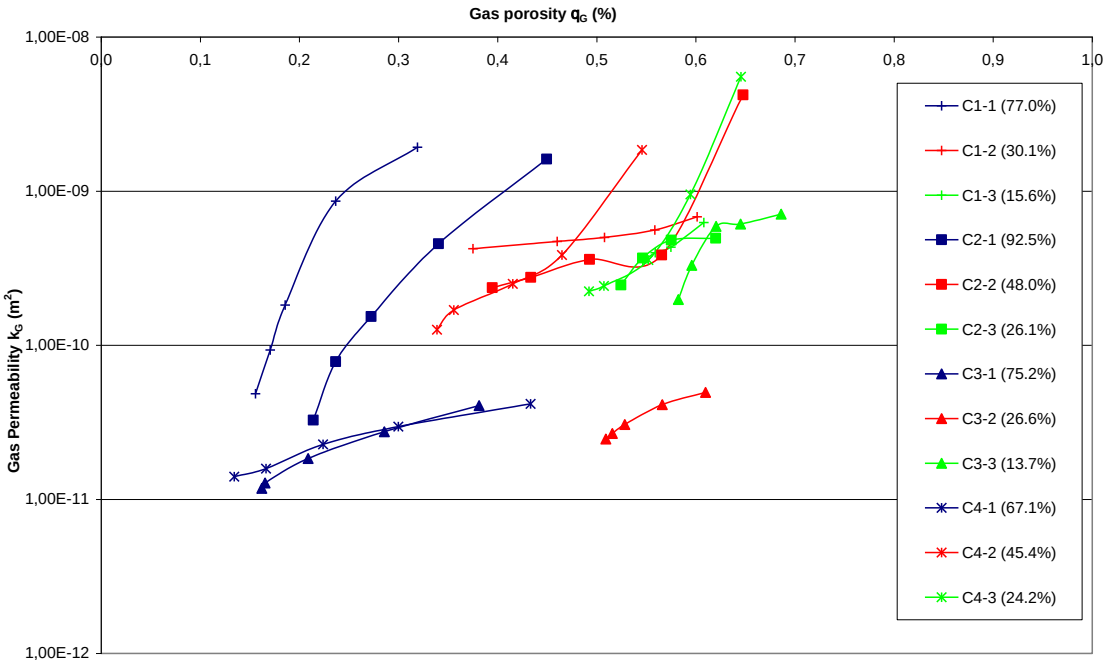

Graph III- 25: Evolution of gas permeability as a function of gas porosity during compression-gas permeability.

The cluster of lines highlights the fact that whichever the method of reduction of porosity either through increase in water content or by the decrease in total porosity through compression, the values of gas permeability obtained are in the same scale of variation. For a given total porosity 'n' for the compressed samples (Table III-9), the decrease in degree of gas saturation (S_G) through the increase in initial moisture content 'w_0' produces a decrease in the gas permeability. This can be related to the decrease in the porous structure at the macro scale rather than on micro scale of the sample. The double effect of compression and increased moisture content produces larger decrease in gas permeability as for comparison between the sample C2-1 (w = 92.5%) and sample C2-3 (w = 13.7%) the decrease in the gas permeability due to compression is more for sample C2-1 which has an initial moisture content almost six times higher than the sample C2-3.

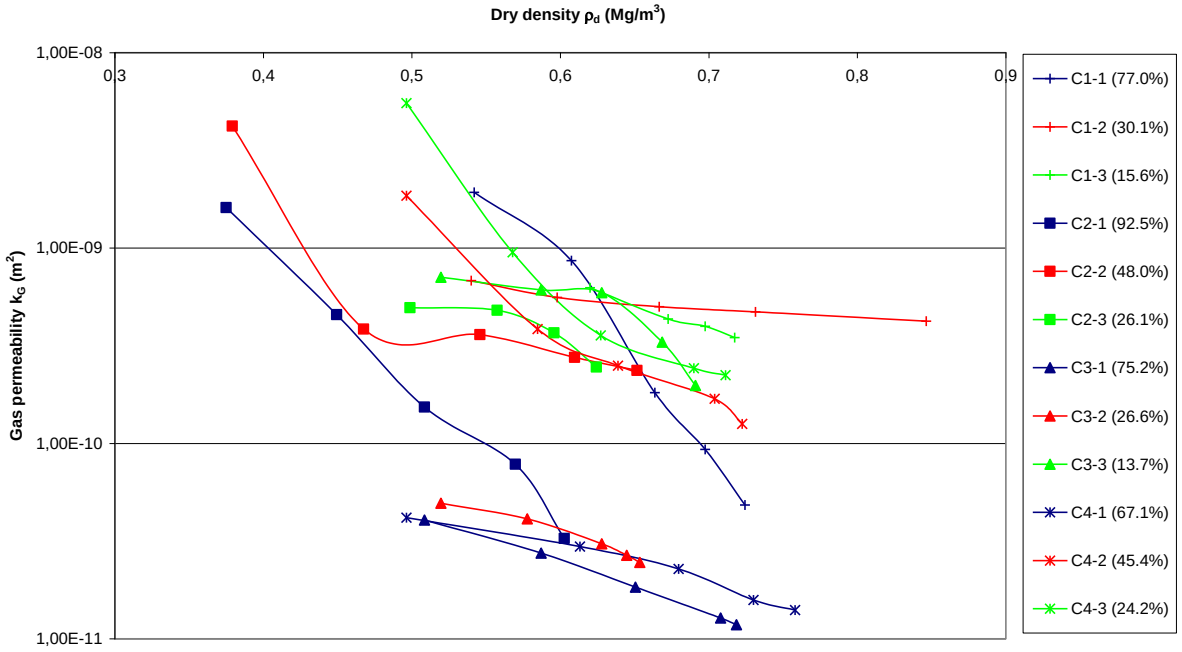

Graph III- 26: Evolution of gas permeability as a function of dry density during compression-gas permeability.

In Graph III-26 change in gas permeability is studied as a function of dry density of the sample. It can be noted that samples with high initial moisture content go under a change in gas permeability on a larger scale than for the samples where the initial moisture content is smaller, even if the dry density varies on a larger scale.

III-2.7 Comparison of Hydro-Mechanical Parameters determined through Oedopermeameter

The present study has helped in highlighting the bio-hydro-mechanical phenomena which all together influence the behaviour of MSW in the landfills. Below the parameters studied in the present study are presented in comparison in order to better comprehend their interaction.

III-2.7.1 Coefficient of Primary Compression C^*_R

An important mechanical parameter of MSW analyzed in the present study is the coefficient of primary compression C^*_R. The coefficient of primary compression is defined by the relation $\frac{\Delta H^P}{H_0} = C_R^* \log \frac{\sigma}{\sigma_{PC}}$.

Within the framework of research study, Stoltz (2009) determined the coefficient of primary compression of two different types of MSW, one being the fresh MSW while the other one was the MSW extracted from an old landfill. The average coefficient of primary compression calculated for the fresh MSW was C^*_R = 0.318, while this value for the old MSW was equal to 0.395.

The value of coefficient of primary compression calculated in the present study for the fresh waste is 0.308 while the average value, for all four test cells of the old waste type, range between 0.15 and 0.33 as detailed in Table III-8. The comparison between these values suggests that the values obtained in the present study are comparable with the earlier values cited keeping in view the difference of age of the waste. A large difference is observed in the values calculated in the present study for old waste but it should be kept in mind that these samples belong to four different cells where the waste was placed either initially untreated or mechanically biologically treated.

III-2.7.2 Comparison of Solids Density ρ_S

The parameter of solids density ρ_S is a characteristic and intrinsic parameter of the waste. This physical parameter itself is affected by the composition and the phase of biodegradation of the MSW. Moreover different methods can be used for its determination out of which the method of determination of ρ_S through the composition of waste is most frequently used in the literature. However the determination of ρ_S through pycnometer was defined and applied by Stoltz in his thesis report (2009) and it was shown that this method is more accurate than the analytical method of determination of solids density ρ_S, related to the proportion of each component and their own solid density.

The solids density ρ_S for a fresh MSW as calculated by Stoltz (2009) through pycnometer resulted in 1.65 Mg/m^3, whereas the solids density for 8 different samples retrieved from the old landfill site values range between 1.95 Mg/m^3 and 2.15 Mg/m^3. Factors affecting these values such as depth, age and state of biodegradation need to be kept in mind while comparing these different values obtained for different landfills. The higher value of solids density in comparison with the fresh waste could be attributed to the loss of organic mass due to degradation which originally exhibits lower of ρ_S. The values determined through the pycnometer in the present study for the fresh waste was equal to 1.81 Mg/m^3 while its calculation through the waste composition resulted in a value of 1.372 Mg/m^3. The solids density values for the old waste are presented in Table III-9 which range between 2.02 Mg/m^3 and 2.14 Mg/m^3. All these values of solids density of the old waste samples remain in the same range when compared with the solids density of fresh waste emphasizing the fact of stabilized organic matter.

III-2.7.3 Comparison of Gas Permeability θ_G

In Graph III-27 the values of gas permeability θ_G as determined for the fresh waste in the present study are presented in comparison with the average values of gas permeability determined by Stoltz (2009) for the fresh waste. The fact that the procedure of tests for the two studies was different from one another should be kept in mind: The tests performed by Stoltz (2009) followed the subsequent humidification of the initial sample while the series of tests carried out in the present study were dried in the oven at 35°C most of the times. However the waste composition was very much similar with the same proportion of organic material so it could be said that similar waste is analysed for both studies. These gas permeability values determined for the waste 'B' are still comparable with the gas porosity θ_G in the same range (70% to 30%) with those determined by Stoltz (2009).

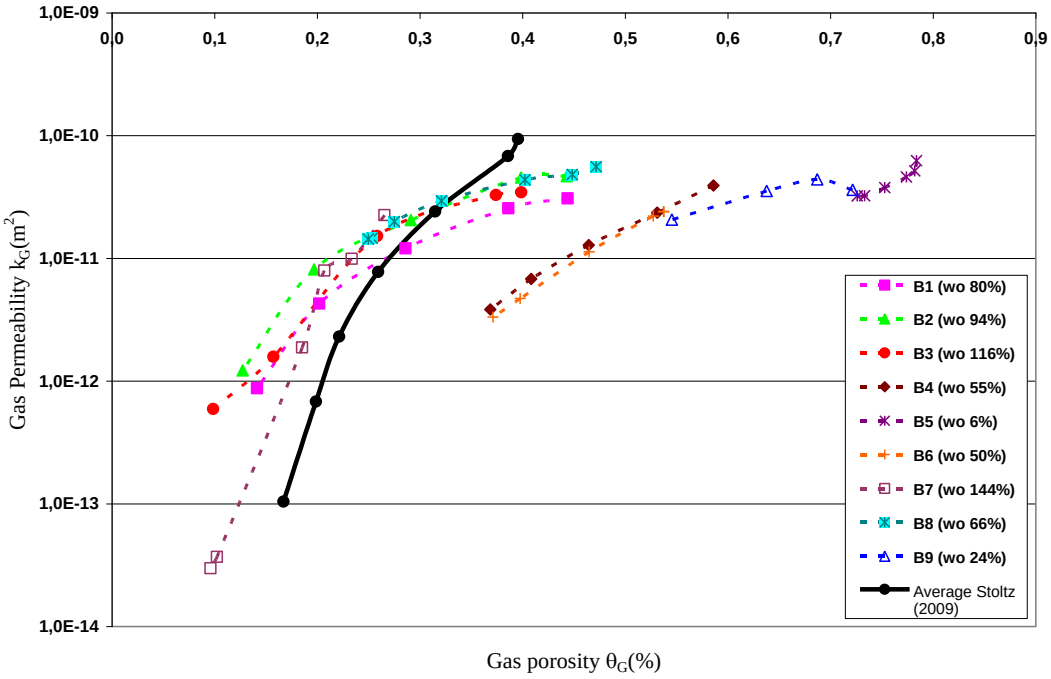

Graph III- 27: Gas permeability (k_G) for waste 'B' as a function of gas porosity (θ_G) in comparison with the values obtained by Stoltz (2009).

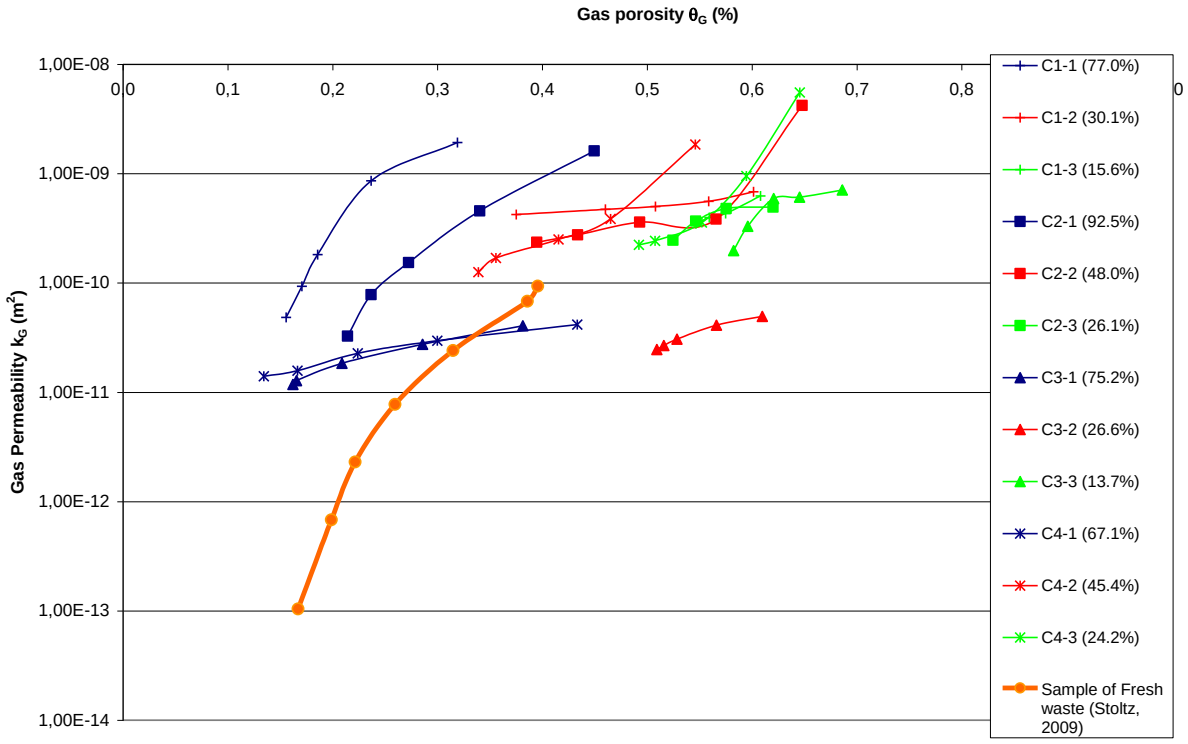

Graph III- 28: Gas permeability (k_G) of test cells ELIA as a function of gas porosity (θ_G) in comparison with the values obtained by Stoltz (2009).

It can be noted in Graph III-28 that the samples of test cells ELIA have a gas permeability range lower than the other samples of waste 'B' as presented in Graph III-27 with the earlier study carried out by Stoltz (2009) which is also related to the initial moisture content. These values of the gas permeability are higher than the values observed for the fresh waste (Graph III-11). The structure of the two kinds of waste is of course different but it is difficult to find a definite explanation for the difference of permeability scale observed between the two waste materials.

From the discussion above it can be concluded that the present study makes quite a noticeable contribution to the multidisciplinary analysis of the hydro-mechanical parameters of the MSW with an objective to better understand this complex medium. In future any study in relevance with the present work done will absolutely help in verifying and confirming the global bio-hydro-mechanical models suggested for studying the MSW.

IV- APPLICATION OF DOUBLE POROSITY MODEL TO LABORATORY EXPERIMENTS

IV-1 MODEL OF DOUBLE POROSITY

In literature multi porosities or double porosities are studied in association with many other parameters which are used interchangeably regarding their different notational terms for example open porosity or effective porosity, or free water or adsorbed water micro pores and macro pores etc. Some hydrological parameters like capillary water or adsorbed water are associated with double porosity without any clear linkage. From the data already available from the recent research work by Stoltz (2009) and the experimental results obtained under the scope of present study discussed in the previous section of this chapter the double porosity model initially proposed by Stoltz (2009) is established in a way to propose a state of the art model for the study of hydrological parameters of the municipal solid waste.

In the model the critical point at the boundary of micro and macro porosity is defined and introduced in reference with the macro porosity for the first time since it has not been studied and defined earlier in the context under study. Likewise a proposition concerning the intrinsic permeability is also put forward here for future detailed analysis.

Various research data already available in the literature and the present study helps in the verification of the presence of double porosity in porous medium of the waste body. This concept of the double porosity is based on the supposition that the porous structure of MSW consists of a matrix of bigger particles separated through the interstitial spaces (macro pores) while within these matrices there is still another fine matrix of micro pores. Furthermore it is supposed that there exists a discontinuity within the distribution of the macro and micro pores. The details of hypotheses and definitions of various parameters as explained within the framework of research study of Stoltz (2009) are reproduced here for reference and subsequent modification are delineated whenever deemed necessary. In the present chapter the applications of this model in the bio-hydro-mechanics are described and an interpretation of the experimental results of the previous section is presented.

IV - 1.1 Other Models available in the Literature

Certain authors consider the water contained in the micro pores of the aggregates as integrated into the “solid” but in the present model, solid phase is distinguished from liquid phase. Though the water of micro porosity is regarded as immobile during the compression application or hydraulic gradient, but

the exchange between the water of micro porosity and the water of the macro porosity is considered possible [the above experimental description of Beaven et al. (2003)]. Moreover, measurements of moisture content by drying in the drying oven take into account the water included in the aggregates.

IV- 1.1.1 Tracer Tests, Beaven et al. (2003)

Beaven et al. (2003) have presented the experimental results of the tracer test with lithium as the tracer injected in the compressed waste samples in a permanent fluid flow re-circulation where lithium concentration at exit point is measured.

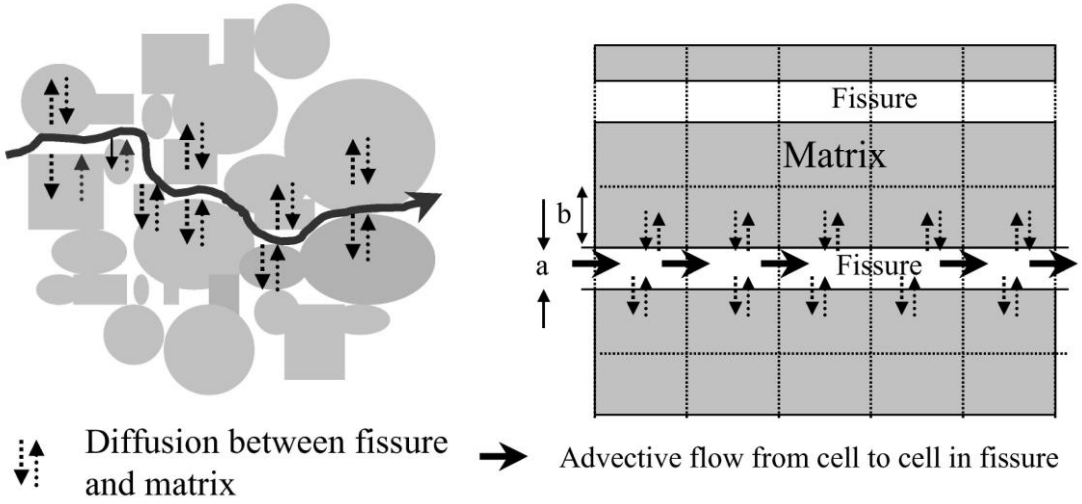

Figure IV- 1: Tracer test, diffusion of Lithium within the fine matrix of the waste sample (Beaven et al., 2003).

They have observed that at the beginning high concentration of lithium is measured at exit due to its rapid flow out of the sample along with leachate flow but even after 90 days of the tracer injection some residual lithium was still present in the leachate collected from the sample. They prove the presence of double porosity and have suggested a double porosity model to analyze the results (Figure IV-1). This model is based on the hypothesis that the water present in the micro pore structure of the medium is immobile.

IV- 1.1.2 Water Saturation Experiments, Capelo et al. (2007)

Capelo et al. (2007) presented the test results of infiltration experiments carried out on a waste column, 3 m high with 60 cm diameter. The flow was kept constant and any change in the moisture content of the sample was measured with the help of neutron probe. They have observed that after 120 minutes of continuous precipitation, the volumetric liquid content of the complete column increased without saturated volumetric liquid content for upper layers which increases afterwards (Figure IV-2).

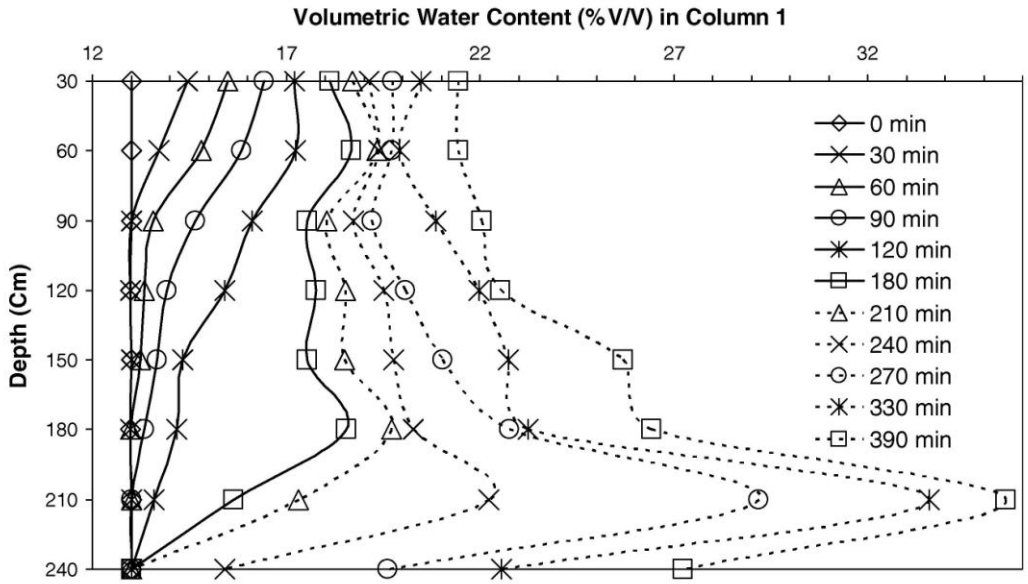

Figure IV- 2: Profile of volumetric liquid content with gradual increase in the layers underneath suggesting the presence of preferential paths (Capelo et al., 2007).

According to classical soil mechanics theory of water infiltration, water initially progressively saturates the upper layers before percolating further towards the bottom layers which was not the case here and hence suggests the presence of preferential paths for liquid flow around the fine matrices of micro pores. These preferential paths are the connected macro pores which allow the quick passage of liquids downwards before it fills the micro pores which it does afterwards as observed from these experimental data showing increased volumetric liquid content of upper layers.

IV - 1.2 Definition of the State Parameters for the Double Porosity Model

IV- 1.2.1 Waste Structure

The porous medium of the waste is composed of different elements of diverse nature. Within this random assembly of various elements two types of porosities can be distinguished: the porosity of the elements of waste and porosity around these elements. If a ruffled sheet of paper is considered, in contact with water, the micro pores of this sheet of paper will soak. Now, if one considers the assembly of several sheets of paper of the same type, confined in order to form an aggregate and if this aggregate is saturated, the water located in the micro pores of the sheets and water located around will not have the same behaviours when the sample is subjected to a compression or a hydraulic head gradient. Schematic diagram of the medium as shown in Figure IV-3 makes it possible to visualize the medium.

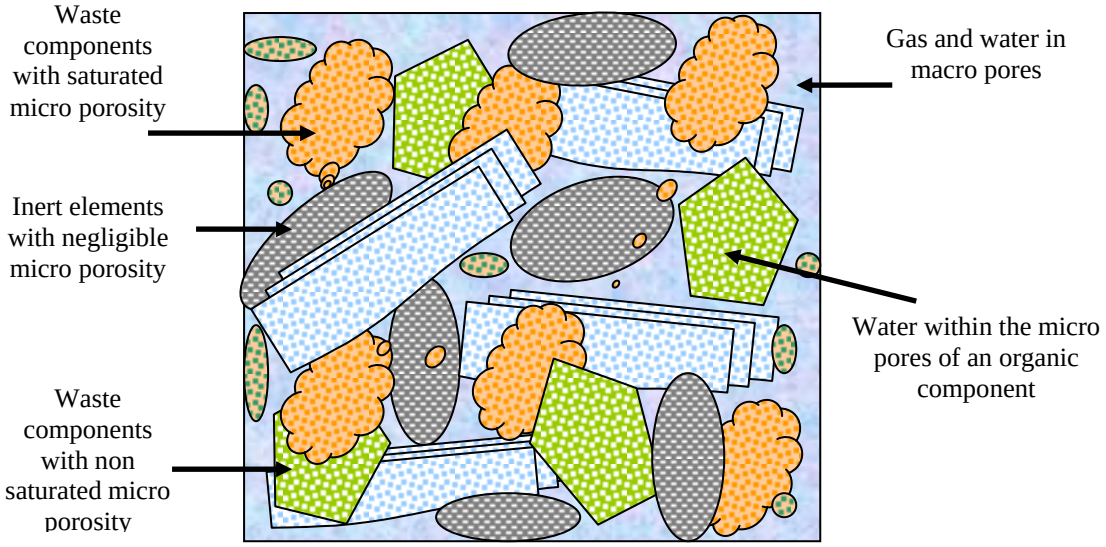

Figure IV- 3: Presentation of the components in the waste medium.

Considering all the aggregates which constitute waste, it is improbable that the micro pores of these aggregates are of the same type (size, form, etc). Characterizing a distribution of size of pores for each aggregate being impossible, two types of porosities are defined:

- A micro porosity located in the fine matrix constituting the aggregates, in major organic part of the waste
- A macro porosity located around the aggregates of waste

The multiple states of water present in micro porosity (hygroscopic water, adsorbed water etc) are not distinguished. The water located in the macro porosity is subjected to the capillary forces and to the gravitational forces.

IV- 1.2.2 Properties of Micro Porosity

The pores of micro porosity for waste 'B' will be arbitrarily supposed to be smaller than 40 µm and this internal micro porosity within the aggregates is supposed to be badly connected. The water contained in this micro porosity is supposed to be immobile during compression, under hydraulic gradient, and at the application of a suction pressure.

With regard to deformation, it was discussed in Chapter II-4.1 that the fact that part of deformation could be due to the compression of the micro porosity of the organic matrix. However, from the experimental results it is noted that the compression of the micro porosity of this micro-porous matrix is negligible compared to the compression of the macro porosity. This observation will be discussed later in detail.

With regard to the liquid flows in saturated conditions, the experiments in laboratory cell can justify the assumption that the water contained in micro porosity is regarded as motionless. The laws of flow in porous media described in Chapter III-5.3 (Kozeny - Carman and Van Genuchten - Mualem) were rewritten by Stoltz (2009) so as to distinguish the porosity mobilized during a flow (the macro porosity) and the one not mobilized (micro porosity). This modification of the laws according to the parameters of state of the model is detailed below and applied to the present study in order to verify the proposition of presence of double porosity.

IV- 1.2.3 Properties of the Macro Porosity

Since the micro pores are assumed to be smaller than 40 µm, the pores of the macro porosity will be arbitrarily considered bigger than 40 µm. This porosity is assumed to be well connected and compressible. The liquid flow is considered to be mainly passing through the macro porosity. The water contained in this macro porosity can be regarded as free. It will be mobile as well during an experiment of compression just as under the effect of a hydraulic gradient.

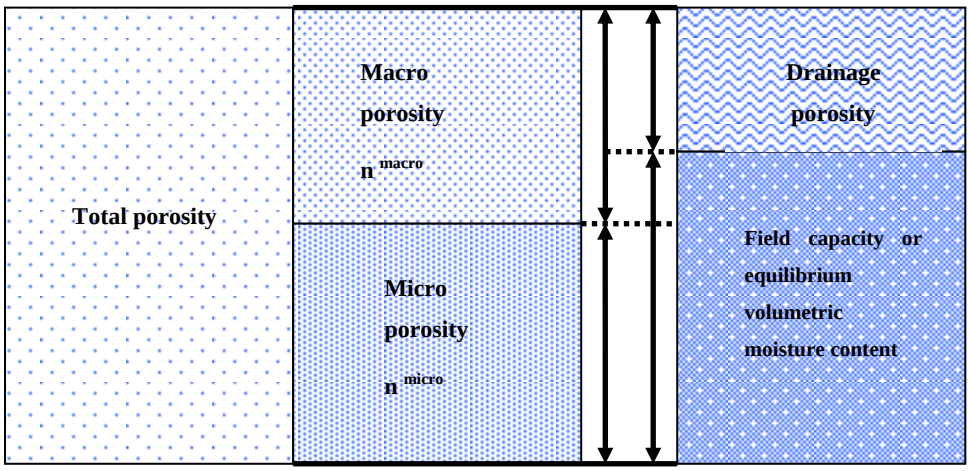

Figure IV- 4: Distribution of micro and macro porosity in contrast with drainage porosity and field capacity within the total porosity.

In the literature, the concept of "drainage porosity" is mentioned. This porosity, for a sample saturated with water, corresponds to the volume of the pores emptied by drainage under the force of gravity. The macro porosity is not the drainage porosity. It can be noticed in Figure IV-4 and Figure IV-5 that for the moisture content at field capacity or rather the state volumetric moisture content, there remains some water with meniscuses retained by capillarity within the pores of the macro porosity. The macro porosity is thus higher than the drainage porosity.

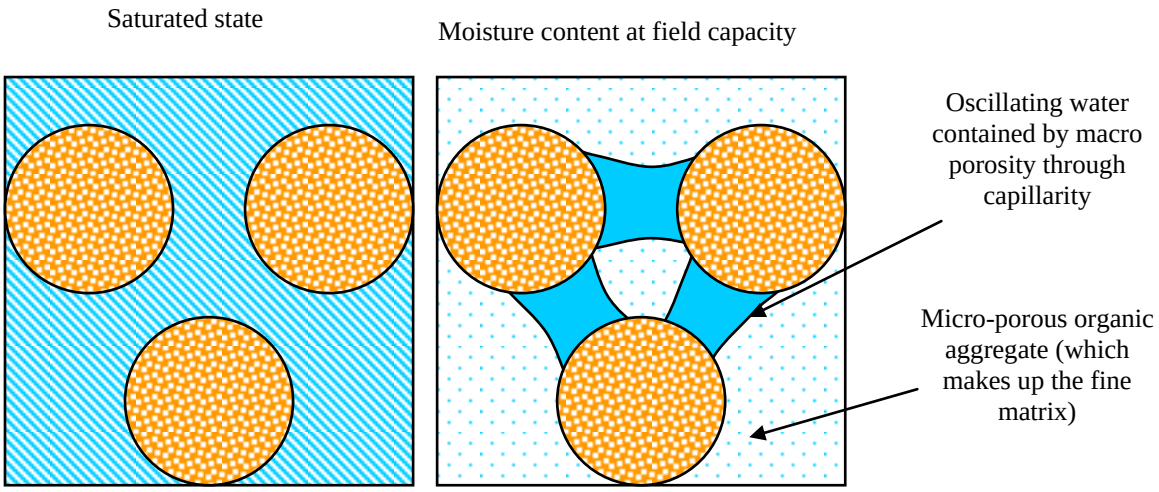

Figure IV- 5: Comparison of saturated moisture content and moisture content at field capacity.

IV - 1.3 Definition of the State Parameters of Macro and Micro Porosity

IV- 1.3.1 Fundamental Parameters

As specified in Chapter II, only three state parameters are sufficient to determine all the other structural parameters:

- density ρ of the sample
- porosity n
- moisture content w

For the double porosity model, w^{micro} is used to determine all the other parameters. Moreover, the evolution under compression of all the parameters of state of the model with double porosity can be given according to the settlement ΔH.

Characteristic state: A characteristic state is the state for which micro porosity is saturated with water along with the macro porosity which is dry:

- $w = w^{micro}$
- $\theta_L = n^{micro}$ and $\theta_G = n - \theta_L = n^{macro}$
- $S_L = S^{micro}$ and $S_G = 1 - S_L = S^{macro}$

IV- 1.3.2 Moisture Contents - Porosities - Degrees of Saturation

In the model, it is supposed that there exists a volume of micro pores noted V_V^{micro} and a volume of macro pores denoted as V_V^{macro} .

These volumes V_V^{micro} and V_V^{macro} make it possible to define:

- a content (mass) of micro pores, denoted as w^{micro} corresponding to the volume of micro pores V_V^{micro} compared on the basis of the dry mass of sample M_S : $\frac{w^{micro}}{\rho_L} = \frac{V_V^{micro}}{M_S}$. It is expressed in $\%_{MS}$ percent dry mass. w^{micro} corresponds to the moisture content when the whole of the volume of the micro pores is filled with water.

- a content (mass) of macro pores, denoted as w^{macro} and corresponding to the volume of macro pores V_V^{macro} compared on the basis of the dry mass of sample M_S : $\frac{w^{macro}}{\rho_L} = \frac{V_V^{macro}}{M_S}$. It is expressed in $\%_{MS}$ percent dry mass. w^{macro} is the complementary to w^{micro}, the sum of w^{micro} and w^{macro} corresponding to the maximum moisture content (at saturation) of the sample $w_{sat} = w^{micro} + w^{macro}$

- w^{micro} is not equal to the moisture content 'w' of the sample (but it is comparable). If $w < w^{micro}$, micro porosity is not saturated with water and if $w > w^{micro}$, it is extremely probable that the micro porosity is saturated with water.

- When considering the micro porosity and the macro porosity, it is the volume of pores divided by a total considered volume. In the model of double porosity, an assumption is made a propos the constant volume of the micro pores of micro porosity, in particular under compression. This results in considering w^{micro} as a constant. However, under compression, total volume varies, which induces a variation of $\frac{V_V^{micro}}{V_T}$. In practice, the w^{micro} term will be largely used to characterize micro porosity, because it can be easily understood, although it is not strictly the porosity.

The situation becomes complex, as presented in Figure IV-6 when $w > w^{micro}$ but the micro porosity is not saturated with water. Since this case can not be verified, this case is simplified by assuming that $w \geq w^{micro}$ which implies that micro porosity is saturated with water.

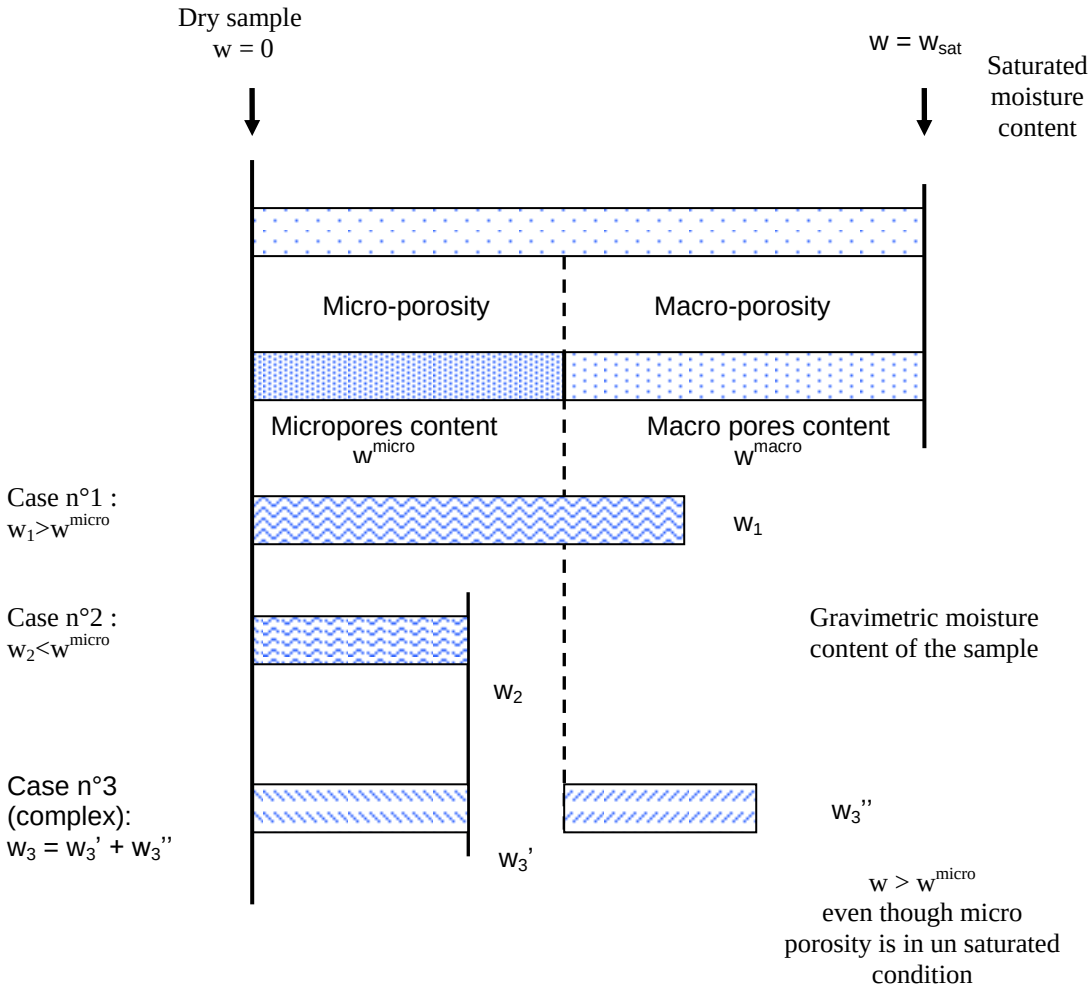

Figure IV- 6 : Comparison of the gravimetric moisture content with the moisture content of micro and macro phase.

From volumes of micro pores V_V^{micro} and macro pores V_V^{macro} two porosities are defined:

- a micro porosity: $n^{micro} = \frac{V_V^{micro}}{V_T}$.
- a macro porosity: $n^{macro} = \frac{V_V^{macro}}{V_T}$.

The sum of micro porosity n^{micro} and macro porosity n^{macro} corresponds to the total porosity, i.e. $n = n^{micro} + n^{macro}$.

Along with the porosity the degrees of saturation are defined as follows:

- a degree of saturation S^{micro} for the micro pores as $S^{micro} = \frac{V_V^{micro}}{V_V} = \frac{n^{micro}}{n}$.

- a degree of saturation for the macro pores S^{macro} as $S^{macro} = \frac{V_V^{macro}}{V_V} = \frac{n^{macro}}{n}$.

In the same way, the sum of S^{micro} and S^{macro} is equal to 1, $S^{micro} + S^{macro} = \frac{n^{micro} + n^{macro}}{n} = 1$

IV- 1.3.3 Relation between the Physical State Parameters

The state parameters of the model of double porosity can be expressed with reference to other parameters. First of all the expression of n^{micro} according to w^{micro} :

$$n^{micro} = \frac{\rho_d}{\rho_L} \times w^{micro} = \frac{\rho_S (1-n)}{\rho_L} w^{micro}$$

Macro porosity n^{macro} is deduced from the total porosity n:

$$n^{macro} = n - n^{micro} = n - \frac{\rho_d}{\rho_L} \times w^{micro} = \frac{\rho_S - \rho_d}{\rho_S} - \frac{\rho_d}{\rho_L} \times w^{micro}$$

IV- 1.3.4 Determination of the Residual Degree of Saturation *SrL*

In the law of capillary pressure of Van Genuchten (1980) and in the laws of relative permeability of Van Genuchten - Mualem, the degree of residual saturation S_{rL} as well as the effective degree of liquid saturation S_{eL} is defined as;

$$S_{eL} = \frac{S_L - S_{rL}}{1 - S_{rL}}$$

These two terms separate the two different sections: the first within which the water is motionless (residual saturation) and the second within which the water is mobile (effective saturation). The model of double porosity proposed by Stoltz (2009) identifies the residual degree of saturation S_{rL} with respect to the degree of saturation of S^{micro} micro pores such that

$$S_{eL} = \frac{S_L - S^{micro}}{1 - S^{micro}}.$$

The effective degree of saturation corresponds thus to the degree of liquid saturation of the macro porosity (Figure IV-7). It can be expressed in the following various ways as shown below

$$S_{eL} = \frac{S_L - S^{micro}}{1 - S^{micro}} = \frac{\theta_L - n^{micro}}{n - n^{micro}} = \frac{w - w^{micro}}{w_{sat} - w^{micro}}$$

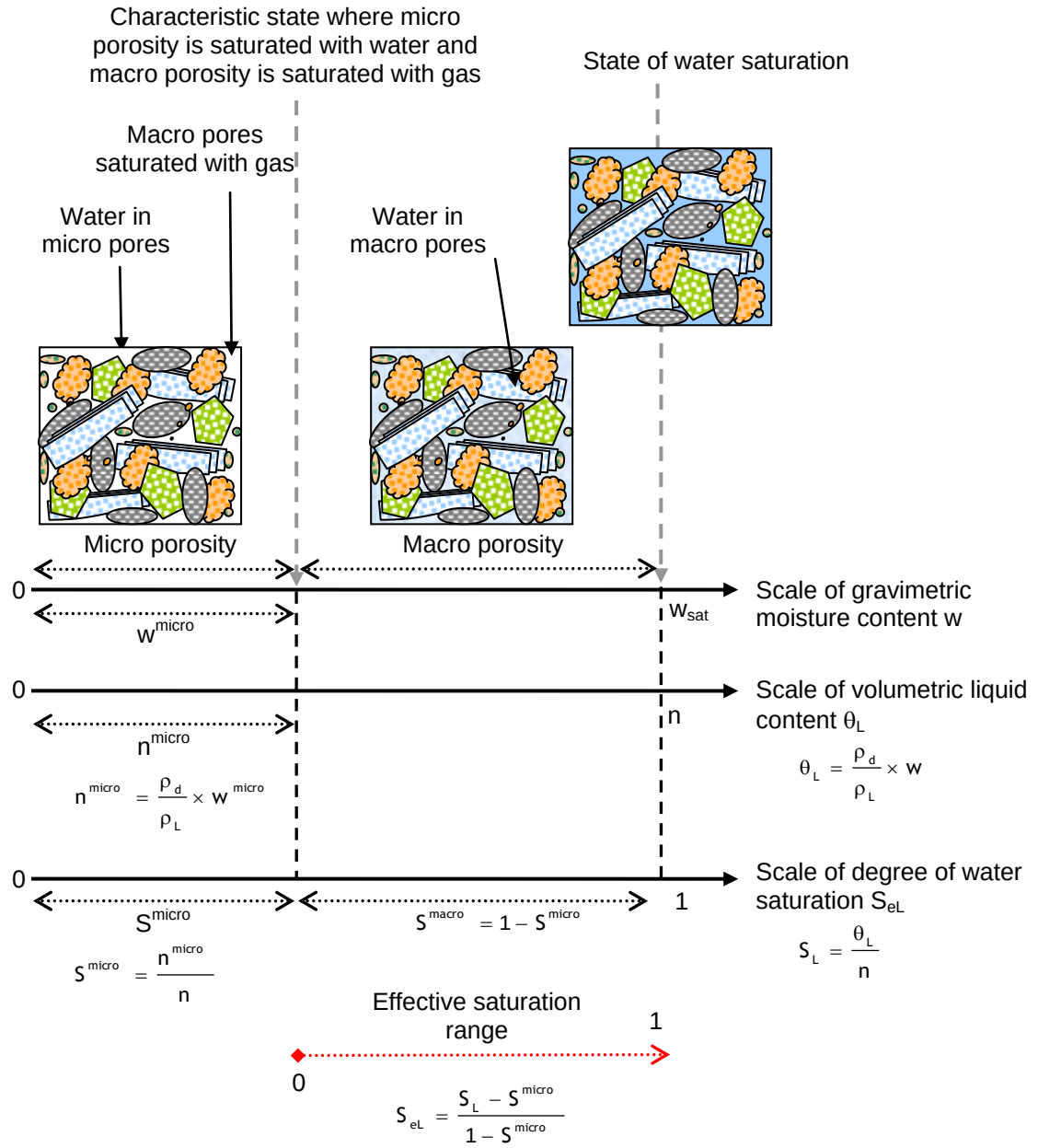

Figure IV- 7: Definition of various effective saturations with respect to the model of double porosity.

For the gas phase, the effective degree of gas saturation is deducted from the effective degree of liquid saturation, as:

$$S_{eG} = 1 - S_{eL} = \frac{S_G}{1 - S^{micro}} = \frac{\theta_G}{n^{macro}}$$

At the characteristic state when micro porosity is saturated with liquid ($w = w^{micro}$) then:

$$S_{eG} = 1 \text{ and } S_{eL} = 0$$

If $w < w^{micro}$ then:

$$S_{eG} > 1 \text{ and } S_{eL} < 0.$$

IV- 1.3.5 Gas Permeability

If the results obtained with the oedopermeameter for the gas permeability are considered not to be influenced by water present in the micro pores then the measurements of gas permeability make it possible to estimate w^{micro}. By considering a sample for given moisture content w undergoing a gas permeability test two cases are distinguished (Figure IV-8):

- When $S_L < S^{micro}$: micro porosity is not entirely saturated. In this case, a measurement of the gas permeability gives a value close to the intrinsic permeability k_i.
- When $S_L \geq S^{micro}$: micro porosity is saturated liquid and the gas permeability decreases with the increase in moisture content.

It is worth noting that the only saturation which influences the gas permeability is the one beyond saturation of micro porosity. The part of the degree of liquid saturation is defined on the basis of the characteristic state (saturation of micro porosity) with reference to the effective degree of saturation as $S_{eL} = \frac{S_L - S^{micro}}{1 - S^{micro}}$.

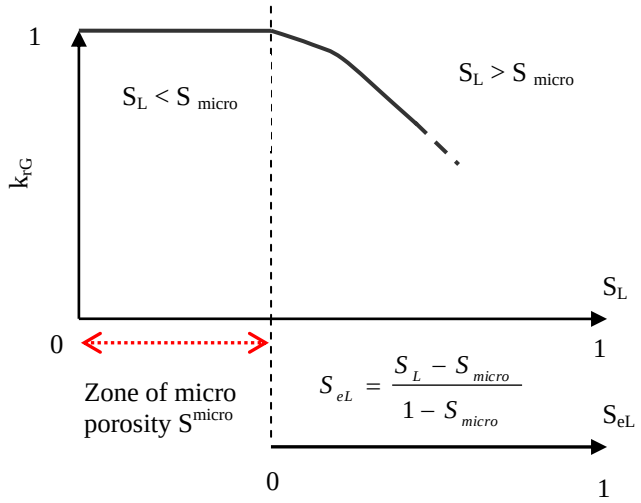

Figure IV- 8: Relative gas permeability trend as a function of degree of saturation for a dual phase medium.

The intrinsic permeability of material can thus be measured with gas if $S_{eL} \leq 0$. The unsaturated gas permeability can be expressed in two manners:

- According to the law of Carman- Kozeny simplified by expressing it according to the gas porosity for the gas flow when $w > w^{micro}$ it is $k_{KC} = C \frac{\theta_G^3}{(1-\theta_G)^2}$.
- According to the law of Van Genuchten - Mualem, with the above stated degree of effective saturation, as $S_{eL} = \frac{S_L - S^{micro}}{1 - S^{micro}}$.

IV-2 INTERPRETATION OF MEASUREMENTS OF GAS PERMEABILITY

IV - 2.1 Determination of the Parameter '*wmicro*'

This is the 'one' major parameter which needs to be determined for the whole analysis and interpretation of the measured gas permeability values for the verification of the model initially proposed by Stoltz (2009). This parameter actually separates the two porosities of the medium, the micro porosity from the macro porosity, in terms of the volumes of the micro pores V_V^{micro} within the fine matrix, $w^{micro} = \rho_L \frac{V_V^{micro}}{M_S}$.

IV- 2.1.1 From the Composition of the Waste

In the same manner as the constitutive density ρ_S of waste 'B' was determined from its composition (Chapter II), w^{micro} can also be estimated from the same composition. The micro pores content w^{micro} is supposed to correspond to the saturated moisture content of all the components.

In Table IV-1 the values of ρ_{dSi}, n_i and w_{sati} determined by Beaven et al. (1995) and Landva et al. (1990) are used for the calculations of w^{micro}. From the physical characteristics of each component '*i*' (dry density ρ_{di} and porosity n_i), the saturated moisture content w_{sati}, of each one of these components is calculated as

$$w_{sati} = n_i \frac{\rho_L}{\rho_{di}}$$

Table IV-1: Calculation of saturated moisture content of each component of the waste 'B' for the determination of 'w^{micro}'

Waste constituent	μ_{Si} (%$_{MS}$)	ρ_{dSi} (Mg/m^3)	n_{Si} (%)	w_{sati} (%)	w_i^{micro} (%)
Paper/carton	17.0	0.4	80	200	34
Plastics	13.2	1.0	0	0	0
Metal	0.7	6.0	0	0	0
Glass	9.8	2.9	0	0	0
Textiles	2.7	0.3	30	100	2.7
Wood	8.2	1.0	20	20	1.64
Food/Fines	39.0	1.0	20	20	7.8
Miscellaneous	9.4	2.6	0	0	0

The content of micro pores, (w_i^{micro}) for each component '*i*' is calculated according to their percentile proportion ($\mu_i = \frac{m_{si}}{m_s}$) with the following equation:

$$w_i^{micro} = w_{sati} \times \mu_i$$

The content of micro pores w^{micro} of the complete sample is calculated by summation of all the contents of micro pores of each component w_i^{micro} with the equation:

$$\overline{w}_{micro} = \frac{\sum_i w_{sati} \times \mu_i}{\sum_i \mu_i} = \frac{\sum_i w_i^{micro}}{\sum_i \mu_i} \text{ with } \sum_i \mu_i = 1$$

From the above values, the value of $\overline{w}^{micro} = 46.14 \ \%_{MS}$ is calculated. It should be noted that certain fractions do not have micro porosity such as plastics, metals, glass. The content of micro pores is mainly due to paper/paperboards and putrescibles (of which major part is contained in the category "fines").

IV- 2.1.2 From all the Measurements of Gas Permeability

For the estimate of the content of micro pores w^{micro} to be more precise, all the gas permeability values obtained from the tests of compression-gas permeability carried out in the oedopermeameter on waste 'B' were considered (section III-1.6). These tests can be characterized as having decreasing total porosity with constant total moisture content through out the length of compression stages (except where it drains during the compression stage).

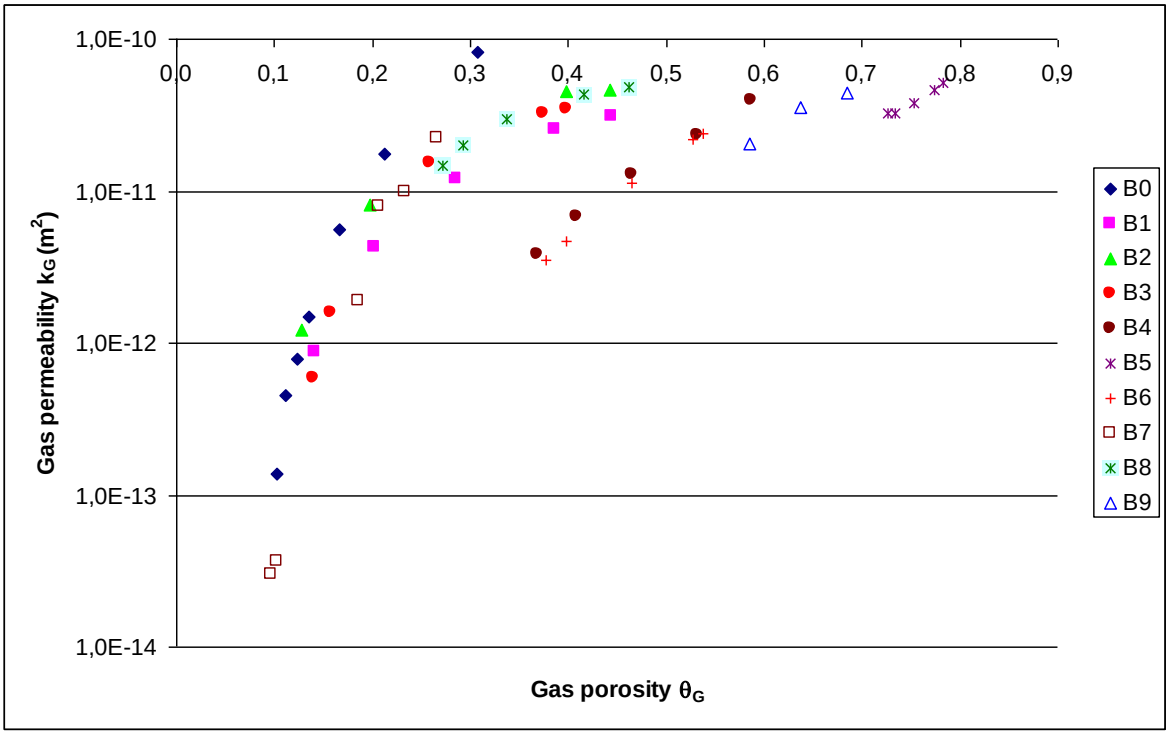

Graph IV- 1: Gas permeability as a function of gas porosity for Waste 'B' presented along the values determined by Stoltz (2009) for the same waste (Sample B0).

In Graph IV-1, only θ_G and k_G are presented while the same gas permeability measurements are plotted in Graph IV-2 as a function of total porosity 'n'. Meanwhile it is important to remember that almost all of the test series were performed on different samples of the waste 'B'. If two values of porosities obtained in experiments fell on two limits of anyone of the porosities quoted above, an interpolation (linear between the porosity and the logarithm of the permeability) needed to be carried out in such a way to determine the parameters n, w, θ_L, θ_G, k_G for the total porosities 77.5%, 75.0%, 72.5%, and 70.0% so that the values of gas permeability k_G fall in the range of same total porosity n.

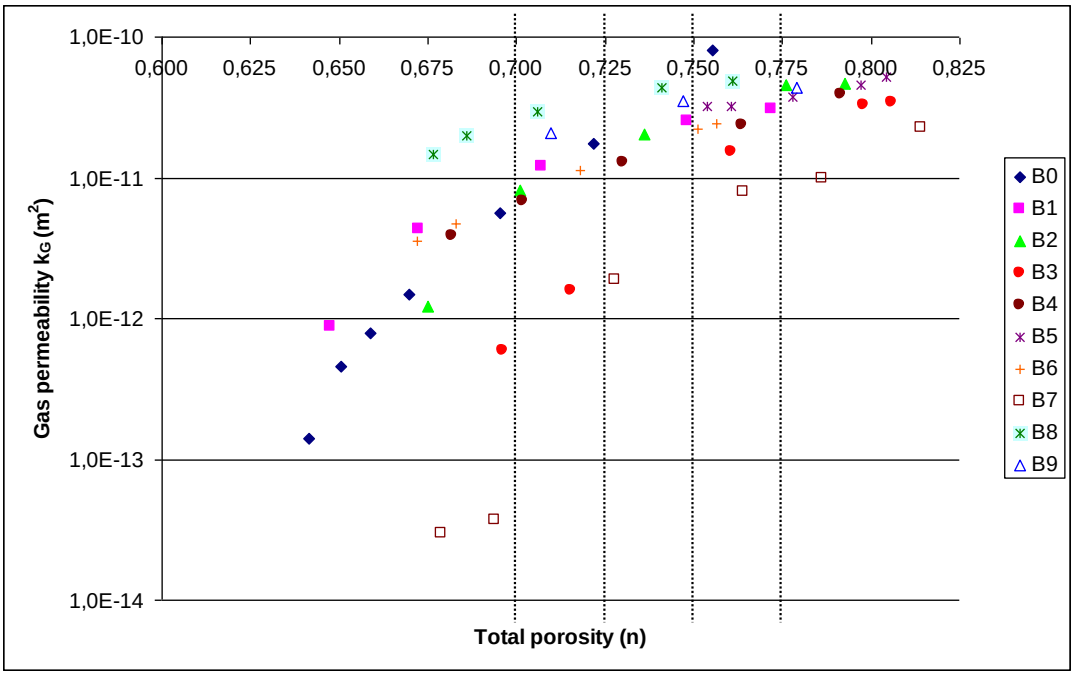

Graph IV- 2: Change in gas permeability as a function of total porosity of the sample during the compression-gas permeability tests Waste 'B'.

For these values of porosities (77.5%, 75.0%, 72.5%, and 70.0%), the gas permeability according to the gravimetric liquid content w are plotted in Graph IV-3. To standardize the graph for a comparison between the various levels of porosity, it is plotted against the ratio $k_{rG} = \frac{k_G}{k_{G\,max}}$. k_{Gmax} corresponds to the maximum gas permeability obtained for a given level of porosity (for example 70.0%).

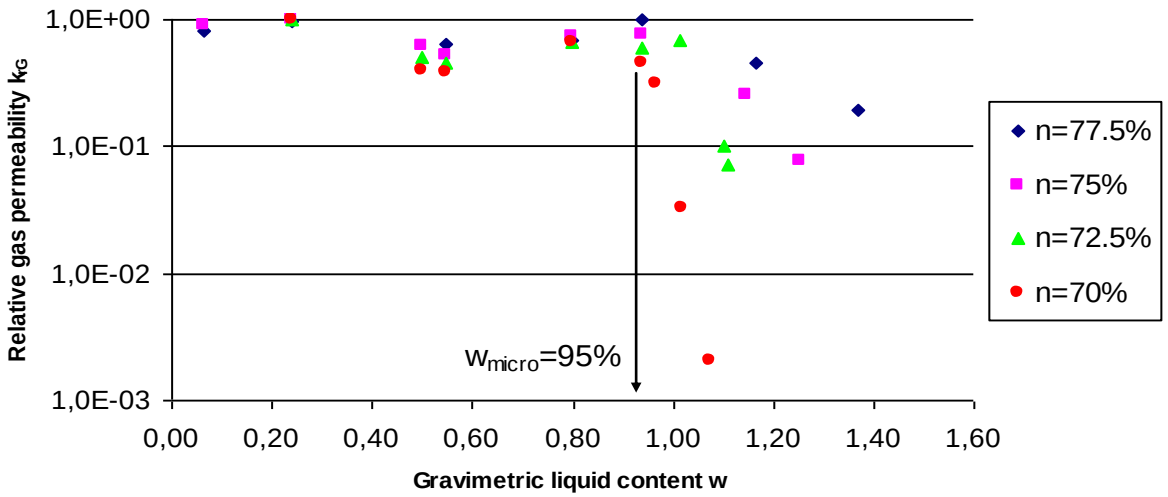

Graph IV- 3: Evolution of relative gas permeability k_{rG} as a function of gravimetric liquid content w for a given total porosity of the waste sample for Waste 'B'.

It can be noted in Graph IV-3 that the relative gas permeability k_G/k_{Gmax} for the gravimetric moisture content w < 95% remains close to the value of 1. Once this moisture content '*w*' exceeds 95%, the relative gas permeability k_{rG} decreases with the increase in the gravimetric moisture content *w*. This is why this gravimetric moisture content is considered as w_{micro} hereafter and the analysis of micro porosity is carried out with this value of w_{micro}.

IV - 2.2 Application of Double Porosity Model to the Gas Permeability Tests

The results obtained from the hydro-mechanical experiments in the oedopermeameter for the waste 'B' and waste 'C' are analyzed with the proposed double porosity model (Stoltz, 2009).

The gas permeability results have been presented keeping in mind the following hypotheses:

- Gas transport takes place strictly in the macro porosity thus any saturation or non saturation of the micro porosity of the medium has no influence over the gas permeability.
- Gas permeability values are corrected and used afterwards for the saturated micro porosity.

w^* corresponds to the corrected moisture content such that;

- For $w < w^{micro}$ (when the macro porosity is smaller than the gas content $n^{macro} < \theta_G$), $w^* = w^{micro}$ thus $\theta^*_G = n^{macro} = n - \rho_d.w^{micro}$
- For $w > w^{micro}$ (when the macro porosity $n^{macro} \geq \theta_G$), it is supposed that the micro porosity is saturated and that $w^* = w$ and $\theta^*_G = \theta_G$

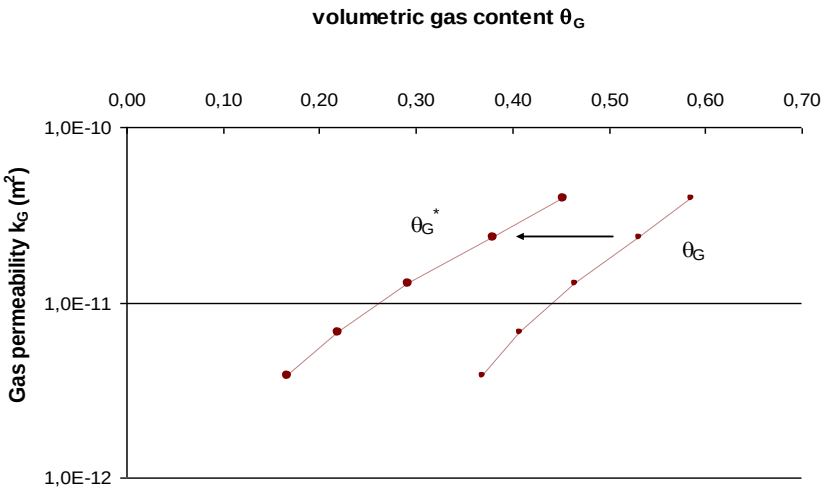

Graph IV- 4: Correction of gas permeability values measured from the compression-gas permeability tests for sample B4.

Table IV-2: Calculation of parameters of micro porosity for sample B4.

Compression stage (kPa)	w ($\%_{MS}$)	ρ_d (Mg/m^3)	n (%)	θ_L (%)	θ_G (%)	n^{macro} (%)	θ^*_G (%)	k_G (m^2)
20	0.55	0.376	0.791	0.205	0.586	0.453	0.453	$3.9\ 10^{-11}$
40	0.55	0.425	0.764	0.233	0.531	0.381	0.381	$2.4\ 10^{-11}$
80	0.55	0.486	0.730	0.266	0.464	0.293	0.293	$1.3\ 10^{-11}$
140	0.55	0.537	0.702	0.294	0.408	0.219	0.219	$6.8\ 10^{-12}$
200	0.55	0.573	0.682	0.313	0.369	0.166	0.166	$3.8\ 10^{-12}$

In Table IV-2 the calculation of corrected values of sample B4 are detailed to portrait the calculation carried out for all the samples of waste 'B'. In Graph IV-5 these corrected values of volumetric gas content are plotted as a function of gas permeability along with the measured values of gas porosity for sample B4.

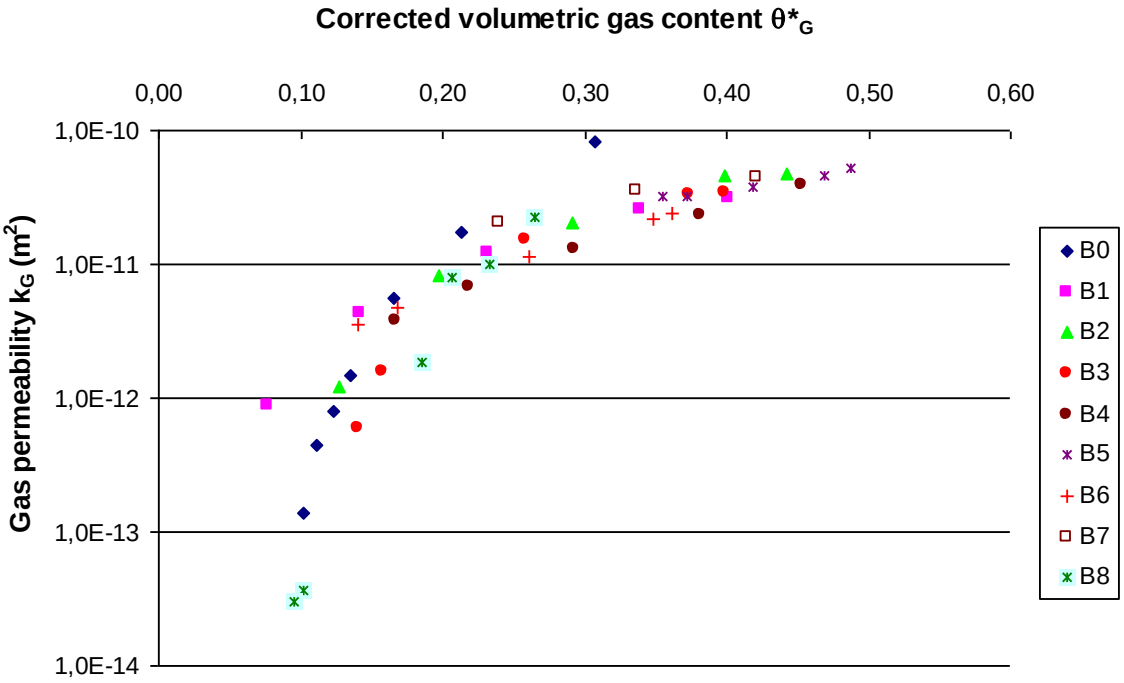

Graph IV- 5: Gas permeability (k_G) measurements plotted against the corrected gas porosity (θ^*_G) for Waste 'B'.

It can easily be observed that all the gas permeability curves which were sparsely located in the Graph IV-1, where it was plotted with calculated gas porosity, are now regrouped together within the same range of gas porosity. It can be stated the micro porosity is not concerned with the gas flow. Furthermore it can be stated that the gas permeability is mainly dependent upon the macro pores within the gas porosity.

IV - 2.3 Gas Permeability Modelling

Power Law

In Graph IV-6 the values of corrected gas porosity are plotted against the values of gas permeability according to the empirical power law. The proposed law suggests:

$$k_G(\theta^*_G) = a \times (\theta^*_G)^b$$

It can be observed in the Graph IV-6 that there is a linear relationship between the two parameters as:

$b = 3.39$ and $\log a = -8.98$ or $a = 1.0 \times 10^{-9}$

Such that $k_G = 1.0 \times 10^{-9} (\theta^*_G)^{3.39}$ with R^2=0.82

Even though till the present time there is no theoretical explanation available for this behaviour but it is interesting to note the linear behaviour of both the parameters according to the power law and any further experimentation and consequent analysis may reveal some explicable correlation.

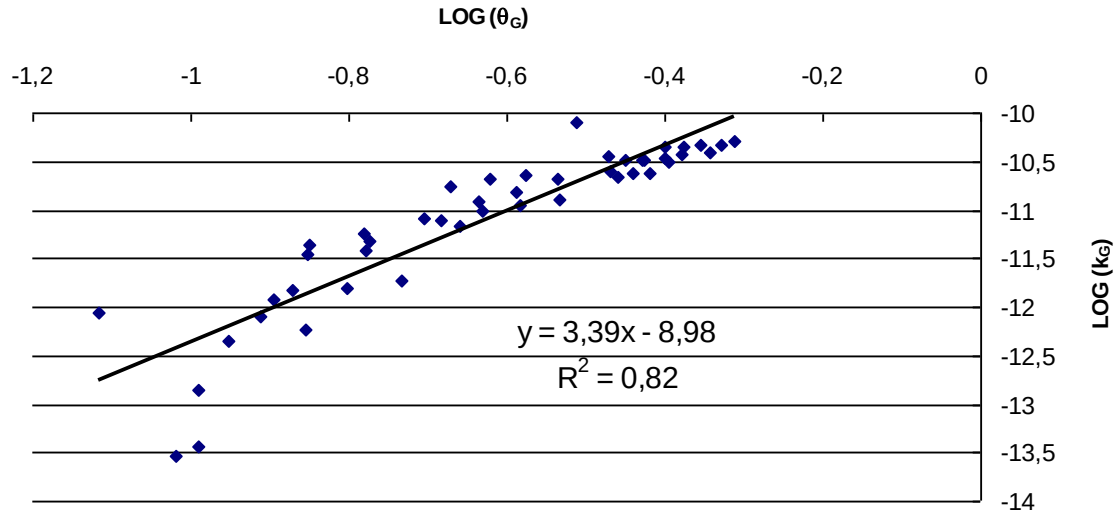

Graph IV- 6: Application of power law to the gas permeability values of waste 'B'.

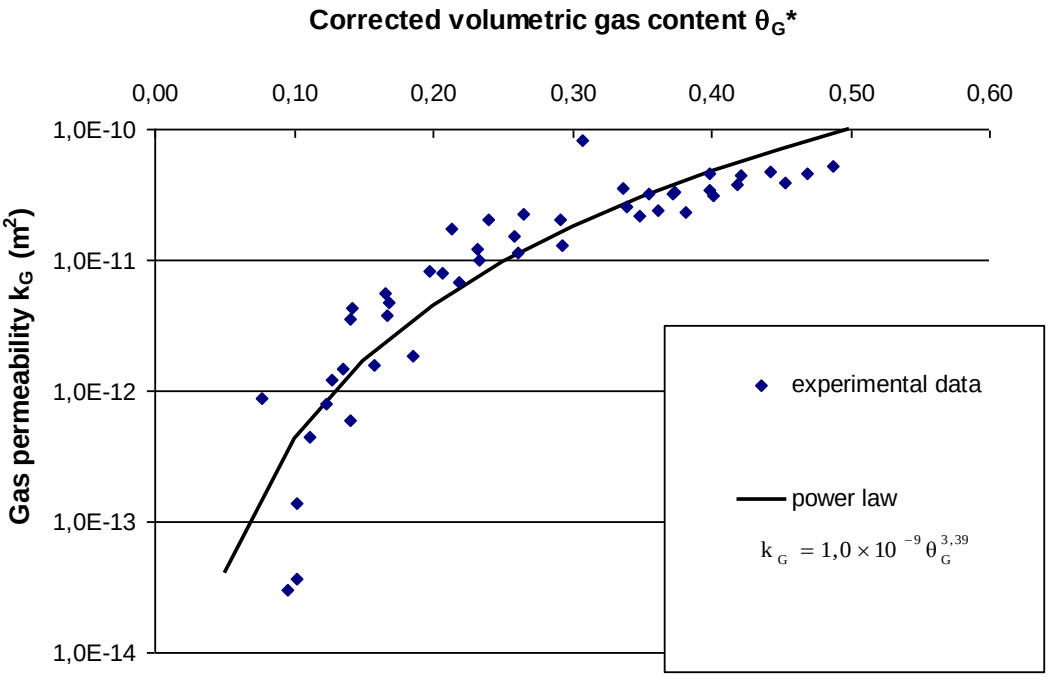

Graph IV- 7: Evolution of gas permeability as a function of corrected gas content of the samples as determined from the power law (waste 'B').

IV - 2.4 Intrinsic Permeability Modelling

Carman - kozeny law: To determine the probable relation of the intrinsic permeability with the micro porosity of the waste sample 'B' all the experimental values determined for the waste are considered such that:

$w \leq w_{micro}$ (non-saturated micro porosity)

thus $\theta^*_G = n_{macro}$ and $k_G = k_i$

Carman - Kozeny model, which is a function of macro porosity (responsible for the gas flow) is defined as:

$$k_i = \frac{1}{\tau}\frac{1}{S_s^2}\frac{(n_{macro})^3}{(1-n_{macro})^2} = C\frac{(n_{macro})^3}{(1-n_{macro})^2}$$

For the permeability measurements carried out in the oedopermeameter neither tortuosity τ, nor specific surface S_s is measured thus the Carman - Kozeny equation is simplified by considering that these two terms remain constant with compression. Thus $k_i = C\frac{n_{macro}^3}{(1-n_{macro})^2}$ where C is taken as a constant $C = \frac{1}{\tau}\frac{1}{S_s^2}$. Plotting the values of intrinsic permeability values of the waste samples as a

function of macro porosity (Graph VI-8) the value of constant C = 1.53E^{-10} m^2 is determined with R^2 = 0.588 so that $k_i = 1.53 \times 10^{-10} \frac{n_{macro}^3}{(1 - n_{macro})^2}$

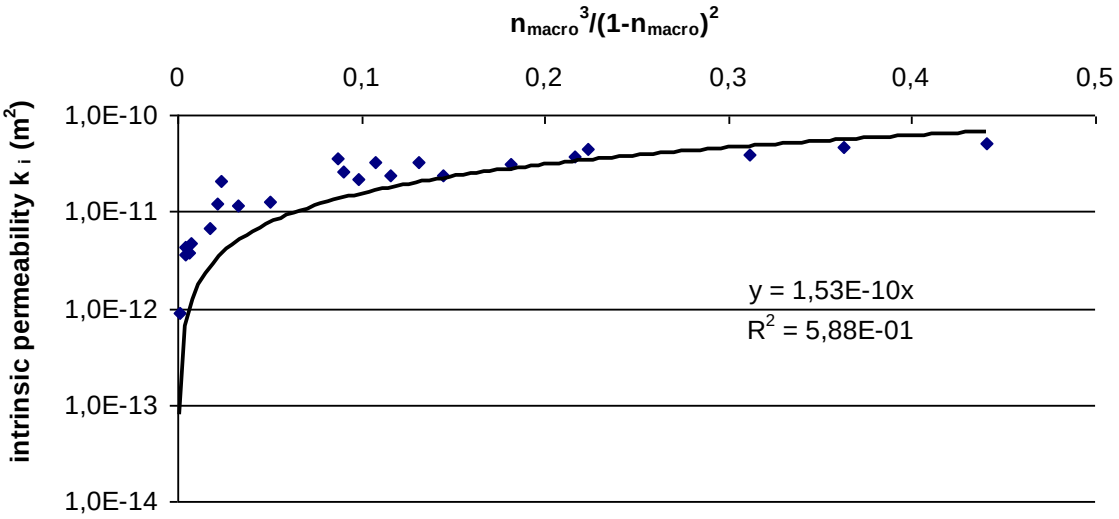

Graph IV- 8: Intrinsic permeability as a function of macro porosity of the waste samples (B).

Power Law: As applied earlier to determine the relationship between the gas permeability (k_G) and the volumetric gas content (θ_G), same power function is applied to the macro porosity of the medium such as:

$$k_i(n_{macro}) = a \times (n_{macro})^b$$

All the calculated values of the intrinsic gas permeability measurements for the waste 'B' plotted as a function of macro porosity (Graph IV-9), suggest the following relationship:

$b = 2.19$ and $\log a = -9.6$ or $a = 2.51 \times 10^{-10}$ such that;

$k_i = 2.51 \times 10^{-10} n_{macro}^{2.19}$ with $R^2 = 0.96$

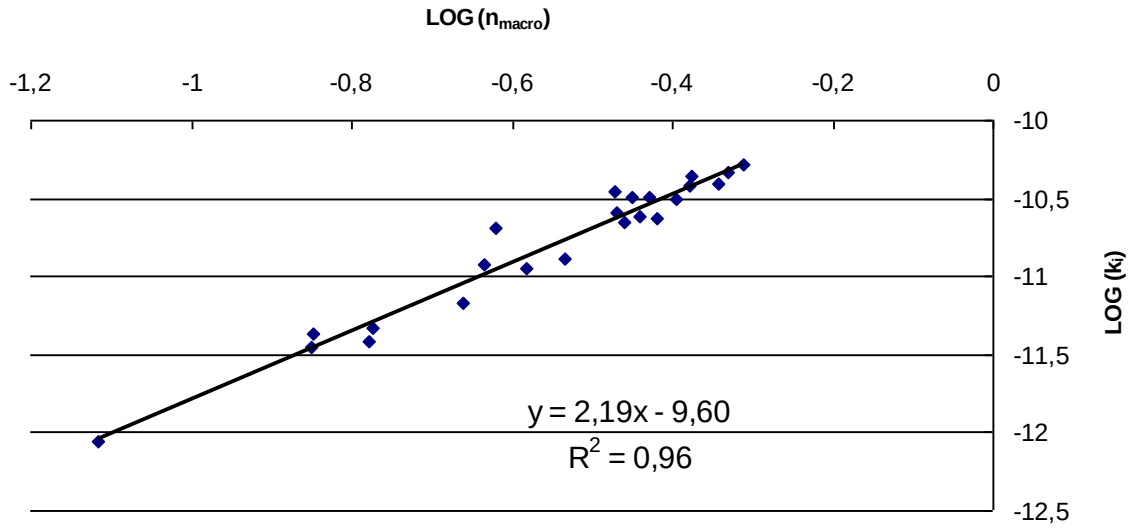

Graph IV- 9: Application of power law to analyse the correlation of macro porosity and the gad porosity of the waste samples (waste 'B').

Finally the two laws, power law and Carman –Kozeny law are plotted on the same graph with the experimental values determined during the present study to observe the best fit out of these two laws (Graph IV-10) and it is observed that the power law describes better the determined values of intrinsic values.

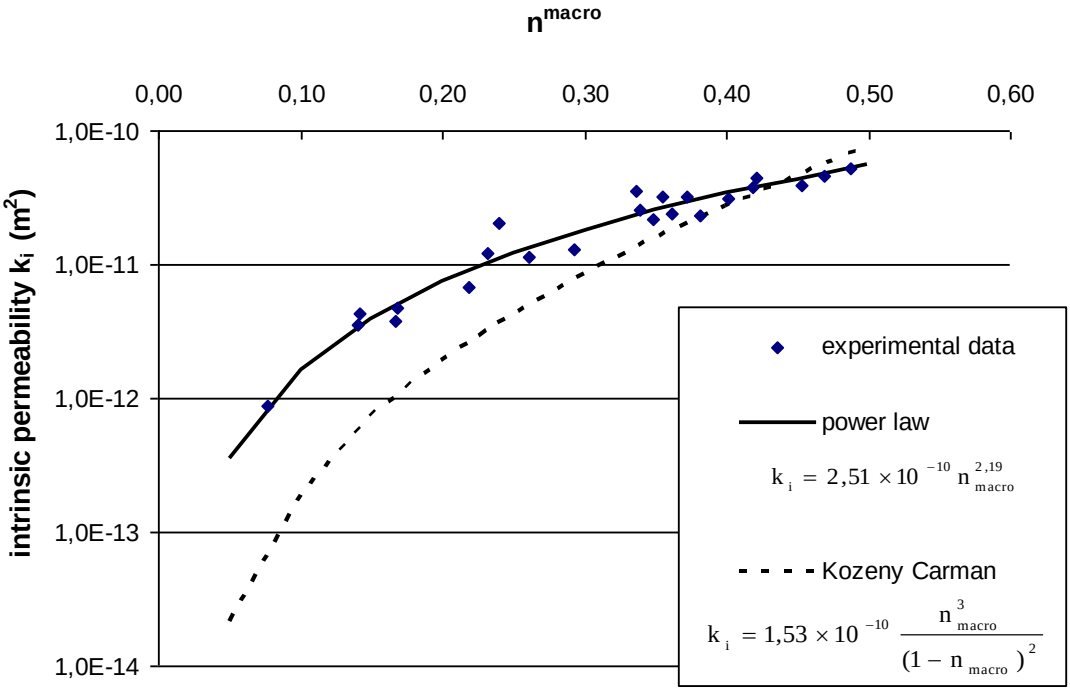

Graph IV- 10: Experimental data along with the power law and the Carman Kozeny law (Waste 'B').

IV - 2.5 Relative Gas Permeability Modelling

For the present modelling, the model of Van Genuchten – Mualem is used. This law is written as $k_{rG} = \frac{k_G}{k_i} = (1 - S_{eL})^{\gamma} (1 - S_{eL}^{1/m})^{2m}$ and is formulated with respect to the total porosity. The model is rewritten in accordance with the assumptions that the residual degree of saturation S_{rL} corresponds to the degree of micro saturation S^{micro} for the characteristic state (saturation of micro porosity). For the experiments carried out for waste 'B', the total porosity values used for the determination of w^{micro} (70.0%, 72.5%, 75.0%, and 77.5%) provided with a set of values of w, θ_G and k_G and thus $S_L = \frac{\theta_L}{n}$ and $S_G = \frac{\theta_G}{n}$ are calculated such that the effective degree of saturation is:

- For the samples where $w < w^{micro}$, $S_{eL} = 0$
- For sample with $w > w^{micro}$, $S_{eL} = \frac{S_L - S^{micro}}{1 - S^{micro}} = \frac{\theta_L - n^{micro}}{n - n^{micro}} = \frac{w - w^{micro}}{w_{sat} - w^{micro}}$

k_{rG} is calculated with the equation $k_{rG} = \frac{k_G}{k_i}$ supposing that the intrinsic permeability k_i corresponds to the moisture content inferior to the moisture content of the micro pores i.e. w^{micro}. Graph IV-10 is presented with the calculated values of relative gas permeability as a function of effective saturation.

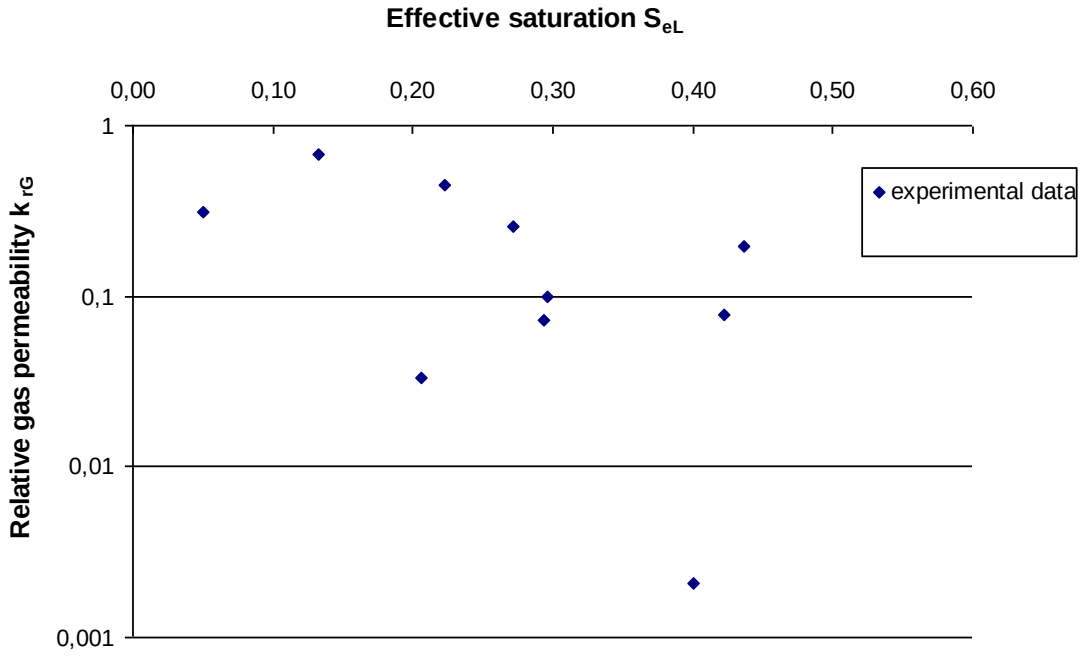

Graph IV- 11: Graph of relative gas permeability values as a function of effective saturation.

From the Graph IV-11 any probable modelling of the experimental data of the present study seems to be delicate as all the values are scattered. In the present case it would be reasonable to contend only with calculated values of the relative gas permeability $k_{rG} = \frac{k_G}{k_i}$ for the calculation of k_G and k_i, which have been presented in § IV-2.3 and IV-2.4 with the power law (i.e. $k_G = 1.0 \times 10^{-9} (\theta_G^*)^{3.39}$ and $k_i = 2.51 \times 10^{-10} n_{macro}^{2.19}$).

IV - 2.6 Conclusions regarding the Model of Double Porosity and Permeability Modelling

The analysis of gas permeability tests for waste 'B' confirms the presence of micro porosity which is calculated for the waste 'B' as equal to w_{micro} = 95%. The application of the double porosity model as proposed by Stoltz (2009) have helped present the gas permeability as a function of the corrected gas porosity θ^*_G. With the help of these corrected gas porosity measurements plotted along the gas permeability measurements, presence of a spindle is observed (Graph IV-5) which suggests the attainment of same gas permeability values through application of various available processes whether it is the increase in the compression of the sample or/and the increase in the moisture content of the medium. This spindle in turn helps in modelling the gas permeability in such a way that there is unique relationship which exists for these gas permeability values and the corrected gas porosity values of the medium. From the analysis of the present study this unique relationship is proved to be the power law.

Similarly according to the hypotheses of double porosity model, the measured value of gas permeability for the case when $w \leq w_{micro}$ makes it possible to evaluate the intrinsic permeability k_i of the medium. This value of intrinsic permeability value has been modelled through two different laws as a function of macro porosity n_{macro} of the medium. One of the laws is an adaptation of Carman-Kozeny's law of double porosity while the other is the power law. The application of these two laws for MSW in landfills would eventually help the landfill operators to predict the permeabilities (intrinsic and gas permeability) within the waste body.

V- MUNICIPAL SOLID WASTE SETTLEMENT BEHAVIOUR

With respect to time the settlement may be broadly divided into 3 phases; instantaneous, primary and secondary settlement. While instantaneous and primary settlements are not a function of time and secondary settlement is dependent upon time. Prediction of long term settlement behaviour is important for a successful future development of the site. Prediction of settlement rate is more important than the total settlement. With a total settlement range of 25% to 50% of the initial waste height, more than half is attributed to secondary settlement Wall and Zeiss (1995). Since settlement is one of the major constraints to the re-use of any landfill it is important to predict settlements accurately to be in a good position for the landfill site development, operation and closure. Furthermore a proper design of gas and leachate collection system requires an accurate prediction of settlement.

Five mechanisms governing the secondary settlement of MSW have long been defined as mechanical, ravelling, physicochemical change, biochemical decay, and interaction among these mechanisms. As ravelling is the process in which after load application, waste particles bend, crush, and relocate themselves to better accommodate the new stress situation forming the mechanical deformation. Also, due to the wide range of waste particle sizes, small particles will tend to move into the voids of larger ones, causing additional settlement especially during compaction. It is usually difficult to distinguish ravelling from other mechanisms. Physicochemical changes (such as corrosion, oxidation, and combustion) and biochemical decay causes a decrease in waste mass, leading to additional vertical deformations. Last but not the least, interactions between these mechanisms may cause further subsidence, such as when methane and heat are released from decay support combustion, or when consolidation triggers ravelling. The mechanism governing the settlement discussed by researchers:

- Physical compression due to bending, pressing reorientation and crushing
- Ravelling settlement due to migration of particles
- Consolidation phenomenon and viscous behaviour
- Decomposition settlement due to organic components
- Collapse of components due to corrosion, oxidation and degradation of inorganic components

V-1 STAGES OF SETTLEMENT

Three main stages of settlement have been identified, namely, initial compression, primary compression, and secondary compression. In literature initial settlement and primary settlement are sometimes considered different phenomena but in the framework of the present study an overall primary settlement is considered since it is not realistic at this scale to distinguish them promptly.

Initial settlement, which is virtually instantaneous, is defined as settlement that occurs directly when an external load is applied to a landfill. It is generally associated with the immediate compaction of void space and particles due to the compaction effort and the superimposed load.

Primary settlement is consolidation generally due to the dissipation of pore water and gas from the void space. In general, it is considered to occur within 30 days after the placement of the final layer. However, there are indications that dissipation processes may not be responsible for primary settlements in MSW landfills. First, waste in municipal landfills is seldom saturated, because traditional management practices prohibit the entry of water in the landfill. Second, the permeability of waste has been characterized in the same order of magnitude as sand and gravel or less for fresh waste; therefore, no pore water pressure should develop, because liquid can readily escape from the landfill mass. In some cases, however, gas pressure is generated due to the initial degradation of the waste. The load induced instantaneous consolidation in landfill is compared to the consolidation settlement of fine grained soils. Many researchers have investigated its comparison e.g. Jessberger et al. (1993), Beaven et al. (1995). In general it is dependent upon composition and age of waste and the compaction effort. The compressibility of the waste is characterised by coefficient of primary compression C_R which is derived from the one dimensional consolidation theory of the pre-consolidated waste.

Secondary settlement is due to creep of the waste skeleton and biological decay. In general, settlement due to secondary compression accounts for 30 to 40 % of the total landfill settlement, and occurs over many years after closure at a continuously decreasing rate, depending on stabilizing process within the landfill. Long term settlement of a landfill is referred to as the secondary settlement which is assumed to be independent of the load but is dependent upon time and biodegradation effects. One dimensional consolidation theory of soils is used for the settlement with the coefficient of secondary compression $C_{\alpha\varepsilon}$ which in turn depends on other parameters such as the time of construction of the waste column, initial degree of compression, recirculation of leachate if any and other bio-chemical factors yet to be correlated with the phenomenon of time dependent settlement. For the post operation settlement it is not the primary settlement which is important since it is almost completely incorporated before landfill closure, but it is the component of secondary settlement which

play an important role throughout the life time of a waste body. On average, settlement of about 15 to 20 % of original landfill thickness is expected due to waste decomposition.

V - 1.1 Settlement Rates

The rate of landfill settlement depends primarily on the waste composition, operational practices, and factors affecting biodegradation of landfill waste, particularly moisture content. While settlement rates usually decrease with time, such rates may increase at a later stage as a landfill undergoes active biological activity. Several factors affect the magnitude and rate of settlement as described in Table V-1.

Table V- 1: Factors affecting magnitude and rate of MSW settlement.

Factors	Observations
Initial void ratio of the waste	Larger initial densities (associated with greater compaction) reduce both the ultimate settlement as well as the rates of primary and secondary settlement.
Waste composition	Waste compressibility increases as the amount of biodegradable material increases.
Applied stress and stress history	Some mechanisms affecting settlement (creep and pressure dissipation) are affected by the ratio of load increase.
Environmental conditions	Waste exposed to favourable decomposition conditions usually exhibits an increase in secondary compressibility behaviour as opposed to waste exposed to unfavourable decomposition conditions.

V - 1.2 Settlement Analyses Available in Literature

The prediction of long term settlement is done making use of one dimensional consolidation theory of soils, with coefficient of secondary compression $C_{\alpha\varepsilon}$ which in turn depend on other parameters namely time of construction of the waste body, initial degree of compression, recirculation of leachate and other bio-chemical factors yet to be correlated with the phenomenon of time dependent settlement. The factors affecting secondary settlement are well known to an environmental engineer, what is uncertain is their inter-dependency. Initially different models have been developed and applied based upon laws of mathematics, mechanics or biochemistry, they all work fairly well within a framework of hypotheses and implications but each one of them has its limits to which its workability is defined and

there is always a need to move one step further in assessing the waste behaviour with respect to the settlement.

V- 1.2.1 Compressibility & Stiffness

For saturated soils it is usually assumed that the particles and pore fluid are incompressible and any change in overall volume results from the rearrangement of the soil skeleton. However this assumption of incompressibility for domestic waste is not appropriate. Likewise soil deformation due to dissipation of pore water pressure is termed as consolidation and continued deformation at constant effective stress is known as secondary compression or creep. Creep is a function of logarithm of time and it is applied in mathematical models to predict long term settlement of solid waste which might not be satisfactory since there are biological as well as chemical factors involved in degradation thus settlement of a domestic waste. So there is a need to correlate settlement to degradation and chemical reactions within the waste in a model. Similarly low stiffness of household waste material results in the movement of a barrier into the waste until equilibrium conditions are established. Landfill barriers are a necessity we cannot avoid, their interaction with the waste confirms the structural integrity and hence performance. The assessment of this interaction between the waste body and barrier system requires the in situ stress information.

Dixon et al. (1999) used the pressure meter to measure horizontal stress, lateral stiffness of the waste and their time dependent variation. The authors performed the self boring pressure meter tests to determine a relationship between the applied pressure and deformation of the material as well as to obtain in situ stress conditions and the deformation properties. In the cylindrical device gas pressure produces outward expansion and radial deformation of the waste along with the applied pressure is used to develop a relation for in-situ conditions and deformation properties of the waste. Radial expansions against applied pressures are logged and plotted as loading curves to report strength and stiffness parameters (shear modulus, shear strength) making use of the coefficient of lateral earth pressure K_0.

Tests were performed on various depths and ages of the waste. Unloading and reloading confirmed the strain hardening effect in the waste while no clear relationship between lateral and vertical stress was obtained, nevertheless a general trend of higher K_0 in the upper layers of the waste column could be assigned. A pronounced relationship between shear modulus and the depth of fresh water was observed that might be a product of additional compaction of the capping layer resulting in higher density and stiffness of upper layers. Likely increase in shear modulus (G) with increasing pressure and lateral stress was noticed. Though a reasonable agreement of values was obtained at laboratory scale and at field, however, the authors suggested that the in-situ measurement of the stiffness

parameter is the most appropriate approach. Finally they recommended a numerical model development for assessment of a range of barrier system performance.

Gotteland et al. (2001) carried out an experimental study on MSW landfill at Montech France to determine compressibility, shear strength parameters and settlements. In situ unit weight was measured and compression-shear box tests were performed to determine C_R and confirm c (cohesion) and φ (angle of internal friction). However no conclusions were made to the models exploited for the determination of secondary settlement.

V- 1.2.2 Study of Settlement Data of MSW

Deformation measurements are performed at site during and after the construction of landfill to estimate the future settlements. There are different measurement techniques available for the instrumental follow-up ranging from surface settlement measurements to a three dimensional laser study of deformation.

Kavazanjian et al. (1999) performed oedometer tests to evaluate different components of compression, immediate compression and the mechanical component of delayed volumetric compression. Both the immediate and the delayed compression were studied and the immediate response was found be following the behaviour of a soil with a mean value of an average modified compression index, Cc = 0.185 (with a range 0.121 to 0.247). They used the average modified coefficient of recompression (C_R = 0.012) to characterise the relationship of immediate volumetric compression and the normal stress during reloading where the range was from 0.003 to 0.017. Likewise they used modified coefficient of secondary compression ($C_{\alpha\varepsilon}$) for the relationship between mechanical component of the delayed volumetric compression and elapsed time. A mean value of 0.0035 was used to characterise the relationship for a range of $C_{\alpha\varepsilon}$ from 0.01 to 0.0000066, though the laboratory rates of secondary compression were less than those back calculated from the field data.

Coumoulos et al. (1999) examined and proposed alternation curves of vertical strain rates to predict long term settlement. The basic assumption of the study was the long term settlement under self weight which can be approximated by a straight line when plotted against logarithm of time (Figure V-1). According to authors observations 'a landfill which is constructed rapidly, has higher settlement rate than the one with longer period of construction'. Settlement slope and vertical strain is expressed as;

$$\Delta H / H = C_{\alpha\varepsilon} \log\left(t / t_1 \right) \qquad \text{(slope of the curve)}$$

With t and t_1 being elapsed time on secondary settlement curve after closure.

$$\frac{d(\Delta H / H)}{dt} = \frac{0.434\, C_{\alpha\varepsilon}}{t}$$

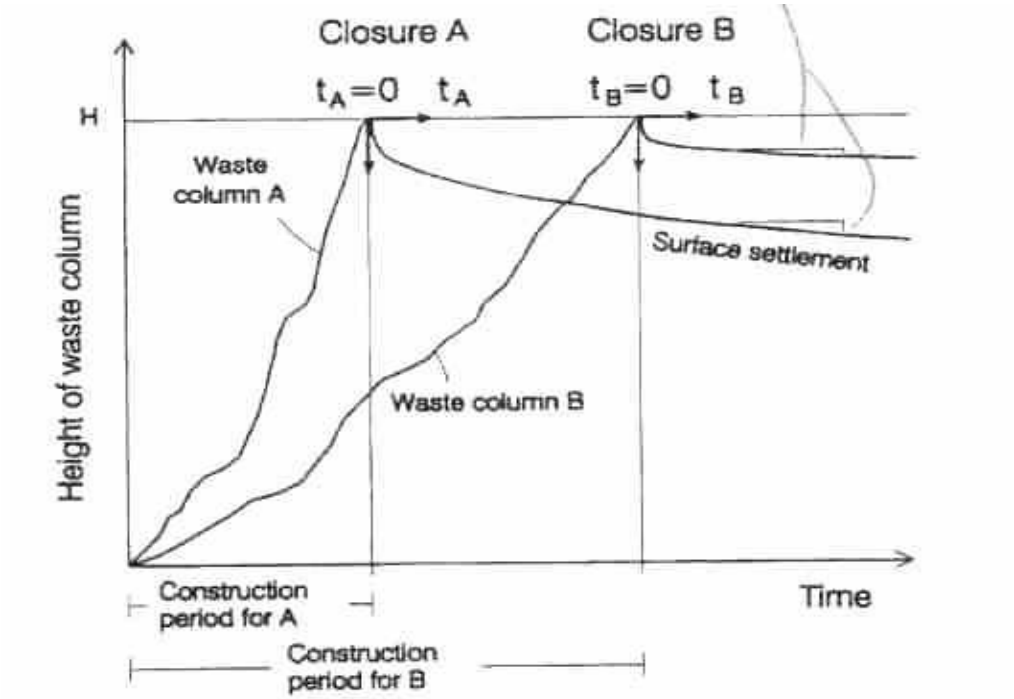

Figure V- 1: Time settlement curves of similar waste columns with different construction periods (Coumoulos et al., 1999).

The authors made use of the above equation as an attenuation equation (Figure V-2) to explain the behaviour of solid waste at already monitored sites to propose $C_{\alpha\varepsilon}$. This analysis was carried out with a range of values of $C_{\alpha\varepsilon}$ and the plotted settlement data confirmed the attenuation affect of vertical strain rate with time; however no data other than construction history were available which could be of help for long term settlement behaviour. As the accuracy of predicting attenuation of vertical strain rate depended upon the accuracy with which $C_{\alpha\varepsilon}$ was determined, (which in turn is accurate when both time settlement data and date of closure is available) it was found that most of the data close to attenuation curve corresponded with $C_{\alpha\varepsilon}$ = 0.07.

The authors compared the value of $C_{\alpha\varepsilon}$ for the waste to those of soils. Since there was no available data to date of $C_{\alpha\varepsilon}$ values for soil under self weight they performed consolidation of thin water clay slurry of (CL) under unified soil classification system with LL of 43 and PL 21 for 99% of fines. It was observed that $C_{\alpha\varepsilon}$ was close to or higher than 0.02 (Figure V-3) and that for denser slurries would further report higher values.

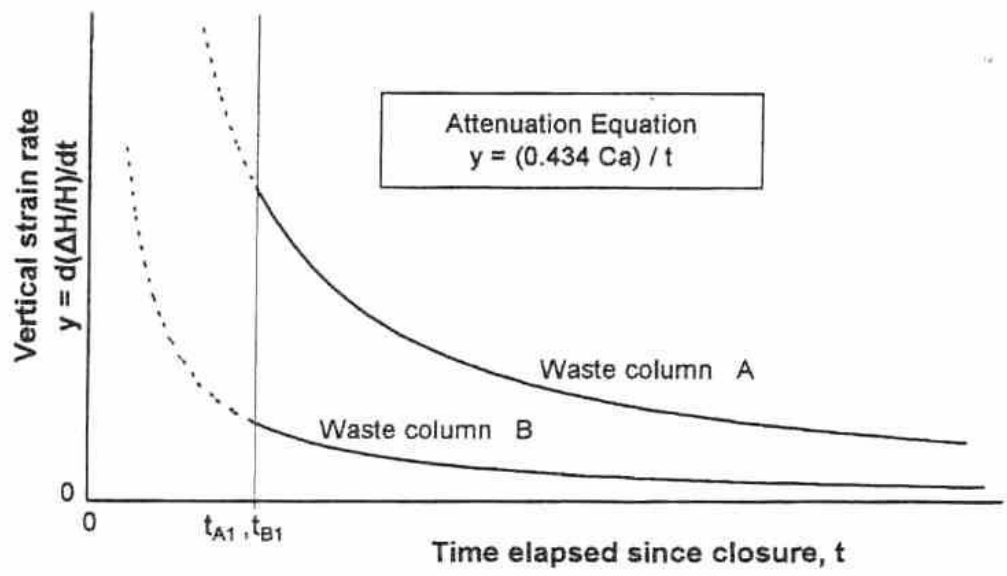

Figure V- 2: Attenuation graph as proposed by Coumoulos et al. (1999).

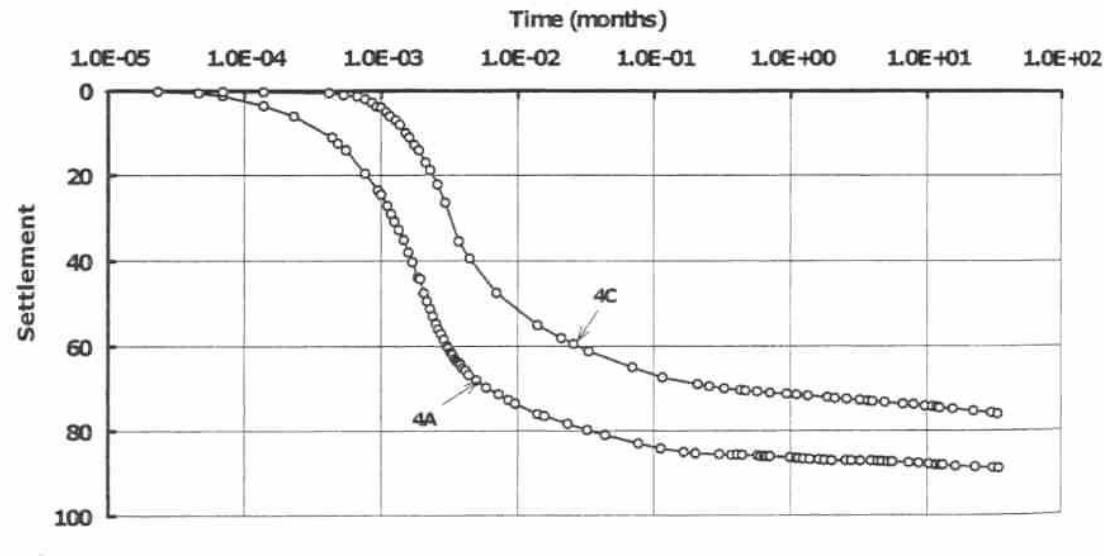

Figure V- 3: Settlement for soils under self weight (Coumoulos et al., 1999).

Table V- 2: Geotechnical data of the slurries (Coumoulos et al., 1999).

Test	Initial dry unit weight (t/m^3)	Dry unit weight at the end of the test (t/m^3)	C_α
4A	0.048	0.43	0.017
4C	0.124	0.54	0.028

Typical values of coefficient of secondary compression for soils under surcharge by different authors e.g. Lambe (1951) as follows were quoted and data for slurries under self weight is summarised in Table V-2.

- Normally consolidated clays $C_{\alpha\varepsilon}$ = 0.005 to 0.02
- Organic soils $C_{\alpha\varepsilon}$ = 0.03 or higher

Ivanova et al. (2003) carried out a prototype settlement study at laboratory scale and investigated various physical and chemical properties of the solid waste which play part in the settlement but they were unable to properly propose reliable results for their findings related to secondary settlement in the MSW. They identified the waste composition utilised for test purpose, calculated the total carbon (TC) and total nitrogen (TN) and determined the calorific values. They performed biochemical methane potential test (BMP) and concluded that the sample with 10% sludge increased the waste decomposition as witnessed through anaerobic methanogenic condition, waste degradation and gas production.

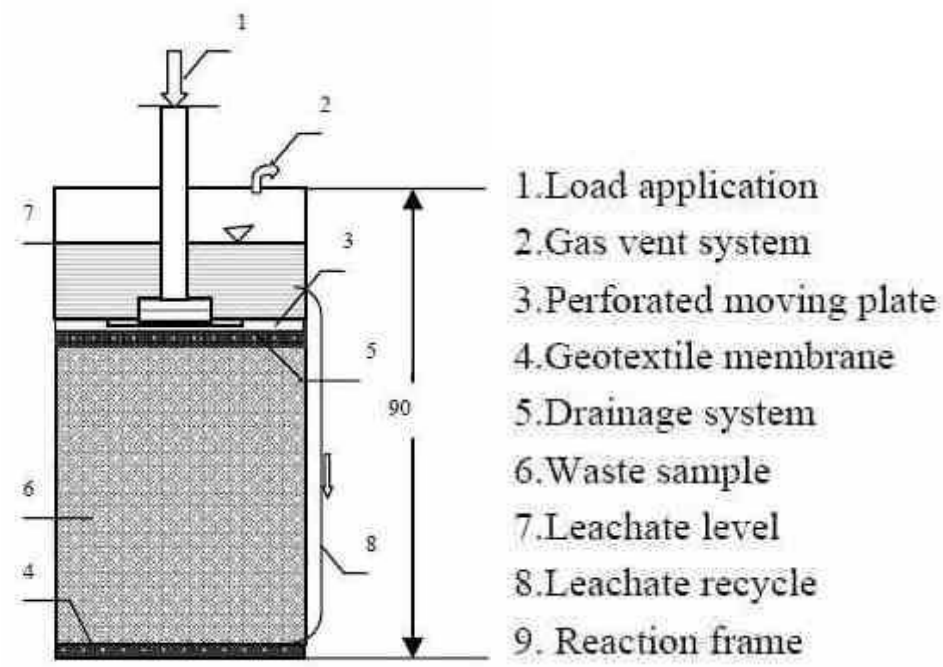

Figure V- 4: Schematic diagram of consolidating anaerobic reactor (Ivanova et al., 2003).

Consolidating anaerobic reactors (CAR) were used to study settlement (Figure V-4), which were, however inadequately compacted. Settlement prediction graphs were analysed (Figure V-5) but due to the new study en route in CARs the authors suggested more investigation rather than drawing any conclusions. They cited the relative importance of various components still to be explored.

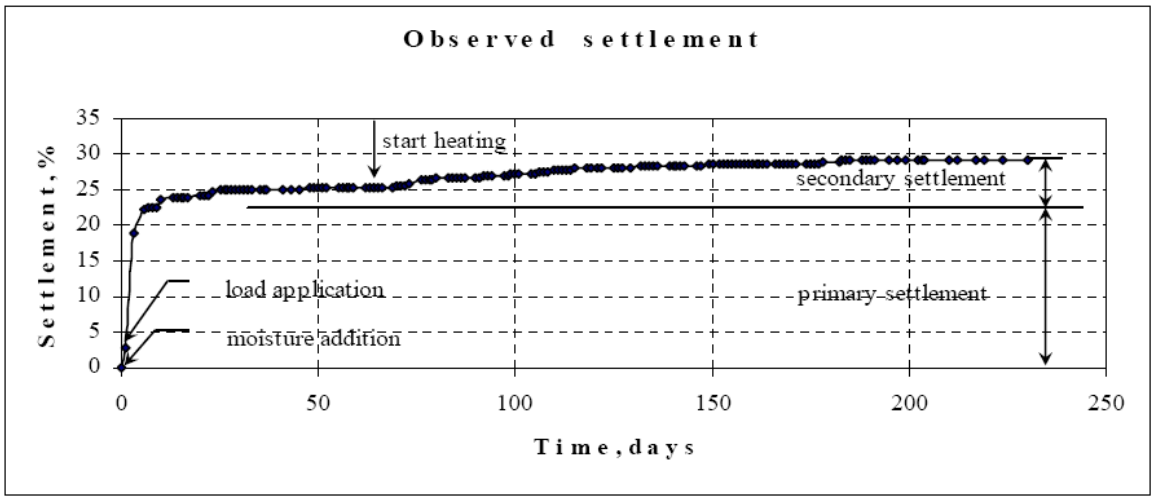

Figure V- 5: Settlement as studied in consolidating anaerobic reactor (Ivanova et al., 2003).

Ivanova et al. (2005) over a period of two years studied a sample of MSW in a way to provide with a quantitative understanding of the influence of waste composition, density, depth, microbial activity and gas production rate on the rate of secondary settlement under constant load. Details of change in chemical composition of leachate were continually recorded to ensure the waste degradation. Samples were obtained from site and put into CARs with a maximum particle size of 40 mm under two different constant loads; 50 and 150 kPa. 10% V/V of sludge was added and leachate was regularly collected and examined, whereas gas was vented and its volumetric calculations were done. Data revealed that gas production can be divided into 3 phases (refer biodegradation stages in chapter I-1.3);

- Day 8-33 : Acetogenic (VFA main product)
- Day 33-150 : Accelerated methanogenic
- Day 150-428 : Decelerated methanogenic

Methane accounted for 58% of volume within the total gas production. The authors measured the settlement for a period of 428 days (Figure V-6) with following features;

- For initial settlement stage sewage sludge was added and a constant load was applied.
- At day 33 completion of primary settlement was assumed (but there was lack of adequate compression)
- Rates for secondary settlement were higher than primary consolidation for both the cells with different load which is an indication of effects related to bio-degradation.

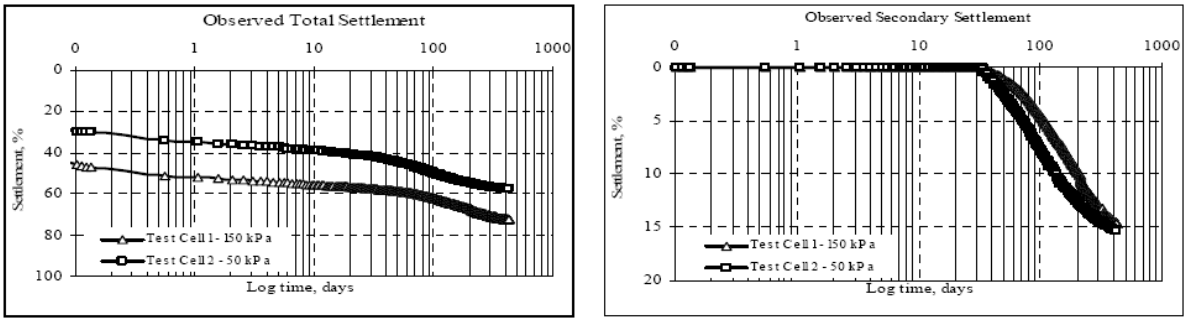

Figure V- 6: Observed total and secondary settlement. (Ivanova et al., 2005).

Olivier et al. (2003) performed the laboratory one-dimensional compression tests on municipal solid waste sample in a fully instrumented oedometer box of a 1 m^3. The authors reported consolidation data for short-term (stress-dependent) and long-term (time-dependent) settlements. The derived compression ratios and coefficient of earth pressure at rest were correlated. The oedometer box (Figure V-7) used had a rigid square cell of size 1 m x 0.98 m with leachate and biogas drainage systems. The waste sample was subjected to a vertical compression (up to 130 kPa). Leachate was removed from the bottom and re-circulated from the top of the waste sample (once to twice a week). Biogas was collected in a discharge-meter, or a biogas analyser with continuous data acquisition. Degradable waste and inert waste were mixed in 55/45 ratio, shredded and placed in layers. Each layer was compacted to a vertical stress of 40 kPa. Recirculation system and cap cover was placed on top of the sample.

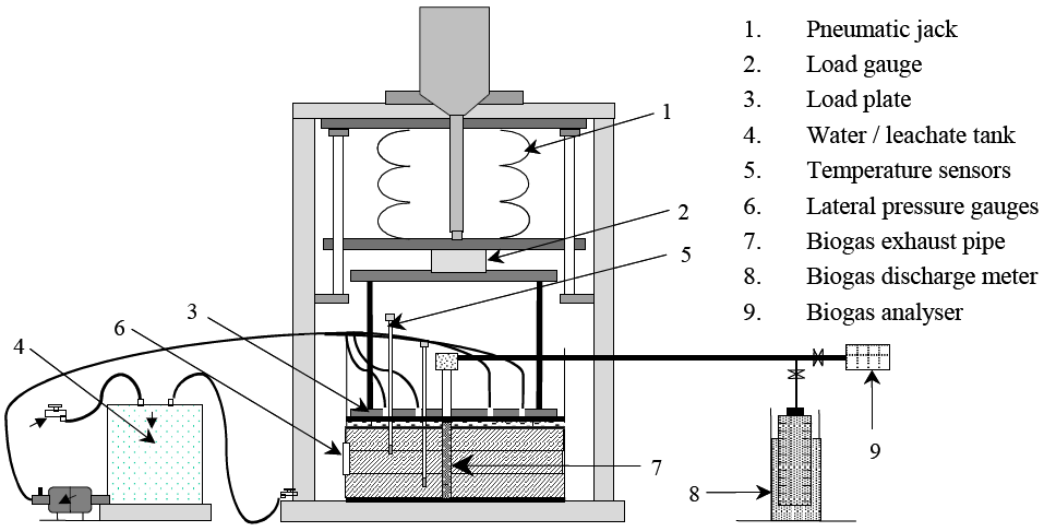

Figure V- 7: Schematic diagram of the compression cell (Olivier et al., 2003).

Considering in detail the physical conditions of the waste; moisture content at the beginning was calculated to study the behaviour of the waste with leachate recirculation. Table V-3 summarises the parameters monitored during the test. Analyses of primary and secondary settlements were done

assuming the primary compression as an instant process and that it ended after passing some time at the end of gradual loading (loaded up to 130 kPa). This assumption of time limit was strengthened by the secondary settlement analysis. Constant cycling of unloading and reloading was followed for purpose of recirculation of leachate.

Table V- 3: Description of monitored data (Olivier et al., 2003)

Characteristics	Monitored data	Unit	Frequency	Description
• Mechanical	- Vertical stress (σ_v)	kPa	daily	continuous record (+/- 3 %)
	- Settlement (Δh)	m	hourly	during the loading and steady phases
	- Lateral stress (σ_h)	kPa	weekly	on vertical plane ; manual monitoring
• Hydrological	- Open porosity (n)	%	occasional	derived from settlement data
	- Water content (w)	%	occasional	derived from w_0 and re-injected vol.
• Thermal	- Internal T°	°C	hourly	2 internal temperature sensors
	- External T°	°C	hourly	Thermometer
• Leachate	- pH	-	weekly	pH-meter probe (manual)
	- Conductivity	mS/cm	weekly	conductivity probe (manual)
• Biogas	- CH_4 content	%	daily	infra-red gas analyser (+/- 2 %)
	- CO_2 content	%	daily	infra-red gas analyser (+/- 2 %)
	- Discharge	l/h	-	Graduated bottle (set in water)

For the secondary settlement, one dimensional consolidation theory is used to predict the long term changes, commonly referred to as 'Sowers Model'. The modified form of coefficient of secondary compression $C^*_{\alpha\varepsilon}$ as proposed by Olivier et al. (2003), (in contrast to Sowers (1973) proposed coefficient of secondary compression $C_{\alpha\varepsilon}$) tends to reach a constant value after a period of time which seems more realistic as the biodegradation and settlement tends to diminish, even though this time period needs to be analysed further in future. The coefficient of secondary compression at various times for the start of secondary settlement (t_1) was used and a period of 2 months was found to be an appropriate estimate for the stabilization of $C^*_{\alpha\varepsilon}$ (Figure V-8).

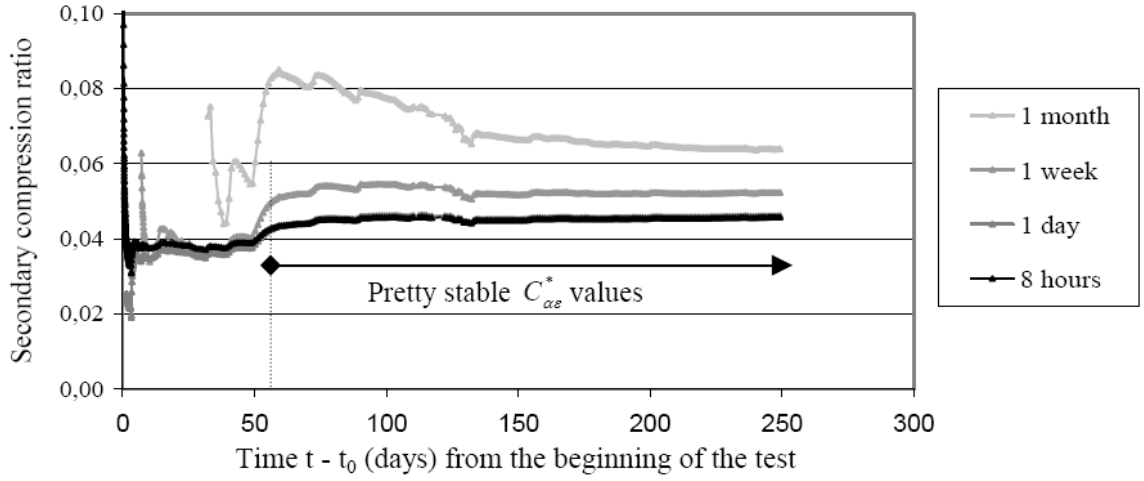

Figure V- 8: Evolution of coefficient of secondary compression with time (Olivier et al., 2003).

Olivier et al. (2007) presented a study of a long term settlement with intensive recirculation of leachate which generated increased settlement rates at and after the recirculation period as presented in Figure V-9.

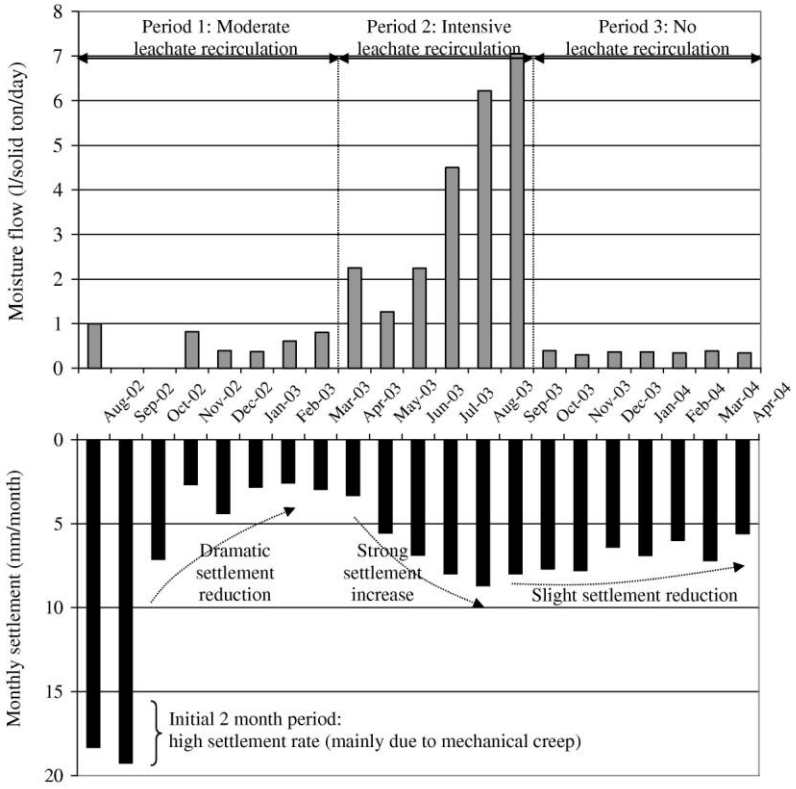

Figure V- 9: Increased rate of settlement at the recirculation period for the long term settlement laboratory tests (Olivier et al., 2007).

Carrubba et al. (2003) conducted a study of compressibility and permeability of pre-treated waste. The authors made use of a mixture of mechanical biological pretreated waste (MBP) with either incinerator sludge or civil depuration plant to analyse the settlement phenomenon. Their experimental study shows that compressibility is more than twice of incinerator slag (S10) than for the sludge (F10), while addition of sludge further increases the compressibility (Figure V-10). Long term compression tests were performed for the sample (S 10) and four phases of secondary compression were identified with a unique value of coefficient of secondary compression $\left((C_{\alpha\varepsilon})_c = {\Delta\varepsilon}/{\Delta \log t} \right)$ as shown in Figure V-11.

- Phase 1 : $C_{\alpha\varepsilon}$ = 3 considered to be effective for 3-4 hrs
- Phase 2 : $C_{\alpha\varepsilon}$ = 1.7 with a duration of 100 hrs
- Phase 3 : $C_{\alpha\varepsilon}$ = 2.3
- Phase 4 : $C_{\alpha\varepsilon}$ = 5

The values of coefficient of secondary compression determined from the short term compression tests were in the range of 2.

Remark: Definition of the coefficient of secondary compression $(C_{\alpha\varepsilon})_c$ is not the same as conventional $C_{\alpha\varepsilon}$.

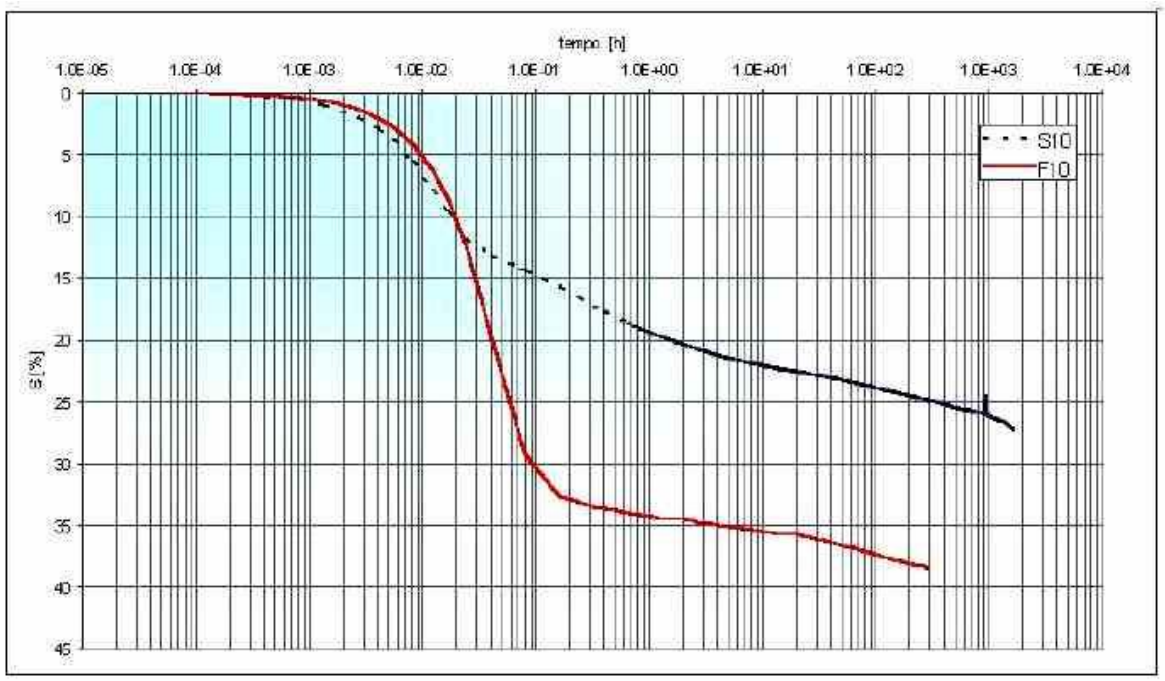

Figure V- 10: Comparison between long term settlements for the two mixtures (S10 and F10) of MBP waste with slag and sludge (Carrubba et al., 2003).

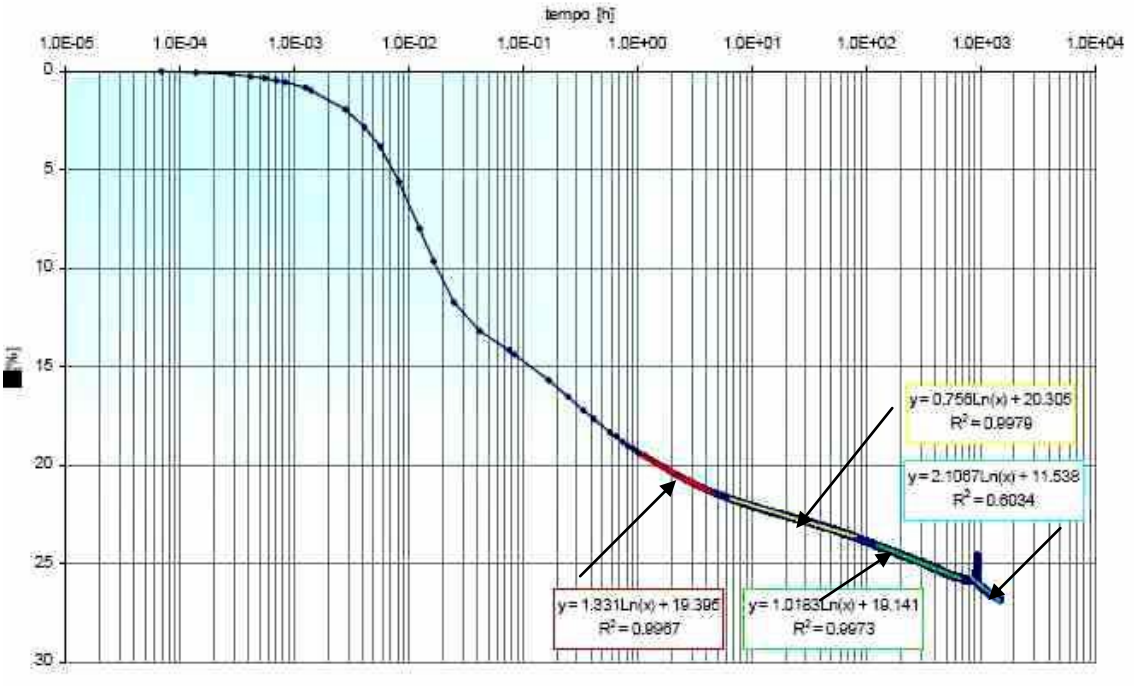

Figure V- 11: Long-term settlements for the mixture S10 during fermentation under a constant stress with calculation of four coefficients of secondary compression (Carrubba et al., 2003).

Moreover they performed drained oedometer tests under a vertical stress of 100 kPa and found out that the biological degradation causes the coefficient of permeability to reduce almost an order of magnitude. The probable explanation might be the reduction of voids in the mechanically biologically treated solid waste.

V- 1.2.3 In-situ Experimentation of Vertical Deformation

Bauer et al. (2005) performed a study to measure vertical deformation inside landfill. According to their study horizontal movements have approximately 75% of settlement values while stating that horizontal settlements are caused by slope geometry and landfill topography. For the purpose of study a ditch in the landfill was excavated and the piping system for leachate and gas collection was placed while from the excavated material, samples were retrieved for laboratory study. Classification of waste was done to evaluate mechanical properties and the composition was determined to estimate slope stability. Similarly biochemical analyses were carried out for modelling of the biochemical reactions. Determination of vertical deformation was done through hydrostatic profile measurement and deformation of ditch wall was recorded through measuring bolts in walls and surface slopes. These pipes served for the measurement of gas amount, composition, relative humidity and temperature. Hydrostatic profile measurement was carried making use of piping system utilised for settlement measurement of leachate collecting pipes.

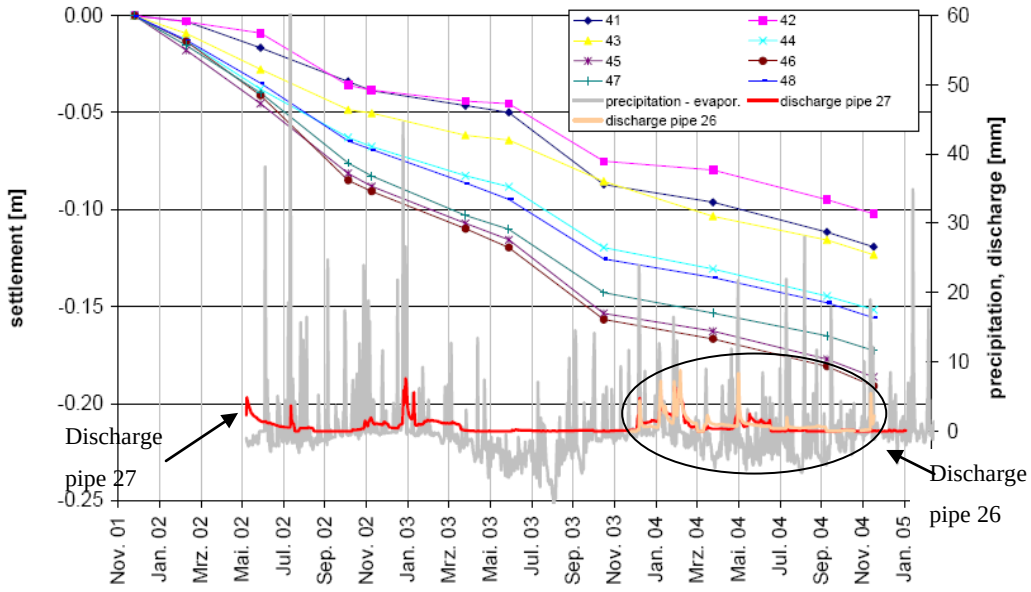

Figure V- 12: Seasonal settlement, precipitation and leachate discharge in different pipes (Bauer et al., 2005).

Settlement data showed velocity of settlement which was not constant for a period of one year (Figure V-12) the reason could be temperature precipitation and water content within waste body. It is worth noticing here that the Figure V-12 is plotted on time scale (t) rather than a log t scale, however, no

relation between horizontal deformation and settlement could be found. In the compression test addition of water resulted in increased settlement velocity which may have chemical and/or physical reasons (Figure V-13) but no further conclusions were made as the influence of water on the behaviour of a waste mass is still insufficiently investigated.

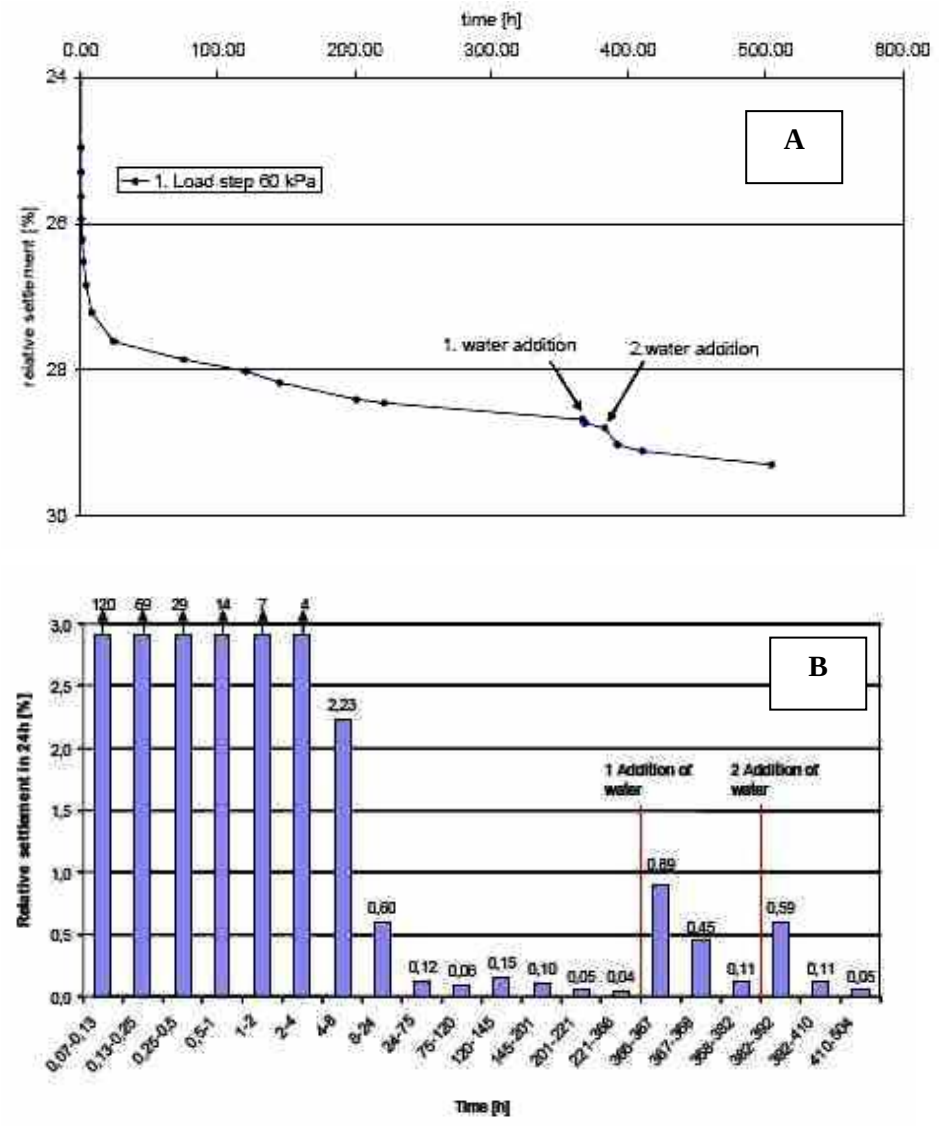

Figure V- 13: Influence of water on the settlement velocity in compression test, over all settlement in figure A and average settlement per day in figure B (Bauer et al., 2005).

Olivier et al. (2005), in complement to other field survey techniques, conducted ground-based 3D laser scanning on a French landfill site proposing a new method of surface modelling for landfill applications. Three out of six waste cells at the landfill were scanned with 3D laser machine and data were interpreted for 2D and 3D applications. 3D application was shown to be useful for the observation of altitude variation within a test zone (Figure V-14) while 2D profiles could help highlight the presence of superficial slip features along lateral slopes. When high resolution is required

the principle of 3D laser could be of benefit over other settlement surveying equipments (inclinometers, buried plates etc) and its point density and ease of implementation are its good assets.

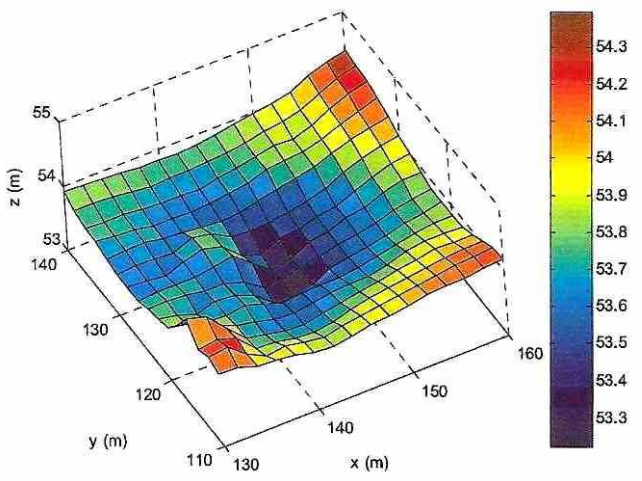

Figure V- 14: Representation of the average altitude of test zone discretised into 2m x 2m elementary grids (Olivier et al., 2005).

By comparison to conventional surveying, the application of the scanner technique in landfills could improve the assessment of cell capacity before and during filling operation as well as the surveillance of covered cells at the post-capping period. A continuous representation of surface settlements with the help of 3D laser scanner (Figure V-15) could be a promising technique to better understand the localised hydro-biophysical and mechanical interactions between waste and structures.

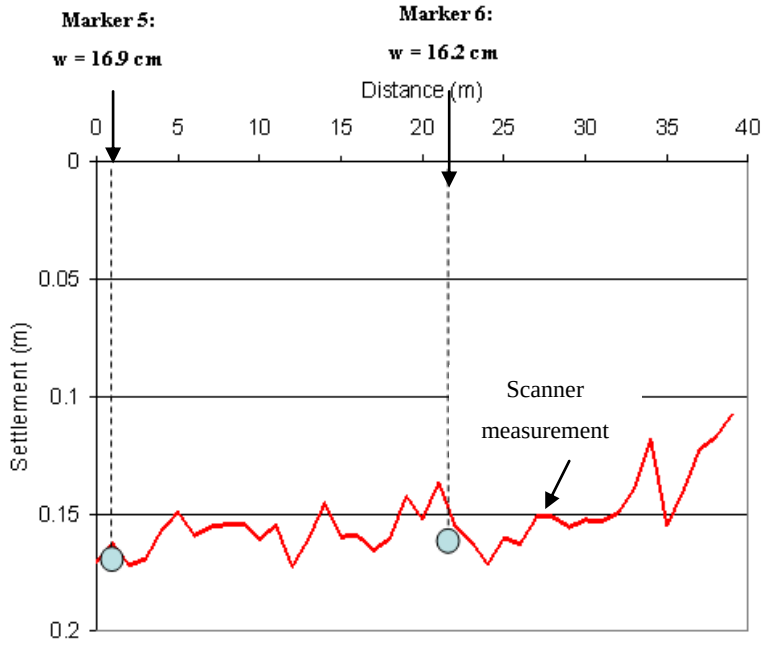

Figure V- 15: Comparison between the settlement measures through conventional survey and 3D laser scanner on waste surface altitudes along a selected section of the landfill (Olivier et al., 2005).

V-2 PREDICTION AND MODELLING OF SETTLEMENT

The control and the prediction of settlement of waste has become very technical with whole share of the follow-up of the modern municipal solid waste due to increasing rationalization of the management of domestic and assimilated wastes. The follow-up and the analysis of these settlements are placed simultaneously in step of a sedentary and economic nature. In addition, research in progress shows that the compressibility of waste with many regards is an indicator of the evolution of the state of material, complementary to the series of hydrological and biochemical measurements.

In the present study, a state of knowledge on the modelling of settlement is drawn in particular the presentation of new version of the Incremental Settlement Prediction Model (ISPM) originally proposed by Olivier (2003) which makes it possible to directly follow-up the MSW in the direction of a better anticipation of long-term settlement. Taking into consideration the recent progress in the field of the measurement of settlement and of their long-term prediction, the calculation of limit of construction (authorized by legislative bodies) deserves to be addressed in a more systematic way. With the help of rigorous procedures of evaluation, it would be possible indeed to take into account post construction settlement by anticipation (by mentioning limits of size after settlement).

V - 2.1 Importance of Settlement Monitoring

The understanding of mechanisms governing municipal solid waste settlement *w* and the development of means to accurately predict the rate and magnitude of settlement have become essential elements in the design and operation of landfills (Figure V-16).

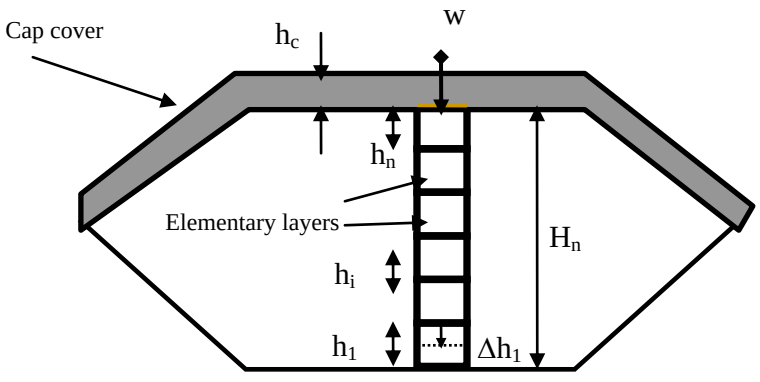

Figure V- 16: Typical landfill scheme, implementation of waste layer by layer and vertical column.

The performance of any structure built on a landfill will depend, to a great extent, on the ability to predict the anticipated settlement. Moreover, prediction of settlement contributes to the determination of the useful lifespan of the landfill and assists in the design of its components, such as cover and liner systems. The occurrence of differential settlements is even more critical than total settlement and is inevitable due primarily to the non homogeneity of solid wastes. Differential settlements eventually result in problems such as water ponding on the cover system and accumulation of water on the drainage layer, hence increasing the rate of water infiltration into the waste and leachate formation. The implementation of a landfill consists in placing waste layer by layer (thickness h_i for layer i) till the landfill is full (maximum height of waste H_n reached), the waste mass is then confined by a cap cover of thickness h_c (clay or geosynthetic).

V - 2.2 Logarithmic Laws in Soil Mechanics

V- 2.2.1 Primary Settlement

Once the phenomenon of dissipation of interstitial pore water pressures in the case of the fine grained soils in 1925 was described, Terzaghi (1943) proposed the following formulation connecting the primary consolidation of the soils to the variations of effective stress (Figure V-17).

[A] $$\frac{\Delta h_p}{h_0} = C_R . \log \frac{\sigma'_0 + \Delta\sigma'}{\sigma'_0}$$

equivalent with $\Delta e_p = C_c . \log \frac{\sigma'_0 + \Delta\sigma'}{\sigma'_0}$ with $\frac{\Delta h_p}{h_0} = \frac{\Delta e_p}{1 + e_0}$ and $C_R = C_c . \frac{1}{1 + e_0}$

Where C_R and C_c represent the coefficient of primary compression and the primary compression index, e_o initial void ratio of a soil sample of height h_o subjected to an initial stress of σ'_0 and $\Delta\sigma'$ as the increase in stress resulting from the application of surcharge. This is only true for a sample of normally consolidated soil, not having undergone previously any effective stress higher than σ'_0. If σ'_{pc} is the pre-consolidation stress of waste, then it is a condition such as $\sigma'_0 > \sigma'_{pc}$. On the other hand, over-consolidated soil (i.e. having undergone a pre-consolidation higher than the current effective stress $\sigma'_0 + \Delta\sigma'$ (i.e. $\sigma'_0 + \Delta\sigma' < \sigma'_{pc}$), eq. [A] becomes:

[B] $$\frac{\Delta h_p}{h_0} = C_S . \log \frac{\sigma'_0 + \Delta\sigma'}{\sigma'_0}$$

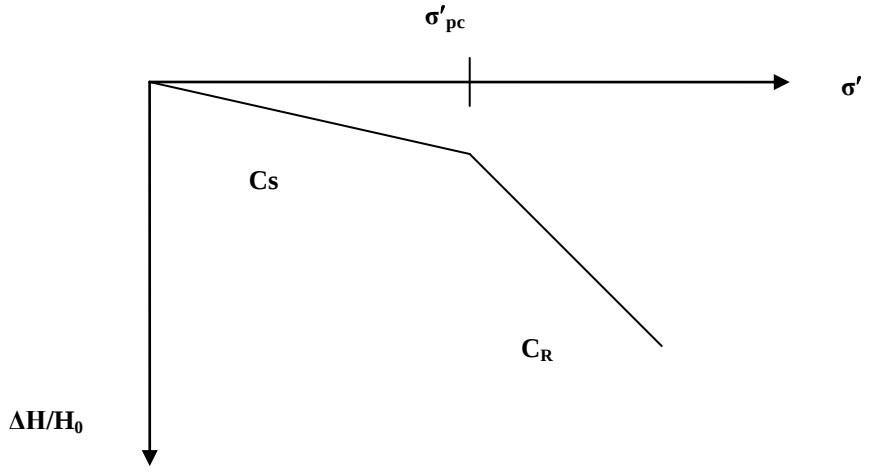

Figure V- 17: Illustration of the primary consolidation according to the Terzaghi theory (1943).

Lastly, in the general case of a pre-consolidated soil sample under an effective stress σ'_{pc} while subjected to an increment of stress ($\Delta\sigma$) such as: $\sigma'_0 < \sigma'_{pc}$ and $\sigma'_0 + \Delta\sigma > \sigma'_{pc}$, following equation is obtained:

[C] $$\frac{\Delta h_p}{h_0} = C_S . \log \frac{\sigma'_{pc}}{\sigma'_0} + C_R . \log \frac{\sigma'_0 + \Delta\sigma'}{\sigma'_{pc}}$$

The coefficients of primary recompression C_S and primary compression C_R are considered as intrinsic parameters of the material, independent of the state of stress. It is not the case of the modulus of oedometric deformation, well-known in soil mechanics, which satisfies the equation:

[D] $$\Delta\sigma' = E_{oed} \frac{\Delta h}{h_0}$$

For a normally consolidated soil, E_{oed} varies with the stress at a constant value of C_R, combining Eq. [A] and [D]

[E] $$E_{oed} = \frac{\Delta\sigma'}{C_R . \log\left(\frac{\sigma'_0 + \Delta\sigma'}{\sigma'_0}\right)}$$

V- 2.2.2 Secondary Settlement

The laboratory tests and the site observations reported by Buisman (1936) and Taylor (1942) showed the effect of time on the compressibility of the fine grained soils. Buisman (1936) in particular highlighted that the settlement of clays and the peats increased linearly with the logarithm of time under constant conditions of effective stress and proposed the following law for secondary settlement:

[F] $$\frac{\Delta h_s}{h_1} = C_{\alpha\varepsilon} . \log \frac{t}{t_1}$$

equivalent to $$\Delta e_s = C_\alpha . \log \frac{t}{t_1} \text{ with } \frac{\Delta h_s}{h_1} = \frac{\Delta e_s}{1 + e_1} \text{ and } C_{\alpha\varepsilon} = \frac{C_\alpha}{1 + e_1}$$

where

- h_1 = the thickness of the soil layer at time t_1 (also called t_{100} in soil mechanics) corresponding to the end of the primary settlement (total dissipation of interstitial overpressures),
- e_1 = void ratio at the beginning of the linear portion of the curve of void ratio according to the logarithm of time,
- finally C_α and $C_{\alpha\varepsilon}$ = coefficient and the intrinsic coefficient of secondary compression.

For practical reasons (due to the difficulty to access the value of h_1 under stress) hereafter h_1 is considered as h_0.

$C_{\alpha\varepsilon}$ is regarded as an intrinsic parameter such that it is independent of the load applied (Leonards and Girault, 1961). Moreover, Mesri and Choi (1985) noted that the ratio $C_{\alpha\varepsilon} / C_R$ varies little for one type of given soil (0.05 ± 0.01 for organic clays). From the equations [C] and [F], the formulation suggested by Garlanger (1972) through addition of primary and secondary settlement is determined:

[G] $$\frac{\Delta h}{h_0} = C_S . \log \frac{\sigma'_{pc}}{\sigma'_0} + C_R . \log \frac{\sigma'_0 + \Delta\sigma'}{\sigma'_{pc}} + C_{\alpha\varepsilon} . \log \frac{t}{t_1}$$

Considering other formulations of primary and secondary settlement proposed like Koppejan (1948) where secondary settlement is dependent on the level of loading, the model however is based on the theory of Buisman (1936) which supposes that once the primary consolidation is completed, settlement varies linearly as a function of logarithm of time. For $t < t_1$ (end of the primary consolidation), settlement follows the theory of the consolidation suggested by Terzaghi. Beyond t_1, the settlement law is written as:

[H] $$\frac{\Delta h}{h_0} = C_{\alpha\varepsilon} . \log \frac{\sigma'_0 + \Delta\sigma'}{\sigma'_{pc}} \log \frac{t}{t_1}$$

which is in the form of $\frac{\Delta h}{h_0} = a + b \log t$

Here it is worth mentioning that the research tasks on the creep of the clays undertaken from Bjerrum (1973) to Leroueil (1985) showed the reduction of void ratio related to creep which involves an increase in the pressure of apparent pre-consolidation whose consequence is such that in the event of additional loading, an old clay will behave like an over-consolidated clay. Similarly if the increase in load remains weak, instantaneous compression will be limited to a weak elastic compression.

V - 2.3 Modelling Landfill Settlement

The prediction and modelling of settlement processes in landfills are predominantly empirical and usually based on measured laboratory and field parameters. There is a lack of one workable theory that accounts for all factors influencing the settlement of waste in landfills. The initial settlement phase is rarely modelled except in the case of foundation design. In this context Eq. 1 applied for partially saturated fine-grained soils and coarse grained soils with large permeability, is used for a landfill that has a relatively large permeability and that experiences a visible immediate compression when surcharged.

$$E_s = \Delta q . \frac{H_0}{w_i} \quad \ldots\ldots\ldots\ldots\ldots\ldots\ldots\ldots\ldots\ldots (1)$$

where,

E_s = waste modulus of elasticity, kPa

Δq = increment of overburden pressure at the mid-level of the layer, kPa

H_0 = initial thickness of the layer under consideration, m

w_i = initial settlement, m

Several models developed to estimate MSW settlement are based on conventional geotechnical theory. **Terzaghi's** theory simulates primary and secondary compression processes for various materials by describing the deformation resulting from consolidation mechanisms. For waste body, it is more a compaction mechanism rather than a consolidation phenomenon with general form of the equation:

$$w(t) = \frac{H_i C_c}{1 + e_o} \log \frac{\sigma_o + \Delta\sigma}{\sigma_0} + \frac{H_p C_a}{1 + e_p} \log \frac{t}{t_p} \quad \ldots\ldots\ldots (2)$$

Where, its first term is related to the primary and the second to secondary settlement.

w = settlement due to primary and secondary consolidation, m;

H_i = thickness of waste layer under consideration after initial compression, m;

C_c = coefficient of primary compression; slope of e-log p curve;

e_0 = void ratio after initial compression, m^3/m^3;

σ_0 = existing overburden stress at mid level of layer, KN/m^2;

$\Delta\sigma$ = overburden at mid level of layer, KN/m^2;

H_p = thickness of waste body after primary consolidation, m;

$C\alpha$ = coefficient of secondary settlement; slope of e-log t curve;

e_p = void ratio after primary consolidation, m^3/m^3;

t = time, $t > t_p$, days;

t_p = time for primary consolidation to occur, days (usually 30).

The complexity of solid waste matrices, the simplicity of the mathematics involved, and the number of case histories that are linked to the conventional techniques are often cited to justify the use of the theory. Although ranges of the consolidation parameters are readily available in the literature, care must be taken when extrapolating results. Actual waste compressibility may differ considerably from values available in the literature. Because it is difficult to reliably predict the initial void ratio of waste, Eq. 2 has been written in different forms to avoid the need to estimate this particular parameter.

Rao et al. (1977) used plots of relative layer thickness vs. the applied stress in order to predict settlement. A major advantage of this approach is to consider a relative height-vertical stress curve which eliminates the estimation of the initial height of a certain layer. Settlement is estimated using Eq.3.

$$w = H_0 \frac{C_S}{H_0 / H_i} \log \frac{\sigma_0 + \Delta\sigma}{\sigma_0} \quad \text{..... (3)}$$

w = settlement due to load application ($\Delta\sigma$), m;

H_0 = existing thickness of waste layer under consideration, m;

C_s = coefficient of compression; slope of relative height-log p curve;

H_0/H_i = relative height corresponding to existing overburden pressure (h_i for surcharge σ_0), m/m;

σ_0 = existing overburden stress, KN/m^2;

$\Delta\sigma$ = increment of stress, KN/m^2;

Remark: The contribution of biodegradation to long-term settlement can account for a large portion of the total settlement. In this regard recent efforts reported mathematical expressions incorporating the effect of decay on settlement (Gourc et al., 2010). The basic assumption underlying these expressions is that the amount of settlement is directly proportional to the amount of solids solubilised. Because solubilisation of organic materials is generally expressed in terms of first-order kinetics, the settlement due to biodegradation is also expressed in terms of first-order kinetics.

V- 2.3.1 Complex Settlement Models for Landfills

Settlement models with a background of derivation based on knowledge of soil mechanics are most practical for civil and geotechnical engineers. Not only they are simple in their mathematical form but also their parameters determination is kept simple and practical. For example in case of the models discussed below much consideration is given to the number of unknown parameters and the ease with which they could be determined in the field so as to keep the model handy for people working at site. And this is one of the reasons why ISPM model developed by LTHE (LIRIGM) is getting appreciation

around the world. The workability of any simple modelling methodology is such that it produces reasonable results with limited data available from the landfill history. In the context of prediction of settlement various models are proposed and developed by the researchers which are sometimes applied solely or in combination with other models. At broader scale these models can be classified as;

- Mathematical model
- Mechanical model
- Biological model

In the near past different models have been proposed for the prediction of settlement in the landfills which follow certain laws. In all the models one technique is common that is to stick to one type of law either a mathematical or mechanical approach. But for sometime now a need to overlap different approaches has been considered much important since waste is a heterogeneous material and it does not strictly follow one law towards its behaviour in the landfills. Different combinations of the individual models include mechanical & mathematical model, Bio-mechanical model or Hydro-bio-mechanical model.

McDougall et al. (2001) discussed in detail a three component model namely hydraulic, biodegradation and mechanical models (HBM) with its implementation in numerical technique of finite element method. In their study they have used an unsaturated flow model for the hydraulic input because of the fact that it correlates moisture content and flow to infiltration and absorptive capacity as well as it develops rate of discharge from leachate exit points. For the biological model anaerobic digestion process is used where quantities of fatty acids and methanogenic biomass are incorporated to determine mass loss. However within the mechanical model there are three components to be handled;

- load induced compression using elastic-plasticity,
- creep settlements under incremental load by an equivalent time method
- and finally biodegradation induced settlement essentially a plastic deformation is catered through depletion of solid organic fraction and current stress state.

But only for the last factor to be realistically incorporated into the model a density dependent phase relation of waste was considered. Keeping in view the diverse structure of waste an extended phase description was proposed with organic and inorganic fractions to provide with a framework for interpretation of volume effects due to biodegradation. The model was tested on Lyndhust sanitary landfill but variations in moisture content in the waste has random nature which was failed to be recognised by the model and hence the associated absorptive capacity as well. Finally their proposal to use a finite element model depends upon the cell lifting history and its corresponding load to envisage more properly the expected settlement upon simulation of filling phase.

McDougall et al. (2005) worked on the HBM model with their previous work to develop a finite element model with three components incorporating simultaneously different parameters responsible for settlement in a landfill (Figure V-18). The point emphasized in their biodegradation induced effects is the rate limitation of decomposition which is a time dependent process however constrained by a maximum rate.

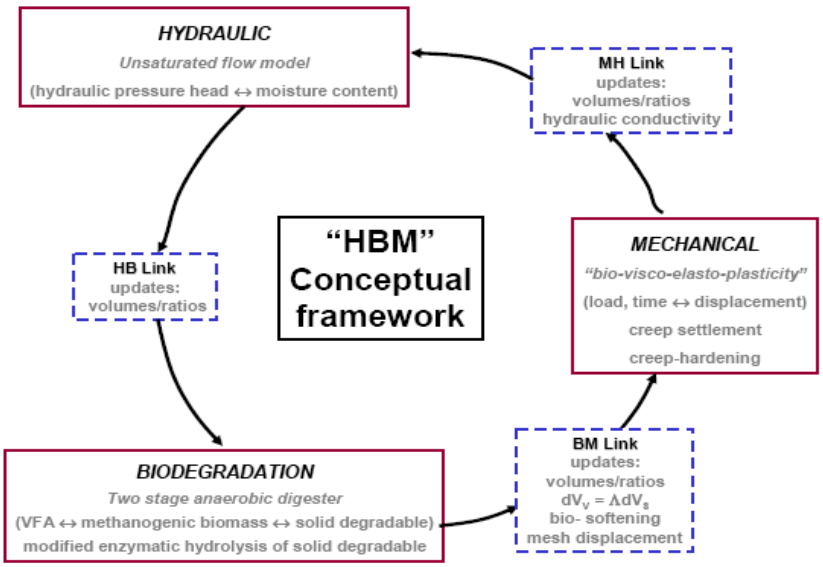

Figure V- 18: Schematic diagram with the components of the HBM model (McDougall et al., 2005).

They formulised the interpretation of mechanical consequences of decomposition by developing a relationship between two volumetric state variables (Figure V-19), the void phase volume and the solid phase volume as $dV_v = \Lambda dV_s$

Λ = void change parameter induced by the decomposition.

The simulation comprised of two parts, firstly it was run without biodegradation effects and afterwards with the biodegradation effects. Since the interest of the study was to see the relative and qualitative behaviour, the absolute decomposition rates are not considered to be the substantial output of the analysis. However an increase in the leachate retention was observed which could be a false case as less organic matter should have a lower leachate holding capacity. Or may be there is need to modify the Van Genuchten parameters in the hydraulic input!!! Moreover the data received for leachate discharge was not coinciding with the retained moisture content within the simulation process so more investigations are needed to be done.

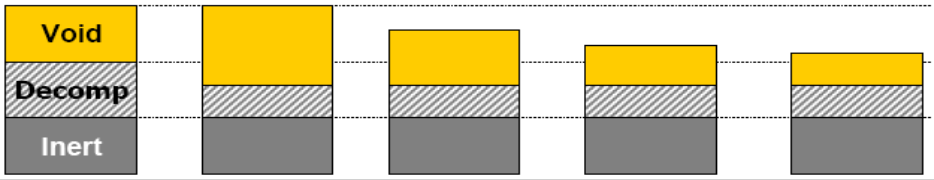

$\Lambda = \frac{dV_V}{dV_S} =$	-1	0	e	> e
Void ratio	Max increase	Increase	No change	Decrease
Overall volume	No change	Reduction		Max reduction
Mechanical condition	Much looser & weaker	Looser & weaker	No change	More compact & stronger

Figure V- 19: Reference values for decomposition induced void change parameter Λ and associated volumetric and mechanical conditions. (McDougall et al., 2005).

Furthermore the diagram showing simulation of settlement in different column heights is very much the same for each point and is uniform over all the time period of simulation (Figure V-20) which implies that there is constant decrease till 500 days as well as end of filling stage and finally at day 1500 it is almost the same tendency. In the end it is suggested that the use of MBP waste may produce better results along with the upgradation of the conventional modelling of moisture retention to interpret leachate retention.

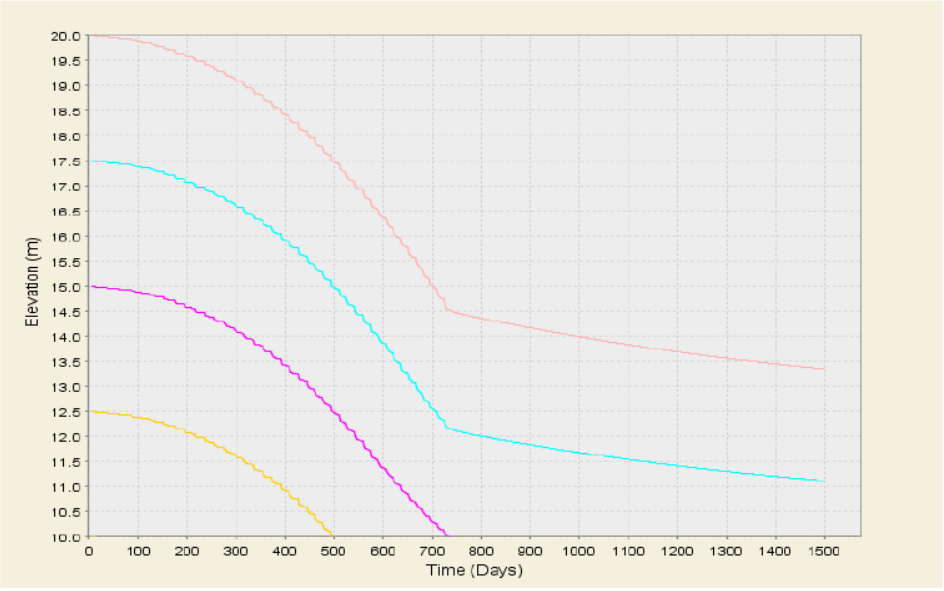

Figure V- 20: Settlement of selective nodal locations by McDougall et al. (2005).

Parker et al. (1999) presented a model for a waste degradation combining two numerical models initially proposed by El-Fadel (1996) and Young (1989). A three stage degradation process with four components coexisting in aqueous phase is modelled (Figure V-21) with assumed rate of degradation

reaction to be determined by the catalytic activity. Law of conservation of mass with respect to carbon is applied and the model constantly calculates the acid concentration of the liquid phase. According to the authors the model can successfully simulate both the cessation and the acceleration of degradation process. The proposed model has various stages catering for different aspects such as;

- Catalytic actions through defined constitutive catalytic equations for each type of biomass;

Lytic, Acidogenic and Methanogenic

- Maintains carbon balance for all stages of chemical changes from solid through aqueous to acidic.
- For each carbon balance there is a stoichiometric correspondence to mass.
- Incremental change of carbon concentrations of all carbon components are converted into mass concentrations.
- And a forward time step calculation for the compensation of any drift to simulate degradation with the course of time.

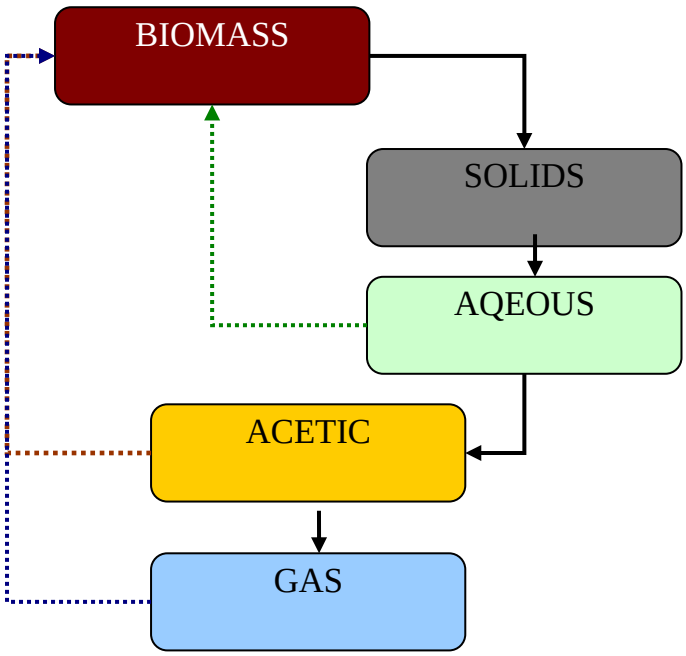

Figure V- 21: Three stage model scheme as proposed by Parker et al. (1999).

The mass balance is generated with incremental change in carbon concentration and subsequent conversion to mass concentration to simulate the degradation with respect to time. The results suggest the model may readily be adapted to other proposed concepts of kinetic and chemical reactions; however, the hydraulic aspect of the model still needs to be developed to cater for the modelling of water components of the process. Moreover it is stated that such a model will never be accurate to simulate precisely the degradation process but may provide with a base for the design of physical test procedures and data interpretations.

V- 2.3.2 Sowers Model (1973) and its Variations

Sowers (1973) was one of the first to propose a transposition of the laws of behaviour of the compressible soils to the waste. This transposition was limited to the unidirectional conditions which corresponded to the conditions of deposit in column (with negligible lateral strain) of a waste sufficiently far from the edges of the waste cell. A conventional soil mechanics approach was adopted to predict waste settlement without coupling any hydrological conditions, since waste is rarely saturated at the time of its placement at site. Even though the physical phenomena concerned are very different yet the application of the compressibility laws of the soils is quite relevant to soils and waste.

The Sowers (1973) method of settlement prediction remains most widely used model in the literature with simple formulation and lesser number of parameters to be introduced. Moreover, its coefficients can be deduced from the observation of a column of waste for one period with an objective of a longer-term prediction. The facility to use Sowers model guaranteed him a broad diffusion in the circle of engineering and design departments specialized in environmental geotechnics due to correct calibrations in a certain number of simple cases. Nevertheless this model suffers from three handicaps of quite importance:

- absence of standardization of its parameters of time, which makes any comparative approach difficult;
- unsatisfactory calibration in the case of columns of waste of complex history (rest period, late expansion), even impossible in the event of delayed topographic follow-up;
- parameter of non-intrinsic compression $C_{\alpha\varepsilon}$ since secondary compression is considered generally only starting from the end of construction of the waste column.

Sowers model breaks up the waste settlement as:

- an instantaneous phase: regarded as pseudo-elastic, it intervenes at the application of a surcharge (new layer of waste or cover);
- a primary phase: resulting mainly from the mechanical actions, its duration is considered less than 3 months (more commonly one month);
- a secondary phase: Resultant of the decomposition of the organic matter, it is supposed to last for about thirty years.

Sowers (1973) proposed to take the definite oedometric model of soils and to apply it directly to the column of waste, comparing column to an instantaneously built single layer. An important and questionable assumption of the Sowers Model is that the primary and secondary settlement are

expressed by extrapolating the laws suggested by Terzaghi (1943) and Buisman (1936), replacing the thickness of a layer h_0 by the column height *H(tc)*.

V - 2.3.2.1 Primary Settlement

Primary settlement is expressed in terms of relative compression (Figure V-22) as given in the following form:

[I] $$\frac{w_p}{H_{ref}} = C_R \log \frac{\sigma'_0 + \Delta\sigma'}{\sigma'_0}$$

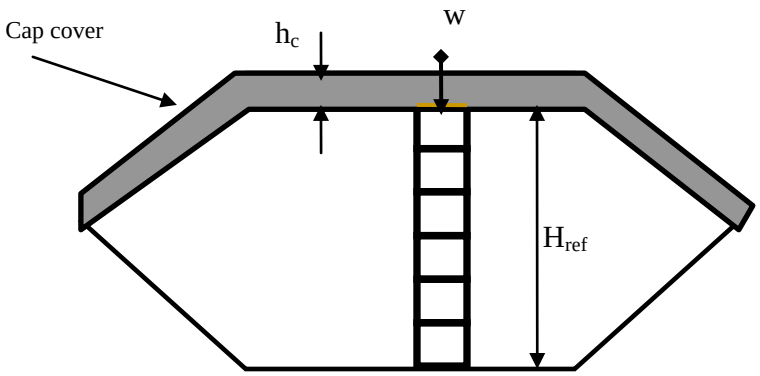

Figure V- 22: Typical landfill waste column construction.

Relative compression depends on the initial stress (σ'_0), the effective surcharge applied ($\Delta\sigma'$). Due to the lack of pore water pressure, effective stresses (σ') are equal to total stress (σ) and the simplified coefficient $C_R = \frac{C_c}{1 + e_0}$ expressed for the soils according to the initial void ratio e_0 is used.

Table V- 4: Summary of the coefficient of primary compression C_R (Olivier, 2003).

Location	Type of waste	Coefficient C_R	
		Range	Average
Sample of 21 sites	Variable	0.13 – 0.47	0.26
Arnouville (France)	MSW	0.20	0.20
Sample of 10 sites	Variable	0.05 – 0.26	0.14
Landfills USA	Unknown	0.15 – 0.26	
Unknown	MSW	0.24 – 0.30	0.27

The coefficient *x:* ($C_C = x.e_0$) with x = 0.15 for a waste low in organic matter and x = 0.55 for a waste rich in organic matter is considered. The richer the material is in organic matter, the more it is thus supposed to be compressible, although the degradation of the organic matter does not intervene in the

primary compression considered as instantaneous. Fasset et al. (1994) suggested that the value of C_R decreases with increasing stress σ'_0. In the case of application of significant loads, it even suggests adopting a linear model by segments, which amounts for considering several values of C_R.

V - 2.3.2.2 Secondary Settlement

Secondary settlement is defined as:

[J] $$\frac{w_s(t)}{H_{ref}} = C_{\alpha\varepsilon} \log \frac{t}{t_{ref}}$$

$C_{\alpha\varepsilon} = \frac{C_\alpha}{1 + e_0}$ can be expressed according to the initial void ratio (after compaction) and an intrinsic coefficient to the material x' :($C_\alpha = x'\, e_0$) with $0.03 < x' < 0.09$ according to whether the conditions are less or more favourable for degradation. The relation of $C_{\alpha\varepsilon} = x'.\frac{e_0}{1 + e_0} = x'.(n_t)_0$ is viable for $(n_t)_0$ initial total porosity of waste with an assumption of linear variation of $C_{\alpha\varepsilon}$ with initial porosity. A spindle was proposed by Sowers (1973) with an aim of determining the values of the coefficients of primary and secondary compression (Figure V-23). Utilizing only one parameter (void ratio) is excessively difficult to characterise the waste; this method thus remains inapplicable. The literature provides a certain number of values of the secondary coefficient of total compression $C_{\alpha\varepsilon}$ for the waste. These values are in general obtained from back-analysis of settlement measured on the surface of waste column and are seldom specified in the literature so that the values of $C_{\alpha\varepsilon}$ published must be considered with much precaution. Moreover the lack of information related to the studied sites (composition of waste, height of storage, construction phases) makes these data un-exploitable.

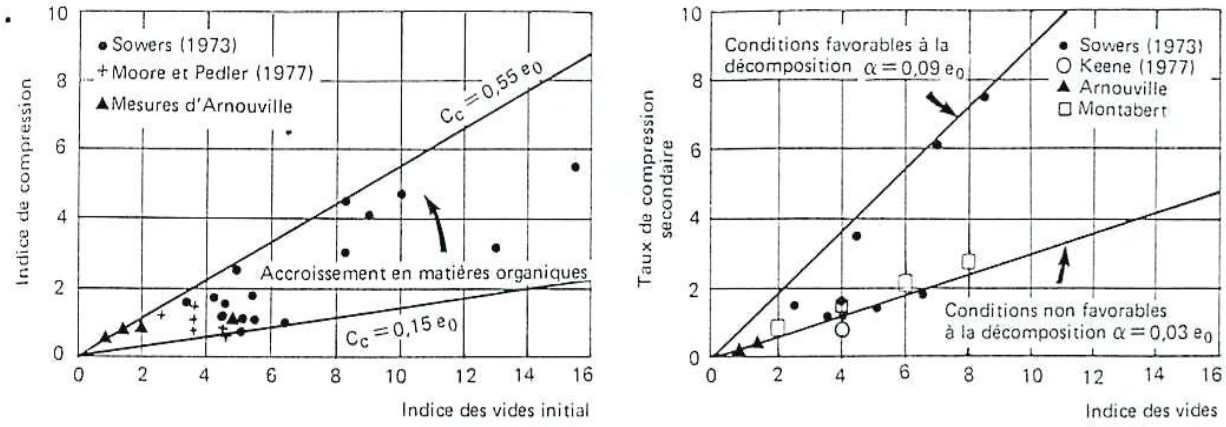

Figure V- 23: Index of primary (Cc) and secondary compression (Cα) for domestic waste according to the initial void ratio e_0 – Spindle of Sowers taken again by Cartier and Baldit (1983).

An evolution of the model of Sowers was proposed by Bjarngard and Edgers (1990), characterized by the introduction of 2 coefficients of secondary compression. One dimension compression tests were carried out to evaluate load and time dependant characteristics of the waste. Data was collected from 24 landfill sites and the relationship drawn with parameters of settlement being calculated by back analysis. For smaller time spans linear curves were observed but for large time periods much greater slopes were observed. The authors pointed out the absence of 's' shape of curve indicative of primary consolidation however it might be due to incomplete saturation.

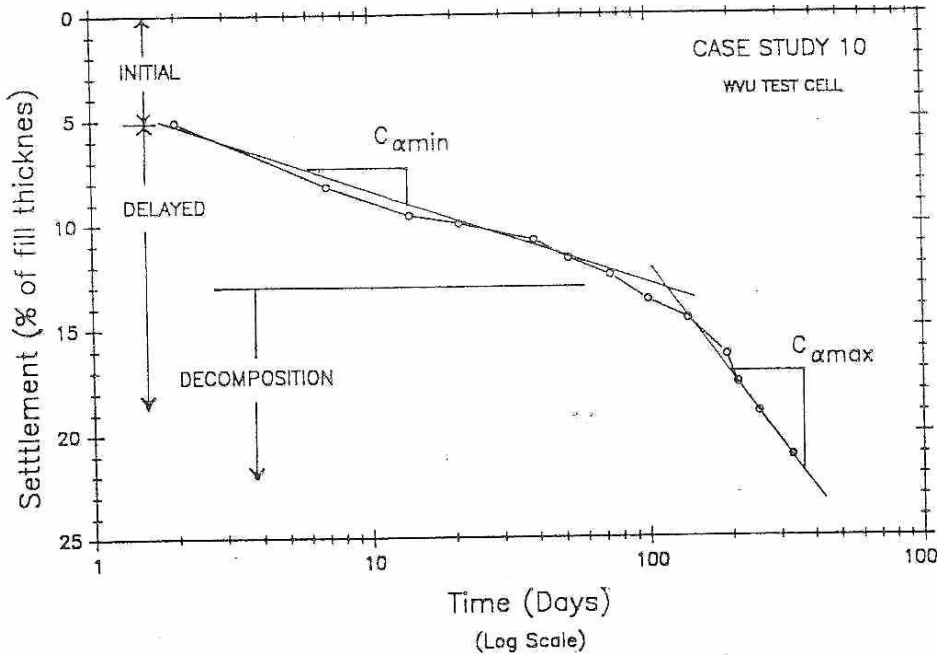

Figure V- 24: Idealised time-settlement curve as suggested by Bjarngard et al. (1990).

In Figure V-24 compression as a three phase process is presented as suggested by Bjarngard et al. (1990). With initial rapid compression and loss of voids some settlement is observed with another slope of delayed compression where the mechanical interaction is the dominating phenomenon with $C_{\alpha min}$ = 0.019. The authors suggested the added effect of decomposition at the last staged to the logarithmic compression rate giving $C_{\alpha max}$ > 0.125. However, it could be shown (Olivier, 2003) that such evolution does nothing but artificially compensates for the error generated by not taking into account the history of construction. From this point of view, ISPM model allows, starting from a single $C^*_{\alpha\varepsilon}$ coefficient, to correctly take into account the evolution of the settlement of the column of waste according to the parameter of time, and it could be considered as a significant improvement vis-à-vis the Sowers model.

In addition to all, the presentation of Sowers model in the literature remains vague with regards to the definition of the parameters of time (t_{ref}) and heights of waste (H_{ref}). A rewriting of the model

following the notations used in the model proposed by LTHE (LIRIGM) is utilized hereafter with the objective of clarifying each parameter of the model (Olivier, 2003):

[K] $$\varepsilon_p = \frac{w_p}{H(t_c)} = C_R \log \frac{\sigma'_0 + \Delta\sigma'}{\sigma'_0}$$

[L] $$\varepsilon_s(t) = \frac{w_s(t)}{H(t_c)} = C_{\alpha\varepsilon} \log \frac{t - t_0}{t_1 - t_0}$$

Where $H(t_c)$ represents the height of the column of waste at the end of the construction with t_c elapsed time for overall construction of the landfill, t_0 origin of time and t_1 the origin of secondary compression. The values of the parameters of time t_0 and t_1 are clarified in Table V-5.

Table V- 5: Values for time parameters of the model of Sowers (1973) as taken from Olivier (2003)

Time parameters	Frequently used approach	Academic approach
Origin of time (t_0)	$t_0 = t_c$	$t_0 < t_c$ $t_c / 2$ or ¾ t_c
Origin of secondary compression (t_1)	t_c + 125 days t_c + 1 month t_c + 1, 2, 3 months	No example in the literature but logically $t_1 = t_c$

Two practical approaches are possible, with regards to the time of end of construction (t_c) either as the origin of time or as origin of secondary compression. In the majority of the cases, both these terms (t_0, t_1) are taken equal to (t_c, t_c + 1 month), and this will be retained in the present numerical applications of Sowers model (except mentioned otherwise). Later the drift of this coefficient compared to the intrinsic coefficient of secondary compression will be discussed according to the origin of selected time and secondary settlement. In Section V-4 the comparison between ISPM model and Sowers model using relationship [K] and [L] will be carried out in detail.

V-3 INCREMENTAL SETTLEMENT PREDICTION MODEL (ISPM)

Morris and Woods (1990) developed a data-processing program (SETT 87) on the basis of equation of Sowers in FORTRAN allowing the calculation of the primary and secondary settlement components by summation of compression of the individual layers. Although this algorithm proceeds in its step as

incremental model ISPM developed hereafter, but it does not remain the same since the history of construction is not taken into account in the expression of the secondary settlement of the various layers. In addition, the determination of the coefficient of secondary compression is not considered by back analysis starting from site data. Its value is fixed arbitrarily by the operator or starting from the void ratio, parameter systematically ignored for a material such as waste.

In addition, Bouazza and Pump (1997) presented a software (FILLS) developed by engineering AGC Woodward-Clyde (Australia). Based on a square grid from 30 to 100 m side to side, this program in Visual BASIC made it possible to obtain a layer by layer projection to the scale of cell to cell, at the landfill site. The results (in the shape of 2 files) include the evolution of the vertical stresses, compression, porosity and the density over the course of time. More broadly, the storage capacity and the construction phase of the site are estimated on the basis of estimated tonnage. As previously, this algorithm works on the basis of global solution identical to that of Sowers and does not allow the user to determine the value of the coefficient of secondary compression by back analysis at the end of one period of topographic follow-up; initial $C_{\alpha\varepsilon}$ on the contrary is preset by the user. Lastly, it does not make it possible to model the vertical expansion of an old waste column.

According to a different approach, Bleiker et al. (1995) suggested an evolution of the model of Gibson and Lo (1961) according to an approach of superimposing the deformations layer by layer. Van Meerten et al. (1995) proposed a complex model of settlement based on the forced theory of the single cell volume. The model integrates well the time of construction of waste column but the construction is implicitly supposed to be linear in the absence of layer construction history. Similarly the increasing load is considered for the whole column in the absence of real construction details. In its ultimate version Van Meerten et al. (1997) suggested a detailed history of material should be taken into account but this model including three parameters of compressibility and two parameters of height (virtual height of uncompressed waste in the course of construction and height at the end of the construction) adds a scale factor to determine the initial rate of deformation of the column which is not practical.

To finish with this short historical retrospective, it should be recalled that this idea of simulation of construction of column of waste in elementary layers (with objective of taking into account the history of material) was also suggested by Green and Jamnejad (1997). The filling of a column of waste is carried out typically over a period of several months to several years where the waste is set up by successive layers compacted and sometimes separated by periodic covers. A deposit of waste thus consists of sub layers of waste of different age and history. The mechanical behaviour of the whole of the deposit thus is considered according to the behaviour of each sub layer.

V - 3.1 Conception of a New Model (LTHE)

Settlements are generally measured on the cap cover and the models of prediction are applied conventionally on column of waste using formula [K] and [L] in place of [A] and [F], without taking into account the history of construction. This corresponds to a coarse simplification whose influence was never quantified. In this context Incremental Settlement Prediction Model (ISPM) was introduced by Gourc et al. (1999) before being developed by Thomas (2000) and Olivier (2003). Based on the placement of elementary layers of waste leading to the formation of total height of the waste (column), this algorithm integrates behaviour in primary and secondary settlement of each elementary layer constituting the column. With the placement of each layer intrinsic parameters of behaviour are affected and the respective layer behaviour is studied individually according to the evolution of the surcharge and time.

The present study contributes to;

- Modelling of a newer version of the construction sequences
- Parametric study and application to case histories using this new version.

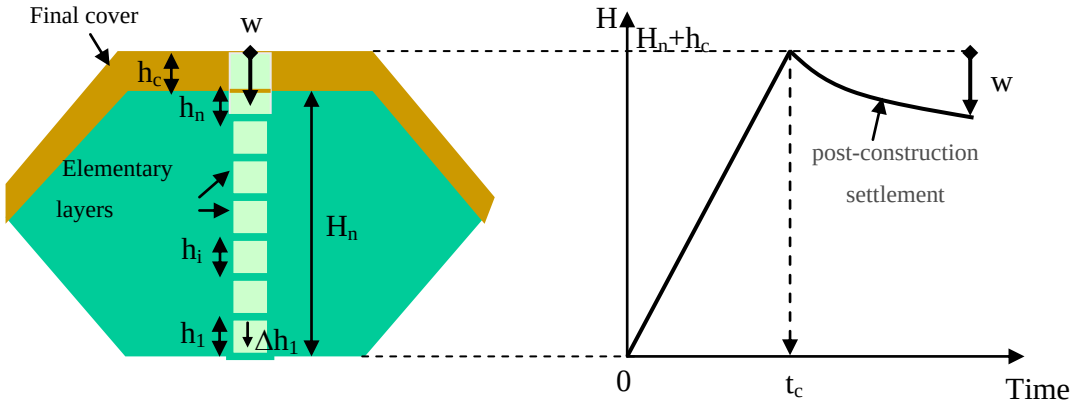

Figure V- 25: Illustration of the waste column division in elementary layers.

V - 3.2 Specific Definitions of ISPM Model

V- 3.2.1 Elementary Layer of Waste

The term ‘elementary’ layer or ‘sub layer’ for a layer of thickness h_i (generally ranging between 50 cm and 2 m) is used to represent the thickness of waste set up and compacted in only one operation at the time of construction of a waste column. The intermediate covers possibly inserted between the elementary layers of waste are not dissociated. The subdivision of elementary layers makes it possible to distinguish the behaviour of waste according to its particular characteristics (age, surcharge and

possibly nature). The parameters relating to the thickness of the layers vary according to the surcharge and time.

V- 3.2.2 Waste Column

'Column' is the waste height H_n of a column of n 'elementary' layers of thickness h_i.

V- 3.2.3 Time and Sequences of Construction of Waste Column

The origin of time (t = 0) coincides, for each waste type, with the date of beginning of construction of the column (i.e. placement of the first waste). An origin of time for every layer is also taken into account as τ_i which is the time of construction of a layer i (Figure V-26) of index i and τ_{ri} to the time of construction likely to intervene at the end of the construction of layer i, $\tau_i = 0$ at the beginning of the construction of layer, t_i corresponds to the time of construction of a column made up of i layers. Lastly, t_c is the time necessary for the construction of a complete column (waste + cover). Moreover t_m^0 is the time corresponding to first measurement of settlement of the landfill cap cover ($t_m^0 > t_c$) and likewise t_m^{ult} is the time corresponding to the ultimate measurement of settlement on site Figure V-26.

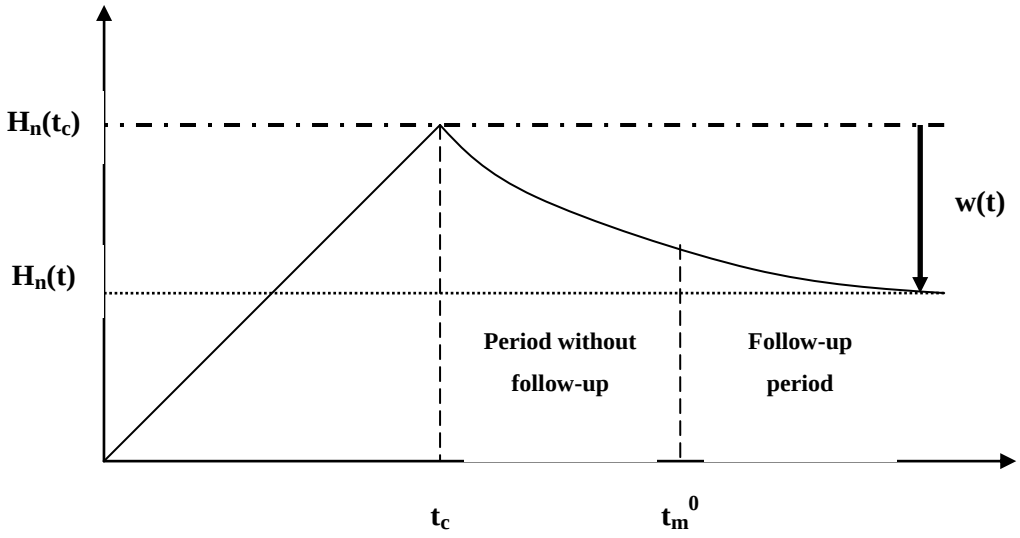

Figure V- 26: Illustration of the differential application of the model of Sowers in the event of delayed follow-up.

V- 3.2.4 Settlement

Settlement is supposed to be vertical (uni-directional), therefore in conditions of zero lateral strain. The settlement of an 'elementary' layer of initial thickness (h_i) is termed as *Δhi* corresponding to the components of primary and secondary compression Δh_i^p and Δh_i^s. The reduction in thickness

compared to the initial thickness (h_{i0}) is obtained after placement and compaction of the considered layer. The components of primary and secondary surface settlement of a 'column' of waste are termed as w_n^p and w_n^s. w is termed as the post construction surface settlement measured from the start of placement of the final cover (t_c) and Δw is the surface settlement measured at a delayed time with reference to the end of construction.

V- 3.2.5 Deformation

The comparison of the data of compression for different thicknesses of waste leads to treat the data in the form of relative strain where deformation ε is the vertical strain of a waste layer brought back to its height of reference. For an elementary layer, this height of reference corresponds to the initial thickness of waste h_0 (after compaction). In the case of a waste column, the height $H(t_c)$ at the end of the construction is considered, generally after the placement of the final cover (or exceptionally before that time).

V - 3.3 Assumptions of ISPM Model

The extension of the application of the settlement models (rigorously applicable to site sample or by analogy to an elementary waste layer) to multi-metric columns comprises of a certain number of difficulties generally not cited in the literature. Settlement model of Terzaghi will be clarified here but others are beyond the scope of the present study. Comparing a column of waste to a superposition of n horizontal layers, ISPM model functions on the following general assumptions:

V- 3.3.1 Geometry of Storage

- The column of waste is supposed to be located away from the slope of waste cell and it has a small height compared to its width so that horizontal strains can be neglected.

V- 3.3.2 Waste Material

- The initial heights h_0 and the initial unit weight γ_0 after the placement of waste (compaction included) are identical for each layer.
- Waste is supposed to be unsaturated at any moment so that the effective stresses σ' are equivalent to the total stresses σ and thus the coefficient of consolidation C_v does not need to be considered.

- Moreover degradation leads to a loss of total mass (fluid included) and is not taken into account over the period of study while waste density is considered constant over the course of time.

V- 3.3.3 Compaction

- The compaction is supposed to affect only the top layers of waste because of the rapid lateral spreading of the compaction energy with depth.
- The pre-consolidation stress of waste resulting from the compaction is supposed to be identical for all the layers of waste ($\sigma_{ci} = \sigma_c$ = constant). It is considered close to 40 kPa for the current sheep foot rollers (Olivier, 2003). The confirmation of this estimate deserves a thorough study. Consequently the compressive strain of the waste layer under vertical stress $\sigma \leq \sigma_c$ is considered negligible.
- Immediate settlement during spreading and compaction of the waste (immediately after disposal) is not taken into account in the modelling of settlement. Initial unit weight γ_0 is measured after compaction.

V- 3.3.4 Soil and Cover Liner

- In the case of sites partially in excavation, the foundation soils supporting the waste column are over-consolidated because of the loss of weight of the excavated ground practically not prone to compression as long as the surcharge coming from waste remains lower than the excavated weight. In the present study, the settlement of the foundation soil, unless otherwise specified, will always be regarded as negligible.
- Although the intermediate/daily covers can represent up to 20 to 25 % of the total stored mass (in particular in the United States, much less in France), it is undoubtedly erroneous to imagine sandwich soil layers between the layers of waste. On the contrary, the clayey soil covers tend to migrate within waste and may mislead to distinguish them from latter (Morris and Wood, 1990). For this reason, these layers of soil are not considered in ISPM modelling. On the other hand, the quantity of soil added to waste (except cap cover) is incorporated for a qualitative account at the stage of the analysis of the compressibility of the material.
- The final cover of unit weight γ_c and thickness h_c is supposed to be incompressible at any moment.

In the context of present study, the vertical compressive stresses σ are considered positive (as in soil mechanics) just as settlements (Δh, w) towards bottom, similarly the deformations in contraction or the reductions in void ratio Δe are considered positive.

V - 3.4 Fundamental Equations of ISPM Model for an Elementary Layer *i*

The research study carried out by Olivier (2003) suggests maintaining the interpretation of two phases in settlement from his own results of research project. In the present study the compression known as 'instantaneous' will not be considered since it is not possible to dissociate it from the primary phase of settlement. It will be thus regarded as included in primary settlement, (the initial thickness h_0 and unit weight γ_0 of an elementary layer of waste both being defined after compaction). Excluding the initial phase of spreading and compaction of waste, the history of an elementary layer includes 2 phases:

- A phase of compression under the actual weight of the overlying elementary layers during which primary settlement and secondary settlement are superimposed;
- a phase of compression known as 'post-construction settlement' at constant load (with the variations of mass relating to the biological breakdown being excluded as well as the evolution of the water content) during which only secondary settlement takes place.

V- 3.4.1 Primary Settlement

Primary settlement results from the mechanical actions related to the application of a surcharge. The response time of material cannot be allocated to dissipations of pore water pressures in the case of waste because it is seldom saturated. On the other hand, it can be due mainly to the significant rearrangements of the materials structure and the compressibility of the different solid elements. The time of primary settlement is considered very short, such as:

- in the case of the construction of a waste column of municipal solid waste, the primary settlement of a layer of waste is supposed to be completed at the end of construction of the layer (time τ_i);
- in the case of laboratory tests on waste samples with thickness of one meter, the end of primary settlement is taken as the offset of the curve $\Delta h = f(t)$. Time t_1 corresponds to the end of primary settlement and varies over a time period of few minutes to few hours after the application of the last load application however additional research is needed to clarify this supposition.

The primary settlement of the layer *i* is described as presented in the theory of Terzaghi developed in soil mechanics as follows (total stresses):

[M] $$\frac{\Delta h_i^p}{h_0} = C_S^* . \log \frac{\sigma_i}{\sigma_0}$$ in over consolidated phase ($\sigma_0 = \sigma_i = \sigma c$) with $C_S^* \cong 0$

[N] $$\frac{\Delta h_i^p}{h_0} = C_R^* . \log \frac{\sigma_i}{\sigma_c}$$ in normally consolidated phase ($\sigma_i > \sigma c$)

Over consolidated waste is supposed to be insensitive of the surcharge (no compression) and C^*_R represents the 'intrinsic' coefficient of primary compression of the waste (different from the Sowers coefficient C_R, Eq.[K]) directly deduced from the equation of a column of waste. Stress σ_i corresponds the pressure applied to the top of layer *i* (on a horizontal face) and corresponds to the weight of the overlying layers of waste column (and the final cover).

V- 3.4.2 Secondary Settlement

Secondary settlement is supposed to be independent of load and varies over the course of time. The secondary settlement, of the layer *i*, is written according to the law of Buisman (1936):

[O] $$\frac{\Delta h_i^s}{h_0} = C^*_{\alpha\varepsilon}.\log\frac{\tau}{\tau_c}$$

Where $C^*_{\alpha\varepsilon}$ represents the 'intrinsic' coefficient of "secondary compression" (creep) of waste, τ_c the time of secondary settlement status and τ is the time since the beginning of the construction of the layer *i* (whose origin coincides consequently with the beginning of the construction of layer *i*). This equation differs from the Sowers equation [L]

V - 3.5 General Formulation of Model ISPM: Modelling of Surface Settlement

V- 3.5.1 Expression of the Primary Settlement of a Waste Column

This part of the modelling was not altered in the ISPM model, as suggested by Olivier (2003). Considering primary settlement independent of stress application mode during the waste placement but only on the compressive stress it can be stated that the placement of waste can be carried out in a regular way or by phases: when waste reaches the height $H(t_c)$ and the cap cover is built, the end value of primary settlement is supposed to be identical whatever the way of loading. Compacted waste will behave, if identical with a soil, as an 'over consolidated' material as long as the pre-consolidation stress (σ_c) resulting from the compaction remains higher than the stress transmitted by the column of waste above it. Or it will compress as a material 'normally consolidated' and its density will thus increase with the depth under the effect of primary settlement.

Considering the history of step by step filling, at the time of the placement of the first elementary layer, it is supposed to be pre-consolidated due to the compaction effort. When the second layer is placed on top of the first, it induces a vertical stress corresponding to its actual weight and so on for the following layers. From a level of stress higher than the pre-consolidation stress σ_c, the application

of the additional layers increases the primary settlement of the normally consolidated layers. Thus, the placement of layer *i*, starts a new phase of primary settlement for layers 1, 2…, i_c -1, index i_c corresponds to the first pre-consolidated layer. The same applies to the placement of the layers *i* + 1 to *n* and final cover. Quantitatively, the vertical stress acting on layer *i* at the end of the construction (*n* layers) corresponds to the actual weight of the overlying strata and cover:

[P] $$\sigma_i = (n - i)\gamma_0 h_0 + \gamma_c h_c$$

Where $\gamma_c h_c$ (noted as *q* hereafter) represents the vertical stress induced by the actual weight of the cover. Taking into account the pre-consolidation stress σ_c induced by the compaction, the elementary layers undergoing a vertical stress $\sigma < \sigma_c$ are supposed to be over consolidated and their primary settlement is considered zero. On the other hand, the layers undergoing a vertical stress $\sigma > \sigma_c$ are supposed normally consolidated. Primary settlement thus relates to the layers of index *i* where $\sigma_i > \sigma_c$ such that for equation [P], the layers satisfying the inequality $i < n - \dfrac{\sigma_c - q}{\gamma h_0}$ with $q = \gamma_c h_c$

In order to define $i_c = ENT\left(n - \dfrac{\sigma_c - q}{\gamma h_0}\right)$ with simplicity, the critical point of over consolidation concerns the layer i_c, it is supposed that layer i_c is over consolidated, this approximation generates a weak error for an elementary thickness where *h* is very small in comparison to *Hn*. Thus $\Delta h_i^p = 0$, $\forall\, i \in [\, i_C \ldots, n\,]$. The expressions of Δh_i^p for $i < i_c$ are illustrated in Figure V-27.

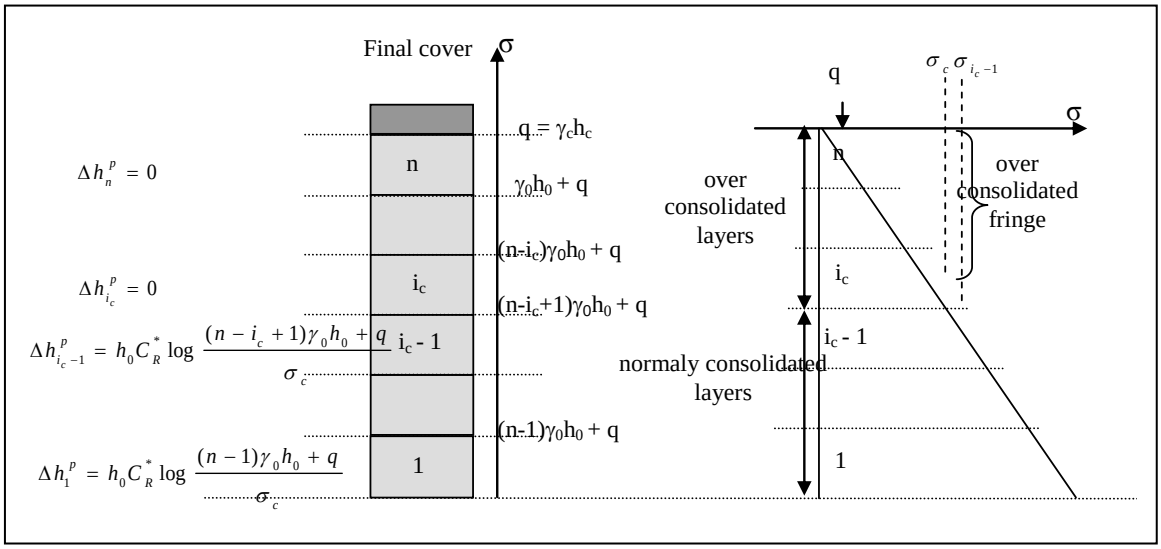

Figure V- 27: Expressions of primary settlement for elementary layers 1 to n (ISPM Olivier, 2003).

If it is considered that the intrinsic coefficients of primary compression are identical for each layer of waste, the expression of the primary settlement (w_n^p) of the complete column while summing Δh_i^p for *i* varying of 1 to $i_c - 1$, is obtained:

[Q] $$w_n^p = \sum_{i=1}^{i_c-1} \Delta h_i^p = h_0 C_R^* X \quad \text{with} \quad X = \log \frac{\prod_{i=1}^{i_c-1} \left((n-i)\gamma_0 h_0 + q\right)}{(\sigma_c)^{i_c-1}}$$

V- 3.5.2 Secondary Settlement Expression for a Column of Waste

To assess the settlement of the multi-layer waste column, modelling of the construction history is required. The modelling of settlement prediction for the present study starts from this section in comparison with the former version of ISPM as developed by Olivier (2003) to the newer one as ISPM 1.1. The fundamental equation modified under the present study is;

$$\frac{\Delta h_i^s}{h_0} = C_{\alpha\varepsilon}^* . \log \frac{\tau}{\tau_c} \quad \text{(Eq. [O])}$$

From the equation [R], the values from t_i and t_c, corresponding respectively to the end of construction of the layer *i* and the end of construction of the complete column (cover included) are deduced Figure V-28.

[R] $$t = \sum_{j=1}^{i-1} \tau_j + \sum_{j=1}^{i-1} \tau_{rj} + \tau$$

where τ_j is the time of construction of layer *j*

τ_{rj} is the rest period between the end of construction of layer *j* and the start of construction of layer *j* + 1. Absolute time (*t*) originates from the time of beginning of construction of the column of waste. Expressing the same parameter according to time τ (considered from the beginning of construction to the last layer), the operating times (τ_j) and the rest periods (τ_{rj}) for each of the sub-layers, τ_{rj} is the rest period between the placement of the layers *j* and *j*+1 ($\tau_{rj} \neq 0$ only for the discontinuity between two successive layers) with the assumption of constant thickness (h_0) for every layer. Figure V-28 presents the overall construction of the landfill, t_i the time corresponding to the end of construction of layer *i* and t'_i corresponds to the beginning of the construction of layer *i+1*.

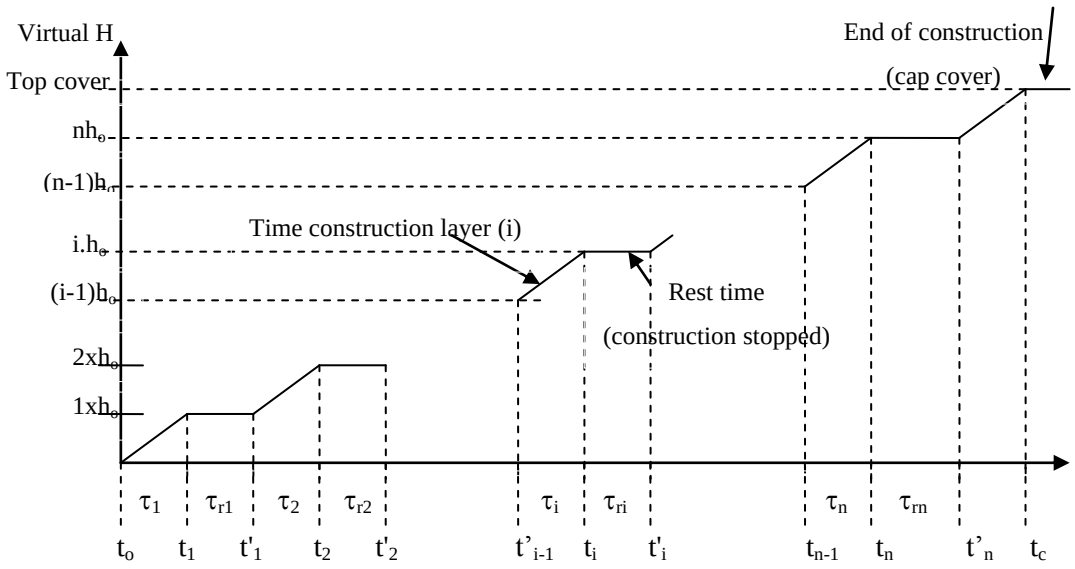

Figure V- 28: Sequence of construction of the overall landfill.

V- 3.5.3 Scheme of Construction

Figure V-28 focuses on the construction of the median column height of the waste, with the assumption that the column under study is situated far from the edge of landfill. By expressing the fundamental equation of secondary settlement [O] according to absolute time *t*, the expression for the secondary settlement of layers 1 to *n* is obtained as shown in Figure V-29. For the median column:

The layer *i* is supposed to be build instantaneously at average time $\left(\frac{t'_{i-1}}{2} + \frac{t_i}{2} \right)$

t'_{i-1} : initial time of construction layer *i* with $t'_{i-1} = t_{i-1} + \tau_{i-1}$

t_i : final time of construction layer *i*

$t'_i - t_i$: rest time, constant height of waste surface

With $t'_{i-1} = \sum_{j=1}^{i-1} \tau_j + \sum_{j=1}^{i-1} \tau_{rj}$ $\qquad$ $t_i = \sum_{j=1}^{i-1} \tau_j + \sum_{j=1}^{i-1} \tau_{rj} + \tau_i$

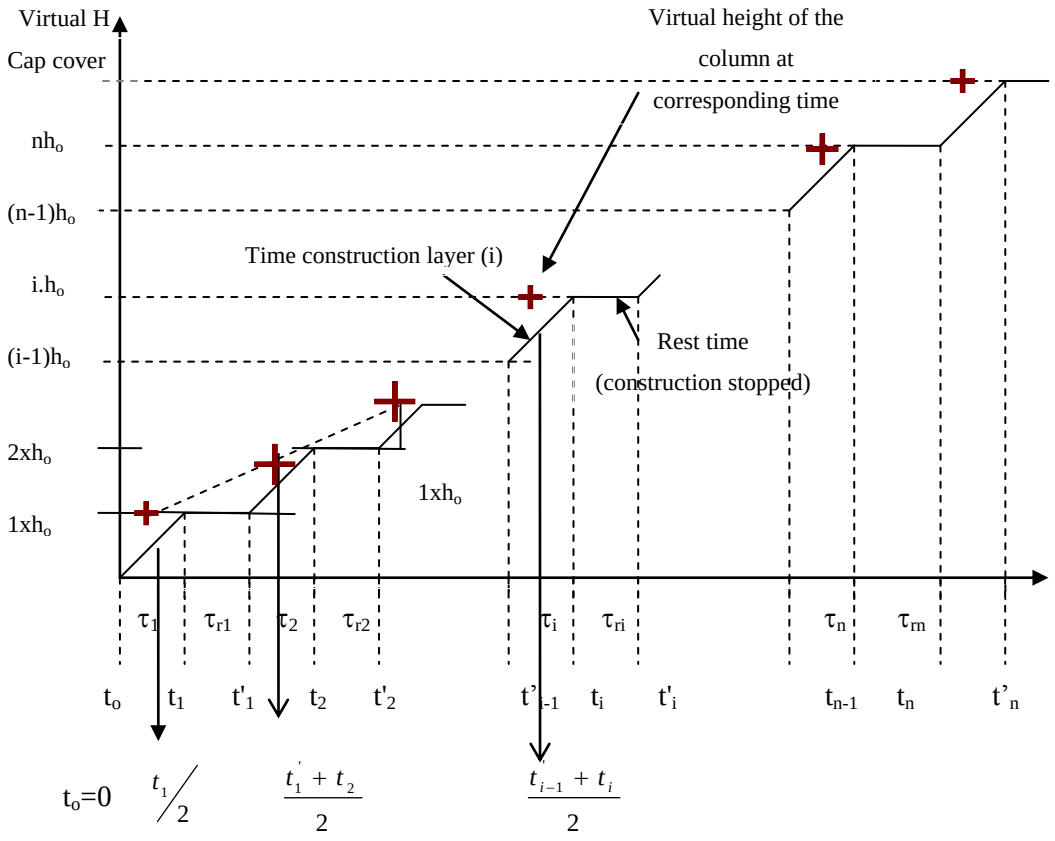

Figure V- 29: Sequence of construction of the median column height.

$$t_i = t_{i-1}^{'} + \tau_i \qquad \left(\frac{t_{i-1}^{'}}{2} + \frac{t_i}{2} \right) = t_i - \frac{\tau_i}{2} = \sum_{j=1}^{i-1} \tau_j + \sum_{j=1}^{i-1} \tau_{rj} + \frac{\tau_i}{2}$$

Secondary settlement for the layer *i* (median column) is defined as:

[S] $$\Delta h_i^s(t) = h_o C_{\alpha\varepsilon}^* \log \frac{\tau}{\tau_c} = h_o C_{\alpha\varepsilon}^* \log \left(\frac{t - \frac{t_{i-1}^{'} + t_i}{2}}{\tau_c} \right)$$

$$\Delta h_i^s(t) = h_o C_{\alpha\varepsilon}^* \log \left\{ \frac{\left(t - \sum_1^{i-1} \tau_j - \sum_1^{i-1} \tau_{rj} - \tau_i/2 \right)}{\tau_c} \right\} \text{ and so}$$

[T] $$w_s^n(t) = \sum_{i=1}^{n} \Delta h_i^s(t)$$

$$w_s^n(t) = h_o . C_{\alpha\varepsilon}^* \left[\sum_{i=1}^{n} \log \left(\frac{t - \frac{t_{i-1}^{'} + t_i}{2}}{\tau_c} \right) \right] = h_o . C_{\alpha\varepsilon}^* \log \left(\frac{\prod_{i=1}^{n} t - \frac{t_{i-1}^{'} + t_i}{2}}{(\tau_c)^n} \right)$$

and

$$w_s^n(t) = h_o.C_{\alpha\varepsilon}^{*} \log\left(\frac{\prod_{i=1}^{n}\left(t - \sum_{j=1}^{i-1}\tau_j - \sum_{j=1}^{i-1}\tau_{rj} - \tau_i/2\right)}{(\tau_c)^n}\right)$$

$$w_s^n(t) = h_o.C_{\alpha\varepsilon}^{*}.Y(t)$$

where

$$Y(t) = \log\left(\frac{\prod_{i=1}^{n}\left(t - \sum_{j=1}^{i-1}\tau_j - \sum_{j=1}^{i-1}\tau_{rj} - \tau_i/2\right)}{(\tau_c)^n}\right)$$

The present study consisted of modifying the calculation methodology of secondary settlement by taking into account the construction phases. Afterwards a parametric study with the new settlement algorithm is carried out and this new version of the ISPM model is named as 'ISPM 1.1', moreover this version is compared for reliable results against the older version 'ISPM 1.0' (Olivier, 2003). The varying parameters for the construction are presented in Table V-6 (thickness proportional with time)

Table V- 6: Details of waste layer construction ISPM 1.1

Waste layer	Thickness	Time of construction
j = 1	$1 \times h_0$	$t_1/2$
j = 2	$2 \times h_0$	$\frac{t_1' + t_2}{2}$
j = i – 1	$(i-1) \times h_0$	$\frac{t_{i-2}' + t_{i-1}}{2}$
j = i	$i \times h_0$	$\frac{t_{i-1}' + t_i}{2}$
j = n	$n \times h_0$	$\frac{t_{n-1}' + t_n}{2}$

V- 3.5.4 Case of Constant Lift Rate for Waste Column Construction

Provided that the speed of rise of the waste column does not fluctuate and in the tangible absence of information on the history of construction, an average operating time per layer ($\tau = t_n / n$) can be considered (Figure V-30) in the place of the operating times τ_i and the rest periods τ_{ri}, simplifying thus significantly the expression of the equation [U].

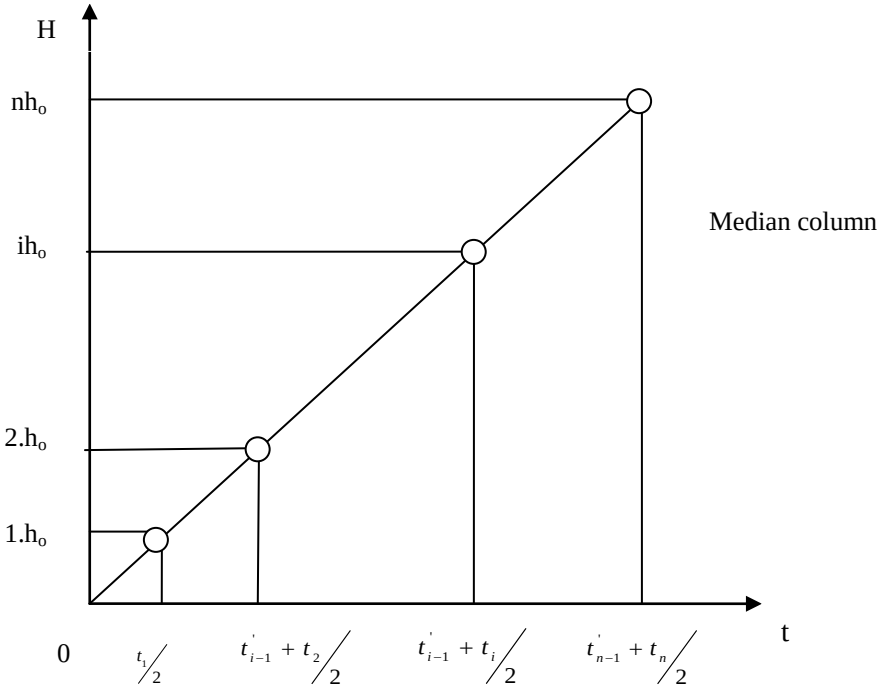

Figure V- 30: Median Column rise with reference to the time of construction.

For $\tau_j = \tau$ and $\tau_{rj} = \tau_r$ and $t_n = n\tau(n-1)\tau_r$

[U] $$w_s^n(t) = h_o.C_{\alpha\varepsilon}^* \log\left\{\frac{\prod_{i=1}^{n}\left(t-(i-1)\tau-(i-1)\tau_r-\tau_i/2\right)}{(\tau_c)^n}\right\}$$

$$w_s^n(t) = h_o.C_{\alpha\varepsilon}^*(Y(t))$$

For linear construction $\tau_{ri} = 0$

Settlement after completion of construction (t = $t_n = n\tau$)

[V] $$w_s^n(t) - w_s^n(n\tau) = h_o.C_{\alpha\varepsilon}^* \log\left\{\frac{\prod_{i=1}^{n}\left(t-(i-\frac{1}{2})\tau\right)}{\prod_{i=1}^{n}\left(n-i+\frac{1}{2}\right)\tau}\right\} = h_o.C_{\alpha\varepsilon}^* \log\left\{\frac{\prod_{i=1}^{n}\left(t/\tau-i+\frac{1}{2}\right)}{\prod_{i=1}^{n}\left(n-i+\frac{1}{2}\right)}\right\}$$

V-4 APPLICATION OF THE MODEL FOR A DIRECT EVALUATION OF SETTLEMENT

The objective of the present parametric study was to evaluate the post construction settlement *w(t)*.

V - 4.1 Definition of the Surface Settlement

As explained previously, the primary compression of a column of waste (w_p) is supposed to be completed at time t_c. Consequently, post-construction settlement *w(t)* when $t > t_c$ (measured using reference marker at surface) can be compared to an exclusively secondary compression for $t \geq t_c$

[W]

$$w(t) = w_n^s(t) - w_n^s(t_c) = h_0 C_{\alpha\varepsilon}^* \left[Y(t) - Y(t_c) \right] = h_0 C_{\alpha\varepsilon}^* \log \left\{ \frac{\prod_{i=1}^{n} \left(t - \sum_{j=1}^{i} \tau_j - \sum_{j=1}^{i} \tau_{rj} - \tau_i / 2 \right)}{\prod_{i=1}^{n} \left(t_c - \sum_{j=1}^{i} \tau_j - \sum_{j=1}^{i} \tau_{rj} - \tau_i / 2 \right)} \right\}$$

In addition, the height of the column of waste (cap cover excluded) is equivalent to:

[X] $$H_n(t) = nh_0 - w_n^p - w_n^s(t)$$

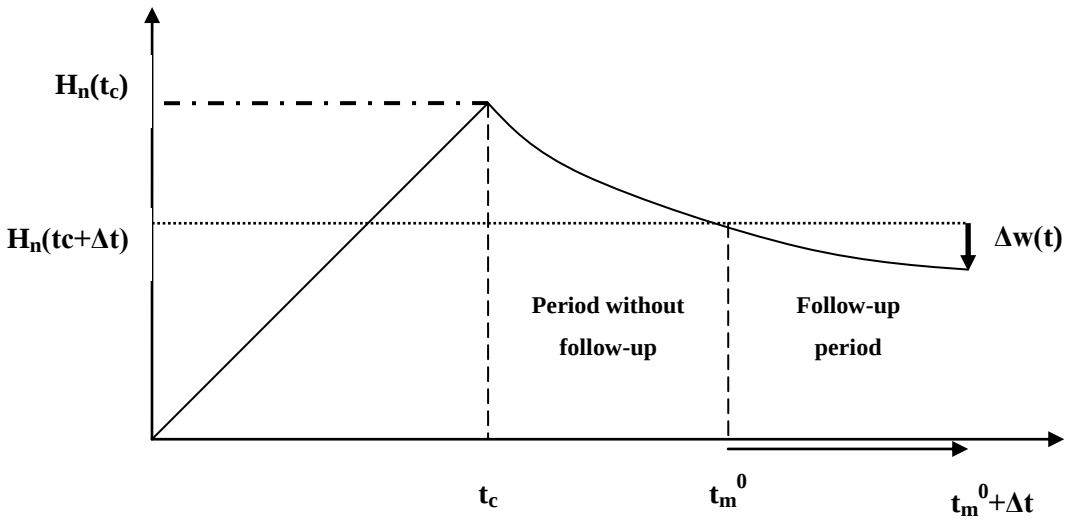

Figure V- 31: Measurement of settlement at a delayed period of follow-up at site at time t_m^0.

Lastly, the post-construction deformation *ε(t)* of average height of the column is calculated by determining the settlement measured at the surface *w(t)* for the total height of waste H_n (cover excluded) at time t_c (and sometimes at time t_n):

[Y] $$\varepsilon(t) = w(t) / H_n(t_c)$$

If for an unspecified reason the topographic follow-up is delayed for time (Δt) after the cover placement, the compression measured on the surface is not equivalent to post-construction settlement *w(t)*. Supposing that the first topographic measurement of surface is carried out at time $t_m^0 > t_c$, where t_m refers to an unspecified intermediate measurement, measured settlement is then equivalent to:

[Z] $$\Delta w(t) = w(t) - w(t_m^0) = w_n^s(t) - w_n^s(t_m^0)$$

V - 4.2 Influence of Different Parameters of the Study

The durations of construction τ_i of each layer are seldom known in detail by the landfill operators. In practice, the researcher must reconstitute the history of construction as precisely as possible, while making use of:

- intermediate plans of construction;
- stored flows of waste (periodic tonnages);
- evolution of the surface of construction of the waste column in activity in the course of time.

If somehow the reconstitution of construction history is not possible, ISPM model can be applied by supposing a rise of waste column at constant speed ($\tau_i = \tau$ = constant and $t_c = n\tau + \tau_c$). Additionally the settlement is dependent on the value of $C^*_{\alpha\varepsilon}$. It still remains difficult to correlate the values of $C^*_{\alpha\varepsilon}$ with the composition of the waste stored and its modification during/after construction. It is mainly due to the difference in conditions of construction (nature and intensity of compaction) and in landfill storage (moisture content of waste, heat flux, biogas drainage, etc.)

V- 4.2.1 Influence of Waste Column Height

In this section the variation of the settlement Δw (Equation [Z]) corresponding to the settlement after construction is considered in detail (i.e. after closure of the landfill, time $t = t_c$). Objective of the study is to observe the influence of total height of waste on the deformation of the waste column after the construction. For this purpose the time of construction of waste column is fixed (Figure V-32), with varying heights of the waste column.

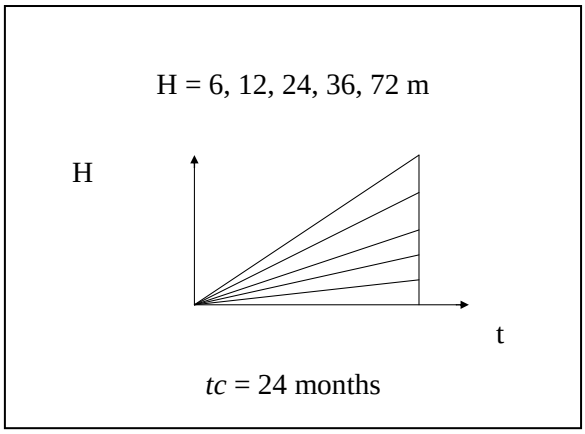

Figure V- 32: Varying the height of waste column for a given constant time of construction

The curves obtained show the influence of column height while keeping the other parameters constant. It can be observed in Graph V-1 that change in height of a waste column affects the relative settlement which is a direct relation, $\varepsilon = {}^{\Delta w}\!/_{H_n(t_c)}$ that is to say more the column is high more will be the settlement since initial part of the secondary settlement is more significant.

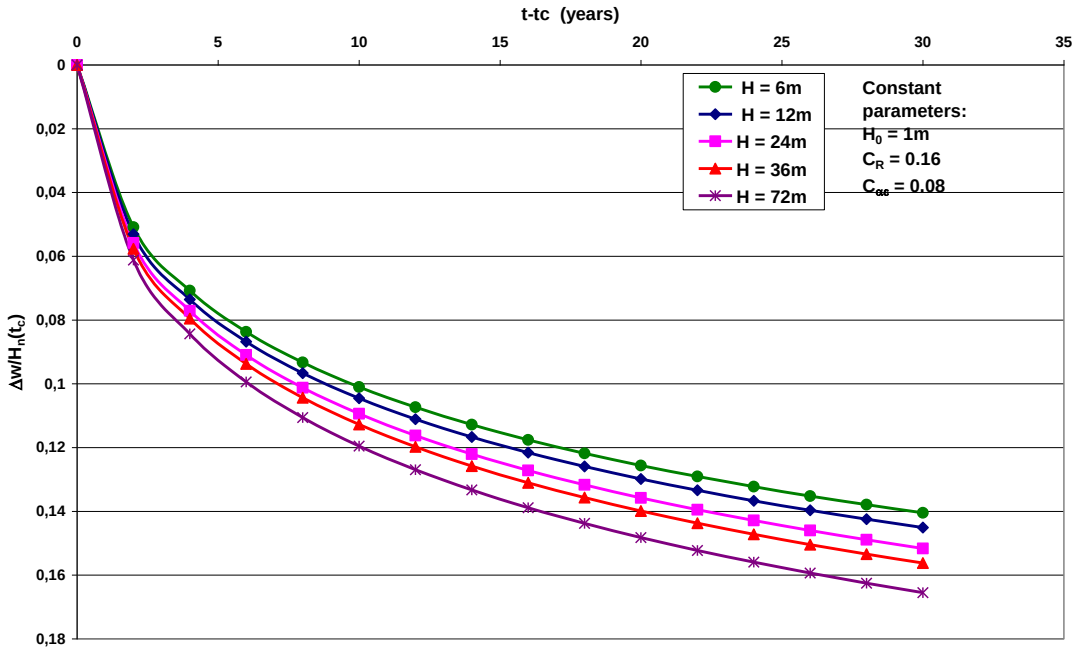

Graph V- 1: Evolution of deformation as a function of the waste column height (t_c = 24 months).

V- 4.2.2 Influence of Column Height for a Constant Lift Rate

To observe the variation in the settlement for a constant lift rate, theoretical cases of waste column were studied with varying heights and construction time so as to achieve a constant lift rate, i.e. H/t_c = 1 m/month as presented in Figure V-33.

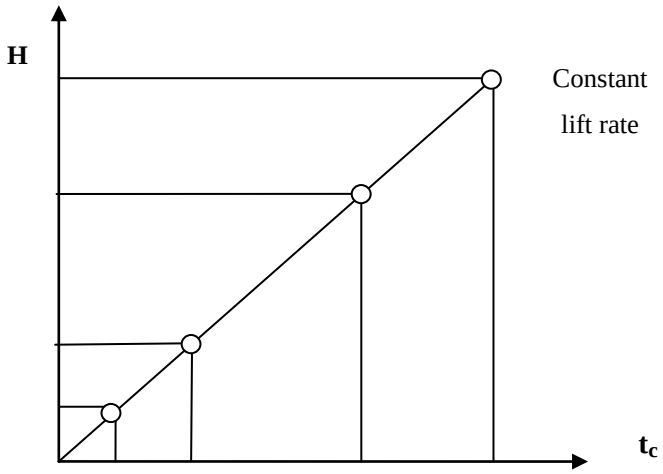

Figure V- 33: Construction history of a waste column with a constant lift rate.

The results as plotted in Graph V-2 show that the relative settlement decreases when the height of the column increases for the same lift rate. Hence for the same lift rate the waste column smallest in height will have the biggest amount of settlement than the tallest waste column. This explains the effect of quick construction of the waste column as each layer is placed without giving the precedent layer enough time to settle so the overall settlement component will be small.

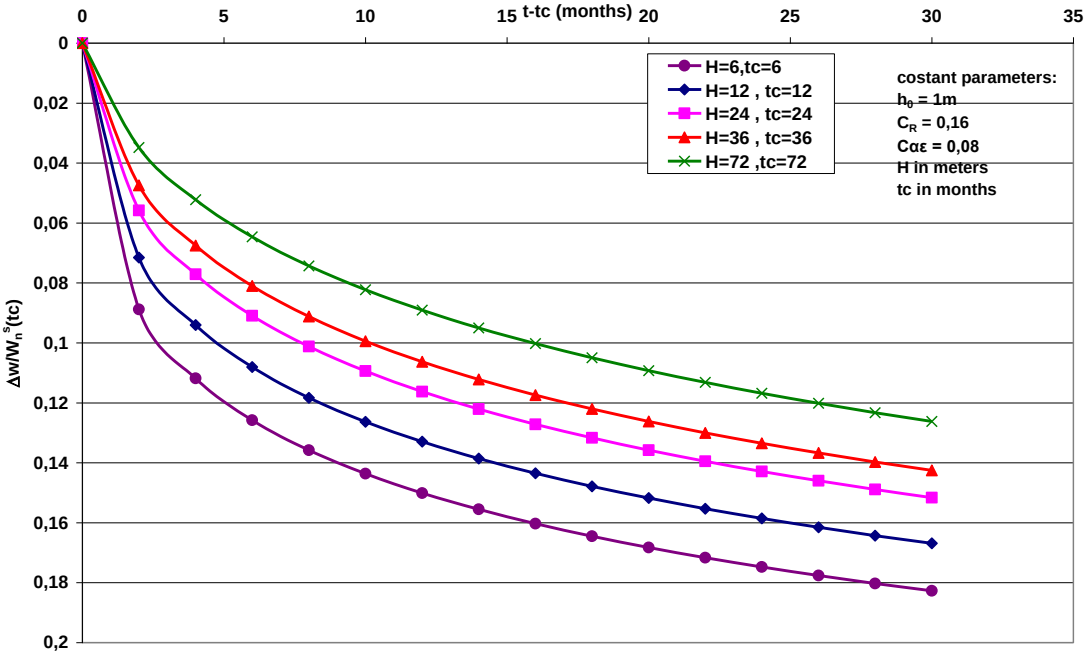

Graph V- 2: Influence of column height on post construction settlement for a constant lift rate.

V- 4.2.3 Influence of Time of Waste Column Construction

To analyse the effect of time of construction on the settlement behaviour the column height was fixed and time of construction was varied. Graph V-3 plotted for settlement as a function of column height clearly shows that faster the construction time faster will be the secondary settlement. And thus it will have a secondary settlement which will be more influential than the part of the settlement already occurred during the construction phase. The similar results observed in Graph V-3 strengthen the earlier findings in Graph V-2.

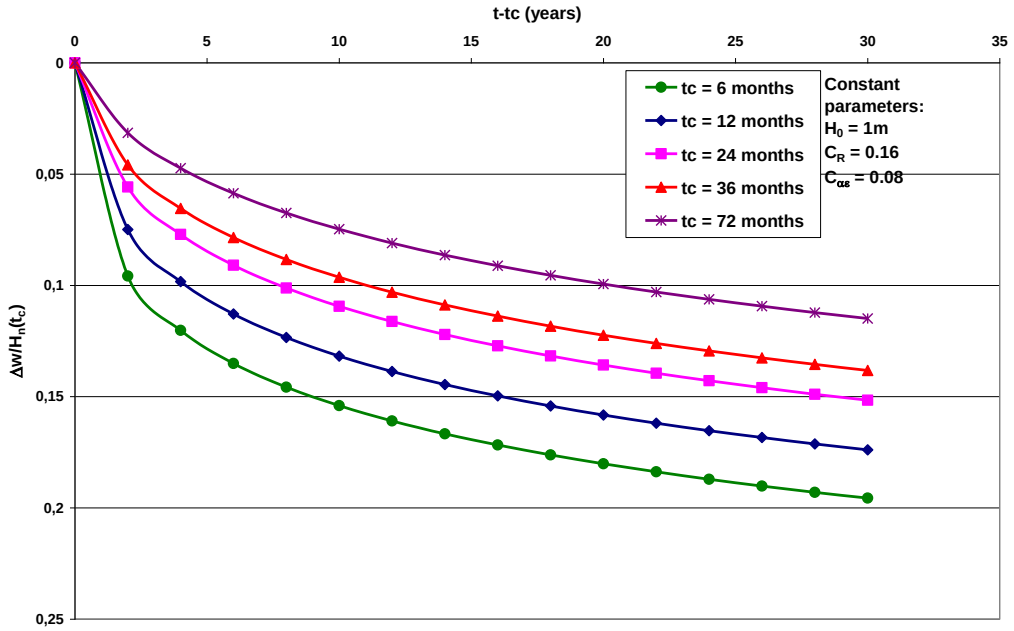

Graph V- 3: Evolution of deformation $\Delta w/H_n(t_c)$ as function of t_c, (H=24m)

V- 4.2.4 Influence of τ_c (origin of time for secondary compression)

Since this parameter was modified from the one used in the older version of ISPM model a large range of the stated time parameter (starting from one day to six months) was studied so as to reach a conclusion about its best suited value for modelling. A number of cases were theoretically calculated with varying waste column heights and time of construction and plotted against τ_c so as to see percentile variation of the parameter.

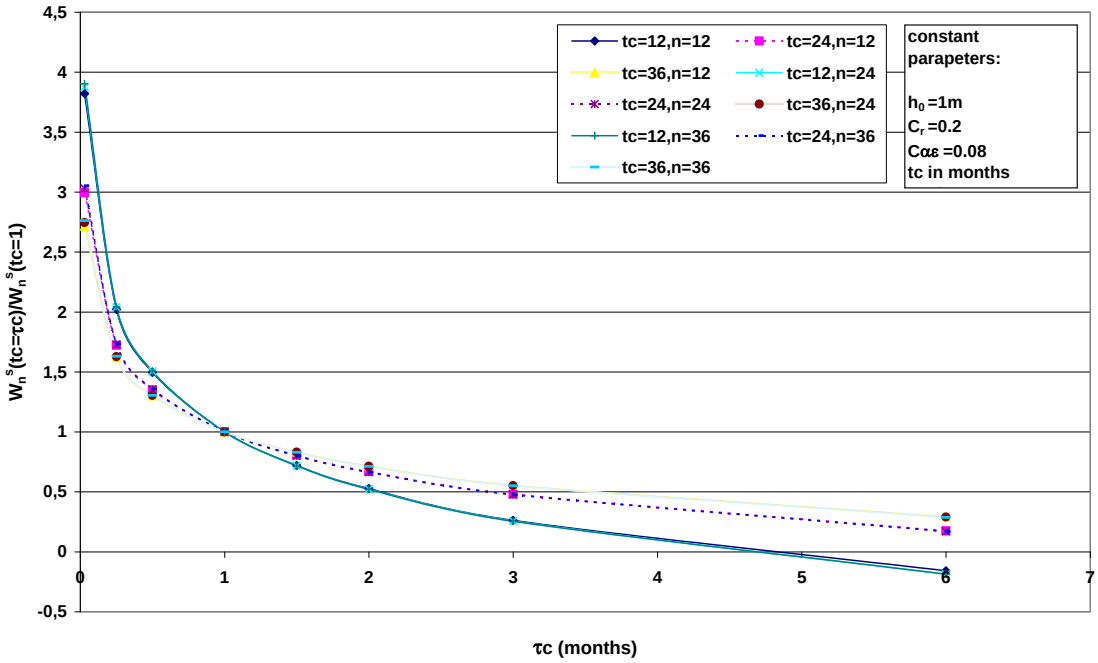

Graph V- 4: Influence of τ_c on settlement ratio for τ_c = 1 month at the end of construction.

While going through this parametric study it was noted that secondary settlement was independent of the chosen value of τ_c and it was then proved analytically, as shown in Graph V-4. Its effect on the back analysis was then proved to be linked to the virtual height of the waste column nh_0 rather than any other parameter involved in waste settlement modelling (Graph V-5) leading to the conclusion that it was only the first part of the secondary settlement which is dependent on τ_c.

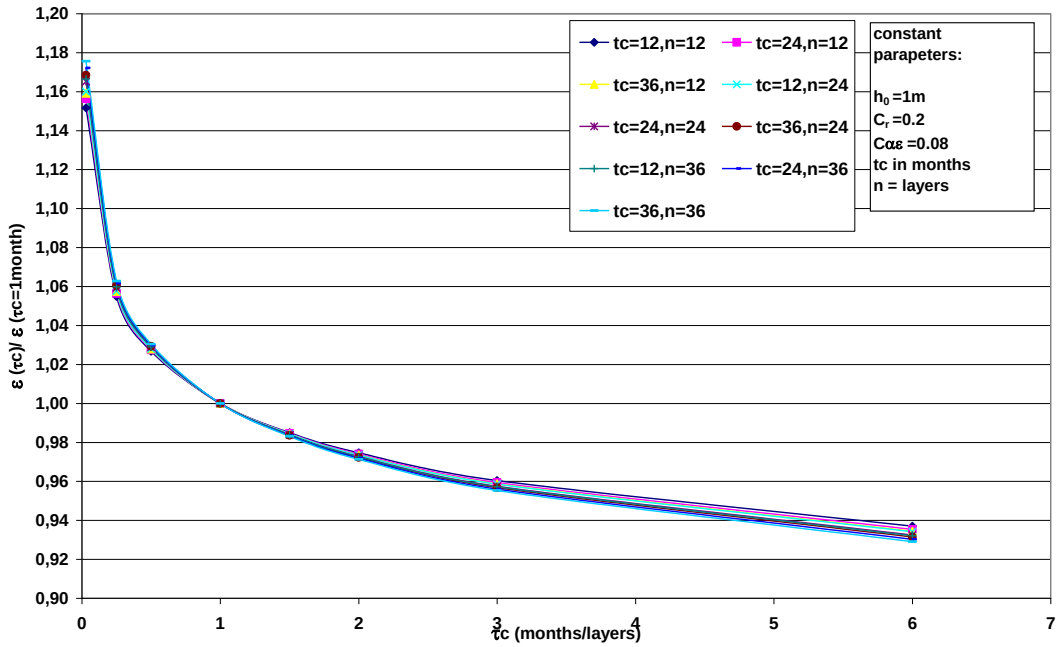

Graph V- 5: Influence of τc on the ratio of post construction deformation ε(t).

V-5 APPLICATION OF ISPM MODEL BY BACK ANALYSIS FOR AN EVALUATION OF $C^*_{\alpha\varepsilon}$

Though $C^*_{\alpha\varepsilon}$ (Eq. [S]) in the present time remains difficult to be fixed for a prediction of the settlement *w* of a waste column and consequently it is proposed here to use case histories where settlement is recorded by monitoring and to deduce $C^*_{\alpha\varepsilon}$ by back analysis. The application of ISPM model by back-analysis consists in determining the values of $C^*_{\alpha\varepsilon}$ starting from data of settlement $w(t_m)$ drawn from measurements on the landfill cap cover. In the case of the modern MSW, the majority of other parameters of the law of settlement relationship can be calculated starting from information available with the landfill operators and by fixing certain parameters (having a limited influence) such as $C^*_{\alpha\varepsilon}$ and σ_c by approximation (Table V-7).

Table V- 7: Synthesis of the parameters of ISPM model and mode of determination.

Category	Parameter	Symbol	Unit	Mode of determination
Geometrical parameters	number of layers	n	-	Approximated
	initial thickness of a layer	h_0	m	Back-analysis
	height of waste at time t_c	$H_n(t_c)$	m	Landfill operator
Parameters of time	Period of construction	τ_i	month	Landfill operator
	durations of stop of construction	τ_{ri}	month	Landfill operator
	total operating time	t_c	month	Landfill operator
	time of measurement	t_m^0, t_m, t_m^{ult}	month	Geometer
Parameters relating to the loading of waste	initial unit weight of waste	γ_0	kN/m^3	Back-analysis
	average unit weight of waste (t_c)	$\bar{\gamma}(t_c)$	kN/m^3	Landfill operator
	compaction stress	σ_c	kPa	Supposed (≅ 40 kPa)
	surcharge due to the cover	q	kPa	Landfill operator
Parameters relating to the compressibility of waste	coefficient of primary compression	C_R^*	-	Measured(≅0.15–0.20)
	coefficient of secondary compression	$C_{\alpha\varepsilon}^*$	-	Back-analysis
	post-construction settlement	$w(t_m)$	m	Geometer

V - 5.1 Case Study of Different Sites for Linear Construction

The back analysis is based on settlement monitored during the period (end of construction t_c) until time t_m^{ult}. For every settlement value $C^*_{\alpha\varepsilon}$ is evaluated by back analysis (Figure V-34): generally for ($t_m^{ult} - t_c$) higher than 9 months $C^*_{\alpha\varepsilon}$ value is stabilized and can be used as a long term value of $C^*_{\alpha\varepsilon}$. This method is applied here for some well-documented case histories (Table V-8).

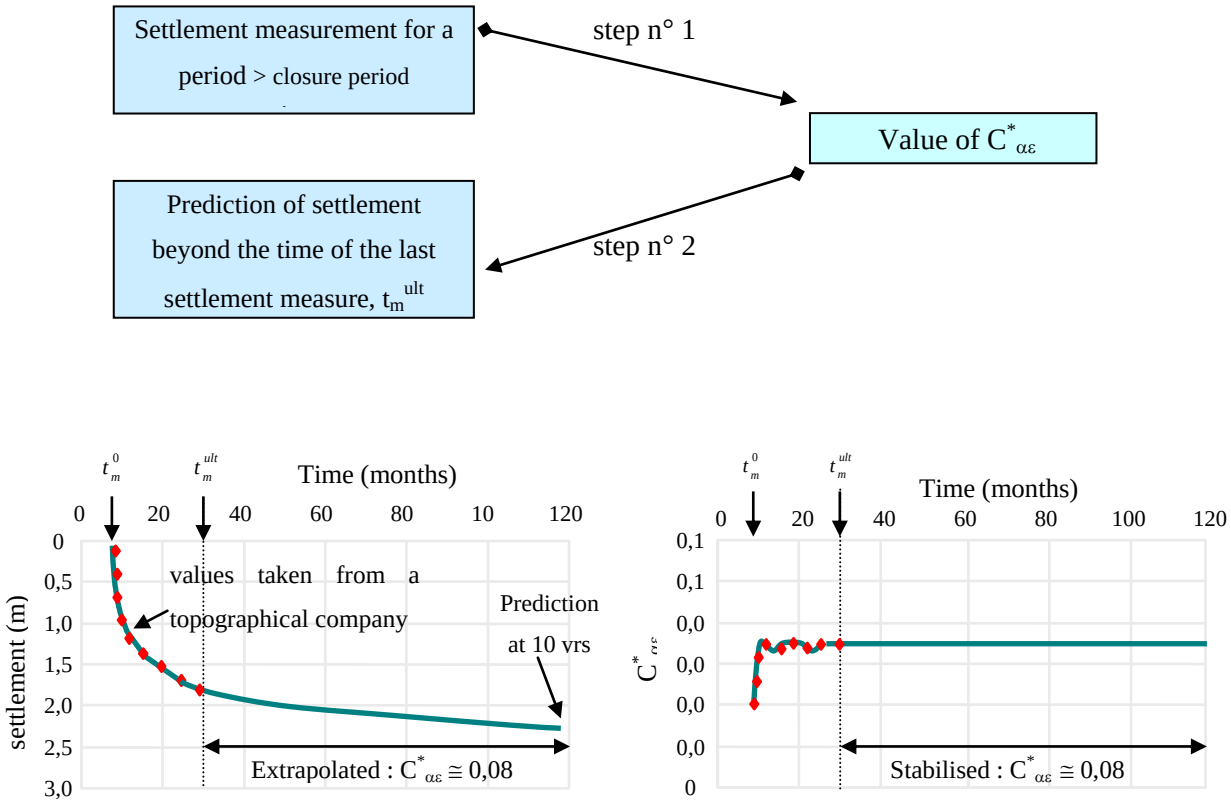

Figure V- 34: Illustration of the prediction of settlement by back analysis (ISPM model, Olivier, 2003).

Table V- 8: Description of different case histories considered in the back calculation.

Parameters	Sites			
	Collier Road	Montreal	Novellara	Yolo county
t_c (months)	188.67	73.87	21.97	6.1
H (m)	15.2	78.92	9.04	13.06
C_R	0.2	0.2	0.2	0.2
γ_0 (Kn/m^3)	6	8	7	8
τ_c (months)	1	1	1	1

Knowing the values of settlement and the construction history of the column of waste, it is possible to determine the value of $C^*_{\alpha\varepsilon}$ making use of the equation [W]. Generally, the height of the column $Hn\,(t_c)$ at the end of the construction and the corresponding average unit weight change $\bar{\gamma}(t_c)$ are estimated starting from the total data resulting from the geometer (thickness of waste and volume of storage) and from the landfill operator (tonnage of waste) at time t_c (or sometimes t_n). It could be shown that a variation of the number of layers have no effect on modelling, in condition that nh_0 satisfies the equation [W] and that n makes it possible to model in a realistic way the rise of column. In addition, supposing the conservation of the mass of the matter during the period of construction, the following equation can be deduced:

[AA] $$\bar{\gamma}(t_c).H_n(t_c) = \gamma_0 nh_0$$

Ultimately, back analysis consists of solving a system made up of 3 equations [W], [X] and [AA] together these equations make it possible to determine the 3 parameters h_0, γ_0 and $C^*_{\alpha\varepsilon}$. By combination of the preceding system with the equation [X], the expression from the coefficient of intrinsic secondary compression according to the deformation ε at time t can be deduced:

[AB] $$C^*_{\alpha\varepsilon}(t) = \frac{\varepsilon(t)(n - C^*_R X)}{Y(t) - Y(t_c)[1-\varepsilon(t)]}$$

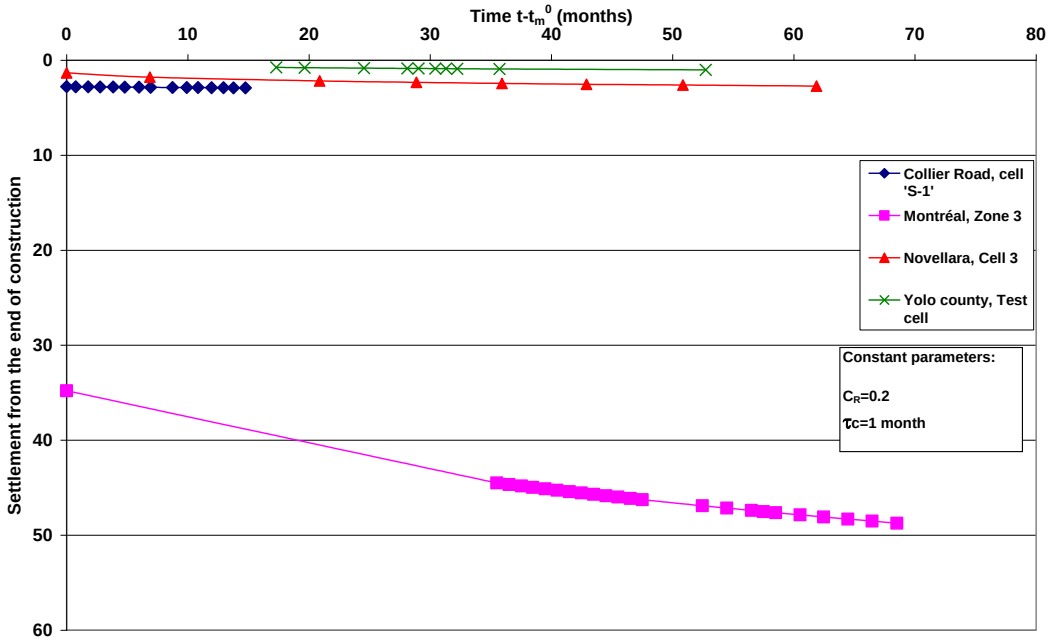

Graph V- 6: Effect of time on the evolution of settlement as analysed through Model ISPM 1.1.

Normally the first topographic measure on the cap cover after the closure of the landfill ($t = t_c$) is generally postponed where $t = t_m^{\,0}$ is time for the first measurement and $t = t_m^{\,ult}$ is the ultimate measurement.

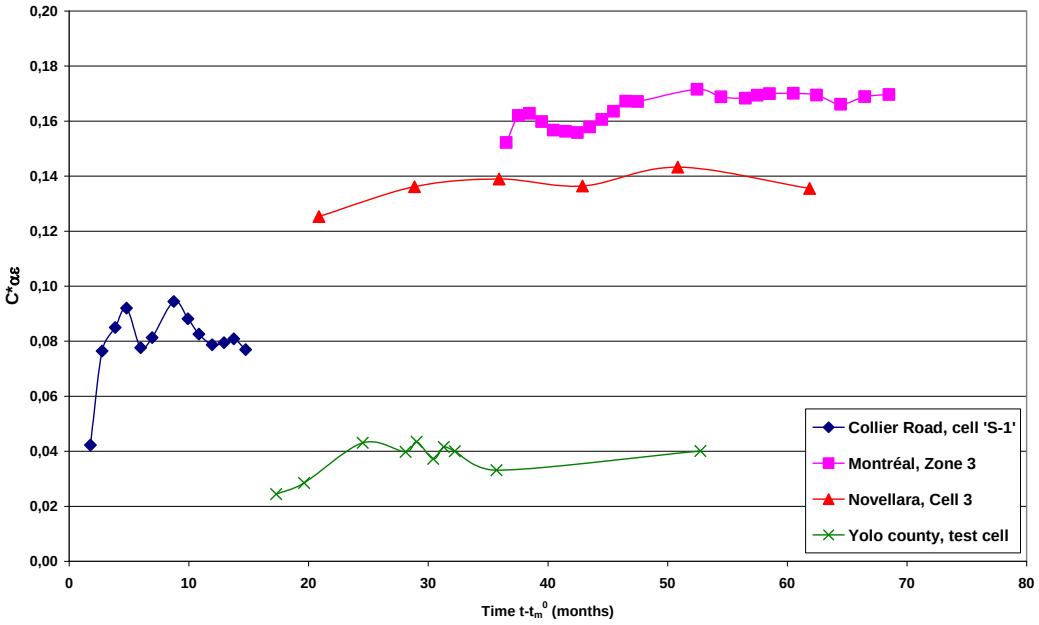

Graph V- 7: Evolution of $C^*_{\alpha\varepsilon}$ as a function of time.

For each value of surface settlement $w(t_m)$ ($t_m^0 \leq tm \leq t_m^{ult}$) (Graph V-7), the resolution of the preceding system provides a value of $C^*_{\alpha\varepsilon}(t_m^{ult})$ as presented in Graph V-8. The treated cases showed that $C^*_{\alpha\varepsilon}$ generally tended towards a stabilized value at the end of a time t sufficiently large, which confirms the intrinsic character of the parameter $C^*_{\alpha\varepsilon}$ obtained. If $t_m^{ult} - t_m^0$ is sufficiently large, one thus obtains a stable value of $C^*_{\alpha\varepsilon}$ allowing extrapolation to predict long-term settlement by extending the experimental curve of settlement.

Remaining problem is the influence of time τ_c corresponding to the beginning of the secondary settlement in the relationship [U]. In the Graph V-7, τ_c is assumed to be equal to 1 month while in Graph V-8 and Graph V-9, the influence of τ_c on the ultimate value of $C^*_{\alpha\varepsilon}(t_m^{ult})$ is presented.

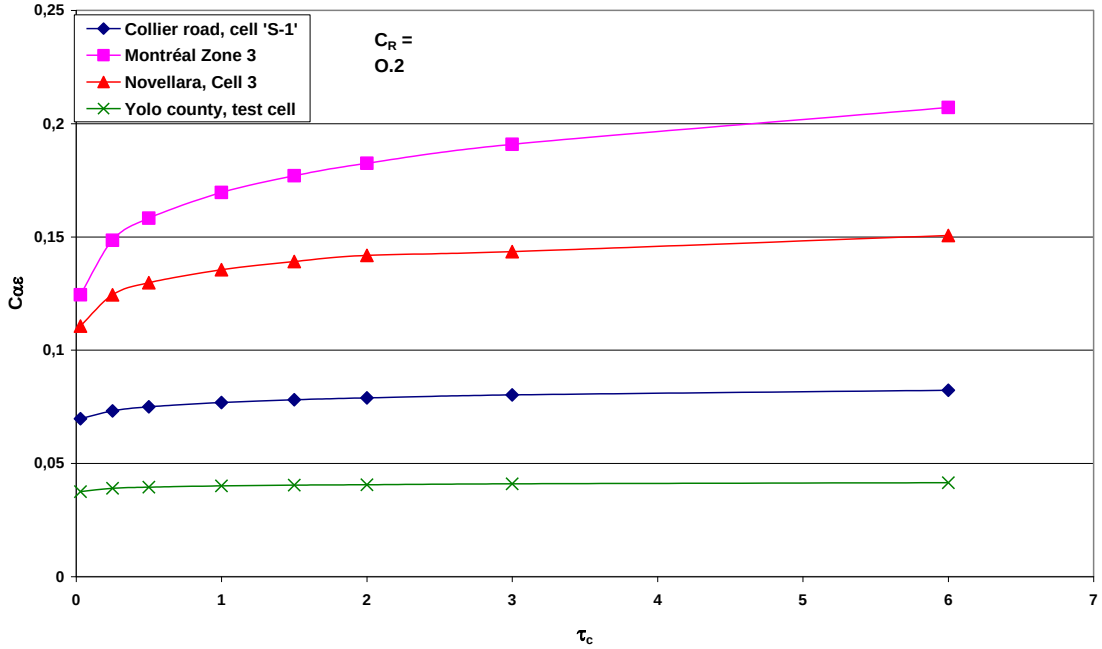

Graph V- 8: Evolution of Cαε obtained for t = t_m^{ult} as a function of τc

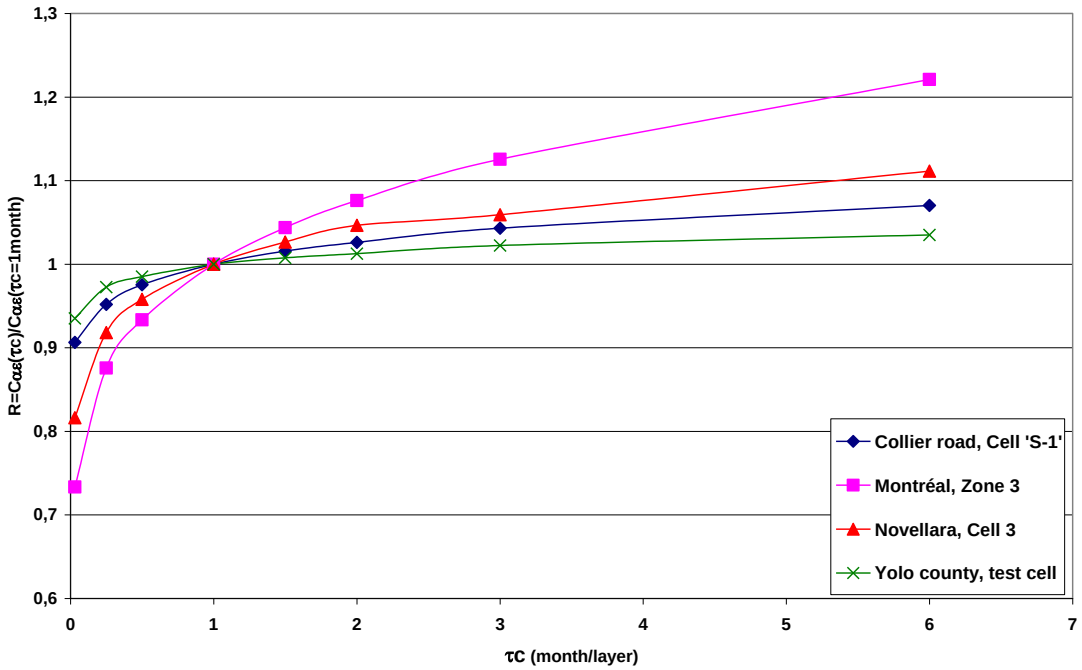

Graph V- 9: Relative evolution of C*αε as function of τ_c.

In Graph V-8 final values of $C^*_{\alpha\varepsilon}$ are shown against a range of values of τ_c which helped consider certain value for $C^*_{\alpha\varepsilon}$ from experimental point of view as the ratio between different τ_c plotted in Graph V-9 which showed the convergence of these measured values such that the suggest the intrinsic characteristic of the parameters $C^*_{\alpha\varepsilon}$. Furthermore this value of τ_c was determined physically from the

laboratory experiments which further justified the view point of considering $C^*_{\alpha\varepsilon}$ as an intrinsic coefficient.

V - 5.2 ISPM Application on 2 Phases Construction for the Evaluation of C_R and $C^*_{\alpha\varepsilon}$

In general, the follow-up of settlement is carried out by means of surface reference marks installed at the end of the construction phase (once cap cover is placed). Consequently, the topographic follow-up includes exclusively the measurement of secondary settlement, primary settlement being completed at the time of the survey of reference (with t_m^0 as in the section V-4.3). Nevertheless, a reactivation of primary settlement is possible in the case of extensions (or vertical reload) of waste columns or in the case of rehabilitation of old landfills including the construction of various works (earth fills, light constructions, roads, etc). In practice, primary settlement made the object of few terrain surveys [Watts and Charles (1990), Coumoulos et al. (1999), Yuen (1999), Bowders et al. (2000)] and their interpretation often was not satisfactory. Similar research was undertaken by LIRIGM on 3 French sites (Torcy, Lapouyade and Chatuzange) by means of internal instrumentations (monitoring of the settlement at the interface between two phases, Figure V-35).

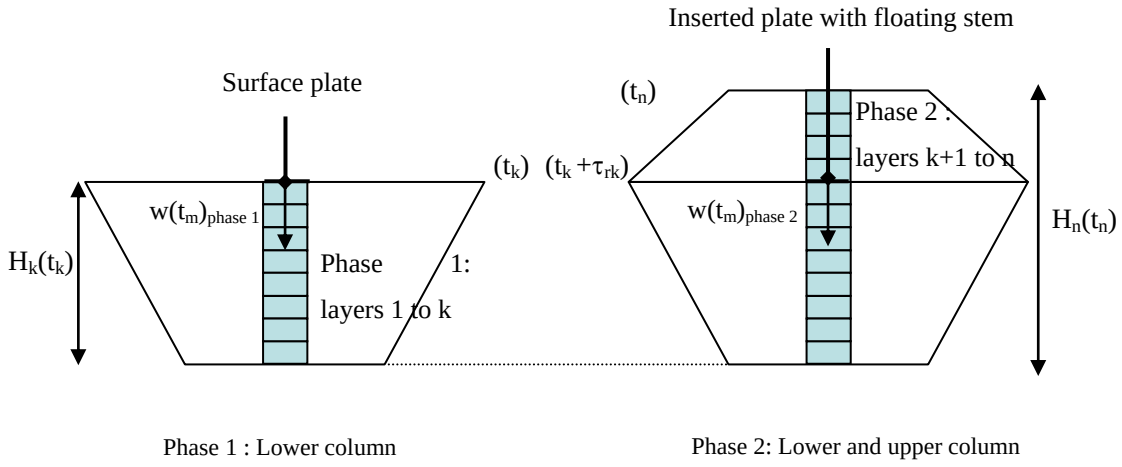

Figure V- 35: Schematic diagram of construction in 2 phases separated by one rest period.

V- 5.2.1 ISPM Settlement Modelling for a 2 Phase Construction (Cell 'B'-Chatuzange

The formulation of model ISPM is kept broad so as to allow the modelling of a landfill in 2 phases. The present application concerns cell 'B' at Chatuzange landfill site (Figure V-36) with the storage of waste in 2 distinct phases (phase 1: placement of layers from 1 to *k*; phase 2: placement of layers from *k+1* to *n*) separated by one rest period of τ_{rk} duration as considered in the example of Graph V-11.

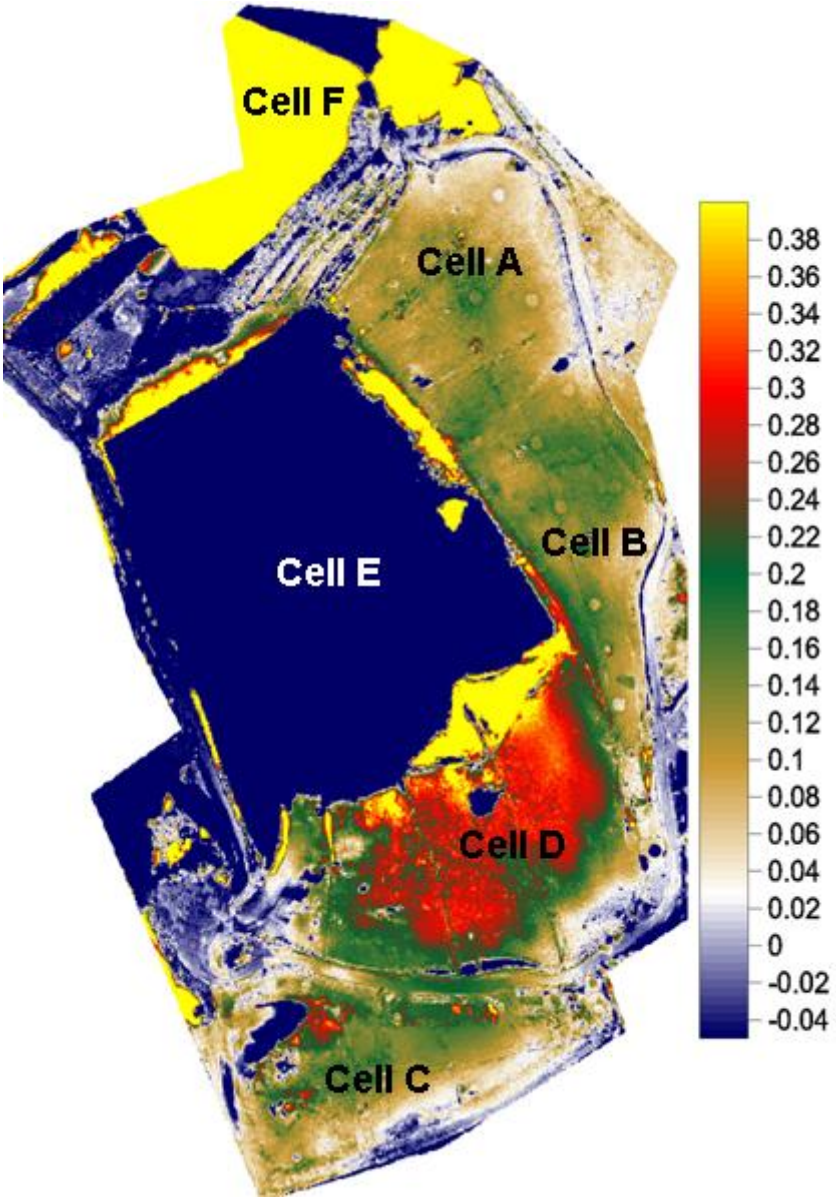

Figure V- 36: Plan of Chatuzange landfill site.

The originality of this example holds in the fact that it is possible to solve independently the system formed by the equations [W] [X] and [AA] during the intermediate period of rest (and the settlement monitoring at the surface of the lower column by surface instrumentation), during and after the phase of refill (phase 2) for internal follow-up. The values of $C^*_{\alpha\varepsilon Phase2}$ can be compared with the values of

$C^*_{\alpha\varepsilon Phase1}$ with an aim of confirming the assumption of the independence of $C^*_{\alpha\varepsilon}$ with respect to the surcharge. The coefficient of primary compression C^*_R can in addition be given with the provision of not stopping the topographic follow-up during construction of the second phase.

Provided an instrumentation of surface is laid out at the top of the waste column on the cap cover of the landfill (with the vertical reference marks) after the end of construction (phase 2), the values $C^*_{\alpha\varepsilon}$ relative to the complete column (layers 1 to *n*) can finally be evaluated. Both settlement of the lower column (layer 1 to *k*) and the upper column (layer *k+1* to *n*) are monitored. In this specific case it is possible to plot the settlement of the lower column for the phase 1 and phase 2 (Graph V-10). The settlement during the phase 1 is exclusively secondary settlement whereas the settlement during the phase 2 is the combination of a primary settlement and a secondary settlement in continuation of the phase 1. The part of the settlement due to overloading can be subtracted, using the primary settlement relationship [N]. An assumed value of C^*_R = 0.13 is considered for the calculations.

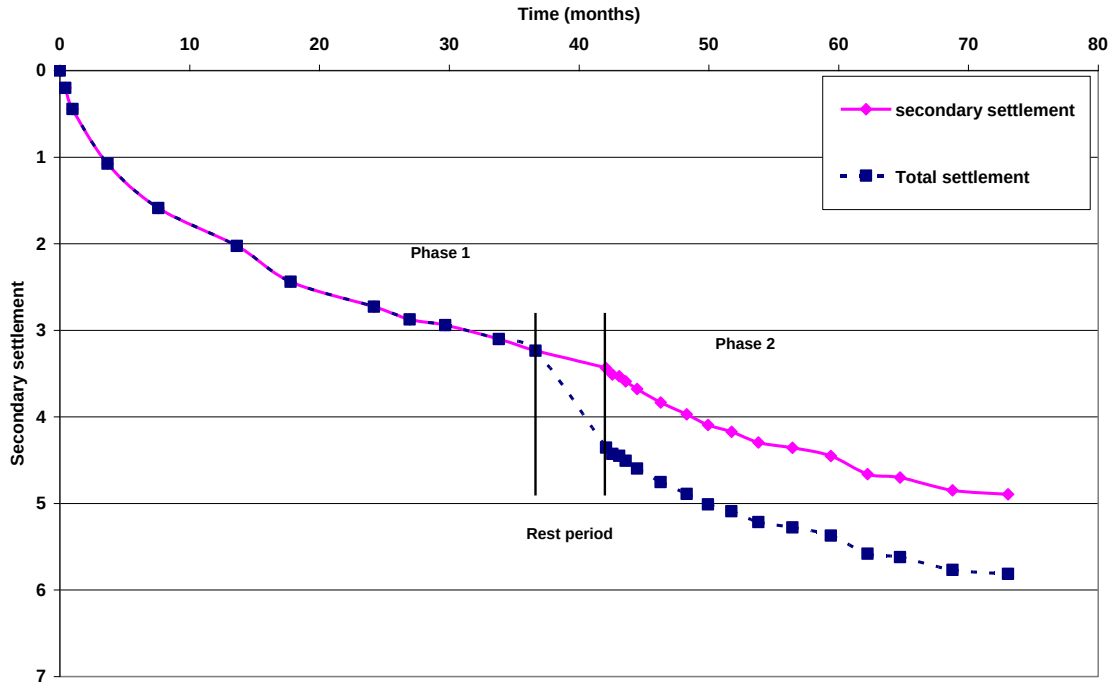

Graph V- 10: Influence of surcharge over secondary settlement of the lower column for a given value of C^*_R (0.13).

In Graph V-11 these results are plotted. In the second step by back analysis it is possible to assess $C^*_{\alpha\varepsilon}$ from the diagram of secondary settlement as in the previous section. It is specifically worth noticing that value of $C^*_{\alpha\varepsilon}$ is becoming constant independent of the surcharge. It is a key point since it is demonstrated in this example that the parameter $C^*_{\alpha\varepsilon}$ should be considered an intrinsic characteristic of the waste material which is independent of the waste column construction sequence.

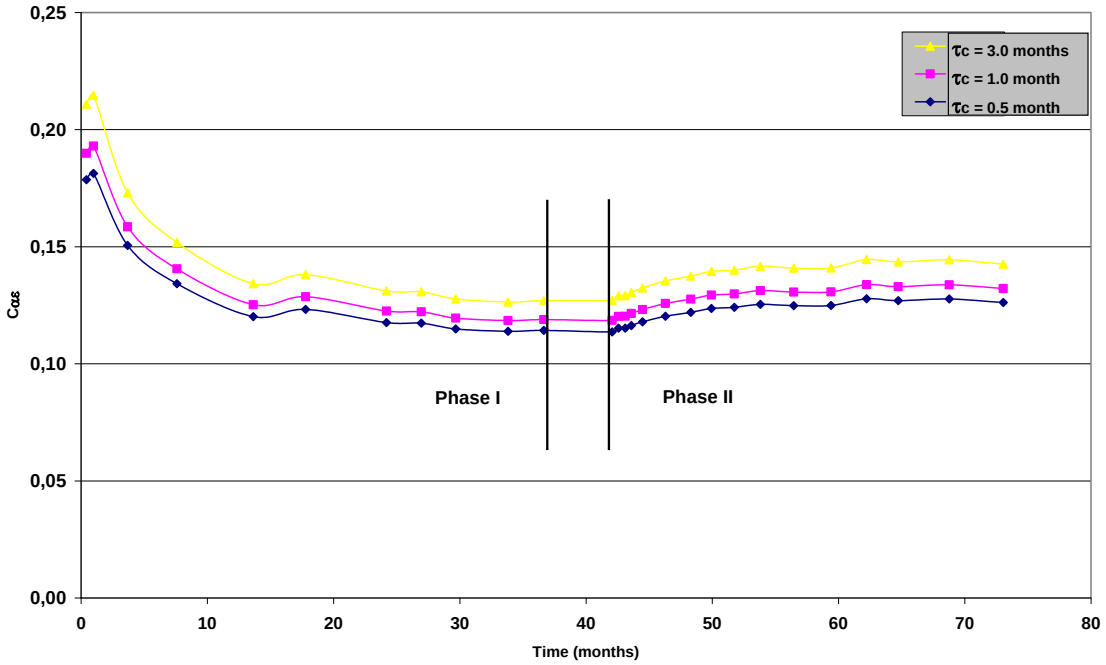

Graph V- 11: Influence of τ_c on $C^*_{\alpha\varepsilon}$ for C^*_R (0.13), the case of marker 12 Chatuzange landfill site.

V- 5.2.2 ISPM Settlement Modelling for a 2 Phase Construction (Cell 'C'- Chatuzange

This application is related to the two phase construction for the cell 'C' at Chatuzange landfill. Different experimentations have been carried out on this cell ranging from sample extractions through drill-holes to the monitoring of biogas, humidity measurements by neutron technique and measurement of density through geophysical technique (Descloitres et al. 2008). This cell has been filled in two stages, the first one between June to September 1998 and 2000, and the second one between 2005 and 2006 for the upper layer (4 m thick). Waste deposits are covered using a geosynthetic clay liner and 1 m of silty-soil. Data received from the scanner is integrated at regular periods for the determination of compressibility. In addition to that, sample extractions are carried out intermittently to study the evolution of waste material with regard to degradation phase, moisture content, leachate and gas generation as well as shear strength parameters.

A number of topographic markers were placed at the end of construction phase I (t_1) which were removed after placement of new layers (t_2), a final cap cover was build after the end of phase II (t_3) (Figure V-37) and the monitoring of the cell was started with the 3D laser scanner. Terrain survey for this objective was undertaken by LTHE on Chatuzange landfill by means of internal instrumentations and regular scanning surveys. Four markers at the former horizontal positions are being selected for

present study, the topographic follow-up includes exclusively the measurement of the secondary settlement. Nevertheless, a reactivation of primary settlement is induced in the case of vertical expansion of cell or in the case of rehabilitation of old landfills including the construction of various works (earth fills, light constructions, roads, etc). From the data available for a series of markers installed for the laser scanner markers (5, 6, 12, 14) located at different topographic locations, are selected for settlement prediction through the ISPM model (Figure V-39).

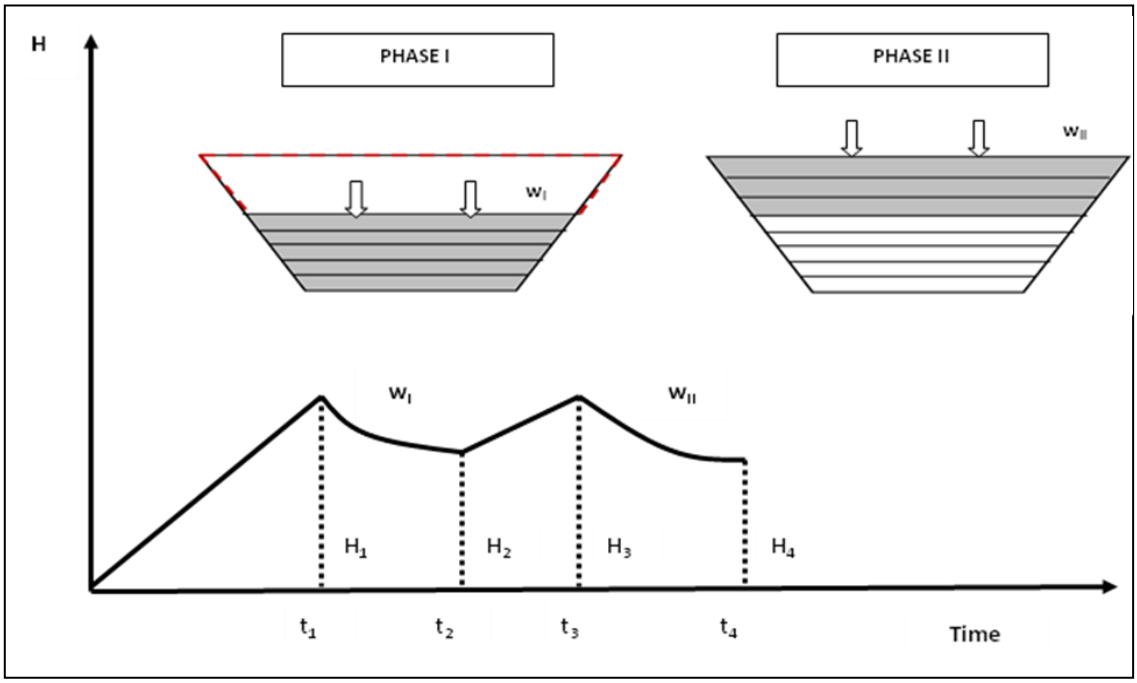

Figure V- 37: Construction of waste column in two phases for Cell 'C' of chatuzange landfill site.

Table V- 9: Calculation of the compressibility coefficient through ISPM model (parameters of Figure V-32)

PHASE I						
Markers	**t_1 (months)**	**H_1 (m)**	**t_2-t_1 (months)**	**w_I (m)**	**H_2 (m)**	**$C^*_{\alpha\varepsilon}$**
5	19.15	22.52	65.18	2.79	19.73	0.114
6	20.11	23.93	65.18	3.23	20.70	0.113
12	16.26	19.16	65.18	3.40	15.76	0.160
14	20.11	27.28	65.18	3.55	23.73	0.108

The successive steps of the calculations are summarised as below;

Phase I: Monitoring of settlement obtained by topographic plates located at the top of the first phase waste body between t_1 end of construction and t_2 start of the construction of phase II. It is possible by back analysis, taking into account the layer by layer construction, to calculate the value of compressibility coefficient $C^*_{\alpha\varepsilon}$ from the settlement values (Figure V-34 & Table V-9).

Phase II: This phase corresponds to the vertical expansion of the landfill cell 'C' (surcharge ΔH). There is some primary settlement. The primary coefficient of compression C^*_R is estimated from the measurements on other cells which resulted in a value 0.14. $C^*_{\alpha\varepsilon}$ is assumed to be the same for every marker taken from the phase I i.e. $C^*_{\alpha\varepsilon}$ (II) = $C^*_{\alpha\varepsilon}$ (I).

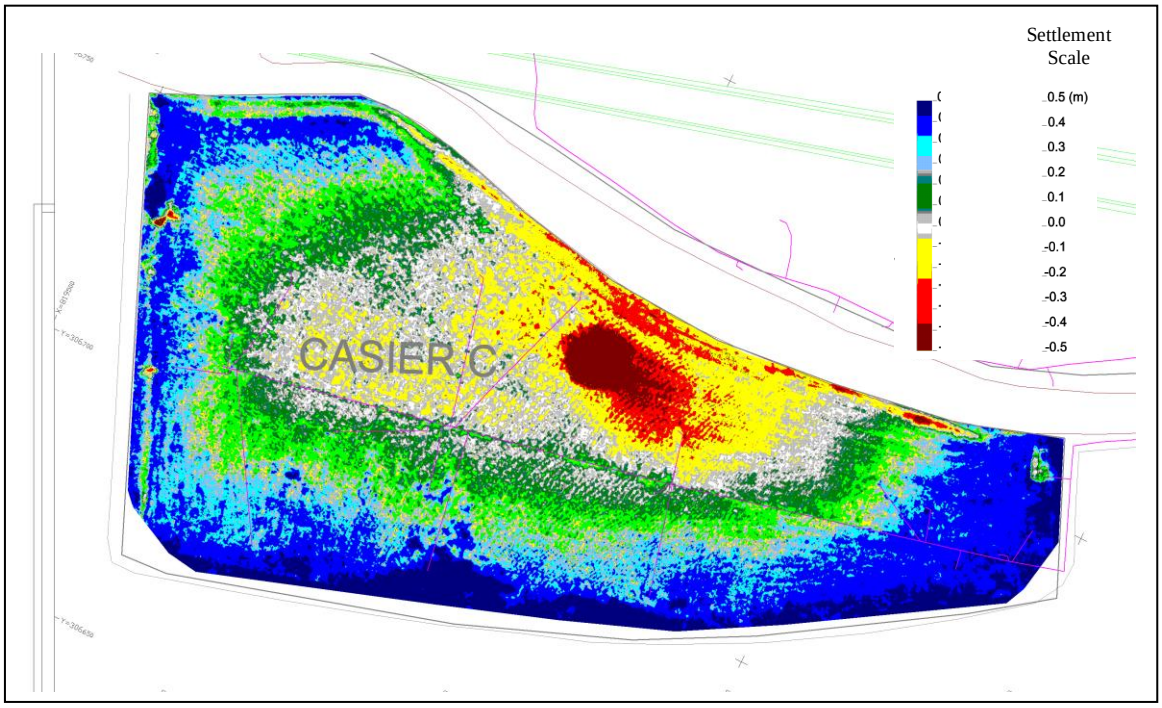

Figure V- 38: Laser Scanning; 3D settlement map after 6 months (t_4-t_3) from the beginning of Phase II

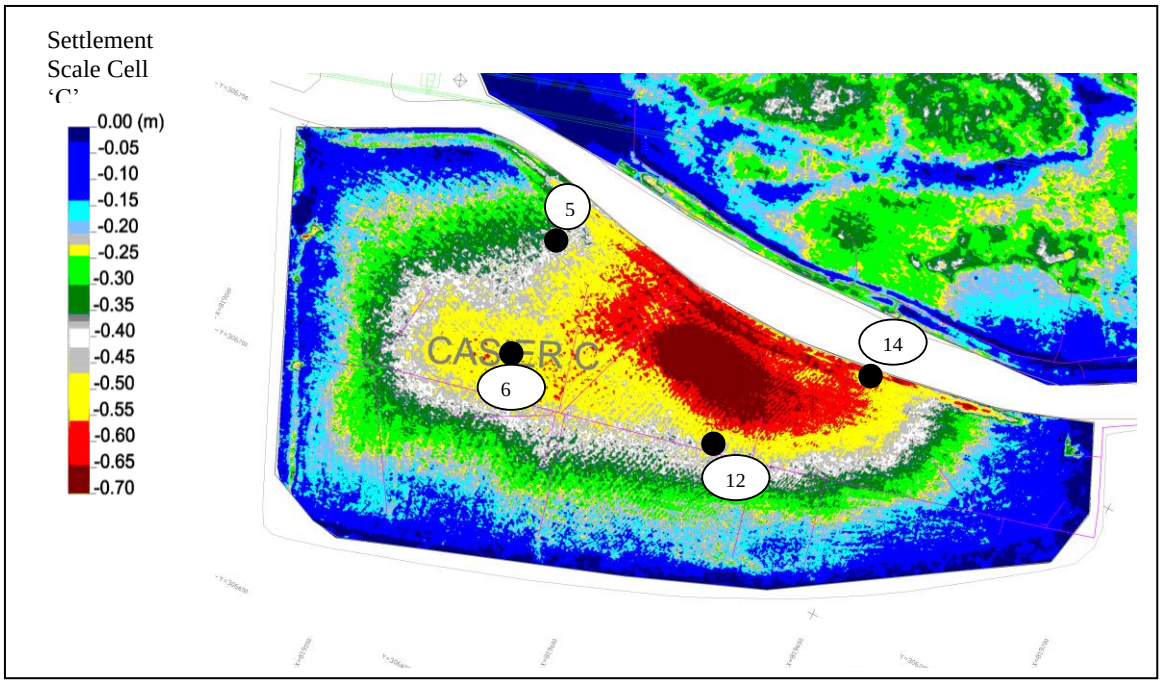

Figure V- 39: Laser Scanning; Settlement map after 18 months from the beginning of Phase II

Table V- 10: Settlement prediction through ISPM model in comparison with the measured values (parameters of the Figure V-32).

PHASE II							
Markers	**$C^*_{\alpha\varepsilon}$**	**t_3-t_2 (months)**	**H_3 (m)**	**ΔH^* (m)**	**t_4-t_3 (months)**	**w_{II} exp. (m)**	**w_{II} pred. (m)**
5	0.114	12	22.35	4.89	18	0.45	0.44
6	0.113	12	23.37	4.71	18	0.50	0.45
12	0.160	12	19.10	6.18	18	0.55	0.60
14	0.108	12	25.94	3.91	18	0.55	0.48

*$[H_3 - H_2 + (w_p(t_3) - w_p(t_2)) + (w_s(t_3) - w_s(t_2))]$

Table V-10 shows settlements obtained during the beginning of phase II (t_4-t_3 = 18 months), w_{II} exp. are in correspondence to w_{II} predict. determined using the ISPM model. As it can been seen that a 4% to 15% of error is produced from the prediction model which is quite a reasonable difference keeping in view the history of cell construction where first phase was constructed over longer period in contrast to the construction in second phase. Considering the good agreement between the experimental values of w_{II} and the predicted w_{II} values, ISPM model is further used for the prediction of settlement for 30 years, with results presented in Graph V-12.

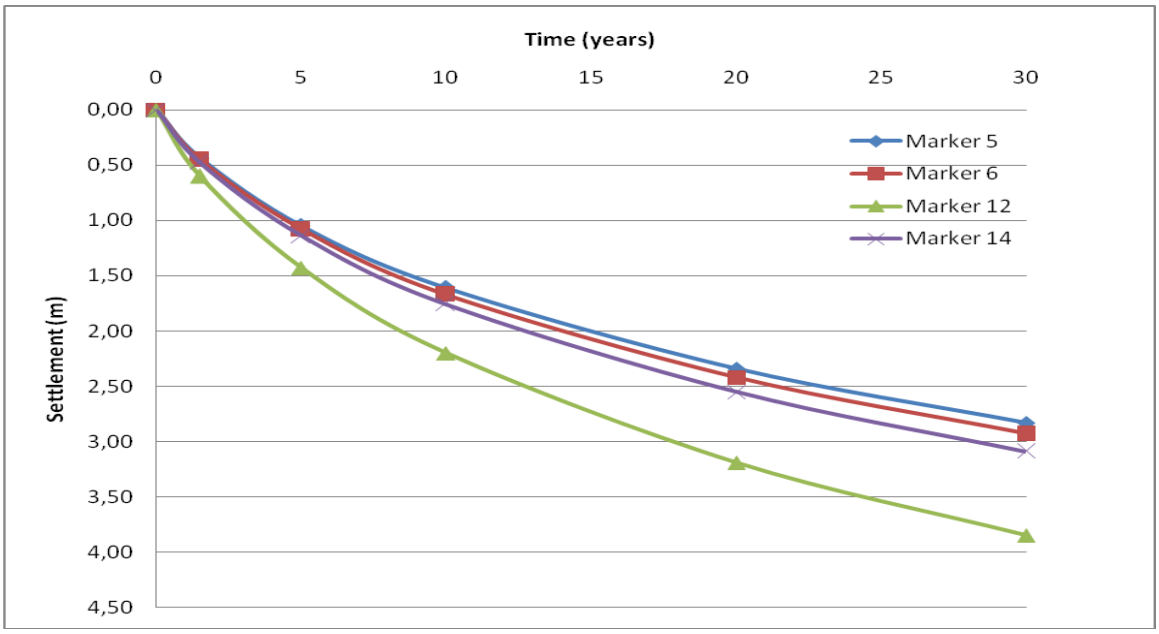

Graph V- 12: Settlement prediction through ISPM model for 30 years.

V-6 COMPARISON OF ISPM MODEL WITH THE SOWERS MODEL

The settlement model of Sowers (1973) remains most commonly used for the long-term prediction of settlement of domestic and assimilated waste. It rises directly from the application of the unidirectional theory of the soils to columns of multi-metric waste. In this model, the evolution of secondary settlement according to time depends on a coefficient of secondary compression $C_{\alpha\varepsilon}$ known as 'global' generally given starting from measurements of settlement of surface realized in period of post-construction.

Previously it was suggested in the literature that this coefficient $C_{\alpha\varepsilon}$ is not 'intrinsic' for waste since it depends in particular on the time of construction and the height of the column. Now in this chapter we will compare the post-construction deformation (or relative settlement) ε_{Sowers} with ε_{ISPM}, as well as the 'global' coefficient of secondary compression $C_{\alpha\varepsilon}$ with the 'intrinsic' coefficient $C^*_{\alpha\varepsilon}$ from the ISPM model. Post-construction secondary settlement is expressed in the form:

- ISPM model:

[1] $$\varepsilon_{ISPM} = \frac{w(t)}{H_n(t_c)} = \frac{w_n^s(t) - w_n^s(t_c)}{nh_0 - w_n^p - w_n^s(t_c)}$$

- Sowers Global model:

[2] $$\varepsilon_{Sowers} = \frac{w(t)}{H(t_c)} = C_{\alpha\varepsilon} . \log\left(\frac{t - t_0}{t_1 - t_0}\right)$$

The assumptions adopted for the model of Sowers are:

- Origin of time $t = 0$: beginning of construction of the column of waste (same for ISPM);
- $t_0 = t_c$ (time of construction) though for certain authors, the definition of t_0 is different;
- Origin of secondary settlement $\Rightarrow t_1 = t_c + x$ (months), with x variable from one author to another. In the present report we use $x = 1$ month.

It is understood that the formula of Sowers, being the subject of divergences on the level of the parameters t_0 and t_1, the value of $C_{\alpha\varepsilon}$ varies for the same case according to assumptions of the authors, which makes the comparisons even more difficult.

V - 6.1 Assessment of the Coefficient of Secondary Compression $(C_{\alpha\varepsilon})_{Sowers}$ for constant $(C^*_{\alpha\varepsilon})_{ISPM}$

From hereafter, except stated otherwise, ISPM model is regarded as model of reference. This is to say that the behaviour in settlement is considered to be correctly modelled by ISPM model with intrinsic coefficient $C^*_{\alpha\varepsilon}$ considered as independent of time and the height of the waste column. The value of $(C_{\alpha\varepsilon})_{sowers}$ is searched such that it gives at the same time (t_m) the same value of settlement. Equating the expressions [1] and [2] this time for t_m,:

[3] $$\varepsilon_{ISPM} = \frac{C^*_{\alpha\varepsilon} . [Y(t_m) - Y(t_c)]}{n - C^*_R X - C^*_{\alpha\varepsilon} Y(t_c)} = \varepsilon_{Sowers} = C_{\alpha\varepsilon} . \log\left(\frac{t_m - t_0}{t_1 - t_0}\right)$$

$C_{\alpha\varepsilon}$ is correlated to $C^*_{\alpha\varepsilon}$ value.

To facilitate the demonstration, 4 examples of the Table V-11 are analysed where the variable parameters are the height of the column of waste (virtual height nh_0 = 12, 24, 48 m), the time of construction (t_c = 24 and 48 months) and the speed of virtual construction (nh_0 / t_c).

For clarity, the columns of waste considered previously will be characterized moreover by:

- a rise of construction at constant speed $\Rightarrow \tau_i = \tau = t_n / n$
- the absence of rest period of construction $\Rightarrow \tau_{ri} = 0$
- instantaneously placement of the final cover $\Rightarrow t_c = t_n$

Table V- 11: Parameters for theoretical cases under consideration.

Characteristics	Units	A1	A2	B1	B2
Initial virtual height (h_0)	m	1	1	1	1
Number of column layers	Layer	24	24	48	48
Time of construction ($t_c = t_n$)	month	12	24	24	48
Lift rate (nh_0 / t_n)	m/month	2	1	2	1

So as to allow numerical applications, the following parameters will be fixed once for all:

$C^*_R = 0.20$ $\gamma_0 = 8$ kN/m ^{3} $q = \gamma_c h_c$ 18 kPa $\sigma_c = 40$ kPa and $C^*_{\alpha\varepsilon} = 0.08$.

Taking into account the previous assumptions, the influence of the three following parameters on the value of the coefficient $(C_{\alpha\varepsilon})_{Sowers}$ is illustrated:

- the time of construction of the column (t_c)
- the virtual height of the column (nh_0)
- the origin of secondary compression (t_1)

It is worth noticing that this coefficient is wrongly considered as a geo-mechanical characteristic of the waste material by all the users of this model of settlement prediction. In the following application the variation of $(C_{\alpha\varepsilon})_{Sowers}$ due to the variation of the parameters described above is displayed.

V- 6.1.1 Influence of Time of Construction (t_c) (Cases A1 & A2)

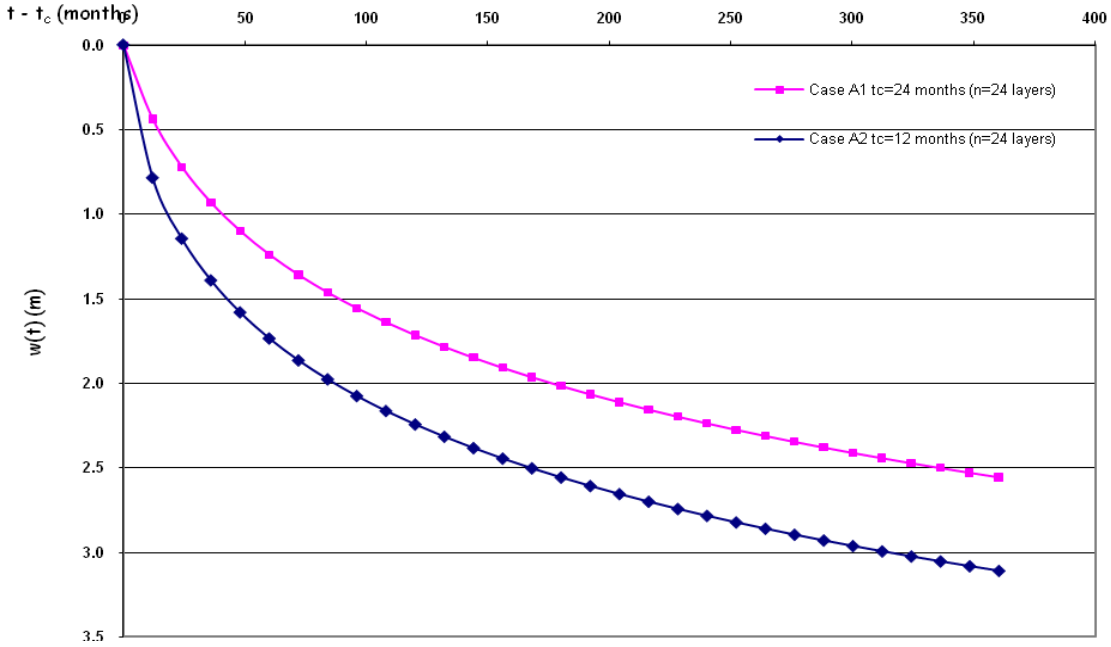

Graph V- 13: Evolution of Settlement as function of time (ISPM 1.1) with constant $C^*_{\alpha\varepsilon}$ (0.08).

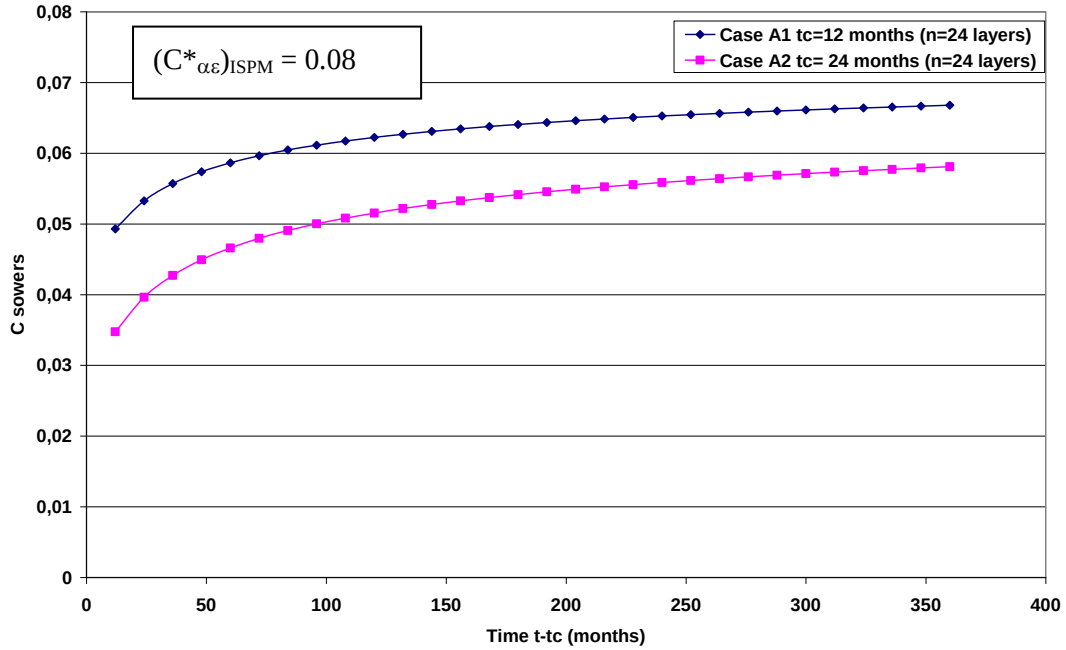

Graph V- 14: Coefficient of secondary compression calculated by the method of Sowers with the calculated values of settlement by ISPM as presented in Graph V-13.

In Graph V-13 numerical values used for the assessment of $(C_{\alpha\varepsilon})_{Sowers}$ show the evolution of the waste column settlement corresponding to two different construction times t_c with a constant value of $C^*_{\alpha\varepsilon}$ = 0.08. From Eq. [3] it is possible by back analysis to deduce the corresponding value, whereas $(C^*_{\alpha\varepsilon})_{ISPM}$ remains constant (Graph V-13). On the other hand $(C_{\alpha\varepsilon})_{Sowers}$ value is significantly different from $(C^*_{\alpha\varepsilon})_{ISPM}$ value =0.08. For every value of t_m-t_c it is possible to evaluate a different $(C_{\alpha\varepsilon})_{Sowers}$. In

Graph V-14 it can be observed that there is a significant variation for the parameter $(C_{\alpha\varepsilon})_{Sowers}$ with the change in duration of construction and with the time.

V- 6.1.2 Influence of Waste Column Height (Cases A2 and B1)

Graph V-15 shows the evolution of settlement using the ISPM model for $C^*_{\alpha\varepsilon} = 0.08$ and two different column heights. Graph V-16 represents the evolution of both $C_{\alpha\varepsilon}$ for model of Sowers as a function of $t - t_c$ for both cases corresponding at two different heights for the same lift rate (equivalent with t_c = 24 and 48 months) and it is observed that the coefficient $C_{\alpha\varepsilon}$ varies with the course of time.

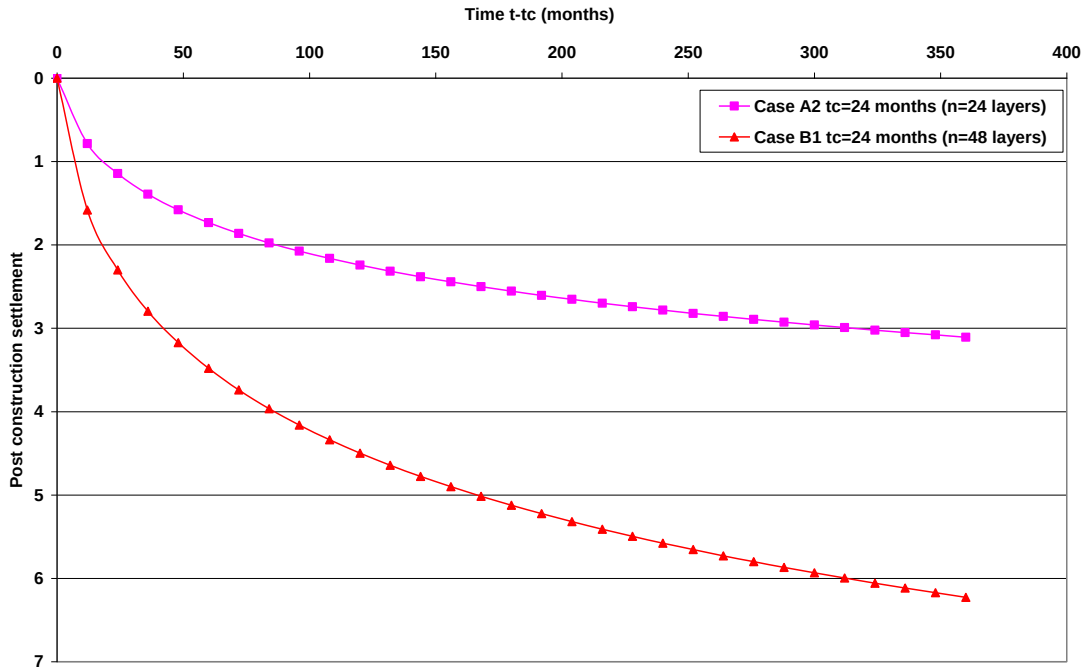

Graph V- 15: Evolution of settlement as function of waste column height (ISPM Model) with constant C*αε (0.08).

The value of time t_m used for the calibration influences the value of $C_{\alpha\varepsilon}$ of the law of Sowers. A law with constant $C_{\alpha\varepsilon}$ will not correctly translate the behaviour of waste in secondary settlement since:

- in all the cases, the secondary settlement modelled by the formula of Sowers begins at $t = t_c + x$ months whereas it begins at the end of the placement of the 1st layer of waste in the case of ISPM model and that w_{ISPM} starts when the moment the construction of the waste column is finished ($t = t_c$).
- $(C_{\alpha\varepsilon})_{sowers}$ is stabilized roughly with a constant value only at the end of a rather long time.

The two laws being distinct, it is not astonishing to obtain different coefficients of secondary settlement but it is better not to confuse them.

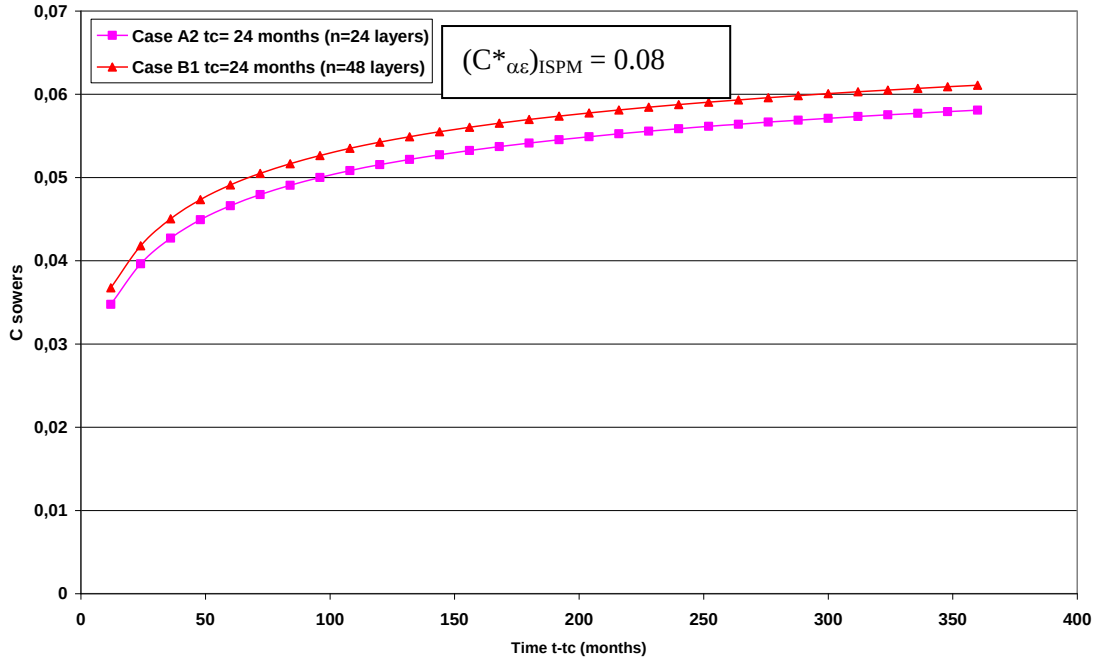

Graph V- 16: Coefficient of secondary compression calculated by the method of Sowers using the values of settlement by ISPM (C*αε = 0.08).

V- 6.1.3 Influence of Lift Rate (Cases B1 & B2)

This time the columns B1 and B2, both characterized by a speed of virtual elevation (nh_0 / t_c) of 1 m/month are considered. Once again different values of $C_{\alpha\varepsilon}$ are obtained for both the models and it is noted that the gap between $C_{\alpha\varepsilon}(t_m)$ and $(C^*_{\alpha\varepsilon})_{ISPM}$ decreases systematically when t_c decreases. The fact that $C_{\alpha\varepsilon}(t_m)$ is a function of thickness (nh_0) testifies owing to the fact that, in the case of the ISPM model, relative post-construction settlements are not proportional to the height of waste.

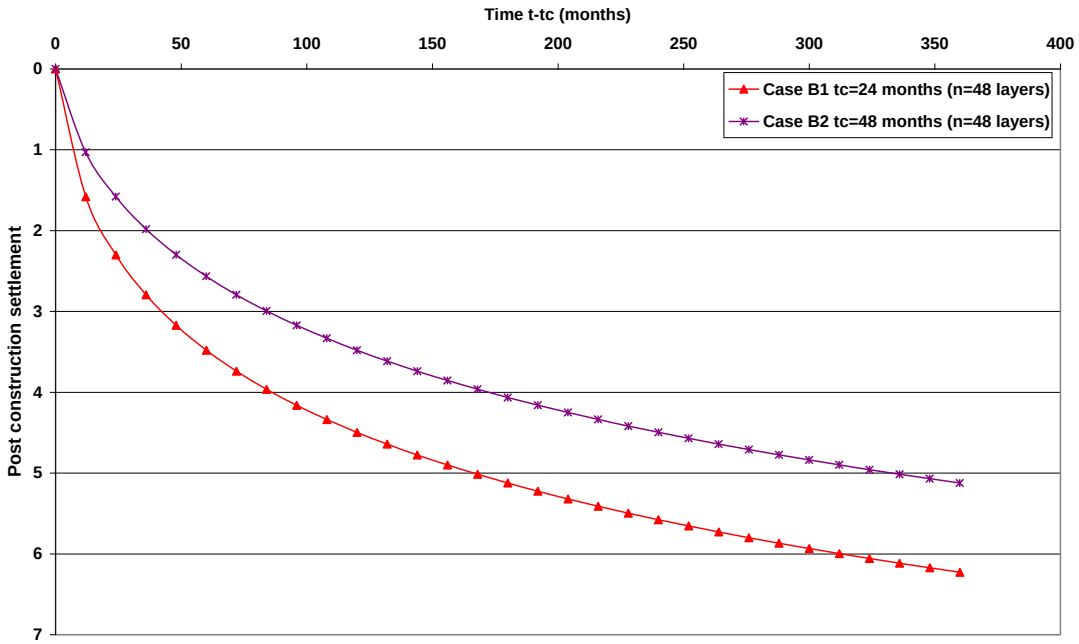

Graph V- 17: Evolution of settlement as function of time.

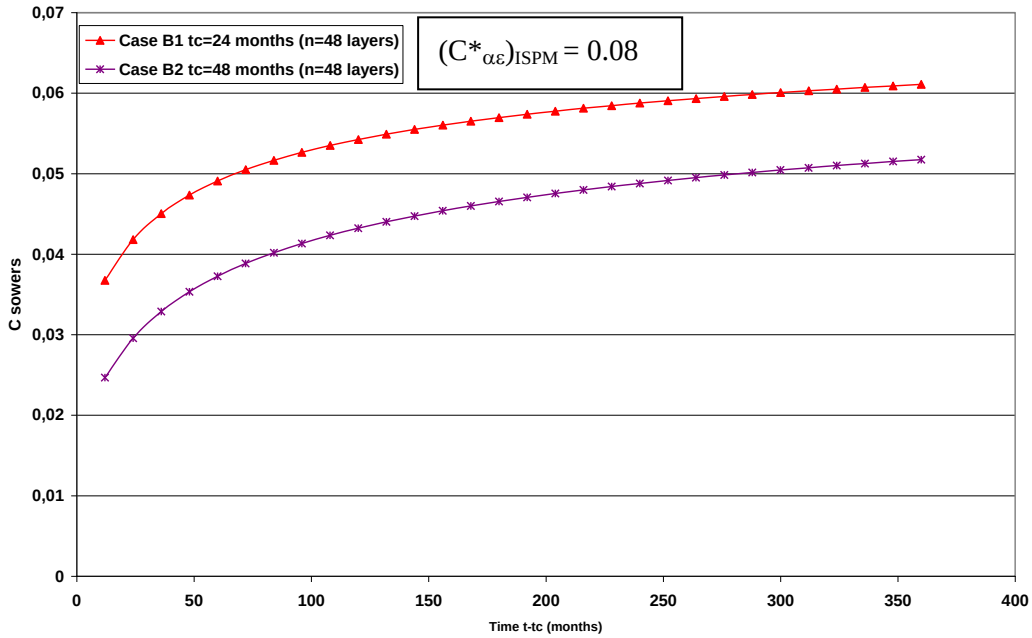

Graph V- 18: Coefficient of secondary compression calculated by the method of Sowers with the values of settlement by ISPM ($C^*_{\alpha\varepsilon}$ = 0.08).

V- 6.1.4 Influence of Time for Start of Settlement (t_1)

The selection of the conventional parameters of time in a model such as that proposed by Sowers (1973) has a considerable importance, although this point was almost systematically overlooked in the conventional applications. Sowers (1973) did not specify at which moment of the life of the column of

waste this origin is applicable. With the exception of very rare authors [(Watts and Charles, 1990) and (Sanchez-Alciturri et al., 1993a)], all considered in fact the model of Sowers on the basis of a time origin at the end of the construction of column ($t_0 = t_c$). A specific study on the influence of this parameter was carried out but taking into account its limited interest, this point is not discussed here. Here $t_0 = t_c$ is supposed with varied origin of time of secondary compression (t_1) so as to illustrate the sensitivity of the Sowers model with respect to the concerned time parameter.

V - 6.2 Comparison ISPM – Sowers Model: Site Studies

In section V-4.4 $(C_{\alpha\varepsilon})_{Sowers}$ was calculated from theoretical values of settlement determined using the ISPM model. In the present case, settlement data is obtained from the available measurement in the case histories and then $(C_{\alpha\varepsilon})_{Sowers}$ and $(C_{\alpha\varepsilon})_{ISPM}$ are both determined by back analysis.

V- 6.2.1 Principle of the Back Analysis for Case Studies

$(C^*_{\alpha\varepsilon})_{ISPM}$ and $(C_{\alpha\varepsilon})_{Sowers}$ are given for a time t_m starting from the experimental value of relative compression $\varepsilon = \frac{w(t_m)}{H(t_c)}$, by applying the formulae explained earlier. Very often there is no settlement measurement immediately at the end of operation.

The first topographic measurement of surface takes place at the time t_m^0 delayed by Δt after the end of construction (t_c). $C^*_{\alpha\varepsilon}(t_m)$, this coefficient is determined by back-analysis for $t = t_m$ as explained in last section. For the model of Sowers, following equation is applied:

[4]

$$\frac{\Delta w(t_m)}{H(t_c)} = \frac{w(t_m) - w(t_m^0)}{H(t_c)} = C_{\alpha\varepsilon}(t_m).\log\frac{t_m - t_c}{t_1 - t_c} - C_{\alpha\varepsilon}(t_m^0).\log\frac{t_m^0 - t_c}{t_1 - t_c} \cong C_{\alpha\varepsilon}(t_m).\log\frac{t_m - t_c}{t_m^0 - t_c}$$

Below the comparative study, starting from models ISPM and Sowers for three real sites with two French sites (Montech and Lapouyade) which were monitored by LTHE(LIRIGM) and a foreign site (Montreal) is presented, for which data were available (Table V-12). These sites have the advantage of presenting columns of waste of different heights and age (for different cells). The Sowers models of prediction of the compression does not take into account the specificity of the material waste, characterized by its consolidation state (partial over consolidation) and its history (age growing with the depth). The ultimate values of the settlement are used to deduce the values of $(C_{\alpha\varepsilon})_{Sowers}$ and

$(C^*_{\alpha\varepsilon})_{ISPM}$ in Graph V-19 and Graph V-20 the ratio of these coefficients is plotted against (t_c) and H_n (t_c).

Table V- 12: Characteristic parameters of different cells from the case histories.

Site	$H_n(t_c)$	t_c	t_m^0	t_m^{ult}	$(C^*_{\alpha\varepsilon})$ ISPM	$(C_{\alpha\varepsilon})$ Sowers
Montech	18.52	3.93	14.93	54.42	0.08	0.086
	19.83	8.23	17.83	62.77	0.11	0.1485
	20.76	10.63	21.50	33.86	0.09	0.084
	21.03	10.97	28.47	84.87	0.089	0.0914
	21.46	11.07	28.09	43.43	0.083	0.083
	21.76	13.93	30.03	58.89	0.091	0.092
	21.86	17.00	54.67	96.30	0.098	0.1173
	22.32	23.83	70.30	61.27	0.10	0.08
Montreal	76.00	36.05	108.57	33.01	0.193	0.4873
	78.73	60.86	181.66	33.01	0.181	0.3883
	80.01	60.90	242.47	33.01	0.1414	0.2512
	95.55	73.07	242.47	33.01	0.179	0.2145
	109.73	85.23	303.37	33.01	0.167	0.2577
Lapouyade	9.89	10.82	23.41	14.49	0.0876	0.0674
	11.44	11.70	25.74	14.49	0.1707	0.1599
	11.65	13.41	28.80	14.49	0.1424	0.1351
	13.22	15.88	31.10	14.49	0.1449	0.1191
	13.61	25.84	34.32	14.49	0.1094	0.0752
	13.62	26.24	37.31	14.49	0.1116	0.0829
	14.23	36.62	41.13	14.49	0.1052	0.0584
	15.33	36.89	43.92	14.49	0.1266	0.0791

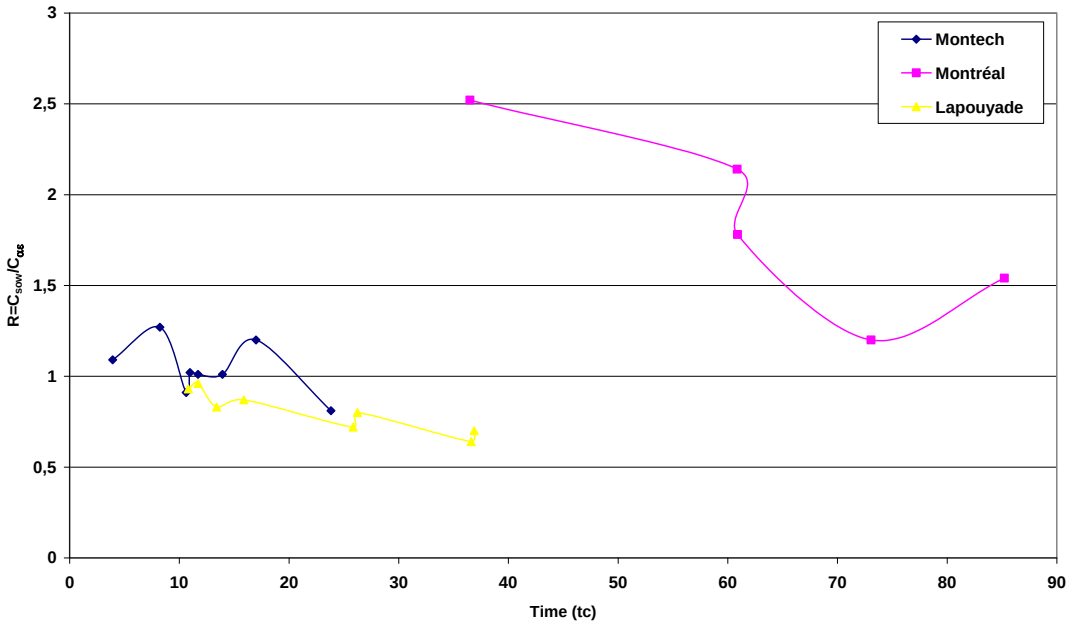

Graph V- 19: Evolution of ratio C_{sow}/ $C^*_{\alpha\varepsilon}$ as function of time.

This variation of ratio of both coefficients of secondary compression shows the dependency of the coefficient of secondary compression of Sowers model on the parameters of time and the waste column height suggesting that this parameter is not the intrinsic parameter of the waste medium.

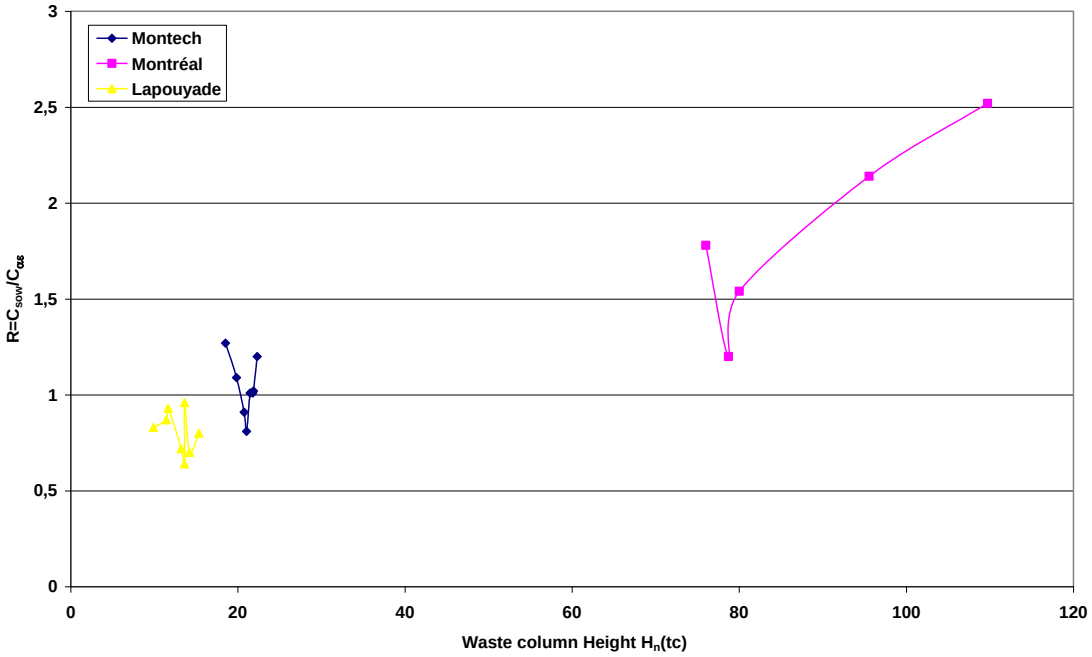

Graph V- 20: Evolution of ratio $C_{sow}/C^*_{\alpha\varepsilon}$ as function of final height of waste column $H_n(t_o)$

V- 6.2.2 Conclusion and Perspective of Practical Application of ISPM Model

According to the level of advancement of the project considered, following aspects regarding the update of existing model of settlement prediction ISPM are of interest:

- **at the stage of the preliminary draft** by the prediction of the total settlement of the column of waste, with the objective of estimating the storage capacity of the waste cell and the effective control of the construction phases $\Rightarrow w_n(t) = w_n^p(t) + w_n^s(t)$

- **in post-construction phase** by the prediction of the settlement of surface (w) taken as starting from the placement of the cover, with the objective of the evaluation of settlement for later time period $\Rightarrow w(t) = w_n(t) - w_n(t_c) = w_n^s(t) - w_n^s(t_c)$ since primary settlement has diminished at the end of the construction.

If a cell at the stage of the preliminary layer construction or in post-construction is considered, the application of ISPM model concentrates initially on the determination of the coefficient of secondary compression $C^*_{\alpha\varepsilon}$ which can be carried out according to one of the following two approaches:

- by **direct analysis**: on the basis of pre-gauged or supposed coefficient of compression (only approach applicable to the stage of the preliminary construction phase or the case of non instrumented waste columns). New progress is needed for research of assumed value of coefficient of compressibility $C^*_{\alpha\varepsilon}$ which is further dependent on the type of waste.

- by **back analysis**: after calibration of $C^*_{\alpha\varepsilon}$ from a topographic campaign starting from one year to a few years (approach privileged for the modern MSW). The systematic use of the ISPM model on case histories would allow to get a correlation between the type of waste and a value of $C^*_{\alpha\varepsilon}$.

The application of ISPM model requires a relatively precise knowledge of the history of construction. This condition can prove to be problematic in the case of old or orphan sites, but this difficulty disappears in modern MSW. Today the ultimate stage of development of ISPM model is launched with prospect for the application of this model by means of software and abacuses. This objective represents an asset for the landfill operators because with the help of the preliminary evaluation of some operating parameters (flow, composition, implemented and hydrous management of waste) it

should be possible to evaluate the storage capacity of the cells (on the basis of excavation campaigns available) and the anticipation on the construction phases of the sites would be an easy task.

- The ISPM model proves the importance of the fact that the parameter $C^*_{\alpha\varepsilon}$ has a dominating influence.
- The range of variation of the coefficient $C^*_{\alpha\varepsilon}$ tends to be rather reduced
- The influence of the initial unit weight of waste (γ_0) is not very significant: it can be shown that a fluctuation of 50 % in its value (0.8 T/m ^{3} ± 50 %) induce a maximum prediction error of 2.5 %, all being equal in addition. However compressibility of waste is of course significantly dependent on the waste density.
- The influence of the value of h_0 (fixed by default at 1 m) is moderate as taking into account a thickness h_0 equal to 50 cm induces an increase in $\varepsilon(t)$ with height at 4.5 %.
- Finally height of the column can be deduced with the help of nh_0 and $C^*_{\alpha\varepsilon}$.

VI- MUNICIPAL SOLID WASTE SHEAR STRENGTH

VI-1 SHEAR STRENGTH-APPLICATION TO SITE STABILITY

Shear strength in reference to soil is used to describe the maximum strength of soil when significant plastic deformation or yielding occurs due to an applied shear stress. There is no definitive "shear strength" of a soil as it depends on a number of factors affecting the soil at any given time and frame of reference, in particular the rate at which the shearing occurs. Factors affecting the shear strength of soils are:

- Soil composition (basic soil material): Mineralogy, grain size distribution, shape of particles, pore fluid type and content, ions on grain and in pore fluid.
- State (initial): Define by the initial void ratio, effective normal stress and shear stress (stress history). State can be describe by terms such as: loose, dense, over-consolidated, normally consolidated, stiff, soft, contractive, dilative, etc.
- Structure: Refers to the arrangement of particles within the soil mass; the manner the particles are packed or distributed. Features such as layers, joints, fissures, slicken sides, voids, pockets, cementation, etc, are part of the structure. Structure of soils is described by terms such as: undisturbed, disturbed, remoulded, compacted, cemented; flocculent, honey-combed, single-grained; flocculated, deflocculated; stratified, layered, laminated; isotropic and anisotropic.
- Loading conditions: Effective stress path i.e., drained, and un-drained; and type of loading, i.e., magnitude, rate (static, dynamic), and time history (monotonic, cyclic)).

The drained strength is the strength of the soil when pore water pressures, generated during the course of shearing the soil, are able to rapidly dissipate. It also applies where no pore water exists in the soil (the soil is dry). It is commonly defined using Mohr-Coulomb theory and termed as "Coulomb's equation" by Terzaghi (1942) combined with the principle of effective stress.

Drained strength is defined as: $\tau = \sigma' \tan(\varphi') + c'$

Where $\sigma' = (\sigma - u)$, known as the principle of effective stress;

σ is the total stress applied normal to the shear plane;

u is the pore water pressure acting on the same plane;

φ' = the effective angle of shearing resistance. (Formerly termed 'angle of internal friction' after Coulomb friction)

The coefficient of friction μ is equal to tan (φ), which is proportional to the normal force on a plane but independent of its area and c' = apparent cohesion which allows the soil to possess some shear strength in the absence of confining stress, or even under tensile stress. Commonly it is referred to as temporary negative pore water pressure (suction) that dissipates over time. When shear tests are conducted on an over-consolidated or dense soil, and peak strengths are plotted on a stress stain plot, it appears that cohesion exists as the y-intercept is non-zero. However, what is being plotted is not "true" cohesion, but it is actually due to interlock of particles in the case of sands and inter-particle attractive forces in the case of clays.

VI-1.1 Analogy of Soils' Shear Strength and MSW

In soil mechanics shear strength and compressibility of most saturated soils are governed by effective stress σ' which is calculated by subtracting pore water pressure u_w from the total stresses. Whereas the behaviour of unsaturated soils depends upon two stress parameters (σ-u_a) and (u_a-u_w) where σ is the total stress, u_a is the pore air pressure and u_w is pore water pressure which may be more comparable to a gassing waste than the saturated soils.

Various researches have tried to analyse the shear strength of MSW both in-situ and at laboratory. Determination of shear strength properties for MSW is difficult due to the heterogeneity of disposed wastes, the difficulty in obtaining and testing representative samples, time-varying properties, and strain incompatibility between the MSW and underlying materials (Eid et al., 2000). Even an approximate evaluation of slope stability for municipal landfills may be useful despite limited or missing data regarding geometry, leachate pressure, solid waste material shear strength, and/or subsurface soil information.

Generally the shear strength is determined through three methods: in-situ testing, laboratory experiments and back calculations from failure and observation of slopes. Within the laboratory testing methods, direst shear test, triaxial tests and simple shear tests are applied for the analysis of shear strength parameters. The problem with these testing methods is that the specimens tested are the disturbed samples and they often need appropriation before their placement in the apparatus. Due the fact that often slope stability problems arise during the post closure period of the landfill, shear strength assessment is significant in the mechanical characterisation of the MSW. Below is a brief study of the research work available in literature.

VI-1.2 Stability Analysis available in Literature

The stability parameters influence the landfill slope design. A slope is geotechnically stable if it does not physically collapse. The long-term stability may need to be checked especially if significant rise in leachate level and seepage are occurring like in some old abandoned refuse fills. Stability problems often are the consequence of excess water percolation in the landfills. Shallow surface ravelling type of failures is also likely to penetrate into the waste below the cover, especially in areas of emerging seepage. The excess water results in saturation of the waste mass changing the unit weight of the waste body, the excess pore water pressure is created which in turn affects the slope stability. Similarly the water saturation of the voids volume may cause the gas pressure and interact with the gas flow. Due to the ever changing nature of the waste medium different deformation and settlement behaviour are observed at site, however most stability analyses have shown that the slopes are the most critical areas (Bauer et al., 2007). The instability of the slope may be caused due to the following reasons:

- Any change in the slope profile due to the decomposition of waste.
- An increase in the moisture content which may cause the reduction of resistance.
- Progressive decrease of shear strength due to leaching or creep.
- Any vibrations or liquefaction effects.

Major slope failures can occur due to natural or landfill management problems and the assessment of waste mass stability is a critical step in reducing the risk to the landfill operators and the general public. The stability analyses rely on site specific simple estimates of the unit weight of waste and the pore pressure conditions and use shear strength envelopes of the municipal waste already available in the literature or obtained through the shear tests. The objective of the present study is to evaluate the potential use of very simple stability analyses which can be used to study the potential for slumps and slides within the waste mass and which may represent a significant constraint on construction and development of the landfill. The issue of slope stability is critical for the safety of the landfill operators and the people living near the base slopes of the landfill but for the protection of investments involved in the equipment to collect the biogas for energy recovery and prevention of large remediation costs.

BISHOP Simplified Method of Stability Analysis

The method of slices and the finite element method are the most frequently used methods for estimating the stability of slopes. Although the potential failure parts of a slope can be obtained by means of a finite element analysis the determination of a suitable measure and a set of rules from a finite element analysis to estimate the stability of slopes need to be further studied. The Factor of Safety is a measure of the confidence that collapse will not occur. Method of slices is very simple and

a quantitative index for stability (factor of safety). The stability analysis for such cases is performed following the method of finite slope analysis.

Hypotheses of BISHOP's model are:

- Shear strength along the failure is uniformly distributed
- Failure plane is an arc of the circle
- The interslice forces including pore water pressure are assumed to be horizontal:

$Y_i = 0 \qquad \forall\, i$ (in Figure VI-1)

- Effective normal stress is determined by summation of all forcing acting perpendicular to the surface = 0

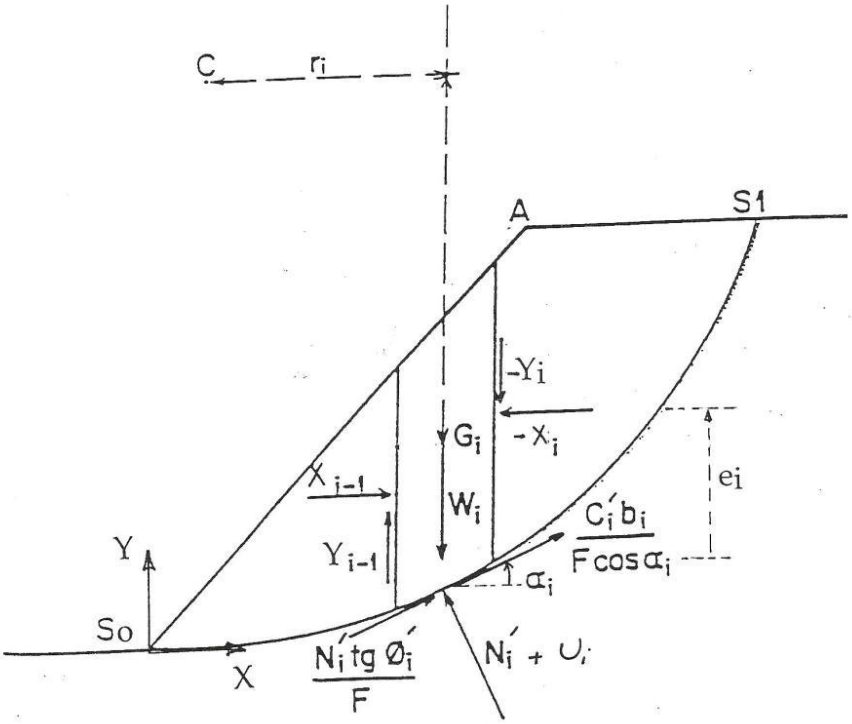

Figure VI- 1: Forcing acting on the sliding surface (BISHOP's simplified model).

In Figure VI-1, W_i is the weight of the slice i

with N_i = normal component of W_i acting perpendicular to the sliding surface;

U_i is the force integrating the pore water at the bottom of the slice and ρ is the density of the material.

$\frac{b_i}{\cos \alpha_i}$ = arc length of the slice.

Considering one slice as indicated in Figure VI-1, vertical equilibrium for all the effective stresses is calculated using the following equation

$$W_i - U_i \cos \alpha_i = N_i' \cos \alpha_i + \left[N_i' tg \phi_{ic}' + c_{ic}' \frac{b_i}{\cos \alpha_i} \right] \sin \alpha_i \qquad (1)$$

And the factor of safety is defined as

$$F = \frac{tg \phi_i'}{tg \phi_{ic}'} = \frac{\phi_c^i}{\phi_{ic}'} \qquad (2)$$

Equation (2) is used for effective stress analysis

Equilibrium of moments is calculated as follows

$$\sum_i (W_i \sin \alpha_i) \rho = \sum_i \left[c_{ic}' \frac{b_i}{\cos \alpha_i} + N_i' tg \phi_{ic}' \right] \rho \qquad (3)$$

From equation (1)

$$N_i' = \frac{(W_i - U_i \cos \alpha_i) - c_i' / F . b_i . tg \alpha_i}{\cos \alpha_i + tg \phi_i' / F . \sin \alpha_i}$$

Summing up equation (1) and (3) gives the Factor of safety 'F' as

$$F = \frac{\sum_i \frac{1}{\cos \alpha_i} \left[c_i' b_i + tg \phi_i' \frac{W_i - U_i \cos \alpha_i - \frac{c_i'}{F} b_i tg \alpha_i}{1 + tg \alpha_i . \frac{tg \phi_i'}{F}} \right]}{\sum_i W_i \sin \alpha_i}$$

The value of factor of safety is then calculated through iterations.

VI-1.3 Shear Strength Parameters and Stability Analyses in Literature

Knowledge of shear strength of MSW is required for the design and probable failure planes in the landfills. When considering the long term stability of the landfill, the impact of degradation on the shear strength of the MSW is of importance. Landva and Clark (1990) observed the decrease in shear strength parameters for the specimens left in the containers for one year with the friction angle value of 9° in comparison with the shear strength of fresh waste (friction angle 24° to 42°) with a cohesion between 10 to 23 kPa. Shear strength of a soil is conventionally described by Mohr-Coulomb failure envelope. But there are reasons that the characterization of shear strength of domestic waste through cohesion and internal friction may not be appropriate such as; behaviour of waste components at the application of normal stresses and reinforcing effect of sheet like components (plastics, textiles) within the waste as described by Kölsch (1995) according to which there has to be no shear strength at zero normal stress.

Likewise the strength of MSW is calculated as a soil like material and the shear behaviour is analysed on the basis of peak shear strength or residual shear strength of the material. In the presence of fibre like components (plastics, textile), which have a reinforcing effect on the behaviour of MSW, the shear behaviour of the waste results in ductile shear response as opposed to the residual shear resistance of the material. In this case no peak stress is observed and the shear stress tends to increase even at 40% of the shear strain during the tests (Gotteland et al., 1995 and Machado et al. 2007) as shown in Figure VI-2.

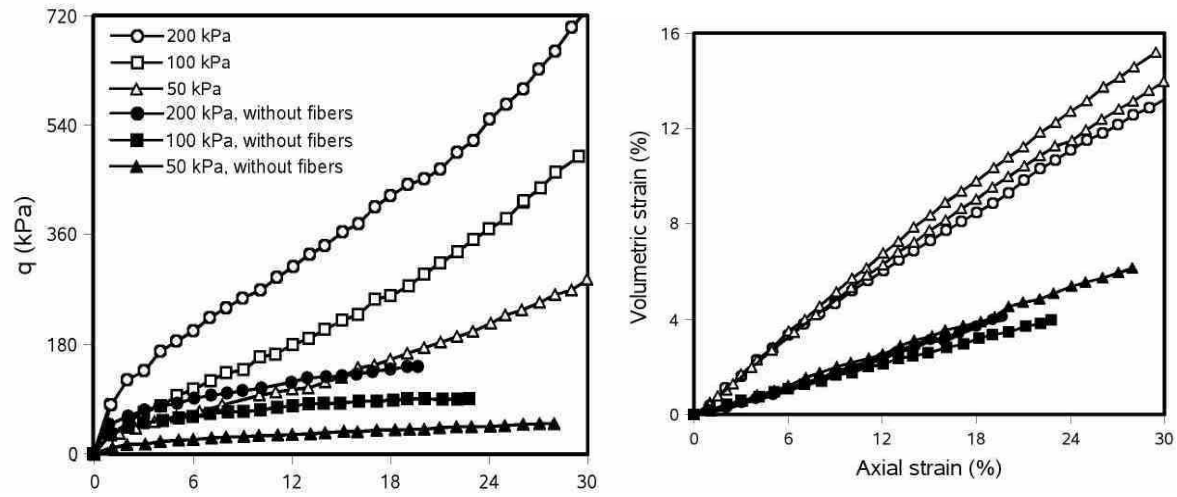

Figure VI- 2: Effect of fibre components on the shear strength parameters of the waste (axial strain on x-axis) (Machado et al., 2007).

Gabr and Valero (1995) tested 15-30-years old waste specimens in direct shear tests. These specimens exhibited continued strength gain at horizontal displacements well in excess of 10% of the specimen's diameter. As a consequence, no peak strength was detected. Therefore, the authors evaluated the values of c' and φ' at strain of 5 and 10%, respectively and suggested that the friction angle increases as a function of increasing horizontal displacement while cohesion remains essentially constant. They however stated that a wide variation in the measured friction angles could result from the inconsistent choice of a horizontal displacement magnitude for data reduction.

Gotteland et al. (1995) Determination of mechanical properties at site: Gotteland et al., (1995) performed geotechnical investigations to summarize stability parameters for a French landfill. Pressure meter tests were carried out to characterise the waste resistance and the values found were comparable to those obtained by other authors. Keeping in view the heterogeneous nature of the waste in-situ determination of the density is difficult and the authors suggest their study could be considered realistic with a degree of uncertainty between 10 to 20%.

Large scale shear box tests were performed, however, even after a displacement of 35% maximum shear strength was not attained. Shear section of (1 x 1 m^2) with a height of 35 cm was tested (Figure

VI-3) under a confining stress of 100 kPa with a maximum shear stress of 100 kPa (Figure VI-4). Both remoulded and undisturbed samples were tested. There was not much to be recommended but it provided an insight to waste mechanics so far developed.

Figure VI- 3: Large scale in-situ direct shear box (Gotteland et al., 1995).

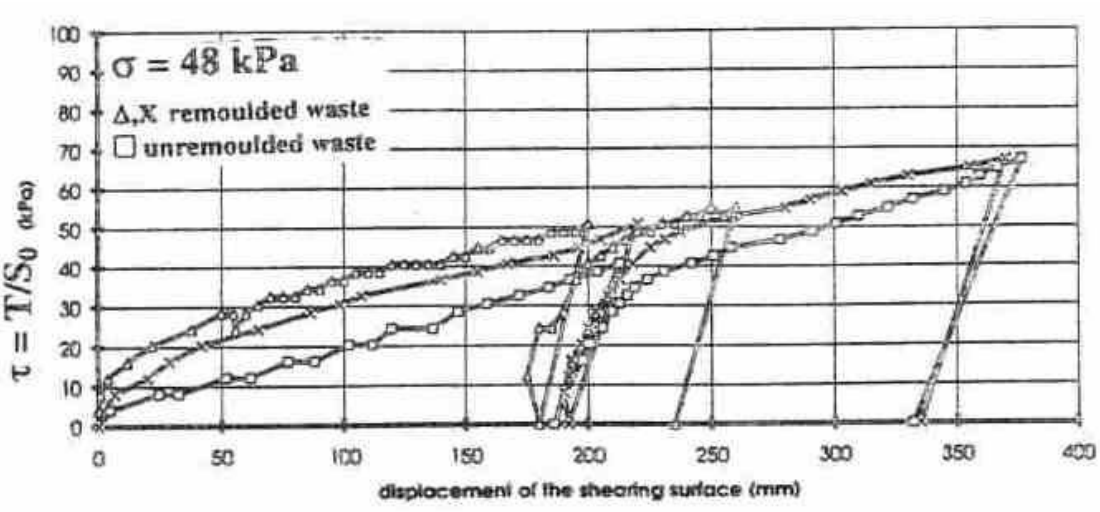

Figure VI- 4: Shear test results (Gotteland et al. 1995).

Kölsch (1995) Bearing model: Kölsch (1995) worked in detail for the development of a bearing model for wastes in general, making use of conventional laws and superimposing new parameters of tensile forces such as fibre cohesion and internal tensile forces. The author conducted a number of tension tests, shear box tests and slope stability analyses to come up with a formulation and possible modelling of the bearing behaviour of wastes. In the proposed model fibrous materials (e.g. plastics)

are supposed to incorporate tensile forces and transmit the same out of the deformation zone. Tensile forces depending upon the normal stresses and friction in the shear plane together make up the total shearing resistance (Figure VI-5). The author explained the shear behaviour of the waste with the concept of tensile resistance that is caused by the fibrous particles interlocking various materials when shear stresses are mobilised. This tensile strength adds up to the Coulomb's equation as a percentage of both the angle of tensile strength and fibre cohesion as follows;

$$\tau = c + \Delta Z^{*}\sigma^{*} \tan \zeta + \sigma^{*} \tan \varphi$$

where Δz = fibre cohesion

$\tan\zeta$ = angle of tensile forces

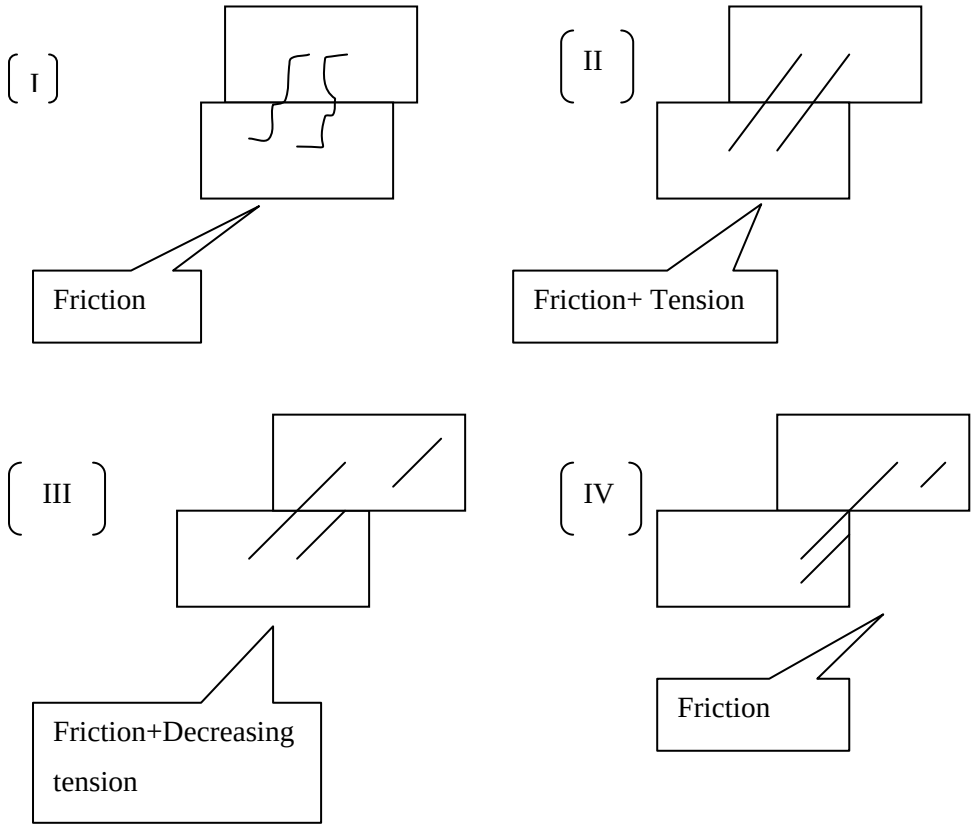

Figure VI- 5: Shearing behaviour of waste sample with the interaction of frictional and tensile forces (Kölsch, 1995).

The total shearing resistance is composed of the friction in the shear plane and tensile forces in the fibres. But the relationship between total shearing stress and normal stress is a nonlinear discontinuous one whereas for the frictional resistance and normal stress it is a linear correlation described by the angle of internal friction φ. Table VI-1 summarises different stages of the shear strength in the waste as a function of shear displacement. According to the author the triaxial test and the direct shear test do not describe the behaviour of a waste the best, and the bearing behaviour of the wastes is affected by

the various processes causing the frictional and shear forces to be changing all the time so these two components were analysed separately through direct shear test and tension test respectively.

New tension test equipment was developed to study tensile forces of the waste within four different wastes with respect to their composition and age or treatment applied namely fresh, residual, rotten and site excavated sample. Sample box of a size (3 x 1 x 1.5) m^3 was filled in 20-30 cm thick layers and pulled with a maximum normal stress of 50 t/m^2. In the absence of shear box results, the results of the tensile test indicate elastic-plastic deformation behaviour.

Table VI- 1: Bearing model description as proposed by Kölsch, 1995.

Displacement Stage	Dominating force	Description
I	Friction	Only the frictional forces arise in the beginning of deformation.
II	Friction + Tension	Increase in deformation produces more stresses in the fibres increasing the tensile force.
III	Friction + decreasing tension	When the tensile strength is exceeded, tearing or slipping is produced reaching the maximum shear stress level.
IV	Friction	Further deformation results in reduction of shear stress down to friction only.

Table VI- 2: Summary of shear tests (Kölsch, 1995).

Sample	Age (years)	Description	Density (t/m^3)	Moisture content %	Internal angle of tensile forces ζ (°)
FRESH	New	Un-treated & without separation of organic components.	0.58-0.72	44	15>°<35
RESIDUAL	New	Un-treated with separation of organic material.	0.54-0.72	32	35
ROTTED	1.5	Aerobic pre-treatment	0.89-1.01	32	15-18
SITE	5	Urban waste excavated from landfill.	1.04-1.1	32	<15

Tensile strength is considered to be independent of waste density in contrast to the shear strength. The maximum tensile stress was 230 kN/m^2 for normal stress 284 kN/m^2. The angle of tensile strength determined through the tension test was termed as ζ instead of φ and the values of φ as stated in other research studies were used in addition to the internal angle of tensile stress ζ. The measured shear strength values are presented in Figure VI-6. It can be noted that the samples 'Residual' (without organic matter) have high cohesion values accompanying high internal angle of tensile forces (ζ) or 'fibres cohesion'; the fibre cohesion depends on the angle between the fibres direction and the sliding surface.

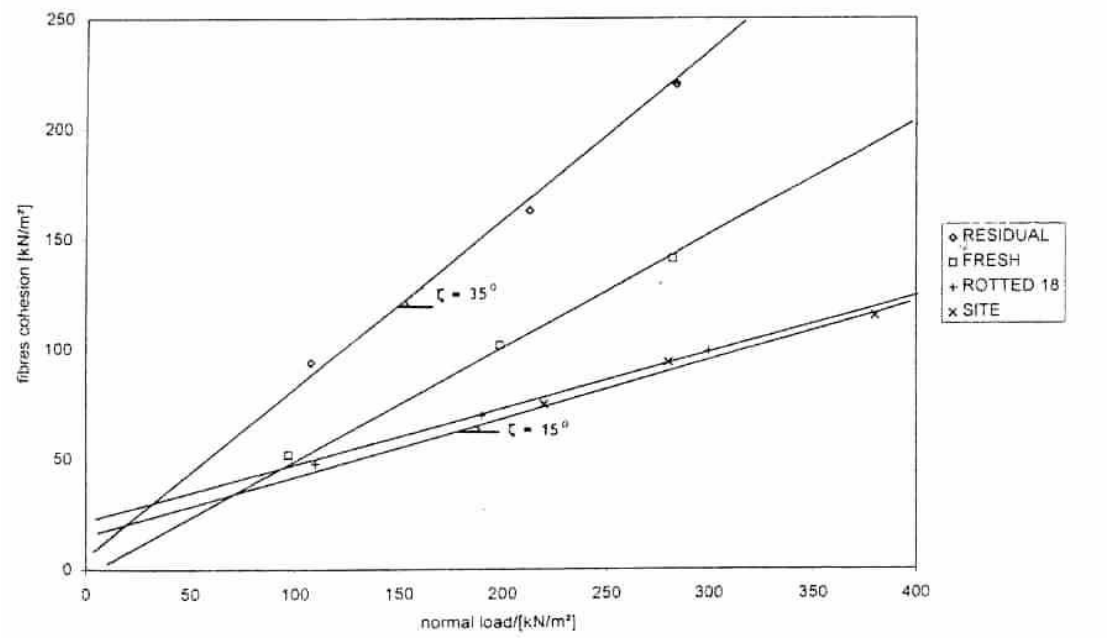

Figure VI- 6: Results of tension tests-relation between fibre cohesion and normal load (Kölsch, 1995).

For the slope failure calculations Kölsch (1995) used available values of angle of internal friction in literature and the calculation were conducted on the sliding figures with two plane sliding surfaces. A number of simplifications in the calculations were made such as;

- No influence of the angle between fibres directions and sliding surface for active tensile forces.
- No tensile forces were considered in the deep sliding surfaces.
- An equal occurrence of maximum tensile and frictional forces was considered.
- Over the reduction of frictional forces by 50% there may be non equal occurrence of different bearing effects.

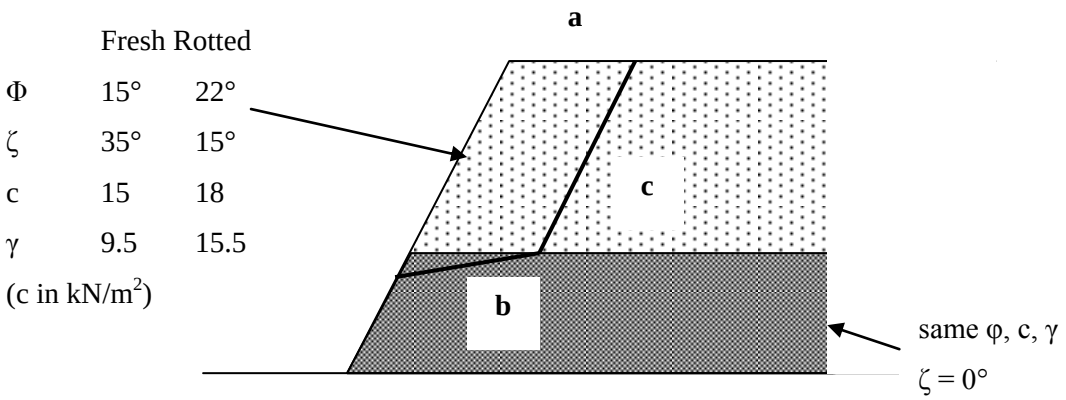

Figure VI- 7: Slope failure calculations from material characteristic values for fresh and rotted waste samples (Kölsch, 1995).

With all these simplifications the results are more critical as otherwise higher stability is observed with exact calculations. For all these figures waste height of 30 m was used for the calculation with angle of slope varying from 30° to 90°. Figure VI-7 describes the material values and the plane surface used for calculations; both angle of internal friction φ and angle of tensile forces ζ were summed up to obtain one value (φ_{sum}). Table VI-3 summarises the different proportions of the sliding figures with reference to Figure VI-8.

Table VI- 3: Slope failure calculations-proportion of sliding figures (Kölsch, 1995)

Figure	Distance between bottom and crossover (a)	Inclination of deep sliding surface (b)	Inclination of upper sliding surface (c)
1	20	10	43
2	40	9	64
3	50	21	61

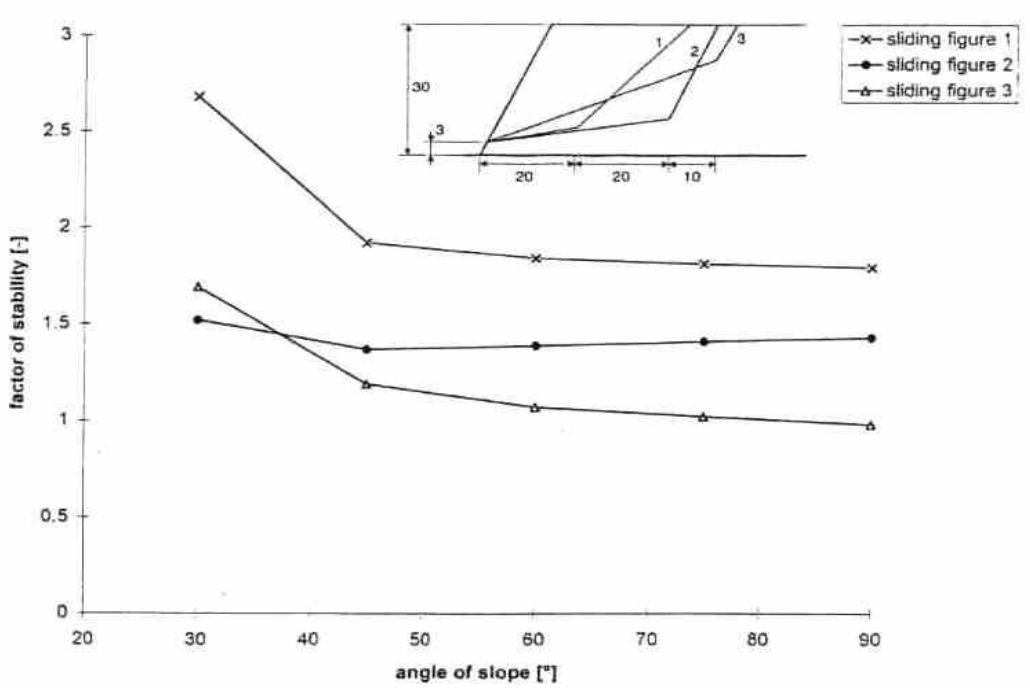

Figure VI- 8: Slope failure calculations for different sliding figures with material values of fresh waste (Kölsch, 1995).

Figure VI-8 shows the slope failure calculations on the three sliding surfaces with material values of fresh waste. The slopes show stability for almost all the sliding figures and slope angles and no considerable influence of slope angle is observed. The most unfavourable case is observed to be the sliding figure 3 because the upper sliding surface is extremely short where the high tensile forces are effective. Similarly for sliding figure 1 with short deep surface and long steep upper surface, high stability values are observed. However due to restriction of tensile forces by a tensile strength as explained in the model, extrapolation of the mechanical values for higher normal loads is not recommended by the author. The author concluded

- The change in mechanical properties of the waste while undergoing decomposition results in lower stabilities for the sliding figures with dominating tensile forces as the internal angle of tensile forces ζ decreases (but the internal angle of friction increases) for an older waste in comparison with a fresh one.
- There is a restriction of a tensile force in the bearing model so much higher normal stresses were not incorporated for the calculations. Stability was found for 90° slope inclination with a waste height of almost 15 m (Figure VI-8).
- For the steep upper sliding surface, high portion of active fibre cohesion generates stability up to the extent that production of failure was literally impossible during the onsite previous testing.
- Since the results of these calculations were comparable to those already observed, the author suggested that the use of this proposed model would be safe.

Kölsch et al. (2005) Stability application to a slope failure case history: When at site the failure has already taken place and researchers and geotechnical experts develop the probable scenario leading to that failure, this forensic study is referred to as the back analysis of the stability. Kölsch et al. (2005) performed a forensic analysis for a dumpsite disaster in Indonesia to check the German advanced calculation model against stability of the landfills. The landfill site was constructed in a narrow valley which was suitable according to the hydrological point of view. Subsoil consisted of rock covered with a clay material with worked as a natural barrier. However the condition of the compacting machines posed the question that whether they were in use or not. The natural landscape showed a slope of 5 to 10% in the bottom of the dump site.

The collapse occurred, after a heavy rainfall which lasted 3 days, like an avalanche killing 147 people but landfill fires hindered the rescue work for weeks. Observations showed a fairly good mineralization and fibres and foils which are considered reinforcements. Upper waste layers were saturated with water which showed that it could hold water back for quite sometime, therefore, shear strength was unlikely to be significantly affected by water pressure. But because of high internal strength the surface between subsoil and waste body becomes critical shear plane. However the geometry of site does not allow this displacement since its outer edge acts as a funnel. There were reports of landfill burns which lasted for months. With these details stability calculations were done using the German technical recommendations. The calculation method considers the reinforcement effect, which is generated by tensile forces in fibres and foils. Tensile stress and normal stress are related by a linear function with an internal angle of tensile stress (ζ) as described earlier by Kölsch (1995).

The shape of the sliding figure corresponds to the situation found at site. Hundreds of alternative sliding figures were calculated, particularly those forming shear planes through the waste. Simulation which best suits the scenario is when landfill fire destroys reinforcement particles in upper layers bringing stability down to 1.0 (Figure VI -10). It was assumed that all tension based components of shear resistance (Tensile angle ζ and cohesion c) had reduced to zero. The shear resistance which is drawn on the bottom of each slice shows clearly the impact of fire at slice 2 and 3 in the upper end of the sliding figure in Figure VI-9 which has disappeared in Figure VI-10 and only the resistance due to friction is left.

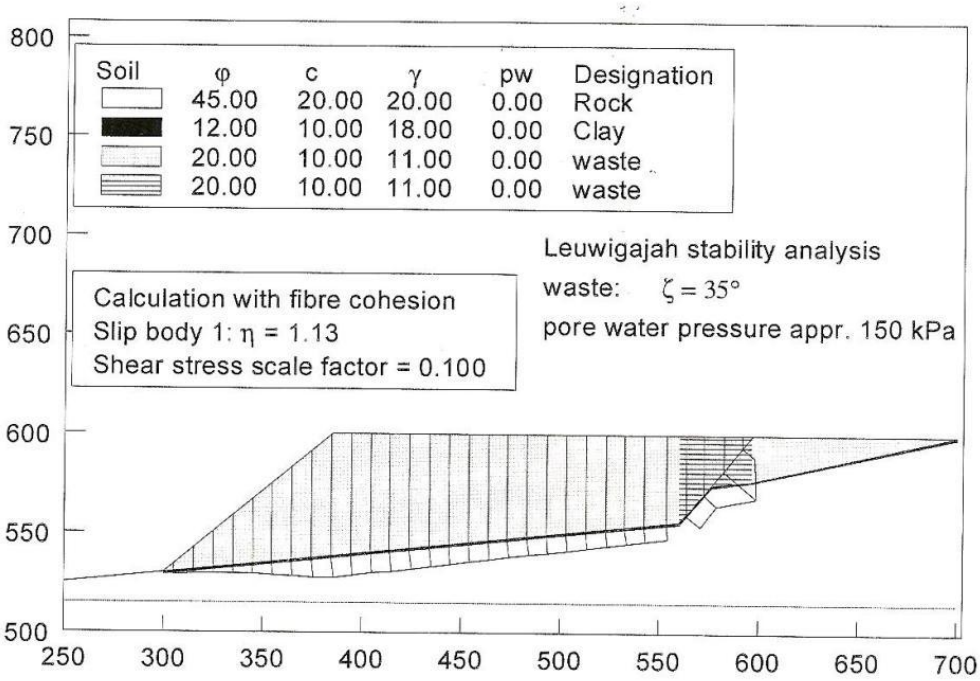

Figure VI- 9: Calculations of the slope stability in the presence of tensile forces acting within the unburned waste body 1:η = factor of safety 'F' (Kölsch et al., 2005).

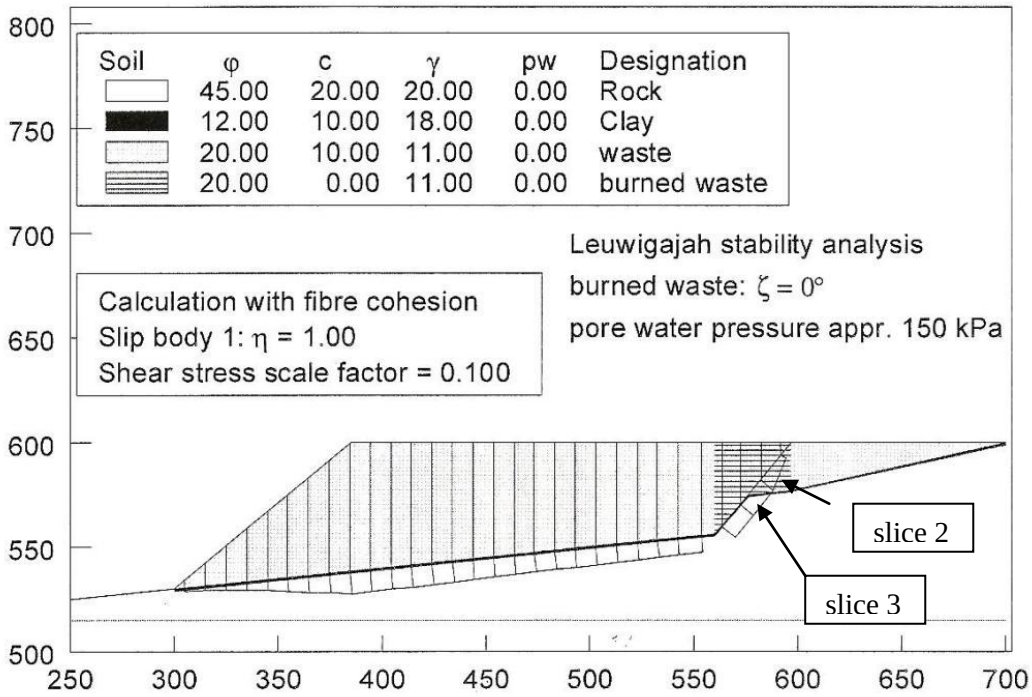

Figure VI- 10: Calculations of slope stability considering the case of burnt waste within the waste body 1: η = factor of safety 'F' (Kölsch et al., 2005).

The calculations indicate that pore water pressure inside the subsoil were more important for the collapse which could have been avoided simply with proper construction and operation of the site. In contrast for a situation with proper drainage and no fire overall stability reaches a value of 1.63 (Figure VI-11). Regarding construction it is important to ensure proper drainage whereas soft soil no matter if a natural deposit or a technical barrier needs protection. Last but not the least is to avoid landfill fires.

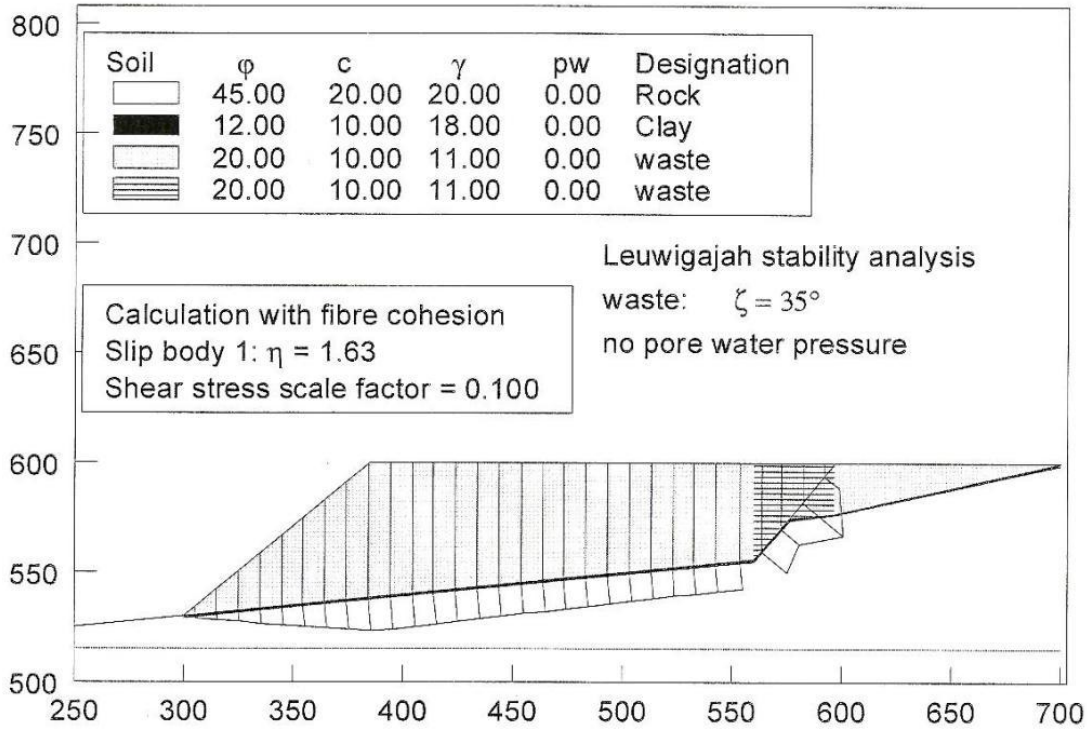

Figure VI- 11: Calculation of slope stability suggesting a stable slope with 1:η =FOS > 1.5 (if proper construction procedure was followed) proposed by Kölsch et al., 2005.

Milanov et al. (1997) Phicometer test and back analysis of slope failure: Milanov et al. (1997) studied in detail a slope failure in a waste fill where apparently fire fighting caused the collapse. Landfill failure caused mixing of leachate into fresh water stream which resulted into pollution of waterworks at the downstream localities. The accident took place when a fire broke out in the landfill body. Their findings regarding the scenario were quite thought provoking such as;

- The waste was tipped and not spread as it should have been.
- There was no incorporation of effluent management techniques.
- The apparent factor of safety (volume ~slope angle) was close to 1.0 which was already weak.

For waste shearing characteristics it was shredded and tipped without compaction so there was no possibility of interlocking between the particles. In situ tests with phicometer were performed which involves application of radial pressure for the teeth of the probe to penetrate the waste; then a tensile

force is applied at controlled speed at the surface of the ground. The strength mobilised under stress σ gives the shear strength as τ = T/S. The principle of the phicometer and the subsequent determination of shear strength parameters are shown in Figure VI-12. But for such less rigidity it was useless to rely on the results, as values of C and φ (φ = 17° and c = 0 kPa) did not permit existence of slope of 50° thus it could be stated that it was under-estimated.

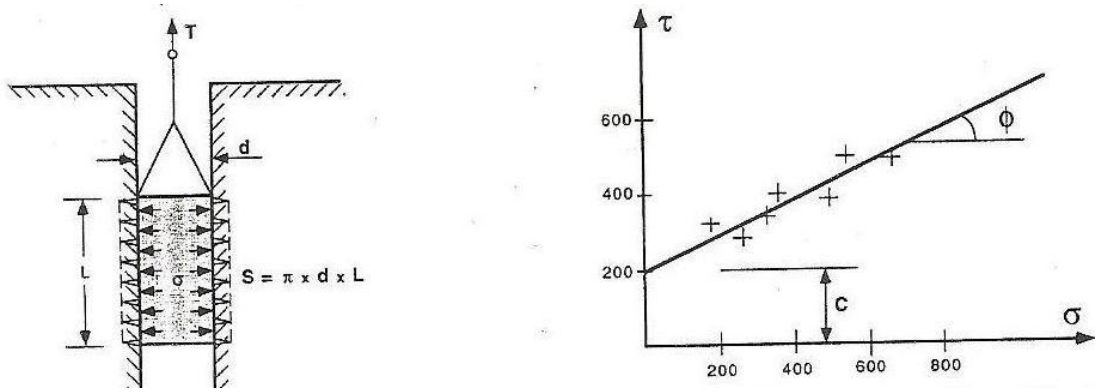

Figure VI- 12: Principle of the shear apparatus with typical graph of shear stress and shear strain (Milanov et al., 1997).

The shear strength values were assumed while considering that fact that a minimum of cohesion is necessary for the stability of the waste body. Table VI-4 gives different combinations of shear strength parameters for a factor of safety of one, assuming;

- Height of the slope = 10 m
- Inclination of the slope = 50°
- Density of the waste = 0.65 t/m^3
- No pore water pressure.

The calculations of factor of safety were carried out using stand-up abacuses with the limit analysis of Druker and Prager criterion for soils.

Table VI- 4: Friction angle and cohesion for FS = 1 (Milanov et al., 1997).

Friction angle φ (°)	Cohesion c (kPa)
30	2.5
35	1.7
40	1.0
45	0.4

Considering the values quoted by other authors e.g. Jessberger et al. 1993 shear strength with cohesion of 1.7 and 1.0 kPa were assumed to be the most probable values. To estimate the absorption capacity

average pressure of 32.5 kPa was used resulting in 115% by dry weight taking into account a linear distribution between 0 and 90 kPa. With original water content assumed at 40% of the dry weight and increase in unit weight with spraying of 50% brings the density from 0.65 t/m^3 to 1.0 t/m^3 which is alone sufficient to lead to rupture (with a reduced factor of safety of 0.65 and 0.7); this condition corresponds to the site situation where abundant water was used to put out the fire (Table VI-5).

Table VI- 5: Decrease of factor of safety after the increase of the density due to water absorption (Milanov et al. 1997).

Factor of safety	Friction angle (°)	Cohesion (kPa)	Density (t/m^3)
0.65	35	1.7	1.0
0.7	40	1.0	1.0

The principle reasons of failure include water absorption (spraying of huge amounts during fire fighting) and subsequent development of pore water pressure. Since water absorption increases unit weight thus reducing factor of safety of the slope and the infiltration in the non compacted waste reaching the bottom generated pore water pressure in saturated zone (assuming the hydraulic conductivity = 10^{-4} m/s to 10^{-5} as quoted by Beaven et al. 1995) and hydrodynamic pressure due to flow at bottom at clayey subsoil. Above complications though less common can have serious consequences if not promptly and properly managed and the authors suggested that well defined protocol precautions and safety measures can help eliminate these complications.

Reuter et al. (1995) Slope stability calculation following triaxial tests: Reuter et al. (1995) performed triaxial tests on the waste samples obtained from Hanover central landfill (Figure VI-13) to determine tension-related shear parameter for the stability analysis. For stability purposes a model (1:50) was constructed to be tested in the centrifuge and the results showed no break but an occurrence of number of distortions in the vertical direction. This distortion behaviour was then confirmed with the help of the waste samples of three different ages (aM = 20 years, zM = 1-3 years and uM = 7-10 years) in triaxial tests (Figure VI-14) and the distortion-dependent parameter of shear stress as calculated in the laboratory was used for the assessment of static stability. Since the investigations did not produce any failure the shear parameters were denoted as the theoretical or apparent parameters i.e. C* or φ*.

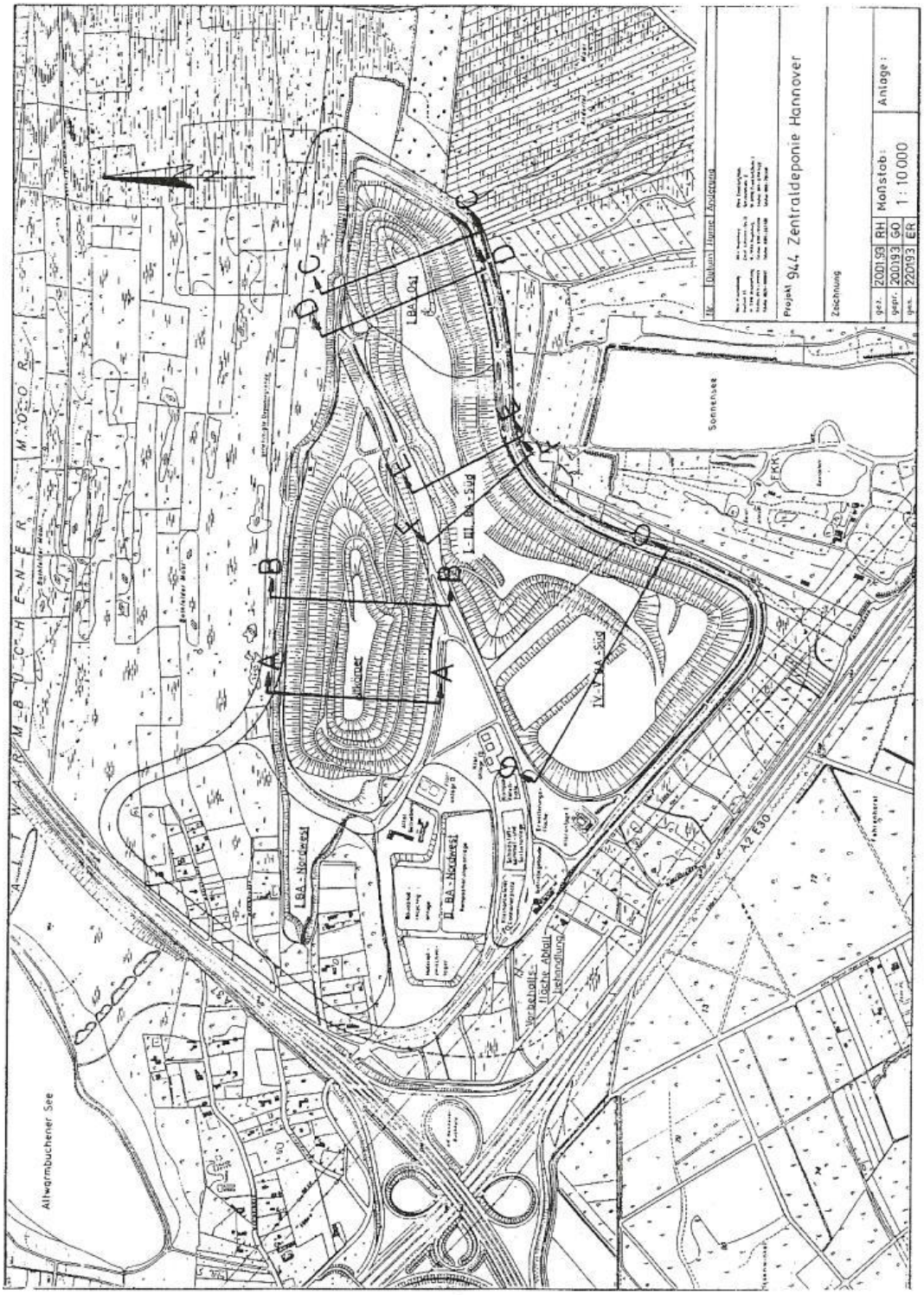

Figure VI- 13: Different sections of landfill studied for the slope stability through distortion analysis (Reuter et al., 1995).

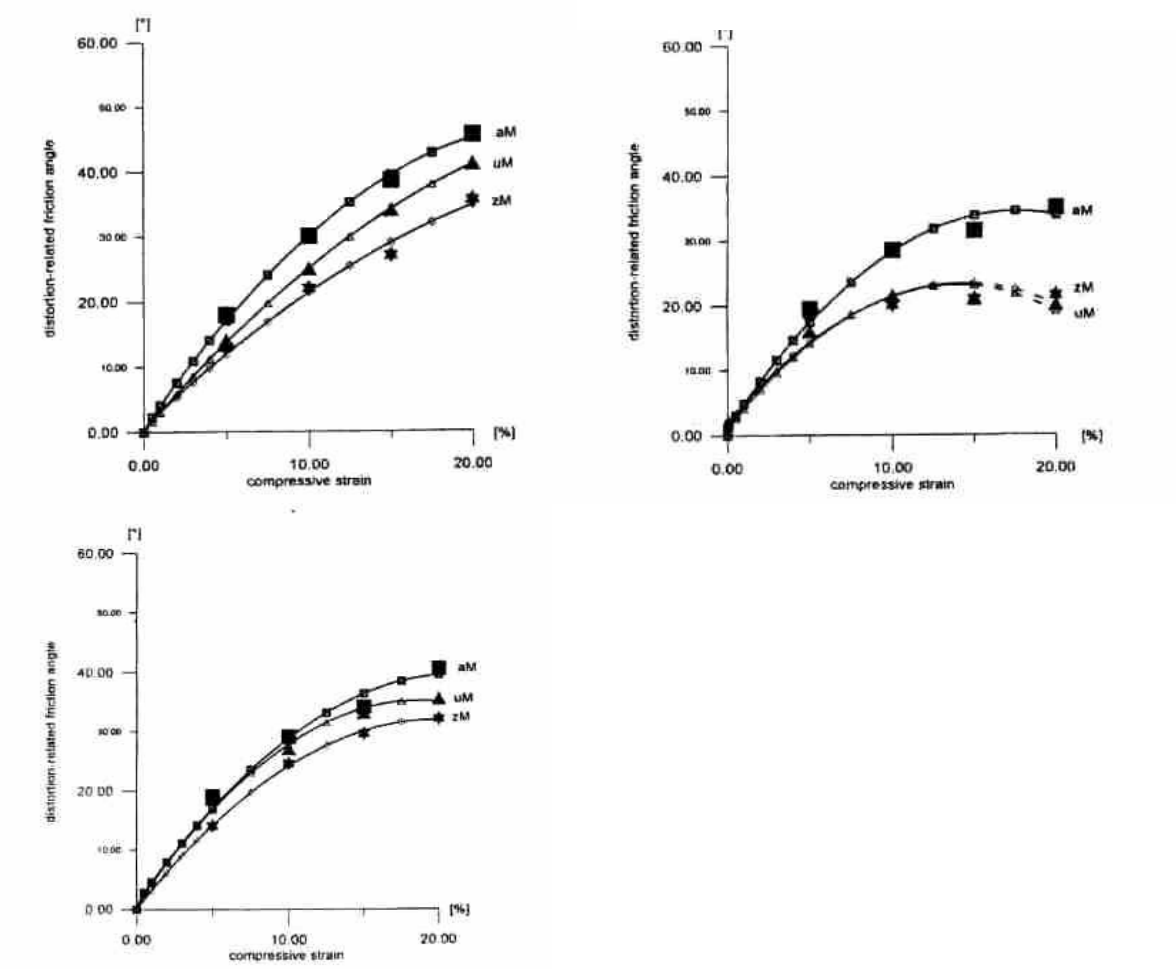

Figure VI- 14: Angle of internal friction as determined through triaxial tests (σ_3 = 300 kPa) of different wastes (aM, uM and zM) having different ages (Reuter et al., 1995).

Observing the results of triaxial tests the authors stated that considerable degree of stability was observed but it mobilised after the major linear strains had developed. Moreover the rise in internal angle of friction can be observed with increasing linear strain. In contrast to the observed angle of internal friction the calculated values indicated cohesion component of shear strength but due to high degree of scattered results any uniform trend in cohesion with increasing linear strain was not possible to identify. The incline failure calculations were performed using BISHOP process with other support programs. Table VI-6 details these calculated results.

Table VI- 6: Calculated values for 15-20 years old untreated waste (Reuter et al., 1995)

Rate of distortion (%)	Bulk unit weight (kN/m^3)	Cal φ* (°)	Cal c* (kN/m^2)
5	15	16.92	15.77
10	15	24.85	31.54
15	15	30.56	51.15

Moreover there is a contrasting data for angle of friction and cohesion and it appears that the identification of any uniform trend in cohesion with increasing linear strain might have not been possible because of the scattered investigations. However no failure was observed (FOS = 1.6) even with the high values of distortion so there may be no stability risk attributing to distortions (Figure VI-15).

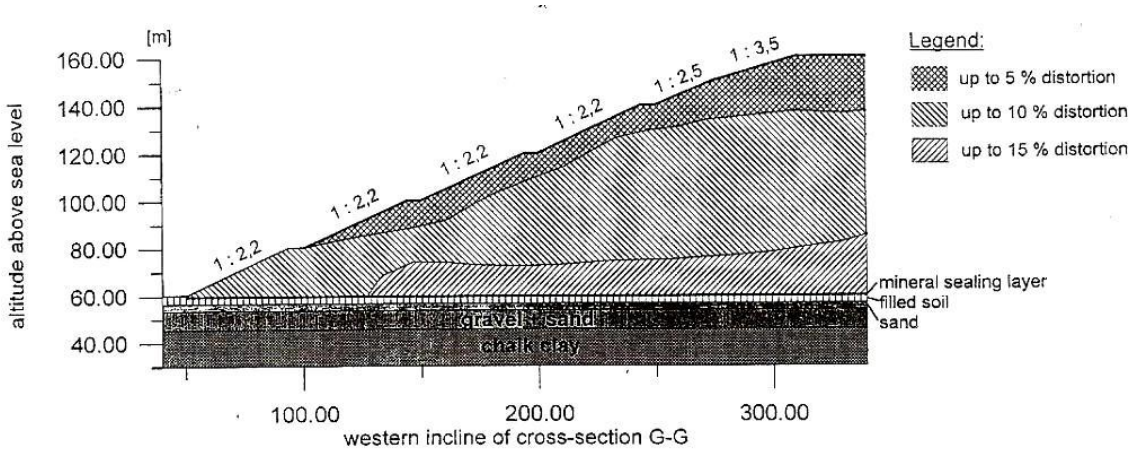

Figure VI- 15: Distribution of distortion in cross-section G-G as calculated by Reuter et al., 1995.

Eid et al. (2000) Shear strength from field and laboratory tests: Eid et al. (2000) studied the shear strength parameters cited by various researchers. The authors assumed the Mohr-Coulomb strength criterion to be applicable because of the fact that the shear resistance of MSW increased with increasing normal stress. Using regression analysis of the data the shear strength of MSW was defined by a narrow band with an effective stress friction angle, φ', of approximately 35°, and the cohesion, c', that ranges from 0 to 50 kPa. Based on the literature study and back-calculation of field case histories, they proposed an average c' of 25 kPa and φ' of 35°, for the design of municipal solid waste containment facilities, which is slightly higher than other published combinations. The lower and upper bounds shown in Figure VI-16 could represent the shear strength of MSW that contains more soil, sludge, and/or other soil-like materials and plastics, respectively. The authors did not state clearly about the mechanisms that yield high shear strength in MSW, but the interconnection of the plastics and other materials is assumed to be a probable contributing factor.

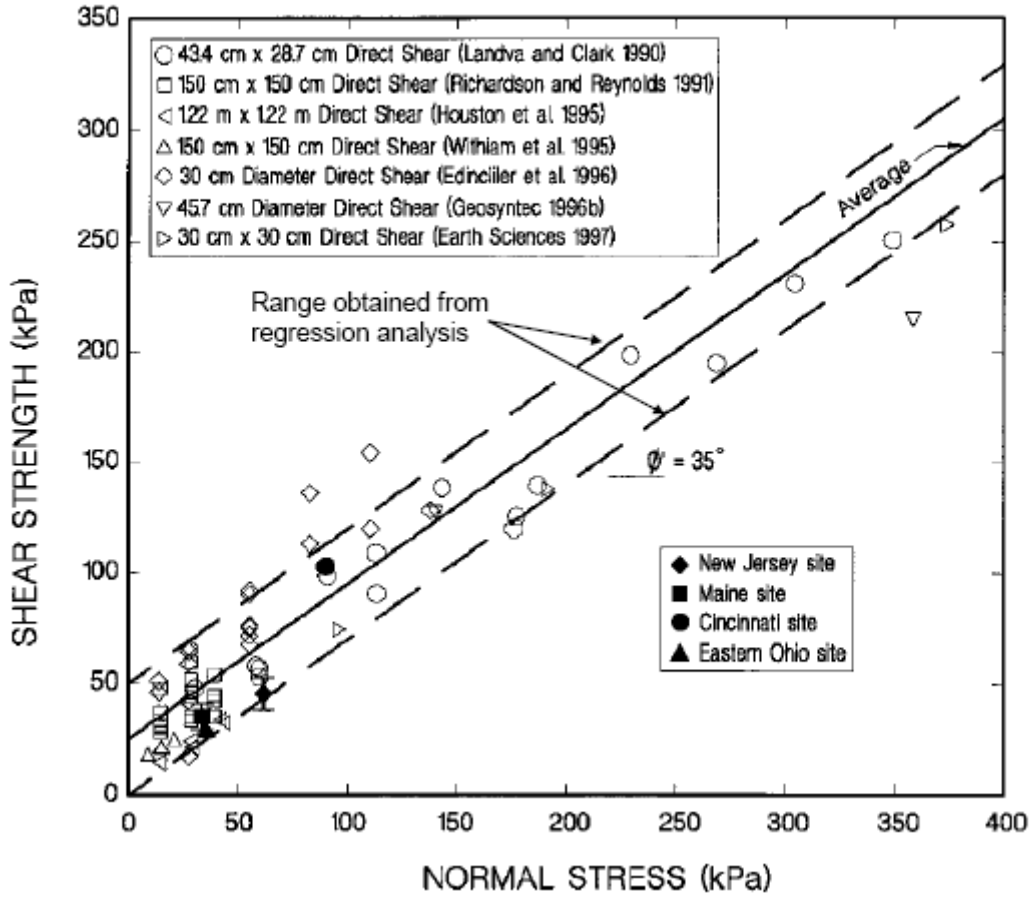

Figure VI- 16: Values of cohesion (c) and friction angle (φ) of the retro analyses from slope failures of waste (Eid et al., 2000).

Eid et al. (2000) indicated that strain incompatibility and progressive failure can occur between MSW and underlying materials and lead to a reduction in mobilized shear strength and failure. The failure studied was found to be a translational failure. Native soils on the bottom and sides of the ravine were not excavated prior to waste placement, thus the mobilisation of post peak shear strength in the brown native soil was suggested to be the primary reason for failure.

Kavazanjian et al. (1999) Shear strength envelope: Kavazanjian et al. (1999) performed a number of laboratory tests regarding shear strength analysis of the waste. They performed a series of direct shear and direct simple shear tests and determined a trend of higher strength towards higher percentage of refuse material. Their testing programme was scheduled such that a number of parameters were interrelated and on non dependency of one parameter they cut short the experiments. Direct shear tests were performed to assess deformation response, evaluate shear data and compare results with those of any other landfill. Two samples were reconstituted with two different unit weights (70% and 90% of the estimates in situ unit weight) but the results indicate that the

reconstitution of samples leads to the field conditions provided the normal stress in enough to compress the sample. Direct simple shear tests (DSS) were performed with monotonic and cyclic loading to evaluate characteristics of waste, stress-strain properties and to provide with the field specific data for subsequent use in deformation and stability analyses. Each DSS test included three to five stages of strained controlled cyclic loading with each stage consisting of 25 cycles. The hysteresis loop for cyclic loading did not degrade with increasing cycles at constant strain due to the reason of volumetric compression and strain hardening (Figure VI-17).

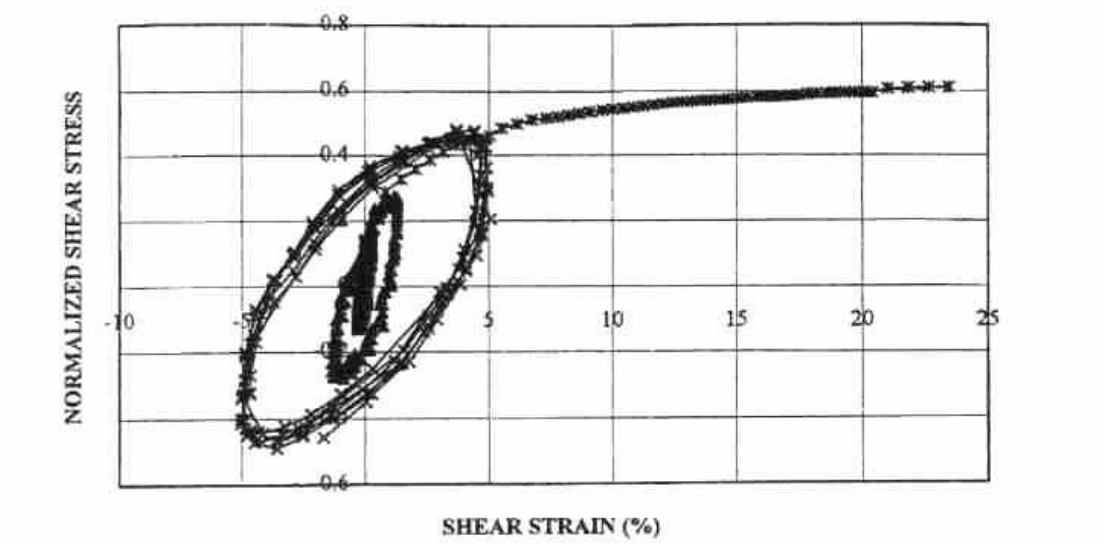

Figure VI- 17: Trend of normalised shear stress as a function of shear strain (Kavazanjian Jr. et al., 1999).

Two interpretations were used for the Mohr circles, firstly based on the assumption that the shear strength is anisotropic and the shear failure occurs on a weak horizontal plane due to structure of the waste and secondly on the assumption that the shear failure occurs on the plane within the test specimen with the largest principle stress ratio. This interpretation was done with cam-clay theory using a K_0 = 0.6. Figure VI-18 explains both these interpretations of the Mohr circle. The results concluded that shear strength on non-horizontal planes may be significantly greater than the shear strength on the horizontal plane (the plane of waste placement). And finally they state that the solid waste mainly remains elastic with little modulus reduction and damping in the cyclic tests.

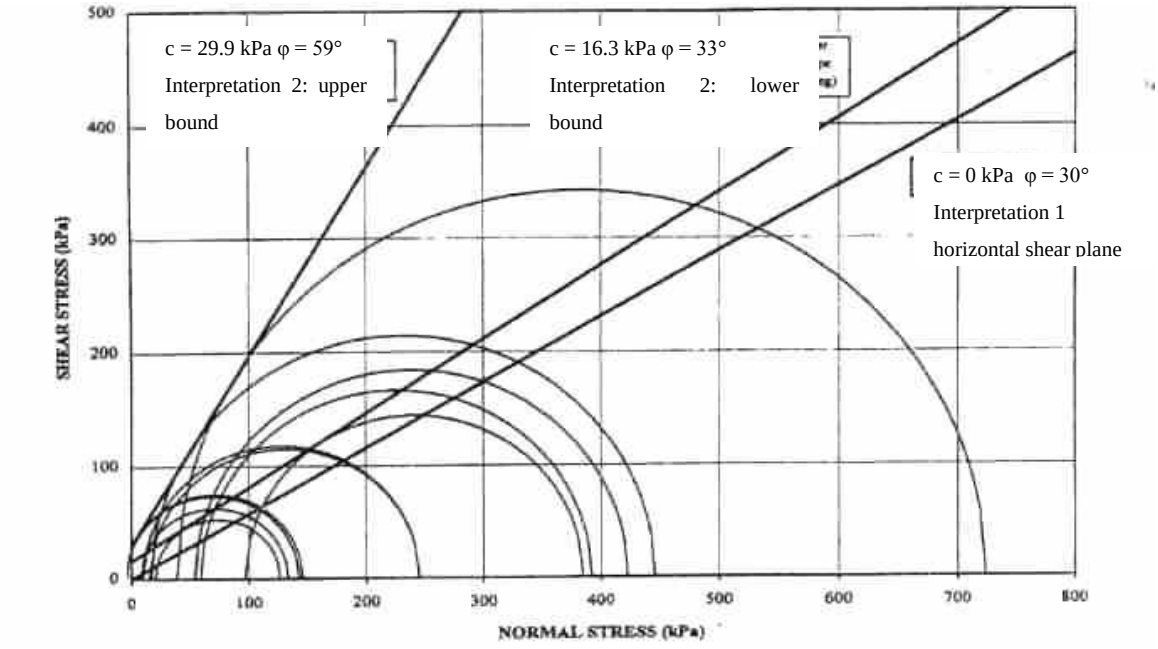

Figure VI- 18: Mohr-coulomb stress envelope, different approaches (Kavazanjian et al., 1999).

The lower bound failure envelope is based on the results of fully saturated MSW samples. The lower bound failure envelope is frictional whereas for effective normal stresses less than 30 kPa, the bilinear failure envelope becomes cohesive. This difference in the two failure envelopes may be caused by the fact that the bilinear failure envelope is based on the back-analyses of landfill failures keeping in view that the MSW was not saturated. It is, therefore, likely that the 'cohesive' portion of the bilinear failure envelope includes some effect of apparent cohesion associated with negative pore water pressures in the MSW under conditions of partial saturation. Furthermore the calculation were carried out with reference to their earlier study of the shear strength parameters Kavazanjian et al. (1995) as presented in Figure VI-19 with c = 24 kPa and φ = 0° for normal stress upto 30 kPa and c = 0 and φ = 33 for normal stress beyond 30 kPa.

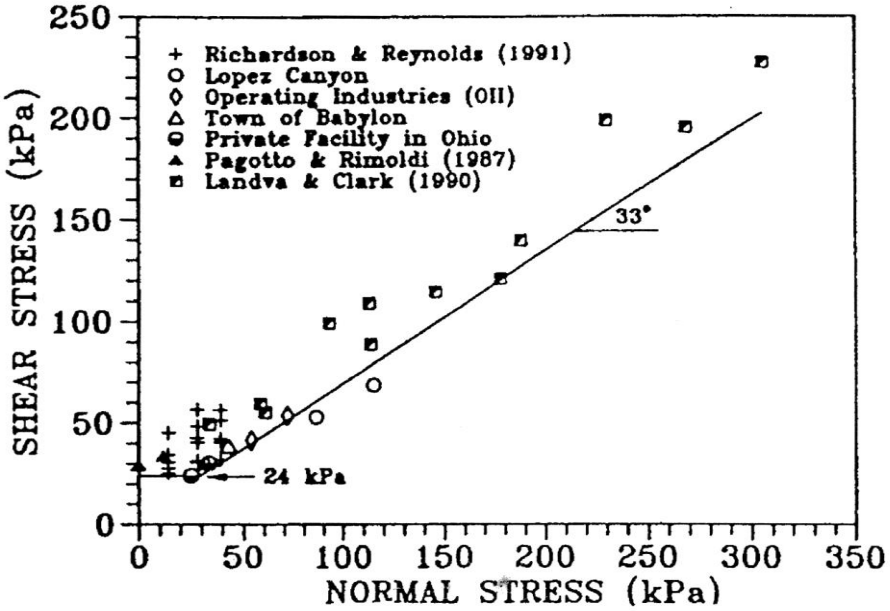

Figure VI- 19: Values of shear strength parameters from shear tests in laboratory (Kavazanjian et al., 1995).

Mahler et al. (2003) Shear strength of MBP waste: Mahler et al. (2003) studied the shear resistance of MBP waste. The MBP process consisted of a sequence of:

- separation of the largest pieces visible in the waste;
- mechanical treatment with minimisation and homogenisation of the mass with input of water/sewage water;
- static biological degradation, enabled by mounting mechanically the windrows, to ensure continuous aeration (in this step the wetting of the material is monitored, as well as the gas production and temperature at different levels and points)
- sieving the material after it is inert.

Table VI- 7: Summary of shear strength parameters determined in the shear box as a function of increasing shear displacement (Mahler et al., 2003).

Parameters	Horizontal displacements (mm)			
	10	20	30	40
φ (°)	21.48	30.7	35.45	35.45
c (kPa)	2.5	3.0	3.5	4.0
τ (kPa)	43.66	60.77	72.49	84.5

Values for the parameters of *c* and *φ* are summarised in Table VI-7, they show the increasing tendency with increase in normal stress. It is worth noticing in Figure VI-20 that unlike conventional MSW the

mechanically biologically pretreated waste did not displayed a ductile behaviour of shear strength as the samples attained the peak shear stress.

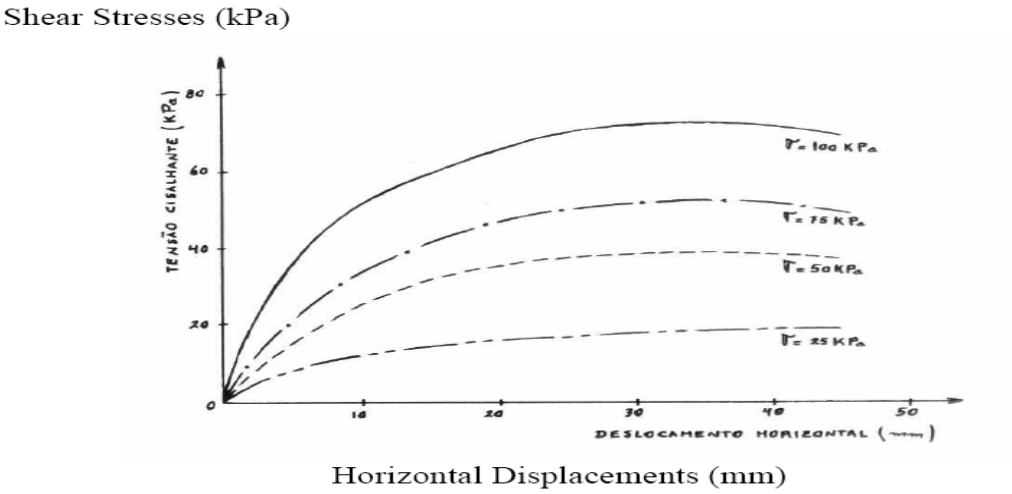

Figure VI- 20: Influence of normal stress on the shear behaviour of the MBP waste (Mahler et al., 2003).

Fucale et al. (2007) Influence of fibre component on shear strength of MBP waste: Fucale et al. (2007) studied the effect of fibre component on the shear strength of the MBP waste. Different samples were testes in the large scale direct shear box (300 mm x 300 mm) including MPB waste at natural composition, samples with 10% of fibre composition and samples with 20% of fibre components (Figure VI-20). The values determined for these different samples are detailed in Table VI-8.

Table VI- 8: Shear strength parameters as determined by Fucale et al. (2007).

Solid Waste	γ_{dry} (kN/m^2)	ϕ' (°)	c' (kN/m^2)
Basic Matrix	9,2	40,1	16,0
Compound Matrix 1	7,5 – 7,8	45,4	34,7
Compound Matrix 2	8,5 – 8,9	48,1	63,1

The MBP waste was sieved to < 8 mm to use the as basic matrix and the reinforcing elements were added to the basic matrix in two percents (10% and 20%) by weight termed as compound matrix 1 and compound matrix 2 respectively. The results showed that the higher proportion of reinforcing elements reduced the stiffness of the material and the reinforced samples did not reach the peak strength over the range of tested displacement. It is in confirmation with the previous research e.g. Kölsch (1995) Grisolia et al. (1995) and Zekkos (2005). The increase in mobilised strength with increasing strain is

though to be due to the low stiffness of the plastic and paper material of the reinforcing component. This finding is strengthened by the observed low values of stiffness with increased proportion of the reinforcing components.

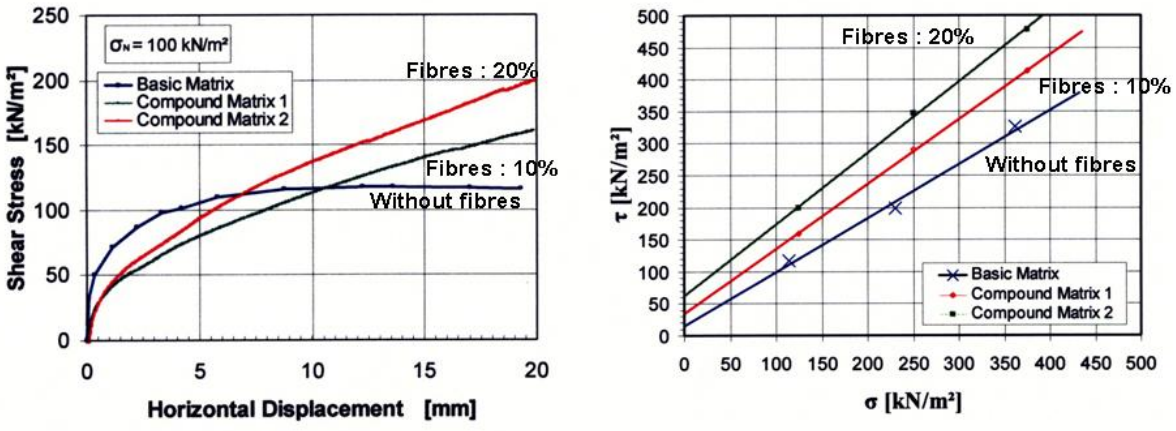

Figure VI- 21: Influence of fibres component on the shear strength parameters of the waste (Fucale et al., 2007).

Caicedo et al. (2002 and 2007) In-Situ analysis of MSW shear strength: Laboratory tests are generally controlled method of testing and manageable than large-scale in-situ tests or back-calculation, but the latter comprises a large amount of sample material, which increases the representativeness of the results. For the purpose of in-situ tests not only the boundary conditions have to be known, but they also have to be set appropriately for examination of the waste material.

Caicedo et al. (2002 and 2007) performed large scale in-situ and laboratory shear tests, as well as phicometer tests. The shear box used in-situ was specifically designed for the purpose and the waste specimens were carved to scale to test in the box (Figure VI-22). Triaxial shear tests were also performed in the laboratory, however, the upper values were obtained with the fresh waste and corresponded to the measurements obtained with the direct shear tests. The effect of the stage of decomposition of the organic fraction of the MSW in Dona Juana on the shear strength or the waste was visible.

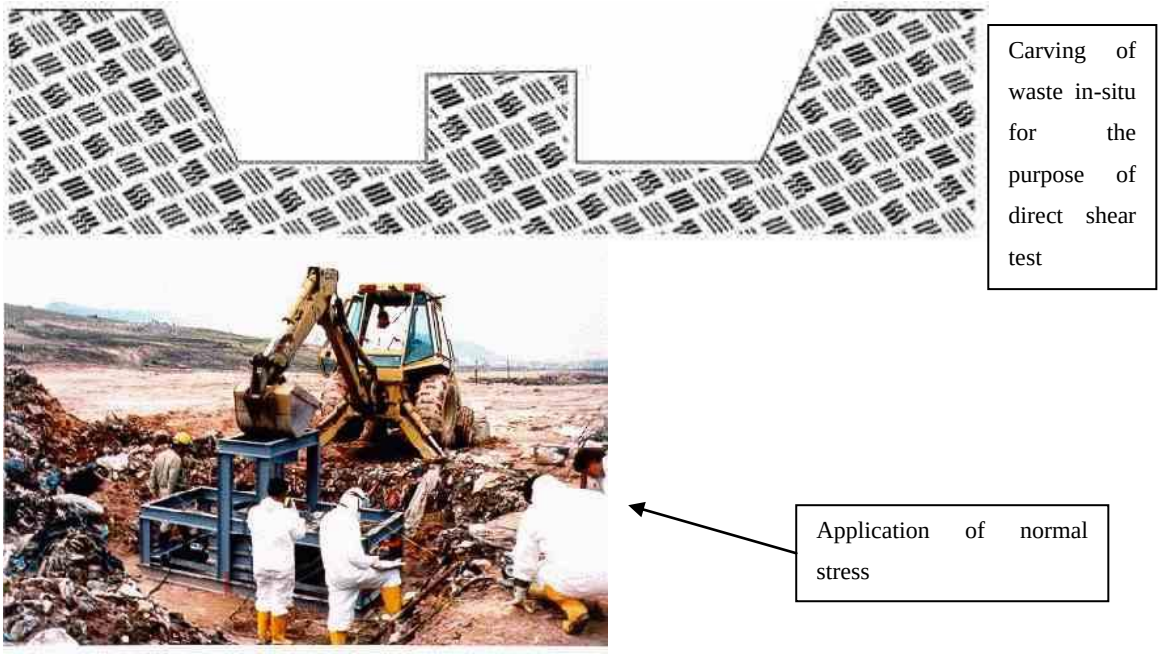

Figure VI- 22: In-Situ direct shear test. (Caicedo et al., 2007).

The comparison of all the shear strength parameters as determined through different test procedures is summarised in Figure VI-23. The results suggested higher shear strength envelope (Figure VI-24) for in-situ direct shear tests, however these tests highlight the importance of site specific testing of the shear strength. The slope stability calculations were performed using the method of Bishop for circular surfaces and Janbu for non-circular.

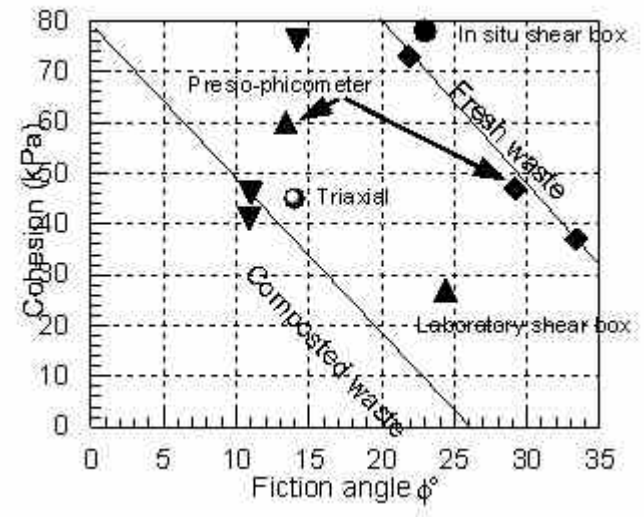

Figure VI- 23: Summary of shear strength results obtained for Dona Juana MSW using different methodologies (Caicedo et al., 2007).

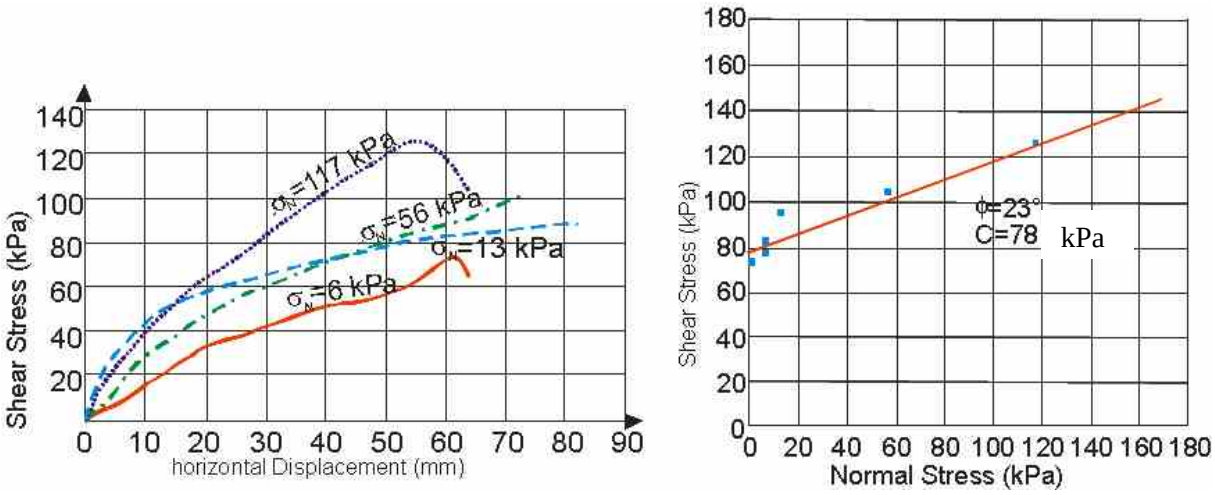

Figure VI- 24: In-situ shear strength parameters as determined by caicedo et al. (2007).

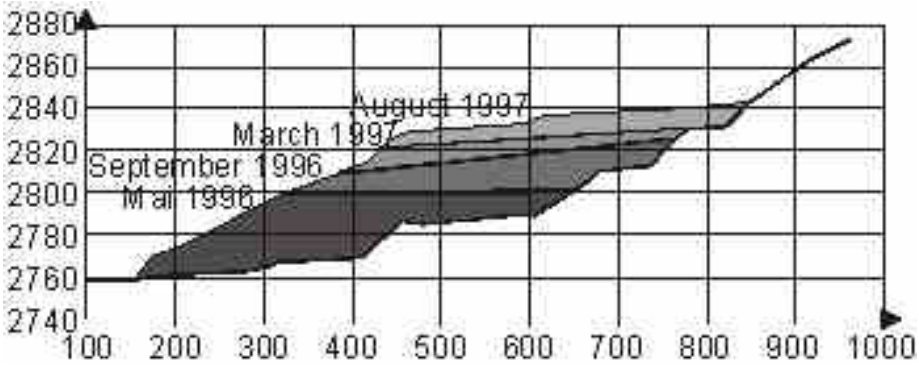

Figure VI- 25: Longitudinal section of Zona II with details of construction periods.

The safety factor decreased consistently due to the constant increase in the gas pressure inside the landfill. For the case of circular surface failure a decrease in safety factor from 1.31 to 1.27 was observed. The decrease in the safety factor was more pronounced when the process of recirculation of leachate through the vertical wells was simulated. The non-circular failure surface presents a more critical behaviour with respect to the circular one. In this case the safety factors for the last two months are 1.2 and 1.16 respectively. When the recirculation of leachate is simulated the safety factor decreases to 1.2 and 0.99 indicating the collapse of the slope. In the collapse and avalanche of the solid waste of Zona II of Doña Juana sanitary landfill several factors combined to generate the effect but mainly the pore pressure was responsible for the instability of the landfill.

VI-2 SHEAR TEST MATERIALS AND METHODS

Large Direct shear box of size 300 mm x 300 mm is used for the shear tests, it includes the following;

- A box of 300 mm x300 mm which may contain up to a thickness of 180 mm of the test material. The box includes two half boxes, lower half box has a height of 100 mm which is the mobile section and the other immobile half is 80 mm thick (Figure VI-26). The sliding of upper half over the lower in a horizontal plane gives the relative movement Δl. To maintain the hydro-static equilibrium, two plates are placed on top and bottom of the boxes.
- A hydraulic motor mobilizes tangential shear force F and allows a maximum speed of v = $\Delta l / \Delta t$ = 5.99 mm / min. The shear rate during a test is kept constant (e.g. 1mm/min).
- A force sensor is installed between the two hydraulic arms of the direct shear machine to measure the shear strength.
- The rigid vertical loading plate is equipped with a sensor for displacement of shear axis to measure the vertical displacement.
- A horizontal sensor located at the edge of the box measures the horizontal displacement Δl of the box. The lower half box due to a horizontal effort can travel up to 60 mm.

In the shear box test the two blocks slide over each other. This sliding mobilizes a tangential resistance. Since the plane of sliding is basically at the separation of the two halves, the rupture plane is actually induced on the sample. During the shear, the surface area under F_n changes, however it is assumed that there is uniform stress distribution on the sliding plane i.e.

Normal stress = $\sigma' = F_n/S$

Tangential stress = $\tau = F/S$

where S is the surface area of the sample

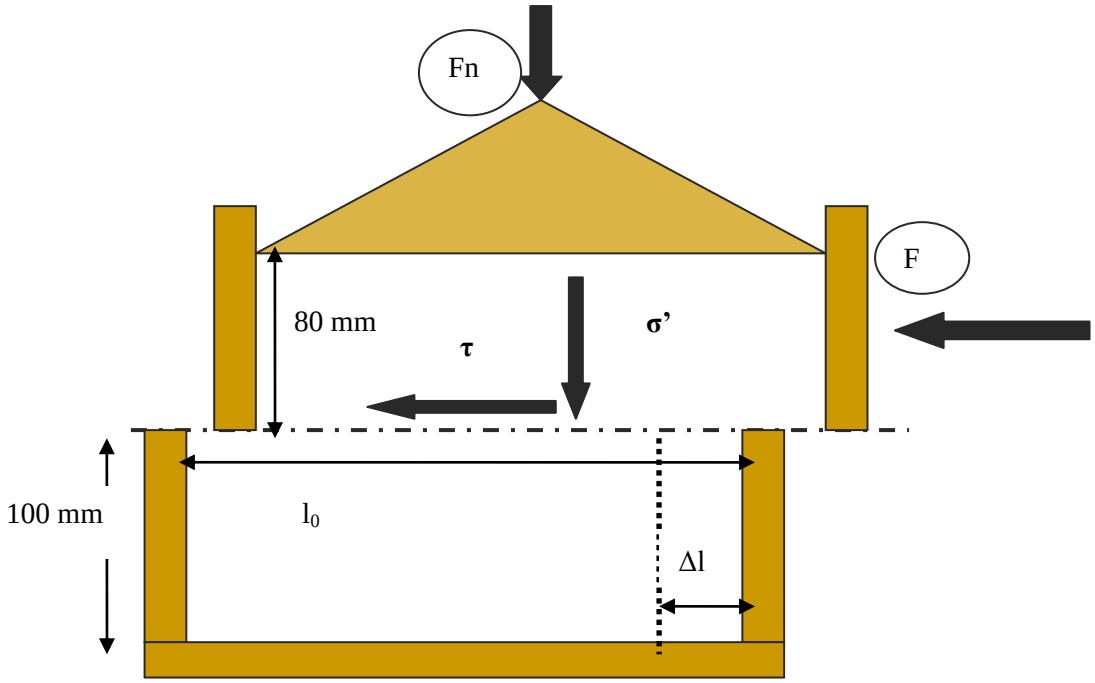

Figure VI- 26: Schematic diagram of direct shear box.

The shear box tests are short term laboratory experiments and no degradation effects are considered during the test. Though simple to realise, however there are various possibilities of changing the parameters to analyse their influence on the shear strength parameters as detailed in section VI-2.2.

VI-2.1 Shear Box Measurements

Data acquisition software transfers the following set of data in tabular form which are automatically stored to the computer and are readily available for further analysis (Figure VI-27).

- Vertical Force (Fn)
- Horizontal Force (F)
- Vertical Displacement (ΔV)
- Horizontal Displacement (Δl)

The rupture can either be characterised by the appearance of a peak point on the stress displacement graph or by the consistent shear level attained. This corresponding stress is termed as residual shear strength. Unlike soils, strain hardening behaviour is systematically observed for waste which can be considered as a ductile material and therefore no peak or residual stress is observed (Figure VI-28). The results in the present study are analysed at the limit defined by the maximum horizontal displacement reached at the end of test (normally 11% deformation).

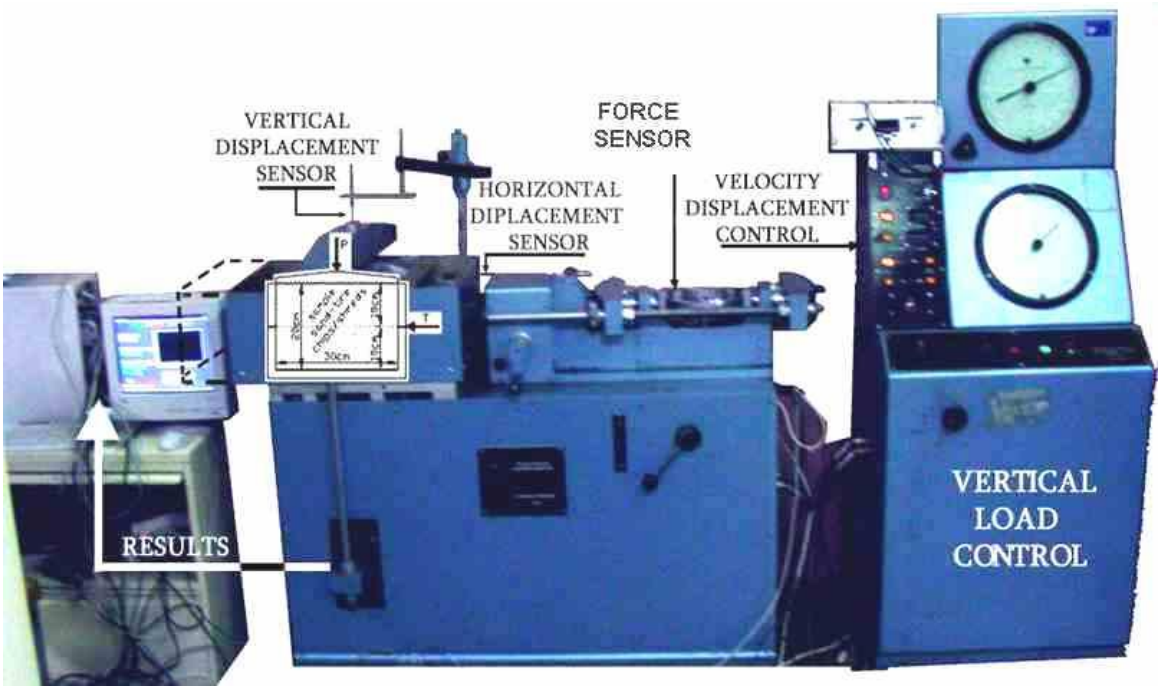

Figure VI- 27: Shear box apparatus along with complementary equipment (LTHE).

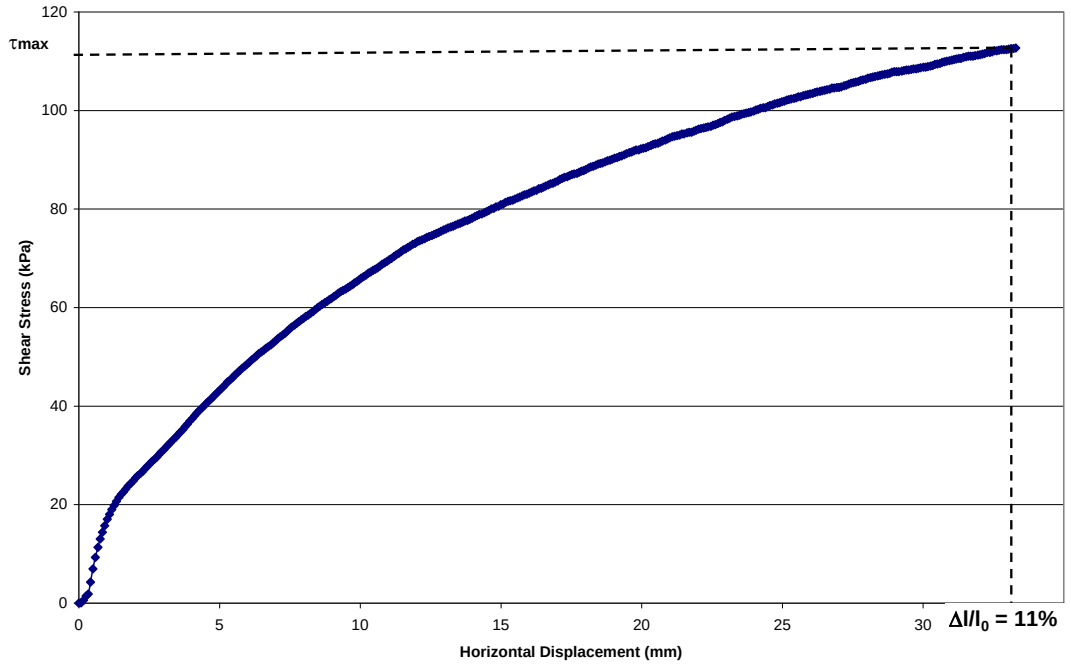

Figure VI- 28: Determination of τ_{max} for shear displacement of $\Delta l/l_0 = 11\%$.

A number of experiments, each time with a different normal stress, give a series of normal stress σ' and residual shear strength (limiting stress) τ_{max} values. Plotting these τ_{max} against σ' on abscise with same scale gives the values for the parameters of Coulomb's equation with φ as the slope of the line and 'c' as the vertical intercept (Figure VI-29).

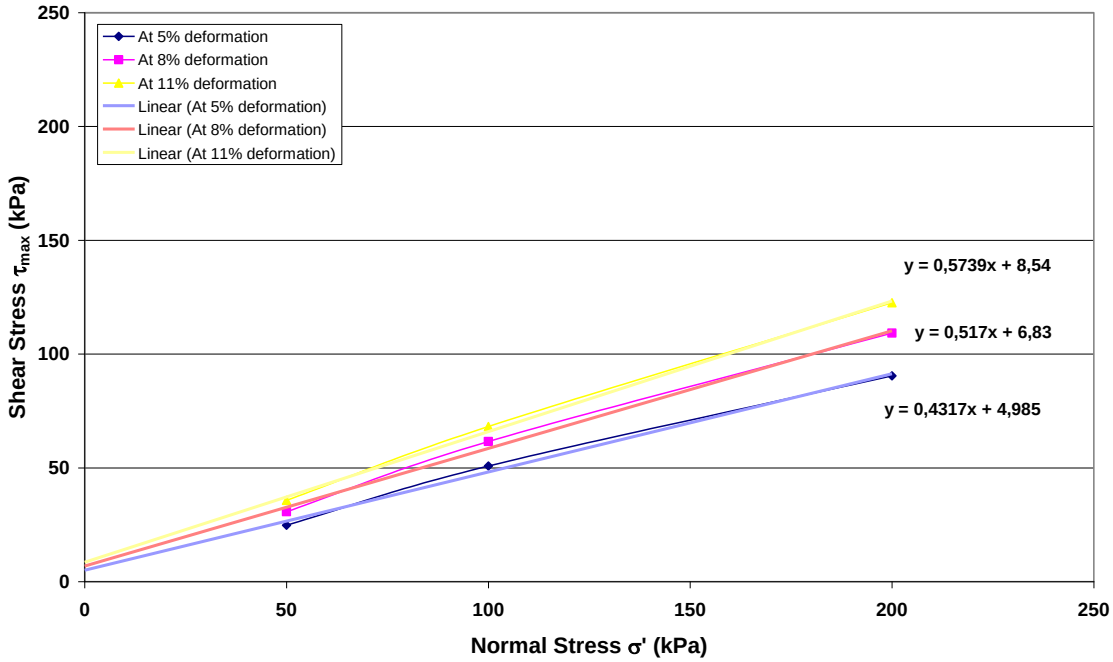

Figure VI- 29: Determination of shear strength values (cohesion c and friction angle φ) from the graph of normal stress and shear stress (test sample LMD-0, § VI-3.2.5).

VI-2.2 Methods: Variable Parameters

Shear strength of MSW depends on many factors such as waste composition, type and age, moisture content and leachate management and compaction level and the type of cover systems. Direct shear test is a simple yet valuable tool for evaluating the geo-mechanical properties of the municipal solid waste. There is a wide range of effective stress shear strength values available in the literature which are used both for the static and seismic stability analysis, however the present study is aimed at analysing the slope stability of the landfills due to any future modifications planned for the landfills.

Shear tests were carried out for different conditions of the waste extracted from number of French landfill sites. Keeping in view the size of the shear box the waste excavated from the landfill sites sometimes needed to be restructured for;

- better representation of waste composition as retrieved from the site.
- to avoid inappropriate waste particle sizes in the shear box.

For this purpose bigger particles, which in general happened to be plastics/textiles, baby dippers and cardboards, were removed and shredded with scissors to reduce to a size not greater than one third of the length of the box. They were then mixed with the waste again to obtain a composition representative as received from the site. The series of shear tests were carried out with different normal

stress on the waste composition obtained from landfill sites as well as the waste further sieved or shredded to either reduce to waste size passing a sieve of 20 mm or reducing the size of the whole sample by shredding (< 50 mm) and finally the waste samples with additional water.

VI-2.2.1 Effect of Waste Composition

In the context of studying the waste behaviour with reference to shear strength at landfill, the waste with initial composition as extracted was subjected to direct shear test. The effect of different waste composition was studied through the variation of waste samples excavated from different location of the landfills.

VI-2.2.2 Effect of Normal Stress

The normal stress is kept constant for one test but it varies for a number of tests to analyse the shear strength variation with respect to density change keeping in view the depth of the waste sample as well as the overload resulting from the vertical expansion of waste cells. The general trend for the waste behaviour under shear stress is considered to be the same as soil thus change of normal stress for the same composition was done to analyse the shear strength evolution with respect to depth.

Pre-consolidation Stress: Prior to shearing all the samples were pre-compacted at a constant stress σ'. In case of over consolidation $\sigma'_{pc} > \sigma'$ was used for pre-consolidation. The sample is placed in the box either at natural moisture content or at additional moisture content. The pre-consolidation of the samples includes:

For normally consolidated samples (σ'): duration of pre-consolidation = 2 – 4 hrs

For over consolidated samples (σ'_{pc}): duration of pre-consolidation = 4 – 16 hrs

VI-2.2.3 Effect of Density

The effect of density change is related to the rheological behaviour of waste similar to that of soils where it has either contracting or dilating effect. With the increase in stress work hardening in the sample is observed i.e. less amount of shear accompanied with the depression of sample which increases the sample density. But due to the over consolidation the waste tends to expand during the shear, known as dilation for soils, sometimes this increase in volume is restricted by the confining pressure.

Determination of density: The volume of the waste material (v) is measured both at start and end of the test and knowing the total weight of the waste sample placed in the box, the global wet density of the sample ρ_h is obtained at the initial step of the test as ρ_{hi} and at the end of the test as ρ_{hf}. Finally with the determined moisture content *w* the dry density is calculated for both initial and final state.

$\rho_d = \frac{\rho_h}{(1+w)}$. ρ_{di} and ρ_{df} are included in the table of shear strength values comparison for all the tests.

VI-2.2.4 Effect of Moisture Content

The series of tests was divided into samples with initial moisture content and samples with experimental moisture content where additional water was added to analyse the change in behaviour of the waste samples.

Determination of moisture content: At the end of each experiment, a sample of waste was weighed and put in the over for the moisture content determination. Though this is an approximate method for the determination of the sample moisture content but due to limitation in waste quantity for every composition and the assumption that moisture content differs a little for little difference of depth, determination of moisture content was compromised. The sample for the determination of moisture content was taken at the shear band level. Even though it is one of the most important parameters of the waste, there is no defined protocol for the determination of moisture content. Due to these difficulties a uniform protocol was adopted for all the samples during this research study, i.e. drying at 80°C in an oven for a period necessary until the stabilisation of the weight.

VI-2.2.5 Effect of Shear Rate

To analyse the effect of shear rate on change of geotechnical parameters some series of tests were carried out with a shear rate other than the one usually maintained. With generally adopted shear rate to be 1 mm/min, other slower or faster shear rate were used for comparison, with 0.5 mm/min for the slower shear rate and 3 mm/min or 5 mm/min for the faster rates. Moreover the change of shear rate was combined with the modification of moisture content to observe the effect of these two parameters in parallel.

VI-3 SHEAR BEHAVIOUR OF SAMPLES RETRIEVED FROM SITES

VI-3.1 Landfill Site 'B'

The details related to the composition and other state parameters have already been established in chapter III under the section related to hydrological analysis. The analysis of compressibility tests (carried out at the same time) for the waste in chapter III resulted in the range of coefficient of primary compression C^*_R = 0.21 to 0.39. The samples from the same landfill were also analysed for the shear behaviour and their results are discussed here.

VI-3.1.1 Shear Tests Results and Discussion

Following series of shear tests were performed on the samples of waste 'B'

- Samples with initial moisture content, sheared at normally consolidated stress.
- Samples saturated with water and left for 48 hours, sheared at normally consolidated stress. Normal confining stresses of 50 kPa, 75 kPa, 100 kPa and 200 kPa.
- Samples saturated (during 48 hours) and sheared while initially consolidated at 200 kPa. Description of the samples of waste 'B' is detailed in Table VI-9.

Table VI- 9: Description of samples of waste 'B' for direct shear tests.

Sample	*w*	σ'_{pc} (kPa)	Shear rate
B0	Natural moisture content	σ'	1 mm/min
B1	Saturated	σ'	1 mm/min
B2	Saturated	200	1 mm /min 5 mm /min

Influence of saturation: It can be noted in Graph VI-1 that as an indirect effect of saturation is the increase of the density of the samples consequently the increase in shear strength with the increase in normal stress is observed for both types of samples as shown in Table VI-10. On the other hand the cohesion of the saturated samples resulted in higher values than the samples at natural moisture content. The internal angle of friction however is observed to be reduced for the saturated samples.

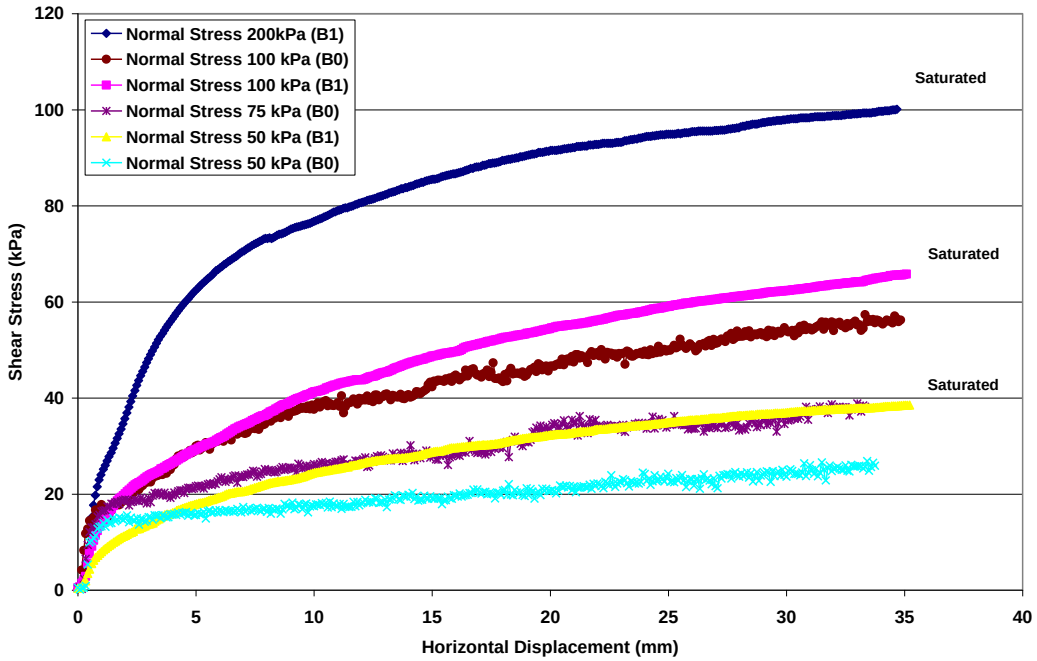

Graph VI- 1: Comparison of samples at initial moisture content (B0) with saturated samples (B1) normally consolidated for waste 'B'.

Table VI- 10: Comparison of samples at natural moisture content (B0) and samples with saturated moisture content (B1) both normally consolidated.

Sample	B0			B1		
σ'_{pc} (kPa)	50	75	100	50	100	200
σ'(kPa)	50	75	100	50	100	200
ρ_{di} (Mg/m^3)	0.36	0.36	0.49	0.56	0.55	0.57
ρ_{df} (Mg/m^3)	0.41	0.43	0.57	0.57	0.57	0.56
w (%)	110.5	-	85.0	102.1	-	97.7
% Deformation	11%			11%		
c (kPa)	0			20.4		
φ	28.2			21.8		

Influence of over consolidation: The shear strength for the samples saturated and consolidated at 200 kPa is observed to increase more that the samples initially normally consolidated. On the one hand this pre-consolidation stress increases the density of the sample but on the other hand it results in evacuation of more liquid from the sample, thus reducing the moisture content of the sample as it can be noted in the Table VI-11. The increase in cohesion of the samples may be attributed to this

reduction in moisture content, but the internal angle of friction seems to have no significant effect of the pre-consolidation stress as it remains in the same range as for the samples normally consolidated or the samples at initial moisture content. This parameter is more difficult to characterise and is influenced by many other physical and mechanical parameters of the waste in parallel.

Influence of pre-consolidation: For the samples tested at normal consolidation stress of 50 and 100 kPa; over-consolidation increases the shear strength values however for the sample with $\sigma'_{pc} = \sigma' =$ 200 kPa the difference between sample B1 and B2 remains difficult to explain.

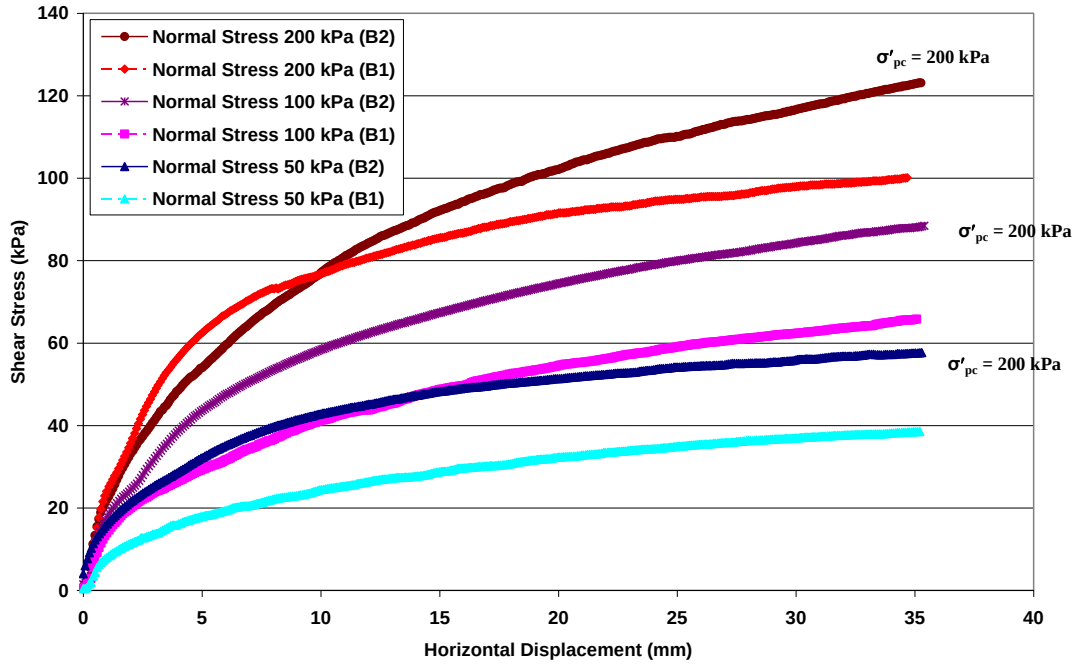

Graph VI- 2: Comparison of saturated samples consolidated at 200 kPa (B2) with initially normally consolidated samples (B1) for shear rate = 1 mm/min.

Table VI- 11: Comparison of saturated samples normally consolidated (B1) and the samples pre-consolidated at 200 kPa (B2) sheared at 1 mm/min and 5 mm/min.

Sample	B1 (1 mm/min)			B2 (1 mm/min)			B2 (5 mm/min)		
σ'_{pc} (kPa)	50	100	200	200	200	200	200	200	200
σ '(kPa)	50	100	200	50	100	200	50	100	200
ρ_{di} (Mg/m^3)	0.56	0.55	0.57	0.69	0.65	0.64	0.63	0.58	0.63
ρ_{df} (Mg/m^3)	0.57	0.57	0.56	0.67	0.65	0.66	0.61	0.58	0.66
w (%)	102.1	-	97.7	85.2	-	-	98.4	-	90.5
% Deformation	11%			11%			11%		
c (kPa)	20.4			40.4			50.5		
φ	21.8			22.3			16.1		

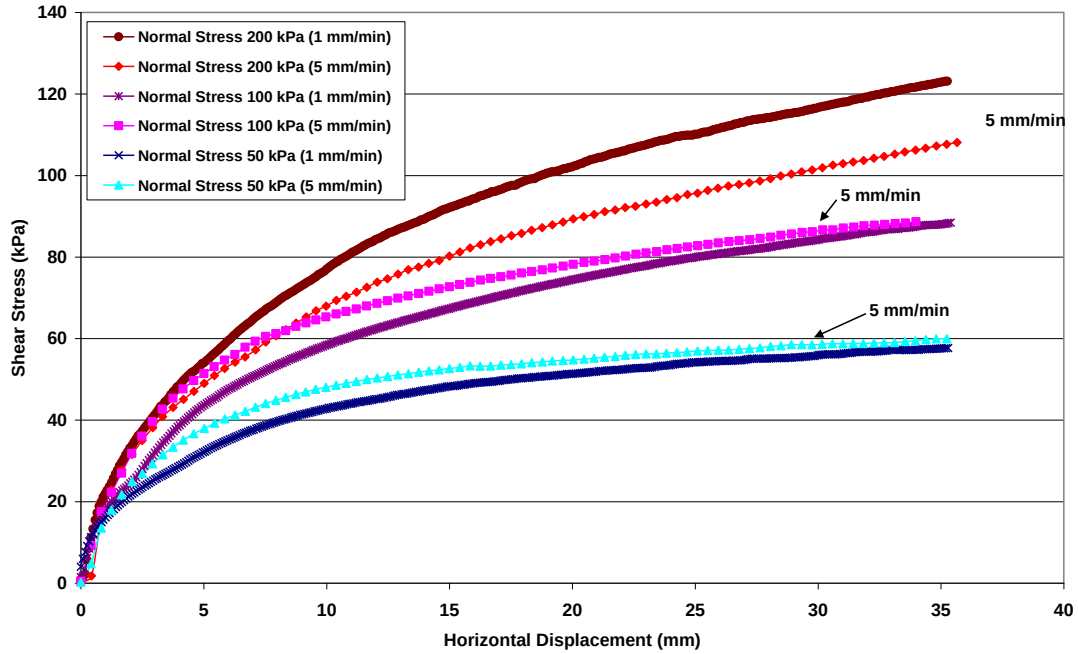

Graph VI- 3: Comparison of samples B2 tested at displacement rate of 1 mm/min and 5 mm/min.

Influence of Displacement rate: There is slight influence of the dry density of the samples with lower values for sample B2. At σ' = 200 kPa the influence of shear rate with a decrease of shear strength with increasing normal stress could be linked to development of over pressures in the material. For the samples which were saturated and sheared at the displacement rate of 5 mm/min it is observed in the Graph VI-3 that they tend to approach the residual shear strength at the axial strain of 11%. But at the same time the two critical parameters of additional water and displacement rate increase the cohesion of the samples (Table VI-11) while the internal friction angle is reduced for high displacement rate.

VI-3.2 Landfill Site ‘LM’

Municipal solid waste degrades over time however the relation of decomposition phase with the shear strength is yet to be developed that whether it decreases, increases or remains the same. More data is on shear strength is needed to analyse this relation and this is the whole different approach to be considered. A detailed sample extraction campaign was carried out on a French landfill ‘LM’ with the objective to analyse shear strength parameters of the old waste body. In addition to the sample extraction, penetrometer tests were also performed to estimate the strength parameters in terms of resistance. In Figure VI-30 the plan of the site marked with location and mode of extraction of samples is presented.

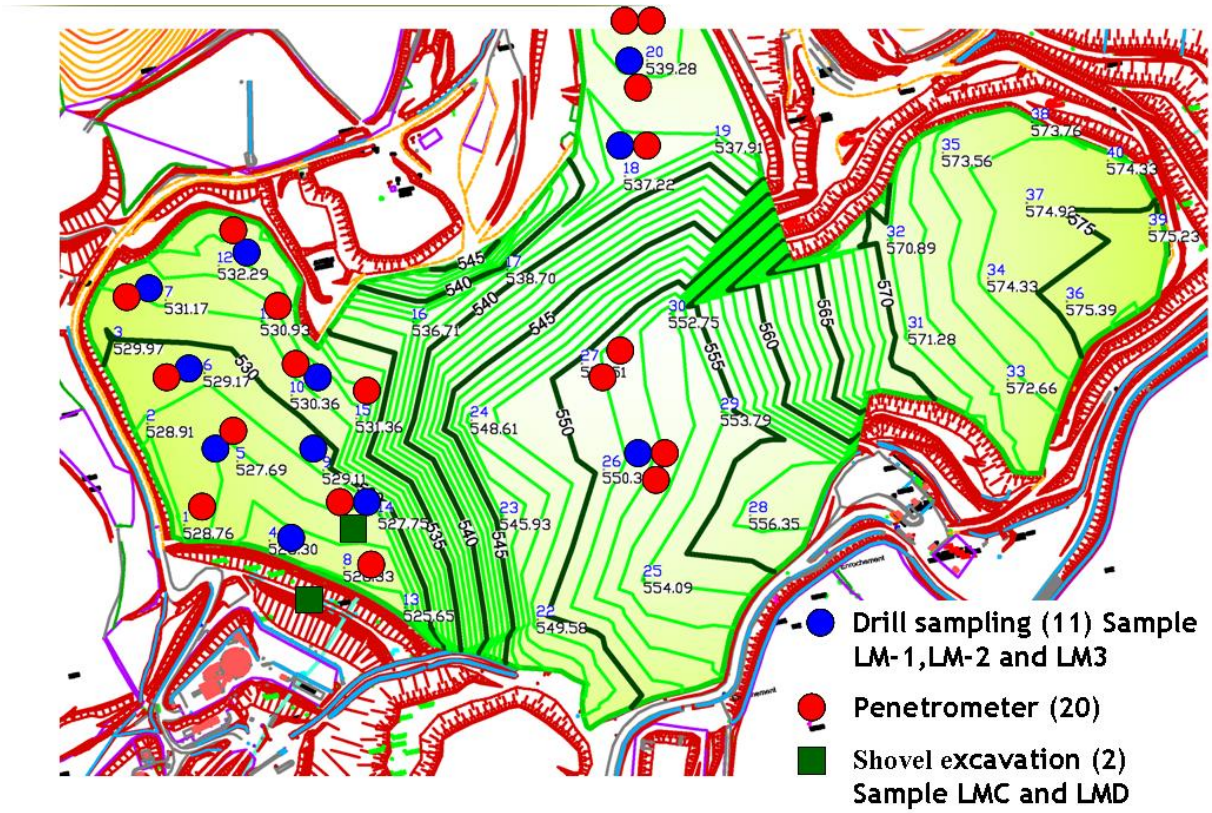

Figure VI- 30: Landfill site ‘LM’ with sample retrieval details.

VI-3.2.1 Sample Retrieval

The detail of sample collection procedure is as under:

- 2 samples were collected with the help of shovel tractor. One sample was excavated from the dike of the downstream slope (age of waste 17 years), while the other sample was collected from the crest of the downstream slope (age of the waste 13 years).

- 50 samples were excavated with the drilling equipment at 11 points; with two to eleven samples retrieved at each drilling point at different depths (Figure VI-30).

Remark: The samples extracted with the drill are classified as the disturbed samples as the drilling not only shreds the particles but also crushes and thus results in change in the composition and grain size distribution of the samples. During the sample preparation it was observed that the samples excavated with the drill had high percentage of fine particles and for that reason all the samples were dried in full once the shear tests series were completed and the composition of the samples were determined only to confirm the initial supposition.

Figure VI- 31: Samples retrieved through shovel and boring.

The shear tests series were carried out on the two different types of sample retrieval processes separately due to following reasons

- To observe the effect of sampling procedure in the first place.
- Due to the grinding effect of the drill, mixing of these samples would have altered the physical properties of the excavated samples by large due to combining two types of disturbed samples.

However mixing of the same type of samples did not pose the problem as all the samples went through the similar sample retrieval effects.

VI-3.2.2 Drilled Samples

For the samples retrieved through drilling, initial moisture content was determined for all the samples, and according to the moisture content profile three zones were identified according to the moisture content as shown in Figure VI-32.

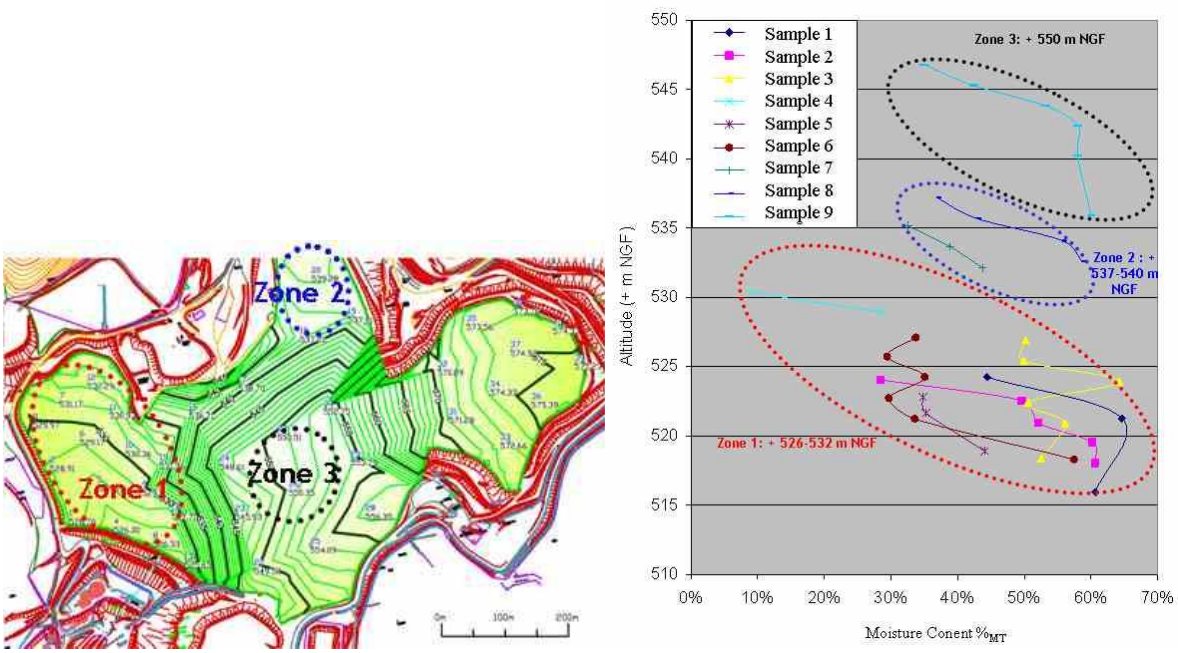

Figure VI- 32: Identification of different moisture zones at landfill site 'LM'.

Due to small quantities of samples retrieved from landfill it was not possible to use a single sample for one shear box test, therefore, mixing of different samples was required. Different approaches were analysed with respect to different influential parameters of shear strength such as geographical location, moisture content and age of the samples (Figure VI-32, VI-33).

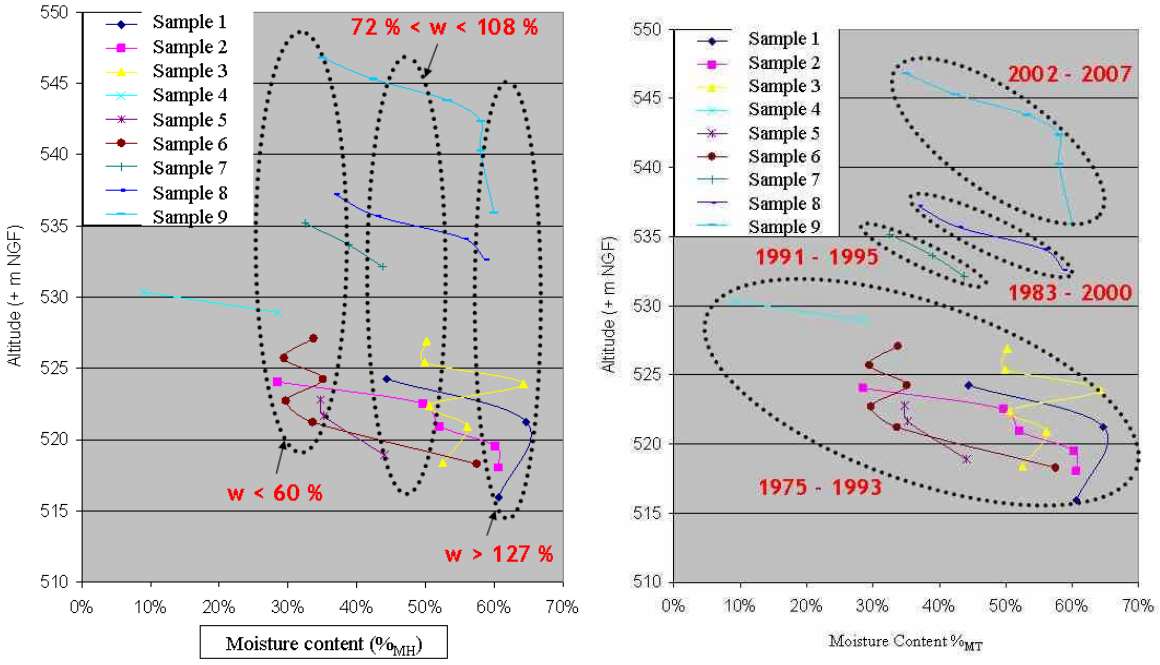

Figure VI- 33: Three range of moisture content for drilled samples LM-1, LM-2 and LM-3.

Finally the regrouping of the sample on the basis of their same range of moisture content was adopted for the present study as this regrouping of samples was observed to be more pragmatic because of huge differences in level of moisture content rather than regrouping the samples according to their age

or location at site. The samples belonging to these three ranges were further mixed together in such a way that three combinations of samples were achieved with the same moisture content range as follows:

- One sample (LM-1) was prepared through mixing of samples with initial moisture content in the range of > 60 $\%_{MS}$ and the average age of 17 years.
- One sample (LM-2) was prepared through mixing of samples with the initial moisture content in the range of 72 – 108 $\%_{MS}$ and the average age of 20 years.
- One sample (LM-3) was prepared through mixing of samples with initial moisture content above 127 $\%_{MS}$ and an average age of 13 years.

Once the samples were tested in shear box for the determination of strength parameters; they were dried in the oven at 80°C until the weight stabilisation. After drying these samples, they were sorted according to the waste composition classification to analyse the influence of composition. The compositions of these samples are presented in Figure VI-34, VI-35 and VI-36.

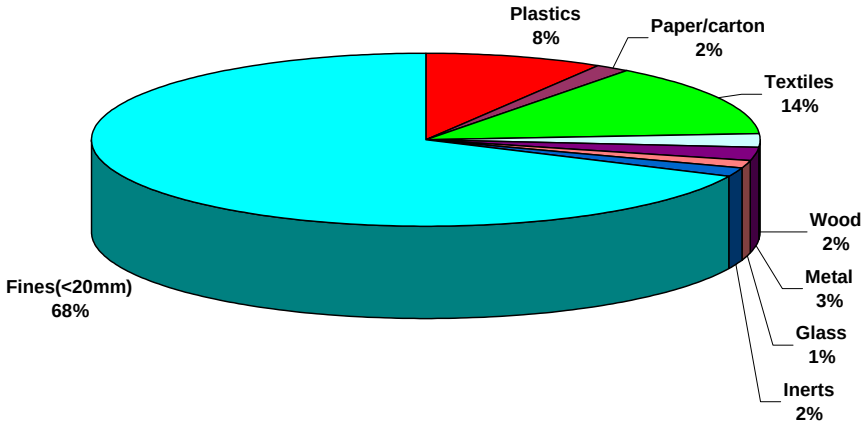

Figure VI- 34: Composition of sample LM-1.

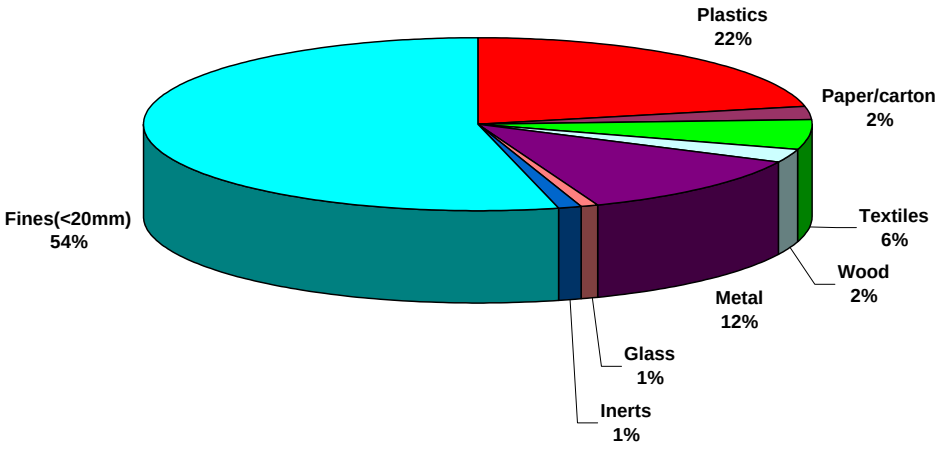

Figure VI- 35: Composition of sample LM-2.

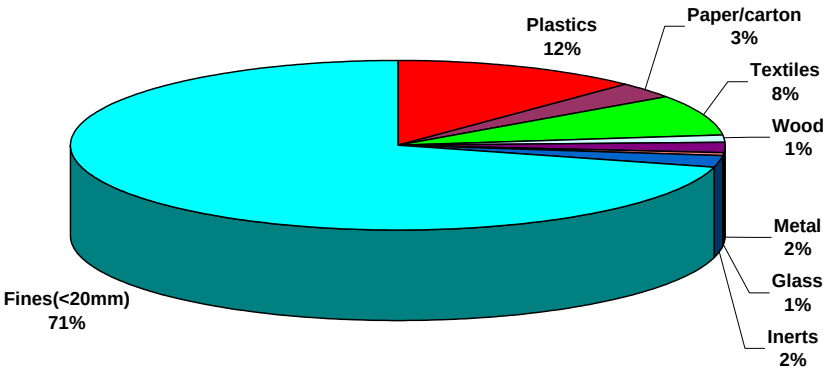

Figure VI- 36: Composition of sample LM-3.

VI-3.2.3 Shear Tests Results and Discussion

Influence of waste composition, age and depth: All the drilled samples have the same trend of shear strength parameters for different normal stresses. Even though the difference in the moisture content of the samples LM-1 and LM3 is around 20% still the cohesion is nearly the same. Similarly the internal angle of friction for both the samples is in the same range of 30-34°, even though for sample LM-2 the shear strength parameters have lower values than the other two combinations. This may be linked with the lesser percentage of fine particles as well as the presence of high percentage of metallic and plastic components (Table VI-10) and consequently high cohesion is observed.

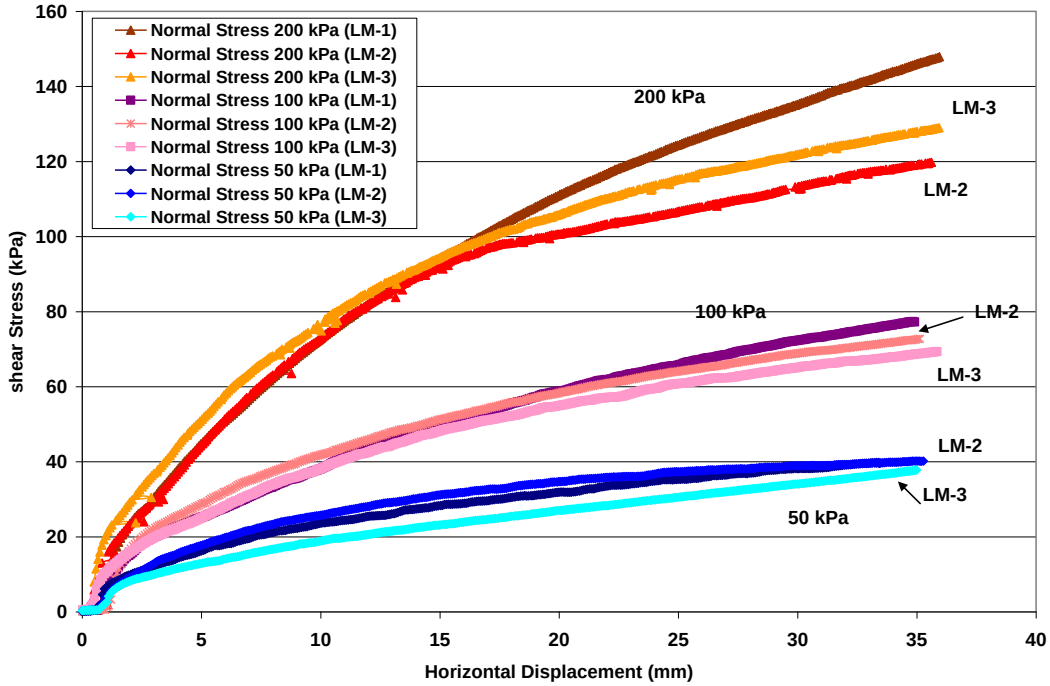

Graph VI- 4: Stress Displacement comparison between all three drilled samples different range of moisture content (LM-1, LM-2 and LM-3).

Table VI- 12: Comparison of shear strength parameters for three drilled samples (LM-1, LM-2, LM-3).

σ'_{pc} (kPa)	50	100	200	50	100	200	50	100	200
Sample	LM-1			LM-2			LM-3		
Depth (m)	0-8.9			1.35-10			0-12.1		
Age of waste(yr)	17			20			13		
σ' (kPa)	50	100	200	50	100	200	50	100	200
ρ_{di} (Mg/m^3)	0.63	0.76	0.89	0.68	0.76	0.94	0.76	0.80	0.84
ρ_{df} (Mg/m^3)	0.65	0.77	0.91	0.68	0.79	0.96	0.78	0.82	0.87
w (%)	62.34	52.23	51.51	77.78	66.67	52.09	78.57	73.79	67.25
% Deformation	11%			11%			11%		
c (kPa)	6.4			16.5			7.0		
φ	34.2			27.0			30.7		

VI-3.2.4 Excavated Samples

The two samples excavated from the slope of the site were tested for their shear strength parameters as follows:

- Both the samples were tested in the shear box at their initial moisture content and their initial state without any modification to their composition.
- In second series of test, the samples were shredded in the laboratory and then the shear box tests were performed. For the samples retrieved from the top of the slope (LM-C) shredding was carried out in the laboratory in two steps to obtain < 50 mm and the shear box tests were performed.
- These samples were humidified with additional moisture and tested in the shear box to analyse the influence of additional moisture. Moreover the displacement rate was altered to observe its influence over the shear strength parameters.
- From the tested samples, representative samples of weight 500 to 1000 g were taken to analyse their moisture content at the end of the shear test.

These series of tests were carried out with the aim to find relevance between the different physical parameters, the effect of composition and the grain size of the waste samples with the combination of moisture content of the samples (Table VI-13).

Table VI- 13: Detailed description of the excavated samples from Landfill 'LM', prepared for the direct shear tests.

Sample Notation	Description
LMC-0	Initial sample as retrieved from site at in-situ moisture content.
LMC-1	Sample LMC-0 shredded to particle size < 5 cm.
LMC-2	Sample LMC-1 saturated for 48 hrs and drained before placement in the shear box.
LMD-0	Initial sample as retrieved from site at in-situ moisture content.
LMD-1	Sample LMD-0 shredded to a particle size < 5 cm.
LMD-2	Sample LMD-1 saturated during 48 hrs and drained before placement in shear box.

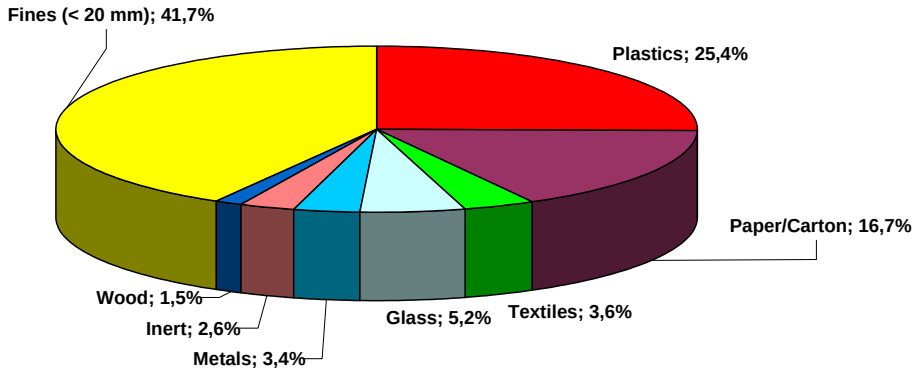

Figure VI- 37: Waste composition of sample LMC.

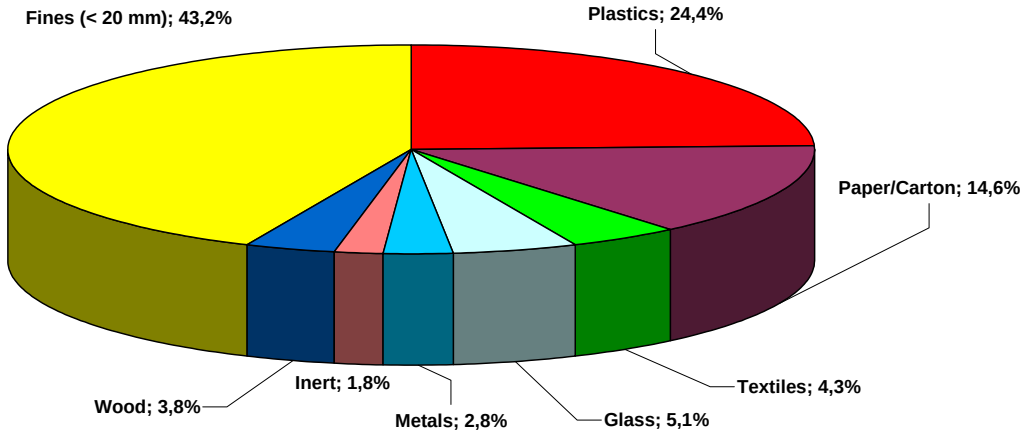

Figure VI- 38: Waste composition of sample LMD.

VI-3.2.5 Shear Tests Results and Discussion

Comparison of samples LMC and LMD: It is noted that the composition of the samples is very similar with the same percentage of fines, plastics and paper (Figure VI-33, VI-34). The same composition of waste resulted in same range of density for all the samples in the shear box. Even though the size of the plastic or paper component in both the samples can not possibly be the same still it can be noted in Table VI-14 that both the samples have the same range of cohesion and the friction angle. In Graph VI-5 the shear test results for both the excavated samples at natural moisture content is presented.

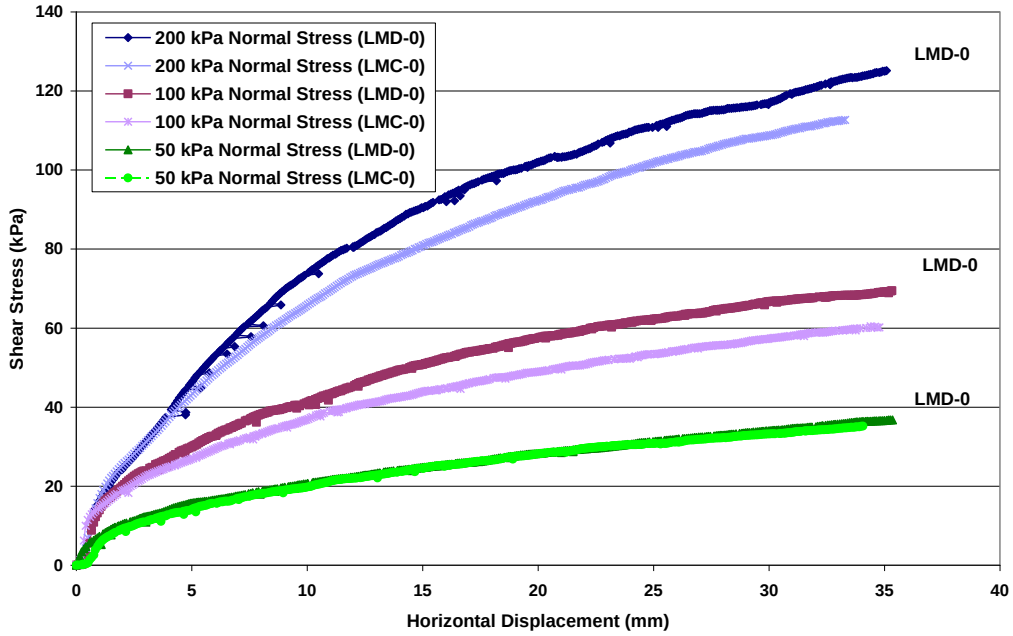

Graph VI- 5: Comparison of shear behaviour of the excavated waste samples 'LMC-0' and 'LMD-0' normally consolidated.

Table VI- 14: Comparison of shear strength parameters of the excavated waste samples 'LMC-0' and 'LMD-0' normally consolidated.

Sample	LMD-0			LMC-0		
Depth (m)	1-1.5			1-1.5		
Age of waste(yr)	17			13		
σ'_{pc} (kPa)	50	100	200	50	100	200
σ' (kPa)	50	100	200	50	100	200
ρ_{di} (Mg/m^3)	0.46	0.56	0.68	0.49	0.54	0.67
ρ_{df} (Mg/m^3)	0.47	0.58	0.68	0.52	0.56	0.68
w (%)	117.39	92.31	66.67	92.31	112.77	85.19
%Deformation	11%					
c (kPa)	8.5			8.1		
φ	29.9			27.5		

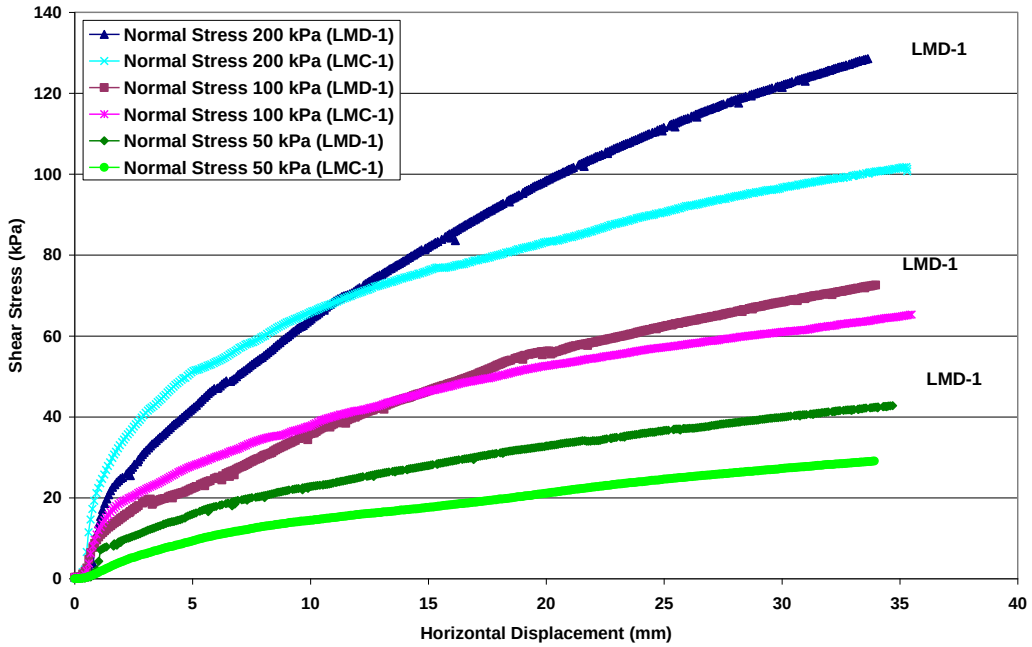

Graph VI- 6: Comparison of shear strength for the two shredded samples (LMC-1) and (LMD-1).

Individual comparison of different parameters for both samples LMC and LMD: Once the comparison of the two samples is presented, both the samples LMC and LMD are analysed hereafter for different parameters individually.

Influence of shredded particles: For the second series of tests the samples LMC-0 and LMD-0 were shredded in the laboratory to the particle size < 50 mm and tested while normally consolidated. The change in the shear strength parameters for the two samples (LMC-0 and LMC-1) and (LMD-0 and LMD-1) due to the change in particle size through shredding is observed in Graphs VI-7 and Graph VI-8. It can be noted that the cohesion of the samples increase with the decrease in the particle size with the consequential reduction in the friction angle.

It can be noted that the shredding mainly affects the immediate compression of the samples Graph VI-7 and that the initial samples have the shear strength of primarily frictional nature which is due to the nature of old waste however this effect is reduced for the shredded samples which have a more pronounced cohesion (Table VI-15). The other reason is the increased density of the shredded samples which influenced positively for the cohesion of the samples but the influence of shredding is not significant.

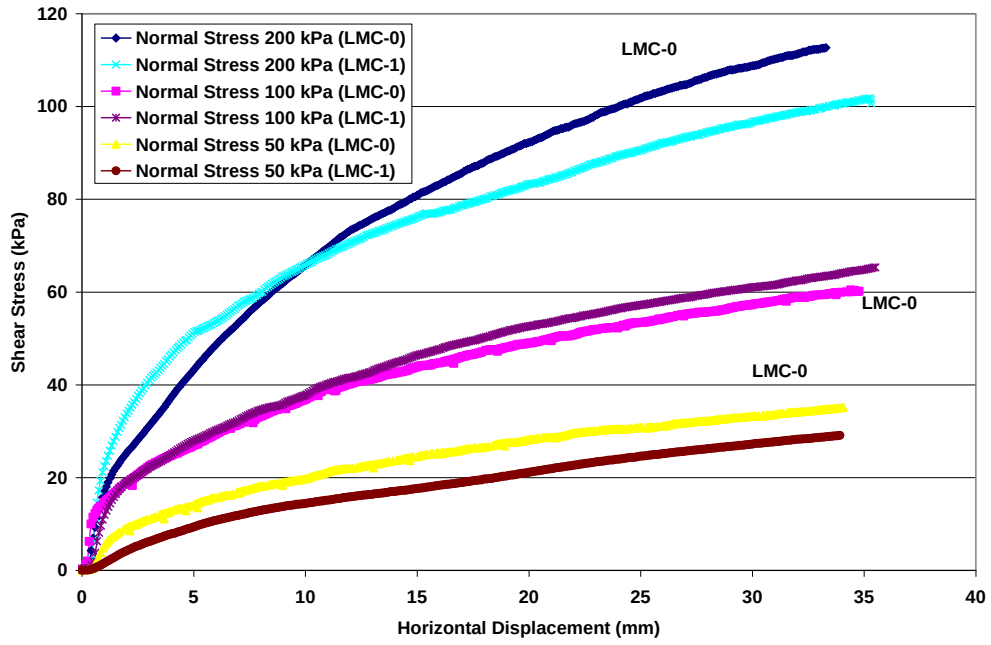

Graph VI- 7: Comparison of shear behaviour of excavated samples (LMC-0) with the shredded samples (LMC-1).

Table VI- 15: Comparison of shear strength parameters of excavated samples (LMC-0) with the shredded samples (LMC-1).

Sample	LMC-0			LMC-1 (Shredded)		
Depth (m)	1-1.5					
Age of waste(yr)	13					
σ'_{OC} (kPa)	50	100	200	50	100	200
σ' (kPa)	50	100	200	50	100	200
ρ_{di} (Mg/m^3)	0.49	0.54	0.67	0.53	0.65	0.69
ρ_{df} (Mg/m^3)	0.52	0.56	0.68	0.57	0.66	0.71
w (%)	92.31	112.77	85.19	78.02	-	-
%Deformation	11%			11%		
c (kPa)	8.1			10.4		
φ	27.5			24.6		

These results were confirmed with the same series of tests performed on the other excavated sample LMD (from the slope of the embankment) and are presented below. First of all the samples at natural moisture content as retrieved from the landfill were tested in shear box and then the samples were shredded and tested in the shear box.

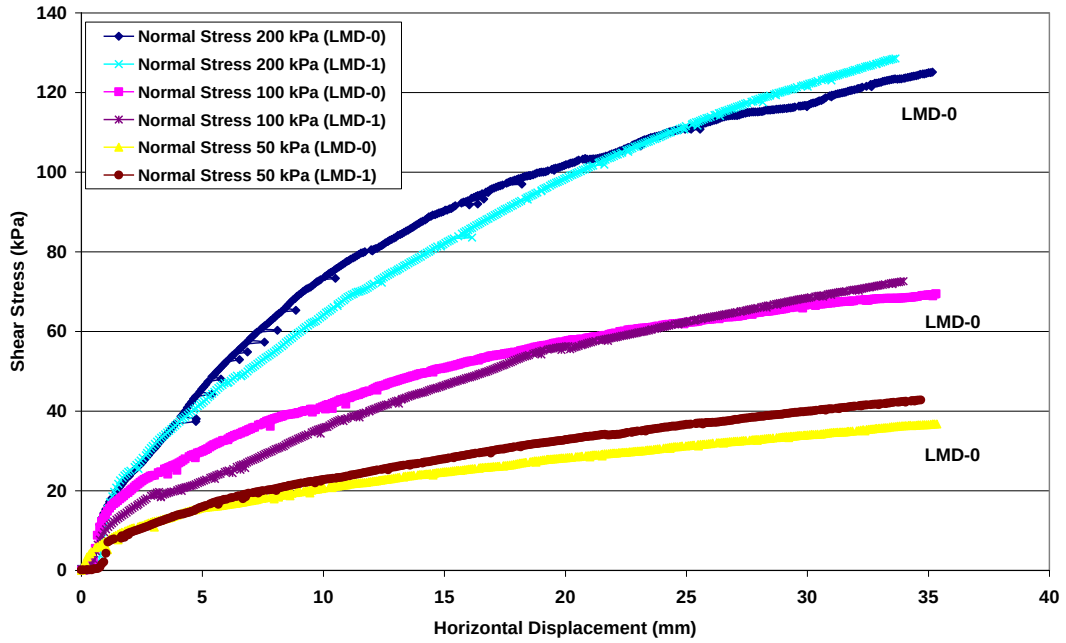

Graph VI- 8: Comparison of shear behaviour of excavated samples (LMD-0) with the shredded samples (LMD-1).

Table VI- 16: Comparison of shear strength parameters of excavated samples (LMD-0) with shredded samples (LMD-1).

Sample	LMD-0			LMD-1 (Shredded)		
Depth (m)	1-1.5					
Age of waste(yr)	17					
σ'_{OC} (kPa)	50	100	200	50	100	200
σ' (kPa)	50	100	200	50	100	200
ρ_{di} (Mg/m^3)	0.46	0.56	0.68	0.52	0.57	0.69
ρ_{df} (Mg/m^3)	0.47	0.58	0.68	0.54	0.60	0.69
w (%)	117.39	92.31	66.67	81.82	79.21	79.21
%Deformation	11%			11%		
c (kPa)	8.5			13.8		
φ	29.9			29.7		

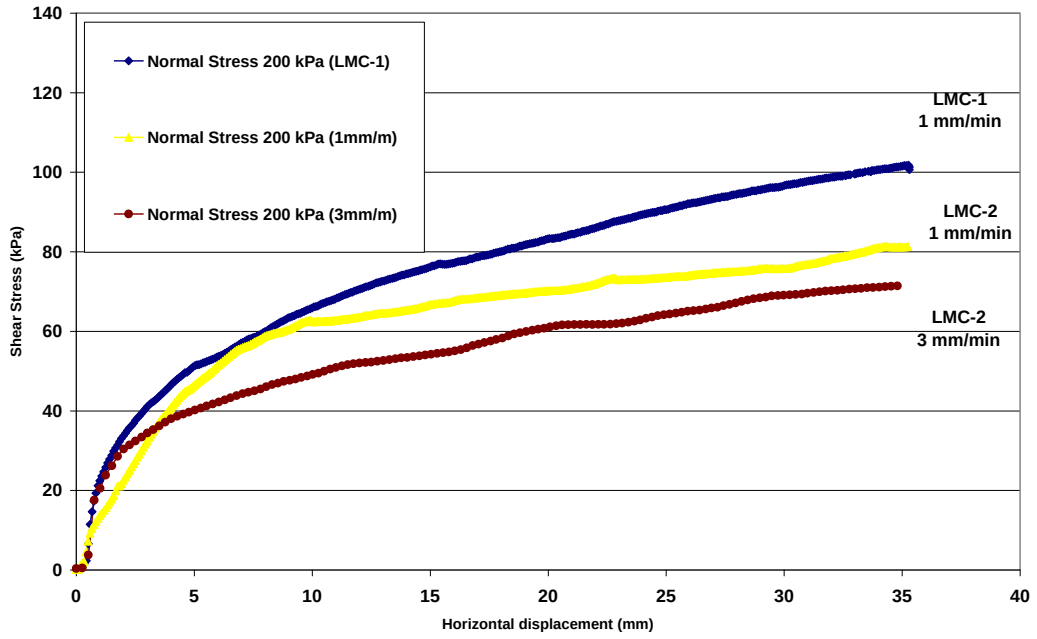

Graph VI- 9: Comparison of shear behaviour of sample "LMC-2" (shredded saturated and over consolidated at 200 kPa) sheared at 1mm/min and the sample sheared at 3mm/min with the sample LMC-1 which was normally consolidated.

Table VI- 17: Comparison of shear strength parameters for shredded saturated sample (LMC-2) initially over consolidated at 200 kPa and sheared at two displacement rates (1 mm/min and 3 mm/min).

Sample	LMC-2 (1 mm/min)			LMC-2 (3 mm/min)		
Depth (m)	1-1.5					
Age of waste(yr)	13					
σ'_{OC} (kPa)	200	200	200	200	200	200
σ' (kPa)	50	100	200	50	100	200
ρ_{di} (Mg/m^3)	0.78	0.77	0.77	0.65	0.65	0.64
ρ_{df} (Mg/m^3)	0.77	0.77	0.80	0.63	0.65	0.66
w (%)	92	-	-	119.3	-	-
%Deformation	11%			11%		
c (kPa)	46.7			49.5		
φ	10.1			6.3		

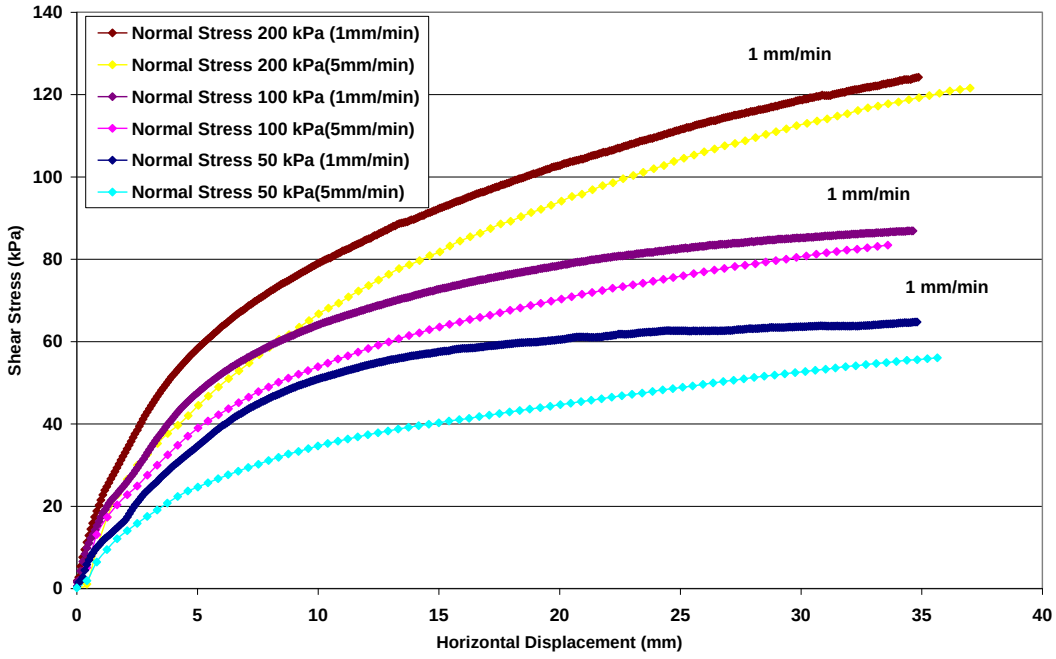

Graph VI- 10: Comparison of shear behaviour of the waste sample "LMD-2" at shear rate 1 mm/min and shear rate of 5 mm/min.

Influence of displacement rate: The samples were saturated and consolidated at 200 kPa before testing in the direct shear box. The comparison between three samples LMC-1, LMC-2 sheared at 1

mm/min and LMC-3 sheared at 3 mm/min is presented in Graph VI-8. It can be noted in Table VI-17 the increased shear rate reduced the frictional effect of the particles which was already reduced due to saturation. This reduction in shear strength values could be linked to a probable generation of over pressures in the samples at high displacement rate.

It is worth noticing from all the shear strength parameters of sample LMC that the cohesion of the samples increased constantly from lowest for the initial samples to highest value for the samples which were shredded, saturated and sheared at the displacement rate of 3 mm/min. On the other hand the sample LMD followed the same pattern of shear strength parameters except for the displacement rate where the cohesion decreased for 3 mm/min as presented in Table VI-18.

Table VI- 18: Comparison of shear strength parameters of shredded saturated sample "LMD-2" initially over consolidated sheared at 1 mm/min with the sample sheared at 5 mm/min.

Sample	LMD-2 (1 mm/min)			LMD-2 (5 mm/min)		
Depth (m)	1-1.5					
Age of waste(yr)	17					
σ'_{OC} (kPa)	200	200	200	200	200	200
σ' (kPa)	50	100	200	50	100	200
ρ_{di} (Mg/m^3)	0.66	0.67	0.67	0.67	0.66	0.69
ρ_{df} (Mg/m^3)	0.64	0.66	0.68	0.66	0.66	0.71
w (%)	84.5	-	-	83.15	-	-
%Deformation	11%			11%		
c (kPa)	45.38			37.625		
φ	22.56			22.10		

Even though these shear test results have largely contributed to the already available data, however research is needed to be carried out with the approach of studying the relation of three phase (Solid, liquid and gas) degradation with the effective stresses.

VI-3.3 Landfill Site ‘N’

Established in a small valley, concerned section of French landfill site (N) represents a maximum surface of 9.3 ha (93 000 m ^{2}). This section spreads out in its central part of an inferior coast ranging between + 131 and + 133 m NGL to a coastal projection of + 184 m for a maximum height of 50 m (Figure VI-39). Starting in 2001, the exploitation of section of the landfill was programmed before this study roughly up to 2010, for a flow of waste stored near 270 000 tons / year (except in 2007: 325 000 tons). Composed of household refuse (~60 %), non-hazardous industrial waste and residues of cleaning, waste is placed and compressed by means of a compactor Caterpillar 836 sheep foot roller (45 tons) in the shape of fine layers consolidated by intermediate cover layers of ten meters approximately. The landfill site is covered by a geo-synthetic membrane and a layer of drainage material to evacuate the leachate, which is protected by a geo-grid against altering the drainage layer by waste. Household waste is discharged without any treatment on site. The biogas production due to anaerobic processes is responsible for the odours, which are recovered by networks of pipes and sent up to flares to be burned.

Site maintenance: The landfill site terrain is surrounded by a circle of pipes for spraying chemicals to minimize odours. This site will produce biogas for thirty years, time necessary for the decomposition of household waste. During this period, drains, wells, sumps, flares, ponds of water, leachate and other management techniques required for the recovery and treatment of leachate and gas will be checked and maintained permanently.

Water treatment: Regarding water treatment, there exist two systems at the landfill site: one for rainwater before they reach the waste, other for the leachate, resulting from the fermentation of waste.

- The rainwater is collected in a basin and after checks for contaminations is released.
- The leachate is pumped to another pond, where they are oxidized and treated with products that destroy odours and evacuated to a treatment plant.

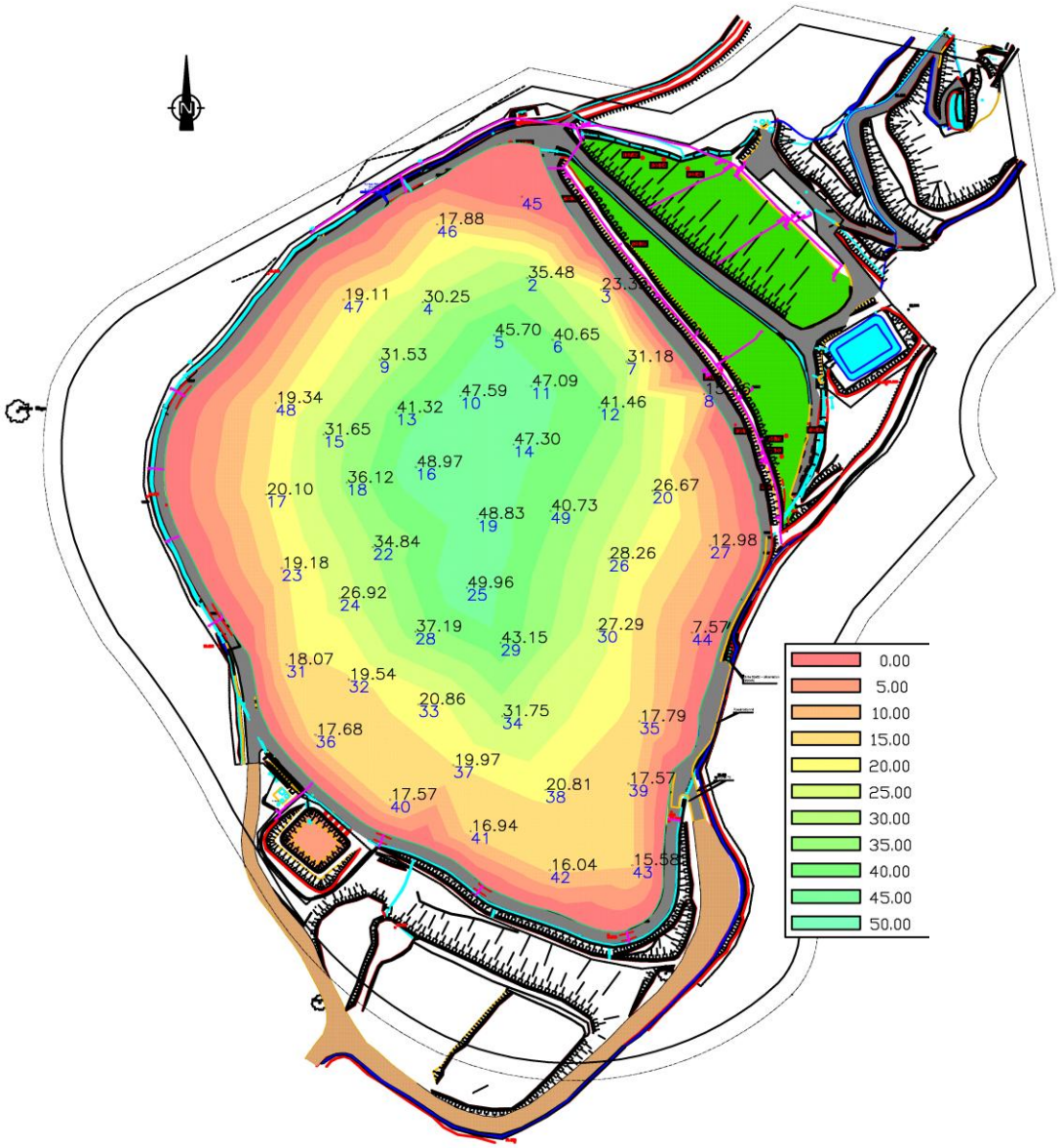

Figure VI- 39: Landfill site profile (waste height with respect to NGL).

VI-3.3.1 Context of the Study

The installation of domestic waste has become increasingly a technical task in which there is a complex interaction of natural materials (clay, sand), artificial materials (geosynthetic membranes) and waste whose behaviour is variable at the same time with respect to time and space. These works require a rigorous analysis, in particular with regard to the control of settlement which pose environmental (deformation of the covers under the effect of the relative settlements, waste structures deformation, leakage of biogas and leachate) and economic problems at the same time (estimation of the storage capacity, optimization of the waste installation process).

The objectives of the study have two dimension, firstly any future installation at site and secondly the possibility of modification of waste stabilisation after its placement at site. It is worth mentioning here that since the commencement of placement works, no treatment of waste prior to installation was carried out as a principle procedure except the compaction. Moreover the waste was neither sorted for recyclables not shredded.

Vertical expansion: Sine the landfill site is one of the largest available approved sites in the region; it takes the waste from all four corners of the region. One of the major concerns of the site manager is to envisage further installation of waste at already existing waste cells. For this purpose future predictions of settlement of the existing waste column as well as the settlement predictions with additional waste columns needed to be carried out to confirm the waste behaviour for long period of time (approximately 30 years). Further the stability issue is important for the waste cells at the borders of landfill which include the slope edges of the cells. In the present study, the settlement analysis is not considered however a stability analysis is carried out for the site, detailed in section VI-4, incorporating the results obtained from the shear tests.

Figure VI- 40: Drilling operation at site.

VI-3.3.2 Sample Retrieval through Drilling

For the purpose of carrying out the laboratory tests, waste from different locations of the landfill site was drilled and brought to the laboratory by the maintenance team working at site. The sampling campaign was performed during spring 2008. Various drills were carried out at different locations and depths of the waste to collect a number of samples differing in age and composition. The drilling was done using a drill core which does not damage, during the process, the elements of waste by grinding them. Column drilling was divided into eight sections (two for each depth range) with moisture content and density determination performed for each section at every 5 or 6 m. Moreover all the waste was weighed to have a density profile for that section of the waste. Moreover sorting of waste was carried out with three meshes of size > 50 mm, 20-50 mm and <20 mm as well as sorting of the following components;

- Kitchen waste
- Garden trimmings, wood
- Paper, carton and composites
- Textiles and sanitary textiles
- Plastics, metals, glass and inert

Figure VI- 41: Location of drilled samples N3 and N6.

Moisture content for each component type was determined at site while moisture content of fines was determined in the laboratory. For each section, some forty kilos of waste was brought to the laboratory for testing purpose. In Figure VI-45 the location of drill holes is marked as 3 and 6 for Sample N3 and N6 respectively. Waste samples were collected at different locations out of which only two waste column of different depths were used for shear strength characteristic determination, while others were used for permeability profile determination and hydraulic conductivity tests performed in LTHE laboratory by other research colleagues. For the ease of denomination, these two drills will be referred to as N3 and N6.

Figure VI- 42: Waste extraction at landfill site 'N'.

VI-3.3.3 Determination of In-situ Unit Weight

Following the drilling process an average dry density was calculated at site for various sections of the drills of different thickness. An average of 1.15 Mg/m^3 was obtained (Table VI-19). For the purpose of simulations of various sections of the waste column, to be as representative as possible for the site conditions, the average density for the corresponding section was used.

Table VI- 19: Densities of the samples of waste determined from drillings according to the depth considered.

Drilling	N3	N6	Average
0 - 7 m	0.84	-	0.84
7 - 14 m	1.06	1.25	1.15
14 - 23 m	1.24	1.26	1.25
23 - 33 m	1.14	1.19	1.65
Average	1.07	1.23	1.15

Figure VI- 43: Collection of waste from the drilling process for the in-situ density calculation.

VI-3.3.4 Drilled Samples N3

From the figures of the drilling operation, it can be noticed that the waste is an old waste and further the grain size distribution is inclined towards fine particles. The percentage composition on the basis of dry weight is presented in Figure VI-44.

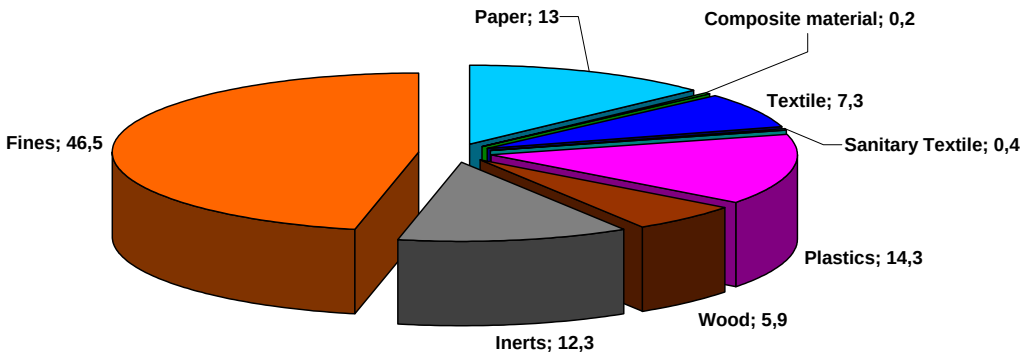

Figure VI- 44: Composition of Waste of drilled samples N3.

The calculated average moisture content of the waste was 25% (Table VI-20), while the range of the age of the waste was determined as from 2001 to 2007, the age of the waste in drill N3 with respect to

depth is shown in Figure VI-45. The overall density for the waste column of 33 m deep was calculated at site to be 1.02 Mg/m^3.

Table VI- 20: In-situ values of physical characteristics for drilled samples N3.

Drill Sample	N3-1	N3-2	Average
Depth	0-7 m	23-33 m	0-33 m
Density	0.84	1.24	1.04
Humidity	27%	23%	25%
Age of Waste	1-2	7	1-7

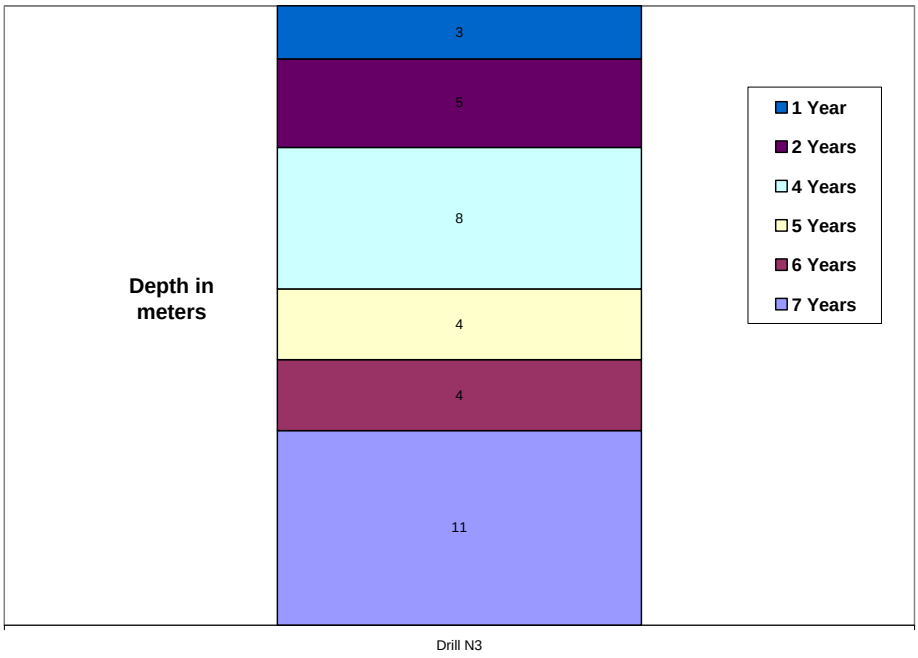

Figure VI- 45: Age of waste as a function of depth for drilled samples N3.

VI-3.3.5 Drilled Samples N6

For the samples received from drill N6, composition of the waste was similar to that of drill N3 with fines making almost fifty percent of the whole waste composition. The moisture content was calculated to be 27.5% with a humid density of 1.2 Mg/m^3, while the age of the waste was determined to be 2003 for the given depth. The data regarding the sample in-situ moisture content and density with reference to depth of the waste column is presented in Table VI-21, the age of the waste as a function of depth is presented in Figure VI-46 whereas the percentage composition of drill N6 is presented in Figure VI-47.

Table VI- 21: In-situ values of physical characteristics for Drill Sample N6.

Drill Sample	N6-1	N6-2	Average
Depth	12.3-17 m	22-32.7 m	12.3-32.7 m
Density	1.26	1.19	1.22
Humidity	28%	27%	27.5%
Age of Waste	5	5	5

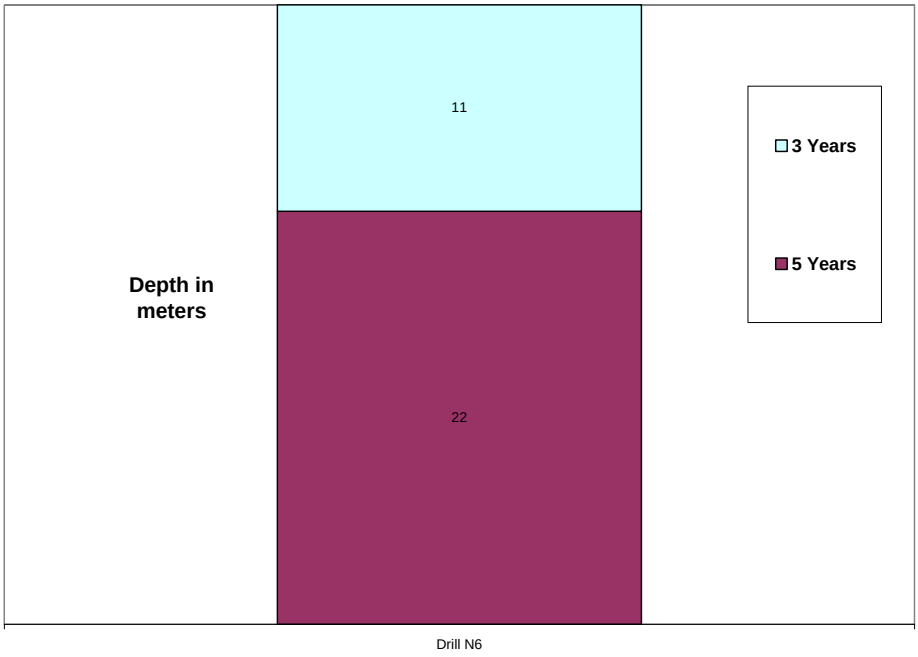

Figure VI- 46: Age of waste as function of depth for drilled samples N6.

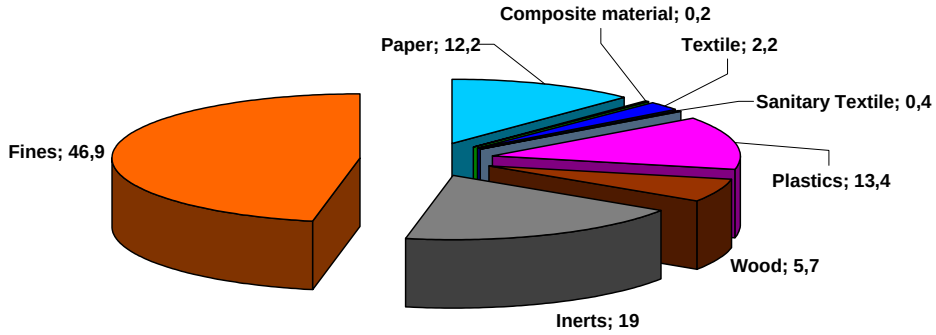

Figure VI- 47: Percentage composition by dry weight of Drill Sample N6.

VI-3.3.6 Shear Test Results and Discussion

In Table VI-22 tests descriptions are summarised with the sample notations and the following series of shear tests were performed:

- Initially the unprocessed waste was tested at different normal stresses.
- Second series of tests was carried out on the waste of fine composition i.e. passing 20 mm. For this purpose the waste of initial composition (N3-1 + N3-2 and samples of two different depths of drill N6) was sieved manually to separate the particles bigger than 20 mm and the fine composition of both the samples was mixed.
- Third series of tests was performed on the waste composed of fines particles with additional moisture content.
- The same fines composition with additional moisture content was tested at slow displacement rate to complete the test series.

Table VI- 22: Description of samples tested for the shear strength for waste 'N'.

Sample	Description
N3-1	Sample retrieved from 0-7 m, tested at natural moisture content.
N3-2	Sample retrieved from 23-33 m, tested at natural moisture content.
N3-3	Sample prepared through mixing the composition of N3-1 and N3-2 passing sieve < 20 mm with additional moisture content.
N3-4	Sample N3-3 with additional moisture content (higher than N3-3)
N6-1	Sample retrieved from Drill N6 (depth 22-32.7 m), tested at natural moisture content.
N6-2	Sample prepared through mixing the samples from two different depths of N6 passing sieve < 20 mm.
N6-3	Sample N6-2 with higher moisture content.

Initially the direct shear tests were carried out on waste samples as collected on site. For the determination of τ_{max} the shear stress at 11% deformation (Table VI-23) was considered in all cases but no peak of shear stress is observed at this level. Graph VI-12 presents the set of curves for the three types of samples and the three levels of stresses.

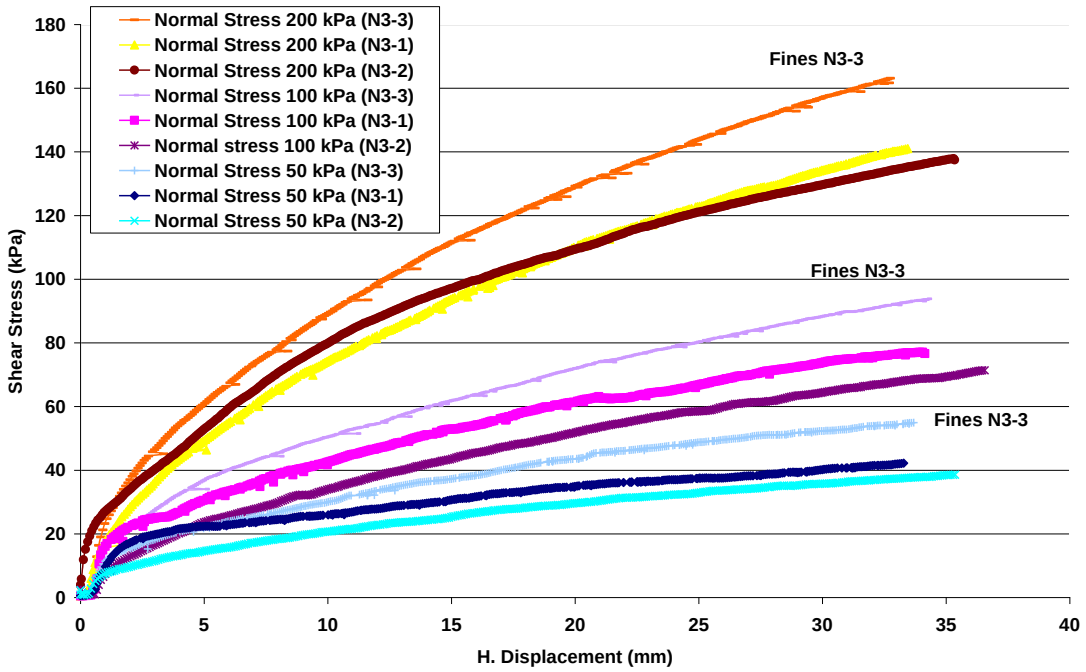

Graph VI- 11: Comparison of shear strength of samples at initial grain size and composition (N3-1 and N3-2) with the sample after sieving < 20 mm (N3-3) normally consolidated at a displacement rate of 1 mm/min.

Table VI- 23: Details of the shear strength parameters of the tests for initial samples N3-1, sample N3-2 and N3-3.

Sample	N3-1			N3-2			N3-3		
Depth (m)	0-7			23-33			0-33		
Age of waste (yr)	1-2			7			1-7		
% < 20mm	46 .45			45 .05			100		
σ'_{pc} (kPa)	50	100	200	50	100	200	65	120	200
σ' (kPa)	50	100	200	50	100	200	65	120	200
ρ_{di} (Mg/m^3)	0.65	0.75	0.75	0.68	0.71	0.81	-	-	-
ρ_{df} (Mg/m^3)	0.68	0.78	0.82	0.69	0.77	0.88	0.75	0.82	0.93
w (%)	25.2	25.6	25.1	21.9	22.1	22.1	36.7	36.2	36.0
%deformation	11%			11%			11%		
c (kPa)	10.0			3.9			0		
φ	33.2			33.0			38.9		

Influence of Sieving: Samples (N3-1 and N3-2) were then passed through the sieve < 20 mm to separate the fines particles and additional water was added to this fraction of fines and tested for the shear strength (N3-3) of samples comprising only of fine particles. The same series of tests were performed for the sieved composition of drill samples 'N6'. In general it is expected that the removal of the fibrous components reduces the frictional component of the shear strength of the waste body but these results suggest otherwise. The cohesion for the tests samples, comprising of fines only, reduced to zero but on the other hand the friction increased. It should be noted on the same time that these test samples were tested with additional moisture which is supposed to be another negatively influencing parameters in terms of the shear strength of the material.

Including the fibrous particles or testing the composition comprising only of fines does not change the shear strength parameters significantly which is due to the fact that fibrous material tend to orient in the horizontal direction. The results derived for sample N6-1 show the increase in friction angle with increasing consolidation stress (Table VI-24). This behaviour could be justified by the increasing test densities (ρ_{df}) with normal stresses for normally consolidated samples.

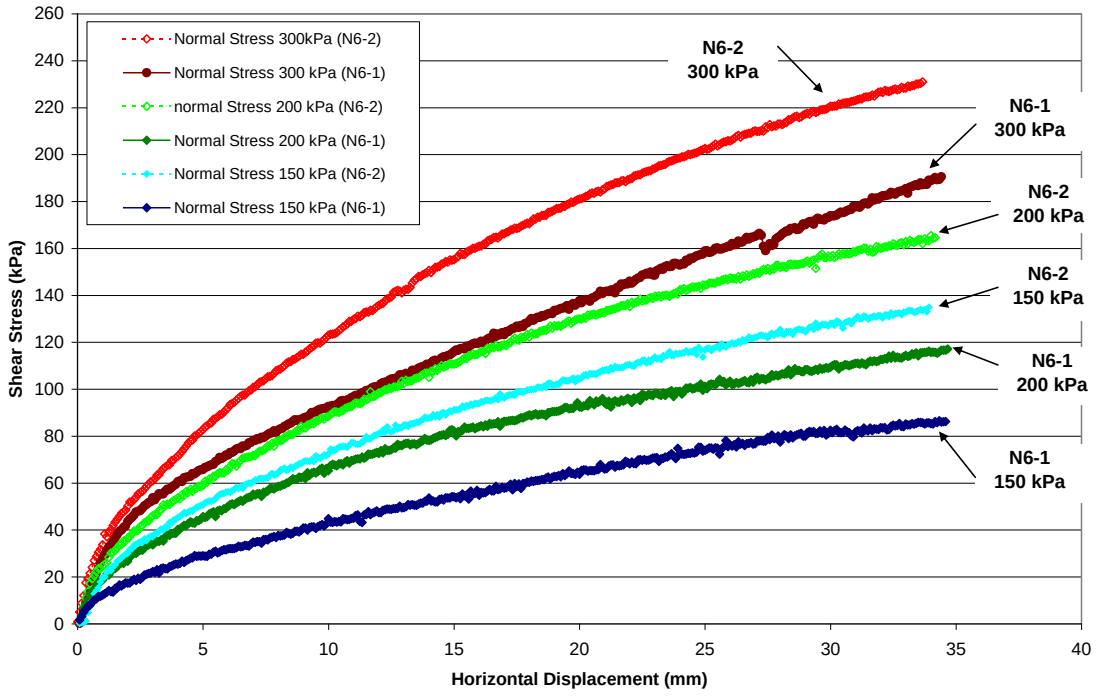

Graph VI- 12: Comparison graph for stress displacement curve of sample N6-1 with initial composition, and the sample N6-2 (fines passing < 20 mm).

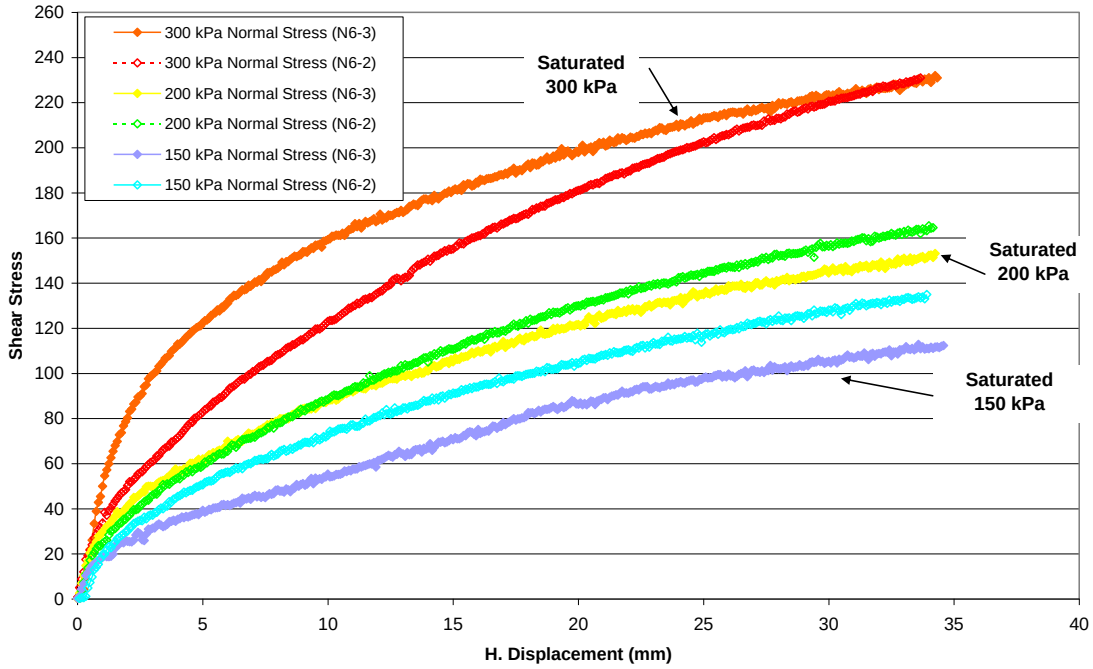

Graph VI- 13: Comparison of sample comprising of fines (< 20 mm) at natural moisture content N6-2 with the samples comprising of fines at saturated moisture content N6-3.

Table VI- 24: Shear strength parameters for the initial samples at natural moisture content (N6-1), the samples comprising of fines (< 20 mm) at natural moisture content N6-2 and the samples at higher moisture content (N6-3) at the same displacement rate 1 mm/min.

Sample	N6-1			N6-2			N6-3		
Depth (m)	22-32.7			12.3-32.7			12.3-32.7		
Age of waste (yr)	5			5			5		
% < 20 mm	47.4			100			100		
σ'_{pc} (kPa)	150	200	300	150	200	300	150	200	300
σ' (kPa)	150	200	300	150	200	300	150	200	300
ρ_{di} (Mg/m^3)	0.63	0.68	0.71	0.79	0.85	0.97	-	-	-
ρ_{df} (Mg/m^3)	0.69	0.75	0.80	0.88	0.96	0.99	0.73	0.76	0.83
w (%)	35.13	-	-	30.43	-	-	52.7	52.7	44.0
%Deformation	11%			11%			11%		
c (kPa)	4.8			36.0			0		
φ	31.4			32.3			37.0		

Influence of displacement rate: The fines composition (N3-3) was further tested with more moisture added to the samples at two different displacement rates (N3-4). The samples were normally consolidated and tested at usual speed of 1 mm/min and at slower speed of 0.5 mm/min. The shear strength parameters do not vary significantly however it is noted that the slower displacement rate slightly increased the density of the samples during the test in comparison with the samples tested at 1 mm/min Table VI-25).

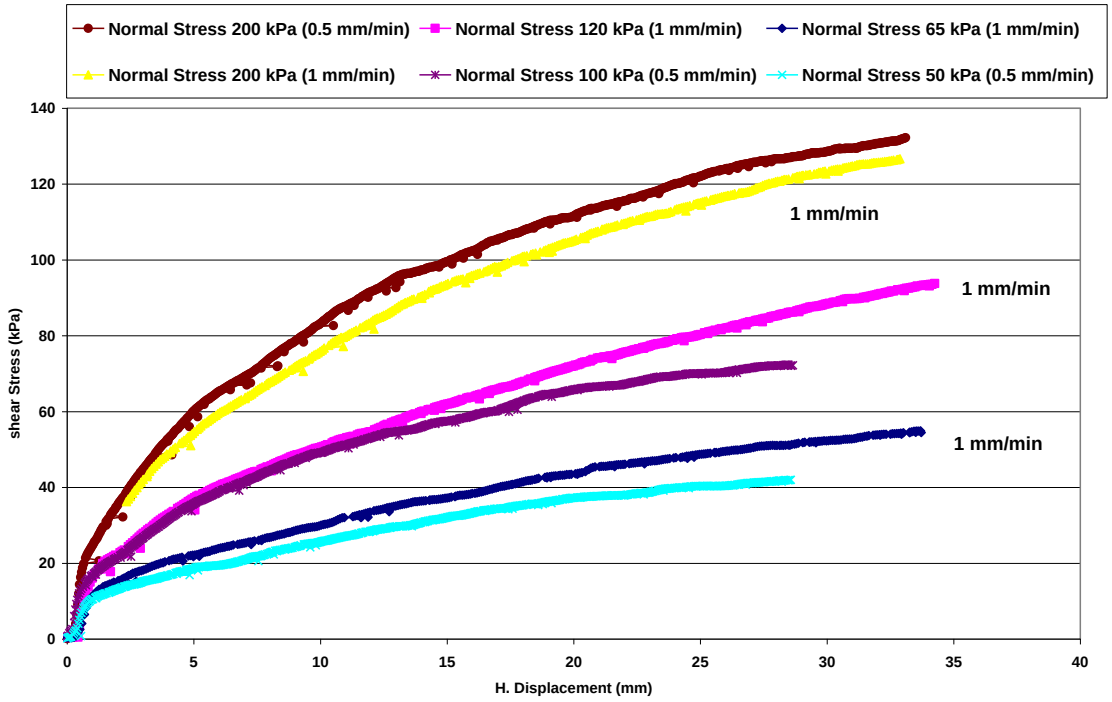

Graph VI- 14: Comparison of stress-displacement trends for sample N3-4 for two different displacement rates (1 mm/min and 0.5 mm/min)

Between the two displacement rates of 1 mm/min and 0.5 mm/min, no significant difference is observed due to the low value of displacement rates.

Table VI- 25: Details of the parameters of the shear tests for samples with enhanced moisture content at 1 mm/min and at 0.5 mm/min displacement rate.

Sample	N3-4 (1 mm/min)			N3-4 (0.5 mm/min)		
Depth (m)	0-33			0-33		
Age of waste(yr)	1-7			1-7		
% < 20mm	100			100		
σ'_{pc} (kPa)	50	100	200	50	100	200
σ' (kPa)	50	100	200	50	100	200
ρ_{di} (Mg/m^3)	0.77	0.81	0.84	0.75	0.79	0.87
ρ_{df} (Mg/m^3)	0.78	0.82	0.86	0.85	0.84	0.90
w (%)	69.3	66.4	66.8	66.7	69.2	65.0
%deformation	11%			11%		
c (kPa)	16.3			14.7		
φ	28.9			29.4		

Analysing all the tests series N3 and N6 it is interesting to note that even though the parameter modification were the same as for the other two landfill sites ‘B’ and ‘LM’ but the shear strength results do not follow the same behaviour. For the two sites tested ‘B’ and ‘LM’ cohesion increased under the effect of shredding but for landfill ‘N’ sieving the samples for the purpose of testing only the fine composition reduced the cohesion of the samples. Moreover addition of moisture increased the cohesion which is probably due to the reason that the initial moisture content was probably lower than the field capacity of the waste samples and it played a positive role in improving the shear strength of the samples however the friction was subsequently reduced.

VI-3.4 Synthesis of Shear Strength Test Results

The shear tests results from the present study are plotted with other values available in literature in comparison with the proposed range of shear strength parameters by Singh and Murphy (1990).

It can be noted that the shear strength parameters determined in the present study are mainly in the range of high frictional component and lower cohesion. This is mainly due to the fact that the samples tested contained considerable percentage of the fibrous components. On the same time other series of the tests performed included saturated samples which reduced the cohesion of the samples. The increased displacement rate has the similar effect on the shear strength parameters.

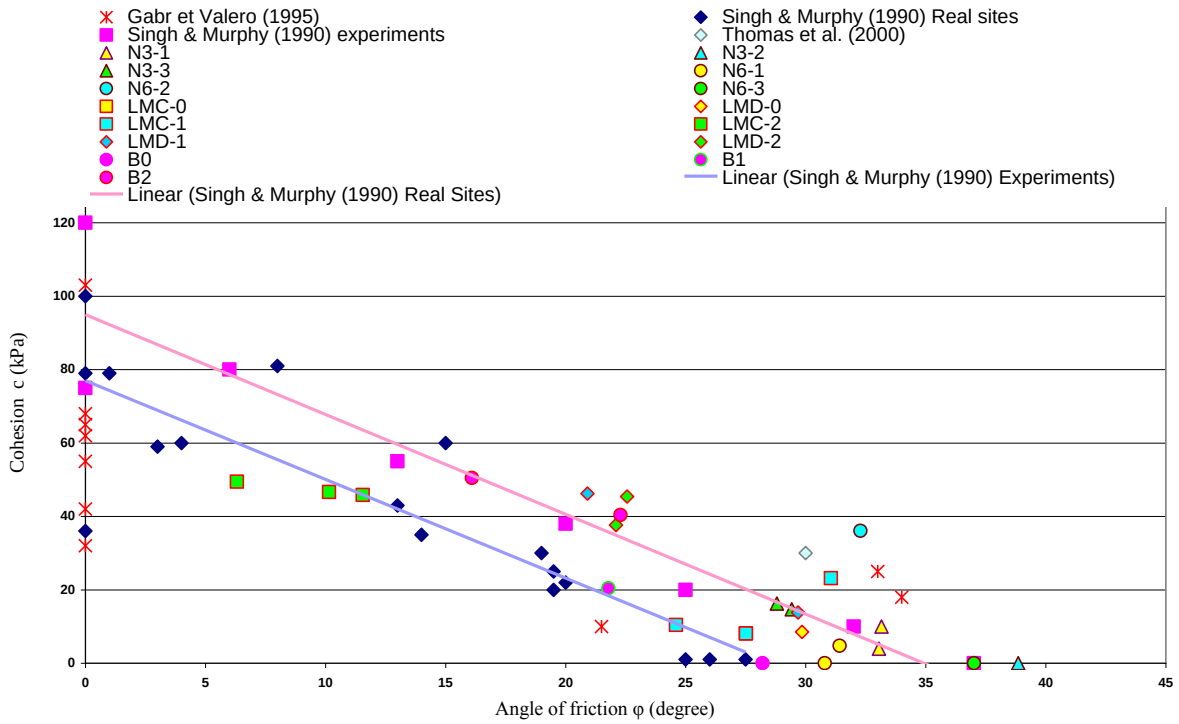

Figure VI- 48: Effective shear strength parameters of test data from the present study (adapted from Singh and Murphy, 1990).

These data presented in Figure VI-48 are subdivided into other figures according to the parametric variation adopted for the present study and are detailed underneath.

Effect of size reduction: Comparison of samples tested at natural composition and the samples reduced in size to obtain the composition < 50 mm is presented in Graph VI-15. It was expected that the smaller fibrous elements would result in the decrease of tensile friction and thus an increase in cohesion however these results are not as flagrant as it was assumed to be an obvious result.

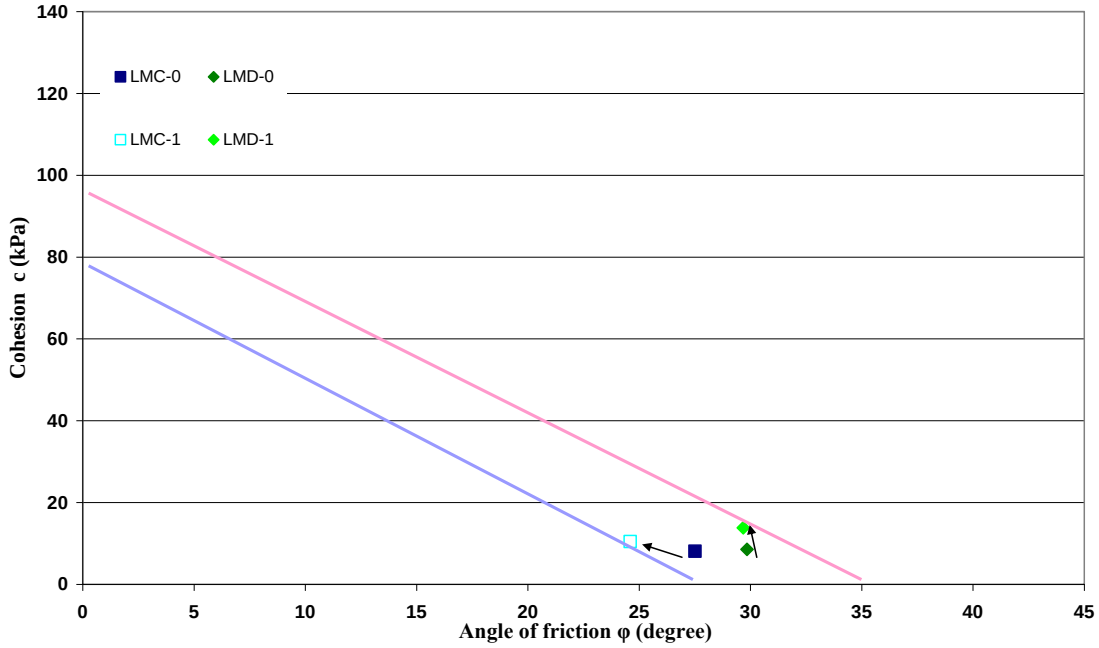

Graph VI- 15: Effect of size reduction on all the shear strength values determined in the present study.

Effect of saturation: For the comparison of samples at natural moisture content and saturated state, one thing needs to be kept in mind while observing these results and it is the fact that most of the samples tested at saturated conditions had undergone other parametric variation as well. Such as the difference in the sample N3-1 and N3-4 is that not only N3-4 is saturated but it is the sample prepared by mixing two samples of a composition < 20 mm the same is true for the samples LMC-2 and LMD-2 which are the samples prepared by size reduction to the composition < 50 mm. An increase in cohesion is observed for the saturated samples with consequent decrease in friction angle however one of the values (sample N6-1 and N6-3) show different behaviour.

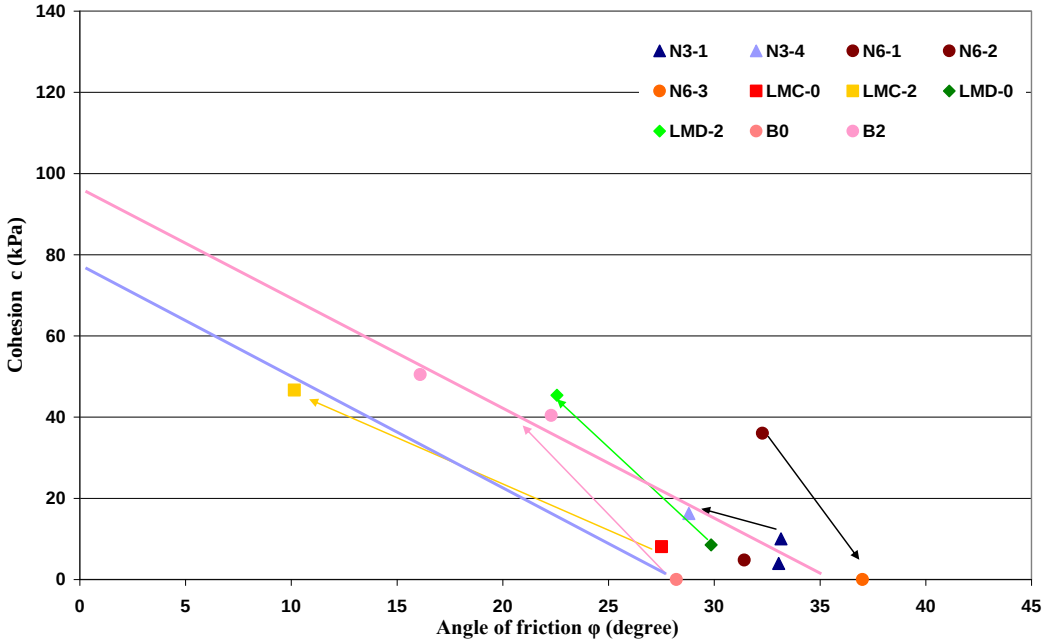

Graph VI- 16: Effect of saturation on shear strength values of all the samples of the present study.

Effect of displacement rate: All the saturated samples were tested at two different displacement rate considering 1mm/min as a consistent protocol displacement rate other displacement rates of 0.5mm/min, 3 mm/min and 5 mm/min were adopted to observe their influence. It can be noted in Graph VI-17 that the samples tested at a faster displacement rate have a reduced friction angle and increased cohesion.

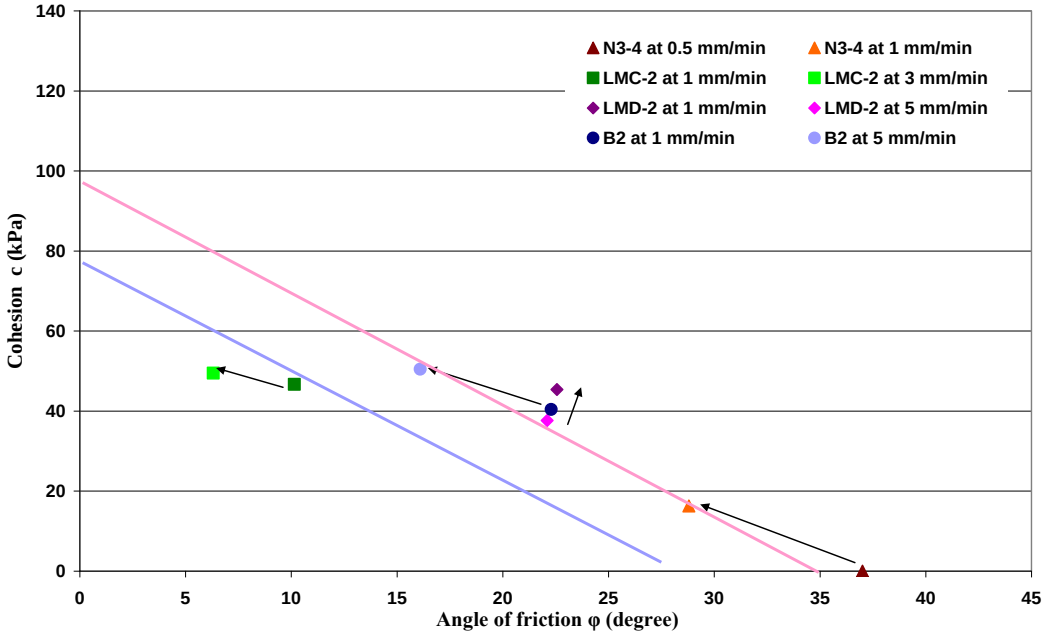

Graph VI- 17: Effect of displacement rate (Δl/Δt) on the shear strength values for all the samples of the present study.

VI-3.5 Influence of Anisotropic Behaviour on Slope Stability

Due to anisotropy of MSW, shear strength is assumed minimum for the horizontal slip surface. The values of shear strength obtained in the present study are used here to analyse the slope stability according to the Bishop's Simplified Stability Method. As shown in Figure VI-49 for the given height of 20 m of waste column and γ = 12 kN/m^3 the stability is analysed with limiting factor of safety at 1 and cohesion as a ratio of c'/γH is plotted against tanφ'.

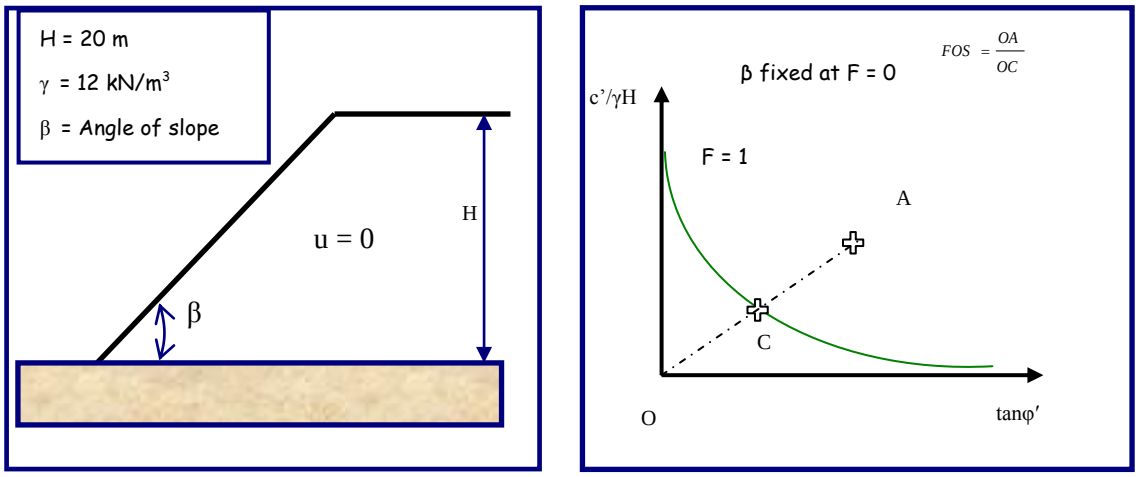

Figure VI- 49: Stability analysis for horizontal slip surface using the limit safety factor.

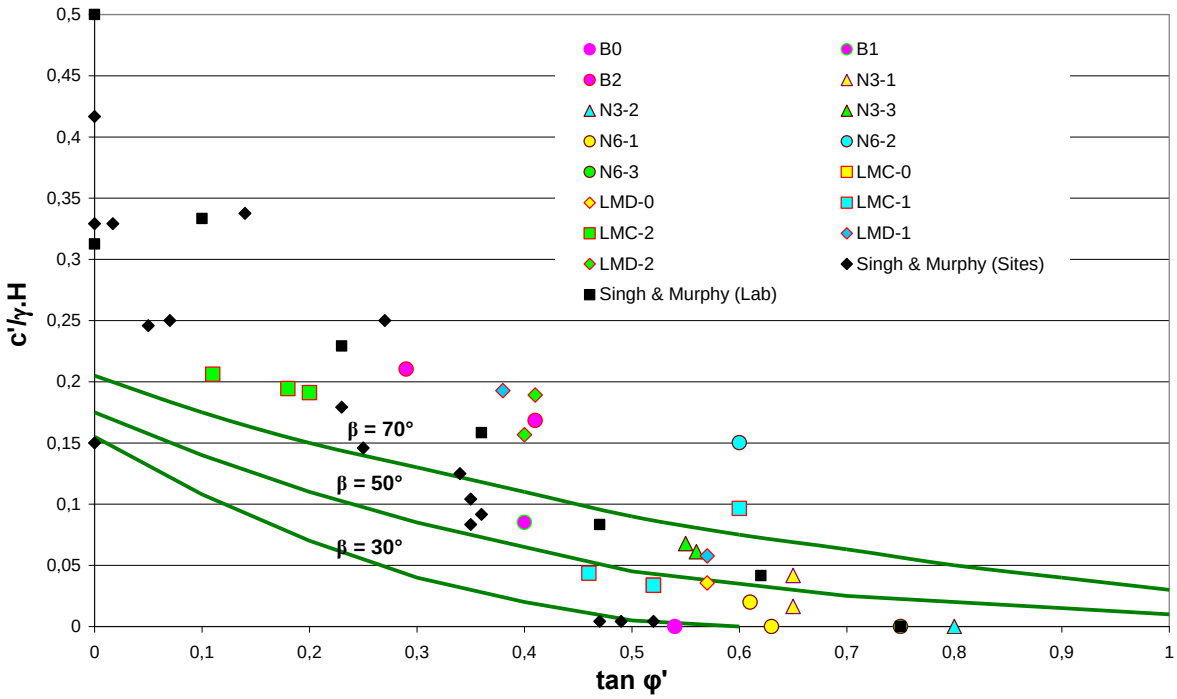

Graph VI- 18: Shear strength values of the present study with data of other researchers on the Bishop's simplified number chart.

These limiting factors of safety for three different slope angles at 30°, 50° and 70° are plotted in Graph VI-18 along with the data. It can be noted that almost all the shear strength values determined in the present study are stable for a slope of β = 30° with some of the values at limit and overall high shear strength values observed for the most of the data showing stable values for an angle of slope at 50° and even 70°. However future research on the shear strength of municipal solid waste should include more laboratory testing and back analyses of landfill failures to further refine the MSW shear strength parameters proposed herein.

VI-4 SPECIFIC STABILITY DESIGN FOR LANDFILL SITE 'N'

From the present study on shear strength parameters, it was found out that, initially the geotechnical characteristics of waste are improved in a significant way by the contribution of the fibres which play a role of reinforcement of structure in a manner similar to that of the reinforced soils. Thus in case of high initial deformation, a high cohesion of fibres sometimes [up to 140 kPa according to Duchêne et al., (1998)] is mobilized which has the advantage of stopping the phenomenon (stabilizing properties). Three sections of the landfill were initially considered as shown in Figure VI-49 but to simplify the task only section 3 was considered in stability calculations for both drilled samples N3 and N6.

VI-4.1 Slope stability analysis – application to the vertical expansion of a landfill site

The slope stability analysis for the landfills is performed to verify that the idealized configuration has an adequate factor of safety against failure under static loading conditions. Solid waste placed within a landfill will have a gravitational weight component that may cause an internal stability problem. A rotational stability failure within the waste itself is a possibility depending on the strength, height, surface grading, and level of leachate within the waste body.

Sine the landfill site is one of the largest available approved sites in the region; it takes the waste from all four corners of the region. One of the major concerns of the site manager is to envisage further installation of waste at already existing waste cells. For this purpose future predictions of stability of the existing waste column as well as the stability analyses with additional waste columns needed to be carried out to confirm the waste behaviour for any possible stability concerns. Further the stability issue is important for the waste cells at the borders of landfill which include the slope edges of the cells.

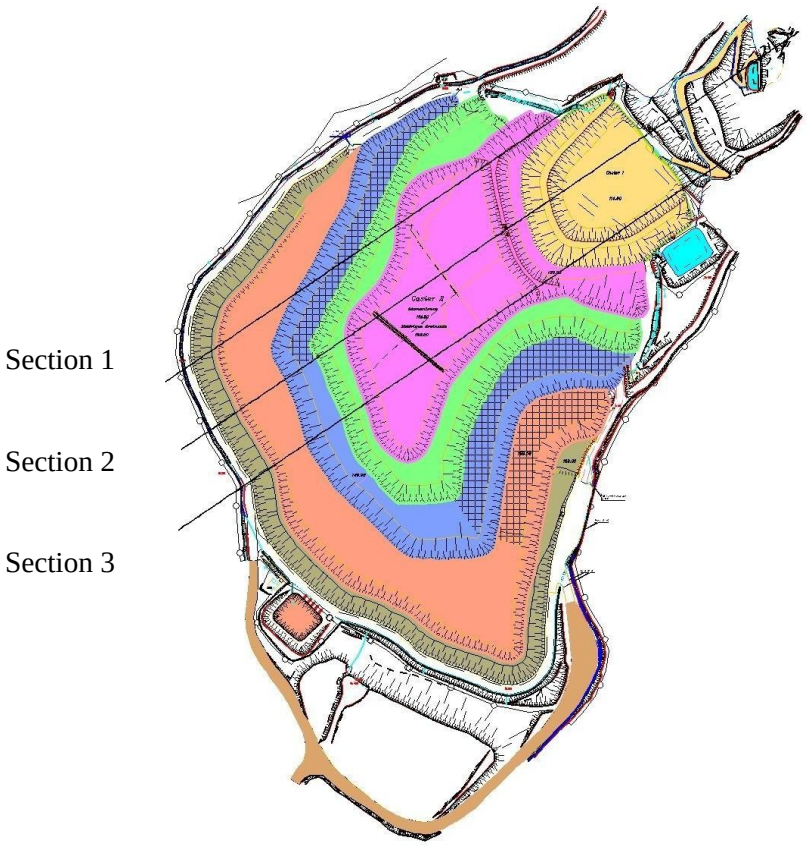

Figure VI- 50: Different probable sections for stability analysis.

Keeping in view the vertical expansion of the landfill, four different case scenarios of waste structure were investigated against the stability of section 3 for landfill 'N' (Figure VI-50) with two distinguished cases of stability analyses incorporating the presence of fresh waste column over the old waste. These cases are termed as:

- **Case 1:** Present height of the waste column at site with a thickness range between 18 to 50 m.
- **Case 2:** Present height of the waste with a rise in the leachate level (5 m).
- **Case 3:** Vertical expansion with fresh waste with a thickness range of 10 to 32 m.
- **Case 4:** Rise of the leachate level of 5 m thickness (with exceptional conditions of leachate accumulated in base uncorrected parameters used in extreme conditions).

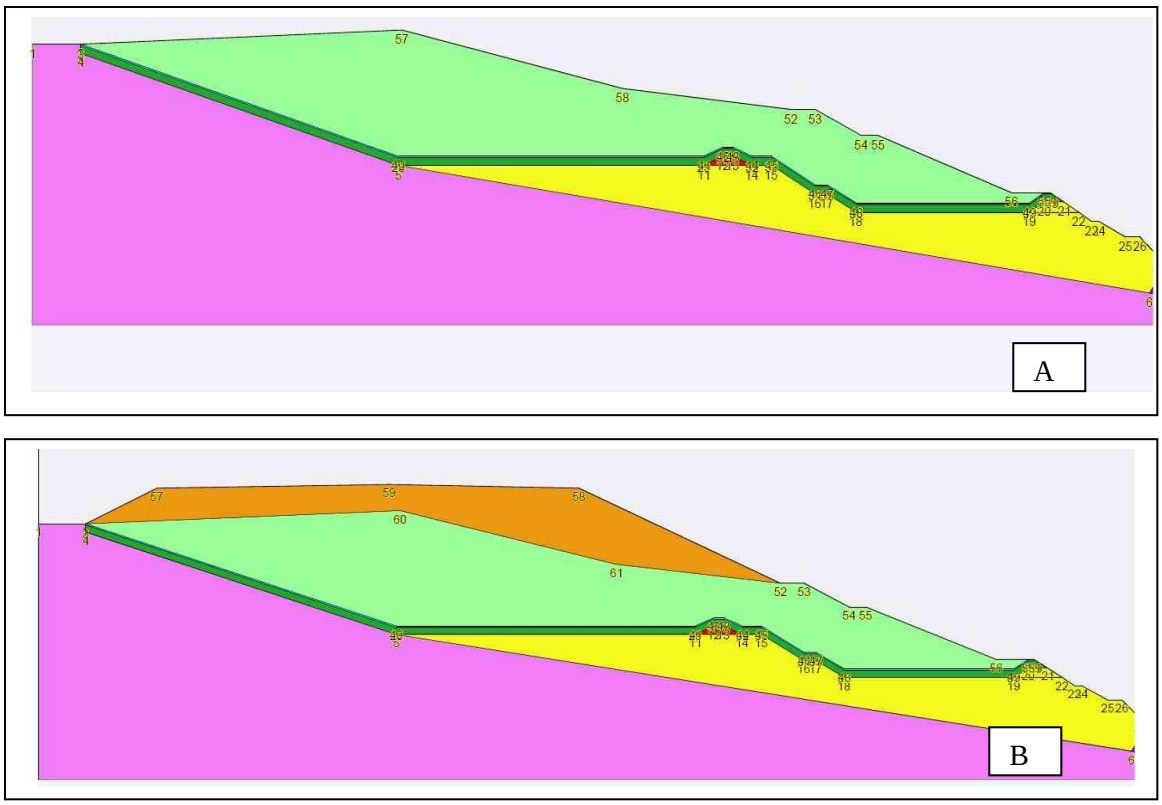

Figure VI- 51: Profile of Landfill section 3 without vertical expansion (A) and with the vertical expansion (B).

VI-4.2 Parameters of Stability

VI-4.2.1 Shear Strength Parameters

In the present study of stability design, the data for shear strength as determined in the previous study and detailed in § VI-3.3.6 was considered for the four case scenarios discussed above. The waste present at site is termed as 'old waste' in comparison with the fresh waste to be placed in the case of vertical expansion and the shear strength values determined earlier are used without any modification to analyse the probable worst case scenario. It is worth mentioning here that the waste samples retrieved from the site for shear test were analysed with modified parameters such as increased moisture content, and absence of fibrous particles which helped in considering the concerned values for change in shear strength. All variations in shear strength values for the four case scenarios are detailed in Table VI-26.

Accidental rise of the leachate level: Considering an event of temporary dysfunction of the leachate pumping system, the incidence of the formation of leachate level saturated at a 5 m height within the bottom of the waste column is analysed through TALREN software for any potentially dangerous condition. Moreover to carry out the analysis for the worst conditions, the waste at the bottom of the waste column was defined having smaller shear strength parameters as compared to the upper section for fresh waste (c = 30 and 33 kPa) Table VI-26.

Table VI- 26: Geotechnical parameters of landfill components used in the analyses (Refer § VI-3.3.6).

Layer	Cohesion (kPa)	Friction (°)	Unit weight (kN/m^3)
Fresh waste (Drilled Sample N3 & N6)	30	25	12.5
Old waste (Drilled sample N3)	10	30	14.0
- with leachate layer	4		
Old waste (drilled sample N6)	5	33	14.0
- with leachate layer	2		
Inert waste	7.5	28	18.0

These properties of resistance are attested besides by the tensile behaviour of fibrous waste in configuration of slope, which led the preceding authors to propose higher values of shear strength characteristics. Nevertheless the results of Jones et al. (1997) which after having carried out a significant work of back analyses from site as well as laboratory tests suggested rupture characteristics appreciably weaker, namely a cohesion of 12 kPa and an friction angle close to 29°.
Taking into consideration:

- The nature of the waste stored at site with strongly reinforced fibrous material, cloths, plastics and textile (Figure VI-44, VI-46)
- The strength of the compaction applied (compactor > 45 T) which supports the interconnection of the fibrous elements of waste
- And low moisture content of waste which consequently appears not to reach saturation under the effect of further surcharge

VI-4.2.2 Calculation of Factor of Safety

The state of stability of the slope is determined by the calculation of factor of safety according to the method of Bishop. This factor corresponds to the total resistant forces (being opposed to sliding) and the sum of the driving forces which can generate the slide on a circular rough surface. Calculations are carried out for many surface geometries having potential of acceptable kinematic rupture which make it possible to deduce the minimum factor of safety F characterizing this state of stability.
If $F < 1$, the slope is instable,
If $F > 1$, the slope is stable.
In practice and for this type of waste body, a minimum factor of 1.5 is necessary for long-term stability, and temporarily to 1.3 for exceptional conditions (for example; higher leachate levels resulting from a breakdown of the pumping system or earthquake). Reinforcements (cover liners and geosynthetics in bottom of waste column) are generally considered stable, therefore, no stability coefficient is being used in the following calculations. With Talren software, calculations of stability were carried out in two-dimensions and following parameters were used:

- geometry of slope (slope, height, intermediate embankment, etc…)
- geometry of various layers of the slope
- mechanical characteristics of constitutive materials of various layers of the slope and the base
- conditions of pore water pressure and/or dynamic stresses in the slope if necessary.

Generally the failure surface is taken as circular or sometimes a combination of straight and circular surfaces. The failure surface passing through the weak material is more likely to be critical. Calculations were done for various radii of circular failure surfaces covering a wider area of the landfill slopes. The factor of safety of landfill slopes is determined by assuming various positions and

shapes of the failure surfaces. The forces acting on the landfill waste include: Self weight and Pore pressures. The calculated factor of safety using the methods of slices and assuming the circular failure surfaces for all of the above cited cases are summarised in Table VI-27.

VI-4.3 Summary of Results

On the basis of assumption described above, numerous simulations with the limiting states of stability were carried out (Table VI-27) according to the section 3 since it was more critical section among the two sections considered while taking into account:

- the slope at 40% downstream
- the possible presence of leachate at 5 m height in bottom of waste column

Table VI- 27: Factors of safety determined from the stability analyses of the four case scenarios at section 3 of the landfill 'N'.

Stability scenario Section 3	Sample	F
Case 1	N3	2.20
	N6	1.89
Case 2 Leachate	N3	1.67
	N6	1.35
Case 3 Vertical expansion	N3	2.20
	N6	1.89
Case 4 Vertical expansion+ Leachate	N3	1.67
	N6	1.35

These results from the simulations for section 3 corresponding to drilled samples N6 (sliding circles and associated factor of safety) are presented below in Figure VI-51, VI-52, VI-53 and VI-54.

VI-4.4 Stability Design Discussion

Within the scope of the results presented in Tables VI-27, following observations are made:

- It is interesting to note that for the present study of stability analysis, the factor of safety determined for the section 3 remains the same both for the present waste column height and the vertical expansion (ranging between 10 to 30 m) that emphasises on no change in the slip

line position of the waste body. However it should be kept in mind that the shear strength of the fresh waste to be placed at the time of vertical expansion is assumed to have high shear strength than the old waste already present as site (Table VI-26).

- In present conditions of storage (without leachate at the bottom) the average factor of safety calculated for both drilled samples N3 and N6 is clearly higher than 1.5.
- In exceptional conditions (with 5 m thick leachate at the bottom) the factor of safety reduces to 1.67 for drilled sample N3 but is 1.35 for the drilled sample N6 which is the critical condition of the slope stability. But it should be kept in mind that the cohesion of 2 kPa was used for the calculation as determined from the shear tests.

Leachate control in the bottom of the waste column: Concerning the stability of the slope downstream, most significant factor lies with the maintenance of favourable hydro-physical conditions in the long run. From this point of view, the experiments show that with the help of an effective drainage of the leachate, the present slope of waste on the site can remain stable even under strong slope conditions. As the majority of slope failures of waste observed all over the world arise from the formation and the rise in leachate levels in the solid mass of waste.

Consequently, throughout the maintenance period of the site, it is important to control the leachate levels and to pump regularly in order to ensure the maintenance of waste above the water table. In addition to that, to be able to react quickly in the event of blockade or filling of the drain and/or sudden arrival of great quantities of leachate (significant storm, leakage at surface) in the bottom of the waste column, it is important to set up a series of mixed wells being able to receive the equipment of mobile pumps (or equipped permanently). Lastly, any measurement making it possible to limit the fire hazard within the solid mass of waste must be prioritised and in the event of proven internal combustion, it is important not to inject great quantities of water as there is the risk of internal pore pressures and loss of mechanical resistance.

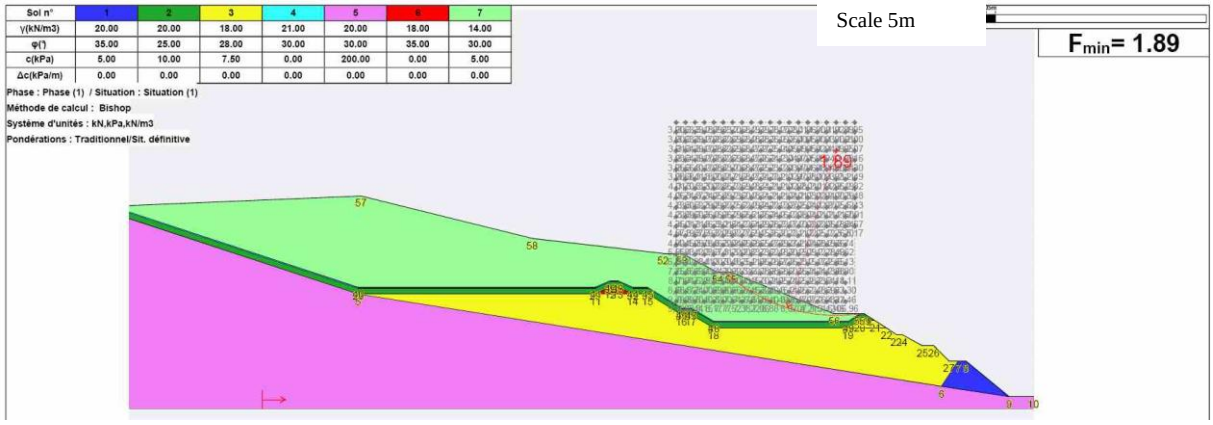

Figure VI- 52: Stability analysis of Case 1 for sample N6 with a calculated factor of safety = 1.89.

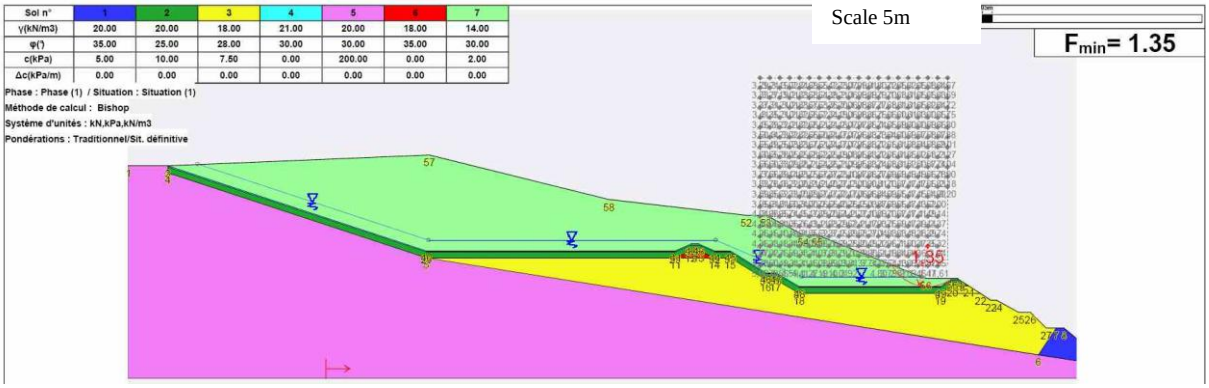

Figure VI- 53: Stability analysis Case 2 for drilled sample N6 with a calculated factor of safety = 1.35.

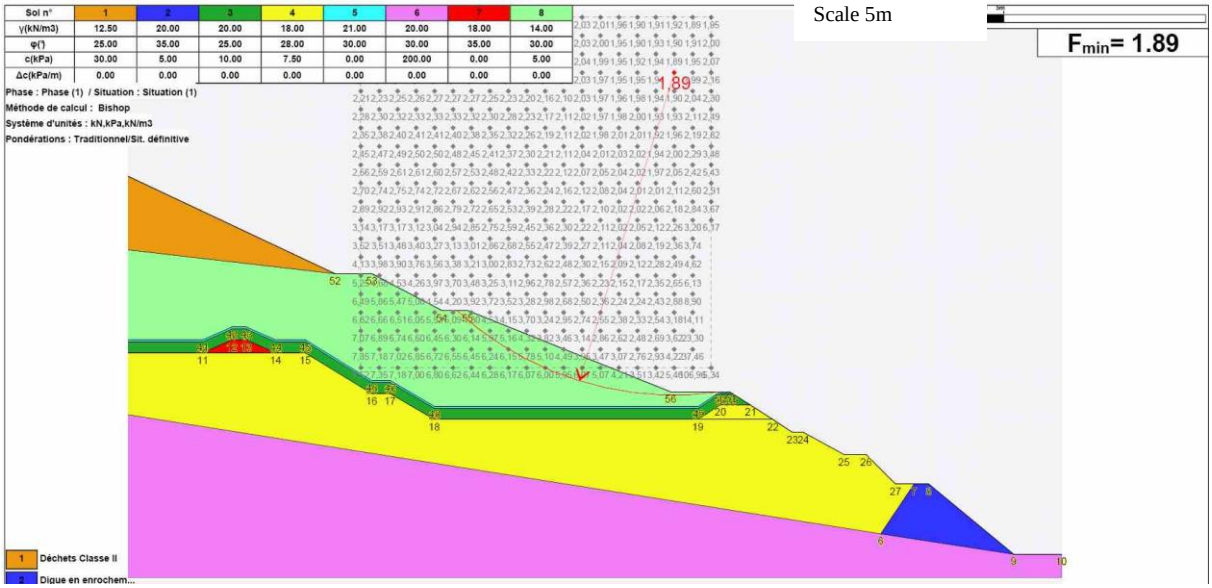

Figure VI- 54: Stability analysis of Case 3 for sample N6 with a calculated factor of safety = 1.89.

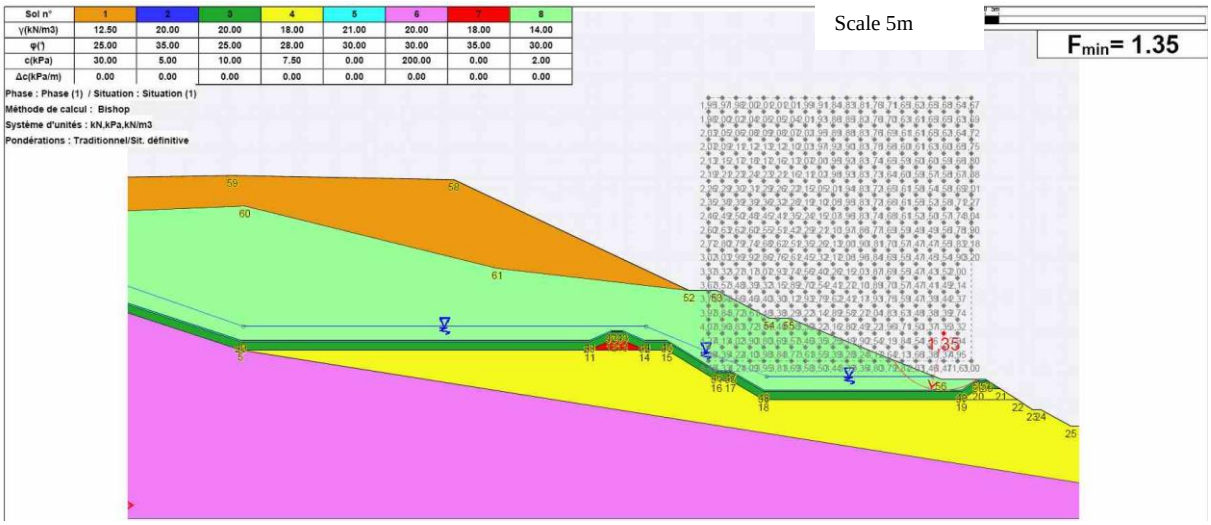

Figure VI- 55: Stability analysis of Case 4 for sample N6 with a calculated factor of safety = 1.35.

Conclusions and Perspectives

Conclusions

The present research study has made it possible to underline different hydro-mechanical aspects of municipal solid waste in correlation and thus the need to study them in conjunction in order to better understand the various phenomena in landfills. The comprehension of these interrelated phenomena is indispensable for the management of conventional landfills in general and the modern landfills in particular.

Within the scope of the present study following hydro-mechanical parameters were studied which made it possible to propose the characterisation of MSW.

Compressibility: Theoretical and actual site cases were analysed to propose a modified version of ISPM settlement prediction model.

- The parameter of time of origin necessary for the start of secondary settlement τ_c is suggested to be fixed at 1 month.
- $C^*\alpha\varepsilon$ ISPM can be assumed intrinsic and its scale of variation is small in relation to the exploitation history of the landfills.
- $C\alpha\varepsilon$ Sowers was determined as "not intrinsic" contrary to ISPM.

Shear Strength: Shear strength values were determined through large scale direct shear box and applied to site stability design.

- Complex testing program included samples retrieved from different sites and different techniques.
- c and φ values obtained, are in a higher range in comparison with the soil.

Gas Permeability/Structural Parameters: Permeability tests on different wastes were performed to validate of the double porosity model hypothesis.

- C^*_R showed small variation in its values for different types of waste samples, analysed during previous as well as present study. Higher values of calculated C^*_R in laboratory show the difficulty of achieving the comparable compaction vis-à-vis the in-situ measurements.

- The comparison of the parameter of solid density ρ_S suggests its relevance with the state of degradation of the waste. It can be stated that this parameter is a good indicator of degradation.
- A characteristic state of moisture content w_{micro} is defined corresponding to the saturation of the micro porosity of the medium.
- It is suggested that the moisture content $w < w_{micro}$ does not influence gas transfer (concept of double porosity).

Perspective of the present study on getting back to Pakistan

As detailed in the general introduction of the status of MSW management in Pakistan, the present study will serve as a reference document to start numerous research projects. At present time following projects are envisaged:

- To launch a MSW research laboratory.
- To develop a data base for Pakistan MSW characterisation efforts to date.
- To develop some public awareness campaigns regarding MSW management.
- To collaborate with the universities of international standings for future research possibilities.
- To propose the improvement techniques to the present environmental safety at landfill sites.
- To suggest the implementation and amelioration techniques for the barrier systems.

BIBLIOGRAPHY

Chapter I:

ARAN C. (2001) Fluid flow and heat transfer modelling for MSW. Application to leachate reinjection in the landfills (Modélisation des écoulements de fluides et des transferts de chaleur au sein des déchets ménagers. Application à la réinjection de lixiviats dans un centre de stockage) Doctoral Thesis, INP Toulouse. p. 248.

BARLAZ M. and HAM R. (1987) Gas Production Parameters in Sanitary Landfill. Waste Management Research. pp 27-39.

COSSU R., RAGA R. and ROSSETTI D. (2003) Full scale application of in situ aerobic stabilization of old landfills. 9th International Waste Management and Landfill Symposium, Cagliari Italy, Proceedings Sardinia.

COSSU R. and ROSSETTI D. (2003) Pilot Scale Experiences with sustainable landfilling based on the PAF conceptual model, 9th International Waste Management and Landfill Symposium, Cagliari, Italy, Proceedings Sardinia.

CHRISTENSEN T. and KJELDSEN P. (1989) Basic Biochemical Processes in Landfills. Academic Press Ltd., Toronto. pp 29-49.

FARQUHAR G. J. (1989) Leachate: production and characterization, Can. J. Civ. Engg, 16, pp 317–325.

GRISOLIA M., NAPOLEONI Q. and TANCREDI G. (1995) Contribution to a technical classification of MSW. 5th International Landfill Symposium, Cagliari Italy. Proceedings Sardinia 95 Vol. II, pp 703-710.

GAWANDE N. A. (2008): https://pegasus.cc.ucf.edu/~ngawande/research.htm

HEYER K.-U., HUPE K., RITZKOWSKI M. and STEGMANN R. (2001) Technical Implementation and Operation of the Low Pressure Aeration of Landfills. 8th International Waste Management and Landfill Symposium, Cagliari Italy, Proceedings Sardinia.

HEYER K.-U., HUPE K., KOOP A. and STEGMANN R.(2005) Aerobic in situ stabilisation of landfills in the closure and aftercare period. 10th International Waste Management and Landfill Symposium, Cagliari Italy, Proceedings Sardinia.

IGES: http://www.iges.or.jp/en/ltp/pdf/activity08/06_pakistan.pdf

JARAMILLO G. J., (Adapted and edited by: Francisco Zepeda Washington, D.C. 1993)
http://www.bvsde.paho.org/bvsars/i/fulltext/manual/manual.html
http://www.bvsde.paho.org/bvsair/e/repindex/repi49-50/lesson8/lesson8.html

JESSBERGER H.L., KOCKEL R., (1993) Determination and assessment of the mechanical properties of waste materials. 4th International Landfill Symposium Sardinia Italy, CISA. pp 167-177.

KJELDSEN P., BARLAZ MA., ROOKER AP., BAUN A., LEDIN A. and CHRISTENSEN TH. (2002) Present and long-term composition of MSW landfill leachate: a review. Crit Rev Environ Sci Technol 2002; 32: pp 297-336.

KÖLSCH F. (1995) Material values for some mechanical properties of domestic waste. Proc Sardinia 95, 5th International Landfill Symposium, Cagliari, Vol. II, p 711-729.

LANDVA A.O. and CLARK J.I. (1990) Geotechnics of waste Fill - Theory and Practice, ASTM, Special Technical Publication 1070, p 86-103.

LANGER U., (2005) Shear and compression behaviour of undegraded Municipal Solid Waste, Doctoral Thesis Loughborough University, p 115-122.

LORBER K. E., NUELLES M., RAGOSSNIG A., RANINGER B. and SCHULTIK J. (2001) Longterm comparison between mechanical biological pretreated and non pretreated landfill. 8th International Waste Management and Landfill Symposium, Cagliari Italy, Proceedings Sardinia, Vol. 1, pp 239-246.

MARSHAL A., (2007), http://en.wikipedia.org/wiki/File:Stages_of_anaerobic_digestion.JPG

NAKASAKI K., YAGUCHI H., SASAKI Y. and KUBOTA H. (1993) Effects of pH control on composting of garbage. Waste Management & Research 11, pp 117-125.

OECD(2004):
http://maps.grida.no/go/graphic/projected_trends_in_regional_municipal_waste_generation

OWEIS I.S. and KHERA R.P. (1990) Geotechnology of waste management. PWS Publishing Company, Boston, Mass.

PERCELL B.E. (2000) Wastes Management March 2000, pp 25-27.

PURCELL B.E. and WALKER N. (2004) Further demonstrations of aerox waste treatment. Waste 2004 - Integrated Waste Management and Pollution Control: Policy and Practice, Research and Solutions, Stratford-upon-Avon, UK, pp 13-21.

RITZKOWSKI M. and STEGMANN R. (2005) Mechanisms affecting the leachate quality in the course of landfill in-situ aeration. 10th International Waste Management and Landfill Symposium Proceedings Sardinia, Cagliari, Italy.

RUNCO. (2007). RUNCO Waste Industries Inc. Consulted 2007, ON Runco Environmental Inc. web site: http://runcoenv.com/home.htm

STEGMANN R., (2005) Mechanical biological pretreatment of municipal solid waste, 10th International Waste Management and Landfill Symposium, CISA, Cagliari, Italy, Proceedings Sardinia.

TCHOBANOGLOUS G. and THEISEN H., VIGIL S. (1993) Integrated Solid Waste Management, 1st ed.; McGraw-Hill Inc., New York, 1993.

TCHOBANOGLOUS G., THEISEN H. and VIGIL (1993); EPA 1995.

WILLIAMS P.T. (2005) "Waste Treatment and Disposal", 2nd ed. John Wiley & Sons Ltd, England, ISBN 0-470-84912-6, pp 171-244.

Chapter II:

ARIGALA SG., TSOTSIS TT. and WEBSTER IA. (1995) Gas generation, transport, and extraction in landfills, Journal of the Environmental Engineering-ASCE, 121 (1), pp 33-44.

BEAVEN R.P. and POWRIE W. (1995) Hydrogeological and geotechnical properties of refuse using a large scale compression cell. 5th International Waste Management and Landfill Symposium Cagliari Italy, Proceedings Sardinia.

BROOKS R. H. and COREY A. T. (1964) Hydraulic properties of porous media. Hydrology Paper n° 3, Colorado State University, Fort Collins.

BUISMAN A.S.K. (1936) Results of long duration settlement tests. Proc. 1st International Conference on Soil Mechanics and Foundation Engineering, Harvard University, Cambridge Massachusetts, Vol. 1, pp 103-106.

DURMUSOGLU E., CORAPCIOGLU MY. and TUNCAY K. (2005) Landfill settlement with decomposition and gas generation, Journal of the Environmental Engineering, 131 (9), pp 1311-1321.

GRISOLIA M., NAPOLEONI Q. and TANCREDI, G. (1995) Contribution to a technical classification of MSW. 5th International Landfill Symposium, Cagliari, Proceedings Sardinia 95 Vol. II, pp 703-710.

JESSBERGER H.L. and KOCKEL R. (1993) Determination and assessment of the mechanical properties of waste materials. 4th International Landfill Symposium, Sardinia, Italy, CISA. Proceedings Sardinia, pp 167-177.

KÖLSCH F. (1995) Material values for some mechanical properties of domestic waste, 5th International Landfill Symposium, Cagliari, Italy, Proceedings Sardinia 95, Vol. II, pp 711-729.

LANGER U. (2005) Shear and compression behaviour of undegraded Municipal Solid Waste, Doctoral Thesis Loughborough University, p 166.

LORNAGE R. (2006) Comparative study of three domestic waste filling techniques- Study of semi industrial pilot scale cells to characterise the associated liquid and gas emissions. (Comparaison de trois filières de stockage d'ordures ménagères – Etude du comportement en pilotes semi industriels et caractérisation des émissions liquides et gazeuses associées), Doctoral Thesis, Ecole Doctorale de Chimie de Lyon, p 266.

MANOUKIAN A. (2008) Evaluation of in-situ and pilot scale emissions of volatile organic compounds (VOCs) of biodegradable waste : Quantification of BTEX (Evaluation des émissions de

composes organiques volatils sur site de stockage et sur pilotes contenant des déchets en cours de dégradation : quantification des BTEX), M2R Thesis report, Université de Grenoble 1.

McDOUGALL J. (2007) A hydro-bio-mechanical model for settlement and other behaviour in landfilled waste, Computers and geotechnics, Volume 34, pp 229-246.

MÜNNICH K., ZIEHMANN G. and FRICKE K. (2003) Hydraulic behaviour of mechanical biological pre-treated waste. 9th International Waste Management and Landfill Symposium, Cagliari Italy, Proceedings Sardinia.

POWRIE W., HUDSON A.P. and BEAVEN R.P. (2000) Development of sustainable landfill practices and engineering technology, Final report to the Engineering and Physical Sciences Research Council (Grant reference GR/L 16149), p 27 .

STOLTZ G. (2009) Transport processes in biodegradable porous, un-saturated and deformable medium with double porosity: Application to landfill sites. (Transferts en milieu poreux biodégradable, non saturé, déformable et a double porosité : application aux ISND (installation de stockage de déchets non dangereux)), Doctoral Thesis LTHE-Université de Grenoble.

TOWNSEND TG., WISE WR. and JAIN P. (2005) One-dimensional gas flow model for horizontal gas collection systems at municipal solid waste landfills, Journal of environmental engineering, Vol 131, Issue 12, pp 1716-1723.

USEPA: **www.USEPA.org**

VAN GENUCHTEN M. (1980) A closed-form equation for predicting the hydraulic conductivity of unsaturated soils, Soil Sci. So. Am. J., vol. 44, pp 892-898.

VIGNERON V. (2005) Ways of reducing nitrogen oxide from MSW body when injected into the medium. (Voies de réduction des oxydes d'azote lors de leur injection dans un massif de déchets ménagers et assimilés), Doctoral Thesis, Université de Paris-XII, 336 p.

WALL D. K. and ZEISS C. (1995) Municipal landfill biodegradation and settlement, Journal of Environmental Engineering, 121 (3), pp 214-224.

WARRICK A.W. (2001) Soil physics companion, CRC Press, Boca Raton, p 398.

WATSON G.V., POWRIE W. and BLADES A.P. (2007) An investigation into the effects of degradation on waste structure. 11th International Waste Management and Landfill Symposium. Cagliari, Italy? Proceedings Sardinia.

WEAST R.C. (1981) Handbook of chemistry and physics. 61st ed. Boca Raton, FL: CRC Press, 1981.

ZORNBERG J.G., JERNIGAN B.L., SANGLERAT T.R. and COOLET B.H. (1999) Retention of free liquids in landfills undergoing vertical expansion, ASCE Journal of Geotechnical and Geoenvironmental Engineering, Vol.125, No.7, pp 583-594.

Chapter III:

BARLAZ M.A, HAM R.K. and SCHAEFER D.M. (1990) Methane production from municipal refuse: a review of enhancement techniques and microbial dynamics. C.r.i.e. Control, Vol. 19, n°6, pp 557-586.

BEAVEN R.P. and POWRIE W. (1995) Hydrogeological and geotechnical properties of refuse using a large scale compression cell. 5th International Waste Management and Landfill Symposium, Cagliari Italy, Proceedings Sardinia.

KAZIMOGLU Y.K., McDOUGALL J.R. and PYRAH I.C. (2005) Moisture retention and movement in landfilled waste, International Conf. Problematic Soils, Eastern Mediterranean University, North Cyprus, Proceedings GeoProb pp 307-314.

LANDVA A.O. and CLARK J.I. (1990) Geotechnics of waste fill. In: Landva AO, Knowles GD (eds) Geotechnics of waste fills, ASTM STP 1070, American Society for Testing and Materials, Philadelphia, pp 86-103.

LORNAGE R. (2006) Comparative study of three domestic waste filling techniques- Study of semi industrial pilot scale cells to characterise the associated liquid and gas emissions. (Comparaison de trois filières de stockage d'ordures ménagères – Etude du comportement en pilotes semi industriels et caractérisation des émissions liquides et gazeuses associées), Doctoral Thesis, Ecole Doctorale de Chimie de Lyon, p 266.

STOLTZ G. (2009) Transport processes in biodegradable porous, un-saturated and deformable medium with double porosity: Application to landfill sites. (Transferts en milieu poreux

biodégradable, non saturé, déformable et a double porosité : application aux ISND (installation de stockage de déchets non dangereux)), Doctoral Thesis LTHE-Université de Grenoble.

WATSON G. V., POWRIE W. and BLADES A. P. (2007). An investigation into the effects of degradation on waste structure. 11th International Waste Management and Landfill Symposium, Cagliari Italy: CISA, Proceedings Sardinia 2007

Chapter IV :

BEAVEN R.P., BARKER J.A. and HUDSON A. (2003) Description of a tracer test trough waste and application of a double porosity model. 9th International Waste management and Landfill Symposium, Cagliari Italy. Proceeding Sardinia.

CAPELO J. and DE CASTRO M.A.H. (2007) Measuring transient water flow in unsaturated municipal solid waste – A new experimental approach. Waste Management, Vol. 27, pp 818-819.

STOLTZ G. (2009) Transport processes in biodegradable porous, un-saturated and deformable medium with double porosity: Application to landfill sites. (Transferts en milieu poreux biodégradable, non saturé, déformable et a double porosité : application aux ISND (installation de stockage de déchets non dangereux)), Doctoral Thesis LTHE-Université de Grenoble.

VAN GENUCHTEN M. (1980) A closed-form equation for predicting the hydraulic conductivity of unsaturated soils, Soil Sci. So. Am. J., vol. 44, pp 892-898.

Chapter V :

BAUER J., MÜNNICH K. and FRICKE K. (2005) Settlement processes of landfill bodies-long term survey of a slope deformation. 10th International Waste Management and Landfill Symposium, 2005, Cagliari, Italy, Proceedings Sardinia.

BEAVEN R.P. and POWRIE W. (1995) Hydrogeological and geotechnical properties of refuse using a large scale compression cell. 5th International Waste Management and Landfill Symposium, Cagliari Italy, Proceedings Sardinia.

BJARNGARD A. and EDGERS L. (1990) Settlement of municipal solid waste landfills. Proceedings 13th Annual Madison Waste Conference, Madison, pp 192-205.

BJERRUM L. (1973) Problems of soil mechanics and construction on soft clays and structurally unstable soils State of the art report, Session 4). Proc 8th International Conference on Soil Mechanics and Foundation Engineering, Moscow, Vol. 3.

BLEIKER D.E., FARQUAHR G. and McBEAN E. (1995) Landfill settlement and the impact on site capacity and waste hydraulic conductivity. Waste Management and Research, Vol. 13

BOUAZZA A. and PUMP W.L. (1997) Settlement and the design of municipal solid waste landfills. Proc. Conference Geo-Environment 97, Melbourne.

BOWDERS J. J., BOUAZZA M., LOEHR E. and RUSSEL M. (2000) Settlement of municipal solid waste landfills. Proc. 4th Kansay Geotechnical Forum, Kyoto, pp 101-106.

BOWLES J. E., (1998) Foundation Analysis and Design, McGraw-Hill, New York, 1998.

BUISMAN A.S.K. (1936) Results of long duration settlements tests. Proc. 1st International Conference on Soil Mechanics and Foundation Engineering, Harvard University, Cambridge Massachusetts,

CARRUBBA P. and COSSU R. (2003) Investigation on compressibility and permeability of pre-treated waste mixture. 8th International Waste Management and Landfill Symposium, Cagliari Italy, Proceedings Sardinia.

CARTIER G. and BALDIT R. (1983) Comportement géotechnique des décharges du résidus urbains. Bulletin de liaison des laboratoires routiers des ponts et chaussées, Vol. 128 pp 55-64

CHEYNEY A. C. Settlement of landfill, Landfill Completion, Symposium Proceedings, Harwell, UK, 1983

COSSU R., Di MAIO R., FAIS S., FRAGHI A., LIGAS P. MENGHINI A. (2005) Physical and structural characterisation of an old landfill site by a multi-methodological geophysical approach. 10th International Waste Management and Landfill Symposium, 2005, Cagliari, Italy, Proceedings Sardinia.

COUMOULOS D. G. and KORYALOS T.P. (1999) Prediction of Long-Term Settlement Behaviour of Landfill Covers After Closure. 7th International Landfill Symposium, Cagliari, Italy, Proceedings Sardinia.

DESCLOITRES M. (2008) Prospections geophysiques (méthodes de résistivité). Project ANR « Bioreactor ». Laboratoire d'Etude des Transferts en Hydrologie et Environnement – LTHE.

DIXON N., JONES D.R.V. and WHITTLE R.W. (1999) Mechanical properties of household waste: in-situ assessment using pressuremeters. 7th International Waste Management and Landfill Symposium, Cagliari Italy. Proceeding Sardinia Vol. III, pp 453-460.

FASSETT J.B., LEONARDS G.A. and REPETTO P.C. (1994) Geotechnical properties of municipal solid wastes and their use in landfill designs. Proc., Waste Tech 94 Conference, Silver Springs.

GARLANGER J.E. (1972) The consolidation of soils exhibiting creep under constant effective stress Geo-Technique, Vol. 22

GIBSON R.E. and LO K.Y. (1961) A theory of soils exhibiting secondary compression. Acta Polytechnica Scandinavica, C:10, n° 296

GOTTELAND P., GACHET C. and VUILLEMIN M., (2001) Mechanical Study of Municipal Solid Waste Landfill. 8th International Waste Management and Landfill Symposium, Cagliari, Italy, Proceeding Sardinia pp 425-433.

GOURC J.P., STAUB M.J. and CONTE, M. (2010) Decoupling MSW Settlement into mechanical and biochemical processes – modelling and validation on large-scale setups. Waste Management 2010 (submitted)

GOURC J.P., THOMAS S. and VUILLEMIN M. (1999) Proposal of a waste settlement survey methodology. Proc. Geo-Environmental conference, Lisbon, Vol. I

GREEN D. and JAMENJAD G. (1997) Settlement characteristics of domestic waste. Shear strength of waste and its use in landfill stability analysis. Proceedings; Conference on Contaminated Ground, British Geotechnical Society, pp 319-324.

http://www.dgi-menard.com/landfill2000.html

IVANOVA L.K., RICHARDS D.J. and SMALLMAN D.J. (2003) Quantification of factors affecting rate and magnitude of secondary settlement of landfills. 9th International Waste Management and Landfill Symposium, Cagliari Italy, Proceedings Sardinia.

IVANOVA L.K., RICHARDS D.J. and SMALLMAN D.J. (2005) A preliminary analysis of waste biodegradation and landfill settlement rate using consolidating anaerobic reactors. 10th International Waste Management and Landfill Symposium, Cagliari Italy, Proceedings Sardinia.

JESSBERGER H.L. and KOCKEL R. (1993) Determination and assessment of the mechanical properties of waste materials. 4th International Landfill Symposium, Italy, CISA. Proceedings Sardinia, pp 167-177.

KAVAZANJIAN E.J., MATASOVIC N. and BACHUS R.C. (1999) Large-Diameter Static and Cyclic Laboratory Testing of Municipal Solid Waste. 7th International Landfill Symposium, Cagliari Italy, Proceeding Sardinia, pp 437-444.

KOPPEJAN A.W. (1948) A formula combining the Terzaghi's load compression relationship and the Buisman's secular time effect. Proc. 2nd International conference on Soil Mechanics and Foundation Engineering, Rotterdam.

LAMBE T.W. (1951) Soil testing for engineers. Wiley, New-York

LEONARDS G. A. and GIRAULT P. (1961) A study of the one dimensional consolidation test. Proceedings 5th International Conference on Soil Mechanics and Foundation Engineering, Paris, Vol. 1, pp. 213-218

LEROUEIL S., MAGNAN J.P. and TAVENAS F. (1985) Remblais sur argiles molles. Technique et Documentation, Lavoisier, p 342.

McDOUGALL J., SILVER R. (2005) Hydro-bio-mechanical modelling landfilled waste: Real insights? 10th International Waste Management and Landfill Symposium, Cagliari, Italy, Proceeding Sardinia.

McDOUGALL J. and PYRAH I.C. (2001) Settlement in landfilled waste: Extending the geotechnical approach . 8th International Waste Management and Landfill Symposium, Cagliari Italy, Proceeding Sardinia.

MERZ R.C. and STONE R. (1962) Landfill settlement rates. Journal of Public Works, Vol. 93, n°9.

MESRI G. and CHOI G. K. (1985) The uniqueness of the end of primary void ratio – effective stress relationships. Proceedings 11th International Conference on Soil Mechanics and Foundational Engineering, San Francisco, Vol. 2, pp 537 – 550.

MORRIS D.V. and WOODS C. E. (1990) Settlement and engineering considerations in landfill and final cover design, in Geotechnics of Waste Fills–Theory and practice, Landva, A. and Knowles, D. Eds., ASTM Special Technical Publication 1070, American Society of Testing and Materials, Philadelphia, Pennsylvania, 1990

OLIVIER F. and GOURC J.P. (2007) Hydro-mechanical behaviour of municipal solid waste subject to leachate recirculation in a large-scale compression cell, Waste Management, vol.27, n°1, pp 44-58.

OLIVIER F., LHOMME D., GOURC J.P. and HIDRA M. (2005) The measurement of landfill settlement using terrestrial 3D laser scanner imaging. 10th International Waste Management and fill Symposium, Cagliari, Italy, Proceedings Sardinia.

OLIVIER F., GOURC J.P., MUNOZ M.L., BUDKA A. and DENECHEAU P. (2003) Validation of a new MSW settlement prediction model from four monitored landfills. Proc. 13th European Conference on Soil Mechanics and Geotechnical Engineering, Prague.

OLIVIER F. (2003) Tassement des déchets en CSD de classe II : du site au modèle. (Settlement of biodegradable waste : From landfill site to modelling) Doctoral Thesis, Laboratoire Lirigm, Université de Grenoble.

OLIVIER F., GOURC J.P., LOPEZ S., BENHAMIDA S. And VAN WYCK D. (2003) Mechanical behaviour of solid waste in a fully instrumented prototype compression box. 9th International Waste Management and Landfill Symposium, Cagliari, Italy. Proceedings Sardinia.

OWEIS I.S. and KHERA R.P. (1986) Criteria for geotechnical construction on sanitary landfills, International Symposium on Environmental Geotechnology, Allentown, Pennsylvania Vol. I p 16.

PARKER L.J., WHITE J.K. and POWRIE W. (1999) The measurement of the geotechnical and hydro-geological properties of degrading solid waste. 7th International Waste Management and Landfill Symposium Cagliari, Italy: Proceedings Sardinia pp 469-478.

RAO S.K., MOULTON L.K. and SEALS R.K. (1977) Settlement of waste landfills, in Proceedings of the Conference on Geotechnical Practice for Disposal of Solid Waste Materials, ASCE.

SANCHEZ-ALCITURRI J.M., PALMA J., SAGASETA C. and CANIZAL J. (1993) Three years of deformation monitoring at Meruelo landfill. Proc. Green'93, Geotechnics related to the Environment, Bolton, pp 365-371.

SOWERS G. F. (1968) Foundation problems in sanitary landfills, J. Sanitary Eng. Div., ASCE, 94(1), 1968.

SOWERS G.F. (1973) Settlement of waste disposal fills. Proc. 3rd International Conference on Soil Mechanics and Foundation Engineering, Moscow.

TERZAGHI K. (1943) Theoretical Soil Mechanics, John Wiley and Sons, New York (1943)

THOMAS S. (2000) Centres de stockage de Déchets – Geo-mecanique des déchets et de leur couverture (Expérimentations sur sites et modélisation) Doctoral Thesis, Laboratoire Lirigm, Université de Grenoble.

VAN MERTEEN J.J., SELLMEIJIER J.B. and PEREBOOM D. (1995) Prediction of landfill settlement, 5th International Landfill Symposium, Calgiari Italy Proceedings Sardinia Vol. III, pp 823-831.

VAN MERTEEN J.J., SELLMEIJIER J.B. and PEREBOOM D. (1997) Prediction of landfill settlement, 6th International Landfill Symposium, Calgiari Italy Proceedings Sardinia Vol. III, pp 525-544.

WALL D.K., and ZEISS C. (1995) Municipal landfill biodegradation and settlement, Journal of Environmental Engineering, 121 (3), pp 214-224.

WATTS K.S., and CHARLES A. (1990) Settlement of recently placed domestic refuse landfill. Proceedings of the Institution of Civil Engineers, Part I, Vol. 88, n° 1, pp 971-993.

YUEN S.T.S. (1999) Bioreactor landfills promoted by leachate recirculation: a full-scale study. Doctoral Thesis, Department of Civil and Environmental Engineering, University of Melbourne.

ZAMISKIE E. M., KABIR M. G. and HADDAD A. (1994) Settlement evaluation for cap closure performance, in Vertical and Horizontal Deformations of Foundations and Embankments, Yeung, A. T. and Felio, G. Y., Eds., Geotechnical Special Publication 40, ASCE, 1994.

Chapter VI:

BAUER J., MÜNNICH K. and FRICKE K. (2007) Influence of hydraulic properties on the stability of landfills. 11th International Waste Management and Landfill Symposium, Cagliari Italy, Proceedings Sardinia.

BEAVEN R.P. and POWRIE W. (1995) Hydrogeological and geotechnical properties of refuse using a large scale compression cell. 5th International Waste Management and Landfill Symposium, Cagliari Italy, Proceedings Sardinia, pp 745-760.

CAICEDO B., YAMIN L., GIRALDO E. and CORONADO O. (2002) Geo-mechanical properties of municipal solid waste in Dona Juana sanitary landfill. Proc. 4th International Congress on Environmental Geotechnics, Brazil, 1: pp 177-182.

DIXON N., JONES D.R. and WHITTLE R.W. (1999) Mechanical properties of household waste: In-situ assessment using pressuremetres. 7th International Waste Management and Landfill Symposium Cagliari, Italy, Proceedings Sardinia pp 453-460.

DURMUSOGLU E., CORAPCIOGLU M.Y. and SANCHEZ I.N. (2005) Permeability of municipal solid waste sample. 10th International Waste Management and Landfill Symposium, Cagliari, Italy: Proceedings Sardinia.

EID H.T., STARK T.D., EVANS W.D. and SHERRY P.E. (2000) Municipal solid waste slope failure – I: Waste and foundation soil properties. Journal of Geotechnical and Geoenvironmental Engineering, ASCE, 126(5): pp 397-407.

FUCALE S.P., JUCA J.F.T., MUNNICH K. and BAUER J. (2007) Study of the mechanical behaviour of MBT – waste In: R. Cossu, L.F. Diaz & R. Stegmann (Eds.) Proceedings Sardinia 2007, 11th International waste Management and Landfill symposium Cagliari Italy, pp 1180.

GABR M.A. and VALERO S.N. (1995) Geotechnical Properties of Municipal Solid Waste. Geotechnical Testing Journal, ASTM, 18(2): pp 241-251.

GOTTELAND P., LEMARECHAL D. and RICHARD P. (1995) Analysis and monitoring of the stability of a domestic waste landfill. 5th International Landfill Symposium Cagliari, Italy, Proceedings Sardinia pp 777-787.

IVANOVA I.K., RICHARDS D.J. and SMALLMAN D.J. (2003) An investigation into the factors affecting secondary settlement of wastes. 9th International Waste Management and Landfill Symposium, Cagliari, Italy, Proceedings Sardinia.

JANBU N. (1963) Soil compressibility as determined by odeometer and triaxial tests. Proc. 3rd European Conference on Soil Mechanics, Wiesbaden, Germany, Vol. 1 pp 19-25

JESSBERGER H.L. and KOCKEL R. (1993) Determination and assessment of the mechanical properties of waste materials. 4th International Waste management and Landfill Symposium. Proceedings Sardinia, pp 1383-1392.

JONES D.R. and DIXON N. (1997) The long term stability of landfill site slopes. 6th International Landfill Symposium Cagliari Italy, Proceedings Sardinia, pp 517-523.

KAVAZANJIAN Jr.E., MATAZOVIC N. and BACHUS R.C. (1999) Large-diameter static and cyclic laboratory testing of municipal solid waste. 7th International Waste Management and Landfill Symposium, Cagliari Italy. Proceedings Sardinia, pp 437-444.

KÖLSCH F., FRICKE K., MAHLER C. and DAMANHURI E. (2005) Stability of landfills -The Bandung dumpsite disaster. 10th International Waste Management and Landill Symposium, Cagliari Italy. Proceedings Sardinia.

KÖLSCH F. (1995) Material values for some mechanical properties of domestic waste. 5th International Landfill Symposium, Cagliari Italy. Proceedings Sardinia, pp 712-729.

LANDVA A. and CLARK J. (1990) Geotechnics of waste fills-theory and practice. ASTM, Geotechnics of waste fills. Baltimore: ASTM.

LANGER U., DIXON N., GOTTELAND P. and GOURC J. P. (2005) Waste mechanics: investigation using synthetic MSW. 10th International Waste Management and Landfill Symposium, Cagliari Italy. Proceedings Sardinia.

MACHADO S.L., VILAR O.M. and CARVALHO M.F. (2008) Constitutive model for long term municipal solid waste mechanical behaviour, Computers and Geotechnics 35 pp 775-790.

MAHLER C.F. and De LAMARE NETTO A. (2003) Sheer resistance of mechanical biological pretreated domestic urban waste. 9th International Waste Management and Landfill Symposium, Cagliari Italy. Proceedings Sardinia.

MILANOV V., CORADE J.M., BRUYAT-KORDA F. and FALKENERECK G. (1997) Waste slope failure analysis at the Rubastens landfill sites. 6th International Landfill Symposium Cagliari, Italy: Proceedings Sardinia, pp 551-556..

POWRIE W., BEAVEN R.P. and HARKNESS R.M. (1999) Applicability of soil mechanics principles to household waste. 7th International Waste Management and Landfill Symposium Cagliari, Italy: Proceedings Sardinia, pp 429-436.

REUTER E. and NOLTE H.C. (1995) Conception of a stability analysis for large landfills: Case study in Hannover. 7th International Landfill Symposium, Cagliari Italy. Proceedings Sardinia, pp 801-812.

SINGH S. and MURPHY B. (1990) Evaluation of the stability of the sanitary landfills. Geotechnics of the waste fills – theory and practice, STP 1070, Landva and Knowles, eds., ASTM, pp 240-258.

TCHOBANOGLOUS G. (1986) Municipal Solid Waste. H. S. Peavy, D. R. Rowe, & G. Tchobanoglous, Environmental Engineering (p. 579). Singapore: McGraw-Hill.

TERZAGHI K. (1943) Theoretical Soil Mechanics, John Wiley and Sons, New York.

THOMAS S., ABOURA A.A., GOURC J.P., GOTTELAND P., BILLARD H. and DELINEAU T. (2000). An in-situ waste mechanical experimentation of a French landfill. 7th International Waste Management and Landfill Symposium, Cagliari Italy. Proceedings Sardinia, pp 445-452.

ZEKKOS D.P., (2005) Evaluation of static and dynamic properties of Municipal Solid Waste, PhD thesis, Department of Civil and Environmental Engineering, University of California at Berkeley.

Nomenclature

Index $_G$ represents the gas phase and the index $_L$ represents the liquid phase.

A	Sample cross section	m^2
BOD	Biochemical oxygen demand	mg/l
BMP	Biochemical methane potential	Nl/kg MS
COD	Chemical oxygen demand	mg/l
NH4+	Ammonia production	mg/l
α	Empirical parameter of Van Genuchten model	-
c	Cohesion	kPa
C_c	Coefficient of primary compression	-
C_s	Coefficient of primary recompression	-
C^*_R	Intrinsic coefficient of primary compression (ISPM model)	-
$C^*_{\alpha\varepsilon}$	Intrinsic coefficient of secondary compression (ISPM model)	-
d_p	Pore diameter	m
e	Void ratio	-
ε	Strain	-
γ	Van Genuchten – Mualem coefficient	-
ΔH	Settlement	m
ΔH^P	Primary settlement	m
ΔH^S,	Secondary settlement	m
$\eta_{G,L}$	Gas/Liquid dynamic viscosity	kg/(m x s)
K_w	Hydraulic conductivity	m/s
$k_{G,L}$	Gas/Liquid permeability	m^2
k_i	Intrinsic permeability	m^2
$k_{rG,L}$	Gas/liquid relative permeability	-
k_{KC}	Permeability (carman-Kozeny model)	m^2
M_L	Mass of liquid phase	kg
M_S	Mass of solid phase	kg
M_T	Total mass of the sample	kg
m	Van Genuchten – Mualem model parameter	-
n	Total porosity	%
n^{micro}	Micro porosity	%

n^{macro}	Macro porosity	%
p_c	Capillary pressure	kPa
p_{cp}	Back pressure	kPa
$P_{G,L}$	Absolute pressure for Gas/Liquid phase	kPa
p_G	Relative gas pressure (with respect to atmospheric pressure)	kPa
p_L	Relative liquid pressure (with respect to absolute gas pressure)	kPa
θ_G	Gas porosity	%
θ_G^*	Corrected gas porosity	%
θ_L	Volumetric liquid content	%
θ_S	Volumetric solid content	%
q	Flow rate	m/s
ρ	Density	Mg/m^3
ρ_s	Solids density	Mg/m^3
ρ_d	Dry density	Mg/m^3
ρ_{di}	Dry density of constituent i	Mg/m^3
$\rho_{G,L}$	Gas/Liquid density	Mg/m^3
ρ_{sat}	Saturated density	Mg/m^3
S_{eL}	Effective degree of liquid saturation	%
$S_{G,L}$	Degree of gas/liquid saturation	%
S_s	Specific surface	m^{-1}
S^{macro}	Macro saturation	%
S^{micro}	Micro saturation	%
σ'	Effective stress	kPa
σ'_{PC}	Pre-consolidation stress	kPa
σ'_c	Consolidation stress	kPa
T	Temperature	°C ou °K
TN	Total nitrogen	mg/kg MS
t	Time	s
t_{fp}	Time at the end of primary settlement	s
τ	Tortuosity	-
τ	Origin of time for waste column layer history (ISPM)	months
τ_{max}	Maximum shear stress	kPa
v_P	Water speed in pores	kPa
μ_i	Percent constituent i (with respect to M_S of the sample)	$\%_{MS}$
v	Speed	m/s
$V_{G,L}$	Gas/Liquid volume	m^3
V_S	Solid volume	m^3

V_T	Total volume of the sample	m^3
V_V	Voids volume	m^3
v_v^{macro}	Volume of macro voids	m^3
v_v^{micro}	Volume of micro voids	m^3
φ	Angle of internal friction	°
w	Settlement at the top of waste column	m
w_{MH}	Moisture content as a ratio of wet mass	$\%_{MH}$
w_{MS} ou w	Moisture content as a ratio of dry mass	$\%_{MS}$
w_{sat}	Saturated moisture content	$\%_{MS}$
w^{macro}	Macro pore moisture content	$\%_{MS}$
w^{micro}	Micro pore moisture content	$\%_{MS}$
$x_i^{molaire}$	Molar fraction of constituent ‘i’	-
ζ	Angle of tensile forces	°

Perfect gas constant R = 8.31 J/(mol x K)

Acceleration due to gravity g = 10 m/s^2 (g = 9.81 m/s^2)